NEI 04-07

PRESSURIZED WATER REACTOR SUMP PERFORMANCE EVALUATION METHODOLOGY

Revision 0
December 2004

Volume 1 – Pressurized Water Reactor Sump Performance Evaluation Methodology

Volume 2 – Safety Evaluation by the Office of Nuclear Reactor Regulation Related to NRC Generic Letter 2004-02, Revision 0, December 6, 2004

This page intentionally left blank.

December 6, 2004

Mr. Anthony R. Pietrangelo
Nuclear Energy Institute
1776 I Street, NW
Suite 400
Washington, DC 20006-3798

SUBJECT: PRESSURIZED WATER REACTOR CONTAINMENT SUMP EVALUATION METHODOLOGY

Dear Mr. Pietrangelo:

By letter dated May 28, 2004, you submitted a guidance report, “Pressurized Water Reactor Sump Performance Evaluation Methodology,” that is intended to allow pressurized water reactor plant licensees to address and resolve Generic Safety Issue (GSI) 191 in an expeditious manner. The report and the enclosed U.S. Nuclear Regulatory Commission (NRC) staff safety evaluation (SE) of the report relate to NRC Generic Letter 2004-02, “Potential Impact of Debris Blockage on Emergency Recirculation During Design Basis Accidents at Pressurized-Water Reactors,” issued September 13, 2004.

The guidance report is divided into two primary parts, the baseline evaluation and the refinements section. The NRC staff has reviewed the report and determined that portions of the report are acceptable as is and other portions needed additional justification and/or modification. Therefore, the staff has identified conditions and limitations and required modifications in the SE for those report portions that needed additional justification and/or required modifications.

The staff concludes that the guidance report, as approved in accordance with the staff SE, provides an acceptable overall guidance methodology for the plant-specific evaluation of emergency core cooling system or core spray system sump performance following postulated design basis accidents.

Contact Mr. John N. Hannon at 301-415-1992 if you have any questions.

Sincerely,

//RA//

Suzanne C. Black, Director
Division of Safety Systems Analysis
Office of Nuclear Reactor Regulation

Enclosure: Safety Evaluation

This page intentionally left blank.

SAFETY EVALUATION BY

THE OFFICE OF NUCLEAR REACTOR REGULATION

RELATED TO NRC GENERIC LETTER 2004-02,

NUCLEAR ENERGY INSTITUTE

GUIDANCE REPORT

(PROPOSED DOCUMENT NUMBER NEI 04-07),

“PRESSURIZED WATER REACTOR

SUMP PERFORMANCE EVALUATION METHODOLOGY”

FOREWORD

The Nuclear Energy Institute (NEI) submitted its report, “Pressurized Water Reactor Sump Performance Evaluation Methodology,” (proposed document number NEI 04-07) in May 2004 to the U.S. Nuclear Regulatory Commission (NRC or the staff) for review (NEI, 2004a). The objective of this safety evaluation (SE) is to document the staff’s review of methodology guidance for licensees of pressurized water reactors (PWRs). This SE relates to NRC Generic Letter (GL) 2004-02, “Potential Impact of Debris Blockage on Emergency Recirculation During Design Basis Accidents at Pressurized-Water Reactors,” issued September 13, 2004 (GL-04-02).

In the staff’s review of the NEI submission, it found that portions of the proposed guidance were acceptable as is; other portions needed additional justification and/or modification. Therefore, in an effort to expedite the resolution of Generic Safety Issue (GSI)-191, “Assessment of Debris Accumulation on PWR Sump Performance,” (issued in September 1996), the staff has identified conditions and limitations and required modifications, including alternative guidance to supplement those portions of the proposed guidance that the staff determined required additional justification and/or modification. The NEI submission, as approved in accordance with the staff safety evaluation, provides an acceptable overall guidance methodology for the plant-specific evaluation of emergency core cooling system (ECCS) or core spray system (CSS) sump performance following any postulated accident for which ECCS or CSS recirculation is required, with specific attention given to the potential for debris accumulation that could impede or prevent the ECCS or CSS from performing its intended safety functions.

EXECUTIVE SUMMARY

In May 2004, the Nuclear Energy Institute (NEI) submitted the report, “Pressurized Water Reactor Sump Performance Evaluation Methodology” (proposed document number NEI 04-07, (NEI, 2004a), referred to herein as the Guidance Report or GR), for review by the U.S. Nuclear Regulatory Commission (NRC or the staff). The NRC’s approval of this methodology guidance would allow licensees of pressurized water reactors (PWRs) to use the document to respond to the NRC Generic Letter (GL) 2004-02, “Potential Impact of Debris Blockage on Emergency Recirculation During Design Basis Accidents at Pressurized-Water Reactors” (GL-04-02), issued on September 13, 2004, as the cited NRC-approved methodology for evaluating plant-specific sump performance. The GL identifies inadequacies in previous approaches for modeling sump-screen debris blockage and related effects, such that the staff no longer considers many licensing-basis analyses acceptable for confirming compliance with the NRC regulations. The NEI submission offers guidance to all PWR licensees in response to those inadequacies, identified during the resolution of Generic Safety Issue (GSI)-191, “Assessment of Debris Accumulation on PWR Sump Performance,” issued in September 1996.

The NEI submission, as approved in accordance with the staff’s safety evaluation, provides an acceptable overall guidance methodology for the plant-specific evaluation of the emergency core cooling system (ECCS) or containment spray system (CSS) sump performance following all postulated accidents for which ECCS or CSS recirculation is required, with specific attention given to the potential for debris accumulation that could impede or prevent the ECCS or CSS from performing its intended safety functions.

The GR is divided into two primary parts, the baseline evaluation and the refinements sections. The baseline is intended by NEI to provide a conservative approach for utilities to perform a “baseline evaluation” of their PWR containment sump using a sample calculation for a consistent and simplified first-step in determining susceptibility to head loss. The refinements sections are intended to address, for those plants that do not “pass” the baseline evaluation, options for refinements to the baseline calculation that either lead to acceptable results, or identify hardware “fixes” to provide acceptable results. The NEI submission addresses the following major areas:

- pipe break characterization
- debris generation/zone-of-influence (ZOI)
- latent debris accumulation within containment
- debris transport to the sump screen(s)
- head loss as a result of debris accumulation
- analytical refinements to remove conservatism(s) from the evaluation
- physical refinements to plant
- alternate evaluation (realistic and risk-informed)
- sump structural analysis
- upstream effects of debris accumulation

- downstream effects of debris accumulation
- chemical precipitation effects of debris accumulation

The following is a brief summary of each major area of the staff's evaluation.

ES.1 PIPE BREAK CHARACTERIZATION

Analysis of the most challenging postulated accident with regard to sump performance during long-term core cooling involves selection of the most limiting pipe break size, location, and debris combination within containment. For a PWR, Section C, Regulatory Position 1.3.2.3 of Regulatory Guide (RG) 1.82, Revision 3, "Water Sources for Long-Term Recirculation Cooling Following a Loss-of-Coolant Accident," issued November 2003, specifies that a sufficient number of breaks in each high-pressure system that relies on recirculation should be considered to reasonably bound variations in debris generation by size, quantity, and type of debris (RG 1.82-3). RG 1.82, Revision 3, stipulates the following maximum set of break locations to be considered:

- breaks in the reactor coolant system (RCS) and, depending on the plant licensing basis, main steam and main feedwater lines with the largest amount of potential debris within the postulated Zone of Influence (ZOI)
- large breaks with the most variety of debris within the expected ZOI
- breaks in areas with the most direct path to the sump
- medium and large breaks with the largest potential particulate debris to insulation ratio by weight
- breaks that generate an amount of fibrous debris that, after transport to the sump screen, could form a uniform thin bed (i.e., usually 1/8 in. thick) that could subsequently filter sufficient particulate debris to create a relatively high head loss referred to as the "thin-bed effect".

The GR states that the objective of the break selection process is to identify the break size and location which results in debris generation that produces the maximum head loss across the sump screen. All phases of the accident scenario must be considered for each postulated break location, including debris generation, debris transport, and sump-screen head-loss calculations. The break selection process outlined in the GR identifies limiting break locations as those that result in the following effects:

- the maximum amount of debris that is transported to the sump screen
- the worst combination of debris mixes that are transported to the sump screen

The GR also provides the following guidance:

- Disregard break exclusion zones for this evaluation (pipe breaks must be postulated in pre-existing break exclusion zones).
- Exclude consideration of NRC Branch Technical Position (BTP) MEB 3-1, "Postulated Rupture Locations In Fluid System Piping Inside and Outside

Containment," (MEB 3-1) as a basis, because limiting conditions for ECCS sump concerns are not related to the pipe vulnerability issues addressed in MEB 3-1.

- For plants needing to consider main steam and feedwater line breaks, break locations should be consistent with the plant's current licensing basis.
- Consider locations that result in a unique debris source term (i.e., not multiple. identical locations).
- Consider locations with high concentrations of problematic insulation.
- Consider breaks that generate an amount of fibrous debris that could create a thin-bed effect.
- Do not consider small breaks less than 2 inches in diameter (for piping attached to the RCS).
- If a significant amount of fibrous debris is not generated, consider breaks that produce the greatest contribution of latent debris sources which may produce the limiting debris loading condition for sump screen blockage concerns.

The staff finds that the GR is consistent with NRC's positions, with the following two exceptions:

1. The GR does not provide guidance for those plants that can substantiate no thin-bed effect, which may impact head loss results and limiting break location.
2. For plants needing to evaluate secondary-side piping such as main steam and feedwater pipe breaks, break locations should be postulated in a manner consistent with the guidance in Section 3.3 of this SE.

To address these exceptions, the staff provided enhanced guidance in the appropriate sections of this SE. Additionally, Appendix VIII to this SE provides a description of a thin bed, including its formation and effects. The guidance provided in the GR, in accordance with the enhanced guidance offered in this SE, provides an acceptable overall approach.

ES.2 DEBRIS GENERATION/ZONE-OF-INFLUENCE

With the rupture of piping comes shock waves and jets of coolant that project from within the piping via the closed system pressure, until that pressure dissipates. Debris is generated as the shock waves and jets impact surrounding insulation, coatings, surfaces, and other materials within the zone. The volume of space affected by this impact, or zone-of-influence, is modeled to define and characterize the debris generated.

The ZOI recommended in GR Section 3.4 is a spherical boundary with the center of the sphere located at the break site. The use of a spherical ZOI is intended to encompass the effects of jet expansion resulting from impingement on structures and components, truncating the sphere wherever it intersects any structural boundary or large robust equipment. The GR recommends that ZOI sizing be determined using the American National Standards Institute/American Nuclear Society (ANSI/ANS) 58.2-1988 standard for a freely expanding jet (ANSI/ANS 58.2-1988). The baseline ZOI comprises the insulation type that generates the largest ZOI of all potentially affected insulation types located inside containment—(i.e., the insulation type with the lowest destruction pressure). The resulting ZOI will then be applied to all insulation types.

Coating debris generation, however, is treated separately. The GR indicates that coating debris is generated from postulated failure (destruction) of both design-basis accident (DBA)-qualified and unqualified coatings within the ZOI and from postulated failure of all unqualified coatings outside the ZOI. For coatings, the GR recommends a ZOI destruction pressure of 1000 pounds per square inch (psi), with a corresponding ZOI radius of 1 pipe diameter. The GR assumes that all coating debris will fail to a particulate size equivalent to the basic material constituent.

The GR describes the debris characteristics in terms of size distribution, size and shape, and density. The GR identifies two size distributions for material within the ZOI, small fines and large pieces. Small fines are defined as debris able to pass through the largest openings of the gratings, trash racks, and radiological fences, which are less than a nominal 4 inches. Debris that cannot pass through these barriers is classified as large pieces.

For sizing fibrous debris within the ZOI, most fiber is assumed to degrade to 60 percent small fines and 40 percent large pieces. Some fiber is considered to degrade to 100 percent small fines and no large pieces. Reflective metallic insulation (RMI) is assumed to degrade to 75 percent small fines and 25 percent large pieces. Most other debris types are considered to degrade to 100 percent small fines and no large pieces. Erosion is neglected based on the assumption that the small fines are already reduced to their basic constituents of individual particles and fibers. Jacketed large debris is also assumed not to erode.

The GR tabulated debris material densities and size distributions for select debris types. The GR lists properties of materials for which limited data are available as “best available.” For those materials for which no data are available, the GR assumes maximum destruction.

The GR assumes that coatings will fail as particulate. The amount of particulate is a function of coating properties, including the thickness and area. The GR indicates that when plant-specific data do not exist regarding the thickness of unqualified coatings, an equivalent thickness of 3 mils of inorganic zinc (IOZ) be used.

The staff has reviewed the use of a spherical model sized in accordance with the ANSI/ANS standard and finds this approach acceptable. The spherical geometry proposed encompasses a zone which considers multiple jet reflections at targets, offset between broken ends of a guillotine break, and pipe whip. The staff’s confirmatory analysis (see Appendix I to this SE) verifies the applicability of the ANSI/ANS standard for determining the size of this zone. The staff found the use of a ZOI model to be an acceptable approach for analyzing debris generation in accordance with RG 1.82, Revision 3 (The staff also used and approved this approach in the boiling-water reactor (BWR) sump performance SE). The GR recommendation to truncate the spherical ZOI when a robust barrier or large piece of equipment is encountered is acceptable to the staff. The refinement offered in the GR to apply spherical ZOIs that correspond to material-specific destruction pressures for each material that may be affected in the vicinity of a break, is also acceptable.

A light-water reactor (LWR) loss-of-coolant accident (LOCA) jet is a two-phase steam/water jet. The destruction pressures, cited in the GR and referenced from the Boiling Water Reactors Owners Group (BWROG) Utility Resolution Guide (URG), were determined using an air jet. Based on staff study of this difference and because of limited experimental evidence from two-phase jets, the BWROG destruction pressures could be too high and thus could underestimate debris quantities. The staff position in this SE is to lower the debris destruction pressure by 40 percent to account for two-phase jet effects (see Section 3.4.2.2 of this SE).

With regard to coatings, the staff agrees with the approach taken in the GR; however, the staff considers there to be insufficient technical justification to support a value of 1000 psi as a destruction pressure, with a corresponding ZOI of 1 pipe diameter. The staff position is that the licensees should use a coatings ZOI spherical equivalent determined by plant-specific analysis, based on experimental data that correlate to plant materials over the range of temperatures and pressures of concern, or 10D (10 pipe diameters.)

The staff concurs with the characterization of debris in GR Section 3.4.3. Confirmatory analyses provided in Appendix II to this SE verify the acceptability of the size distributions recommended in the GR. However, the staff position is that licensees apply insulation-specific debris size information when available.

For the characterization of coatings in Section 3.4.3.4, the staff position is that the alternative offered to the use of plant-specific data for the determination of coatings thicknesses should include plant-specific justification. The recommended equivalent inorganic zinc (IOZ) thickness of 3 mils may be nonconservative and unsubstantiated because, although the assumption that all “unqualified” coatings outside the ZOI fail is consistent with the position provided in NUREG-0800, “Standard Review Plan for the Review of Safety Analysis Reports for Nuclear Power Plants,” Section 6.1.2, “Protective Coatings Systems,” the staff is aware of numerous cases in which containment coatings, “qualified” and “unqualified”, are much thicker than the recommended 3 mil IOZ-equivalent thickness.

In addition, for those plants that can substantiate no formation of a fibrous thin bed, the assumptions and guidance provided in the GR for coatings may be nonconservative in that the particulate-sized debris assumed would simply pass through the screens and not cause a head-loss concern. Therefore, for any such plant, the staff position is that assumptions related to coatings characterization be realistically-conservative based upon the plant-specific susceptibilities and data identified by the licensee, or that a default area equivalent to the area of the sump-screen openings be used for coatings size.

ES.3 LATENT DEBRIS

Section 3.5 of the GR provides guidance for estimating the amount of latent debris as a contributing source to head loss across the ECCS sump screen. Generally, miscellaneous fiber, dust, and dirt are primary sources of this debris type. For all-RMI plants, latent debris sources may provide the primary contribution of fibrous debris toward formation of a thin bed.

The staff has reviewed the guidance provided for estimating the impact of latent debris and agrees that it is necessary to determine the types, quantities, and locations of latent debris. The staff also agrees that it is not appropriate for licensees to assume that their existing foreign material exclusion (FME) programs have entirely eliminated miscellaneous debris. Results from plant-specific walkdowns should be used to determine a realistic amount of latent debris in containment and to monitor cleanliness programs for consistency with committed estimates.

The staff considers the guidance provided in the GR for consideration of the effects of latent debris to be acceptable for (1) general considerations for latent debris, (2) estimates of some surface areas for evaluation of latent debris, and (3) some attributes associated with evaluation of debris buildup, quantity of miscellaneous debris, and defining debris characteristics. Section 3.5 of this SE provides alternate guidance for sampling techniques and analysis to allow licensees to more accurately determine the impact of latent debris on sump-screen performance. This revised approach is based on generic characterization of actual PWR debris samples. If desired, a licensee could pursue plant-specific characterization as a refinement.

ES.4 DEBRIS TRANSPORT

Section 3.6 describes debris transport which is separately specified for each of three containment types—highly-compartmentalized, mostly uncompartmentalized, and ice condenser containments. The staff's review of debris transport considers the transport of the two size distributions identified in ES.2 above, and discussed in Section 3.4.3 (i.e., small fines and large pieces).

The staff finds that the transport guidance for small fines of debris is acceptable. However, the guidance for the large pieces of debris is unacceptable because of the unrealistic assumption that large pieces of debris cannot be transported. Specifically, plants with configurations conducive to fast pool velocities will realistically transport some large pieces, therefore the staff position is that consideration of the transportability of large pieces of debris is necessary.

The staff also finds that the method recommended for determining the quantity of fine debris trapped in inactive pools based on the volume ratio of inactive pools to the total pools is unrealistic for plants with large inactive pools. Therefore the staff position is that licensees should limit the maximum fraction of fine debris being trapped in inactive pools to 15 percent to avoid nonconservative results.

ES.5 HEAD LOSS

Computation of head loss in the GR involves input of design characteristics and thermal-hydraulic conditions into a head loss correlation (NUREG/CR-6224). The approach is acceptable to the staff, with specific areas of additional guidance offered in Sections 3.7.2.2 and 3.7.2.3 of this SE. The licensees should ensure the validity of the NUREG/CR-6224 correlation for the application of specific types of insulation and the range of parameters using the guidance provided in Appendix V to this SE.

The following additional guidance on fibrous thin bed formation should be considered:

- use of the appropriate density in the determination of the quantity of debris needed to form a thin bed (i.e., the as-manufactured density)
- careful evaluation of the limiting porosity for the particular particulate or mixture of particulates in the debris bed
- consideration of uncertainties in specifying a 1/8-in. bed thickness criteria (e.g., the indication that calcium silicate can form a debris bed without supporting fibers)
- consideration of other uncertainties (e.g., uncertainties associated with mixing of constituents, or uncertainties associated with latent debris data collection)

Before using the NUREG/CR-6224 correlation that is recommended in the GR or any other head-loss correlation, licensees should ensure that the correlation is applicable for the type of insulation and the range of parameters. If the correlation has been validated for the type of insulation and the range of parameters, licensees may use it without further validation. If the correlation has not been validated for the type of insulations and the range of parameters, licensees should validate it using head- loss data from tests performed on the particular type of insulations.

ES.6 ANALYTICAL REFINEMENTS

Three analytical topics are identified in this section—i.e., debris generation, debris transport, and head loss. A fourth, break selection, is addressed in Section 4.2.1.

For debris generation, the GR recommends two refinements for insulation materials. First, the GR proposes use of debris-specific ZOIs versus use of the most conservative debris type applied to all. Second, the GR proposes use of two freely expanding jets emanating from each broken pipe section versus use of a spherical ZOI. The staff finds both debris generation refinements to be acceptable.

For debris transport, the analytical refinements section of the GR provides two methods for computing flow velocities in a sump pool, the network method and the computational fluid dynamics (CFD) method. The staff finds both methods to be acceptable for predicting sump pool flow velocities provided the models are properly applied. However, neither method adequately addressed the estimation of debris transport once sump pool hydraulic conditions were determined. The network method lacked any debris transport guidance. The CFD method included debris transport guidance, which did not address two key aspects of the evaluation, i.e., where and when the debris enters the sump pool and debris size distributions appropriate for sump pool debris transport. For this reason, the staff provided alternative methods.

For head loss, only refinements discussed in GR Section 3.7.2.3.2.3, “Thin Fibrous Beds,” are offered. This section addresses the need to consider fibrous thin-bed formation, and the alternative consideration of latent debris as the primary contributor to this thin bed for all-RMI plants.

ES.7 PHYSICAL REFINEMENTS TO PLANT

GR Section 5.0 provides guidance for refinements in the areas of debris source term, debris transport obstructions, and screen modifications.

The following areas for refinement are offered for the debris source term:

- housekeeping and foreign material exclusion (FME) programs
- change-out of insulation
- modification of existing insulation
- modification of other equipment or systems
- modification of or improve coatings program

The staff has reviewed these refinements and finds them to be acceptable. However, with regard to insulation change-out or modification, the staff emphasizes consideration of the minimum loadings required to form a thin bed. In addition, the statement that DBA-qualified coatings have very high destruction pressures has not been demonstrated (see Sections 3.4.2, and 4.2.2.2.3).

This section of the GR also discusses the potential use of floor obstructions to provide barriers to prevent debris transport to the sump. It mentions that barriers can be used either near the sump or closer to the debris source. Key considerations regarding the use of floor obstructions and barriers include; (1) that the barrier be located where flow velocities and turbulence are insufficient to lift debris over the barriers, and (2) that the barrier should cover the entire cross section of flow.

To credit debris transport obstructions for trapping debris, plant specific documentation should be available on site to demonstrate an appropriate correlation to the test results in terms of debris type and velocity limits.

The staff finds the screen modifications discussed in the GR to be acceptable; however, licensees are not limited to those identified.

ES.8 ALTERNATE EVALUATION

NEI has proposed an alternative evaluation approach which incorporates realistic and risk-informed elements to the PWR sump analysis. The following three steps are proposed for this alternative approach, or “Option B”:

- Define a “debris generation” LOCA break size to distinguish between customary and more realistic design-basis PWR sump analyses.
- Perform customary design-basis analyses for break sizes up through the debris generation break size identified above (i.e., Region I analyses).
- Perform analyses demonstrating long-term cooling and mitigative capability for break sizes larger than the debris generation break size up through the double-ended rupture of the largest RCS piping (i.e., Region II analyses).

The GR proposes realistic treatment of Region II break sizes based on the low probability of these larger breaks. The models, assumptions, and equipment availability for mitigation used for this analysis are proposed to be realistic and demonstrated as functionally reliable, and may not necessarily be safety related or single failure proof. Licensees would perform risk evaluations as a basis for plant modifications and credit taken for operator actions. Such analyses may require plant-specific exemption and/or license amendment requests.

In considering the risk-informing aspects of the resolution of GSI-191, the staff recognized that the potential exists for the containment sump to clog if the mitigation capability credited in the Region II analysis does not function properly. Based on the industry-proposed approach in the Region II analysis, which also uses the conservative large-break (LBLOCA) frequency reported in NUREG-1150 to calculate the target reliability of the mitigation capability, and using the related generic study information, the largest LBLOCA core damage frequency (CDF) would be 1.4x10-5/year. This indicates that at a minimum the risk associated with LBLOCAs will be reduced from the current condition by nearly an order of magnitude.

- The staff concludes that GR Section 6.0 provides an acceptable approach for evaluating PWR sump performance. Application of more realistic and risk-informed elements is technically justified based on the low likelihood of such breaks occurring.

ES.9 <u>SUMP STRUCTURAL ANALYSIS</u>

The staff provides information in this section to show that structural loads on a sump screen should be computed using the total pressure drop across the screen. The limiting conditions correspond to the break location and debris source term that induce the maximum total head loss at the sump screen after full consideration of transport and degradation mechanisms. This represents the minimum required performance criterion for judging recirculation-sump operability. In other words, the recirculation sump must be able to accommodate both the clean-screen head loss and the debris-induced head loss associated with the limiting break while providing adequate flow through both the ECCS injection pumps and the CSS pumps if needed. For some licensees, the minimum structural design criterion for the sump screen can depend on the plant's net positive suction head (NPSH) margin. Revised plant-specific licensing bases may dictate the structural capacity of the sump screen for supporting water flow through a debris bed under recirculation velocities, depending on screen geometry (i.e., fully submerged versus partially submerged designs).

ES.10 <u>UPSTREAM EFFECTS</u>

The GR states that certain holdup or choke points exist which could reduce flow to and possibly cause blockage upstream of the sump. Such areas within containment are: (1) narrowing of hallways or passages, (2) gates or screens that restrict access to areas of containment, such as behind the bioshield or crane wall, and (3) the refueling canal drain.

The staff finds the guidance with respect to upstream blockage to be acceptable.

ES.11 DOWNSTREAM EFFECTS

This section provides guidance on the evaluation of entrained debris downstream of the sump causing downstream blockage. The three areas of concern identified are: (1) blockage of flowpaths in equipment, such as containment spray nozzles and tight-clearance valves, (2) wear and abrasion of surfaces, such as pump running surfaces, and heat exchanger tubes and orifices, and (3) blockage of flow clearances through fuel assemblies.

The staff finds that this section requires clarification and additional considerations and provides the following alternative guidance with regard to downstream blockage:

- Licensees should consider the potential for particles larger than the flow openings in a sump screen to deform and flow through or orient axially and flow through the screen, and determine what percentage of debris would likely pass through their sump screen and be available for blockage of piping, core spray nozzles, and instrument tubing at downstream locations.
- Licensees should consider the term of operating line-up (short or long), conditions of operation, and mission times.
- Licensees should consider wear and abrasion of pumps and rotating equipment, piping, spray nozzles, instrumentation tubing, and high-pressure safety injection (HPSI) throttle valves. The potential for wear to alter system flow distribution and/or form plating of slurry materials (in heat exchangers) should be included.
- An overall ECCS or CSS evaluation should be performed considering the potential for reduced pump/system capacity resulting from internal bypass leakage or through external leakage.
- Licensees should consider flow blockage associated with core grid supports, mixing vanes, and debris filters, and their effects on fuel rod temperature.

ES.12 CHEMICAL EFFECTS

GR Section 7.4 addresses how reaction products formed in a post-LOCA environment can contribute to blockage of the sump screens and increase the associated head loss across the screens. The GR also defers guidance for dealing with these effects until current testing is complete and the data have been appropriately evaluated.

The staff has considered the NEI response and finds that chemical effects should be addressed on a plant-specific basis. Initially, licensees should evaluate whether the current chemical test parameters are sufficiently bounding for their plant-specific conditions. If they are not, then licensees should justify the use of test results in their plant-specific evaluation. If chemical effects are observed during these tests, then licensees should evaluate the sump-screen head-loss consequences of this effect. A licensee who chooses to modify its sump screen before tests are complete should consider potential chemical effects to avoid additional screen modification should deleterious chemical effects be observed during testing.

GUIDANCE DEVELOPMENT BACKGROUND

The staff of the U.S. Nuclear Regulatory Commission (NRC or the staff) began working with the Nuclear Energy Institute (NEI) on the resolution of Generic Safety Issue (GSI)-191 in 1997 with the establishment of the PWR Industry Sump Performance Task Force. The staff also conducted a study on the susceptibility of pressurized-water reactors (PWRs) to emergency core cooling system (ECCS) sump blockage following a loss-of-coolant accident (LOCA). This study was entitled, “GSI-191: Parametric Evaluations for Pressurized Water Reactor Recirculation Sump Performance” (Rao, 2001), and was performed by Los Alamos National Laboratory (LANL) in support of the NRC’s GSI-191 technical assessment to determine if sump failure is a plausible concern for PWRs.

On July 26 and 27, 2001, the NRC held a public meeting with the industry and other stakeholders including NEI, the Westinghouse Owners Group, the Babcock and Wilcox Owners Group, and the Combustion Engineering Owners Group, on the preliminary findings of that study. This meeting was documented in a meeting summary dated August 14, 2001 (Mtg, 2001). The preliminary results of the study indicated that significant quantities of fibrous and particulate debris will be generated during various size LOCAs, and that a sufficient fraction of this debris may be transported to the sump screen and cause sump screen blockage. However, before determining what regulatory action was needed, the staff presented the results to the industry and interested stakeholders, to discuss the assumptions and calculations in the report. Since that time, the parametric report was approved and issued (NUREG/CR-6762), and the staff concluded that GSI-191 is a credible concern for the population of domestic PWRs and that detailed plant-specific evaluations are needed to determine the susceptibility of each U.S.-licensed PWR to ECCS sump blockage.

The staff has worked closely with NEI, providing feedback in the development of an acceptable approach to the resolution of GSI-191, through a series of public meetings held between July 2001 and October 2003, until the submission of NEI’s October 31, 2003, report entitled “PWR Containment Sump Evaluation Methodology” (NEI, 2003b). Following the public meeting on July 26 and 27, 2001, described above, which involved discussions of risk considerations, as well as the parametric evaluation results, a public meeting was held on March 28, 2002, which was described in a meeting summary dated April 16, 2002 (Mtg, 2002a). The staff presented its approach toward the resolution of GSI-191, as did the industry, making references to the revision of Regulatory Guide (RG) 1.82 “Water Sources for Long-Term Recirculation Cooling Following a Loss-of-Coolant Accident,” the issuance of a generic letter, the update of NUREG-0800, “Standard Review Plan,” (SRP), chemical testing, data collection guidance, and evaluation guidance. The industry also committed to take the lead in resolving this issue.

By the next meeting on May 30, 2002, NEI had issued NEI 02-01, “Condition Assessment Guidelines: Debris Sources Inside PWR Containments,” dated April 19, 2002 (NEI, 2002a). The staff’s comments in response to NEI 02-01 identified minor concerns with a lack of firm direction in some areas of data collection; however, the staff considered that NEI 02-01 provided reasonable overall guidance. Attachment 3 to the meeting summary dated June 6, 2002, includes the staff’s conclusion, as well as status presentations from the staff, NEI, and the industry (Mtg, 2002b).

In the next two public meetings, held on July 2, 2002, and August 29, 2002, the staff discussed the schedule for the draft generic letter, the development of temporary instructions for NRC inspectors regarding GSI-191, concerns surrounding downstream effects, such as high-pressure safety injection (HPSI) throttle valve blockage, and presented fault tree modeling for ECCS injection. The NEI discussion focused on interim plant assessment templates and guidance on related compensatory measures, as well as its response to the staff's comments on NEI 02-01. Meeting summaries dated July 31, 2002 (Mtg, 2002c), and September 5, 2002 (Mtg, 2002d), respectively, document the discussions of both meetings.

The next two public meetings, held on October 24, 2002, and December 12, 2002, revolved around the NEI proposed ground rules for the sump evaluation guidance and discussion of head-loss behavior and leak before break (LBB) considerations for break selection, as well as the HPSI issue. The staff objected to the use of LBB as applied to break selection assumptions. NEI issued "NEI Draft Evaluation Methodology Ground Rules" on December 12, 2002 (NEI, 2002b). Meeting summaries dated October 31, 2002 (Mtg, 2002e), and December 31, 2002 (Mtg, 2002f), respectively, include the material presented during both meetings.

The staff, NEI, LANL, and interested stakeholders participated in discussions of GSI-191 issues and toured the University of New Mexico experimental facilities on March 5, 2003. The NRC presented the schedule for generic letter issuance, chemical testing status and expectations, its response to the NEI ground rules for sump evaluation guidance, and supporting data and research by LANL, including debris accumulation, ECCS vulnerability, and pool flow analysis. NEI presented material on the use of LBB for break selection, the use of a nodal network method as an alternative to computational fluid dynamics computer modeling for debris transport analysis, and the use of fracture mechanics for debris generation. The meeting summary, issued April 24, 2004, documented several individual presentations (Mtg, 2003a).

NEI requested a meeting on April 29, 2003, summarized in a meeting summary dated May 15, 2003 (Mtg, 2003b), where the technical basis for using LBB arguments for break selection was discussed at length. The staff recommended that NEI provide for staff consideration an official submission on its proposed approach to break selection. The staff presented the proposed bulletin in the meeting, which was titled "Potential Impact of Debris Blockage on Emergency Sump Recirculation at Pressurized-Water Reactors."

On June 30, 2003, the staff held a public meeting with NEI and interested stakeholders on the issuance of NRC Bulletin 2003-01, "Potential Impact of Debris Blockage on Emergency Recirculation during Design-Basis Accidents at Pressurized-Water Reactors," dated June 9, 2003 (NRCB, 2003). NEI had forwarded 73 industry questions and comments on the bulletin, to which the staff responded in a handout distributed at this meeting. The public also questioned the effect of the bulletin on the overall GSI-191 resolution schedule. All meeting material was attached to the meeting summary dated August 12, 2003 (Mtg, 2003c).

On July 1, 2003, the staff held a separate public meeting with NEI and industry representatives. NEI presented sections of the draft methodology to the staff. The staff discussed progress in four major regulatory areas: the issuance of RG 1.82 Revision 3, head-loss task report, debris characterization project, and chemical effects testing. The credibility of metal corrosion, precipitation of low-solubility lead, and significant head-loss effects from fiber debris beds were also addressed. The public raised the question of ranking the plants' susceptibility to sump blockage, to which the staff replied that no ranking was intended beyond the parametric study results for 69 cases which had already been issued. The associated meeting summary is dated August 11, 2003 (Mtg, 2003d).

The NRC participated in a public workshop on debris impact on ECCS recirculation held in Baltimore, Maryland, on July 30 and 31, 2003, at which the NRC and LANL presented material on sump evaluation methodology and the use of computer codes and volunteer plant studies in sump evaluation analyses. (See Wkshp, 2003 for documentation of the NRC presentations.

The staff held a public meeting with NEI and industry representatives on September 10, 2003, the results of which are documented in a meeting summary dated October 16, 2003 (Mtg, 2003e). The NRC staff expressed concern over chemical effects on sump-screen blockage based on testing. NEI and the industry also presented material on chemical effects. Considerable discussion centered on the formation of gelatinous material due to chemical effects.

On October 31, 2003, NEI submitted to the staff the "PWR Containment Sump Evaluation Methodology" (NEI, 2003b). The staff provided NEI a preliminary review of the October 31, 2003, submission, by letter dated February 9, 2004 (NRC, 2004a). The staff transmitted two requests for additional information (RAIs) by electronic mail to NEI on March 10, 2004, and June 28, 2004. The staff met with NEI and stakeholders in a public meeting on March 23 and 24, 2004, to discuss the draft submission and the March 10, 2004, RAIs. A meeting summary dated April 22, 2004 (Mtg, 2004a) describes the results of this meeting. NEI responded to the staff's RAIs by letters dated June 10, 2004 (NEI, 2004c), and July 8, 2004 (NEI, 2004d), respectively.

On April 19, 2004, NEI submitted to the staff a preliminary version of a baseline evaluation method (NEI, 2004b), found in Section 3.0 of the proposed guidance report (GR). On May 28, 2004, NEI submitted the final version of the "PWR Containment Sump Evaluation Methodology" (NEI, 2004a), including a revised Section 3.0 and a draft version of Section 6.0. On July 7, 2004, NEI provided the staff with a "Table of Refinements," via electronic mail, clarifying what refinements were being offered in the GR. On July 13, 2004, NEI submitted a final version of the risk-informed section, or Section 6.0 (NEI, 2004e), of the GR.

NEI submitted a total of three draft versions of the GR, which the staff reviewed, including a draft of key sections of the evaluation guidance submitted July 1, 2003 (NEI, 2003a); a first draft of the "PWR Containment Sump Evaluation Methodology," submitted October 31, 2003 (NEI, 2003b); and a preliminary version of the current baseline evaluation method, or Section 3.0, of the proposed GR, submitted April 19, 2004 (NEI, 2004b). NEI submitted the final GR to the NRC staff for review on May 28, 2004 (except Section 6.0, which was submitted to the staff on July 13, 2004), and is the subject of this safety evaluation. The final GR provides baseline guidance to utilities for evaluating plant-specific issues of pipe break selection, debris generation, latent debris, debris transport, sump-screen head loss, and ECCS pump net positive suction head. In addition, the GR provides supplemental guidance to be used by licensees to refine their analysis and evaluations. The GR baseline guidance does not provide detailed guidance for several important related issues, including long-term chemical effects and head-loss correlations for particular insulation materials (e.g., calcium silicate), nor does it provide guidance for evaluating the impact of debris passing through the screens and being ingested into the ECCS (downstream effects). The GR does note that licensees must consider these additional elements in the overall performance evaluation in their plant-specific analyses.

The process used between the industry and the staff involved (1) direct discussions between the industry and the staff on key issues, (2) the NRC staff's independent research in support of the GSI-191 resolution effort, and (3) the submission by NEI of three separate versions of the GR, which significantly contributed to the development of the technical basis for an acceptable methodology, which is described in this safety evaluation.

Table of Contents

Review of NEI Guidance Appendices

Confirmatory Analysis and Alternative Guidance Appendices

List of Figures

List of Tables

Acronym List

ACRS	Advisory Committee on Reactor Safeguards
AJIT	air jet impact test
ANSI	American National Standards Institute
ASME	American Society of Mechanical Engineers
BWR	boiling water reactor
BWROG	Boiling Water Reactor Owners' Group
B&W	Babcock and Wilcox
CalSil	calcium silicate
CDF	core damage frequency
CFD	computational fluid dynamics
CP	corrosion products
CS	containment spray
CSS	containment spray system
DBA	design basis accident
DGBS	"debris generation" break size
DDTS	Drywell Debris Transport Study
DEGB	double-ended guillotine break
DPSC	Diamond Power Specialty Co.
ECC	emergency core cooling
ECCS	emergency core cooling system
GDC	General Design Criteria
GR	NEI PWR Sump Performance Evaluation Methodology guidance report
GSI	Generic Safety Issue
HELB	high-energy line break
HPSI	high-pressure safety injection
IEF	initiating event frequency
IOZ	inorganic zinc
LANL	Los Alamos National Laboratory
LBB	leak before break
LBLOCA	large break loss of coolant accident
LDFG	low density fiberglass
LERF	large early release frequency

LOCA	loss-of-coolant accident
NEI	Nuclear Energy Institute
NIST	National Institute for Standards and Technology
NPSH	net positive suction head
NRC	Nuclear Regulatory Commission
PE	Parametric Evaluation
PWR	pressurized water reactor
RAI	Request for Additional Information
RCS	Reactor Coolant System
RG	Regulatory Guide
RMI	reflective metal insulation
SEM	scanning electron microscope
SE	Safety Evaluation
SMC:FP	sump mitigation capability failure probability
SRP	Standard Review Plan
SS	stainless steel
TMI	Three Mile Island
TPI	Transco Products, Inc.
TR	target reliability
UNM	University of New Mexico
ZOI	zone of influence

Intentionally blank

SAFETY EVALUATION BY THE OFFICE OF NUCLEAR REACTOR REGULATION

RELATED TO NRC GENERIC LETTER 2004-02,

NUCLEAR ENERGY INSTITUTE

GUIDANCE REPORT (PROPOSED DOCUMENT NUMBER NEI 04-07)

"PRESSURIZED WATER REACTOR SUMP PERFORMANCE

EVALUATION METHODOLOGY"

1.0 INTRODUCTION

By letter dated May 28, 2004, the Nuclear Energy Institute (NEI) submitted a document entitled, "Pressurized Water Reactor Sump Performance Evaluation Methodology" (proposed document number NEI 04-07) (NEI, 2004a), to the U.S. Nuclear Regulatory Commission (NRC or the staff) for review. This document is herein referred to as the guidance report (GR). NRC approval of the GR would allow licensees of pressurized-water reactors (PWRs) to use the GR to respond to NRC Generic Letter (GL) 2004-02, "Potential Impact of Debris Blockage on Emergency Recirculation During Design Basis Accidents at Pressurized-Water Reactors" (GL-04-02), as the cited NRC-approved methodology for their evaluation of plant-specific sump performance. The GL identifies inadequacies in many of the current PWR licensing-basis analyses for modeling sump-screen debris blockage and related effects, such that the staff no longer considers those analyses acceptable for confirming compliance with NRC regulations. The NEI GR offers guidance to all PWR licensees in response to those inadequacies raised during the resolution of Generic Safety Issue (GSI)-191, "Assessment of Debris Accumulation on PWR Sump Performance," which were documented in the generic letter.

The staff has completed its review of the GR and associated documentation, and this safety evaluation (SE) outlines the staff's conclusions. In general, the staff found that portions of the GR are acceptable for use in conducting plant-specific analyses of emergency core cooling system (ECCS) sump-screen blockage and resultant ECCS and/or containment spray system (CSS) loss of net positive suction head (NPSH) for pumps required following a loss-of-coolant-accident (LOCA). However, the staff found that several portions of the GR are not acceptable because the proposed methods lack sufficient guidance, supporting data, or analysis to justify their technical bases. For each of these areas, the staff has provided a recommendation and/or alternative guidance to that offered in the GR. This SE addresses each section of the GR, discusses the staff's evaluation of the proposed methodologies, and documents the basis for the staff's conclusions.

This SE addresses each part of a plant-specific analysis of sump performance and is organized so that its discussions parallel the guidance discussions presented in the GR. The SE includes sections on each of the following topics:

- pipe break characterization (Section 3.3)
- debris generation/zone of influence (Section 3.4)
- latent debris (Section 3.5)
- debris transport (Section 3.6)
- head loss (Section 3.7)
- analytical refinements (Section 4.0)
- design and administrative control refinements (Section 5.0)
- debris source term refinements (Section 5.1)
- refinements by use of debris transport obstructions (Section 5.2)
- refinements via sump screen modifications (Section 5.3)
- risk-informed evaluation (Section 6.0)
- sump structural analysis (Section 7.1)
- upstream effects (Section 7.2)
- downstream effects (Section 7.3)
- chemical effects (Section 7.4)

1.1 BACKGROUND

In 1979, Unresolved Safety Issue (USI) A-43, "Containment Emergency Sump Performance," was established as a result of evolving staff concerns related to the adequacy of PWR recirculation sump designs. After extensive research, the staff found that the design assumption of 50-percent sump blockage used by licensees was nonconservative under certain conditions, and published the technical findings in NUREG-0897, "Containment Emergency Sump Performance," dated October 1985 (NUREG-0897). Although the staff's regulatory analysis concerning USI A-43 did not support imposing new sump performance requirements, the staff issued GL 85-22, "Potential for Loss of Post-LOCA Recirculation Capability Due to Insulation Debris Blockage," dated December 3, 1985 (GL 85-22). GL 85-22 documented the resolution of USI A-43, recommending that all reactor licensees replace the 50 percent blockage assumption with a comprehensive mechanistic assessment of plant-specific debris blockage potential for future modifications related to sump performance, such as thermal insulation change-outs. The staff also updated the NRC's regulatory guidance, including Section 6.2.2 of NUREG-0800, "Standard Review Plan for the Review of Safety Analysis Reports for Nuclear Power Plants" (hereafter referred to as the Standard Review Plan or SRP) (NUREG-0800) and Regulatory Guide (RG) 1.82, "Water Sources for Long-Term Recirculation Cooling Following a Loss-of-Coolant Accident" (RG 1.82), to reflect the USI A-43 technical findings documented in NUREG-0897.

Following the resolution of USI A-43 in 1985, several events challenged the staff's conclusion that no new requirements were necessary to prevent the clogging of ECCS strainers at operating boiling-water reactors (BWRs).

- On July 28, 1992, at Barseback Unit 2, a Swedish BWR, the spurious opening of a pilot-operated relief valve led to the plugging of two containment vessel spray system suction strainers with mineral wool and required operators to shut down the spray pumps and backflush the strainers.
- In 1993, at Perry Unit 1, ECCS strainers twice became plugged with debris. On January 16, 1993, ECCS strainers were plugged with suppression pool particulate matter, and on April 14, 1993, an ECCS strainer was plugged with glass fiber from ventilation filters that had fallen into the suppression pool. On both occasions, the affected ECCS strainers were deformed by excessive differential pressure created by the debris plugging.
- On September 11, 1995, at Limerick Unit 1, following a manual scram caused by a stuck-open safety/relief valve, operators observed fluctuating flow and pump motor current on the “A” loop of suppression pool cooling. The licensee later attributed these indications to a thin mat of fiber and sludge that had accumulated on the suction strainer.

In response to these ECCS suction strainer plugging events, the NRC issued several generic communications, including Bulletin 93-02, Supplement 1, “Debris Plugging of Emergency Core Cooling Suction Strainers,” dated February 18, 1994; Bulletin 95-02, “Unexpected Clogging of a Residual Heat Removal (RHR) Pump Strainer While Operating in Suppression Pool Cooling Mode,” dated October 17, 1995; and Bulletin 96-03, “Potential Plugging of Emergency Core Cooling Suction Strainers by Debris in Boiling-Water Reactors,” dated May 6, 1996. Through these bulletins, the staff requested that BWR licensees implement appropriate procedural measures, maintenance practices, and plant modifications to minimize the potential for the clogging of ECCS suction strainers by debris accumulation following a LOCA. Bulletin 96-03, in particular, noted the experience-based finding that clogging by fibrous debris is not limited to fibrous insulation as a debris source. All BWR licensees adequately addressed these bulletins.

However, findings from research to resolve the BWR strainer clogging issue in the 1990s raised questions concerning the adequacy of PWR sump designs by confirming what the aforementioned BWR strainer clogging events had earlier indicated: (1) that the amount of debris generated by a high-energy line break (HELB) could be greater than estimated by the USI A-43 research program, (2) that the debris could be finer (and thus more easily transportable), and (3) that certain combinations of debris (e.g., fibrous material plus particulate material) could result in a substantially greater head loss than an equivalent amount of either type of debris alone. Therefore, in 1996, the staff identified GSI-191, to ensure that post accident debris blockage would not impede or prevent the operation of the ECCS and CSS in the recirculation mode at PWRs in the event of a LOCA or other HELB accidents for which sump recirculation is required. The staff began evaluating the potential vulnerability of PWRs and contracted Los Alamos National Laboratory (LANL) to evaluate the potential for debris to cause degraded PWR recirculating sump performance. In July 2001, preliminary parametric calculations were completed on PWR sump performance, which confirmed the potential for debris accumulation in a representative number of operating PWRs. A number of studies (e.g., NUREG/CR-6771, LA-UR-02-7562) have been performed to evaluate the potential for sump clogging and the concerns associated with GSI-191. Designing the containment sump so that it is not susceptible to clogging has been generically estimated in the above studies to reduce the risk associated with large-break LOCAs (LBLOCAs) by a factor of 45. Using the conservative NUREG-1150 LBLOCA frequency (i.e., 5x10-4/year) in the generic calculation results in a risk reduction from 1.6x10-4/year to 3.6x10-6/year. Using a current (more realistic) LBLOCA frequency (4x10-6/year) would result in a risk reduction from 1.2x10-6/year to 2.6x10-8/year.

On June 9, 2003, having completed its technical assessment of GSI-191 (summarized in the next section), the NRC issued Bulletin 2003-01, "Potential Impact of Debris Blockage on Emergency Recirculation During Design-Basis Accidents at Pressurized-Water Reactors," requesting an expedited response from PWR licensees regarding the status of their compliance with regulatory requirements concerning the ECCS and CSS recirculation functions. PWR licensees unable to assure regulatory compliance pending further analysis were asked to describe any interim compensatory measures that they had implemented, or would implement, to reduce risk until the analysis could be completed. All PWR licensees have since responded to Bulletin 2003-01.

In developing Bulletin 2003-01, the NRC staff recognized that it might be necessary for PWR licensees to undertake complex evaluations to determine whether regulatory compliance exists in light of the concerns identified in the bulletin, and that the methodology to perform such evaluations was not currently available. As a result, the NRC did not request such information in the bulletin, but PWR licensees were informed that the staff was preparing a generic letter that would request this information. On September 13, 2004, the staff issued GL 2004-02, "Potential Impact of Debris Blockage on Emergency Recirculation During Design Basis Accidents at Pressurized-Water Reactors" (GL 04-02).

1.2 OVERVIEW

In the event of a HELB inside the containment of a PWR, energetic pressure waves and fluid jets would impinge upon materials in the vicinity of the break, such as thermal insulation, coatings, and concrete, causing them to become damaged and dislodged. Debris could also be generated through secondary mechanisms, such as severe post-accident temperature and humidity conditions, flooding of the lower containment, and the impact of containment spray droplets. In addition to debris generated by jet forces from the pipe rupture, debris can be created by the chemical reaction between the chemically reactive spray solutions used following a LOCA and the materials in containment. These reactions may result in additional debris, such as disbonded coatings and chemical precipitants, being generated. Through transport methods, such as entrainment in the steam/water flows issuing from the break and containment spray washdown, a fraction of the generated debris and foreign material in the containment would be transported to the pool of water formed on the containment floor. Subsequently, if the ECCS or CSS pumps were to take suction from the recirculation sump, the debris suspended in the containment pool would begin to accumulate on the sump screen or be transported through the associated system. The accumulation of this suspended debris on the sump screen could create a roughly uniform covering on the screen, referred to as a debris bed, which would tend to increase the head loss across the screen through a filtering action. If a sufficient amount of debris were to accumulate, the debris bed would reach a critical thickness at which the head loss across the debris bed would exceed the NPSH margin required to ensure the successful operation of the ECCS and CSS pumps in recirculation mode. A loss of NPSH margin for the ECCS or CSS pumps as a result of the accumulation of debris on the recirculation sump screen, referred to as sump clogging, could result in degraded pump performance and eventual pump failure. Debris could also plug or wear close tolerance components within the ECCS or CSS. The effect of this plugging or wear may cause a component to degrade to the point where it may be unable to perform its designated function (e.g., pump fluid, maintain system pressure, or pass and control system flow).

The primary objective of the NRC's technical assessment of GSI-191 was to assess the likelihood that the ECCS and CSS pumps at domestic PWRs would experience a debris-induced loss of NPSH margin during sump recirculation. The NRC's technical assessment culminated in a parametric study that mechanistically treated phenomena associated with debris blockage using analytical models of domestic PWRs generated with a combination of generic and plant-specific data. As documented in Volume 1 of NUREG/CR-6762, "GSI-191 Technical Assessment: Parametric Evaluations for Pressurized Water Reactor Recirculation Sump Performance," dated August 2002 (NUREG/CR-6762-1), the GSI-191 parametric study concludes that recirculation sump clogging is a credible concern for domestic PWRs. As a result of limitations with respect to plant-specific data and other modeling uncertainties, however, the parametric study does not definitively identify whether or not particular PWR plants are vulnerable to sump clogging when phenomena associated with debris blockage are modeled mechanistically.

The methodology employed by the GSI-191 parametric study is based upon the substantial body of test data and analyses documented in technical reports generated during the NRC's GSI-191 research program, as well as earlier technical reports generated by the NRC and the industry during the resolution of the BWR strainer clogging issue and USI A-43. The GSI-191 parametric study references the following pertinent technical reports, which cover debris generation, transport, accumulation, and head loss:

- NUREG/CR-6770, "GSI-191: Thermal-Hydraulic Response of PWR Reactor Coolant System and Containments to Selected Accident Sequences," dated August 2002
- NUREG/CR-6762, Volume 3, "GSI-191 Technical Assessment: Development of Debris Generation Quantities in Support of the Parametric Evaluation," dated August 2002
- NUREG/CR-6762, Volume 4, "GSI-191 Technical Assessment: Development of Debris Transport Fractions in Support of the Parametric Evaluation," dated August 2002
- NUREG/CR-6224, "Parametric Study of the Potential for BWR ECCS Strainer Blockage Due to LOCA Generated Debris," dated October 1995

In light of the new information identified during the efforts to resolve GSI-191, the NRC staff determined that the previous guidance used to develop current licensing-basis analyses did not adequately and completely model sump screen debris blockage and related effects. As a result, because of the deficiencies in the previous guidance, an analytical error could be introduced that would result in ECCS and CSS performance that does not conform to the existing applicable regulatory requirements outlined in GL 04-02. Therefore, the staff revised its guidance for determining the susceptibility of PWR recirculation sump screens to the adverse effects of debris blockage during design-basis accidents (DBAs) requiring recirculation operation of the ECCS or CSS (RG 1.82-3). The NRC staff determined that it was appropriate to request that addressees perform new, more realistic analyses and submit information to confirm their plant-specific compliance with NRC regulations and other existing regulatory requirements listed in GL-04-02 pertaining to post-accident debris blockage.

In addition to demonstrating the potential for debris to clog containment recirculation sumps, operational experience and the NRC's technical assessment of GSI-191 have also identified three integrally related modes by which post-accident debris blockage could adversely affect the sump screen's design function of intercepting debris that could impede or prevent the operation of the ECCS and CSS in recirculation mode.

First, as a result of the 50-percent blockage assumption, most PWR sump screens were designed assuming that relatively small structural loadings would result from the differential pressure associated with debris blockage. Consequently, PWR sump screens may not be capable of accommodating the increased structural loadings that would occur from mechanistically determined debris beds that cover essentially the entire screen surface. Inadequate structural reinforcement of a sump screen may result in its deformation, damage, or failure, which could allow large quantities of debris to be ingested into the ECCS and CSS piping, pumps, and other components, potentially leading to their clogging or failure. The ECCS strainer plugging and deformation events that occurred at Perry Unit 1 (further described in Information Notice [IN] 93-34, "Potential for Loss of Emergency Cooling Function Due to a Combination of Operational and Post-LOCA Debris in Containment," dated April 26, 1993, and licensee event report (LER) 50-440/93-011, "Excessive Strainer Differential Pressure Across the RHR Suction Strainer Could Have Compromised Long Term Cooling During Post LOCA Operation," submitted May 19, 1993,), demonstrate the credibility of this concern for screens and strainers that have not been designed with adequate reinforcement.

Second, in some PWR containments, the flowpaths by which containment spray or break flows return to the recirculation sump may include "choke points" where the flowpath becomes so constricted that it could become blocked with debris following a HELB. Examples of potential choke points are drains for pools, cavities, isolated containment compartments, and constricted drainage paths between physically separated containment elevations. Debris blockage at certain choke points could hold up substantial amounts of water required for adequate recirculation or cause the water to be diverted into containment volumes that do not drain to the recirculation sump. The holdup or diversion of water assumed to be available to support sump recirculation could result in an available NPSH for ECCS and CSS pumps that is lower than the analyzed value, thereby reducing assurance that recirculation would successfully function. A reduced available NPSH directly concerns sump screen design because the NPSH margin of the ECCS and CSS pumps must be conservatively calculated to determine correctly the required surface area of passive sump screens when mechanistically determined debris loadings are considered. Although the parametric study (NUREG/CR-6762-1) did not analyze in detail the potential for the holdup or diversion of recirculation sump inventory, the NRC's GSI-191 research identified this phenomenon as an important and potentially credible concern. A number of LERs associated with this concern have also been generated, which further confirms its credibility and potential significance:

- LER 50-369/90-012, “Loose Material Was Located in Upper Containment During Unit Operation Because of an Inappropriate Action,” McGuire Unit 1, submitted August 30, 1990
- LER 50-266/97-006, “Potential Refueling Cavity Drain Failure Could Affect Accident Mitigation,” Point Beach Unit 1, submitted February 19, 1997
- LER 50-455/97-001, “Unit 2 Containment Drain System Clogged Due to Debris,” Byron Unit 2, submitted April 17, 1997
- LER 50-269/97-010, “Inadequate Analysis of ECCS Sump Inventory Due to Inadequate Design Analysis,” Oconee Unit 1, submitted January 8, 1998
- LER 50-315/98-017, “Debris Recovered from Ice Condenser Represents Unanalyzed Condition,” D.C. Cook Unit 1, submitted July 1, 1998

Third, debris blockage at flow restrictions within the ECCS recirculation flowpath downstream of the sump screen is a potential concern for PWRs. Debris that is capable of passing through the recirculation sump screen may have the potential to become lodged at a downstream flow restriction, such as a high-pressure safety injection (HPSI) throttle valve or fuel assembly inlet debris screen. Debris blockage at such flow restrictions in the ECCS flowpath could impede or prevent the recirculation of coolant to the reactor core, thereby leading to inadequate core cooling. Similarly, debris blockage at flow restrictions in the CSS flowpath, such as a containment spray nozzle, could impede or prevent CSS recirculation, thereby leading to inadequate containment heat removal. Debris may also accumulate in close tolerance subcomponents of pumps and valves. The effect may either be to plug the subcomponent, thereby rendering the component unable to perform its function, or to wear critical close tolerance subcomponents to the point at which the component or system operation is degraded and unable to fully perform its function. Considering the recirculation sump screen’s design function of intercepting potentially harmful debris, it is essential that the screen openings are adequately sized and that the sump screen’s current configuration is free of gaps or breaches which could compromise the ECCS and CSS recirculation functions. It is also essential that system components are designed and evaluated to be able to operate with debris-laden fluid as necessary post-LOCA.

To assist in determining, on a plant-specific basis, whether compliance exists with Title 10, Section 40.46(b)(5), of the *Code of Federal Regulations* (10 CFR 50.46(b)(5)), licensees may use the guidance contained in RG 1.82, Revision 3, “Water Sources for Long-Term Recirculation Cooling Following a Loss-of-Coolant Accident,” dated November 2003. RG 1.82, Revision 3, enhances the debris blockage evaluation guidance for PWRs provided in Revision 1 of the RG to better model sump-screen debris blockage and related effects. The NRC staff determined after the issuance of RG 1.82, Revision 2, that research for PWRs indicated that the guidance in this revision was not comprehensive enough to ensure adequate evaluation of a PWR plant’s susceptibility to the detrimental effects caused by debris accumulation on debris interceptors (e.g., trash racks and sump screens). RG 1.82, Revision 2, altered the debris blockage evaluation guidance found in Revision 1 of the guide following the evaluation of blockage events, such as the Barseback Unit 2 event mentioned above, but for BWRs only. RG1.82, Revision 1, replaced the 50-percent blockage assumption in Revision 0 of the guide with a comprehensive, mechanistic assessment of plant-specific debris blockage potential for future modifications related to sump performance, such as thermal insulation change-outs. This was in response to the findings of USI A-43.

The NEI GR expands on RG 1.82, Revision 3 (requirements for long-term cooling), using portions of NUREG/CR-6808 (knowledge-base report) and other NRC and industry-related documents. The NEI research contributions are (1) in the area of alternate break size, including options for risk informing the analysis as it relates to the initial postulated break size, and (2) on the behavior of protective coatings (a potential debris type) under high-pressure, two-phase jet impact.

In support of the GSI-191 resolution effort, the staff also conducted research, for a plant-specific sump performance analysis based on sample plant data. Although the work was not published, some of it was completed and simply not documented. Therefore, the staff has provided results from specific aspects of this research to supplement areas in the GR that lack supporting data and experimentation as a basis for alternative guidance. Appendices III and VI to this SE provide details of such cases.

2.0 REGULATORY EVALUATION

This section details the regulatory requirements, associated guidance, and precedent upon which the staff based its review of the GR submitted by NEI to be used for the evaluation of PWR sump recirculation performance.

In accordance with 10 CFR50.46(b)(5), licensees of domestic nuclear power plants are required to provide long-term cooling of the reactor core. Specifically, this regulation provides that "after any calculated successful initial operation of the ECCS," the "calculated core temperature shall be maintained at an acceptably low value and decay heat shall be removed for the extended period of time required by the long-lived radioactivity remaining in the core." For this evaluation of PWR recirculation performance, the staff considers this extended time to be 30 days, and requires cooling by recirculation of coolant using the ECCS sump, where coolant is accumulated for this purpose. However, if debris collects and clogs the sump screen or other components or pathways that prevent adequate suction for the ECCS or CSS pumps, then compliance with this regulation may be in question.

RG 1.82, Revision 3, provides guidance for determining compliance with 10 CFR 50.46(b)(5). Section 6.22, "Containment Heat Removal Systems," of the SRP includes the staff's review guidance for evaluating licensee compliance with 10 CFR 50.46(b)(5) Additionally, SRP Section 6.1.1, "Engineered Safety Features Materials," provides the review process for thermal insulation and coating systems, which impact long-term cooling evaluation; SRP 9.2.5, "Ultimate Heat Sink," provides review guidance from which the extended time for recirculation performance is derived; and SRP 6.1.2, "Protective Coating Systems (Paints)," provides review guidance for coating systems, a debris type evaluated in the sump analysis.

For PWRs licensed to the General Design Criteria (GDC) listed in Appendix A to 10 CFR 50; GDC 35 "Emergency Core Cooling" specifies additional ECCS requirements, GDC 38 "Containment Heat Removal" specifies heat removal systems requirements, and GDC 41 "Containment Atmosphere Cleanup" provides requirements for ensuring a clean containment atmosphere. Many PWR licensees credit a CSS, at least in part, with performing the safety functions to satisfy these requirements. PWRs that are not licensed to the GDC may credit a CSS to satisfy similar, plant-specific licensing-basis requirements. In addition, PWR licensees may credit a CSS with reducing the accident source term to meet the limits of 10 CFR 100 or 10 CFR 50.67.

Technical specifications pertain to the ECCS and CSS insofar as they require the operability of these systems for the mitigation of certain DBAs. The final safety analysis report also documents other plant-specific licensing commitments concerning the ECCS and CSS.

The staff considered the NRC's August 28, 1998, SE on the "Utility Resolution Guidance (URG) for ECCS Suction Strainer Blockage (NEDO-32686-A)" (URG SE) used to resolve the related strainer blockage issue for BWRs in its evaluation of the GR. This approach helped to assure consistency and efficiency. In some areas, departures from the GR and the URG SE were warranted because of differences in the design features of BWRs and PWRs, as well as later information obtained through regulatory research.

The staff considered the Commission's staff requirements memorandum (SRM) from A.L. Vietti-Cook to L.A. Reyes, SECY-04-0037, "Issues Related to Proposed Rulemaking to Risk-Inform Requirements Related to Large Break Loss-of-Coolant-Accident (LOCA) Break Size and Plans for Rulemaking on LOCA with Coincident Loss-of-Offsite-Power," dated July 1, 2004 (SECY-04-0037) and RG 1.174, "An Approach for Using Probabilistic Risk Assessment in Risk-Informed Decisions on Plant-Specific Changes to the Licensing Basis," dated July 1998 (RG 1.174), in the review of industry-proposed alternatives, and in the realistic and risk-informed options with regard to break size selection and mitigative equipment requirements.

3.0 BASELINE EVALUATION

Section 3 of the GR provides an evaluation methodology referred to as a baseline set of methods that help identify the dominant design factors for a given plant. The baseline evaluation methodology is intended to provide an approach that includes sufficient conservatism to allow the use of simpler analytical methods.

3.1 INTRODUCTION

Section 3.1 of the GR describes the purpose of the baseline and presents background information regarding general accident scenarios of concern and accident phenomena. This section also notes the limitations of the evaluation method. It makes reference to supplemental guidance for refinements, and data collection to support base evaluations.

Key introductory points include the following:

1. This section states, “If a plant uses this method and guidance to determine that sufficient head-loss margin exists for proper long-term Emergency Core Cooling (ECC) and Containment Spray (CS) function, no additional evaluation for head loss is required.”
2. The baseline evaluation method only addresses the phenomena and issues up to and including head loss across the sump screen. Insufficient information presently exists to evaluate the effects of chemical reaction products on head loss across a sump screen and the associated debris bed. In addition, the baseline methodology does not include the evaluation of holdup of flow by debris upstream of the sump screen, the structural integrity of the sump screen, or the effects resulting from debris passing through the sump screen and being ingested into the ECCS or CSS.
3. The baseline evaluation guidance provides a conservative approach for evaluating the generation and transport of debris and the resulting head loss across the sump screen. If a plant determines that the results of the baseline approach are not acceptable, or additional design margin is desirable, the refinement guidance provided in subsequent sections may be used to further evaluate the post-accident performance of the ECC sump.

Staff Evaluation of GR Section 3.1: The baseline guidance acknowledges that the chemical reaction product effects on head loss, downstream effects, and upstream effects are not fully considered in the baseline evaluation methodology. However, the guidance does not make it explicitly clear that the plant must still address these issues, even if the licensee successfully applied the baseline method to the plant. Therefore, the staff position is that licensees address these effects in accordance with the staff positions specified in Section 7.0 of this SE.

The staff questions the GR statement that the baseline provides a conservative approach. Aspects of the baseline guidance have been identified that are clearly not conservative, while other aspects are conservative. The subject aspects are identified at the appropriate locations in this SE. Acceptance of the baseline evaluation requires that the baseline approach results in an evaluation that, overall, is realistically conservative.

The staff has sponsored research to confirm whether or not specific aspects of the guidance are truly conservative, as stated by the guidance. Results of this research are included in Appendices I, II, IV, and V, to this SE; and are referenced appropriately in the pertinent sections of this document. Section 3.8 of this SE documents the staff's evaluation of assumptions for which conservatism is in question, and provides alternative guidance toward ensuring an overall realistic conservatism for the baseline.

3.2 METHOD OVERVIEW

Section 3.2 of the GR presents the five major areas of the baseline guidance as break selection, debris generation, latent debris, debris transport, and head loss.

3.3 BREAK SELECTION

This section of the GR presents considerations and guidance for selecting an appropriate postulated break size and location for use in the baseline analysis. The stated objective of the selection process is to identify the break conditions that present the greatest challenge to post-accident sump performance.

The staff review resulted in two exceptions to the proposed GR guidance for break selection. These two exceptions involved the treatment of secondary-side breaks and the guidance for plants that can substantiate that no thin bed develops. A discussion of the evaluation of secondary-side breaks is included in this section of the SE. Other sections of this SE discuss guidance for thin-bed considerations, including those on debris generation, latent debris, transport, and head loss. Additionally, Appendix VIII to this SE provides a description of a thin bed, including its formation and effects.

3.3.1 Introduction

The GR describes break selection as a two-step process involving selection of (1) the size of the break and (2) the location of the break.

Staff Evaluation of GR Section 3.3.1 The staff notes that double-ended guillotine breaks (DEGBs) need to be assumed for the baseline analysis of primary system piping (GR Section 3.3.3), so the size of the break is then determined by the diameter of the pipe. Other break-size criteria may be adopted for postulated breaks in secondary piping, depending on assumptions in the plant licensing basis.

The GR states that the objective of the break selection process is to identify the break size and location which results in debris generation that is determined to produce the maximum head loss across the sump screen. The staff finds this objective to be acceptable. Because the assessment will address several complex phenomena for each break location, the location of the most challenging break cannot be identified with confidence until a number of postulated break locations have been evaluated.

3.3.2 Discussion

As stated in the GR, the criterion used to define the most challenging break conditions is the estimated head loss across the sump screen. The break location that maximizes estimated head loss is referred to in the GR as the "limiting break location." All phases of the accident scenario must be considered for each postulated break location, including debris generation, debris transport, and sump-screen head loss calculations. The outcome of head-loss predictions from each candidate break location should be performed systematically and should be self-contained.

Two attributes of break selection which are emphasized in the GR that can contribute to head loss are (1) the maximum amount of debris transported to the screen and (2) the worst combination of debris mixes that are transported to the screen. The GR emphasizes the proper metric for comparison, head-loss effect upon arrival at the screen. The GR requires that break locations be surveyed to provide for both items 1 and 2, above, because under given circumstances, either could represent the limiting break. For example, relatively small quantities of fiber, in combination with LOCA-generated or latent-debris particulate, can induce head losses which exceed the effects of much larger debris beds. RG 1.82, Revision 3 itemizes additional features of a break that may dominate effects on the screen, but these two GR criteria encompass quantity, type, transport, and mixed composition as key issues.

3.3.3 Postulated Break Size

Staff Evaluation of GR Section 3.3.3 The NRC agrees that DEGBs with full piping separation and offset should be used for baseline evaluation of LOCA debris generation for breaks assumed to occur in primary system piping (reactor coolant system (RCS) main loop piping and attached auxiliary piping). For plants that require recirculation to maintain long-term cooling after secondary-system pipe ruptures, either DEGB conditions may be assumed, or conditions consistent with the plant’s licensing basis for breaks may be used to characterize the break size (typically, a spectrum of break sizes is evaluated, up through a double ended rupture). The staff finds that the GR guidance with respect to break size is acceptable because this approach provides for large volumes of debris and the worst combinations of debris.

3.3.4 Identifying Break Locations

Staff Evaluation of GR Section 3.3.4 The NRC agrees that, in accordance with 10 CFR 50.46, all RCS piping and connected piping, must be considered in the evaluation of locations to identify the limiting break. As stated in the GR, some plant designs require eventual coolant recirculation from the sump for pipe ruptures other than a LOCA. If recirculation is required under the plant’s licensing-basis to mitigate these events, then breaks must be examined in this piping, as well. Any actuation of the recirculation pumps implies an initiating event that should be examined for potential debris generation, regardless of whether the recirculation supplies containment spray or safety injection systems.

3.3.4.1 General Guidance

The staff position is provided for each of the following seven principles of break selection guidance offered in the GR.

1. The GR states that break exclusion zones must be disregarded for this evaluation. The staff finds this to be acceptable because all piping locations should be considered. The GR also states that for main steam and feedwater line breaks, licensees should evaluate the licensing basis and include potential break locations in the evaluation, if necessary. The staff finds this to be

acceptable. However, the staff position is that if secondary breaches (i.e., main steam and feedwater line breaks), rely on sump recirculation, as described in the plant licensing basis, breaks should be postulated in these systems at locations chosen in a manner consistent with the remaining guidance in this section.

2. The GR states that application of NRC Branch Technical Position (BTP) MEB 3-1 is not appropriate for determining potential LOCA break locations. The staff finds this to be acceptable (see Section 4.2.1 of this SE for a more detailed discussion of the staff position).

3. The GR states that for plants for which secondary-system breaks (i.e., main steam and feedwater line breaks) rely on sump recirculation as described in the licensing basis, postulated break locations should be consistent with the plant's current licensing basis. The staff finds this position to be unacceptable. The staff position is that secondary-side break locations should be postulated in a manner consistent with the remaining guidance in this section. The reason supporting this position is that inclusion of secondary-break scenarios in the licensing basis acknowledges the possible need for recirculation, but the break locations evaluated in the licensing basis may not have been defined specific to sump performance and could not have anticipated the range of concerns identified in the course of resolving GSI-191. Although secondary side breaks are not analyzed in accordance with the requirements of 10 CFR 50.46 or to demonstrate compliance with these requirements, the staff's position is that licensees relying on the ECCS sumps to mitigate the consequences of secondary-side breaks (e.g., for EEQ purposes) should identify and evaluate the limiting break locations to ensure acceptable sump performance.

4. The GR recommends that pipe breaks be postulated at locations that result in unique debris source terms to avoid multiple locations with identical composition and quantity of debris. The staff considers that in order to assess the potential head loss on the sump screen, the break location must also be judged based on the degree of transport that is expected. Licensees may analyze the first few break locations in full detail, quantifying all phases of the accident sequence. A licensee may then evaluate additional breaks by comparing debris composition, debris quantity, and debris transport potential. This approach will avoid some duplication of effort and will permit a systematic survey of break locations.

5. The GR states that licensees must postulate pipe breaks that affect locations containing high concentrations of problematic insulation (microporous insulation, calcium silicate, fire barrier material, etc.). The staff finds this position to be acceptable. Additionally, in keeping with the objective of identifying limiting break conditions, zones of problematic insulation might be affected by smaller breaks in their vicinity or by larger breaks that encompass them. Both possibilities should be considered because the overall composition of the debris arriving at the screen may be different.

6. As discussed above, the initial quantity and composition of the debris source are important attributes of break selection, but potential transport must also be considered. The GR states that "pipe breaks shall be postulated with the goal of creating the largest quantity of debris and/or the worst-case combination of debris types at the sump screen." The staff agrees that these conditions should

be evaluated. The GR correctly notes that the largest quantity at the screen may not produce the highest head loss. Additional discussion of screen head loss analysis found in Section 3.7 of the SE may help guide the selection of break locations that could create adverse conditions at the sump screen.

7. The GR proposes that piping less than 2 inches in diameter need not be considered in order to identify the limiting break conditions. The staff finds this to be acceptable. While it may be possible for a 2-in. break to challenge NPSH margins for some existing screens, larger breaks postulated with minimal transport would pose an identical challenge. Larger breaks with higher transport potential will certainly bound the maximum on-screen debris permitted by a 2-in. break. Eliminating 2-in. diameter breaks from the baseline greatly simplifies the systematic survey.

3.3.4.2 Piping Runs to Consider

The staff agrees that breaks, ruptures and leaks other than a LOCA will be considered in this analysis, if these scenarios eventually require recirculation for any purpose and if they are part of the plant licensing basis.

The staff's position is that all broken lines, regardless of piping system, that (1) are incorporated in the licensing basis, (2) are capable of generating debris, and (3) lead to a recirculation demand on the sumps should be considered. This position is not meant to imply that breaks must be fully analyzed in every length of every system. Many postulated locations will be eliminated by comparison with other collocated break possibilities of their respective debris volume, composition, and transport potential. However all piping in containment should be considered, regardless of its location within containment because breaks in secondary systems may also be of interest if the above criteria for consideration are satisfied (e.g., main steam and feedwater piping).

The level of detail pursued in the application of breaks in alternative piping systems depends largely on assumptions made in other steps of the accident analysis. For example, if assumptions made in the transport and head-loss analyses both require the assessment of thin bed formation, then break selection can focus on (1) particulate sources that may contribute to the thin-bed, and (2) maximum debris quantities that may dominate the debris bed. An example of a case in which detailed examination of an alternative system might be required is a high-energy line with debris generation potential that is either insulated with or that might affect problematic or diverse insulation types in locations outside the range of larger pipe breaks. Locations of this type might be found in upper containment near component cooling lines close to the pressurizer, for example. Scenarios of this type could be conservatively analyzed using bounding jet parameters relevant to the primary system piping or a new jet calculation could be performed specific to the conditions of the line in question. The actuation of spray for breaks postulated in alternative systems is also a key consideration in their assessment as potentially limiting conditions because containment spray will enhance transport to the recirculation pool and to the sump screen. This discussion is intended to recognize that there may be candidate break locations outside of the larger break zone of influence (ZOI). Conversely, if such locations are already considered within larger postulated breaks with a large ZOI, then detailed examination may not be required.
The explicit assumption of thin-bed formation, regardless of break size or location, offers a significant simplification for break selection because more focus can be placed on the

larger piping systems that envelop more spatial volume. Breaks outside of the crane wall may require more detailed examination for pipe size, pipe pressure, nearby insulation types, and transport potential.

3.3.4.3 Other Considerations for Selecting Break Locations

The GR presents three additional considerations for selecting break. The staff's position regarding each respective consideration is discussed below.

1. The staff finds that the GR correctly emphasizes proper consideration of relative locations between the postulated break location and the affected containment material targets. Additionally, the staff notes that a good understanding of spatial volume obtained from the ZOI discussion in Section 3.4.2 of this SE and related calculations will assist in determining the level of detail needed for the break location survey.
2. The second consideration focuses on the potential for the formation of a thin fiber layer on the screen that filters particulates very efficiently, the so-called thin-bed effect. In general, state-of-the art debris transport methods are not sufficiently advanced to preclude the formation of a thin bed when fibrous insulation is damaged within any ZOI. The degree of vulnerability to this effect is specific to the sump screen in question. This GR consideration for break selection sets a marginal value for debris generation that might already be bounded by larger breaks with minimal transport. The staff agrees that the thin-bed effect should be evaluated. Additionally, the staff's position is that smaller breaks affecting unique combinations of insulation not encompassed by larger breaks should still be examined for potential thin-bed formation. When computing the volume of fibrous debris needed to form a 1/8-inch thick uniform layer on a given sump screen, the dry-bed, or as-manufactured, density should be used, and only the wetted screen area relevant to the break in question should be credited.
3. The GR offers an additional consideration that recognizes the importance of latent debris inventory as a potentially limiting debris source for plants with little or no fibrous insulation. The staff agrees with this consideration, and refers to Section 3.5 of this SE for a more complete discussion of latent debris characterization. The staff notes that plants with non-fiber insulation can use an appropriate dry-bed density for latent fiber and a wetted screen area to establish a plant cleanliness criterion for their foreign material exclusion (FME) programs.

3.3.4.4 Selecting the Initial Break Locations

The staff finds that the guidance offered in the GR for initial break location selection is acceptable and notes that spatial perspectives gained from implementation of the ZOI models will be helpful at directing the break-location survey further. In general, the survey should first consider larger breaks with more complex debris composition and proceed down to smaller breaks with more unique debris compositions that have not yet been captured in the survey. The degree of transport, which can be affected by the use of containment spray, should be considered during the comparison of potential break locations. Starting with this initial break location and moving to other large breaks that envelop any previously identified debris-source concerns will quickly build a set of comparative source-term and transport factors that can be used to judge other locations and classes of postulated breaks without as much detailed quantification. Comparative rationale that disqualifies a candidate location from designation as a limiting break condition should be documented to illustrate the systematic and comprehensive scope of the break-selection survey.

3.3.5 Evaluation of Break Consequences

Staff Evaluation of GR Section 3.3.5 The staff finds that the GR emphasizes the proper metric of comparison between break locations (i.e., head loss across the sump screen as a result of generation, transport, and accumulation of debris on the sump screen). Break locations cannot be eliminated from consideration based on any single attribute alone. The staff agrees that all breaks should be evaluated in the context of the complete accident sequence and the potential effect on sump-screen head loss. Nevertheless, many comparisons will be found that are useful. For example, all large break locations within a compartment may be found to have similar transport characteristics and spatial volume, so only one or two locations within the compartment are needed to bound the variation in debris composition.

3.3.5.1 Purpose of Break Consequence Evaluation

Once the limiting break condition(s) has been identified, the corresponding head loss will be compared to the required NPSH either as a measure of vulnerability to sump blockage or as a design criterion for sump-screen modifications. The staff finds that the GR provides an acceptable and concise summary in this section of the steps involved with evaluating each candidate break location against the criterion of maximum sump-screen head loss.

3.3.5.2 Selection of Intervals for Additional Break Locations

This section of the GR describes a systematic approach to break selection along individual piping runs that starts at an initial location along a pipe, generally a terminal end, and steps along in equal increments (3-ft increments), placing breaks at each sequential location. The staff position is that break intervals can be relaxed to 5-ft increments along the pipe in question and notes that the concept of equal increments is only a reminder to be systematic and thorough. Earlier work reported by NRC contractors using automated analysis tools to evaluate higher spatial resolution (1 to 3 ft increments) was motivated by a risk assessment approach that required an accurate sampling of piping lengths and break sizes to represent the proportional contribution to the overall frequency of sump screen failure. For the purpose of identifying limiting break conditions, a more discrete approach driven by the comparison of debris source term and transport potential can be effective at placing postulated breaks. The key difference between many breaks (especially large breaks) will not be the exact location along the pipe, but rather the envelope of containment material targets that is affected.

The staff agrees that as the plant-specific analysis develops, many break locations along a pipe will be determined by inspection of potential debris inventory, similarity of transport paths, and piping physical characteristics compared to a smaller number of fully quantified break scenarios.

As discussed previously, the staff does not accept the GR position regarding the treatment of secondary-break locations. The staff position is that if secondary-break scenarios involve a recirculation-sump demand, and if these scenarios are part of the plant licensing basis, the same considerations for break location must be applied as discussed in this section for LOCA events in primary piping. The reason supporting this position is that inclusion of secondary-break scenarios in the licensing basis acknowledges the possible need for recirculation, but the break locations evaluated in the licensing basis may not have been defined specific to sump performance and could not have anticipated the range of concerns identified in the course of resolving GSI-191. Although secondary-side breaks are not analyzed in accordance with the requirements of 10 CFR 50.46 or to demonstrate compliance with these requirements, the staff's position is that licensees relying on the ECCS sumps to mitigate the consequences of secondary-side breaks (e.g., for EEQ purposes) should identify and evaluate the limiting break locations to ensure acceptable sump performance.

The staff accepts the GR-stated position regarding breaks in attached piping beyond isolation points, provided there is no possible need for recirculation should a break occur in these sections. The decision whether to include piping segments beyond the isolation points should consider possible failure of the isolation valves in a manner consistent with the licensing basis.

3.4 DEBRIS GENERATION

3.4.1 Introduction

This section of the GR discusses the process of determining, for each postulated pipe break location, the zone within which the break jet forces will be sufficient to damage materials and create debris, the amount of debris generated by the break jet forces and the need to determine the characteristics of the debris.

3.4.2 Zone of Influence

The GR in Section 3.4.2 recommends a spherical boundary for the ZOI with the center of the sphere located at the break site. The ZOI is defined as the volume about the break in which the fluid escaping from the break has sufficient energy to generate debris from insulation, coatings, and other materials within the zone. The use of a spherical ZOI is intended to encompass the effects of jet expansion resulting from impingement on structures and components.

Staff Evaluation of GR Section 3.4.2 The recommended spherical ZOI is a key feature of the baseline evaluation and any alternatives other than spherical or alternatives specifically reviewed and approved by the staff for use within the baseline as described in Section 6.0 of this SE will not be considered valid for the baseline. Section 4.2.2 of this SE addresses the staff's evaluation of refinements to the spherical ZOI.

The spherical zone is a practical convenience that accounts for multiple jet reflections and mutual interference of jets from opposing sides of a guillotine break, as well as pipe whip. It is important to note that when the spherical volume is computed using an acceptable approximation for unimpeded free-jet expansion, the actual energy loss involved in multiple reflections is conservatively neglected to maximize the size of the

ZOI. The staff concurs with the use of a spherical ZOI as a practical approximation for jet impingement damage zones.

3.4.2.1 Recommended Size of Zone of Influence

The GR recommends using the ANSI/ANS 58.2-1988 standard to determine the radius of the spherical ZOI that represents the effects of the jet originating from a postulated pipe break. Appendices B, C, and D of the ANSI/ANS standard provide guidance necessary to determine the geometry of a freely expanding jet for jets originating from a variety of reservoir conditions, including subcooled conditions. This section of the GR reviews the key steps used in the ANSI/ANS 58.2-1988 procedure to determine the size of the ZOI.

Section 3.4.2.1 of the GR also specifically addresses the break jet pressures that will result in coating debris generation within the ZOI.

Table 3-1 of the GR contains the recommended destruction pressures for typical protective coatings and for several types of insulation.

Staff Evaluation of GR Section 3.4.2.1 The staff agrees that the ANSI/ANS 58.2-1988 standard (cited as Reference 3 in the GR) provides a suitable basis for computing spatial volumes inside a damage zone defined by a jet impingement pressure isobar. Appendices in the standard do provide a set of equations that can be evaluated for this purpose, but the presentation is somewhat confusing, and the physical limitations of the model are not discussed thoroughly. For these reasons, Appendix I to this SE adds guidance on the proper evaluation and interpretation of results from the ANSI model.

The GR outlines the following six steps for performing ZOI calculations using the ANSI jet model:

1. The mass flux from the postulated break was determined using the Henry-Fauske model, as recommended in Appendix B to the standard, for subcooled water blowdown through nozzles, based on a homogeneous, none-equilibrium flow process. No irreversible losses were considered.
2. The initial and steady-state thrust forces were calculated based on the guidance in Appendix B to the standard, with reservoir conditions postulated.
3. The jet outer boundary and regions were mapped using the guidance in Section 1.1 of Appendix C, to the standard for a circumferential break with full separation.
4. A spectrum of isobars was mapped using the guidance in Appendix D to the standard.
5. The volume encompassed by the various isobars was calculated using a trapezoidal approximation to the integral with results doubled to represent a DEGB.
6. The radius of an equivalent sphere was calculated to encompass the same volume as twice the volume of a freely expanding jet.

The staff finds these steps acceptable for generic implementation of the model and conversion of isobar volumes to a volume-equivalent spherical radius. However, this SE provides the following observations which concern the implementation details of this method that should be considered when using the model. Appendix I to this SE further explains these details:

1. Plots of metrics related to the Henry-Fauske mass flux presented in the standard do not extend to the desired state point, so it is not clear exactly how the GR evaluated the mass flux. Licensees using this technique should refer to confirmatory Appendix I to this SE for guidance.

2. It should be noted that neglect of irreversible losses refers to internal pipe and pipe component friction losses between the upstream reservoir and the location of the break.

3. Only the steady-state thrust coefficient should be used in this calculation as a conservative bound.

4. Insulation damage pressures, such as the 10 psi cited for Nukon fiberglass, can only be interpreted with a full understanding of the test conditions under which they were experimentally measured. The computed jet conditions will not match the experimental test conditions; therefore, care should be taken to assure that equivalent damage effects are considered. Finally, it should be noted that the GR exercised the model for a spectrum of pressure isobar values because different materials have different resistances to damage from jet impingement.

Regarding the three conditions offered for jet expansion calculations, the staff agrees that DEGB configurations with circular geometries, and full separation and offset between the broken ends, provides the maximum debris generation volume. However, as further discussed in Appendix I to this SE, the choice of fluid reservoir conditions is not justified as bounding for the baseline evaluation, and the reported thermodynamic properties do not match the stated conditions. Using automated National Institute for Standards and Technology (NIST)/American Society of Mechanical Engineers (ASME) steam tables (NIS96), the stagnation enthalpy and degree of subcooling for the stated conditions of 2250 psia and 540°F are 534.9 Btu/lbm and 112.7°F, respectively. Appendix I to this SE confirms that these conditions bound nominal conditions for a hot-leg break, and offers some guidance for licensees to estimate the effects of minor system pressure increases without the need for reevaluating the model.

The staff agrees with the GR's choice of ambient containment pressure versus crediting containment backpressure. The staff considers this choice important because ZOI volumes are strongly driven by the system stagnation pressure, which is highest when the containment is at ambient conditions. The maximum debris generation would occur instantaneously within this ZOI. Furthermore, the use of atmospheric pressure may not be conservative for subatmospheric containment designs that would permit the discharge of a slightly higher mass flux across a break. However, the effect is judged to be small and is compensated by jet-pressure equations in the standard that do neglect ambient pressure in containment. See Appendix I to this SE for a discussion of mass flux calculations and the dependence of ANSI correlations for thrust coefficient on the choice of psia.

The staff finds that the citation of 10-diameter limits for jet damage recommended in NUREG/CR-2913 (WEI83) for structural loadings on equipment and components is not applicable to the present concern regarding insulation damage. The criteria for onset of damage and the implications of structural damage versus debris generation are not directly related. Furthermore, any comparison of conservatism between methods should consider the range of damage pressures for various insulation types. Therefore, the 10-diameter limit for jet damage may only be used for structural loading and for coatings as described below.

Protective Coatings Destruction

The potential debris term generated by failed coatings can be a significant contributor to the total containment sump debris term for some plants. The GR assumes the following LOCA effects on coatings:

- all coatings in the ZOI will fail
- all “qualified” (DBA-qualified or acceptable) coatings outside the ZOI will remain intact
- all “unqualified” coatings will fail

The GR also assumes that coating failure will generate debris in the form of fine particulate which is equivalent in size to the basic material constituents. This is descriptive of the size of the average zinc particle in inorganic zinc (IOZ) coatings or the pigment used in epoxy coatings, which is approximately a 10μm (in diameter) spherical particle in both cases. The GR states that because there is a lack of experimental data regarding coating debris size values, a debris size distribution of 100 percent small fines (10μm IOZ equivalent) is adopted for all coatings inside the ZOI. For coatings outside the ZOI, the GR states that all indeterminate and “DBA-unqualified” and “unacceptable” coatings should be treated as a single coating category which produces debris of the same characteristic, independent of the type of coating. As such, the coating debris size within the ZOI is applicable to all “unqualified”, indeterminate, and “unacceptable” coatings that fail outside the ZOI, as well.

Outside the ZOI, the GR assumes that all “qualified” coatings remain intact and do not contribute to the debris term. Although the GR assumes that all “unqualified” coatings will fail and break down into 10μm particles, it also indicates that plant-specific data should be used to estimate the area and thickness of the “unqualified” coating to determine the amount of debris generated.

The GR indicates that “the ZOI for DBA-qualified coatings or coatings determined to be ‘Acceptable,’ applied to PWR containment surfaces, which results from fluid impingement from the break jet, has not been clearly defined.” However, two key pieces of evidence are offered in the GR to support the argument that “DBA–qualified” and “acceptable” coatings are resistant to direct jet impingement, (1) DBA qualification tests subject samples to elevated temperatures with no apparent loss of structural integrity or performance degradation, and (2) water jet pressures in excess of 2250 psia are commonly required to efficiently remove coatings in industrial applications.

This GR-assumed destruction pressure is tied to experience for removing coatings by the commercial water blast industry and industry waterjet testing detailed in Appendix A to the GR. This testing was performed using a 3500 psig positive displacement pump, hose, and nozzle attachment (high-pressure washer) at two temperatures, approximately 80 °F and 150 °F, to investigate coating degradation under jet impingement conditions. The test apparatus was used at various distances from substrates coated with “qualified” coatings. The testing indicated that coating debris generated in the ZOI would fail as the result of erosion and would generate debris sized roughly equivalent to the coating pigment size. Both IOZ and epoxy were tested. The testing also indicated that coating degradation was influenced by temperature.

Staff Evaluation of Protective Coatings Destruction The staff finds the spherical modeling of the ZOI to be consistent with the approach approved in Section 3.4.2 of this SE, and therefore an acceptable approach for application to coatings. The staff finds that the following assumptions should be applied with regard to coating debris destruction subjected to a LOCA jet:

- “Qualified” coatings outside the ZOI are assumed to remain intact and will not contribute to the sump debris load during a postulated event.
- All “unqualified” coatings outside the ZOI are assumed to fail and act as a potential contributor to the debris load during a postulated event.
- All coatings, regardless of qualification are assumed to fail within the LOCA jet ZOI. The baseline guidance does not provide sufficient technical justification to support use of a 1000 psig coating destruction pressure and corresponding ZOI equivalent to 1 pipe diameter. The staff position is that licensees should use a coatings ZOI spherical equivalent determined by plant specific analysis, or 10D. The specified ZOI of 10D is based upon the previous staff position used for BWR sump analysis (even though there may be differences between the spherical ZOI geometry proposed in this SE and the geometry that may have been used at some BWRs). Any plant specific analysis should incorporate at a minimum the temperature and pressure effects of the jet on plant coating systems in the ZOI. Such an analysis should be based on experimental data over the range of pressures and temperatures of concern using coating samples that can be correlated to coatings found at the plant. The analysis should also seek to accurately estimate the amount of coating on a plant specific basis within the ZOI. If a realistically conservative approach is taken, the basis and justification for why the method is realistically conservative should be provided.

The staff agrees that it is conservative to treat coating debris as highly transportable particulates in the range of 10 to 50 µm in diameter, based on plant susceptibility to thin bed formation at the sump screen. However, for those plants that can substantiate no formation of a thin bed at the sump, this assumption may be non-conservative with regard to sump blockage because fine particulates would pass through the sump screen and generate no blockage concerns. Therefore, for those plants that are susceptible to thin bed formation at the sump screen, use of the basic material constituent (i.e., 10 µm sphere) to size coating debris is acceptable. However, for those plants that can substantiate no formation of a thin bed at which particulate debris can collect, the staff finds that coating debris should be sized based on plant-specific analyses for debris generated from within the ZOI and from outside the ZOI. Such an analysis should conservatively assess the coating debris generated with appropriate justification for the assumed particulate size or debris size distribution. Degraded “qualified” coatings that have not been remediated should be treated as unqualified coatings. Finally, testing regarding jet interaction and coating debris formation could provide insight into coating debris formation and help remove some of the potential conservatism associated with treating coatings debris as highly transportable particulate. If coatings, when tested at corresponding LOCA jet pressures and temperatures, are found to fail by means other than erosion, or the erosion is limited, the majority of debris may be larger, less transportable, or pose less of a concern for head loss.

The staff agrees with the assumption that “qualified” coatings outside the ZOI remain intact during a postulated event and will not contribute to the ECCS sump debris load, because it is based on qualified coatings meeting established quality criteria and acceptance testing and is consistent with the position outlined in Section 6.1.2, “Protective Coating Systems,” of the Standard Review Plan. The assumption is also based on the coatings being in good condition at the initiation of the postulated LOCA. However, operating experience indicates “qualified” coatings require periodic maintenance throughout the coating service life, and operating experience has identified cases in which “qualified” coatings have exhibited significant degradation during the coatings’ normal service life. Therefore, the staff position is that a periodic coating condition assessment be identified, described, and implemented during routine outages, to assure that “qualified” coatings remain capable of performing in a manner consistent with assumptions used to evaluate sump debris loads. Further, the staff has concluded that “qualified” coatings which have degraded, but which have not yet been remediated, should be considered to fail during a postulated accident and will potentially contribute to the debris load. The staff finds that the estimated quantity of debris from degraded qualified coatings (if any) should be based on plant-specific data and should follow the guidance for debris resulting from unqualified coatings.

The staff agrees with the assumption that all “unqualified” coatings outside the ZOI fail, based on the position outlined in SRP Section 6.1.2.

The staff agrees with the assumption that all coatings, regardless of type and qualification will fail within the ZOI because it conservatively addresses the LOCA jet interaction with all coatings (“unqualified” coatings are assumed to fail regardless of location) in this zone; however, the staff believes there is insufficient technical justification for the assumption of a 1000 psig destruction pressure and corresponding spherical ZOI with a radius equivalent to 1 pipe diameter.

Although Appendix A to the GR provides useful test data illustrating the erosion effects of high-pressure water-jets on coating systems, no test data are offered that combine both the effects of mechanical insult and elevated temperature in the same test, and no data appear to be available on the effects of very rapid thermal transients on coating performance. Specifically, the initial conditions of the LOCA jet established in the baseline methodology are 540 °F and 2250 psig, while industry testing referenced in Appendix A to the GR was performed at approximately 3500 psig and 150 °F. Although the initial LOCA jet pressure is expected to be lower than the industry test pressure used (approximately 3500 psig) and waterjet pressure data, the initial LOCA jet temperature expected is significantly higher than the industry test temperatures used (150 °F). The NEI baseline methodology provided no correlation or extrapolation illustrating how the elevated test pressure accounts for the reduced test temperature to produce a similar damage mechanism and degree of damage as the combined temperature and pressure from a LOCA jet. Thus, to the test results do not adequately establish the coating ZOI, and the staff finds the results of the water jet testing to be inconclusive in this regard.

Additional information offered in Appendix I to this SE presents spatial contours of estimated jet impingement temperature for a reference cold-leg break condition. Temperature zones exceeding 300°F are observed to extend out to 10 pipe diameters from the break, and exceed 220°F for most of the jet envelope. Given the small thickness of the paint and the differences in heat conduction between the layer and the substrate, it is presumed that the coating would reach the impingement temperature almost instantly when directly hit by the break jet. Thermal shock may affect bonding with the substrate, induce expansion cracking in the coating layer, and change its tensile properties. All of these potential effects increase the vulnerability of paint to jet impingement. The occurrence of very rapid thermal transients in combination with the mechanical insult of water-laden jet impact is a unique environment that should be subject to experimental study.

The NRC staff acknowledges that the five reasons given to defend the selection of 1000 psig as a destruction pressure for DBA-qualified or acceptable coatings are factual, while the GR arguments do not address important phenomenology of the accident environment. It is premature to accept the proposed value of 1000 psig as either appropriate or conservative. Individual licensees should provide data to support the robustness of their DBA-qualified and acceptable coatings system for use in the baseline analysis. Spatial contours of jet impingement temperature, such as that offered in Appendix I to this SE, may be useful in judging the cost-benefit of alternative test conditions.

Because (1) the temperature effect may be influenced by the coating system (i.e., IOZ alone, IOZ topcoated with epoxy, or multiple coats of epoxy), (2) epoxy and IOZ each would be expected to have a different temperature response, and (3) no testing replicating the effects of LOCA jet pressures and temperatures on coatings (epoxy, IOZ, qualified, or unqualified coatings) have been performed or referenced; the staff position is that either a coating spherical ZOI of 10D be used, or a ZOI be determined by plant-specific analysis. If an analysis is performed, it should incorporate, at a minimum, the combined temperature and pressure effects of the jet on potential coating systems in the ZOI. Such an analysis should be based on experimental data over the range of pressures and temperatures of concern using coating samples that can be correlated to plant materials. The analysis should also seek to accurately estimate the amount of coating on a plant-specific basis within the ZOI. If a bounding approach is taken, it is the staff's position that the basis and justification why the method is conservatively bounding must be provided. The staff believes that a comprehensive test program investigating the effects of direct impingement of a LOCA jet (accounting for jet pressure and temperature) on coating degradation should be performed to have a sound basis for the destruction pressure and size of the coating ZOI.

3.4.2.2 Selecting a Zone of Influence

Section 3.4.2.2 of the GR recommends that for the baseline calculation, the ZOI for a break be selected based on the potentially affected insulation inside containment with the minimum destruction pressure. This ZOI is then applied to all insulation types.

Staff Evaluation of GR Section 3.4.2.2 The staff accepts the baseline approach of selecting ZOI size based on the potentially affected insulation type in containment with the lowest destruction pressure, provided that (1) there are no other materials in containment more fragile than insulation that might pose a debris generation potential, and that (2) defensible damage pressures are available or can be ascertained conservatively with engineering judgment, for all insulation types, coatings and other materials of concern. The implication of the assumption that the presence of a single vulnerable material is that all candidate debris materials should be presumed damaged to the same level. Credit for the individual response of well-characterized insulation types can be given under the refinement offered in Section 4 of the GR.

GR Table 3-1 can be used to match experimentally determined damage pressures with "calculated" values of volume-equivalent spherical ZOI radii. Presumably, the calculations were performed in the manner described in Appendix D to the GR, but no cross reference or explanation is offered. Appendix D cites an evaluation of the ANSI/ANS 58.2-1988 standard that was used to generate spatial jet-pressure contours, but the GR offers no insights for interpreting the resulting pressures with respect to material damage.

In order to confirm that the ANSI jet model was implemented properly, the model was independently programmed and the results compared with the isobar map tabulated in Table D-1 of the GR. This comparison is shown in Figure 3-1 in which the blue contour lines represent the GR evaluation of a break at 2250 psia and 540°F and the red contour lines represent a reference cold-leg break at 2250 psia and 530°F. Appendix I to this SE provides further explanation of the independent calculation and additional guidance on interpreting the results of the ANSI jet model.

Good agreement is seen between the calculations for downrange behavior (Zone 3), but discrepancies exist in Zones 1 and 2. It appears that contour termination points on the centerline are not accurate and that the quadratic behavior of the Zone 2 isobar equations is not implemented correctly. These differences will have a negligible effect on volume integrals for jet pressures less than 20 psig, but may become more of a concern for higher pressures near the break. To quantify the magnitude of the difference, Table 3-1 below presents a comparison of ZOI radii computed from both methods. In particular, the GR approach may not have preserved the system stagnation pressure throughout the volume of the liquid core region, as specified by the standard. However, the GR recommended values essentially bound both sets of calculated values.

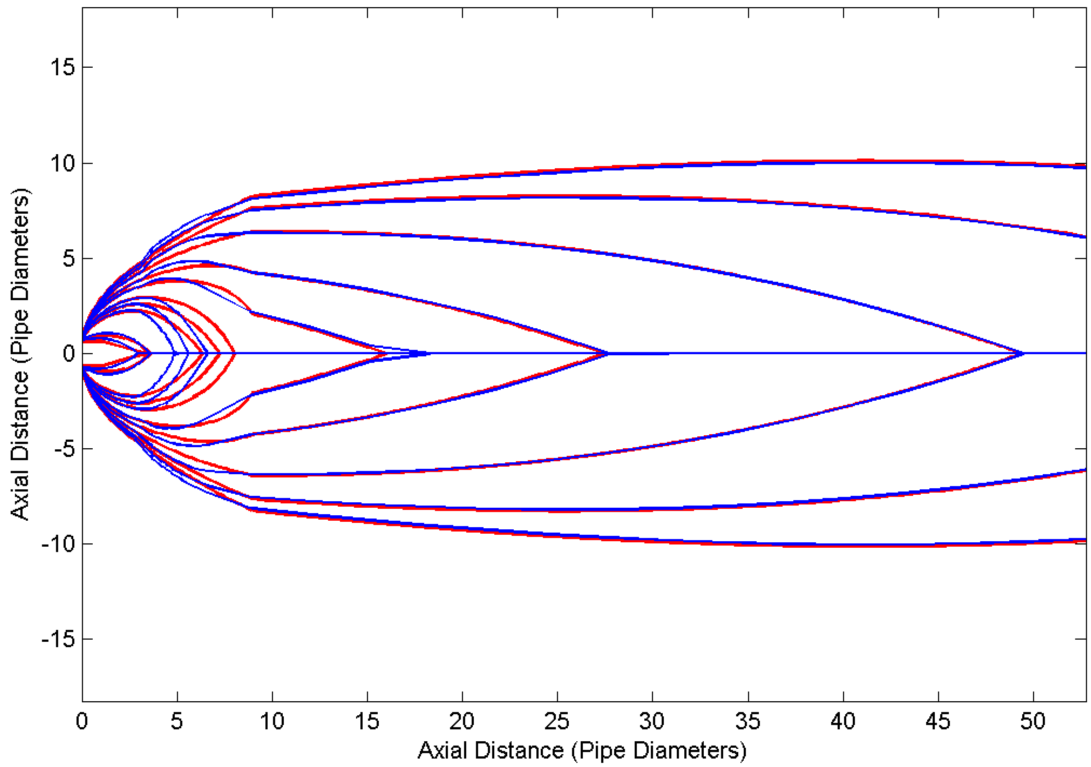

Outside to Inside Contour Values (psig)
4, 6, 10, 17, 24, 40, 50, 64, 150, 190

Figure 3-1. Comparison of GR Isobar Map (Blue) with Isobars from Independently Evaluated ANSI Jet Model (Red)

Table 3-1 Comparison of Computed Spherical ZOI Radii from Independent Evaluations of the ANSI Jet Model

Impingement Pressure (psig)	ZOI Radius/Break Diameter		
	Guidance Report Recommendation	Calculated Value	SE Appendix I
1000	1.0	0.24	0.89[a]
333	1.0	0.55	0.90
190	1.3	1.11	1.05
150	1.6	1.51	1.46
40	3.8	3.73	4.00
24	5.5	5.45	5.40
17	7.8	7.72	7.49
10	12.1	12.07	11.92
6	17	16.97	16.95
4	21.6	21.53	21.60

[a] The core volume at stagnation pressure P0 gives a minimum possible ZOI radius of 0.88 diameters.

The larger question of what damage pressure to recommend for each material type requires an understanding of both the limits of the jet model and the knowledge base of existing experimental data.

First, as discussed in Appendix I to this SE, the jet model predicts impingement pressures in the longitudinal (downstream) direction only and may underestimate the radial extent of isobars in Zones 1 and 2 when considering the impingement pressure that would develop on the face of a target perpendicular to the local flow velocity.

Second, the ANSI model appears to be unbounded in the downstream direction. This means that for very small impingement pressures, the isobar volume will grow unrealistically large. These two limitations compensate to some extent when volume-equivalent spherical radii are computed; because the jet envelope provides a rigid constraint to radial growth of the contours, unbounded downstream growth will eventually dominate.

Unreasonable growth of low-pressure isobars can be illustrated by comparing the spherical radius plot in Figure I-26 (Appendix I) to Figure 3-3 in the parametric evaluation (PE) supplement (NUREG/CR-6762-3). The PE study plots a function of spherical ZOI radii that was determined by the Boiling Water Reactor Owners Group (BWROG) using the NPARC computational fluid dynamics (CFD) model for BWR blowdown conditions. Despite the differences in thermodynamic state point, the differences in qualitative behavior for target pressures less than 20 psig is evident; the ANSI trend appears to be diverging, while the BWROG correlation appears to approach a finite maximum at zero pressure. The NRC reviewed the BWROG calculations and found the NPARC code to be a more capable method of modeling steam jets than the ANSI model.

The staff notes that a comparison using a CFD model for PWR break conditions was not performed for either the GR or this safety evaluation. Caution should be used in comparing calculated and experimentally determined pressures to ensure that the computed parameter of the field matches the measured parameter as closely as possible. For example, while it is trivial to fractionate a computed pressure into static and dynamic components over any incident angle, it may be difficult to obtain high-fidelity measurements under equivalent conditions and diagnostic orientations.

Third, the correlation between any prediction of jet pressure and an experimental observation of damage pressure depends on how the measurements were taken, how the debris was characterized, and what the thermodynamic conditions of the test actually were. Data from the references cited in Table 3-1 of the GR are dominated by tests conducted for resolving the strainer blockage issue for BWRs using high-pressure air as a working fluid. Therefore, much of the test data are not directly applicable to PWR or BWR blowdown conditions in which jets consist of steam and water mixtures. Without directly applicable data and/or high-fidelity predictive models, this surrogate information can only be applied with appropriate caution. The NRC was concerned about potential differences in debris generation between air surrogates and two-phase jets, and therefore initiated a joint test program with Ontario Power Generation (OPG). Testing of low-density fiberglass ended prematurely after only one test, and the concerns were not fully resolved, but Volume 3 of the PE report (NUREG/CR-6762-3 and Reference 7 of the GR document the available results. GR Table 3-1 cites, but does not discuss, these data in reference to damage pressures for calcium silicate. Therefore, there is a very limited set of data to evaluate the effects of two-phase jets on low-density fiberglass.

Destruction pressure is the threshold pressure for the onset of damage. This is normally determined by experimentally measuring the differential pressure on the face of a target. One recurring problem with defining damage pressure is inconsistency in the degree of damage that is correlated to the pressure value. Two obvious choices exist. The first option is to define the minimum pressure (threshold) at which jacketing is breached in any way. Issues regarding contribution to potential screen blockage are then handled with a complete description of the debris size distribution from fines to partially intact cassettes and blankets. The second option is to presume a debris size that is suspected to contribute to the blockage potential and to report the damage pressure as the point at which significant quantities of this debris size are generated. The second option will have higher values of damage pressure than the first, and the debris size distribution will be skewed towards smaller, and therefore more transportable, pieces, if the two options are to give equivalent results in a vulnerability assessment. The second method also requires more a priori subjective judgment. Table 3-1 of the GR reports damage-pressure values based on the second approach. The single fiberglass test performed by OPG resulted in conversion of approximately 50 percent of the insulation volume into debris of sufficiently small size to be a concern. It is assumed that this test meets, by a significant margin, the criteria for significant quantity implicit in the second damage-pressure definition.

The OPG test for fiberglass was conducted at a distance of 10D on the centerline downstream of a heated vessel of water at 1450 psia. Comparisons with more extensive OPG data for calcium silicate suggested that the lower threshold for fiberglass damage in two-phase jets might be as low as 4 psig (NUREG/CR-6762-3). The actual range can only be determined by bracketing with two tests at differing distance the transition from significant damage to negligible damage. While it is true that the insulation products tested by OPG were not identical to those tested in the BWROG air jet tests, substantially different debris characteristics were observed.

In the absence of more complete test data, it is prudent to attribute the observed effects to the differences in the jet medium (i.e. the difference between air used in the BWROG tests and the two-phase steam/water mixture used by OPG). Several plausible physical mechanisms may contribute to enhanced debris generation in two-phase jets, including penetration and erosion from impingement of entrained droplets, increased shear forces within the jet caused by radial velocity components of the expanding fluid, and higher local velocities because of the lower density of water vapor compared to air. To judge the potential contributions of these effects without more extensive data would be speculative, as would be any counter arguments offered to refute their importance. The GR has already acknowledged the potential for material degradation by erosion in relation to coatings damage. Although offered there as an ostensible conservatism, the same phenomenon should be considered for all material types.

Based on the OPG test results, an argument could be made for reducing damage pressures determined through air-jet testing by a factor of 2 or more. In fact, the PE study recommended this approach by reducing the damage pressure for fiberglass from 10 psig to 4 psig. A corresponding spherical ZOI radius was then recommended based, not on the ANSI model for PWR break conditions, but rather on the BWROG correlation for BWR break conditions that were similar to the OPG test. The corresponding radius was reported to be 12-D for an incident pressure of 4 psig, while the ANSI model predicted a 21.6D radius for nominal PWR break conditions at the same impingement pressure. Hence, there appears to be an inconsistency in the PE report because no compensation was made for increased ZOI volume induced by the higher initial pressure of a PWR break.

Given the uncertainties discussed above regarding (1) interpretations and applicability of the ANSI jet model and its performance compared to CFD correlations for very low impingement pressures, (2) the dissimilarity of insulation types, jacketing and target orientation used in the OPG test compared to U.S. PWRs, and (3) the practical definition of damage pressure and its empirical correlation to the degree of insult, it would be speculative to assess the full damage-pressure reduction derived in the PE report. Therefore, based on the 50 percent destruction of fiberglass observed in the only publicly accessible two-phase debris generation test for this insulation type, comparison with OPG data on greater than 40 percent reduction in damage pressure for calcium-silicate insulation, and on the similarity of this degree of damage to the definitions used in Table 3-1 of the GR, the NRC staff position is that damage pressures for all material types characterized with air jet testing should be reduced by 40 percent to account for potentially enhanced debris generation in a two-phase PWR jet.

Of course, specific materials may respond differently (if at all) to the effects of a two-phase jet, but this reduction in damage pressure provides adequate recognition of the issue and could focus some attention on the remediation or mitigation of high-debris volume accident scenarios. When available, the reduced damage pressure thresholds should be replaced with material-specific test data, so the GR recommendation of 24 psig for the damage pressure of calcium silicate is appropriate, based on the findings of the OPG study. Table 3-2 lists the revised destruction pressures and the corresponding ZOI diameters computed as described in Appendix I to this SE for the reference cold-leg break.

Table 3-2 Revised Damage Pressures and Corresponding Volume-Equivalent Spherical ZOI Radii

Insulation Types	Destruction Pressure (psig)	ZOI Radius/ Break Diameter
Protective Coatings (epoxy and epoxy-phenolic paints)	TBD[1]	NA[2]
Protective Coatings (untopcoated inorganic zinc)	TBD[1]	NA[2]
Transco RMI Darchem DARMET	114	2.0
Jacketed Nukon with Sure-Hold® bands Mirror® with Sure-Hold® bands	90	2.4
K-wool	24	5.4
Cal-Sil (Al. cladding, SS bands)	24	5.45
Temp-Mat with stainless steel wire retainer	10.2	11.7
Unjacketed Nukon, Jacketed Nukon with standard bands Knaupf ET Panel	6	17.0
Koolphen-K	3.6	22.9
Min-K Mirror® with standard bands	2.4	28.6

[1] To be determined by experiment.
[2] Not available for evaluation at this time.

Formal debris generation studies have confirmed that insulation products having outer casings, jackets, or other similar mechanical barriers resistant to jet impingement yield smaller quantities of debris than do less robust materials. Various studies have also demonstrated dependence between the orientation of the jacketing seam relative to the jet and the amount of debris generation. This suggests that the integrity of the jacket during impingement is an important feature for minimizing debris generation. Russell reports, for example, that double jacketing an insulation product with a second overcladding of stainless steel having a rotated, opposing seam was very effective at minimizing the distance from the jet to the onset of damage (OPG, 2001). As mentioned in Appendix I to this SE, any improvement in the mechanical resistance of the insulation product will help to avoid inflated ZOI volumes predicted by the ANSI jet model for very low damage pressures.

As noted above, the ANSI/ANS jet model has been proposed in the GR and found acceptable by the staff for the purpose of estimating potential damage volumes associated with empirically measured damage pressures. Various attributes and interpretations of the ANSI jet model are presented in Appendix I to this SE. Among those observations is the explanation of potentially exaggerated conservatism for very low damage pressures. While this is conservative, it may be detrimental for the identification and design of practical mitigation strategies. The staff notes that the use of robust insulation materials is one possible approach for avoiding excess conservatism. Another approach, which can be accomplished concurrently with the testing of specific insulation products, is to properly instrument jet tests for the purpose of refining the ANSI model for the specific application of debris generation. Particular emphasis should be placed on the measurement of impingement pressures on small targets placed both perpendicular to the jet centerline and at radial locations parallel to the jet centerline. A test program such as this would be most effective when combined with concurrent insights gained from models including ANSI-58.2-1988 and CFD.

In a letter dated October 18, 2004, the Advisory Committee on Reactor Safeguards (ACRS) provided its view on the draft SE. Regarding the ANSI/ANS 1988 standard, the ACRS noted several inconsistencies and errors in the models described in the standard. These included no definition of "impingement pressure;" assumed flow patterns which do not correspond to observed and computed patterns for supersonic jets; inconsistent conditions in a free jet compared with a jet impinging on a large target; an unrealistic representation of the physics and inappropriate one-dimensional approximations for an "asymptotic plane;" and that the density at this fictional "asymptotic plane" is evaluated as if the fluid were at rest, whereas in reality it is flowing at a high Mach number. The staff agrees with the ACRS comment on the ANSI/ANS model and observes that additional model inaccuracies, such as unrealistically large isobars calculated for lower stagnation pressures, are noted in Appendix I.

Notwithstanding these technical points, the staff considers the standard acceptable for use in determining the ZOI to be used for modeling debris generation during design basis accidents. This determination is based in large part on the method which is used to approximate the debris generation resulting from postulated breaks. To account for jet reflections, shadowing effects, directionally changing discharge from a whipping pipe, and the difficulty of assessing all potential orientations of breaks, the GR proposes using a spherical volume equivalent to a volume determined using the ANSI/ANS model using the demonstrated destruction pressure of debris sources. This volume translation conservatively ignores the energy that would be lost in multiple reflections and in the generation of debris.

The precision that could be gained by the development of a more accurate method to determine the characteristics of a freely expanding jet is more than offset by conservatism in using an equivalent volume approach for determining ZOI. This is because in reality, damage does not occur throughout a volume but rather on a surface. Although reflection of jets will occur, and can even result in pressure pulses above stagnation pressure in front of particular targets, energy will also be lost in generating debris and redirection of the jets. The staff's position is that the overall approach to determining ZOI is sufficiently conservative (by conserving the volume of a freely expanding jet to isobars of demonstrated destruction pressure) to allow use of the ANSI/ANS standard for determining ZOI. However, the staff remains open to licensee use of alternatives which more accurately model two-phase jets. Such models could be used to significantly reduce the ZOI for low-damage pressure debris sources such as NUKON insulation.

3.4.2.3 The Zone of Influence and Robust Barriers

Section 3.4.2.3 of the GR recommends truncating the spherical ZOI whenever the ZOI intersects a robust barrier such as walls, or components, such as supports, pressurizers, steam generators, reactor coolant pumps or jet shields. Such barriers will terminate further expansion of the ZOI. The area in the shadow of the component or structure will be free from damage. The baseline assumes there is sufficient conservatism in drawing the sphere that it is not reasonable that a jet reflected off of a wall or structure would extend further than the unrestrained sphere.

<u>Staff Evaluation of GR Section 3.4.2.3</u> Conceptually, the volume integral under a computed jet expansion isobar represents the potential for material degradation at pressures equal to the isobar value and higher. Multiple reflections and deflections of a LOCA jet within a confined space would dissipate energy, so conservation of the jet volume under an impingement pressure isobar provides an upper bound on the integral volume of the spatial damage zone, regardless of the shape it is mapped into either by the local geometry of obstacles or by convention for the purpose of analysis. Spherical zones were originally conceived as an adequate approximation for opposing jets from each side of a guillotine break in the congested piping environment of a BWR containment structure. Spherical zones also provide significant convenience for mapping onto piping layouts.

The only conservatism inherent to the ZOI mapping within containment is the conservation of damage potential computed as the volume under a relevant damage-pressure isobar. The degree of conservatism depends on the piping and equipment congestion in the vicinity of the break. More deflections and redirections lead to greater local deposition of energy, and hence, to greater conservatism in the preservation of damage volume, which maximizes the size of the ZOI by assuming no interference with jet development. It is difficult to quantify the degree of conservatism introduced by ignoring jet reflections, but for BWR break conditions, CFD calculations were performed in a spatial domain with contrived obstacles and flow paths to demonstrate rapid dissipation of the potential damage volume. Similar examples have not been offered in the GR to quantify the conservatism that would rationalize the truncation of spherical ZOI. Relevant attributes of this calculation would include representative spatial complexity and scale relative to the damage volume for PWR break conditions.

PWR containment structures often have structural paths that are designed to direct the principal expansion flow. These features include the ice columns in ice condenser plants and steam generator compartments in large dry plants that are vented to upper containment domes with spray deluge systems. Given the potentially large damage volumes that may be predicted from the previous section, it seems reasonable that these spherical ZOI will be redirected along the designed flowpaths for many break scenarios.

The potential benefits of shadowing by equipment and components are also difficult to quantify. Undoubtedly, shadowing is a relevant effect for impingement on a large steam generator from one side in a relatively unconfined location, but within a doghouse enclosure, flows may accelerate completely around the generator causing damage on all sides. Shadowing effects cannot be approximated by strict geometric obstruction angles. The GR provides limited guidance on the practical implementation of the proposed method.

For the baseline analysis, the NRC staff position is that licensees should center the spherical ZOI at the location of the break. Where the sphere extends beyond robust barriers, such as walls, or encompasses large components, such as tanks and steam generators, the extended volume can be truncated. This truncation should be conservatively determined with a goal of +0/–25 percent accuracy, and only large obstructions should be considered. The shadow surfaces of components should be included in this analysis and not truncated, as debris generation tests clearly demonstrate damage to shadowed surfaces of components.

3.4.2.4 Simplifying the Determination of the Zone of Influence

GR Section 3.4.2.4 offers a conservative simplification for the determination of the ZOI. Given the complexity of the analysis as a whole, it may be desirable to make conservative assumptions with the goal of simplifying the analysis. For example, for some breaks it may be only slightly more conservative and much simpler to assume that an entire subcompartment (but not outside the subcompartment) becomes the ZOI.

Staff Evaluation of GR Section 3.4.2.4 The staff concurs that simplifications may be desirable. As a point of practical guidance, it may be useful to precalculate the free volume of subcompartments and rooms that could host a break location or be affected by an adjacent break location. This will facilitate cumulative volume estimates for the total affected zone.

The staff finds the example simplification acceptable; provided the simplification procedure properly justifies that significant jet destruction cannot occur beyond the assumed boundaries of the affected compartments.

3.4.2.5 Evaluating Debris Generation within the Zone of Influence

Section 3.4.2.5 of the GR provides a general statement regarding the assessments of debris within the ZOI and refers to GR Section 3.4.3. It notes that plant-specific information on the type, location, and amount of debris sources within containment is needed. This information is obtained from plant drawings and the results of condition assessment walkdowns.

Staff Evaluation of GR Section 3.4.2.5 The staff finds the general statement in GR Section 3.4.2.5 to be acceptable. To further clarify, the staff suggests that once the spatial region of the ZOI has been determined, the next step is to calculate the volume of insulation, the surface area of coatings (both qualified and unqualified), and the amounts of any other potentially frangible debris sources within that ZOI. Guidance provided in other sections determines how this insulation is distributed by size and character into debris.

3.4.2.6 Sample Calculation

GR Section 3.4.2.6 provides a sample calculation. The sample postulates the break of a 10-inch diameter pipe attached to the RCS. The break occurs at the base of a steam generator. Two types of insulation materials are specified (Nukon and reflective metallic insulation (RMI)), and the quantities of each in the affected zone are given. A ZOI radius is determined based on the pertinent ZOI/break diameter values given in Table 3-1 of the GR. All of the insulation material within the affected zone is assumed to be damaged and becomes debris. The sample also calculates the surface area of coatings estimated to be destructed by the break jet forces.

Staff Evaluation of GR Section 3.4.2.6 Separation of the containment into inventory zones appears to be a very effective aide in moving through the break selection and ZOI mapping processes in a systematic way. Alternative segmentation schemes (or useful subdivisions), other than the uniform grid shown in Figure 3-1 of the GR, might be based on structural barriers or groupings of diverse, but collocated, insulation types. In step 4 of the calculation, the volume of the evaluation zone and the estimated surface area of coatings (both qualified and unqualified) are not provided, even though this step should represent all available information about the potential impacts of a break in the postulated location.

The sample calculation is inconsistent with the baseline methodology discussed above because it implies that the potentially affected insulation type with the minimum destruction pressure can be selected from within an accounting region in the vicinity of the break, rather than from the entire containment inventory, as specified in Section 3.4.2.2. For example, if Min-K were present in an adjacent evaluation zone (or anywhere else in containment), the ZOI radius would have to be larger to account for the lower damage pressure of this particular insulation type. The ZOI may easily overlap several evaluation zones for large breaks.

If NUKON™ is the most fragile insulation in containment, then the example is consistent through step 5 except that, using the revised damage pressures presented in Table 3-2 above for two-phase jet impingement, the ZOI radius would be 17 pipe diameters, the ZOI radius would be 14.1 ft, and the ZOI spherical volume would be 11,742 ft^3. The debris inventory should include all potential debris generation materials within this zone.

Step 6 appears to invoke the simplification of assuming 100 percent inventory within the zone. The decision to make this simplification might be assisted by comparing the ratio of the ZOI volume to the volume of the evaluation zone. It is further reinforced by considering the relative volume of the ZOI obstructed by the steam generator and major piping. When this additional volume is added back to account for flow divergence, the ZOI occupies an even larger proportion of the evaluation zone.

For strict compliance with the baseline methodology, step 6 should also include all of the coatings within the evaluation zone as debris, both qualified and unqualified. Instead, step 7 illustrates an example of a proposed refinement presented in Section 4 of the GR for which a ZOI specific to a material type is computed to account for the possible higher resistance of coatings to jet impact. Under this refinement, a separate ZOI radius can be computed for each potentially affected debris source. It is likely that many licensees will choose this refinement rather than accept the conservatism of applying, at all break locations, damage zones defined by the most vulnerable material in containment.

Because acceptable damage pressures for coatings have not been developed, the staff does not agree with step 7 of the calculation. However, once a ZOI has been established, the total area (or equivalent mass) of qualified paint within the spherical zone should be added to the initial debris inventory. There is no basis for the assumption of a coating area equal to the surface area of the ZOI except to satisfy the intent of conservatism for very small damage zones. This assumption of a minimum coating contribution is not necessary if no paint is present within the potential ZOI that is eventually defined by a coatings damage pressure.

3.4.3 Quantification of Debris Characteristics

3.4.3.1 Definition

Section 3.4.3.1 of the GR defines debris characteristics as post-accident size distribution of material, material size and shape, and material densities. The input information needed to determine debris characteristics is also noted.

3.4.3.2 Discussion

GR Section 3.4.3.2 provides a discussion of the debris size distributions that have been used in various studies and specifies the distribution recommended for the baseline evaluation. The GR adopts a two-size distribution for material inside the ZOI of a postulated break. These two size groups are small fines and large pieces. Small fines are defined as any material that could transport through gratings, trash racks, or radiological protection fences by blowdown, containment sprays, or post accident pool flows. Furthermore, small fines are assumed to be the basic constituent of the material for fibrous blankets and coatings (i.e., individual fibers and pigments, respectively). The GR assumes the largest openings of the gratings, trash racks, or radiological protection fences to be less than a nominal 4 inches (less than 20 square inches total open area). The GR classifies the remaining material that cannot pass through gratings, trash racks, and radiological fences as large pieces.

Section 3.4.3.2 of the GR also discusses the erosion and potential disintegration of some debris materials by post-DBA environment water flows. Because the small fines were already classified as reduced down to the basic constituent, further erosion of the small fines does not apply (e.g., for fibrous and coating debris). For fibrous insulation material, the large pieces are assumed to be jacketed or canvassed. According to NUREG/CR-6369, jacketed pieces are not subjected to further erosion. In addition, for material outside the ZOI, all insulation material that is jacketed is assumed not to undergo erosion or disintegration by containment spray or break flow.

The discussion noted the NUKON™ debris size distribution from the test as the insulation that had the most data points and that produced the smallest fines. This distribution was then adapted as the bounding value of fines production for unjacketed fibrous blankets. The GR references the OPG testing (OPG, 2001) for a low-density fiberglass, which indicated that 52 percent of the debris was in the category defined as small fines.

The GR assumes that if a material has a higher destruction pressure than NUKON™, then it signifies that the material has a higher resistance to damage, hence the size distribution would be larger than a more fragile material indicated by a lower destruction pressure. Therefore, it is conservative to adopt the NUKON™ blanket size distribution for material with a higher destruction pressure.

Staff Evaluation of GR Section 3.4.3.2 The categories in any size distribution must correlate to the transport model assumptions. The recommended two-category size distribution (i.e., small fines and larger pieces) adapted by the NEI baseline for material inside the ZOI of a postulated break is suitable to the baseline transport assumptions, which are based on the transport of either the basic constituent (e.g. individual fibers) or large pieces. The division between the two categories of a nominal 4-in. size is adequate in that it agrees well with debris generation testing data. The two-category size distribution, however, is likely to become highly problematic for debris transport refinements that more realistically treat the transport processes. For example, a transport model designed to treat small fibrous debris that transport along the pool floor rather than as suspended fibers will require the small fines in the NEI baseline to be further subdivided into suspended fines and small pieces. The staff finds the two-category size distribution suitable to the baseline; but the use of this size distribution should be reevaluated when debris transport refinements are proposed, such as those discussed in Section 4 of the GR.

The baseline approach contains the assumption that all large pieces of fibrous insulation material would be jacketed or canvassed and therefore would not be subject to further erosion resulting from water flows. Although this assumption is inconsistent with debris generation data acquired through NRC-sponsored tests, the staff position is that the overall impact of this nonconservatism on the results of the analysis is relatively minor in terms of the acceptance of the baseline guidance, and therefore acceptable. This is based on GR assumptions which include a large fraction of small debris (60 percent), all of which is assumed to be small fines. These are unrealistically conservative assumptions which substantiate the minor importance of addressing degradation of large debris. Further, it is agreed that for material outside the ZOI, all insulation material that is jacketed will not undergo significant erosion or disintegration by containment spray or break flow.

The NEI baseline guidance for determining a conservative fraction for the small fines based on one insulation type (i.e., NUKON™), is not realistic even though the 60 percent determination is adequate. The GR indicates that the debris generation test with the most destruction for the determination is the low-density fiberglass test conducted by OPG and documented in NUREG/CR-6808, which indicated 52 percent of the debris was in the category defined as small fines, which is in close agreement with the GR assumption of 60 percent. During the debris generation for the drywell debris transport tests documented in NUREG/CR-6369, Transco™ fiberglass blankets (similar to NUKON™ blankets) were located at a distance in front of the air jet nozzle so that the blankets were routinely completely or nearly completely destroyed (seepage 3-20 in NUREG/CR-6369). Therefore, it must be concluded that fiberglass blankets will be essentially totally destructed into small fines given sufficient jet pressures (approximately 17 psi for Transco™). However, because this testing was based on a small distance between the nozzle and the insulation target, a realistic determination of the fraction of the insulation in a spherical ZOI that would be destructed to small fines requires integration over the sphere based on damage versus pressure and a mapping of the test jets into the spherical ZOI. Analyses documented in Appendix II to this SE confirmed the adequacy of the recommendation of 60 percent for the fraction of small fines debris generation for NUKON™ fiberglass insulation. Further, this analysis confirmed the 60 percent number for Transco™ and Knauf insulations, which are similar to NUKON™ (all low-density fiberglass insulations). The Appendix II analyses also illustrate the correct process to determine the debris size recommendation.

The baseline guidance assumes it is conservative to adopt the NUKON™ blanket size distribution for other materials with a higher destruction pressure than NUKON™. This assumption has been supported, but not conclusively assured, by the debris generation confirmatory analyses documented in Appendix II to this SE. This assumption should only be applied if insulation-specific debris size information is not available.

In addition, although the GR provides damage pressures for a number of insulation products, this list reflects only those products that have received some type of prior testing. The list is not comprehensive either in trade name or by mechanical insulation type. Acceptable default assumptions regarding material damage have been discussed, but product-specific testing can be performed to avoid unnecessary conservatism. Test data should be used to quantify the performance of mitigation strategies, such as double cladding, double banding, or other redesigned insulation-application methods.

3.4.3.3 Size Distribution

Section 3.4.3.3 of the GR provides the recommended size distributions (i.e., percentages that are small fines versus large pieces) for fibrous materials in a ZOI, reflective metallic insulation (RMI) in a ZOI, other material in ZOI, and material outside the ZOI. Table 3-3 summarizes these recommendations.

Table 3-3 NEI Recommended Debris Size Distributions

Material	Percentage Small Fines	Percentage Large Pieces
Fibrous Materials in a ZOI		
NUKON™ Fiber Blankets	60	40
Transco™ Fiber Blankets	60	40
Knaupf	60	40
Temp-Mat	60	40
K-Wool	60	40
Min-K	100	0
Generic Low-Density Fiberglass	100	0
Generic High-Density Fiberglass	100	0
Generic Mineral Wool	100	0
Reflective Metallic Insulation in a ZOI		
All Types	75	25
Other Material in a ZOI		
Calcium Silicate	100	0
Microtherm	100	0
Koolphen	100	0
Fire Barrier	100	0
Lead Wool	100	0
Coatings	100	0
Material outside a ZOI		
Covered Undamaged Insulation	0	0
Fire Barrier (Covered)	0	0
Fire Barrier (Uncovered)	100	0
Lead Wool (Covered)	0	0
Unjacketed Insulation	100	0
“Qualified” Coatings	0	0
“Unqualified” Coatings	100	0

Staff Evaluation of GR Section 3.4.3.3: The baseline recommendations can be grouped as follows:

- Materials for which adequate debris generation data exists to evaluate the debris size distribution, i.e., NUKON™ fiberglass and DPSC Mirror™ RMI insulations.
- Materials deemed to have a size distribution no finer than the materials for which debris generation data is available.

- Materials for which the debris generation is not known well enough to conservatively estimate debris size distributions, therefore maximum destruction is assumed.
- Materials outside the ZOI that are not expected to form debris due to qualification of or lack of protective coverings.

For section 3.4.3.3 of the GR, the staff finds the following:

1. Analyses documented in Appendix II confirmed the adequacy of the recommendation of 60% for the fraction of small fines debris generation for NUKON™ fiberglass insulation. Further, this analysis confirmed the 60% number for Transco and Knauf insulations, which are similar to NUKON™. The small fine generation fraction of 60% is a realistic value that is only slightly conservative.
2. The GR assumes it is conservative to adopt the NUKON™ blanket size distribution for other materials with a higher destruction pressure than NUKON™. This NEI assumption has been supported but not conclusively assured by debris generation confirmatory analyses documented in Appendix II. This assumption should only be applied if insulation-specific debris size information is not available.
3. The staff agrees with the assumption of 100% of the materials becoming small fines for materials for which the debris generation is not known well enough to conservatively estimate debris size distributions. However, for those plants that can substantiate no formation of a thin bed at the sump, this assumption would be nonconservative with regard to sump blockage because fine particulates would pass through the sump screen and generate no blockage concerns. Therefore, for those plants that can substantiate no formation of a thin bed at the sump at which particulate debris can collect, the staff finds that debris generated should be assumed to be sized with realistic conservatism based on the plant-specific environment and susceptibilities identified for that facility, with appropriate justification for the sizing used.
4. The staff agrees that covered insulations and fire barrier material outside the ZOI will not form significant debris, provided the covering is substantial enough to remain intact and to stop significant water from passing through the insulating materials. For example, an exception would be a vinyl covering of fibrous or particulate material that might melt at post-LOCA containment temperatures, and thus would not protect the materials inside from the effects of water erosion.

3.4.3.4 Calculate Quantities of Each Size Distribution

Section 3.4.3.4 of the GR provides guidance for estimating the quantities of debris for each material and each size distribution category. For materials located within the ZOI, other than coatings, the volumes of materials are simply multiplied by the respective size distribution fractions for either small fines debris or large piece debris to obtain the debris volumes of small fines and large pieces, respectively.

Staff Evaluation of GR Section 3.4.3.4 The staff agrees that for materials other than coatings, it is appropriate to multiply the volumes of the ZOI by the appropriate debris size distribution fractions to determine the volumes of debris.

Protective Coatings Quantification

The ZOI for protective coatings is based on the coating destruction pressure assumed in the GR. The same approach used to map the ZOI for other debris types (described in GR Section 3.4.2) is also used to map the ZOI for coatings, specifically, modeling the ZOI as a spherical volume resulting from the freely expanding LOCA jet that will be exposed to pressures greater than or equal to the assumed destruction pressure. Depending on the break location, coated components may or may not exist within this sphere. Where plant-specific data do not exist regarding the amount of coating within the ZOI, the GR assumes that coated components equivalent to the surface area of the sphere will exist within this volume and will fail, generating fine particulate debris. The amount of coating debris is a function of the coating thickness, as well as the surface area. If plant-specific coating thicknesses are not available, then the GR provides guidance on assuming a coating thickness in the ZOI that consists of 3 mils of IOZ primer plus 6 mils of epoxy topcoat.

Staff Evaluation for Protective Coatings Quantification The staff finds that the quantity of coating debris that will be generated as a result of a LOCA jet should be based on the following:

- For plants that can substantiate the formation of a thin bed, use of the basic material constituent (10 µm sphere) to size coating debris is acceptable.
- For those plants that can substantiate that the formation of a thin bed which can collect particulate debris will not occur, the staff finds that coating debris should be sized based on plant specific analyses for debris generated from within the ZOI and from outside the ZOI, or that a default area equivalent to the area of the sump-screen openings, be used for coatings size. If analyzed, then such an analysis should conservatively assess the coating debris generated with appropriate justification for the assumed particulate size or debris size distribution. Degraded “qualified” coatings that have not been remediated should be treated as “unqualified” coatings. Finally, testing regarding jet interaction and coating debris formation could provide insight into coating debris formation and help remove some of the potential conservatism associated with treating coatings debris as highly transportable particulate. If coatings, when tested at corresponding LOCA jet pressures and temperatures, fail by means other than erosion or the erosion is limited, the majority of debris may be larger, less transportable, or pose less of a concern for head loss.

The GR stipulates that all “unqualified” coatings outside the ZOI are assumed to fail. This assumption is consistent with the position provided in Section 6.1.2 of the Standard Review Plan. The amount of debris will be a function of the area of “unqualified” coating and the coating thickness as described in the GR, but the staff recommends that plant-specific values regarding the “unqualified” coating properties and thickness be used. The GR recommendation to use 3 mils of IOZ as a default thickness for “unqualified” coatings outside of the ZOI was based on the fact that 3 mils of IOZ, being 4.5 to 5 times denser than epoxy, epoxy phenolic, or alkyd coatings, would yield approximately the same mass as 13.5 to 15 mils of epoxy coating film. This concept of an “IOZ-equivalent” coatings quantity can lead to inaccurate results in the calculation of the amount of debris generated because the GR does no clearly explain that the mass of coatings debris estimated in this way must then be combined with the actual coating density (not the density of IOZ) to accurately determine the amount of particulate that may impact sump-screen head loss.

Further, the staff is aware of numerous instances in which containment coatings, “qualified” and “unqualified”, are much thicker than the assumed equivalent thickness of 13.5 to 15 mils, so the assumed equivalent thickness may not be conservative. The staff concludes that the GR alternative is not acceptable without plant-specific justification and recommends that plant-specific evaluation of the plant’s “unqualified” coatings be performed to determine conservative coating properties and thicknesses. The staff recognizes that the amount of “unqualified” coating in a plant may vary as a result of changes in plant equipment and modifications which could affect the sump-debris load. Therefore, the staff recommends that licensees periodically assess the amount of “unqualified” coating identified and used in the sump analysis to ensure the quantity remains bounding, and if nonconservative changes in the amount of “unqualified” coating occur, that the impact of this change be evaluated.

Staff Conclusions Regarding GR Section 3.4.3.4 The staff concludes that the baseline alternatives to plant-specific data for the determination of the coatings thickness may not be conservative and are not acceptable without plant-specific justification. The staff further concludes that each plant should perform a plant-specific evaluation of its respective coatings to determine realistically conservative coating thicknesses. The staff drew this conclusion despite the perceived conservatism of the recommendations of assuming all the unqualified coatings in containment fail and all coating debris forms a fine, 10 µm particulate. It is considered reasonable for each plant to assess its respective coating thicknesses, as well as the soundness of its coatings, rather than assume a default recommendation which may not be conservative.

3.4.3.5 Sample Calculation

Section 3.4.3.5 of the GR provides a sample calculation for estimating the quantities of debris from the ZOI by size category and for the “DBA-unqualified” coatings outside the ZOI.

Staff Evaluation of GR Section 3.4.3.5 The staff found the sample calculation presented in this section of the GR to be adequate in concept and practice, but numerically inconsistent with revised guidance explained in this SE, particularly in its treatment of coatings debris. First, the size distribution of fine and large pieces for both fiberglass and RMI insulation should be reviewed for consistency with the recommendations found in Section 3.4.3 of this SE. Second, the estimate of coating debris from within the ZOI should be based on plant-specific characterization of coating thickness and a defensible ZOI radius. Finally, the estimate of coating debris from outside the ZOI should also be based on a plant-specific characterization of unqualified coating thickness and total inventory, rather than the suggested default thickness.

3.4.3.6 Debris Characteristics for Use in Debris Transport and Head Loss

GR Section 3.4.3.6 provides Tables 3-2 and 3-3, which present selected debris characteristics for a variety of materials, specifically material densities and characteristic sizes. The baseline guidance declared the characteristic sizes to be the most conservative values that can be associated with debris transport and head loss. The tables include data for fibrous, cellular, RMI, and particulate (granular) insulation materials. It is noted that the manufacturer should be contacted to obtain information for materials not listed.

<u>Staff Evaluation of GR Section 3.4.3.6</u> The staff notes the following concerns regarding the use of the data in GR Tables 3-2 and 3-3:

1. The range of variation for several data entries is substantial (e.g., the as-fabricated density for Kaowool ranges from 3 to 12 lb/ft^3). The reason for such wide variation was not provided, but is likely caused by the variability in the manufacture of that insulation. Further, the specification of such a wide range is not specific enough for head-loss predictions because using 3 lb/ft^3 versus 12 lb/ft^3 for an as-manufactured density could easily make a drastic difference in the prediction. For example, it would take 4 times the volume of insulation to form a uniform 1/8-in. thick layer if the density were 12 rather than 3. It is important that each plant locate data specific to its installed insulation.

2. An inconsistency exists in the guidance regarding the particulate size for coatings debris outside the ZOI. GR Table 3-3 lists the characteristic size for epoxy and epoxy phenolic coating chips (outside the ZOI) as 25 µm. However, the discussion on page 3-25 of the GR appears to recommend a 10 µm particulate size for all unqualified coatings. It is the staff's understanding that the intent of the baseline guidance was to recommend the 10 µm size for the coating particulate; therefore, acceptance of the baseline is based on the 10 µm recommendation.

3. Table 3-2 recommends a range of 5 to 12 lb/ft^3 for as-fabricated densities for Microtherm. However, GR Reference 13 provides several ranges (i.e., 8 to 25 lb/ft^3, 12.5 to 22 lb/ft^3, and 15 to 22 lb/ft^3), none of which match the range recommended in the GR. Therefore, the value used for Microtherm should be confirmed by the licensee before its application.

4. The data tables provide a characteristic size to represent the material in head-loss calculations, rather than the specific surface area required when using a correlation such as the NUREG/CR-6224 head loss correlation. In the discussion of head loss in Section 3.7 of the GR, the characteristic size is used to estimate the specific surface area from simple geometric formulas. The staff is concerned with the method of converting characteristic dimensions into specific surface area because it has been demonstrated that the method shown in GR Section 3.7 is not reliable. This concern is particularly important when estimating a specific surface area for a particulate with a distribution of particle sizes for which the tendency of using the mean of the size distribution is incorrect and leads to an underestimate of the specific surface area that, in turn, can lead to an underestimate of the head loss. The staff evaluation in Section 3.7 of this SE further discusses this issue. Confirmatory research presented in Appendix V of this SE was performed and illustrates the application of simple geometric equations (e.g., 4/d for fibers and 6/d for particles).

Staff Conclusions Regarding GR Section 3.4.3.6 The staff concludes that acceptance of this section depends upon each plant-specific evaluation properly determining that the parameters selected for the analysis adequately reflect the insulation types actually used in that containment, and that the specific surface area used in the head loss calculation is properly determined.

The staff did not independently verify all the data contained in GR Tables 3-2 and 3-3, however, the values presented agree with analyst perceptions for these materials.

Failed Coatings

The GR assumes that all failed coatings generate debris sizes equivalent to the coatings' basic constituent or pigment sizes which the methodology identifies as 10μm. The GR chose this value because experimental evidence was lacking regarding coating debris size generation during a postulated event. The industry pressure wash testing detailed in Appendix A to the GR provided some insight that coatings within the ZOI will likely fail by erosion resulting in debris sized in the range of 10μm–50μm spheres. The testing also provided insight that the "qualified" epoxy and "qualified" IOZ coatings that were tested would not fail as chips or sheets during simulated jet-impingement testing. Coatings outside the ZOI that fail are also assumed to generate debris in sizes equivalent to their basic constituents or pigment sizes. This debris is on the order of 10μm spheres.

Staff Conclusions Regarding Failed Coatings: For plants that substantiate a thin bed, use of the basic material constituent (10 μm sphere) to size coating debris is acceptable.

For those plants that can substantiate no formation of a thin bed that can collect particulate debris, the staff finds that coating debris should be sized based on plant-specific analyses for debris generated from within the ZOI and from outside the ZOI, or that a default area equivalent to the area of the sump screen openings should be used. Such an analysis should conservatively assess the coating debris generated with appropriate justification for the assumed particulate size or debris size distribution. Degraded, "qualified" coatings that have not been remediated should be treated as "unqualified" coatings.

Finally, testing of jet impingement on coatings could provide insight into how coating debris is formed and could help remove some of the potential conservatism associated with treating coatings debris as highly transportable particulates. If coatings, when tested at corresponding LOCA jet pressures and temperatures, are found to fail by means other than erosion, or the erosion is limited, the majority of debris may be larger, less transportable, or pose less of a concern for head loss.

3.5 LATENT DEBRIS

3.5.1 Discussion

Section 3.5.1 of the GR discusses general considerations for latent debris in terms of its potential impact on sump-screen blockage, as well as some variables that should be addressed on a plant-specific basis. The GR outlines the following five generic activities needed to quantify and characterize latent debris inside containment: (1) Estimate horizontal and vertical surface area; (2) Evaluate resident debris buildup; (3) Define debris characteristics; (4) Determine fractional surface area susceptible to debris buildup; and (5) Calculate total quantity and composition of debris—provide a working outline of the process.

Staff Evaluation of GR Section 3.5.1 The staff finds the GR guidance with respect to general considerations for latent debris to be acceptable. The staff agrees with the position in the GR that latent debris present in containment during operation may contribute to head loss across the ECCS sump screens, and that it is necessary to determine the types, quantities and locations of latent debris. The staff also agrees that it is not appropriate for licensees to claim that their existing FME programs have entirely eliminated miscellaneous latent debris. Results from plant-specific walkdowns should be used to determine a realistic amount of dust and dirt in containment and to monitor cleanliness metrics that may be deemed necessary following the overall sump-screen blockage vulnerability assessment.

For more detailed analysis, the staff believes that when characterizing the resident debris buildup, it would be useful to partition the inventory not only by vertical and horizontal location, but also by relationship to spray impingement and washing by containment-spray drainage.

3.5.2 Baseline Approach

The introduction provided in this section of the GR provides practical insights into the level of importance that latent debris may take in the overall vulnerability assessment and helps licensees to judge the level of effort needed to characterize their plants. In this section, NEI acknowledges that latent debris should be considered as an input to sump-screen head loss, and recommends the use of conservative strategies rather than evaluating the effects of latent debris to a high level of detail.

Staff Evaluation of GR Section 3.5.2: The staff finds the GR guidance with respect to the introduction of the baseline approach for consideration of latent debris to be acceptable. For plants that expect to have fibrous insulation debris generated in the ZOI, the additional contribution to head loss from the latent fiber component may be small by comparison, and reasonable approximations of inventory will suffice. However, for predominantly RMI plants, the latent fiber component represents the dominant potential for thin-bed formation across the screen. In any case, accurate fiber inventories can provide valuable insight for critical decisions regarding sump-screen vulnerability.

3.5.2.1 Estimate Horizontal and Vertical Surface Area inside Containment

This section of the GR provides a general outline of steps required to estimate the horizontal and vertical surface areas in containment. The bulleted list of items that should be included in the surface area calculation (floor area, walls, cable trays, major ductwork, control rod drive mechanism coolers, tops of reactor coolant pumps, and equipment, such as valve operators, air handlers, etc.) provides a starting point for licensees to consider for major inputs. The five steps provided for surface-area calculations (flat surface considerations, round surface area considerations, vertical surface area considerations, thorough calculation of surface areas in containment, and use of estimated dimensions when exact dimensions are unavailable) are informative.

<u>Staff Evaluation of GR Section 3.5.2.1</u>: The staff finds the GR guidance for estimating surface areas within containment to be acceptable with the provisions outlined below for specific sections/attributes.

The staff agrees that the quantity of ambient dust and dirt collected on vertical surfaces by settling from the air is small compared to that collected on horizontal surfaces in the absence of factors that promote adhesion to those vertical surfaces. Any special factors that might promote adhesion to vertical surfaces should be noted and examined more carefully for dust accumulation. A list of potential adhesive factors includes oil leaks, moisture- or condensate-laden surfaces, residue from previously sprayed oils or solutions, and detergent films. Dust that accumulates on vertical surfaces is very small and should be assumed to be 100 percent transportable, if affected by water during a LOCA.

Other surfaces that should be considered for inclusion in plant-specific inventory estimates include steam generators; pressurizers and pressurizer relief tanks; cooling fans; other large equipment; structural supports, such as I-beams and seismic restraint collars; access gratings and steps; and piping. In general, the area inventory refers to external surfaces that can be affected by spray wash down. Internal compartments and cabinets with known loadings of dust and debris which are not typical of most surface conditions after containment closeout should be examined carefully for water infiltration and potential flushing. Areas of this type include inlet-air filter housings and confined crawl spaces that are accessed infrequently.

The guidance provided in the GR for surface-area calculations treats the contribution of vertical surfaces in an inconsistent manner. In general, the staff agrees that practical simplifications can be made to make estimating surface area easier; however, the 10 percent factor proposed for general vertical surfaces does not provide complete guidance for debris estimation. The method the staff finds acceptable is discussed in Section 3.5.2.2.1. Vertical surfaces that are subject to enhanced dust and debris accumulation should be added to the latent debris load estimation separately as part of the resident debris buildup evaluation explained in GR Section 3.5.2.2. This section also provides additional guidance for considerations to be included in containment surveys for latent debris loading.

The staff agrees that the containment dome does not need to be considered from the point of view of dust accumulation. However, the dome may be a contributor of degraded coatings that are dislodged during vapor expansion and should be addressed as such in the determination of the coatings debris source term.

The staff agrees with step 2 in the GR regarding the treatment of round surfaces, but notes that piping surfaces should be considered. Steps 4 and 5 also provide some practical recommendations that are acceptable.

3.5.2.2 Evaluate Resident Debris Buildup

Section 3.5.2.2 of the GR provides a high-level discussion of general practices needed to evaluate latent debris buildup in containment. The GR cites recent sampling of surfaces inside the containment at a number of plants, and recommends that surveys of the containment be performed to determine the quantity of latent debris. As this information is not available in the public domain to allow confirmation of consistency in sampling methods and reporting practices, any statement of expected maximum dust inventory should be considered speculative. The GR references NEI 02-01 to provide guidance for conduct of these containment surveys and evaluation of the presence of foreign material found. The GR also suggests that the degree of rigor for containment survey and surface swiping be applied in inverse proportion to the attention given to foreign material exclusion under normal operations.

Staff Evaluation of GR Section 3.5.2.2 The staff finds the GR guidance with respect to the practices for overall evaluation of latent debris to be acceptable, provided the provisions outlined below are incorporated into the site-specific surveys for latent debris in containment. These surveys will produce opportunities to maximize credit for plant cleanliness, and identify areas of higher than expected debris loadings.

In its present form, the baseline guidance requires detailed calculations of both horizontal and vertical surface areas and physical surveys of dust accumulation on horizontal surfaces (see GR Section 3.5.2.2.1). To improve consistency in the treatment of vertical surfaces, the staff provides the following two acceptable alternative options for baseline analysis based on the best available information documented by the industry:

Option 1. Adopt a default vertical-surface debris inventory of 30 pounds to be characterized by the smallest size fraction found in the horizontal surface inventory, and document a simplified, but realistic calculation of vertical surface area. Consideration should still be given to the unique deposition areas discussed above and the results should be added to the default vertical debris inventory. This value is approximately 5 times (established by using a 2-standard deviation expansion from the mean of the reported sample data set to achieve a 95 percent coverage of the expected data curve and, then doubling the result for conservatism) higher than the vertical inventory reported in Appendix B to the GR for concrete walls and the containment liner and should be sufficiently high to bound variations in surface area, plant cleanliness and the additional vertical areas represented by piping and equipment.

Option 2. Conduct swipes for three categories (a, b, c) of vertical surfaces in the manner illustrated in Appendix B to the GR. It should be noted that repeated wiping with a lint-free cloth (Masolin) under manual pressure or high-efficiency particulate air (HEPA)-filtered vacuuming with mild brush agitation of the surface are both effective methods for collecting the full spectrum of particle sizes found on surfaces. Both methods provide collection media that can be weighed before and after collection to determine the mass of debris in the sample (see Appendix VII to this SE). Concrete walls (a), the liner (b), and vertical piping/equipment (c) should each be sampled at a minimum of three locations selected and documented by a simple rationale to represent typical variations in expected dust loadings within containment. For example, walls near the equipment hatch might represent maxima, and the upper containment liner might represent minima. A simplified, but realistic, calculation of vertical surface area for each category of surface that is sampled should be documented and the average of the three (or more) measurements should be used to determine the mass present on vertical surfaces of each surface category. The three subtotals are then added to the inventory estimate obtained from any unique deposition areas (as identified below). If recently cleaned surfaces are used to establish the minima for a surface category, a documented cleanliness plan should be referenced that describes the frequency of this cleaning treatment. This option represents a minimal increase in effort over that required in the

GR, specifically the collection of vertical-surface swipes, and yet allows maximum credit for individual variations in plant cleanliness.

To ensure a comprehensive evaluation of containment debris, the following items should be considered as part of the containment survey. Phenomena that can enhance dust collection on both vertical and horizontal surfaces include temperature gradients (thermophoresis) and static electrical charge (electrophoresis). The vertical surfaces of cooling fins, heat exchangers, and warm electrical panels may attract higher concentrations of dust than painted concrete structures. Hanging lamp shades inside containment are a common location for enhanced dust collection caused by the thermal gradient. Static charge may accumulate on any surface exposed regularly to air flow. Dielectric materials, such as plastics and exposed cable jackets, may be principle candidates for inspection. For some plants, these effects and locations may be minor contributors to the total dust inventory and can be dismissed with proper examination. However, these issues should be considered and their disposition documented.

For the purposes of latent debris characterization, surveys taken after every second outage should be sufficient. Exceptions to this schedule warrant surveys after any invasive or extended maintenance such as steam generator replacement.

3.5.2.2.1 Evaluate the Resident Debris Buildup on Surfaces

This section of the GR focuses on the measurement of dust and dirt found on horizontal surfaces of containment. The GR presents the following four steps for this purpose:—(1) Divide the containment into areas based on robust barriers; (2) Determine representative surfaces for each section of containment; (3) Survey the representative surfaces in each section to measure debris quantity; and (4) Calculate the thickness of the debris layer—and describe the process. Of these, Steps 1 and 2 offer practical and thorough guidance for performing a systematic survey. The primary method for determining latent debris inventory suggested in Steps 3 and 4 of the GR is direct measurement of debris thickness.

Staff Evaluation of GR Section 3.5.2.2.1 The staff finds the GR guidance to be acceptable with respect to division of containment areas (Step 1) and determination of representative surfaces (Step 2). However, the staff found the methods identified for measuring and evaluating the buildup of debris on surfaces to be unacceptable. The staff considers the recommendation in the GR for direct measurement of dust thickness to be impractical. This SE offers a revised approach for the assessment that is based on generic characterization of actual PWR debris samples. This revised approach also addresses the question of particulate-to-fiber ratio as it relates to the thin-bed effect. If desired, a limited plant-specific characterization can also be pursued as a refinement using this guidance.

Attempting to directly measure latent debris thickness is not recommended because (1) masses can be measured much more accurately than thickness, (2) comparison of dirt layers to reference thickness standards is subjective and prone to error because of heterogeneous small objects that may reside on the surface and because of non-uniform dust thickness across a surface like piping, and (3) in situ estimates of thickness do not characterize size distributions, particulate-to-fiber mass ratios, or densities that are needed to define hydraulic head-loss properties. These problems can be avoided by measuring total masses within a known surface area and then partitioning the fiber and particulate mass fractions either by physical measurement or by generic assumptions described in the next section of this SE.

Statistical sample mass collection is an acceptable method for quantifying latent debris inventories. This approach will not pose an undue burden if planned in advance and incorporated with other survey activities. A list of unique debris sample locations should be developed starting with the previous discussion in Section 3.5.2.1 that can be checked for each evaluation zone that is defined in containment. For convenient cross reference, these evaluation zones should be defined to coincide with the break zones discussed in Section 3.4. For later input in debris transport assessment, the potential for exposure to water from either direct containment-spray, containment-spray drainage, or recirculation-pool immersion should be noted for the surfaces in each evaluation zone. Other areas that should be included in the survey include annular compartments outside of the bioshield and the reactor cavity, if the area participates in circulatory flow with the sump pool during recirculation. Using the practical guidance offered in GR Section 3.4.2.2.1, item 2, for selecting typically loaded surfaces within each inventory evaluation zone, several classes of horizontal surfaces should be defined to represent places where latent debris is found (e.g., high- and low-traffic floor areas, tops of equipment, floor near curbing, cable trays, etc.). At least three samples should be taken from each category as they appear throughout containment, and the results should be treated in the same manner described for vertical surfaces.

The goal of defining debris characteristics is satisfied by collecting swipe or vacuum-filter samples that can be weighed before and after collection to determine the total mass of debris within a measured area. It is important that the collection method adequately captures the full range of particulate sizes from very small (less than 10 µm) up to the large miscellaneous chips and pieces, and all fibers in the sample region. Both HEPA-filtered vacuuming with light-brush agitation of the surface and repeated swiping under manual pressure with a Masolin cloth were found to be effective collection methods for fine particulates and fiber. Vacuuming is considered more efficient for collecting larger grains and miscellaneous objects. Scraping with a metal blade or sweeping with a bristle-type brush will not adequately collect the full range of debris (DIN04).

3.5.2.2.2 Evaluate the Quantity of Other Miscellaneous Debris

Section 3.5.2.2.2 of the GR provides general guidance for the considerations to be used in identifying and evaluating potential sources of miscellaneous debris in containment. The GR refers to and endorses the use of NEI 02-01 to provide guidance for performance of containment surveys. A list of three items, equipment tags, tape, and stickers or placards affixed by adhesives, is used to provide guidance for these specific sources of latent debris.

<u>Staff Evaluation of GR Section 3.5.2.2.2</u> The staff finds the GR guidance acceptable with respect to methods to identify and evaluate miscellaneous debris, provided the guidance is supplemented with the additional direction identified below. The staff agrees that surveys of containment for the presence of miscellaneous debris should be performed and that miscellaneous debris types should be assessed for potential contributions to sump-screen head loss. In addition to the three categories of miscellaneous debris discussed in the GR, the quantity, characteristics, and location of any failed qualified coatings should also be noted in the survey. This issue may be addressed elsewhere in the GR, but it warrants emphasis in this section as well.

- Without specific data to cite regarding the behavior of miscellaneous debris types, the phrases “available for transport” and “transportable debris” should be interpreted as “complete transport to the screen” for fines and particulate debris under the conditions of interaction with water. Larger, miscellaneous debris types must be evaluated on a case-by-case basis for susceptibility to transport as outlined in GR Section 3.6. If data on disintegration and transport become available, they should be documented and used as an acceptable refinement to quantify an assumption of partial degradation or partial transport. If applicable, refinements should include a plausible timeline or necessary operating condition for failure. For example, if adhesives are shown to fail after hours in containment, large or heavy stickers and signs may become detached, but still may not be transportable in low-velocity recirculation conditions. Similarly, delayed failure of adhesives on upper levels of containment may not lead to debris being transported if containment sprays are no longer operating. Proper consideration should be given to the location of these items and the logic of the rationale that is used. For example, slow softening of adhesive in a high-humidity environment is much different than erosion by spray-water cascade or break-jet impingement. The following additional guidance is offered on the evaluation of the GR-listed categories of latent debris.

- Equipment tags. The GR guidance provided on the post-LOCA status of paper tags is ambiguous. There is an implied assumption that complete tags arriving at the screen will induce more head loss than shredded or dissolved paper fiber contributing to a mixed-debris bed. Regardless of their physical condition, tags can only contribute to head loss if they are transportable. Robust lanyards and attachment methods should prevent most equipment tags that exist outside the ZOI from becoming detached (equipment tags within the ZOI shall be assumed to become detached). The size and weight of detached equipment tags and broken lanyards should be evaluated against the criteria in GR Section 3.6 to determine if they should be considered transportable debris. For all equipment tags that are found to be potentially transportable, it is necessary to determine the number and location of tags by type for contribution to screen-head loss. If transportability or the capability of tags to remain intact cannot be determined, it should be assumed that they remain intact and are transported to the sump screen, to preserve conservatism. In other applications, an average mean packing ratio of 0.75 (a 50% overlap of the items stacked on top of each other) has been assumed for larger, flat objects (paint peels), and has been considered reasonably conservative. Consequently, the wetted sump-screen flow area should be reduced by an area equivalent to 75% of the total of the original single-sided surface area of the tags. If there is information that indicates the tags will not remain intact, the staff recommends that the equivalent mass of the tags be treated as latent fiber.

- Tape. The GR mentions some specific applications of tape and recommends that all tape be assumed to fail as transportable debris. The staff agrees that the size, weight, and composition of tape that would interact with water should be evaluated for transportability, as discussed in GR Section 3.6, to determine the realistic amount that would arrive on the sump screen. As stated in the GR for equipment tags, all failed tape that is determined to be transportable should be assumed to arrive on the screen intact and to obstruct an area equivalent to 75% of the total of the original single-sided surface area, unless there is evidence that the tapes will not remain intact. If there is evidence that the tapes will not remain intact (e.g., prior in-service disintegration), then the equivalent mass of the tape should be assumed to be transported to the screen in the form of latent fiber.

- Stickers or placards affixed by adhesives. The staff agrees with the position in the GR that adhesives may fail in post accident conditions. Under the present guidance offered in the GR, all items attached by adhesives should be assumed to fail and be evaluated for transport to the sump screen as outlined in GR Section 3.6. The staff considers this an acceptable position. Where evidence is available that these items will degrade, the equivalent mass of the items in question should be assumed to be transported to the sump screen in the form of latent fiber. Otherwise, the wetted flow area of the sump screen should be reduced by 75% of the total of the original single-sided area of the items in question.

3.5.2.3 Define Debris Characteristics

This section of the GR notes that two generic methods can be applied for defining debris characteristics, Method 1 analysis of samples, or Method 2 assume composition and properties based on conservative values. NEI indicates that Method 2 (assume conservative values for debris composition properties) is preferable, and provides parameter values for fiber density, particle density, and particle diameter. The GR notes that for this option to be used, an appropriate fiber/particulate mix for the plant being evaluated should be employed. The GR goes on to describe some of the difficulties and challenges associated with Method 1.

Staff Evaluation of GR Section 3.5.2.3 The staff finds the GR guidance to be acceptable with respect to defining debris characteristics, provided the method used is supplemented with the additional details outlined below.

It should be noted that conservatism with respect to head-loss potential includes both the aspects of transportability and the hydraulic properties of the material in a mixed-debris bed. The four GR bullets provided in this section for evaluating debris characteristics will be addressed in a parallel format that discusses the Method 1 and Method 2 approaches to each topic concurrently. Both methods first require that adequate surface samples be taken to characterize variability in the plant, and that total masses in containment be estimated by multiplying the empirically determined concentration for each type of collection area (g/ft^2) by the corresponding surface areas before summing to obtain the total inventory. Since the GR indicates that Method 2 is preferred, it will be addressed first for each bullet provided.

First GR Bullet – Use an appropriate fiber/particulate mix for the plant being evaluated.

Method 2 – Assume that fiber contributes 15 percent of the mass of the total estimated inventory. If abnormal qualified coating conditions indicate a dominant presence of paint chips compared to normal dust and dirt at a particular sampling location, that location should be characterized by measurement under Method 1 (See Appendix VII to this SE concerning latent debris for more specific information.)

Method 1 – Characterize the fiber-to-particulate mass ratio in the plant by wet rinsing and manual separation of the fibers from the particulates followed by drying and weighing to obtain mass ratios for samples taken. If this option is chosen, HEPA filtration is recommended as the preferred collection method because of easier separation of the debris from the filter.

Second GR Bullet – Fiber density

- It is conservative to assume that all fiber exposed to water is transported to the screen (unless special circumstances are noted, as discussed earlier), but material buoyancy is not the primary contributing factor and a density equal to that of water should not be assigned.

  Method 2 – Assume that latent fiber material has a mean density of 1.5 g/cm^3.

  Method 1 – Immerse dry fiber samples of known mass in a graduated cylinder with a known quantity of water. Cover with plastic film to prevent evaporation and let stand for several days or heat gently to remove trapped air. Measure new volume of contents and determine fiber material density by displacement.

Third GR Bullet – Particle density

- It is appropriate to assume that latent particulates are primarily geophysical in origin being composed of soil, sand, and dust (i.e., “dirt”).

  Method 2- Assume latent particulate material has a nominal density of 2.7 g/cm^3.

  Method 1 – Measure the particulate density by water displacement as described above for fiber.

Fourth GR Bullet – Particle Diameter

- The principal use of particle diameter is to estimate the hydraulic properties of the debris, such as the specific surface area. This information can also affect judgments regarding transportability and retention in a fibrous debris bed.

  Method 2 – The GR provides the guidance to assume all particulate mass is composed of 10-µm diameter grains. The staff considers this assumption to be acceptable, but this approach is very conservative, especially when much of the mass may be composed of small paint chips, hardware, and visible sand grains. However, this assumption offers the convenience of consistency with baseline assumptions applied to failed coatings as mentioned in the GR. A more refined set of assumptions that would also be considered acceptable are as follows:

- Assume that typical mixtures of latent particulate debris have a specific surface area of 106,000 ft^{-1}, as defined for use in the NUREG/CR-6224 head-loss correlation.

- Assume that 22 percent of the particulate mass determined from the raw samples above the recirculation-pool flood level is non-transportable.
- Under conditions of low sump-screen flow (i.e., less than 0.2 ft/s) and estimated particle-to-fiber mass ratios less than 3, assume that 7.5 percent of the latent particulate debris penetrates the sump screen and is not permanently deposited in the bed to contribute to head loss.

  Method 1 – Dry sieve particulates into size fractions down to 75 µm and characterize the mass distribution as a function of diameter. Assume that the fraction less than 2 mm is not transportable. Assume that 25 percent of the 75 µm diameter mass fraction can penetrate the debris bed. Use scanning electron microscopy (SEM) on subsamples of the 75-µm fraction to determine statistically the fraction of particles below a 10-µm diameter. Compare measured size distributions to literature reported determinations of latent debris size distribution and adjust the Method 2 specific surface area by ratios of estimated masses in each size bin.

The following two additional factors not mentioned in the GR are :

- The dry-bed accumulated density of latent fibers is needed for head-loss calculations. For fiberglass, this density is typically reported as the as-manufactured density, but there is no equivalent definition for latent fiber.

  Method 2 – Assume the dry-bed bulk density for latent fiber is equal to that of fiberglass insulation (2.4 lbm/ft^3=38.4 kg/m^3).

  Method 1 – Using the dry-fiber component obtained from the Method 1 measurement of fiber-to-particulate mass ratios, separate fibers and small flocks from a sample of known mass and drop them successively through several inches of air into a graduated container. Measure the volume after a bed has been formed by random settling and compute the bulk density of this configuration.

- The fiber-specific surface area is also needed for head-loss calculations to compute the contributions to head loss of latent fiber in a mixed debris bed.

  Method 2 – Assume the head-loss properties of latent fiber are the same as reported in NUREG/CR-6224 for commercial fiberglass. Latent fiber will either be dominated by fiberglass present from the break location or it will form the substrate of a thin-bed particulate filter and be dominated by the particulate bed forming on top of the fiber. In either case, the exact properties of the latent fiber are dominated by another debris type, so the error associated with the assumption should be small.

  Method 1 – Measure the hydraulic properties of latent fiber by inference using iterative comparisons of head-loss data and model predictions using the NUREG/CR-6224 head-loss correlation.

The staff agrees with all of the cautionary notes provided in the GR regarding the difficulties of debris characterization, except for the presumptive judgment of extreme expense and little benefit. While cost/benefit is an important practical consideration, the NRC never discourages well-documented testing to obtain site-specific information. For some of the simpler steps of the analysis, it may be an immediate benefit to characterize plant conditions more completely than the default assumptions permit. Improved particulate-to-fiber mass ratios, for example, may offer an immediate potential benefit because of the key role latent fiber plays in the assessment of vulnerability for thin-bed formation in a predominantly RMI-insulated plant.

3.5.2.4 Determine Fraction of Surface Area Susceptible to Debris Accumulation

The guidance in this section of the GR is again offered in the form of a baseline approach. The GR offers the two following options for guidance, (1) assume that 100% of the surface area is susceptible to debris accumulation, and (2) perform an evaluation that consists of estimating fractional surface areas susceptible to debris accumulation on a case-by-case basis. The intent of the guidance in this section is to offer credit for cleanliness programs exercised in certain parts of containment. The GR provides a basic approach for reducing the area considered susceptible to debris accumulation through (1) a calculation of the total surface area, (2) a calculation of the surface area considered to be clean using conservative assumptions, and (3) a calculation of the ratio of potentially dirty area to total area.

<u>Staff Evaluation of GR Section 3.5.2.4</u>: The staff finds the GR guidance acceptable with respect to fractional surface area susceptible to debris accumulation, with the provisions outlined below:

To implement the baseline approach, the GR intended for a measurement to be made of dust thickness on a representative surface within each inventory evaluation zone and that this thickness would be multiplied by the total relevant area in the zone to obtain the volume of debris. This approach is not considered reliable because of the difficulty and subjectivity of measuring a debris thickness, as discussed in Section 3.5.2.2.1.

Either approach presented in this section of the GR for establishing a fractional surface area for debris accumulation is acceptable to the staff with the following caveat--if areas are excluded from the surface inventory, documented cleaning procedures should be in place that are exercised before each restart. If periodic cleaning occurs less frequently, the sampling method outlined earlier in this SE is recommended to determine the minimum dust loading in those areas of a surface type that have been previously cleaned.

An issue similar to accumulation susceptibility that may lead to a credit for reduced latent inventory is transport susceptibility. As recommended earlier in this SE, potential exposure to water should be assessed for each inventory evaluation zone. It is expected that most surfaces will be exposed to either direct spray, spray accumulation flow, or immersion in the recirculation pool but some isolated areas may exist for which little or no water transport can occur (interior cabinets, elevated crawl spaces, locked rooms, etc). For these types of areas where latent debris is known or expected to exist, justification for exemptions from considering the total latent-debris inventory can be documented on a case-by-case basis.

3.5.2.5 Calculate Total Quantity and Composition of Debris

The GR provides four basic steps for calculating the total quantity of latent debris: (1) perform calculations as previously outlined on an area-by-area basis; (2) compute the total quantity of debris using the area/debris thickness method outlined in the GR; (3) include other types of debris from containment survey data as outlined previously in the GR; and (4) categorize and catalog the results for consideration in debris transport evaluation.

<u>Staff evaluation of GR Section 3.5.2.5</u>: The staff finds the general steps identified with respect to the total process acceptable, provided that methods outlined earlier in this SE are used in place of those specific items previously identified for computation of quantity of debris and debris density.

This SE has alluded to the process for integrating survey findings over all surface types several times. Given the revised approach to measurement of debris build up recommended by the staff, the total quantity of debris for each inventory evaluation zone and each surface type will be found by multiplying debris concentration (lbm/ft^2) by the respective areas to obtain the total number of pounds in containment. Proper evaluation of debris for transportability has been discussed previously in other sections of this SE pertaining to evaluation of debris types. Most importantly, the calculation must separate the fiber and particulate components of the debris aggregate. These fractions behave differently during transport, contribute separately to head loss, and introduce separate considerations regarding sump-screen vulnerability.

3.5.3 Sample Calculation

The sample calculation presented in this section of the GR illustrates the concept and systematic process involved with defining categories of surfaces that reside within a given inventory evaluation zone, calculating areas, and summing debris inventories. The following sections offer minor points of clarification.

3.5.3.1 Calculate Horizontal Surface Area

This section of the GR illustrates the appropriate level of simplification for computing structural surface areas in containment.

<u>Staff Evaluation of GR Section 3.5.3.1</u>: The staff finds the sample calculations provided to be acceptable for implementing concepts for determining the horizontal surface areas in containment. The following clarifications are added for licensees to consider when performing these calculations.

Step 4 of the calculation discusses the calculation of additional horizontal surface areas contributed by equipment, piping, cable trays, etc. Where these items are large and obstruct floor areas computed in previous steps, the projected area of the item is effectively included twice. The duplicate area can either be subtracted from the inventory or cited as a conservatism to account for the complexity of the object in question, whichever is most appropriate.

The treatment given to the recirculation sump cover as a projected area accounted for in the floor-area calculation is appropriate.

3.5.3.2 Calculate Quantity of Debris

The example calculation in the GR is consistent with guidance given in previous sections, assuming that a debris-layer thickness can be measured and that in situ densities can be determined; total latent-debris mass is then computed accordingly.

Staff Evaluation of GR Section 3.5.3.2: The staff finds the GR guidance with respect to the total calculation of the quantity of debris to be unacceptable. The problems associated with direct measurement of debris thickness have been explained. If inventory analysis options involving sampling are pursued, it might be practical to conduct calculations like the example provided in this section of the GR.

3.6 DEBRIS TRANSPORT

3.6.1 Definition

Section 3.6 provides guidance for estimating debris that is transported from debris sources to the sump screen. The four major transport modes considered in the GR are blowdown, spray washdown, pool fill-up, and pool recirculation flow.

3.6.2 Discussion

Section 3.6.2 of this GR presents a generic transport logic tree used subsequently in the transport recommendations. In addition, the GR defines the following three containment-type categorizations:

1. Highly compartmentalized containments are defined as those containments that have distinct robust structures and compartments totally surrounding the major components of the RCS. For a main steamline break in a highly compartmentalized containment, the mostly uncompartmentalized containment values should be used.
2. Mostly uncompartmentalized containments are defined as those containments that have partial robust structures surrounding the steam generators.
3. Ice condenser containments are defined as all seven ice condenser plants, which lack lower containment compartmentalization.

Staff Evaluation of GR Section 3.6.2 The staff considers the simple generic debris transport chart shown in GR Figure 3-2 to be acceptable for a schematic representation of the GR baseline debris transport evaluation methodology. However, the distinction between the highly compartmentalized and mostly uncompartmentalized containments has not been clearly defined. Therefore, if the containment category in a plant-specific analysis is not certain, then the evaluation should assume the category which predicts the greater debris accumulation on the sump screens. Section 3.8. of the GR discusses the acceptance of the baseline guidance as a package.

3.6.3 Debris Transport

The introduction to GR Section 3.6.3 introduces the NEI baseline concept for estimating debris trapped in inactive pool volumes which are defined as volumes located below the containment bottom floor (e.g., the cavity under the reactor vessel) that are not affected by drains from the upper part of the containment that may cause them to participate in the active volumes. All volumes at the containment bottom floor elevation are assumed to participate in the recirculation flowpath from the containment sprays and break flow to the sump. The baseline model assumed no preferential direction for water to flow to the sump. Further, the baseline guidance assumes that all debris in the containment bottom floor is uniformly distributed throughout the entire volume of water in containment. This guidance then assumes that the debris transported to the inactive sumps is strictly based on the ratio of the volume of the inactive sumps to the total water volume in containment at the start of recirculation. The baseline guidance states that this assumption is conservative because it ignores the preferential sweeping of the debris on the containment floor to the inactive sumps by the thin sheets of high-velocity water. It was further noted that all small fine debris in active pools on the containment floor is transported to the sump during recirculation.

GR Sections 3.6.3.1, 3.6.3.2, and 3.6.3.3 which address the highly compartmentalized, the mostly uncompartmentalized, and the ice condenser containments, respectively, primarily contain compartmental specific debris transport assumptions. Table 3-4 summarizes these assumptions for the small fines debris generated within the ZOI. The baseline guidance recommends that all debris generated outside the ZOI be treated as small fines debris that is subsequently transported to the sump screens (i.e., 100 percent washdown transport, 100 percent sump pool recirculation transport, and no transport into the inactive pools). The baseline guidance recommends the assumption that all of the large piece debris deposits onto the containment bottom floor where it stays.

Table 3-4. Summary of Debris Transport Assumptions for Small Fines Debris from ZOI

Transport Assumption	Fibrous Debris	RMI Debris	Other Debris
Highly Compartmentalized Containments			
Fraction of Debris Generated	0.6	0.75	1
Fraction of Debris Generated That Transports into Upward Levels by Blowdown	0.25	0.25	0.25
Fraction of Debris Generated That Transports Directly to Sump Pool Floor by Blowdown	0.75	0.75	0.75
Fraction of Debris Generated That Blows into Upper Levels and Washes Down into Sump Pool	1	0	1
Fraction of Debris Generated That Enters into Inactive Sump Pools	Volume Ratio	Volume Ratio	Volume Ratio
Fraction of Debris that Enters Sump Pool That Transports to Sump Screens	1	1	1
Mostly Uncompartmentalized Containments			
Fraction of Debris Generated	0.6	0.75	1
Fraction of Debris Generated That Transports into Upward Levels by Blowdown	0*	0	0
Fraction of Debris Generated That Transports Directly to Sump Pool Floor by Blowdown	1*	1	1
Fraction of Debris Generated That Blows into Upper Levels and Washes Down into Sump Pool	1	0	1
Fraction of Debris Generated That Enters into Inactive Sump Pools	Volume Ratio	Volume Ratio	Volume Ratio
Fraction of Debris that Enters Sump Pool That Transports to Sump Screens	1	1	1
Ice Condenser Containments			
Fraction of Debris Generated	0.6	0.75	1
Fraction of Debris Generated That Transports into Upward Levels by Blowdown	0.1**	0.1**	0.1
Fraction of Debris Generated That Transports Directly to Sump Pool Floor by Blowdown	0.9	0.9	0.9
Fraction of Debris Generated That Blows into Upper Levels and Washes Down into Sump Pool	1	0	1
Fraction of Debris Generated That Enters into Inactive Sump Pools	Volume Ratio	Volume Ratio	Volume Ratio
Fraction of Debris that Enters Sump Pool That Transports to Sump Screens	1	1	1

*Because this value was not actually specified in the baseline guidance (Section 3.6.3.2, fibrous blowdown transport), the table value was assumed to be the same as the stated RMI value.

** Guidance assumes 100% ejected upwards of which 90% returns via ice melt to containment floor.

Staff Evaluation of GR Section 3.6.3 The staff based its evaluation of this section on confirmatory research documented in Appendices IV and VI to this SE and the base of debris transport knowledge documented in NUREG/CR-6808.

Table 3-5 includes the baseline recommendations for the fractions of the debris generated that are transported into upward levels by blowdown, which were 0.25, 0, and 0.1 for highly compartmentalized, mostly uncompartmentalized, and ice condenser containments, respectively. These fractions are conservative. In the detailed analysis performed for the volunteer plant, which was assumed to have a highly compartmentalized containment, the fractions were 0.92 and 0.44 for small fines fibrous and small RMI debris, respectively, as compared to the 0.25 fraction recommended for the baseline analysis (see Appendix VI to this SE). For mostly uncompartmentalized containments, the GR recommends no debris be transported to the upper containment. For ice condenser containments, the GR recommends a value of 0.1, which is conservative because these containments are designed to divert a significantly higher fraction of blowdown flow towards the ice condensers.

The inactive pool debris entrapment model does not represent the realities of debris transport. In the detailed volunteer plant debris blowdown/washdown transport analysis (see Appendix VI to this SE), a majority of the small fines debris was determined to be transported upwards in the containment, where it deposited onto any number of surfaces. Only a few percent of the small fines would likely deposit directly onto the containment bottom floor where the debris would be subjected to pool formation flows into the inactive volumes. In the volunteer plant, the openings into the bottom sump-level floor consisted of two personnel access doorways, which are small compared to the large area that opens directly to the containment dome. The large opening was designed for pressure relief from HELB events in the steam generator compartments housing most of the RCS. A significant time delay would most certainly exist between the blowdown period and the time when major portions of the small fines would be transported down to the sump pool by the containment spray drainage. Therefore, the inactive pools would most likely fill (within the first few minutes) before a large portion of the debris could wash to the sump pool, hence the assumed volume ratio is nonconservative.

The baseline guidance assumes that the debris transported to the inactive sumps is strictly based on the ratio of the volume of the inactive sumps to the total water volume in containment at the start of recirculation. The baseline guidance states that this assumption is conservative because the debris transport methodology ignored the preferential sweeping of the debris on the containment floor to the inactive sumps by the thin sheets of high-velocity water. This basis does not reflect realistic debris transport.

Observations made during the integrated tank tests (NUREG/CR-6773) show debris being directionally driven by the sheeting-flow wave front. Such transport could drive debris across the tank bottom (either away from or to the sump), unless the debris became otherwise trapped along the transport path. With this type of sheeting-flow transport of fine debris, a sharp direction change, such as at an entrance into a hallway leading to the reactor cavity, could easily result in the debris being swept past such an entrance because it was unable to alter direction with flow into the doorway. Because it is difficult to determine how sheeting flow would actually transport debris, the amount of conservatism achieved by ignoring the preferential transport of debris to the inactive volumes is difficult to quantify.

The baseline assumption that all debris in the containment bottom floor is uniformly distributed throughout the entire volume of water in containment also does not reflect reality, certainly not in the general sense of all PWRs. The volunteer plant's detailed analysis of a line break within a steam generator compartment indicated that more of the blowdown-deposited debris on the bottom floor was likely retained within the affected steam generator compartment than was transported outside the compartment. Hence, a substantial concentration of debris would initially be located in the affected steam generator compartment. Although the washdown debris would enter the sump pool at multiple locations with the containment spray drainage, the entry points would place the debris directly into the sump pool flow-stream, rather than into inactive pools or inactive or quieter portions of the sump pool.

The inactive pool debris entrapment model can predict an unrealistically high fraction of debris moving into inactive pools for some plants. Therefore, the licensees should limit the fraction of debris moving into inactive pools to a maximum of 15 percent of the source, unless shown otherwise by analysis as described in Appendix IV of this SE.

Table 3-4 shows that the only distinguishing feature among the highly compartmentalized, mostly uncompartmentalized, and ice condenser containments relative to the debris transport assumptions is the fraction of the debris assumed to deposit directly onto the containment bottom floor as a result of blowdown debris transport. For fibrous debris transport, however, this fraction becomes irrelevant because all the debris transported upwards is conservatively assumed to wash back down to the sump pool, whereas the washdown debris is treated in the same manner as the blowdown floor deposited debris. In summary, for small fines fibrous debris transport (all three containment categories); the overall transport fraction to the sump screens is 1 minus the fraction assumed to enter the inactive pools (based on a water volume ratio). The 100 percent washdown assumption for fibrous (and other) debris is conservative.

For small fines RMI debris transport, the fraction assumed ejected upwards (25 percent) is subsequently assumed to remain in the upper containment areas. In reality, some portion of the small fines RMI debris deposited in the upper reaches of the containment during blowdown would wash back down to the sump pool; therefore, this baseline assumption is non-conservative in isolation. However, based on the confirmatory debris transport research summarized in Appendices IV and VI to this SE, this nonconservative transport assumption, in conjunction with the relatively high fractions of small fines blowdown assumed to be deposited on the bottom floor (0.75, 1.0, or 0.9), represents a conservative estimate of small fines RMI debris placed in the sump pool.

The baseline assumption that the recirculation phase pool transport is 100 percent for small fines is conservative and removes a need to address the effects of the variety of pool geometries and flow velocities associated with the differences among the PWR containments. However, the baseline assumption of zero sump pool transport of the large piece debris is nonconservative for the plants with relatively fast pool velocities that are capable of moving large debris. The implication of this assumption is that absolutely no large piece debris would accumulate on the sump screens. Based on experimental results from testing performed at the University of New Mexico (UNM), the volunteer plant pool model demonstrated that large pieces will degrade and fibers will come out of the large flocks and be transported to the screen (NUREG/CR-6773). As stated in Appendix IV to this SE, the characteristic transport velocities must be compared to typical debris transport velocities to determine whether or not the baseline method should be modified to include the transport of large debris. Characteristic transport velocities can be sufficiently estimated using recirculation flow rates and nominal sump dimensions to determine if a potential exists for substantial portions of the large debris to be transported. If substantial transport of large debris is reasonably possible, and if such transport can alter the outcome of the NPSH margin evaluation, then analytical refinements are needed that evaluate large debris transport.

The baseline guidance recommends a conservative assumption that all debris generated outside the ZOI will consist of small fines debris that subsequently is transported to the sump screens (i.e., 100 percent washdown transport, 100 percent sump pool recirculation transport, and no transport into the inactive pools). This assumption removes a need to address the variability and uncertainties caused by a lack of data on the generation and transport of debris outside the ZOI, especially when considering the differences among the PWR containments.

Staff Conclusions Regarding GR Section 3.6.3: The staff concludes that two of the transport assumptions given in the baseline guidance are non-conservative. These assumptions are (1) that the quantity of fine debris trapped in inactive pools, especially debris washed down from the upper levels of the containment, can be estimated simply by the ratio of the inactive pool volume to the total water volume, and (2) the large piece debris will not transport in the sump pool. To avoid predicting unrealistic results when using these assumptions, the licensees should (1) limit the fraction of debris moving into inactive pools to a maximum of 15 percent of the source, unless shown otherwise by analysis, and (2) evaluate large debris transport if characteristic transport velocities show that substantial transport of large debris is possible.

The baseline assumption that all debris in the containment bottom floor is uniformly distributed throughout the entire volume of water in containment is also not conservative. This assumption was made in the baseline guidance to justify the inactive pool volume ratio, but otherwise does not directly affect the acceptance of the baseline guidance resulting from the 100 percent recirculation pool transport assumption. However, should a plant subsequently perform a pool transport refinement, then this assumption would not apply and alternative approaches, such as those detailed in Appendix III to this SE should be considered.

3.6.4 Calculate Transport Factors

Section 3.6.4 of the GR provides a sample transport calculation. For the sample calculation, it was assumed that the containment was highly compartmentalized, with an inactive pool fraction of 30 percent, and that the ZOI insulation debris included NUKON™ and RMI debris. The unquantified logic chart shown in GR Figure 3-2 was applied to both the NUKON™ and RMI debris in accordance with the guidance outlined in GR Section 3.6.3. GR Figures 3-3 and 3-4 depict quantified transport logic trees for NUKONTM and RMI debris.

Applying the chart to NUKON™ debris, the size distribution is 60 percent small fines and 40 percent large pieces that were assumed not to be transportable. Two transport pathways delivered small fines debris to the sump (1) 75% of the debris was assumed directly deposited to the sump pool floor, and (2) the remaining 25 percent of the debris deposited in the upper containment, but subsequently washed down to the sump pool after 30 percent of each case was sequestered in inactive pools. Therefore, 42 percent of the total NUKON™ debris was assumed to reach the sump with the remaining 58 percent assumed either trapped in the inactive pools (18 percent) or as large pieces (40 percent). Applying the chart to RMI debris, the size distribution is 75 percent small pieces and 25 percent large pieces that were assumed not to transport. Only one transport pathway delivered debris to the sump, resulting in 75 percent of the debris assumed to be directly deposited to the sump pool floor. The 18.75 percent of the RMI assumed deposited in the upper containment was thought to remain, and 30 percent of the small pieces were assumed to reach the lower containment (56 percent was assumed trapped in the inactive pools). Therefore, 39 percent of the total (or 53 percent of the small pieces) RMI debris was assumed to reach the sump. No large debris was transported to the sump. The sample calculation acknowledges 100 percent transport of coatings debris, from both within and outside the ZOI, and all debris material outside the ZOI, including latent debris. A list of all debris by type and size is provided and available for the subsequent sample head-loss calculations.

<u>Staff Evaluation of GR Section 3.6.4</u>: The sample problem is consistent with the baseline methodology discussed above and the specified transport assumptions.

3.7 HEAD LOSS

3.7.1 Introduction and Scope

Section 3.7.1 of the GR consists of an introduction to the head-loss guidance.

3.7.2 Inputs for Head-Loss Evaluation

3.7.2.1 Sump-Screen Design

Section 3.7.2.1 of the GR briefly describes several aspects of sump-screen design pertinent to estimating the head loss across the sump screen. The aspects described include screen construction, screen orientation, screen mesh size, applicable screen area, flat screen versus alternate geometries, such as stacked-disc strainers (circumscribed area versus actual screen area), and clean strainer head-loss estimation.

<u>Staff Evaluation of GR Section 3.7.2.1</u>: The staff finds the general guidance in this section acceptable because it is consistent with general engineering practice.

3.7.2.2 Thermal-Hydraulic Conditions

3.7.2.2.1 Recirculation Pool Water Level

Section 3.7.2.2.1 of the GR recommends using the minimum water level of the recirculation pool in estimating the head loss across the debris bed accumulated on the screen. The minimum water level will yield the smallest surface area for the water flow through the screens that are partially submerged, as well as the lowest available NPSH to the ECCS pumps.

<u>Staff Evaluation of GR Section 3.7.2.2.1:</u> The staff determined that the recommendation of using the minimum water level in the pool is appropriate. For partially submerged sump screens, the water level affects the wetted screen area, which affects the water approach velocity used in the calculation of the head loss resulting from the debris accumulation on the sump screen. A lower water level in the pool would result in a lower wetted screen area giving a higher approach velocity, which would conservatively give a higher head loss across the debris bed. For completely submerged screens, the static water level adds to the NPSH margin. The staff further notes that the determination of the minimum level should consider potential water holdup in the upper levels of the containment including water holdup caused by potential debris blockage at water passages such as drains (e.g., refueling pool drains). The minimum level is not merely a conservative assumption, but is consistent with ensuring adequate NPSH margin when the pool is actually operated at that level.

3.7.2.2.2 ECCS Flow Rate

Section 3.7.2.2.2 of the GR recommends using the highest ECCS flow rate in calculating the head loss across a screen (i.e., the maximum pump flows as identified in current NPSH calculations). For multiple sump screens, the flow rate for the head-loss calculation is the flow through each of the screens.

Staff Evaluation of GR Section 3.7.2.2.2: The staff concludes that the recommendation of using the maximum pump flows in the head-loss calculations is the appropriate assumption, although under certain conditions, those pumps might be throttled back to a lesser flow rate. This maximum pump flow assumption removes the uncertainty that a lesser flow rate will be exceeded. The rate of flow through the screen, along with the screen area, is used to determine the velocity of flow through the screen, which is a primary input to the head-loss calculation.

3.7.2.2.3 Temperature

Section 3.7.2.2.3 of the GR makes the following three recommendations for specifying the water temperature to be used in the head-loss calculations:

1. The temperature at which the head loss is evaluated should be consistent with the temperature used for the NPSH evaluation.
2. The head loss is to be evaluated at multiple times when different temperatures and flows exist during an accident.
3. The maximum expected temperature may be used for the NPSH analysis, whereas the lowest expected temperature during ECCS operation may be taken for the head loss analysis.

Staff Evaluation of GR Section 3.7.2.2.3: The water temperature determines the viscosity of the water, which affects head loss. A head-loss correlation typically either includes the viscosity or is only valid for a distinct range of temperatures. A lower water temperature increases the viscosity and therefore conservatively gives a higher frictional head loss across the debris bed on the sump screen. Therefore, Recommendation 3, above, is acceptable for specifying the water temperature. Licensees should calculate the NPSH margin according to their licensing bases (RG 1.82-3).

The estimation of the minimum water temperature may require a different calculation than the typical plant estimation of the maximum water temperature for the design basis.

In calculating the maximum sump pool water temperature, it is conservative to neglect heat transfer processes or systems (e.g., a nonsafety-related heat removal system) either to simplify the calculation or because a system cannot be relied upon to limit the temperature. But in a minimum water temperature calculation, all heat removal systems and processes should be included.

Recommendation 2 allows the time-dependency of the temperature to be evaluated, i.e., the evaluation of multiple times, temperatures, and flows during an accident. Staff concerns with the approach include the following:

1. Recommendation 2 appears to also suggest that the pump flow can vary with time as well, which is in direct conflict with GR Section 3.7.2.2.2, which states that the maximum pump flow should be used.
2. The debris in the time-dependent calculation must be assumed as the worst-case debris accumulation, because the debris transport evaluation capability is not sufficient to predict time-dependent accumulation.
3. If one calculation is used to estimate the pool temperature, it should be sufficiently realistic to capture all important heat transport processes. The systems specified in the accident scenario and the specification of the accident scenario must address whether or not systems such as nonsafety-related heat removal systems are operating.

Recommendation 1 is unacceptable because it does not in any way specify a minimum temperature for the head loss calculation.   Licensees should calculate the NPSH margin according to their licensing bases (RG 1.82-3).

Staff Conclusions Regarding GR Section 3.7.2.2.3: The staff concludes that Recommendation 3 for determining the pool temperatures is conservative and adequate, if the minimum and maximum temperatures are properly estimated. Recommendation 2 is also a valid approach if properly evaluated, provided (1) that the flow remain that of the maximum pump flow, (2) the debris bed should be the worst-case debris accumulation throughout the time-dependent temperature transient, and (3) the pool temperature is properly determined. Recommendation 1 is incomplete and unacceptable by itself.

3.7.2.2.4 Debris Types, Quantities, and Characteristics

Section 3.7.2.2.4 of the GR provides a general discussion regarding the parameters needed to specify an accumulation of debris on the sump screen.

Staff Evaluation of GR Section 3.7.2.2.4: The staff notes that the list of important head-loss parameters is incomplete. In addition to quantities specified as volumes or masses, the bulk and fiber densities are needed for fibrous debris, the particle density and limiting porosity are needed for the particulate, and the specific surface areas are needed for each debris bed component. Appendix V to this SE offers guidance for determining the specific surface areas.

3.7.2.3 Head-Loss Methodology

3.7.2.3.1 General Theoretical/Empirical Formulas

3.7.2.3.1.1 Fibrous Debris Beds with Particulate

Section 3.7.2.3.1.1 of the GR describes the NUREG/CR-6224 head-loss correlation by providing the basic correlation equation and the supporting constituent equations for solidity (1 minus the porosity). This section also discusses fibrous debris bed compression resulting from the pressure gradient across the sump screen, as well as compression limiting factors.

The baseline guidance offers the following four options for dealing with debris materials or combinations of materials for which the empirical head-loss data do not exist:

1. characterizing the material with SEM analysis and the establishment of a size distribution
2. choosing an alternate material that conservatively represents the material in question, via similitude arguments
3. testing head loss of the particular material to establish a correlation or validate an existing correlation for that material
4. using other information that may exist to establish head-loss data for the material in question

The section contains a discussion for estimating the specific surface area, S_v, from the constituent characteristic dimension (e.g., particle or fiber diameter). A formula is provided for determining S_v for a mixture of debris constituents that is based on volume averaging the squares of the constituent S_v. The baseline guidance states, "it is best to err on the low side for conservative values of S_v." In addition, the guidance describes obtaining the aggregate density for both particulate and fibrous debris using a simple volume averaging procedure. Finally, a computational procedure is described for solving the correlation equations to obtain the head loss.

Staff Evaluation of GR Section 3.7.2.3.1.1: The GR options for obtaining head-loss parameters for materials that have not been previously characterized are all valid methods of learning more about that material. Performing head-loss testing (Option 3 above) that can be subsequently analyzed to determine appropriate head-loss parameters is the best option, since it provides results with the least uncertainty. The other three options will improve knowledge, but can leave substantial uncertainty in the resultant head-loss parameters that must be countered through the use of conservative safety factors.

Confirmatory research presented in Appendix V to this SE and head-loss testing reports LA-UR-04-1227 on CalSil and Appendix VII on Latent Debris illustrate the application of the NUREG/CR-6224 correlation to head-loss data to determine applicable input parameters for the correlation. The confirmatory tests performed so far only provide reasonable assurance that NUREG/CR-6224 can be used as a scoping tool to calculate the pressure drop across CalSil and latent debris beds. Therefore, the NUREG/CR-6224 correlation cannot be used as a design tool to calculate the head loss across a

CalSil or latent debris bed on sump screens. Licensees should use other verifiable methods to calculate the pressure drop across CalSil and latent debris beds in design evaluations.

The baseline adequately presents the concept of compression limiting whereby the compaction of the fiber and particulate effectively prevents further compression of the debris bed (i.e., limiting of the solidity of the debris bed). However, the computational procedure described in the GR for solving the NUREG/CR-6224 correlation equations to obtain head-loss does not include steps for determining whether or not the limiting solidity would occur; as well as how to proceed with the calculation should the limiting solidity condition occur within the iterative solution. The reader is left with the impression that the limiting solidity is approximately 0.2 (i.e., limiting porosity of 0.8), which is correct for BWR iron oxide corrosion products. This impression is reinforced in the sample problem (page 3-71 of the GR) in which the mixed-bed solidity is set to 0.2 for a particulate that consists of latent and coating debris. Common sand, a likely component of latent debris, has an approximate solidity of 0.6 (data available in common soil handbooks), which is greater than the GR-implied limit of 0.2. The surrogate latent debris head-loss testing documented in Appendix VII tested common sand and verified the handbook values for sand solidity. When applying the NUREG/CR-6224 correlation, the correct value for the limiting solidity should be used for the postulated particulate, because the limiting solidity governs the head-loss prediction whenever the correlation predicts compression limiting has occurred, as is the case with thin-bed debris accumulations.

An important aspect for predicting the head loss is determining the specific surface area for the debris bed. The head loss from the NUREG/CR-6224 correlation is directly dependent on S_v; in fact, the leading laminar term uses the S_v^2. For example, at lower flow velocities, if the S_v were under-predicted by a factor of 2, then the head loss could be under-predicted by a factor of 4. The baseline guidance statement that, “it is best to err on the low side for conservative valves of S_v,” should be clarified to indicate that it is the debris size that should be selected on the low side, not the value of S_v. It is conservative to estimate S_v high, rather than low.

The baseline guidance for estimating S_v from the constituent characteristic size dimension (e.g., fiber or particle diameter) has been demonstrated to be unreliable, particularly when a particulate is defined by a size distribution. The use of 6 divided by the diameter is reasonable when specifying S_v for the conservative, all-one-size particulate (10 µm) postulated for coatings debris. However, it is unreasonable when a particulate distribution covers a wide range of sizes (e.g., iron oxide corrosion products range from 1 to 300 µm), typically described by 3 or 4 subgroups. The value of S_v calculated is sensitive to the value of the diameter used to represent the size group in the 6/diameter formula. The natural tendency is to select the mean of the size group, but the mean significantly under estimates the specific surface area because all particles in the group less than the mean make a substantially greater contribution to S_v than do those particles larger than the mean value. Selecting an appropriate value within the range is problematic because it depends upon the size distribution within the size group. A conservative solution to this problem is to use the minimum size of each size group. However, this approach can lead to large estimates of S_v, especially when the particles become very small. For example, assume the size group has a uniform distribution ranging from 5 to 100 µm. Using the 5 µm size results in a S_v of 366,000/ft, which is conservative (but too large), whereas using the mean of 52.5 µm results in a S_v of only

34,800/ft, which is much too small. Smaller particles in a debris bed cause greater head loss than do larger particles. Confirmatory research presented in Appendix V to this SE shows significant error in the S_v calculated using simple geometric equations (e.g., 4/d for fibers and 6/d for particles) compared to the error deduced using head-loss data. Where the particulate for a specific material is defined by a size distribution, licensees should use applicable head loss data to determine S_v.

The formula provided in the baseline for determining S_v for a mixture of debris constituents that is based on volume-averaging the squares of S_v is adequate and conservative relative to the formula actually provided in NUREG/CR-6371.

Before using the NUREG/CR-6224 correlation that is recommended in the GR, or any other head-loss correlation, the licensees should ensure that it is applicable for the types of insulations and the range of parameters. Appendix V to this SE gives the procedures for applying the correlation and the ranges of parameters used to validate it that are publicly available. If the correlation has been validated for the type of insulations and the range of parameters, licensees may use it without further validation. If the correlation has not been validated for the type of insulations and the range or parameters, licensees should validate it using head-loss data from tests performed for the particular type of insulations.

Staff Conclusions Regarding GR Section 3.7.2.3.1.1: The staff agrees with the baseline that the NUREG/CR-6224 correlation is an appropriate method for estimating the head loss associated with a debris bed consisting of fibers and particulates. Using the guidance in Appendix V to this SE, the licensees should ensure the validity of this correlation for the application of their type of insulation and the range of parameters.

3.7.2.3.1.2 RMI Debris Beds

GR Section 3.7.2.3.1.2 provides a head-loss correlation for estimating the head loss across a bed of RMI debris. This correlation and the values for the constant known as the interfoil gap thickness were extracted directly from NUREG/CR-6808.

Staff Evaluation of GR Section 3.7.2.3.1.2: The staff agrees with the baseline that the NUREG/CR-6808 is an appropriate method for estimating the head loss associated with a debris bed consisting of RMI, as documented in NUREG/CR-6808.

3.7.2.3.1.3 Mixed Debris Beds (RMI, Fiber, and Particulates)

Section 3.7.2.3.1.3 of the GR provides guidance for mixed debris beds that include RMI, fibrous, and particulate debris. The baseline guidance recommends that the head loss for the fibrous/particulate debris and the RMI debris be estimated separately, and then added together, to obtain the head loss for the mixed debris bed (i.e., superposition of individual head losses).

Staff Evaluation of GR Section 3.7.2.3.1.3: The NRC-sponsored research found the test data for head loss for mixed debris beds to be bounded by the sum of the head loss of the individual constituents. However, it was noted that the mixed bed tests were not comprehensive with regard to all of the types and combinations of debris that may be possible. NUREG/CR-6808 concluded that the head loss associated with a mixed RMI and fiber debris bed should preferably be based on head-loss measurements, but can alternately be calculated as an algebraic sum of the fiber and RMI components after accurately accounting for the strainer geometry. The potential for forming a fiber/particulate thin bed should be evaluated even when mixed-debris beds are possible because there are insufficient data to substantiate the conclusion that the presence of RMI debris can prevent the formation of a thin bed.

3.7.2.3.1.4 Calcium Silicate Insulation

GR Section 3.7.2.3.1.4 discusses the calculation of head loss for debris beds containing calcium silicate insulation debris. It states, "Based on current information, the NUREG/CR-6224 correlation can be used according to the methods for fibrous debris beds with particulate if the application is limited to particulate mixtures containing up to about 20 percent calcium silicate by mass." The calcium silicate is treated as the particulate in the fiber/particulate debris bed. The guidance referenced the NRC-sponsored calcium silicate test report (issuance pending), which is now available as LA-UR-04-1227.

Staff Evaluation of GR Section 3.7.2.3.1.4: The staff concludes that the baseline guidance regarding the estimation of head loss for debris beds containing calcium silicate debris is not adequate. The staff recognizes that LA-UR-04-1227 was not available in time for it to be reviewed by industry and its results included in the baseline guidance. Therefore, the recommendations from LA-UR-04-1227 are summarized herein. The confirmatory tests performed so far only provide reasonable assurance that NUREG/CR-6224 can be used as a scoping tool to calculate the pressure drop across CalSil debris beds. Therefore, the NUREG/CR-6224 correlation cannot be used as a design tool to calculate the head loss across a CalSil debris bed on sump screens. Licensees should use other verifiable methods to calculate the pressure drop across CalSil debris beds in design evaluations.

Table 3-5 summarizes the staff-recommended parameters for applying the NUREG/CR-6224 correlation to debris beds consisting of fibrous and calcium silicate. The recommendations depend upon whether or not the thin-bed debris configuration is a potential concern. If the potential for a thin-bed debris configuration exists, then the application of the correlation must consider the higher specific surface area deduced from the tests in which the high thin-bed head losses were encountered.

The reproducible thin-bed calcium silicate tests demonstrated that the potential thin-bed accumulation is realistic. Only a small quantity of fibers (or perhaps none) and fine calcium silicate particulate, which tends to remain in suspension, is needed to form a uniform debris bed. The recommended specific surface area of 880,000 ft^{-1} is 10 percent higher than the experimentally deduced area and prudently incorporates a 10 percent to 20 percent safety factor to account for (1) experimental uncertainties, such as instrumentation error, (2) an incomplete examination of the experimental test parameter space, and (3) the variance in the manufacture of calcium silicate insulation.

Table 3-5. Recommended Conservative Calcium Silicate NUREG/CR-6224 Correlation Parameters

Correlation Parameter	Recommended Head-Loss Parameters	
	Thin-Bed Configuration	Other Configurations
Particle Density	115 lbm/ft^3	115 lbm/ft^3
Particulate Sludge Density	22 lbm/ft^3	22 lbm/ft^3
Particulate Specific Surface Area	880,000 ft^{-1}	600,000 ft^{-1}

The sump-screen conditions that cannot form a thin-bed configuration include (1) the advanced strainer designs, for which test data have indicated that thin-bed configurations would not uniformly form because of complex surface design, and (2) flow conditions insufficient for the required debris bed formation, which can be substantiated by applicable test data. Examples of advanced strainer designs include the stacked-disk strainers, for which it has been generally accepted, based on testing of prototypical strainers, that a uniform thin-bed configuration will not form under potential debris loadings. An example of insufficient flow conditions includes a maximum screen/strainer approach velocity of less than 0.1 ft/s and particulate-to-fiber mass ratios of less than 0.5. Under these conditions, a thin bed was not achieved in the calcium silicate head-loss tests because the filtration efficiency apparently was not sufficient to remove enough of the fine calcium silicate from the flow to form a granular debris bed. Beyond these conditions, a thin bed was actually formed during the tests or the tests did not cover that part of the parameter space; thus, it is not known if a thin bed can form.

The specific surface area for calcium silicate is not a fixed value as it is for hardened particulates, such as BWR corrosion products. It was demonstrated that calcium silicate particles are somewhat “spongy,” with interior voids so that when compressed, the particulate deforms to fill inter-particle spaces. A working theory that fits the experimental results is that the compression forces water through smaller and smaller interior voids and increases the effective specific surface area of the calcium silicate particles.

The three parameters recommended in Table 3-5 (i.e., particle density, particulate sludge density, and particulate specific surface area) are a parameter set and should be applied as a set. The experimental determination of the specific surface areas depended upon the specification of the debris densities. It is also important to note that the calcium silicate tested was obtained from only one manufacturer, and that these recommendations do not necessarily apply to all types of calcium silicate insulation debris.

Whether or not there is sufficient fiber to form a thin-bed has been generally based on the NUREG/CR-6224 recommendation that the quantity of fibrous debris available must be sufficient to form an accumulation 1/8-in. thick on the screen. Tests conducted using only calcium silicate fragments have demonstrated that calcium silicate debris can accumulate without the aid of fibrous debris. However, tests conducted using only calcium silicate were not definitive enough to accurately determine the conditions under which a thin-bed can form without the presence of fibrous debris, other than the fibers contained in the calcium silicate insulation.

Staff Conclusions Regarding GR Section 3.7.2.3.1.4: The staff concludes that the recommendations shown in Table 3-5 of this report should be followed for debris beds containing calcium silicate debris, unless other data become available which are more applicable to plant-specific conditions. If it can be demonstrated that a thin-bed configuration cannot be formed with calcium silicate debris, then the mixed-bed configuration recommendations can be followed. Otherwise, the thin-bed configuration should be assumed. In determining whether or not enough fibrous debris is available, the determination that it may be possible to form a bed of calcium silicate debris without other supporting fiber should be factored into the analysis.

3.7.2.3.1.5 Microporous Insulation

Section 3.7.2.3.1.5 of the GR acknowledges that microporous insulation (e.g., MinK and Microtherm) is a granular insulation that is used in PWRs. For guidance, the GR refers to insights gained in a limited series of head-loss experiments for which additional background is provided in the supplemental guidance (see GR Section 4.2.5.2.2).

Staff Evaluation of GR Section 3.7.2.3.1.5: The staff finds that the GR did not provide adequate guidance to predict head loss for microporous insulation debris beds because it did not recommend any methodology. The licensees should develop correlations or use test data for predicting head loss for microporous insulation debris beds.

3.7.2.3.1.6 Microporous and Fiber Debris

Section 3.7.2.3.1.6 of the GR provides limited guidance regarding the application of the NUREG/CR-6224 correlation to light loadings of microporous insulation debris on a sump screen for a particulate to fiber mass ratio less than 0.2.

For ratios larger than 0.2, the baseline guidance recommends the following options:

1. Remove microporous or calcium silicate insulation until the particulate-to-fiber mass ratios drops below 0.2.
2. Seek an alternative head-loss correlation to the NUREG/CR-6224 correlation.
3. Perform head-loss experiments using plant-specific debris mixtures, sump-screen configuration, and thermal-hydraulic conditions.

The baseline guidance in this section also discusses concerns for microporous or calcium silicate debris only (i.e., no additional fibers other than those integral to the microporous or calcium silicate debris). This guidance recommends the same three alternatives noted above for situations in which a debris bed can be accumulated with these insulations without significant other fiber.

The baseline guidance addresses mixtures of granular insulation and RMI debris beds by referring to the superposition guidance presented in GR Section 3.7.2.3.1.3.

Staff Evaluation of GR Section 3.7.2.3.1.6: The staff concludes the following regarding the guidance presented in this section:

1. The baseline guidance is adequate for particulate-to-fiber mass ratios less than 0.2.
2. The alternatives for particulate-to-fiber mass ratios greater than 0.2 are adequate with the caveat relative to option 2, above, that the adequacy of the alternate correlation should be verified using applicable test data.
3. Because a debris bed formed of microporous debris without additional fibrous debris would be similar to a fibrous/microporous debris bed with a high particulate-to-fiber mass ratio, the adequacy of the options is the same as for a debris bed with fibers and a particulate-to-fiber mass ratio greater than 0.2.
4. The acceptance of the baseline guidance for thin beds containing microporous insulation types is also subject to the acceptance of the three options defined above.
5. The superposition guidance for mixtures of granular insulation and RMI debris is acceptable.

3.7.2.3.2 Methodology Application Considerations

3.7.2.3.2.1 Total Sump-Screen Head Loss

Section 3.7.2.3.2.1 of the GR recommends adding the clean-strainer head loss to the debris-bed head loss to get the total head loss across the screen.

Staff Evaluation of GR Section 3.7.2.3.2.1: The staff concludes that this guidance is acceptable because it is consistent with general engineering practice. RG 1.82, Revision 3, recommends a different approach, which is based on NPSH margin. Either approach is acceptable.

3.7.2.3.2.2 Evaluation of Breaks with Different Combinations of Debris

Section 3.7.2.3.2.2 of the GR recommends that analysts evaluate a spectrum of breaks with different combinations of debris types to ensure the identification of the break with the mixture of debris on the screen that causes the highest head loss. The guidance notes that the limiting break is not necessarily the break that generates the largest total quantity of debris.

Staff Evaluation of GR Section 3.7.2.3.2.2: The staff concludes this guidance is acceptable because the break size recommended in the GR gives conservatively higher head loss across the debris bed on the sump screen.

3.7.2.3.2.3 Thin Fibrous Beds

GR Section 3.7.2.3.2.3 recommends that the head loss associated with a thin-bed be calculated as a sensitivity analysis. To analyze a thin fiber bed, a fiber quantity sufficient to form a 1/8-in. thick debris bed should be determined to be available and, if present, could be deposited on the sump screen. The head loss calculations are the same as described for fiber and particulate beds using the full value of particulate matter transported to the sump screen. The particulate matter includes the latent debris such as dirt, concrete dust, rust, inorganic zinc, epoxy fines, etc. The particulate layer is characterized by a high sludge-to-fiber ratio; hence a limiting value for the compression is used. If under these conditions, the thin-bed head loss should exceed the NPSH margin, then the allowable particulate loading can be evaluated by reducing the particulate quantity until the calculated head loss is within the NPSH margin.

Staff Evaluation of GR Section 3.7.2.3.2.3: The staff agrees that the potential for developing a thin-bed head loss must be evaluated, regardless of the composition of the potential containment debris. Appendix VIII to this SE provides detailed staff guidance on evaluation of thin bed effects. The following is a summary:

1. The appropriate density to apply to the fibrous debris in the determination of the quantity of debris needed to form a 1/8-in. bed is the as-manufactured density. The 1/8-inch minimum thickness has been based on the NUREG/CR-6224 (Appendix B, page B-60) finding, "The head loss model is applicable only to fiber bed thicknesses where uniform bed formation is expected. Typically, this is valid for fiber bed thicknesses larger than 0.125" (0.318 cm). Below this value, it appears the bed does not have the required structure to bridge the strainer holes and filter the sludge particles." The NUREG/CR-6224 analysis used the as-manufactured density to specify the "theoretical bed thickness," which is used to specify whether or not a 1/8-in. thick bed exists. For NUKON™ debris, the accepted as-manufactured density has been 2.4 lb/ft^3. For latent debris, the as-manufactured density is not applicable because latent fibers can come from any number of sources. However, after examining the latent fibers collected from volunteer plants Appendix VII conservatively recommended a density of 2.4 lb/ft^3, which is equal to that of NUKON™.
2. For a thin-bed debris accumulation, the limiting bed compression specified as either the limiting porosity or limiting solidity becomes a controlling parameter in the NUREG/CR-6224 correlation (i.e., the bed solidity essentially approaches that of the granular materials). It is important that the limiting solidity be correctly evaluated for the particular particulate or mixture of particulates in the debris bed. For example, the limiting solidity for BWR iron oxide corrosion products is about 0.2 (NUREG/CR-6224), but for common sand, it varies between 0.57 to 0.60 (standard handbook data). Section 3.7.2.3.1.1 of the GR discusses this issue.
3. Because a number of uncertainties are associated with specifying the 1/8-in. bed thickness criteria, the parameter values that go into the bed thickness determination need to be sufficiently conservative to compensate for uncertainties to ensure adequate NPSH margin. One consideration is the fineness of the fibrous debris accumulating on the screen. Tests have been conducted since the NUREG/CR-6224 study was completed where thin-beds have been formed that were somewhat thinner than one-eighth-inch (e.g., 1/10-in.), principally because the bed was formed from suspended individual fibers rather than from the shredded fiber debris used in the NUREG/CR-6224 testing. Another consideration is the fact that the 1/8in. criteria was based on NUKON™ debris and has not been actually determined for other types of fibrous debris. Another consideration is the indication that calcium silicate can

form a debris bed without supporting fibers (other than the fibers integrated into the calcium silicate).

4. In determining the mass of allowable particulate on the sump screen that is needed to overcome the NPSH margin, the uncertainties associated with predicting this value should be noted. Specifically, the determination of the limiting solidity has a significant uncertainty as a result of inaccurate specifications of the densities of the particulate components or perhaps the mixing of constituents, as well as the involvement of fibers interlaced with the particulate.

5. To compensate for these noted uncertainties, sufficient conservatism should be used in estimating the quantities of fibrous debris available to form a thin bed. This point is particularly important for plants that do not have significant fibrous insulation (e.g., an all-RMI plant), so that the main contribution to the fiber quantities on the sump screen comes from latent debris. In such cases, the estimate of the latent fiber becomes a determining factor, but substantial uncertainty is also associated with that estimate.

3.7.2.3.2.4 Sump-Screen Submergence

Section 3.7.2.3.2.4 of the GR describes the applicable characterization for partially versus completely submerged sump screens. The limiting criterion for submerged screens occurs when the combined clean-sump and debris-bed head loss exceeds the NPSH margin. The limiting criterion for a partially submerged screen is when the debris -bed accumulation on the screen reduces the flow to less than the flow requirements for the sump. An effective head loss across the debris, which is approximately equal to one-half of the pool height, is sufficient to prevent adequate water flow. The head-loss estimate is applied to the submerged portion of the sump-screen area.

Staff Evaluation of GR Section 3.7.2.3.2.4: The staff concludes that the baseline guidance in this section regarding partially and completely submerged sump screens is acceptable because it is consistent with RG 1.82, Revision 3.

3.7.2.3.2.5 Buoyant Debris

Section 3.7.2.3.2.5 addresses the conditions in which buoyant debris could become a problem for strainer head loss. For fully submerged screens, buoyant debris is not considered a problem because it would not reach the sump screens. For partially submerged screens in which buoyant debris is determined to reach the screen, the baseline guidance recommends that the effective area be reduced by the thickness of the buoyant debris layer times the length of the covered perimeter, to the extent that it fully envelops the screen.

Staff Evaluation of GR Section 3.7.2.3.2.5: The staff agrees with the necessity of considering the potential for buoyant debris affecting sump-screen head loss. The baseline guidance is acceptable with the exception that shallow, fully submerged sump screens could still draw buoyant debris down to the submerged screen. An analysis should be performed to determine the submerged depth needed to ensure buoyant debris cannot be drawn down onto the sump screen.

3.7.2.3.3 Methodology Limitations and Other Considerations

3.7.2.3.3.1 Flat Screen Assumption

Section 3.7.2.3.3.1 of the GR states that head-loss data obtained using a vertical pipe test section of a closed-loop test apparatus with a horizontally mounted flat screen yielded conservative data for the development of the NUREG/CR-6224 correlation because all debris was forced onto a very small screen. Further, it states that in the alternative design screens, the direct application of the NUREG/CR-6224 correlation may yield overly conservative results, and that for these alternate geometry screens, independent head-loss correlations should be developed based on actual design configurations, debris loads, and test data to reduce conservatism.

Staff Evaluation of GR Section 3.7.2.3.3.1: The staff finds that the guidance in this section needs the following clarification. The development and application of the NUREG/CR-6224 correlation is based on uniform and homogeneous debris beds. Applicable test data must therefore be measured on test debris beds that match these correlation assumptions. The vertical pipe, closed-loop test apparatus generally meets these conditions, provided the debris is introduced in such a manner that it settled uniformly on the test screen. The baseline statement that “all debris was forced onto a very small screen” does not reflect testing realities. The debris is allowed to settle uniformly but the important point is that the correlation is based on the bed thickness and composition as tested.

A uniform debris bed is a realistic and a likely form of debris accumulation when debris accumulation is accomplished by filtering out suspended fibers. For example, during the conduct of the integrated tank tests (NUREG/CR-6773), the typical accumulation of fibrous debris was primarily a result of suspended debris transport and led to a uniform debris buildup on both horizontally and vertically oriented screens. In addition, the operational incidents at Perry (NUREG/CR-6808) where a coating of fine dirt covered most of the surface of the strainers and at Limerick, where a thin mat of material covered the strainer, must be considered. The flat screen assumption is reality based and is not merely a conservative assumption. It is also not overly conservative.

While it is adequate to develop independent head-loss correlations based on actual design configurations, debris loads, and test data for alternative screen designs, it should also be noted that the NUREG/CR-6224 correlation has been successfully applied to these designs without over conservatism. The application of the NUREG/CR-6224 correlation involves the selection of the appropriate screen area versus debris loading (i.e., total screen area, circumscribed area, or some area in between based on test data), as will any other successful correlation that models an alternate design from a clean screen to its fully loaded condition. The NUREG/CR-6224 correlation has been and can be applied to prototype alternate geometry screens/strainers to determine effective screen areas for specific debris loadings that can be subsequently used in plant specific evaluations.

3.7.2.3.3.2 Non-uniform Deposition on Sump-Screen Surfaces

Section 3.7.2.3.3.2 of the GR discusses the conservatism of the assumption that the debris is uniformly distributed on the screen relative to potential nonconservative accumulation associated with vertical and inclined screens.

Staff Evaluation of GR Section 3.7.2.3.3.2: The staff agrees that it is conservative to assume uniform debris accumulation on all types and orientations of screens.

3.7.2.3.3.3 Very Thin Fiber Beds

GR Section 3.7.2.3.3.2 discusses instances in which the fiber loading is less than that required to form a thin bed. It states that experiments have shown that very thin fibrous beds (with a thickness of less than 1/8-in.) are characterized by large scale, non-uniformities on the screen and negligible head losses. The baseline guidance recommends assuming a negligible head loss whenever the debris bed thickness is less 1/8-in.

Staff Evaluation of GR Section 3.7.2.3.3.3: The staff concludes that it is appropriate to neglect the head loss associated with low-density fiberglass insulation debris beds of less than 1/8-in. provided the concerns expressed in the staff's response to Section 3.7.2.3.2.3 regarding the determination of the thin-bed thickness are adequately addressed. These concerns included using the appropriate density to determine the thickness for a given quantity of debris and the uncertainties associated with the original specification of 1/8-in. as the threshold thickness. The uncertainties include the relative fineness of the insulation debris used to make the threshold thickness determination and the fact that the thickness determination was made only for NUKON™ debris and has not been directly determined for other types of insulation debris. An example in which it is not appropriate to neglect the head loss for a debris bed less than 1/8-in. thick is when there is substantial calcium silicate debris in the bed. There have been experimental indications that calcium silicate can form a debris bed without supporting fibers.

3.7.2.3.4 Sample Calculations

Section 3.7.2.3.4 of the GR provides sample head-loss calculations. The sample calculations assume flat-plate strainer geometry, steady-state ECCS flow conditions, and the final debris loadings. The debris sources were developed in the sample problem sections for debris generation (GR Section 3.4.3), latent debris (GR Section 3.5.3), and debris transport (GR Section 3.4). Sample head-loss calculations were presented for a fiber/particulate debris bed, an RMI-debris bed, a mixed RMI, fiber/particulate debris-bed, and a thin-bed debris condition.

Staff Evaluation of GR Section 3.7.2.3.4: The sample problems are consistent with the baseline methodology discussed above and with the specified head-loss calculational assumptions, with the exception that the sample problem used a fiber density of 175 lbs/ft^3 rather than the 159 lbs/ft^3 density recommended in GR Table 3-2. However, the sample problems fail to clarify the differing volumes and densities associated with each constituent. For example, in the fiber/particulate calculation, two volumes are provided for NUKON™ fibers without distinguishing the type of volume quoted (1) 129 ft^3 for the bulk volume, and (2) 1.77 ft^3 for the material (solid) volume. The reader must take care to use the proper volumes and densities in the appropriate calculational steps.

In Section 3.7.2.3.1.1, the GR discusses maximum solidity for particulates as a material-dependent property. However, this section leaves the reader with the impression that 20 percent is a reasonable limiting value for general use. The staff comments on this section pointed out that many particulates have maximum solidities much higher than 20 percent, (e.g., common sand has an approximate solidity of 60 percent). Therefore, the general use of 20 percent is not appropriate. Rather, the maximum solidity should be determined for each particulate constituent, and then the particulate constituent effective average must be determined. It should also be noted that the maximum solidity also depends upon the particulate-size distribution. The sample head-loss calculations, specifically the thin-bed calculation in which the limit is applied, failed to treat material-specific maximum solidities. The failure to correctly treat the maximum solidities can lead to erroneous and nonconservative head-loss predictions for pack-limited debris beds.

3.8 ACCEPTANCE OF NEI BASELINE GUIDANCE

The purpose of the baseline evaluation methodology is to provide PWR licensees in the United States with a common and consistent approach for evaluating the susceptibility of containment sumps to blockage resulting from the effects of postulated LOCA events. The baseline evaluation methodology is the application of a conservative set of methods that help identify the dominant design factors for a given plant (GR Section 3) that could be subsequently followed by separate guidance on possible analytical refinements to the baseline approach (GR Section 4) and potential design/operational refinements (GR Section 5).

The baseline, however, goes beyond the scoping intent with the statement that, “If a plant uses this method and guidance to determine that sufficient head-loss margin exists for proper long-term Emergency Core Cooling (ECC) and Containment Spray (CS) function, no additional evaluation for head loss is required.” Rather, the baseline methodology becomes an acceptance methodology for plant-specific evaluations. Therefore, the NRC staff’s acceptance of the baseline evaluation methodology is based on whether or not any and all PWRs that determine an adequate head-loss margin by applying the baseline evaluation methodology will actually have adequate sump performance capabilities to support long-term cooling functions.

The NRC staff’s acceptance depends upon providing adequate assurance that the baseline assumptions taken as a whole and applied generically to any PWR will not result in a plant operating without adequate ECC or CS head-loss margin. In addition, the staff’s acceptance considers how follow up analytical refinements will affect the baseline methodology retained in the final evaluation. Specifically, the acceptance of the baseline evaluation methodology as a package must balance conservative assumptions against nonconservative assumptions; therefore, an analytical refinement that decreases the degree of conservatism on a particular assumption has the potential to alter the package balance such that the degree of conservatism is reduced or even reversed to nonconservatism.

The primary difficulties with assessing whether the assumptions used in the baseline guidance result in the baseline guidance as a package being conservative with respect to estimating NPSH margin is that each assumption is variable with respect to the plant evaluated. In addition, the conservatism for each assumption cannot be quantified without actually performing a detailed evaluation. Without quantification for at least the more influential assumptions, it is difficult to judge the baseline package conservatism. For example, assuming that all unqualified coatings fail into 10 μ particles could be overly conservative for containments with large quantities of unqualified coatings. However, for plants with little unqualified coatings this assumption does not provide any extra conservatism to counter the non-conservative assumptions in the baseline guidance. Table 3-6 summarizes the more influential assumptions with potential notable conservatism. Table 3-7 summarizes the more influential assumptions that are clearly not conservative.

Table 3-6. Conservative Assumptions in the Baseline Evaluation Methodology

No.	Baseline Guidance Assumption	Rationale for Assumption	Perceived Level of Conservatism
	Debris Generation Assumptions		
1	All unqualified coatings in containment are assumed to fail.	Compensate for lack of data (i.e., no basis for estimating failure of unqualified coatings).	Variable depending upon plant conditions; therefore, the associated conservatism to the baseline package could range from essentially none to excessive.
2	All coatings debris (qualified and unqualified) assumed to become 10µ particulate. The implication of the small particulate size is complete transport to sump screen and complete filtration.	Compensate for lack of data (i.e., no basis for estimating coatings debris-size distributions).	Variable depending upon plant conditions; therefore, the associated conservatism to the baseline package could range from minimal to excessive.
3	100% destruction of materials for which suitable debris generation data are not available, including all such materials inside the ZOI and unprotected materials outside the ZOI.	Compensate for lack of data (i.e., the fraction of the materials that become small fines debris cannot be ascertained without material-specific debris generation data).	Variable, depending upon the types and quantities of such materials. Additionally, it depends upon the relative quantities of such materials compared to dominant insulation with known destruction characteristics. The associated conservatism to the baseline package could range from a minor correction to substantial.

No.	Baseline Guidance Assumption	Rationale for Assumption	Perceived Level of Conservatism
	Debris Transport Assumptions		
4	Washdown transport to the sump pool is 100% for fibrous debris, and a large fraction of the blowdown-transported debris is directed to the sump with the end result that all small fibrous debris fines are transported to the sump pool.	Avoidance of complex analyses.	Variable, depending upon containment design. Some containment designs could result in high-washdown transport, (e.g., the volunteer plant study (see Appendix VI to this SE), while others may retain debris in the upper levels of the containment.
5	100% of small fines within the ZOI not allocated to an inactive pool are transported to the sump screens.	Avoidance of complex analyses.	Variable, depending upon the transport characteristics of the pool. Given a fast-flowing pool, the transport could be high; therefore, this assumption would not necessarily be conservative. But for a slow pool, a substantial portion of the small fines debris could sink to the floor and not be transported to the screen (i.e., substantial conservatism with this assumption).
6	All debris generated outside ZOI assumed to be transported to sump screen.	Avoidance of complex analyses and compensation for lack of data.	Variable, depending upon the types and quantities of such materials. The associated conservatism to the baseline package could range from a minor correction to substantial.

Table 3-7. Non-conservative Assumptions in the Baseline Evaluation Methodology

No.	Baseline Guidance Assumption	Rationale for Assumption	Perceived Level of Non-conservatism
Debris Generation Assumptions			
7	The adaptation of the BWROG URG destruction pressures to PWR LOCA jets.	Lack of BWR- or PWR-specific data. Similar application suggests that the BWR data are appropriate for PWRs.	Because an LWR LOCA jet is a two-phase steam/water jet and the destruction pressures cited in the URG were determined using an air jet and because limited experimental evidence exists from the OPG two-phase jets, the BWROG destruction pressures could be too high. The baseline methodology could underestimate debris quantities. Therefore, based on the study of this issue and testing, the staff position is to lower the debris destruction pressure by 40% in order to account for two-phase jet effects (see Section 3.4.2.2).
8	A spherical ZOI is truncated whenever the ZOI intersects a robust structure. The radius of the remaining ZOI is not increased to compensate for jet-reflection effects.	Assumption that jet reflections off the robust structure would not extend further than the unrestrained sphere. This approach was used for resolving the BWR strainer issue.	Jet reflections off the robust structures would reinforce other components of the LOCA jet. A major portion of the energy of the jet may be preserved.
9	The destruction pressures for coatings within the ZOI were based on high-pressure water-jet data rather than two-phase jets typical of a PWR LOCA.	Lack of applicable data.	The water jet data may not properly address thermal shock effects that spalled concrete in the HDR tests (NUREG-0897, page C-2 and Figure C-5). The ZOI coatings debris quantities may be underestimated. Therefore, the staff position is that either

No.	Baseline Guidance Assumption	Rationale for Assumption	Perceived Level of Non-conservatism
			destruction pressures and spherical ZOI sizing for coatings be determined on a plant-specific basis (based on experimental data as described in Sections 3.4.2 and 3.4.3), or a spherical ZOI of 10D be used.
10	Default worst-case paint thickness of 3 mils for unqualified coatings outside ZOI.	Default alternative when plant-specific coating thickness data are not available.	Not worst-case and the assumption was not properly justified. Therefore, the staff recommends plant-specific justification of this thickness, or plant-specific evaluations to determine unqualified coating properties and thicknesses, as described in Section 3.4.3.
	Debris Transport Assumptions		
11	Debris transport into inactive pools based on the ratio of the inactive pool water volume to the total water volume in the sump pool. Implies a uniform distribution of debris throughout the water pools formed following the LOCA.	Assumptions of uniformly distributed (as opposed to preferential) sweeping of debris on the containment floor into inactive pools by thin sheets of high-velocity water, and of 100% transport of small fines to the sump during recirculation.	Baseline assumption that debris entrapment in inactive pools (e.g., reactor cavity) based on ratio of water volumes is not realistic. Debris will not be uniformly distributed in the sump water and washdown transported debris likely to arrive in sump after inactive pools filled. Potentially large nonconservatism that depends upon inactive pool volume relative to total water volume. In addition, the same sheeting-flow mechanism credited by the GR has the nonconservative result of sweeping debris preferentially to the screens.

No.	Baseline Guidance Assumption	Rationale for Assumption	Perceived Level of Non-conservatism
			Therefore, the staff position is that licensees limit the ratio of debris transported to the inactive pools to 15%, unless a higher fraction is adequately supported by analyses or experimental data (see Section 8).
12	Large piece debris (> 4 in.) is assumed not to be transported in sump pool; hence, large piece debris accumulation on sump screen completely neglected.	Avoidance of complex analyses.	The impact of neglecting all large debris on the baseline conservatism depends upon pool transport characteristics and sump-screen geometry. Little impact for a slowly flowing pool, for which detailed analyses would predict little large-debris transport, but potentially a large impact for a fast-flowing pool, for which substantial large debris could accumulate on the screen, or for geometries such as sump screens protected by gratings at floor level.
Head-Loss Assumptions			
13	The baseline recommends using simple geometric formulas to use characteristic diameters for fibers and particles to determine specific surface areas needed for the NUREG/CR-6224 head loss correlation.	Lack of experimentally determined specific surface areas.	Confirmatory research has demonstrated that this approach is not reliable in that it has the potential to result in large underestimates of debris bed head loss. Therefore, the staff provides additional guidance in Appendix V to this SE to deduce the specific surface areas from applicable head-loss data through the application of the correlation.

The baseline methodology assumptions were apparently made for a variety of reasons. Worst-case conditions were assumed in certain situations for which there is nearly a complete lack of data required to support a more realistic evaluation. These assumptions primarily include the generation of debris, such as the treatment of unqualified coatings, where all unqualified coatings are assumed to fail and then form fine particulate debris that would readily be transported and accumulate in a fibrous bed of debris. In reality, much, if not most, of this coatings debris would either remain attached to the surfaces or would form chip debris that may not be transported so readily. In addition to the unqualified coatings, other materials, both within and outside the ZOI, were assumed to fail into 100-percent small fines debris. The difficulty with judging the impact of these assumptions is that a particular containment may not have much of these materials; therefore the relative conservatism associated with these types of assumptions cannot be quantified for PWR containments in general.

Other baseline assumptions were made so that complex debris transport analyses could be avoided. The baseline methodology does not recommend debris-transport methods, but does credit debris entrapment in inactive pools. In addition, the methodology does not consider washdown transport of RMI debris and does not consider the transport of large pieces of debris. Again, the conservatism and nonconservatism of these assumptions cannot be judged for PWR containments in general, but only by plant-specific analyses. Assuming all fine fibrous and particulate debris washes back down to the sump pool is conservative for all plants. However, neglecting the transport of large piece debris is not conservative for all plants. Judging whether or not a conservative assumption can compensate for a nonconservative assumption requires the consideration of plant-specific features. The assumption that debris entrapment within inactive pools could be made on a simple water volume ratio is not realistic because it does not consider the timing of debris washdown relative to the fill up of the inactive pools, which would occur early in the sequence. The volunteer plant study estimated that a majority of the small fines debris was blown upwards in the containment where it subsequently would be subject to washdown processes. That study estimated a majority portion of the small fines debris returning to the sump pool, but the analytical capabilities cannot determine the timing of the debris entrance into the pool. If the inactive pools filled before the small fines debris washed back to the sump, then only relatively minor quantities might become trapped. Therefore, the inactive pool entrapment assumption is probably non-conservative.

As an illustration of the variability of these assumptions when applied to the fleet of PWR plants, consider the following hypothetical situations. Assume that the application of the baseline guidance to both Plants A and B results in the prediction of adequate NPSH margin. Table 3-8 summarized the importance of the key assumptions. The containment of Plant A is characterized as having relatively large quantities of debris with unknown debris-generation characteristics and debris-transport characteristics, and the containment has debris-transport characteristics that tend to entrap debris, thereby preventing transport to the sump screens. The variability of the baseline assumptions would tend to over predict debris generation and over predict debris transport by substantial amounts. Therefore, if Plant A has sufficient NPSH margin evaluated using the baseline guidance, Plant A should then have an adequate NPSH margin with reasonable certainty. Plant B, however, would be characterized as having limited quantities of debris, other than the ZOI insulation, with reasonably well-known destruction properties. Realistic debris transport fractions to the sump screen would be relatively high. Substantial larger debris transport would be expected with relatively minor quantities trapped in inactive pools. With hypothetical Plant B, there is a concern that the baseline evaluation could predict an adequate NPSH margin, whereas an adequate margin may not actually exist if the collective uncertainties line up in a nonconservative manner.

Table 3-8. Baseline Guidance Application to Divergent Hypothetical Plants A and B

Assumption	Hypothetical Plant A	Hypothetical Plant B
Unqualified coatings (#1 and #2)	Large quantities of unqualified coatings.	Little, if any, unqualified coatings.
100% destruction of ZOI materials with unknown destruction pressures and unprotected materials outside ZOI (#3) and complete transport of the outside ZOI material (#6)	Large quantities of such materials.	Small quantities of such materials.
100% washdown transport for fibrous and particulate small fines debris (#4)	Containment design would likely retain substantial debris at the upper levels	Most debris would likely wash down to the sump pool.
100% pool transport for small fines debris not entrapped in inactive pools (#5)	Relatively slow sump-pool flow velocities result in significant small fines debris entrapment on sump pool floor.	Relatively fast sump-pool flow velocities result in little small fines debris entrapment on sump pool floor.
Debris entrapment in inactive pools (#11)	Inactive pool volumes are relatively small; therefore, debris entrapment in the inactive pools becomes minor consideration.	Inactive pool volumes are relatively large; therefore, debris entrapment in the inactive pools becomes substantial consideration.
Neglect large piece debris (#12)	Relatively slow sump-pool flow velocities result in little actual large piece debris transport.	Relatively fast sump-pool flow velocities result in substantial actual large piece debris transport.

It cannot be conclusively demonstrated that the application of the baseline evaluation methodology can be relied upon to prove that a PWR predicting an adequate NPSH margin will truly have an adequate NSPH margin. However, a reasonable assessment of the methodology is that sufficient overall realistic conservatism exists in the baseline to accept its application with the use of acceptance qualifications or alternative guidance for specific outlier situations, such as the one described below.

For example, consider a hypothetical plant that has extensive unqualified coatings, but insufficient fibrous debris to form a fibrous-debris thin-bed capable of filtering particles.

Under the baseline methodology, all the coating debris would be in the form of 10-μ particles, which would be assumed to simply pass through the screens, thereby not causing a significant head loss. But in a potential LOCA, the coating debris could fail in large quantities and possibly transport as chips that could accumulate on the screen without the aid of fibrous debris, thus resulting in significant head loss.

This example raises two major concerns. First, the baseline guidance excludes transport and blockage of large piece debris. The staff position is that the sump-screen blockage evaluation should address whether outlier scenarios, such as these, exist and evaluate any that are identified. If a plant's sump-pool flow is relatively fast, then neglecting large piece debris could lead to substantially underestimated debris effects. Second, for debris characterization, a caution is needed regarding the determination of whether or not there is sufficient fiber to form a thin bed. If this determination is a close call, then all aspects of that determination become critical. Licensees will need to examine inputs to ensure that each of these aspects is realistic, with appropriate conservatism added before reaching the final conclusion that there is not sufficient fibrous material in containment to form a thin-bed debris accumulation.

The results of supporting confirmatory research and information available in the knowledge base (NUREG/CR-6808) cause concern in several aspects of the baseline guidance acceptability. These concerns include the following:

- Concerns regarding two-phase jet effects, relative to data collected from air jet testing, indicate a potential need to reduce the NEI-recommended destruction pressures (which are based on air-jet testing), unless over-conservatism can be demonstrated in the analytical estimates for debris quantities.
- The baseline evaluation recommendation of truncating a ZOI whenever it intersects a robust structure, without resizing the remaining ZOI to maintain jet volumes, is not conservative. Jet reflections from the robust structure may affect the remaining ZOI.
- The default coating thickness recommended by the baseline evaluation guidance is not the worst-case thickness. Only plant-specific coating thickness evaluations can adequately assess not only the coating debris volumes, but also the appropriate parameters for the head-loss correlation (e.g., the particle densities).
- Because conservative estimates for the debris-specific surface areas used in the NUREG/CR-6224 head-loss correlation are critical to ensuring conservative estimates for the NPSH margins, the staff is concerned that the baseline evaluation methodology recommendations for estimating the areas using only the characteristic diameters will lead to nonconservative head-loss predictions. Confirmatory research recommendations should be addressed.
- The baseline methodology neglects potential erosion of large piece debris by water flows by assuming all large piece debris remains in protective coverings, which debris-generation data clearly show is not realistic. Even though such erosion is not expected to result in large quantities of additional fine debris, it should still be considered in the baseline evaluation, if large portions of the large piece debris are physically located directly below large flows of falling water.

In summary, the baseline evaluation, coupled with the methodology enhancements provided in this SE is acceptable. The baseline evaluation methodology by itself cannot be given a blanket acceptance because (1) the baseline guidance recommends nonconservative assumptions, (2) it is not possible to quantify the degree of conservatism or nonconservatism of each important assumption without performing detailed analyses for comparison, especially considering the diversity in the containment and RCS designs, and (3) confirmatory research has resulted in concerns associated with key aspects of the guidance. Therefore, the baseline evaluation methodology, as modified in accordance with staff positions established in the preceding sections, is acceptable. If the baseline evaluation is based on planned design/operational changes, as opposed to current plant configuration, then acceptance of the evaluation is also based on the implementation of these planned changes. The baseline evaluation guidance does not resolve concerns which are not explicitly addressed by the baseline (e.g., chemical effects and downstream effects).

Subsequent analytical refinements to the baseline evaluation must reconsider the nonconservative assumptions of the baseline evaluation, rather than merely reducing identified over-conservatisms. Supplemental NEI analytical refinements include recommendations for reducing the sump-pool transport fractions by means of evaluating pool-flow velocities and comparing those velocities with test data for threshold velocities for moving debris along the pool floor. If such analyses are performed on small piece debris, then those analyses need to also treat large piece debris transport.

The sample problem developed in the baseline evaluation methodology may serve to illustrate the evaluation process, but is not detailed enough to serve as a template for plant evaluations.

4.0 ANALYTICAL REFINEMENTS

The GR provides some acceptable analytical refinements, and some sections contain additional information to support the development of refinements. For clarity, NEI has presented the following table (Table 4-1) that lists the refinements offered in Sections 4 and 5 of the GR.

For the purpose of this review, the staff provides its position on each of those analytical refinements recognized in this section of the GR for use by the industry. A licensee should present to the staff for approval any analytical refinements in its plant-specific analysis of sump performance which is not addressed by the staff in this section of the SE.

4.1 INTRODUCTION

Section 4.1 defines four main analytical topics for which the GR offers analytical refinements to the baseline evaluation, including (1) break selection, (2) debris generation, (3) debris transport, and (4) head loss.

4.2 METHOD DESCRIPTION

Section 4.2 identifies three main analytical topics for which the GR offers refinements to the baseline evaluation, including (1) debris generation, (2) debris transport, and (3) head loss. Discussions of the other two topics (i.e., break selection and latent debris) are included for completeness.

4.2.1 Break Selection

Section 4.2.1 of the GR discusses an analytical refinement involving pipe break locations to be considered when performing PWR-sump analyses. The proposed guidance suggests application of NRC GL 87-11, “Relaxation in Arbitrary Intermediate Pipe Rupture Requirements,” (GL-87-11) to preclude arbitrary, intermediate pipe break locations from consideration in PWR sump analyses. The refinement suggests consideration of only those break locations which are consistent with BTP MEB 3-1, “Postulated Rupture Locations in Fluid System Piping Inside and Outside Containment,” and SRP Section 3.6.2, “Determination of Rupture Locations and Dynamic Effects Associated with the Postulated Rupture of Piping.” Application of BTP MEB 3-1 for PWR sump analyses is intended to focus attention on high-stress and fatigue break locations, such as at the terminal ends of a piping system and intermediate pipe ruptures at locations of high stress.

Staff Evaluation of GR Section 4.2.1: The staff’s evaluation of this section considered the proposed GR guidance in conjunction with existing, corresponding guidance on this subject. The staff’s review considered the requirements of 10 CFR 50.46, the staff’s evaluation and conclusions for a similar proposal from the BWROG (URG SE), the guidance provided in RG 1.82, Revision 3 and the Commission’s staff requirements memorandum (SRM) regarding a proposed rulemaking to risk-inform requirements related to LBLOCAs (SECY-04-0037).

Table 4-1 Pressurized-Water Reactor Sump Performance Evaluation Methodology Refinements Table

No.	Section	Page	Topic	Description
1	4.2.1	4-1	Break Selection	This section identifies that plants may use Generic Letter 87-11, "Relaxation in Arbitrary Intermediate Pipe Rupture Requirements," consistent with their licensing basis, to select break locations for evaluating post-accident sump operability.
2	4.2.2.1	4-2	Debris Generation	This section identifies that plants may refine the Zone of Influence (ZOI) definition from a single all-encompassing region based on the material with the minimum destruction pressure by assigning multiple ZOIs to each break site. Each ZOI would correspond to the destruction pressure of one insulation species located near the break site.
3	4.2.2.1	4-3	Debris Generation	This section identifies that plants may refine the Zone of Influence (ZOI) definition by modeling two freely-expanding jets, each originating at one end of a postulated DEGB. The ZOI for a specific material would be evaluated as the region enclosed within the calculated isobar corresponding to a given destruction pressure of an insulation species located within the jet.
4	4.2.2.2	4-5	Debris Characteristics	This section provides additional refinements with respect to the characteristics of debris that might be generated from a postulated break. Specifically, the use of plant-specific or publicly available vendor-specific information, where applicable, is identified as source for refining debris sizes considered in the transport and blockage evaluation.
5	4.2.3	4-14	Latent Debris	This section identifies that plant-specific conditions (for example, cleanliness programs) may be used to support improvements to the latent debris source term.
6	4.2.4	4-14	Debris Transport	This section identifies two refinements to evaluate debris transport. • The first refinement is the use of an open channel nodal network to evaluate bulk fluid movement about the containment. • The second refinement is the use of a Computational Fluid Dynamics (CFD) model to calculate a detailed flow field within the containment sump and assess debris transport.

Table 4-1 Pressurized-Water Reactor Sump Performance Evaluation Methodology Refinements Table (Continued)

No.	Section	Page	Topic	Description
7	4.2.4.1	4-14	Debris Transport	This section provides guidance on the development of an open channel network model Guidance is given on: • Use of the physical configuration of the containment geometry to define the model, • Development of boundary conditions based on sources and sinks of cooling water, • Defining hydraulic channels • Calculation of hydraulic losses in the channels, and, • Refinements to the channel pattern. A sample calculation is included for demonstration purposes.
8	4.2.4.2	4-23	Debris Transport	This section provides guidance on the development of detailed flow patterns in the containment pool using state-of-the-art 3D computational fluid dynamics (CFD) codes. Guidance is given on: • Selection of CFD software, • Building a CAD model of the containment to be used as input to the CFD model • Building the CFD model, including mesh generation and selection of material properties and boundary conditions, • Solution convergence considerations, and, • Use of computed results for evaluating debris transport. A sample calculation is included for demonstration purposes.
9	Table 4-2	4-29	Debris Transport	This table provides additional transport data for debris generated from common insulation materials. This information may be used in conjunction with either the Open Channel Nodal Network or CFD models to evaluate debris transport in the sump pool during operation of the ECCS in the recirculation mode.
10	4.2.5.1	4-35	Head Loss	This section identifies that no refinements for evaluating thin bed effects are offered beyond those already given in Section 3.7.2.3.2.3.

Table 4-1 Pressurized-Water Reactor Sump Performance Evaluation Methodology Refinements Table (Continued)

No.	Section	Page	Topic	Description
11	4.2.5.2	4-35	Head Loss	This section presents information that may be helpful in refining the head loss analysis as a whole including a brief background discussion on head loss correlation development. This section identifies the parameters to be considered when developing a head loss correlation. This discussion is given to identify the considerations to be accounted for when developing a design-specific head loss correlation for a sump screen.
12	4.2.5.2.1	4-37	Head Loss	This section presents a summary of early sump screen head loss testing. Included in the discussion is the method of test, a summary of the nature of the tests and the data obtained, and how the data were correlated. This is provided to facilitate understanding of the nature and complexity of head loss testing. Add statement regarding plant-specific basis.
13	4.2.5.2.2	4-39	Head Loss	Several special head loss correlations are presented and discussed. Specifically: • An empirical correlation for fiber-only beds, • The US NRC NUREG/CR-6224 head loss model, • The US BWROG combined debris head loss correlation, and, • Correlations for head loss due to flow through reflective metallic insulation (RMI). The basis for, and considerations to be accounted for, in applying the RMI head loss equations are also listed.
14	4.2.5.2.3	4-50	Head Loss	This section presents information that may be useful in the development of correlations for alternate strainer designs. Two potential improvements identified for head loss modeling for alternate strainer designs are identified: • Accounting for geometry of the screen, if it varies significantly from a flat plate, and, • Non-uniform deposition of debris on the strainer, if appropriate and justifiable.

Table 4-1 Pressurized-Water Reactor Sump Performance Evaluation Methodology Refinements Table (Continued)

No.	Section	Page	Topic	Description
15	5.1	5-1	Debris Source Term	This section identifies possible design and operational activities that may be undertaken to reduce the debris source term, such as: • Improved housekeeping and foreign materials exclusion (FME) programs • Insulation change-out, • Insulation modifications, • System and equipment modifications, and, • Modifications to protective coatings programs.
16	5.2	5-4	Debris Transport	This section identifies information that might be used for debris barriers that might mitigate debris transport about the containment. These barriers include: • Floor obstructions, and, • Debris racks.
17	5.3	5-6	Screen Modifications	This sections identifies options for sump screen modifications, including: • Passive strainer designs, • Backwash strainer designs, and, • Active strainer designs. In addition to the sump screen modification options, a list of considerations for each of the options is identified.

GSI-191 and the concern of PWR sump blockage are directly associated with the long-term cooling acceptance criteria listed in 10 CFR 50.46 (b)(5). To ensure acceptable ECCS cooling capability, 10 CFR 50.46 requires that "ECCS cooling performance must be calculated in accordance with an acceptable evaluation model and must be calculated for a number of postulated loss-of-coolant accidents of different sizes, locations, and other properties sufficient to provide assurance that the most severe postulated loss-of-coolant accidents are calculated." The staff notes that the worst breaks with respect to peak clad temperature and the other acceptance criteria of 10 CFR 50.46 may not necessarily be the limiting breaks for debris generation and sump-head loss. When evaluating ECCS performance for compliance with 10 CFR 50.46, SRP Sections 6.3, "Emergency Core Cooling System," and 15.6.5, "Loss-of-Coolant Accidents Resulting from Spectrum of Postulated Piping Breaks Within the Reactor Coolant Pressure Boundary," should be considered. SRP Section 15.6.5 states that reviewers "evaluate whether the entire break spectrum (break size and location) has been addressed." The proposed GR guidance to consider only those break locations consistent with BTPMEB 3-1 is not in accordance with the requirements of 10 CFR 50.46 because BTP MEB 3-1 may not provide assurance that the most severe postulated LOCAs are calculated.

RG 1.82, Revision 3 provides the NRC's guidance regarding an appropriate spectrum of breaks to be considered when evaluating PWR sump performance. Specifically, Regulatory Position 1.3.2.3 of RG 1.82 states that a "sufficient number of breaks in each high-pressure system that relies on recirculation should be considered to reasonably bound variations in debris generation by the size, quantity, and type of debris." At a minimum, the staff position is that the following postulated break locations should be considered, (1) breaks in the hot leg, cold leg, intermediate leg, and, depending on the plant licensing basis, main steam and main feedwater lines with the largest amount of potential debris within the postulated ZOI; (2) large breaks with two or more different types of debris, including the breaks with the most variety of debris, within the expected ZOI; (3) breaks in areas with the most direct path to the sump; (4) medium and large breaks with the largest potential particulate debris to insulation ratio by weight; and (5) breaks that generate an amount of fibrous debris that, after its transport to the sump screen, creates a minimum uniform thin bed (1/8-in. layer of fiber) to filter particulate debris. The staff considers that RG 1.82 provides the complete scope of breaks which should be evaluated to ensure that the criteria of 10 CFR 50.46 are satisfied. The proposed GR guidance to consider only break locations consistent with BTP MEB 3-1 does not provide an adequate alternative to the guidance provided in RG 1.82, Revision 3, to demonstrate compliance with the requirements of 10 CFR 50.46 because the complete scope of break locations may not be evaluated.

The staff previously reviewed a similar request to apply SRP Section 3.6.2 and BTP MEB 3-1 for identifying break locations to be considered when evaluating ECCS strainer concerns in BWRs. As documented in the staff's SE for the BWRs (URG SE), the staff rejected the BWROG proposal for two reasons. The first reason was that SRP Section 3.6.2 and BTP MEB 3-1 do not provide guidance or acceptance criteria for demonstrating compliance with the requirements of 10 CFR 50.46. The staff noted that the only acceptance criterion specified in SRP Section 3.6.2 is compliance with General Design Criteria (GDC) 4, "Environmental and Dynamic Effects Design Bases." GDC 4 requires that licensees must protect structures, systems, and components important to safety from the dynamic effects (e.g., pipe whip, direct steam jet impingement, etc.) and environmental effects (e.g., temperature, pressure, radiological effects) of postulated pipe ruptures. The staff communicated through GL 87-11, which transmitted the revised SRP Section 3.6.2 and BTP MEB 3-1, that licensees could still provide an adequate and practical level of protection for compliance with GDC 4 by reducing the number of postulated pipe breaks and by physically protecting equipment important to safety from the postulated pipe breaks that have a relatively higher potential for failure (e.g., postulated failures at high-stress and fatigue locations). As a result, when demonstrating compliance with GDC 4, licensees may analyze pipe breaks through the use of pipe-stress analysis methodologies similar to that provided in SRP Section 3.6.2 and BTP MEB 3-1. The staff considers SRP Section 3.6.2 and BTP MEB 3-1 to be inappropriate for postulating break locations for the purpose of determining the extent of debris generated in order to comply with the requirements of 10 CFR 50.46 because these are applied to demonstrate compliance with GDC 4, not 10 CFR 50.46. The second reason given by the staff in rejecting the BWROG proposal was that the BWROG had not demonstrated that break locations selected consistent with SRP Section 3.6.2 and BTP MEB 3-1 would bound the worst-case debris generation scenarios and, therefore, meet the intent of 10 CFR 50.46. The staff finds that this discussion also applies to PWRs and the GR proposal.

Finally, in evaluating the GR proposal, the staff considered the current effort involving a proposed rulemaking to risk-inform requirements related to LBLOCA break size. For a risk-informed 10 CFR 50.46, the staff is revising the design-basis LOCA break size, but does not plan on changing its current position regarding break locations which need to be considered for purposes of meeting the requirements of 10 CFR 50.46. The staff's intention is to ensure that the methodology used to resolve GSI-191 is consistent with the 10 CFR 50.46 rulemaking effort.

Based on the above discussions, the staff concludes that it is inappropriate to cite SRP 3.6.2 and BTP MEB 3-1 as methodology to be applied for determining break locations to be considered for PWR sump analyses because these may not identify the limiting break location. The staff concludes that the guidance regarding break locations, as described in GR Section 3.3 (and as amended in Section 3.3 of the staff's SE) should be followed when performing PWR sump analyses. The staff's conclusion applies for the entire spectrum of pipe-break sizes which are considered. When performing analyses described in Section 6 of the GR, "Alternate Evaluation," this conclusion applies for both Region I and Region II analyses.

4.2.2 Debris Generation

4.2.2.1 Zone of Influence

This section reiterates that, for the baseline calculation, the GR recommends the use of a spherical ZOI to encompass the effects of jet expansion resulting from impingement on structures and components. It notes that two refinements are to be presented for insulation materials, but none are offered relative to coatings.

<u>Staff Evaluation of GR Section 4.2.2.1</u>: The spherical zone is a practical convenience that accounts for multiple jet reflections and mutual interference of jets from opposing sides of a guillotine break. It is important to note that when the spherical volume is computed using an acceptable approximation for unimpeded free jet expansion, the actual energy loss involved in multiple reflections is conservatively neglected to maximize the size of the ZOI. The staff concurs with the use of spherical ZOI as a practical approximation for jet-impingement damage zones.

4.2.2.1.1 Method 1: Debris-Specific Spherical ZOIs

Method 1 refines the evaluation of ZOI by recommending that multiple ZOIs be assigned to each break site, with each corresponding to the destruction pressure of one insulation species located near the break site. The methodology of the ANSI/ANS 58.2-1988 standard determines the pressure isobars used to define the equivalent-volume spherical ZOI pertinent to a particular insulation type. Table 3-1 of the GR presents destruction pressures for several insulation types. This table provides the ratio of the ZOI radius to the break diameter for each insulation type listed. The Method 1 discussion notes that no changes to insulation destruction pressures are to be made to account for differences between dry and saturated-steam jets. Section 3.4 of the GR discusses robust barriers and the effects on the ZOI.

Once the ZOI for each insulation type has been determined, the debris generated within each ZOI is calculated and the individual contributions are summed to arrive at a total debris source term.

Staff Evaluation of GR Section 4.2.2.1.1: The NRC agrees that the definition of multiple, spherical ZOI at each break location that correspond to the damage pressures of potentially affected materials is an appropriate refinement for debris-generation calculations. Furthermore, it is also appropriate to apply this refinement in a selective manner. For example, a separate, well-characterized ZOI can be applied for coatings, and all insulation types can be treated according to the baseline assumption of damage equivalent to the most vulnerable material in containment. The sample calculation presented in GR Section 3.4.2.6 illustrates this approach. Target material inventories within their respective ZOI should be calculated in accordance with the staff evaluations described in Section 3.4 of this SE, including the treatment of robust barriers.

Definition of a Spherical ZOI

Section 3.4 of the GR and Appendix I to this SE review the application of the ANSI/ANS 58.2-1988 jet model, which was found to be an acceptable approach for computing volume-equivalent spherical ZOI. However, material-specific damage pressures that were experimentally determined using high-pressure air as a surrogate working fluid should be treated in a manner similar to that presented in Section 3.4.2.2 to account for potential differences between dry and flashing two-phase water-jets. The listing of damage pressure provided in Table 3-1 of the GR implicitly acknowledges the potential for enhanced destruction by citing two-phase destruction tests for calcium silicate. The staff position to reduce destruction pressure by 40 percent for materials not tested under two-phase conditions is substantial; however, it is less than the decrease measured for calcium silicate.

The following three additional refinements related to the application of the ANSI jet model can be developed on a case-by-case basis for selected breaks if it is advantageous to do so:

1. First, the application of worst-case thermal hydraulic conditions to every break location can be relaxed if there is supporting evidence to demonstrate that a

particular break location or class of break locations exhibits substantially different conditions that can be conservatively calculated or measured. Maximum-damage volumes are generally driven by increased pressure, but these volumes can exhibit unexpected changes related to the degree of subcooling (see Appendix I to this SE).

2. Second, the assumption of equivalent maximum mass flux from both ends of a guillotine break can be relaxed if there are supporting calculations to conservatively substantiate important differences between the thermal-hydraulic conditions upstream in either direction. Damage volumes from each side would be calculated independently and then added similar to the way that damage volumes are doubled for the baseline analysis.

3. Third, some credit can be taken via conservative approximation for friction losses in lines leading to the break location if adequate documentation of roughness coefficients and flow losses in piping components can be provided. This refinement will have the effect of reducing the effective total pressure at the exit plane below the stagnation pressure of the upstream system reservoir. The system stagnation enthalpy should be assumed constant.

It is expected (but not necessary) that these refinements would be pursued on a selective basis for break locations that are found to drive key decision points. For example, limiting breaks identified under the baseline assumptions might be found to impact vulnerable insulation types that are located in high-radiation areas. While replacement of vulnerable insulations with more robust material might be the desired mitigation option, these refinements might demonstrate that the material should be left in place. If these refinements are applied as described for the purpose of exempting specific targets, the corresponding assumed break locations should be located to minimize the flowpath distance between break and target. These refinements can be applied selectively in any combination, and they apply as well to the Method 2 refinement for direct jet impingement.

The ZOI and Robust Barriers

Target material inventories within their respective ZOI or generic ZOI should be calculated as discussed in Section 3.4 of this SE, including the treatment of robust barriers. Section 3.4 does not allow simple truncation for robust barriers, as proposed in the GR.

Evaluating Debris Generation within the ZOI

The NRC agrees that the contributions of each material type to the total debris inventory should be added to determine the debris source term available for transport as described in other sections of the GR. Therefore, this is an acceptable approach.

4.2.2.1.2 Method 2: Direct Jet Impingement Model

This section of the GR offers the refinement of defining the ZOI by modeling two, freely-expanding jets emanating from each broken pipe section as opposed to using the spherical ZOI approach presented in Section 3.4 of the GR. The ANSI/ANS 58.2-1988 standard is recommended for determining the jet geometry. The specific procedures to be followed for determining jet geometry are summarized, and an example calculation is discussed. Appendix D to the GR presents the results of the isobar mapping calculations and an example of a plotted isobar. The treatment of robust barriers and the determination of overall debris generation are the same as for Method 1.

<u>Staff Evaluation of GR Section 4.2.2.1.2</u>: The NRC staff has reviewed this refinement and finds it acceptable. This refinement retains some spatial information inherent to the direction of the severed pipe. It implicitly assumes that the ends of the pipe are fully separated and fully offset, but yet, remain basically aligned in the original direction. The staff notes that there is no specific analysis of pipe-whip potential if this method is used. However, the spherical ZOI approximation carries similar inherent assumptions (basic alignment of pipe segments to create a spherical ZOI from opposing and interfering jets). Although not explicitly stated, the perceived advantage of this method under strict implementation of the GR would follow from truncation of a jet segment that impinges directly on a barrier, such as a wall or floor, as well as the economy associated with the use of ZOI calculations that have already been performed for local dynamic effects (i.e., GDC 4 analyses). Section 3.4 reviewed the practice of ZOI truncation and was judged to be nonconservative compared to the concept of ZOI volume conservation. Licensees electing direct impingement model refinement should retain the volume for conservatism. In fact, the mapping of an independent directional jet segment within containment would be necessary for postulated sidewall ruptures, if they are considered for analysis. Analysis of sidewall ruptures would carry the additional burden of investigating alternative jet directions. In lieu of mapping directional jet segments for sidewall ruptures, Section 6 of this SE reviews the use of directional (worst debris generation) hemispherical break geometry as an acceptable alternative to assuming a sphere for partial breaks in RCS main loop piping (non-DEGB).

The information provided in this section on ANSI jet modeling is identical to that provided in GR Section 3.4.2.1 and was reviewed previously. However, the staff would like to emphasize the GR statement that this refinement relies upon a high degree of rigor in determining what the stagnation pressure to which each insulation type is subjected. The first task is to model unimpeded jet expansion using the ANSI standard and Appendix I to this SE for guidance, and the second task is to map relative spatial geometries of targets and the jet in the vicinity of the break location. It is also true, as stated in the GR, that isobar contours like those presented in Appendix D to the GR and Appendix I to the SE have rotational symmetry and can be rotated about the longitudinal axis to define the three-dimensional surface of equivalent damage potential (i.e., impingement pressure).

As a point of nomenclature consistency, there is a conceptual difference between the classical definition of stagnation pressure in a moving fluid, as approximated by Bernoulli's Law, and the pressures predicted by the ANSI model. The predicted pressures are referred to throughout the SE as impingement pressures because they represent non-isentropic stoppage of the fluid on the face of a target that should be slightly higher than the theoretical stagnation pressure at a free-stream point in the flow field. Other limitations to this interpretation of the predicted jet pressures also apply as, discussed in Appendix I to this SE.

It should be noted that the additional optional refinements discussed above as Method 1 refinements for debris-specific ZOI also apply to Method 2. The choice of using an approximate spherical geometry or the more realistic geometry of a directed jet is largely independent of the thermal-hydraulic assumptions used to compute a jet contour.

The ZOI and Robust Barriers

Target material inventories within their respective ZOI or generic ZOI should be calculated, as discussed in Section 3.4 of this SE. The isobar volume of interest should be mapped and conserved independently for the jet on each side of the break. The total damage volume of the two jets should be preserved in a contiguous region, rather than crediting overlapping reflections.

Evaluating Debris Generation within the ZOI

The guidance offered in this section is identical to that presented in Section 3.4.2.5 and has been reviewed previously. Additionally, the contributions of debris from both independently evaluated jets are added to represent the total debris source term.

4.2.2.2 Debris Characteristics

GR Section 4.2.2.2 provides additional information regarding the characteristics of debris following a postulated break. The section recommends using plant-specific or publicly available vendor-specific information, where applicable, for refining debris sizes considered in the transport and blockage evaluations. The section includes Table 4-1 that contains recommendations for destruction pressures, fabrication and material densities, and debris characteristic sizes. In addition to replicating data presented in baseline Tables 3-1 and 3-2, Table 4-1 includes recommendations for other materials, as well.

Staff Evaluation of GR Section 4.2.2.2: The staff has the following concerns regarding the guidance provided in GR Section 4.2.2.2:

1. In Section 4.2.2.2.1, “Fibrous Insulation,” the guidance states, “Not all generated fibrous debris needs to be assumed to be of a transportable size.” The reality is all debris not specifically attached to a structure can be transported given a sufficient driving force. For example, an entire intact blanket of fibrous debris will move in a pool of water, if the flow velocities are sufficiently fast. Sheeting flows during testing has shown the capability of moving intact RMI cassettes under certain conditions. In short, all debris should be considered transportable until plant-specific analyses determine otherwise.
2. Section 4.2.2.2.2, “Reflective Metallic Insulation (RMI)” cites GR Reference 27 as a source of information for the debris-size distribution for RMI debris. However, Reference 27 is a report on the testing of NUKON™ insulation and does not contain RMI information. Therefore, the GR does not provide an appropriate debris-size distribution for RMI debris. Section 4.2.2.2.3, “Coatings,” also inappropriately cites Reference 27 for evaluating coatings.
3. In Section 4.2.2.2.3.1, “Coatings within the ZOI,” the GR recommends using the properties of a multiple-coating system that produces the post accident debris with the most detrimental effects to the containment sump. However, the GR does not provide guidance regarding which types of properties (e.g., a light- or

heavy-coating density) would produce the most detrimental effects. The most detrimental properties for debris transport may differ from those most detrimental to head loss. The staff is concerned that such ambiguity in the guidance could lead to improperly determined properties from a conservative standpoint and recommends that each component in a multiple-coating system be evaluated separately with its applicable properties. Effective properties for multiple types of debris can then be determined. A similar statement in Section 4.2.2.2.3.2, "Coatings outside the ZOI," directs that the most detrimental properties be assumed for unidentified non-DBA-qualified coatings systems used outside the ZOI; however, more supporting guidance is needed regarding which types of properties are most detrimental.

4. In Section 4.2.2.2.4, the GR recommends assuming that all tape and stickers located in the ZOI are destroyed into small pieces and fibers. The positive aspect of this assumption is that 100 percent of the debris would be subsequently transported to the sump screens. However, it is not a foregone conclusion that assuming the debris is destroyed into small pieces and fibers would cause a higher head loss than if this debris arrived at the screens intact, which is one of the potential realities, at least for no soluble tapes, stickers, and tags. As intact debris, this debris could effectively interdict flow through covered portions of the screen, thereby effectively reducing the size of the screen. Hence, the GR statement that it is conservative to assume that all debris created from tape and stickers is reduced into fine or small pieces or individual fibers is not supported. It is recommended that the head-loss evaluation estimate the head loss by assuming each condition of the debris, and then use the higher head loss in the NPSH margin determination.

5. In Section 4.2.2.2.5, "Fire Barrier Materials," fire barriers consist of many types of insulation and other materials, including board materials, blanket materials, and foam materials. With a few exceptions, debris-generation data do not exist for fire barrier materials that differ from the piping insulations tested. The GR recommends, "For materials that are unique to fire barrier applications and do not have supporting test data, a destruction pressure equal to that of low-density fiberglass may be assumed." While this guidance seems reasonable for fire barrier materials consisting of a low-density fiberglass or even a high-density fiberglass, it is not acceptable to apply data for low-density fiberglass to the variety of fire barrier materials (e.g., board and foam materials).

The staff did not independently verify all the data contained in GR Table 4-1 and has the following concerns:

1. Table 4-1 provides four seam orientation calcium silicate destruction pressures (i.e., 0°, 45°, 180°, and generic orientation) without additional guidance. Furthermore, the 0° reference was not stated. Application of seam-oriented destruction pressures requires orientation-specific jet destruction models. As discussed in Appendix II to this SE, the threshold pressure for destruction is actually less than 24 psi because substantial insulation damage occurred at a jet pressure of 24 psi in the OPG tests (45° orientation), which was the lowest pressure tested. The staff suggests using the recommendation in NUREG/CR-6808 of 20 psi for calcium silicate.

2. Table 4-1 recommends a destruction pressure of 2.5 psi for blanketed and unjacketed Min-K, whereas the baseline Table 3-1 of the GR recommends a destruction pressure of 4 psi. Hence, these two recommendations are in conflict. The staff recommends using a destruction pressure of 2.5 psi for blanketed, unjacketed Min-K in the baseline, as well as in the refinements. The GR-recommended destruction pressure of 6 psi for blanketed, jacketed Min-K with stainless steel bands and latch and strike locks does not specify the jacket construction. Unless a specific jacket construction can be correlated to test data to demonstrate that a pressure of 6 psi or greater is needed to compromise that specific jacket, then the lower destruction pressure of 2.5 psi should be used.

3. It is noted that several data are missing from Table 4-1 that the analyst will require. For example, the material density for Min-K is specified as NA, but will be required when applying the GR-recommended NUREG/CR-6224 head-loss correlation.

4. The destruction pressure for Microtherm was apparently set equal to that of Min-K in Table 4-1, without justifying remarks. Some rationale should have been presented for this action.

5. For Knaupf, with an as-fabricated density of 2.4 lb/ft^3, Table 4-1 recommends a destruction pressure of 10 psi for Knaupf with an as-fabricated density of 4.0 or (blank), the GR does not recommend a destruction pressure. However, in Table 3-1 of the GR, one entry exists for Knaupf which recommends a destruction pressure of 10 psi alone. Because of the inconsistency, application of this guidance for Knaupf should be based on its as-fabricated density, as appropriate.

6. The destruction pressure recommended in Table 4-1 for Kaowool was made without justifying remarks or reference. Some rationale should have been presented for this assumption.

7. Table 4-1 specifies the as-fabricated density of Kaowool as 9.4 lbs/ft^3 which is given as a range of 3 to 12 lbs/ft^3 in baseline Table 3-2. If this density is a manufacturing variable, then the plant-specific, as-applied density should be used. As illustrated in Appendix V to this SE, the head-loss evaluation is very dependent upon this number.

8. The reference number provided for the material density of Kaowool is given as “xx,” which is not listed in the GR references section (i.e., Section 9), and should be corrected and/or provided.

9. Table 3-1 of the GR recommends the destruction pressure for Mirror® with Sure-Hold® bands as 150 psi; however, this item is missing from GR Table 4-1. Section 3.4.2 of this SE provides the staff’s evaluation of this value. The acceptable value provided in Table 3-2 of this SE should also be used, if applied as a refinement.

10. The destruction pressure recommended in Table 4-1 for silicone foam was made without justifying remarks or reference. Some rationale should have been presented for this assumption.

11. The destruction pressure recommended in Table 4-1 for gypsum board was made without justifying remarks or reference. Some rationale should have been presented for this assumption.

<u>Staff Conclusions Regarding Section 4.2.2.2</u>: The staff finds that use of debris-specific characteristics as a refinement to the baseline is acceptable. However, the cautions listed above should be considered in the use of this refinement and debris-specific data should be sought.

4.2.3 Latent Debris

Although the GR does not identify any generic analytical refinements for quantifying latent debris in this section, other methods the staff identified in Section 3.5 of this SE as acceptable alternatives for sampling plans could be viewed as refinements to a conservatively assumed baseline inventory.

4.2.4 Debris Transport

Section 4.2.4 of the GR recommends two methods of analytical refinements for determining the flow characteristics of the sump pool for the purpose of predicting the transport of debris in the sump pool to the recirculation sump screens. These methods include the open channel flow network method (Section 4.2.4.1) and the three-dimensional CFD method (Section 4.2.4.2). Aspects of the network method discussed included the following the analytical approach, model input development, and the network solution. An example network model was superimposed onto a corresponding CFD result. No discussion was provided regarding the use of network-predicted results to estimate debris transport within the sump pool. Aspects of the CFD method discussed included the selection of software, the building of a computer aided design model that could be used to generate the computational mesh, the CFD analysis, and the prediction of debris transport using the CFD results.

The debris transport discussion associated with the CFD modeling included a discussion of plotting velocity magnitude contours for the minimum bulk transport velocity at selected levels within the containment pool. After the area within this transport velocity contour is determined, the debris within this area is assumed to transport to the sump screen.

The GR also includes Table 4-2, “Debris Transport Reference Table,” which provides transport data, such as the minimum velocities needed to transport debris.

<u>Staff Evaluation of GR Section 4.2.4</u>: Of the two methods of analytical refinements for transport of debris in the sump pool, the staff identified the following challenges in using the open channel network method:

1. The implementation of the network method requires the adaptation of multiple correlations for estimating form-loss coefficients and friction factors (correlations typical of piping pressure-loss calculations). At each network node junction, a form-loss coefficient is required that simulates flow for the connecting nodes. The complexity of the sump pool channel will require the analyst to make engineering judgment adaptations for the application of generic

correlations. The complexity of the model input development can severely limit the detail of the model, resulting in a rather coarse nodalization.

The coarseness of the network method, as illustrated by the example nodalization in GR Figure 4-4, limits the simulation of important aspects of the sump pool, such as the complexity of the flow channel, obstacles to flow, and the complex distribution of containment spray drainage entering the pool. The example nodalization ignored portions of the sump pool without providing a rationale for determining which portions of the pool do not need to be modeled.

2. The model coarseness forces the analyst to rely on predicted bulk velocities between coarse nodes, and therefore the model cannot predict localized flow conditions that are capable of moving debris, even if the bulk flow velocities indicate no movement of debris. An example of localized flow is vortices that could be completely internal to a network node. Testing has shown that vortices affect debris transport (NUREG/CR-6773).

3. The network method is not capable of predicting sump-pool turbulence or its effects on debris transport. Sump-pool turbulence has been shown to affect debris suspension within the pool (e.g., water flows falling into the sump pool can suspend debris that would normally settle in calm water) and the rates of erosion (Section III.3.3.3) for certain types of debris (e.g., fiberglass insulation debris).

4. The network method is not capable of predicting pool characteristics during pool formation that affect the transport of debris during this period, such as the initial spreading of water across the floor or the filling of inactive portions of the sump (e.g., reactor cavity).

5. The large number of input parameters associated with specifying a network nodalization model (e.g., inputs to form-loss correlations) could make the performance of a quality sensitivity evaluation for those input values difficult.

Appendix C to the GR compares the results of the open channel network method to the results of the CFD method. The staff concluded that the results do not agree; this is in contrast to the assertion in the GR that the network and CFD results compare favorably. The difference in flow rates of less than 10 percent was calculated by dividing by the total recirculation flow. For example, the GR-quoted error for Channel 156 is 7.7 percent (Table C-1), but the flow for the network method is in the opposite direction to that of the CFD analyses. If the difference for Channel 156 were calculated as the difference between the network and the CFD-predicted flow rates divided by the CFD the result would have been 56 percent instead of 7.7 percent. In addition, the flows of the network and CFD methods are in the opposite direction.

The GR recommends adding 10 percent to the calculated channel flow rates, but the staff recommends that the safety factor applied to the network calculated results be based on benchmark analyses of the network methodology against experimental debris transport results and/or superior analytical methods. In addition, a method is still needed to perform the required analysis that is well beyond the capabilities of the network method.

Regulatory Position 1.3.3.4 of RG 1.82, Revision 3, states the following:

> An acceptable analytical approach to predict debris transport within the sump pool is to use computational fluid dynamics (CFD) simulations in combination with the experimental debris transport data. Examples of this approach are provided in NUREG/CR-6772 and NUREG/CR-6773. Alternative methods for debris transport analyses are also acceptable, provided they are supported by adequate validation of analytical techniques using experimental data to ensure that the debris transport estimates are conservative with respect to the quantities and types of debris transported to the sump screen.

Consistent with the above regulatory position, the staff accepts the nodal network method as an alternative method to calculate debris transport onto the sump screens. However, the licensees should support this method using experimental data to ensure that their estimates are conservative with respect to the quantities and types of debris transported to the sump screen.

The staff finds that the GR discussion regarding the CFD method and analysis is thorough. Specific staff comments include the following:

1. The GR suggests using turbulent turbine kinetic energy (TKE) profiles in the pool as a pool characteristic, but fails to prescribe how this information would be useful in the debris-transport analysis. The staff recommends a potential adaptation of a CFD method employed in the BWR drywell debris-transport study (NUREG/CR-6369, Vol. 3) in which the CFD code is also used to simulate applicable tests with debris settling correlated to the CFD predicted turbulence indicators.
2. The GR discussions regarding the level of detail or analytical fineness to the model does not adequately address potential plant features that can significantly affect sump-pool hydraulics. For example, the GR statement that, “obstructions less than 6 inches in diameter or the equivalent may be omitted,” is too general a statement. If there is a single 6–in. obstacle, it might be argued that it can be neglected, but if there is a series or array of 6–in. objects, then the array may need to be modeled.
3. Other model development aspects should be properly assessed before selecting modeling options, including the type and size of calculational mesh, boundary conditions inflow and outflow options, and convergence criteria. Many of the modeling options depend upon the CFD code selected, and the model development should properly select the best options for the plant-specific sump-pool evaluation.

The GR recommends using a uniform distribution of debris on the sump floor (i.e., the sump pool debris transport fraction is equal to the floor area fraction where the velocity is greater than the minimum transport velocity. (See GR Section 4.2.4.2.5.)) This recommendation is not acceptable because the debris entrance into the pool is not uniform. The staff provided supplemental guidance in Appendices III and VI to this SE addressing sump pool debris transport and blowdown/washdown transport, respectively, in the volunteer plant. Appendix III demonstrates that the GR floor area transport model would under-predict the sump pool debris transport in the volunteer plant by a wide margin. Debris initially deposited onto the sump floor in the volunteer plant was preferentially deposited within or near the break compartment because of the partial confinement of debris in the break compartment, and debris initially deposited in the upper levels of the containment would wash down with the drainage of the containment sprays entering the sump pool at discrete locations, typically in the faster areas of the pool. Licensees should use the debris transport methodologies presented in Appendices III and IV for refined analyses.

In the GR baseline, a two-group size distribution was recommended in which the small fines would completely transport to the sump screens and the large debris would not transport at all. Therefore, the sump pool debris transport refinement cannot be applied to small fines because at least a portion of this group must be treated as suspended fines with complete transport. A refinement can be applied to the large size group, but in the baseline guidance this group is assumed not to be transportable. In order to proceed with a sump pool analytical refinement, a better-defined size distribution that addresses the key aspects of debris transport should be used. In addition, if the analytical refinement is applied to the small debris, it should also be applied to the large debris that is neglected in the baseline methodology. The licensee should use the four size categories used in both Appendices III and VI to this SE for fibrous debris. This size distribution has (1) fines that remain suspended, (2) small piece debris that are transported along the pool floor, (3) large piece debris with the insulation exposed to potential erosion, and (4) large debris with the insulation still protected by a covering, thereby preventing further erosion.

Also, for the situation where coatings debris are assumed to be larger than the basic material constituent size due to the substantiation of no thin bed at the sump screen, and instead sized as chips or flakes; licensees may choose to justify a transport factor of less than 100 percent for those chips or flakes based on experimental data or analysis.

GR Table 4-2 provides useful data and references NRC-published documents as the source of the data. However, one column in the table provides selected values for TKEs required to suspend debris that are not in the referenced NRC-published documents. The staff has not assessed or accepted the TKE values presented in GR Table 4-2.

Staff Conclusions Regarding GR Section 4.2.4: GR Section 4.2.4 recommends the open channel flow network method and the three-dimensional CFD method for refining the analysis for transport of debris in the sump pool to the recirculation sump screens. Consistent with RG 1.82, Revision 3, the staff accepts (1) the CFD method, and (2) the nodal network method as an alternative method to calculate debris transport onto the sump screens. However, the licensees using the nodal network method should support it with experimental data to ensure that the debris transport estimates are conservative with respect to the quantities and types of debris transported to the sump screen. The GR-recommended debris transport model in Section 4.2.4, which assumes a uniform distribution of debris across the sump floor, is not acceptable because the debris entrance into the pool is not uniform. Appendices III and VI to this SE provide additional staff guidance on adapting the debris transport methodologies for refined analyses.

4.2.5 Head Loss

The GR states that no head-loss refinements are offered other than those given in Section 3.7.2.3.2.3. (See SE Section 3.7.2.3.2.3, “Thin Fibrous Beds,” for the staff evaluation of this section of the GR.) The supporting Appendix E repeats the text found in Section 4.2.5, and provides tables that summarize available domestic and international head-loss testing and results.

Staff Evaluation of GR Section 4.2.5: The staff did not identify any specific analytical refinements offered in Section 4.2.5 or Appendix E. Therefore, no evaluation is provided for analytical refinements to the head-loss analysis.

5.0 DESIGN AND ADMINISTRATIVE CONTROL REFINEMENTS

Industry representatives including the NEI, the Westinghouse Owners Group, and various participants from individual utilities have followed the development, research, and resolution process of GSI-191 for several years. Over this time, practical insights have been gained by the participants regarding the relative importance of each stage of the accident sequence to the overall assessment of recirculation sump vulnerability. This section addresses the phenomenology associated with debris generation, debris transport, debris accumulation, and head loss across beds of mixed composition. As the knowledge base of research data and plant survey information has improved, and as analytic methods have developed to address each aspect of the complex accident sequence, so too has the awareness of potential vulnerabilities grown. Recognition and understanding of the principal contributors to sump-screen vulnerabilities has initiated a discussion about possible mitigation strategies that seek to interdict the accident progression at one or more of the aforementioned stages.

Self assessment of recirculation sump vulnerability and the identification of site-specific contributing factors is a responsibility of each licensee, but this section attempts to share the broader industry perspective on possible improvements that a licensee can make to improve its sump performance posture, regardless of the current plant condition.

Based on the findings of individual licensees, the range of mitigative actions pursued across the industry may range from status quo operation to sump-screen replacement. In many cases, though, new awareness of the issues involved with ensuring sump-screen performance will lead to at least procedural changes that help avoid unnecessary exposure to the risk of sump-screen blockage. With improved understanding of a problem comes a new perspective of common sense regarding the simple things that can be done to improve safety, as well as the detailed knowledge required to affect engineered solutions to a specific technical problem. This section provides insights at both levels. This discussion may be sufficient for a given licensee to address any identified problems. For others it may motivate progress towards a site-specific solution of their own devising. However, successful management of sump-screen vulnerability may require a combination of the approaches presented in this section.

Given the diversity of possible responses to this issue and the variety of site-specific solutions that will be developed at varying degrees of complexity, the NRC cannot endorse any one mitigation strategy that is offered here at this time. Assessments of relative effectiveness expressed in the GR are the opinion of the industry representatives. The staff believes that this information improves the practicality of the GR because licensees are immediately motivated to find workable solutions to any problems that are identified during their vulnerability assessments. Any necessary changes to plant configuration, technical specifications, operating procedures, or other licensing basis changes should still consider the need for NRC staff review and approval. Licensees should consider existing regulatory processes, and if necessary, submit any required information for staff review. An important aspect of the existing review process is the need for applicable testing and analysis of any new equipment or materials that are incorporated into the ultimate resolution strategy. In this manner, the NRC can judge the effectiveness of the approaches chosen by each licensee. For these reasons, the staff's review of Section 5 of the GR is limited. The staff found the technical descriptions in this section to be acceptable as an introduction to the topic of mitigating sump-screen vulnerabilities.

5.1 DEBRIS SOURCE TERM

This section examines five categories for design and operational refinements. Staff comments on each category are summarized below.

1. **Housekeeping and FME Programs:** The GR recommends that if housekeeping or FME programs are implemented or revised to reduce the latent/miscellaneous debris burden, then appropriate procedures should be designed to ensure a high level of performance. The staff wishes to emphasize that such procedures and performance metrics, based on swipe sample analyses, for example, should be used if vulnerability assessments rely on periodic cleaning activities to maintain debris loadings below some minimum level of concern.

2. **Change-Out of Insulation:** The staff notes two items in addition to those identified in the GR. First, while change-out of problematic insulation types may address the issue of maximum debris loadings on the screen, it might not address the issue of minimum loadings required to form a thin filtration bed. To satisfy both concerns, a combination of strategies in addition to change–out, might be needed. Second, the large-scale removal of some insulation types may inadvertently increase the latent debris loading of residual insulation materials, unless removal is performed carefully to minimize the spread of fine materials or effective plant cleaning routines are implemented after insulation removal to recover dispersed material.

3. **Modify Existing Insulation:** This action may effectively address the issue of maximum debris loads on the screen without changing the minimum loadings required to form a thin filtration bed. To satisfy both concerns, a combination of strategies, in addition to a modification of existing insulation, may be necessary.

4. **Modify Other Equipment or Systems:** The staff agrees that changes to non-insulation items should be considered in the context of the entire sump performance evaluation. Discussion of latent debris surveys that identify unique collections of particulate or fibrous material, such as filter housings that are vulnerable to water infiltration, suggested another example of beneficial change to equipment. If such sources can be sealed or protected from containment spray, then the internal inventory will not be released to the sump pool.

5. **Modify or Improve Coatings Program:** Under the conservative assumption that 100 percent of unqualified coatings will fail, the staff agrees that conversion to DBA-qualified systems would reduce the source term contributed by failed coatings. Additionally, the staff does not agree with the statement that DBA-qualified coatings have very high destruction pressures. This statement has not been proven for the simultaneous combination of high-temperature and high-pressure jet impingement. See Sections 3.4.4 and 4.2.2.2.3 for more discussion on acceptable coatings destruction pressures.

5.2 DEBRIS TRANSPORT OBSTRUCTIONS

This section examines various options for redirecting or retarding the movement of debris towards the sump screen. The objective of these approaches is to trap or sequester debris so that it cannot reach the sump screen during recirculation. Transport velocities are highest during pool fill-up when sheeting velocities can move large pieces of debris that are initially impacted on the floor near the break or washed to the floor by the break effluent. During this timeframe, flow direction is not preferentially towards the sump. As the containment pool fills, sheeting velocities decrease. With the onset of recirculation flow, debris transport with a preferential direction aligned towards the sump screen is established. Design of obstructions to provide a barrier to debris transport to the sump screens should consider all phases of pool fill and establishment of recirculation flow.

5.2.1 Floor Obstruction Design Considerations

Careful thought must be given to the stability of the holding location with respect to turbulence introduced by cascading containment spray water. For example, if diversion baffles successfully collect debris during fill-up in a drainage zone that is highly agitated by falling water, the net result may be to increase the fraction of individual fibers and fine material available for transport to the screen under low recirculation velocities. During initial fill-up, curbs may be subjected to significant flow velocities, so heights would need to be designed accordingly in order to be effective. Removable structures, such as debris rakes and baffles, may also experience significant hydrodynamic force loadings during fill-up. The test data cited from GR Reference 54 for the effectiveness of curbs are very rudimentary. Significant opportunity exists for optimizing curb designs to accomplish the complementary objectives of debris capture and/or debris diversion.

5.2.1.1 Test Results

During pool fill-up, flow directions are dictated by the location of the break and the containment geometry. During recirculation, there is a directed flowpath towards the sump screens, but perhaps at lower bulk velocities. None of the data apply to turbulence induced from direct water splashing near the curbing. It is noted that curbs could be an especially important strategy for protecting horizontal sump screens from debris buildup while the sump cavity is filling. To effectively design curbing, a reasonable detailed understanding of water velocity and direction is needed during the phase of transport for which the curbs are intended to be effective. The staff also notes that while curbing may be effective at impeding the migration of larger debris along the floor, curbs do not address the problem of suspended fines. Thus, the overall effectiveness of curbing and debris racks (next section) will depend on the site-specific debris types that they were designed to mitigate.

5.2.2 Debris Obstruction Rack Design Considerations

There is ample room for optimization of rack designs for trapping debris before it reaches the sump screen. One conceptual design that has been discussed involves two or more parallel racks placed across the flowpath to act as weirs over which the water must flow while depositing larger debris in the spaces between the racks. For this to be effective, the mesh size and height of the baffles would need to be optimized for the size of the debris and the depth of the pool to prevent obstruction of water flow. This design concept of interstitial capture between vertical risers might also be incorporated directly into a multilayered suction strainer in which the outer layers serve initially to attract and capture debris, leaving the inner layers clear to provide adequate water flow.

5.2.2.1 Test Results

The test results cited from GR Reference 55 focus on tumbling and sliding of debris along the floor. During pool fill, water velocities could be much higher than the incipient velocities listed in GR Table 5-1. The use of racks may effectively manage larger debris items moving along the floor, but would not stop the migration of individual suspended fines.

5.2.2.2 Debris Rack Grating Size

In this section, the GR emphasizes several of the design considerations mentioned above in Section 5.2.2 of this SE.

5.3 SCREEN MODIFICATION

Staff Evaluation of GR Section 5.3: This section of the GR provides guidance regarding potential sump screen designs and features.

The relative effectiveness of curbs and debris racks depends on the characteristics of the debris that challenge the sump screen. While these design features may be effective at preventing the migration of large volumes of debris along the floor, they may not be effective at preventing transport of suspended fines. Therefore, depending on the dominant debris types at a site, licensees could determine that it may be more cost effective to modify screen configurations to manage the entire range of debris size. The GR considers the attributes of three generic design approaches that licensees might pursue. These include passive strainers, backwash strainers, and active strainers.

The staff emphasizes two performance objectives that should be addressed by a sump-screen design. First, the design should accommodate the maximum volume of debris that is predicted to arrive at the screen, given full consideration of debris generation, containment transport, and auxiliary mitigation systems, such as curbing, that may be in place. Second, the design should address the possibility of thin-bed formation. When fibrous debris is expected, the screen should accommodate a large fraction of the expected fines (both from the ZOI and from potential pool degradation) as individual fibers with the potential to form a uniform layer. The difference between these objectives relates to the degree of uncertainty in debris transport methodology that the screen design should accommodate. While it is difficult to argue that debris will not be transported (first objective), it is equally difficult to demonstrate that it will be transported (second objective). Thus, both extremes should be satisfied by the screen design.

5.3.1 Considerations for Passive Strainer Designs

The large appeal of passive strainers relates to the simplicity of their maintenance and their high reliability for an adequately tested design, both important considerations for safety-related equipment. While the GR accurately presents the general attributes of existing passive designs, the presentation is focused on applications of one-dimensional head-loss correlations that have traditionally led to large strainer designs. Water velocity through the debris bed is an important factor in predicting head loss, so larger surface areas imply lower velocity for a given recirculation flow, and hence, lower head-loss. The challenge with this approach is to achieve a large surface-to-volume ratio by using a convoluted screen geometry that traps debris, while providing adequate recirculation flow without taking up too much space in containment.

Given the requirement in some plants to address thin-bed formation for potentially large amounts of fine fibrous debris, large surface areas alone may not be sufficient. Two alternative design concepts may be effective, perhaps in combination with compact geometries that achieve large surface-to-volume ratios. Generically, these design concepts may be described as disrupting the formation of a uniform fiber layer by (1) using a complex porous filter structure to capture fiber, or (2) designing hydraulic flow paths that amplify velocity gradients across the flat surfaces of the strainer where fiber first approaches.

The first design concept can be imagined as a prefilter, made perhaps of crumpled wire net (approximately 1-in. mesh) or similar material that creates a very porous volumetric filter on the face of a standard sump screen for the purpose of capturing fibers with minimal head loss. Porosity and thickness of the prefilter section would require design optimization to accommodate a specific quantity and size of suspended fiber debris. The second concept utilizes small friction losses internal to the body of a convoluted filter structure that has many fins, fingers, plates, or other protuberances on which to capture debris. Small internal friction losses can be enhanced and designed to create velocity gradients across the external surfaces of the filter. If properly designed, this feature might be effective at directing the buildup of fiber in a controlled way that avoids uniform simultaneous coverage of the strainer face. This might be used to efficiently pack material on an essentially sacrificial surface while leaving other flow areas unobstructed. These concepts, and other innovations, share a common need for adequate design testing, but they may offer effective solutions to the drawbacks of large passive strainers presented in the GR.

5.3.2 Considerations for a Backwash Strainer Design

In addition to the practical considerations for a backwash strainer design offered in the GR, the NRC staff observed the following. The staff agrees that backwash systems may need to undergo design testing and possible surveillance testing to demonstrate that they will work as intended.

1. Any design that attempts to clear an existing debris blockage should give careful consideration to the problem of resuspension and redeposition of that debris. If the working fluid is applied too violently, a cloud of debris may temporarily disperse and then reform a bed on the screen. Testing may show that this is acceptable behavior that reduces the screen loading enough to be effective regardless of bed reformation.
2. The GR suggests implicitly that normal recirculation flow will be stopped during backflushing. This may raise concerns about the restart reliability of the ECCS system. Some backflush designs might be able to operate effectively without interrupting ECCS flow. For example, a continuous water-jet curtain directed across the face of the screen might be effective at preventing debris buildup to unacceptable levels. This water flow might be provided as a side stream from

the main ECCS system so that no additional pumps, actuators, or valves need be qualified.

3. Debris beds, especially fiber-based mats, are effective filters of suspended particulate. If the entire debris mat is disturbed very quickly, the local concentration of material that can pass through the screen is suddenly very high. This may represent a unique challenge to downstream components that is not present during normal recirculation flow.

4. Most debris beds studied to date are held to the screen only by the pressure of the water flowing through them. They form no particular adhesive or mechanical attachment to the screen. Fibrous beds have been observed to slump or slough off of the screen in contiguous mats. For designs in which ECCS flow is interrupted, this behavior presents an opportunity for collecting or trapping the debris that loosens from the screen without dispersing it greatly. Debris racks, or bins, might be designed to sequester the debris mats and minimize redeposition. Minimum-flow backflush systems, in combination with inclined screens that provide gravity assist for the detachment, might benefit the most from this behavior.

5. Item 5 in the GR suggests automated control systems to actuate the backwash cycle based on measurement of pressure drop or flow. For backwash systems that function intermittently upon actuation, some degree of information feedback and/or intervention might be given to operators to increase the flexibility and utility of the backflush system as a recovery alternative for potential sump blockage.

5.3.3 Considerations for an Active Strainer Design

Active strainer concepts offer much greater design flexibility for addressing the challenges of debris accumulation in PWR recirculation pools. Therefore, they offer some unique advantages over the other two generic screen designs. The GR presents several such advantages as favorable technical considerations. One contradiction that the staff would point out relates to favorable technical consideration number 3, which offers the opinion that self-cleaning strainers may avoid uncertainties related to various debris generation and transport phenomenology. However, the same active strainer features that indicate success for some phenomena might also exacerbate problems for other phenomena. As an example, adhesive chemical corrosion byproducts might be smeared into a semi-impervious layer across the sump-screen mesh by a scraping device whereas the same debris might be dislodged by an optimized backflush system.

Active designs can carry a greater burden of proof for effectiveness and operability depending on their complexity, and the staff agrees with additional consideration number 1 that experimental studies would be needed to demonstrate the effectiveness of proposed active strainer designs. In general, many of the considerations for an active strainer design like power supply, control system reliability, and functional reliability are similar to those presented in the GR for backwash systems.[1] Many of the staff observations are also similar. For example, active strainers may be most effective when

[1] In fact, after correcting a typographical error near the end, item 6 should read, “Margin must be available to initiate *active strainer mode* before sump blockage affects either ECC or CS operation.”

combined with mechanisms for debris collection and sequestration that over time reduce the local suspended debris concentration that poses a challenge to the strainer surface.

To maintain the generality of this discussion, the NRC prefers the terminology “active strainer” over the description of “self cleaning.” The GR accurately defines an active strainer as a design that incorporates active components to maintain flow to the sump, but there the generality of the presentation ends and discussions of self-cleaning mechanisms begin. Because there are no active strainer applications for either BWR suppression pools or PWR sumps, there should be no preconceptions imposed regarding typical active designs. Similarly, while continuous cleaning of the strainer surface area might be one desirable performance metric of an active design, it is not the only method of maintaining flow to the sump.

Another class of design solutions exists that periodically clean the strainer surface, rather than continuously cleaning the surface. An example of such a design is a set of flat, parallel, inclined sump screens that are latched at the top corners and hinged at the bottom corners. When the outer face is loaded with debris, the latches are released and the screen swings to the floor, exposing a fresh screen for debris collection and trapping its debris inventory from further transport. Other methods may be developed using gravity-assisted debris detachment on downward inclined screen surfaces. Internal flows could be alternately switched between separate chambers of the strainer to permit detachment on one side while drawing flow from the other side. Flow baffles might be switched with actuation mechanisms and control logic systems or by simple rotation of a spindle based on hydraulic flow imbalance between the chambers. The success or failure of any innovative design concept depends on how completely it can satisfy the additional considerations presented in the GR, but once the commitment has been made to facing these design challenges, no restrictions should be placed on the options available for a successful plant-specific solution.

5.3.4 Summary

In combination with staff comments provided in this SE, the NRC finds this section of the GR to be a useful and acceptable introduction to the variations in sump-screen design that an individual licensee may pursue for sump modification. The exact definitions of the generic categories and the particular label given to an innovative design are not as important as the generic attributes defined in the GR. These attributes serve as a basis for comparing the technical challenges and benefits, and the potential programmatic costs of alternative design solutions. Any consideration of screen modifications should be made in the context of the comprehensive site-specific vulnerability assessment. Alternative combinations of source mitigation, design changes, and administrative control should be weighed against existing debris types, containment geometry constraints, and NPSH margins.

6.0 ALTERNATE EVALUATION

6.1 BACKGROUND AND OVERVIEW

Section 6 of the GR describes an alternate evaluation methodology for demonstrating acceptable containment sump performance. Option B in Figure 2-1 of the GR depicts the alternate evaluation methodology described in this section.

For the last several years, the NRC has recognized that probabilistic risk assessment (PRA) has evolved to the point that it can be used increasingly as a tool in regulatory decision making. Through its policy statement on PRA (ADAMS Accession No. ML021980535), the Commission expressed its expectation that enhanced use of PRAs will improve the regulatory process through (1) safety decision making enhanced by the use of PRA insights, (2) more efficient use of agency resources, and (3) a reduction in unnecessary burdens on the licensees.

The NRC staff has considered the development of risk-informed approaches to the technical requirements specified in 10 CFR 50.46, and these considerations are documented in numerous communications between the Commission and the staff (SECY and SRM). The NRC Commissioners, in their March 31, 2003, SRM, directed the staff to undertake several rulemakings, one of which would develop a proposed rule to allow, as a voluntary alternative, a redefinition of the design-basis LOCA break size. In a March 4, 2004, letter to NEI (SB, 2004), the staff stated that it would discuss, in public meetings, the use of current or planned work to risk-inform 10 CFR 50.46 as a suitable technical basis for defining a spectrum of break sizes for debris generation and containment sump strainer performance.

Specific to GSI-191, the Commission recently requested the staff to, “implement an aggressive, realistic plan to achieve resolution and implementation of actions related to PWR ECCS sump concerns.” One such resolution path involves the LOCA break size used in PWR sump analyses. For example, it is well understood that the amount of debris generation to be expected following a LOCA is dependent on the break size, and generally that less debris would be generated with a smaller LOCA break size (although less debris generation may be worse in certain situations when considering debris type and break location). The staff is already working to risk-inform 10 CFR 50.46 to redefine the design-basis LBLOCA break size based on expected LOCA frequencies. A comparable approach for use in GSI-191 resolution would identify a debris generation break size (DGBS) which would be used to distinguish between customary and realistic design-basis analyses. However, it is very important to note that an alternative approach for resolving GSI-191 would not redefine the design-basis LOCA break size in advance of the 10 CFR 50.46 rulemaking effort. In developing an alternate approach for resolving GSI-191, the staff intends to remain at least as conservative as, and consistent with, any forthcoming revision to 10 CFR 50.46.

On May 25, June 17, and June 29, 2004, the staff met with NEI, industry representatives, and stakeholders in category 2 meetings to discuss alternate, realistic, and risk-informed approaches for resolution of the PWR sump issue. Throughout these meetings, both NRC and NEI staff presented proposals and positions regarding the technical and regulatory elements of alternative approaches.

These interactions between the staff, NEI, industry representatives, and stakeholders yielded an alternative approach which includes both realistic and risk-informed elements. For such an approach, licensees would continue to perform design–basis, long-term cooling evaluations and satisfy design-basis criteria for all LOCA break sizes up to a new DGBS that would be smaller than a double-ended guillotine break (DEGB) of the largest pipe in the RCS. This analysis space is referred to as Region I in the GR. Long-term cooling must be assured for breaks between the new DGBS and the double-ended rupture of the largest pipe in the RCS, but the evaluation may be more realistic than a customary design-basis evaluation, consistent with the small likelihood of the break occurring. For breaks larger than the DGBS, licensees could apply more realistic models and assumptions. This analysis space is referred to as Region II in the GR. Additionally, any physical modifications to plant equipment, or operator actions credited to demonstrate mitigative capability for these larger breaks (Region II) would not necessarily need to be safety related or single-failure proof. Changes to the existing facility designs, and credit for operator actions would include risk evaluations consistent with RG 1.174. Licensees should ensure that the changes to the facility design would have sufficient reliability to provide reasonable assurance that they will perform their intended function.

While not a component of the 10 CFR 50.46 ECCS evaluation model, the calculation of sump performance is necessary to determine if the sump and the residual heat removal system are configured properly to provide enough flow to ensure long-term cooling, which is an acceptance criterion of 10 CFR 50.46. Therefore, the staff considers the modeling of sump performance as the validation of assumptions made in the ECCS evaluation model. Since the modeling of sump performance is a boundary calculation for the ECCS evaluation model, and acceptable sump performance is necessary for demonstrating long-term core cooling capability (10 CFR 50.46(b)(5)), the requirements of 10 CFR 50.46 are applicable. Based on this, such an alternative approach might require plant-specific license amendment requests or exemption requests from the regulations, depending on each licensee’s chosen resolution approach. Licensees could request, on a plant-specific basis, exemptions from the requirements associated with demonstrating long-term core cooling capability (10 CFR 50.46(b)(5)). For example, exemptions from the requirements of 10 CFR 50.46(d) may be required if a licensee chooses to classify new equipment as nonsafety related or not single-failure proof. For purposes of resolving GSI-191, exemption requests would not be applicable to the other acceptance criteria of 10 CFR 50.46 (peak cladding temperature, maximum cladding oxidation, maximum hydrogen generation, and coolable geometry), and would be submitted in accordance with existing NRC regulations (10 CFR 50.12). Additionally, changes in analytical methodology or assumptions may also require license amendment requests. Licensees would assess the need for license amendment requests in accordance with the requirements of 10 CFR 50.59.

The NRC staff review and acceptance of such plant-specific license amendment or exemption requests would consider the following elements:

- application of the principles of RG 1.174, ”An Approach for Using Probabilistic Risk Assessment in Risk-Informed Decisions On Plant-Specific Changes to the Licensing Basis,” (e.g., defense-in-depth, safety margins, delta (CDF), delta large early release fraction)

- consistency with SRP Section 19, ”Use of Probabilistic Risk Assessment in Plant-Specific, Risk-Informed Decisionmaking: General Guidance”
- design-basis, deterministic analyses necessary to verify compliance with 10 CFR 50.46(b)(5) for break sizes up through “debris generation” break size
- acceptable mitigative capability up through the DEGB of the largest pipe in the RCS equipment needed for mitigative capability would have some functional reliability requirements, but would not necessarily need to be safety-related or single failure proof

One key element of RG 1.174 involves assurance that defense-in-depth is maintained. Although a DGBS is selected to distinguish between customary and more realistic design-basis analyses, the staff would require that licensees demonstrate acceptable mitigative capability for LOCA break sizes up through the DEGB of the largest pipe in the RCS. This philosophy is consistent with 10 CFR 50.46 (b)(5) and recent recommendations made by the Advisory Committee on Reactor Safeguards (ACRS) in its April 27, 2004, letter to the Chairman. Requiring that mitigative capability be maintained in a realistic and risk-informed evaluation of the PWR sump issue for all LOCA break sizes up through a DEGB of the largest RCS piping ensures that defense-in-depth is maintained.

6.2 ALTERNATE BREAK SIZE

The GR methodology provides the following definition for the alternate break size to be applied for an alternate evaluation of sump performance:

- a complete guillotine break of the largest line connected to the RCS loop piping
- for main-loop piping, a break size assumed to be equivalent to a guillotine break of a 14-in. schedule 160 line, and equating to an effective break area of 196.6 square inches (assuming both sides of the break are pressurized)

In defining these break sizes, the alternate break size to be considered by each licensee for lines connected to the main-loop piping is plant dependent, while the alternate break size to be applied to the main-loop piping is identical for each licensee.

The GR also provides guidance for determining whether a DEGB needs to be considered in attached piping. If sufficient energy for debris generation exists on both sides of the break, a DEGB will be used. The GR criteria for determining whether sufficient energy exists are based on the postulated break distance from a normally closed isolation valve and include the following:

- 10 pipe inside diameters for large-bore piping (i.e., greater than a 2 in. diameter)
- 20 pipe diameters for small-bore piping

If a normally closed isolation valve exists within this number of pipe diameters, then a licensee need only consider a single-ended break. These GR criteria are based on the low stored energy in the pipe section between the break and isolation valve with respect to significant debris generation.

Additionally, the GR provides guidance for consideration of the ongoing 10 CFR 50.46 rulemaking effort. The GR states that, "In using this GSI-191 alternate break size, it is recognized that when the 50.46 rule is finalized, licensees can re-perform the sump performance evaluations with the final break size specified in 50.46 and modify the plant design and operation. This would assure coherence in the implementation of 50.46."

Staff Evaluation of GR Section 6.2: The staff has reviewed the alternate break size proposals as described in the GR and finds them to be acceptable.

The DGBS to distinguish between customary and more realistic design basis analyses is as follows:

1. For all ASME Code Class 1 PWR auxiliary piping (attached to RCS main loop piping) up to and including a DEGB of any of these lines, the design-basis rules apply.
2. For RCS main-loop piping (hot, cold, and crossover piping) up to a size equivalent to the area of a DEGB of a 14 in. schedule 160 pipe (approximately 196.6 square inches), the design-basis rules apply.
3. For breaks in the RCS main-loop piping (hot, cold, and crossover piping) greater than the above size (approximately 196.6 square inches), and up to the DEGB, licensees must demonstrate mitigative capability, but design-basis rules may not necessarily apply.

Several factors comprise the technical basis for the staff's acceptance of the division of the pipe break spectrum for the purpose of evaluating debris generation. First, the staff considered recent information developed by the NRC's Office of Nuclear Regulatory Research (RES) regarding the frequency of RCS ruptures of various sizes. The RES developed this information through an expert elicitation process, as documented in SECY-04-0060, "Loss-of-Coolant Accident Break Frequencies for the Option III Risk-Informed Reevaluation of 10 CFR 50.46, Appendix K to 10 CFR Part 50, and General Design Criteria (GDC) 35." The RES study determined the frequency of primary pressure boundary failures under normal operational loading and transients. Although the results of the expert elicitation are not yet final, the preliminary results support the observation that the probability of a PWR primary-piping system rupture is generally very low and that the break frequency decreases with increasing piping diameter. The selection of a break size equivalent to the area of a DEGB of a 14 in. schedule 160 pipe for RCS main loop piping is consistent with the attached auxiliary piping sizes in PWRs, and is also consistent with the ongoing 10 CFR 50.46 rulemaking direction (at this time).

The staff also considered the fact that there is a substantial difference from a deterministic, "margins to failure" or "flaw tolerance" perspective between 30-in.to 42–in. diameter PWR main coolant loop piping and the next largest ASME Code Class 1 attached auxiliary piping (generally the 12-in. to 14–in. diameter pressurizer surge line). This difference is evident, for example, in leak before break (LBB) evaluations conducted in accordance with NUREG-1061, Volume 3, "Report of the U.S. Nuclear Regulatory Commission Piping Review Committee," wherein main coolant loop piping characteristically passes an LBB evaluation more easily than ASME Code Class 1 auxiliary piping systems. Finally, the staff considered the fact that certain ASME Code

Class 1 auxiliary piping systems may be more susceptible to failure as a result of environmental conditions which are conducive to known degradation mechanisms and/or loading conditions which routinely apply significant stresses to the piping system. An example of both of these considerations would be a typical PWR pressurizer surge line in which Alloy 82/182 dissimilar metal welds are subjected to a high-temperature operating environment known to abet primary water stress-corrosion cracking and which is subjected to significant bending loads during startup/shutdown conditions because of the large temperature gradient between the pressurizer and the hot leg of the main coolant loop.

Based upon the considerations noted above, the staff has determined that the division of the pipe break spectrum proposed for the purpose of evaluating debris generation is acceptable based on operating experience, application of sound engineering judgment, and consideration of risk-informed principles. Licensees using the methods described in Section 6 of the GR can apply the defined DGBS for distinguishing between Region I and Region II analyses.

The staff has reviewed the GR guidance provided regarding the need to consider a DEGB in attached auxiliary piping. The GR provides criteria based on the number of pipe diameters, pipe size, and distance to a normally closed isolation valve for determining if sufficient energy for debris generation exists on both sides of the break. If a normally closed isolation valve exists within a specified number of pipe diameters from a postulated break location, than only a single-ended break needs to be considered. The GR does not provide a technical basis for this criterion. To assess the acceptability of this proposal, the staff considered the fluid volumes available on each side of a DEGB which would fall within the criteria provided in the guidance. Considering that a break occurs at the maximum distance from a normally closed isolation valve, as allowed by the proposed criteria, the staff agrees that there would be an insignificant amount of energy available for destruction from the isolated side of the break when compared to the fluid volume and energy available on the unisolated side of the break. For example, in the case of a DEGB of a 1–ft. diameter auxiliary pipe with a normally closed isolation valve 10 inside pipe diameters away, the fluid volume in the isolated piping portion is less than 10 cubic feet. This fluid volume is insignificant when compared to the RCS fluid volume, which is on the order of 10,000 cubic feet. The fluid and energy blowdown from the isolated side of the break will depressurize and void almost instantaneously, while the blowdown from the RCS side of the break would be significantly larger, on the order of minutes (the staff verified this through a simplified RELAP calculation). Based on this, and considering engineering judgment, the staff finds that the criteria proposed by NEI for evaluating whether a DEGB should be considered in auxiliary piping is acceptable. The staff's engineering judgment takes into consideration that (1) past experiments and analyses have confirmed that debris generation caused by initial blast impulse (which would be from both sides of the postulated break) would be minimal, and (2) that debris generation is dominated by jet loading and/or jet erosion. As confirmed by the staff's estimate, blowdown jet impacts would be dominated by the blowdown from the RCS side of the break.
The staff also considered the GR guidance regarding consideration of the ongoing 10 CFR 50.46 rulemaking effort. The staff agrees with the recommended guidance that licensees may re-perform the sump performance evaluations using the final break size specified in the rulemaking and modify the plant design and operation accordingly. This would assure consistency with the new requirements of 10 CFR 50.46. The staff

expects that the DGBS specified in this section will bound the transition break size specified by these new requirements.

6.3 REGION I ANALYSIS

The Region I analysis of recirculation sump performance includes evaluation of all break sizes up to and including the DGBS defined in Section 6.2. The majority of the analyses to be performed for the Region I break sizes are to be conducted in the manner described in Sections 3, 4, and 5 of the GR. For Region I breaks, the GR states that a full range of break locations will be assessed to determine the limiting location considering both debris generation and debris transport. However, as discussed in Section 6.3.2, the GR refers to a Section 4 refinement proposing that BTP MEB 3-1 may be used to limit the break locations considered. Additionally, any design–basis, secondary-side breaks (main steamline break, feedwater line break, etc.) which rely on sump recirculation will be analyzed in accordance with the Region I analyses.

With respect to break configuration, circumferential breaks will be assumed to result in pipe severance and separation amounting to at least 1-diameter lateral displacement of the ruptured piping sections, unless physically limited by piping restraints and supports, or other plant structural members that can be shown through analysis to limit pipe movement to less than 1-diameter lateral displacement. For pipes with a larger diameter than the maximum break size, the maximum attainable break area would be modeled as a partial pipe break with an area equivalent to the DEGB of a pipe with the same diameter as the DGBS. The worst location of the break in terms of orientation around the break location should be considered.

One area of which the GR Section 6.3 guidance differs from the guidance in the baseline analysis of Section 3 involves the ZOI to be considered for debris generation. The guidance in Section 3 regarding the ZOI presumes a DEGB, and for a DEGB, a spherical ZOI is conservatively postulated. A spherical ZOI is appropriate in the Region I analyses for any auxiliary piping attached to the RCS, since a DEGB of any such piping falls within Region I analysis. However, partial breaks of the RCS main loop piping are also included in Region I (breaks up to the DGBS), and would indicate a limited-displacement circumferential break or a longitudinal break, (i.e., “split break”). The GR proposes that the ZOI for such partial breaks in RCS main loop piping be accounted for by applying one of the following two methods:

- For a ZOI based on a hemisphere, the ZOI is simulated as a hemisphere radius determined by the destruction pressure of the insulation that would be affected by the postulated break. The break orientation needs to be simulated at various angles around the loop piping to determine maximum debris generation.
- For a ZOI based on a sphere, because the worst-case break orientation can be difficult to determine, an alternative to assuming a hemispherical ZOI is to translate the hemispherical volume into an equivalent-volume sphere.

The GR also states that the ZOI refinements discussed in Section 4 are available when performing Region I analyses.

The acceptance criteria for containment sump-screen performance continue to be core cooling based on available NPSH equal to, or greater than, the required NPSH for all pumps needed to operate for long-term core cooling. The calculations of required and available NPSH are based on the models and assumptions currently used in design-basis analyses of sump and core-cooling recirculation performance. Additionally, the GR states that if containment spray is credited in the design-basis analyses, the containment sump-screen performance also includes NPSH margin for the minimum required containment spray.

The Region I analyses also consider the impact of the DGBS on event timings, thermal-hydraulic conditions, and NPSH requirements. For example, use of the DGBS will affect key scenario events, such as the timing of transfer from refueling water storage tank (RWST) injection to recirculation mode, the containment sump water properties (e.g., temperature), and containment back-pressure (if credited in the design-basis analyses). The Region I evaluation will consider these revised timings and parameters as appropriate. The guidance also provides for the impact of operator actions to mitigate containment sump blockage, provided that the operator actions meet the criterion for consideration in design-basis analyses. These considerations would include adequate time for operator action in accordance with design-basis rules, proceduralized guidance, job task analysis, training, and other requirements.

Staff Evaluation of GR Section 6.3: The staff has reviewed the Region I alternate evaluation methodology, as described in the GR. The Region I analysis methods described in Section 6.3 are applicable for any break sizes equal to or smaller than the DGBS defined in Section 6.2. The Region I methodology, therefore, applies to any ASME Code Class 1 auxiliary piping (attached to RCS main-loop piping) up to and including a DEGB of any of these lines, as well as RCS main-loop piping (hot, cold and crossover piping) up to and including a size equivalent to the area of a DEGB of a 14–in. schedule 160 pipe. The majority of the Region I analyses are performed in the same manner as the methods described in Sections 3, 4, and 5 of the GR, and as such, the corresponding sections in this SE are applicable for Region I analysis. For example, the guidance in Sections 3 and 4 of this SE is to be used as part of the Region I analyses to determine the debris generation, transport, and accumulation on the containment sump screens. The staff evaluation described below will focus on the differences between this SE and Sections 3, 4, and 5 of the GR.

For Region I breaks, the GR states that a full range of break locations will be assessed to determine the limiting location, considering both debris generation and debris transport. Additionally, as discussed in Section 6.3.2, the GR refers to a Section 4.2.1 refinement which proposes that BTP MEB 3-1 may be used to limit the break locations considered. As documented in Section 4.2.1 of this SE, the staff concluded that it is inappropriate to cite SRP Section 3.6.2 and BTP MEB 3-1 as methodology to be applied for determining break locations to be considered for PWR sump analyses. The staff concludes that for Region I breaks, which are considered as customary design-basis analyses, a full range of break locations should be assessed to determine the limiting location considering both debris generation and debris transport. Section 4.2.1 of this SE provides further details regarding the staff's position. The staff finds that the GR guidance is acceptable with respect to break configuration because the methodology assures that the limiting break location, considering debris generation, debris transport, and the worst location of the break in terms of orientation around the break location, will be evaluated. This methodology provides reasonable assurance that the limiting break conditions for PWR sump analyses will be evaluated. Additionally, considering piping restraints and supports or other plant structural members that can be shown through analysis to limit pipe movement to less than 1-diameter lateral displacement may be acceptable to the staff; however, because the limiting break location and orientation must be evaluated, these locations may not produce the limiting conditions for sump analyses.

Regarding the ZOI to be considered for attached auxiliary piping breaks, the GR states that a spherical ZOI is postulated for breaks smaller than the DGBS for piping connected to the RCS main loop piping because a DEGB of this piping is postulated. For Region I partial pipe breaks, the GR proposes that one of two methods be applied, either a ZOI based on a hemisphere or a ZOI based on translating the hemispherical volume into an equivalent-volume sphere. The staff evaluated the GR with respect to the ZOI to be considered under these conditions and concludes that applying a hemispherical ZOI is acceptable for such partial breaks, and that when doing so, licensees will need to simulate various directions around the RCS main-loop piping to determine the limiting break location. The staff does not accept the proposed approach of a ZOI based on translating the hemispherical volume into an equivalent-volume sphere. The GR does not provide any technical justification for this approach except that it is a simplification because the worst-case break orientation can be difficult to determine. The staff does not have a technical basis for accepting a translation of the volumes, which would result in a different ZOI, and the staff has no basis to evaluate whether this would be conservative, nonconservative, or realistic. For simplification, the staff would accept application of a spherical ZOI with a radius equivalent to that of a ZOI based on a hemisphere.

The application of the ZOI refinements for Region I analyses should be in accordance with the staff's position discussed in Section 4.0 of this SE.

For the Region I sump analyses, the acceptance criteria for containment sump-screen performance continues to be core cooling based on available NPSH equal to, or greater than, the required NPSH for all pumps required to operate for long-term core cooling. The calculations of required and available NPSH are based on the models and assumptions currently used in design-basis analyses of sump and core cooling recirculation performance, and therefore, the staff finds their continued application for Region I analyses to be acceptable. The staff agrees with the GR that the impact of the DGBS on event timings, thermal-hydraulic conditions, and NPSH requirements, as well as crediting operator actions for demonstrating that the acceptance criteria are satisfied, can be applied for Region I analyses consistent with customary design-basis analysis procedures and requirements. Licensee analyses should consider, at a minimum, the following factors:

1. The accuracy of deterministic analyses performed to calculate DGBS event timings, thermal-hydraulic conditions, and NPSH requirements, and their compliance with 10 CFR 50.46. The staff expects that licensees will document, and if necessary, provide to the staff detailed information regarding the analyses and the modeling assumptions. The GR guidance does not explicitly identify which phenomena and parameters will receive time-dependent treatment and will be considered in-scope for estimating timing of events.

2. The experimental data used for estimating debris generation, transport, and head-loss buildup for breaks other than a DEGB. In general, most experimental data were obtained for jet conditions and transport flow rates prototypical of a DEGB. For example, most of the debris generation data were obtained for jet

durations typical of a DEGB (10–30 seconds). Direct use of such data for insulations where erosion is the dominant generation mechanism (e.g., calcium silicate) may not be appropriate for a DGBS break. Similar limitations on the applicability of available experimental data to a DGBS exist for other phenomena as well, including debris transport and debris buildup, especially when operator actions are to be credited in the mix of the analyses being performed. However, application of GR Section 3 baseline methods ensures conservative treatment of erosion concerns for tabulated materials.

3. Because of uncertainties in various phenomena, the staff believes that it is difficult to judge when maximum head loss would occur (e.g., the maximum debris accumulation and the minimum NPSH margin may or may not occur simultaneously, depending on operator actions). Considerable attention and a broad spectrum of evaluations should be devoted to establish that the analyses conducted are customary design-basis analyses.

4. If credit is to be taken for containment overpressure, underlying analyses should conform with the staff guidance for estimating minimum overpressure, as suggested in RG 1.82, Revision 3.

The staff notes that there is a typographical error in the following sentence of Section 6.3.6 of the GR, "In addition, if containment spray is credited in the design basis analyses (containment pressure, radiological consequence, etc.), the containment sump-screen performance also includes NPSH margin for operation of the minimum required containment spray." The staff believes that this sentence should state that adequate NPSH margin needs to be available for the maximum required containment spray or to allow for an overestimate of the required containment spray.

6.4 REGION II ANALYSIS

The Region II analysis of recirculation sump performance includes evaluations of break sizes in the RCS main loop piping (hot, cold, and crossover piping) greater than the DGBS specified in GR Section 6.2 (approximately 196.6 square inches) and up to a DEGB of the largest pipe in the RCS. Region II considers only RCS main loop piping because all primary-side attached auxiliary piping and secondary-side breaks are fully addressed as part of the Region I analyses. Section 6.4.2 of the GR states that, "if a licensee chooses to use an alternate break size smaller than the largest connected piping to the main coolant loop piping, as discussed in Section 6.2, then connected piping larger than the alternate break size would be addressed as part of the Region II evaluation." The staff finds that this statement is not consistent with the alternate break size, as defined in Section 6.2, and should be clarified. The NEI and industry representatives informed the staff that this statement is included in the GR to allow for the possibility that the forthcoming 10 CFR 50.46 rulemaking would redefine the design-basis LOCA break size to be smaller than the DGBS described in Section 6.2. As discussed in Section 6.2 of this SE, the staff agrees with the recommended guidance that licensees may re-perform the sump performance evaluations using the final break size specified by rulemaking and modify the plant design and operation accordingly.

Section 6.4.2 of the GR refers to a Section 4 refinement proposing that BTP MEB 3-1 may be used to limit the break locations considered. With respect to break configuration, the Region II analyses are limited to a DEGB of the RCS main loop piping.

These circumferential breaks are assumed to result in pipe severance and separation amounting to at least 1-diameter lateral displacement of the ruptured piping sections, unless physically limited by piping restraints and supports, other plant structural members, or piping stiffness as may be demonstrated by analysis. The GR states that existing plant-specific dynamic loads analyses for postulated primary-side breaks are utilized to determine the break configuration for Region II analyses.

The ZOI models and assumptions to be applied for Region II analyses are those described in Sections 3 and 4 of the GR. There are a number of known conservatisms in the ZOI model presented in Sections 3 and 4. However, because development of a technically sound model to more realistically model the ZOI based on existing experimental and analytical data is quite complex and has not been initiated, the GR relies on the models described in Sections 3 and 4.

The guidance in Sections 3 and 4 of the GR is also applied to determine the debris generation, transport, and accumulation on the containment sump screens for Region II evaluations. The models presented in Sections 3 and 4 are considered to be bounding models to assure that the debris generation, transport and accumulation are not under-predicted. There are known conservatisms in each portion of these evaluation models described in Sections 3 and 4. However, development of more realistic models in these areas is difficult because of the limited amount of experimental and analytical information available, and this work has not yet been initiated.

The acceptance criteria for containment sump-screen performance for Region II analyses are continued core and containment cooling. The following criteria to demonstrate retained mitigation capability for long-term cooling capability in Region II analyses:

- Positive NPSH margin is maintained for the minimum number of ECCS pumps necessary to demonstrate adequate core cooling flow.
- Adequate containment cooling capability is demonstrated to provide assurance that the containment boundary remains intact.

The first criterion (i.e., positive NPSH margin is maintained for the minimum number of ECCS pumps) can be met by ensuring that the NPSH margin is maintained for one or more moderate to high-capacity ECCS injection pumps. Additionally, for Region II analyses, the GR states that limited operation without an NPSH margin is acceptable if it can be shown that the pumps can reasonably be expected to survive during the time period of inadequate available NPSH. The suggested technical justification for this statement would include vendor information in the form of test data or engineering judgment derived from tests and/or operational events.

The GR states that the second criterion (i.e., demonstration of adequate containment cooling capability) can be met through credit taken for minimal heat removal pathways, including containment fan coolers, permitted by emergency procedures. Additionally, subatmospheric containment plants would not have to demonstrate that the containment remains below atmospheric pressure for the duration of the accident, if permitted by emergency procedures. The GR also states that, “exceeding nominal transient containment design pressure/temperature and environmental qualification (EQ) envelopes is allowed for Region II analysis, if reasonable assurance is provided that containment pressure boundary failure or vital equipment failure would not be expected."

The Region II analyses also consider more realistic modeling of debris generation, transport, and accumulation on sump screens based on the timing of debris generation, transport, and accumulation in relation to the timing of the available and required NPSH. More realistic modeling of these items considers the following:

- Debris generation, transport, and accumulation are time dependent.
- Available NPSH is time dependent.
- The maximum debris accumulation and the minimum required NPSH may not occur simultaneously.

The GR also allows credit for operator actions and the operation of non-safety equipment.

Staff Evaluation of GR Section 6.4: The staff has reviewed the Region II alternate evaluation methodology described in the GR. The Region II analysis methods described in Section 6.4 are applicable for any breaks in the RCS main loop piping (hot, cold and crossover piping) greater than the DGBS specified in Section 6.2 (approximately 196.6 square inches) and up to a DEGB of the largest pipe in the RCS.

For Region II break locations, Section 6.3.2 of the GR refers to a Section 4.2.1 refinement proposing that BTP MEB 3-1 be used to limit the break locations considered. As documented in Section 4.2.1 of this SE, the staff concludes that it is inappropriate to cite SRP Section 3.6.2 and BTP MEB 3-1 as methodology to be applied for determining break locations to be considered for PWR sump analyses. The staff concludes that for Region II breaks, a full range of break locations should be assessed to determine the limiting location, considering both debris generation and debris transport. Section 4.2.1 of this SE provides further details regarding the staff's position.

The staff finds that the GR guidance is acceptable with respect to break configuration because the limiting break location, considering debris generation, debris transport, and resulting sump-screen head loss, will be evaluated. This methodology provides reasonable assurance that the limiting break conditions for PWR sump analyses will be evaluated. Additionally, considering piping restraints and supports or other plant structural members that can be shown through analysis to limit pipe movement to less than 1-diameter lateral displacement may be acceptable to the staff; however, because the limiting break location must be evaluated, these locations may not produce the limiting conditions for sump analyses.

Certain portions of the Region II analyses are performed in the same manner as the methods described in Sections 3 and 4 of the GR; the corresponding SE sections are applicable for Region II analyses. The guidance in Sections 3 and 4 is to be used as part of the Region II analyses with respect to ZOI models and assumptions, and for determining debris generation, transport, and accumulation on the containment sump screens. There are known conservatisms in each of these models as described in Sections 3 and 4, and the staff finds them to be acceptable for Region II analyses.

Sections 0 and 4.0 of this SE provide further details regarding the staff's position and review of these models.

The GR proposed the following two acceptance criteria for the Region II analysis:

- Maintain positive NPSH margin for the minimum number of ECCS pumps necessary to demonstrate adequate core cooling flow.
- Demonstrate adequate containment cooling capability to provide assurance that the containment boundary remains intact.

The staff considers a positive NPSH margin to mean that the available NPSH is greater than the required NPSH for each pump. The GR has not specified the amount of NPSH margin necessary. Because the staff has previously accepted the available NPSH equal to the required NPSH (i.e., an NPSH margin of zero), this nonspecificity is acceptable for realistic and risk-informed Region II analyses. Sections 6.4.7.1 and 6.4.7.2, respectively, of this SE address the determination of both the available and the required NPSH.

The GR does not specify what is meant by adequate core cooling. The staff interprets adequate core cooling to mean that the acceptance criteria of 10 CFR 50.46 are satisfied. By maintaining a positive NPSH margin to demonstrate adequate core cooling flow, the 10 CFR 50.46 acceptance criteria should not be challenged.

The GR does not specify what is meant by adequate containment cooling. The staff interprets adequate containment cooling to mean that the containment is in a safe and stable state and is preventing risk-significant fission product releases. Further, the containment has not failed structurally. The GR states that containment design pressure and the containment design temperature may be exceeded for analyses of breaks above the DGBS. The staff will consider this, and licensees should determine, on a plant-specific basis, whether exemption and/or license amendment requests are required if the containment design pressure and/or temperature is exceeded. Licensees should determine whether the containment leakage rate exceeds the value of L_a defined in Appendix J to 10 CFR Part 50 and given in the plant's technical specifications. An exemption to this regulation and/or a license amendment request might be required if a licensee determines that this is the case. The staff will evaluate these requests on a plant-specific basis.

The GR states that the second criterion can be met through credit taken for minimal heat removal pathways, including containment fan coolers, permitted by the emergency procedures. The staff finds that credit taken for minimal heat removal pathways permitted by the emergency procedures would be acceptable in a realistic and risk-informed Region II analysis. The staff expects that licensees will provide detailed information regarding plant equipment and/or operator actions credited in their GL responses. The staff will assess credit taken for minimal heat removal pathways as part of the GL response reviews and closeout process.

The GR also states that it is acceptable to exceed the "nominal" environmental qualification (EQ) envelopes. The staff finds that applying a more realistic EQ envelope could be acceptable in a realistic and risk-informed Region II analysis. For Region II analyses, the staff does not consider it necessary to comply with the guidance of

NUREG-0588, Revision 1, which is the basis for the EQ analyses described in plant updated final safety analysis reports (UFSARs). If any equipment exceeds the appropriate EQ envelope, the licensee should consider whether an exemption to 10 CFR 50.49 is required. The staff expects that licensees will provide detailed information with respect to exceeding nominal EQ profiles in their GL responses. The staff will assess the application of EQ envelopes as part of the GL response reviews and closeout process.

For the Region II evaluation, the GR criteria would allow limited ECCS and containment heat removal pump operation without an NPSH margin. Licensees would need to demonstrate that the pumps can reasonably be expected to survive during the time of inadequate available NPSH margin. Test data or engineering judgment derived from tests and/or operating experience should serve as the basis of the technical justification for this conclusion.

The GR points out that the guidance for determining adequate NPSH margin is currently provided in RG 1.1, which is the licensing basis for some operating reactors, and RG 1.82, Revision 3, which contains the current staff guidance. The GR suggests that it is not necessary to apply the conservative guidance provided in these RGs when analyzing the consequences of breaks larger than the DGBS. The remainder of Section 6.4.7 provides guidance on an alternate, more realistic approach.

Section 6.4.7 discusses the application of GL91-18 with respect to determining a realistic NPSH margin. The GR considers that a “nominal” parameter value used in performing Region II analyses could be exceeded. For this situation, the GR proposes that operability assessments in accordance with GL 91-18 are not necessary. The GR establishes a time limit allowing the nominal value to be exceeded for a period of 30 days. LOCA analyses are typically carried out only to 30 days. The staff finds this proposal to be unacceptable because the Region II analyses remain within the design bases. Exceeding the nominal value of a parameter used the Region II analyses may result in decreasing the available NPSH to the degree that there is no longer positive margin for this DBA. Therefore, the staff concludes that the same conditions apply for a Region II analysis as would apply for a Region I analysis, and the guidance in GL 91-18 should also apply.

The GR discusses the realistic assumptions that may be applied in calculating the available NPSH for breaks larger than the DGBS. Section 6.4.7.1 of the GR discusses these assumptions for each of the factors which contribute to the available NPSH, including suction elevation head, absolute pressure head, vapor pressure head, and friction and form-head losses. The staff finds the GR discussion in Section 6.4.7.1 to be acceptable with one caveat. The discussion of friction losses notes that experience has shown that calculations of friction loss based on handbook values tend to overestimate the friction loss. The GR states that these values may be reduced based on engineering judgment or test results. To quantify the available margin in these calculations, the staff’s position is that a more substantive basis than engineering judgment should be used. Engineering judgment by itself, without further technical basis, does not provide adequate justification for removing conservatism in handbook friction loss values. The staff will accept a reduction in head-loss calculations based on accepted handbook values only if its basis is technically justified.

The pump vendor measures the required NPSH of a pump in accordance with applicable standards. It is usually based on a 3 percent drop in the pump total head (first stage for a multi-stage pump). This value has been selected as an easily recognized level of cavitation. It is not the level at which cavitation first appears. The GR states that, since total head is not necessarily a critical parameter for a centrifugal pump in the LOCA recirculation mode, the pump vendor may be able to provide relief in the amount of NPSH required to avoid pump damage, rather than depend on the formal definition of required NPSH. The staff agrees. In the past, the staff has accepted the pump vendor's technical judgment on pump capabilities. In this case, the conditions the pump will experience and the time period during which the pump will experience these conditions should be well defined and evaluated by the pump vendor. In addition, staff believes that vendors' technical judgments should take into consideration the fact that recirculation water may include debris of different kinds and sizes (i.e., combined effects of debris ingestion and cavitation should be factored into decision making).

The GR states that accounting for the decrease in required NPSH with an increase in pumped liquid temperature, as discussed in ANSI/HI 1.1-1.5-1994 (ANSI/HI 1.1-1.5), should not be used. The staff agrees. This is consistent with the guidance in RG 1.82, Revision 3.

The calculational method section (Section 6.4.7.3) of the GR discusses assumptions that could be applied for more realistic available and required NPSH calculations. It is not clear what is meant by calculating required NPSH because the pump vendor typically measures and specifies the required NPSH. Licensees referencing the GR should clarify this. One of the items listed in this section refers to: "containment pressure head based on absolute pressure rather than vapor pressure." Rather than "absolute pressure," the term "pressure of the containment atmosphere," would be clearer. The staff expects that licensees will provide detailed information regarding the application of more realistic analysis assumptions in their GL responses. The staff will assess these assumptions as part of the GL response reviews and closeout process. Additionally, application of certain assumptions may require plant-specific exemptions and/or license amendment requests.

With respect to timing of events, the GR discusses the realistic modeling of debris generation, transport, and accumulation on sump screens. One bullet in this section states that "the maximum debris accumulation and the minimum required NPSH may not occur simultaneously." It appears that this is referring to the minimum available NPSH margin, rather than the minimum required NPSH. Other than this editorial comment, the staff agrees with the report's proposals in this section. The staff expects that licensees will provide detailed information regarding more realistic modeling of event timing in their GL responses. The staff will assess this modeling as part of the GL response reviews and closeout process.

The staff agrees with the GR's proposal of operator actions that may be credited to compensate for the effects of debris generation on the ECCS and the containment spray system. Credit for these actions will be assessed on a plant-specific basis, and risk calculations supporting the credit should be performed in accordance with RG 1.174.

The GR does not address the analytical methods to be used for performing the Region II analyses (e.g., computer codes and models). In particular, the staff has reservations about how the models and methods described in Sections 3 and 4 could be adopted for these types of analyses. The staff will assess the adequacy of methods used during its review of any plant-specific licensing submission and plant-specific audits performed as part of the GSI-191 and GL closeout process. Part of the staff's assessment would include methods, models, and data used to estimate event timings; thermal-hydraulic conditions; and the calculational uncertainties associated with the debris phenomena. It is known that all aspects of debris phenomena (i.e., generation, transport, and head loss) have large uncertainties. In lieu of explicitly treating these uncertainties, staff used engineering judgment to conclude that these uncertainties are typically small compared to the conservatism introduced by DEGB-type limiting analyses. Licensee evaluations performed under Region-II should be cognizant of such issues and address them explicitly. For example, considerable experimental evidence exists in support of increased head loss resulting from long-term operation. Very limited, if any, experiments are carried out to quantify such a factor mechanistically. Instead traditional correlations developed using short-term tests, corrected based on engineering judgment, were used to account for long-term phenomena. In the past, the staff accepted such approximations because of the large margin of conservatism implicit in DEGB-type analyses.

6.5 RISK INSIGHTS

Section 6.5 of the NEI GR guides the determination of risk acceptability for cases in which a licensee relies on sump mitigation capability (including crediting operator actions) for the Region II analysis (i.e., Section 6.4). Section 6.5 of the NEI evaluation guidance uses the acceptance guideline from RG1.174, which is also used to define an acceptably small increase in CDF to establish a target reliability for the sump mitigation capability. To further ensure the acceptability of this approach, the NEI evaluation guidance also uses a conservative value for the LBLOCA initiating event frequency (LBLOCA:IEF), which is taken from NUREG-1150. Thus, the NEI evaluation guidance provides a method by which a licensee can ensure that any increase in CDF resulting from plant modifications, operator actions, etc., and which is credited in Section 6.4, will be small and will meet the RG 1.174 acceptance guideline by demonstrating that the target reliability of the sump mitigation capability is achieved.

The target reliability is established by first calculating the increase in CDF as the combination of the LBLOCA:IEF and the sump mitigation capability failure probability (SMC:FP). This calculation uses a number of conservatisms to make it simple and straightforward, including the following:

- The base case condition represents the condition in which the current sump meets the regulations without needing credit for mitigation capability and is assumed not to clog (i.e., the sump is perfect, with a clogging probability of 0).
- The mitigation condition case represents the condition in which the sump takes credit for mitigation capability and assumes if the mitigation capability fails, the sump will clog (i.e., the sump always clogs if the mitigation capability fails, with a clogging probability of 1). Further, a clogged sump results in core damage (i.e., no credit for potential recovery actions).
- The calculation is performed for the entire LBLOCA break spectrum (i.e., all breaks greater than about 6 inches), while the NEI evaluation guidelines Region II alternate approach is only used for those break sizes greater than the DGBS,

which is only a portion of the LBLOCA break spectrum (i.e., the calculation assumes all LBLOCAs require mitigation, not just those greater than the DGBS).

Based on this approach, the calculation for the increase in CDF can be simplified to:

$$\Delta CDF = LBLOCA{:}IEF \times SMC{:}FP$$

Recognizing that the target reliability (TR) is the complement of the SMC:FP, resolving the equation results in:

$$TR = 1 - SMC{:}FP = 1 - [\Delta CDF / LBLOCA{:}IEF]$$

The RG 1.174 acceptance guideline for a small change in CDF is less than 1.0x10-5/year. This is an appropriate acceptance guideline for plants where the total CDF can be reasonably shown to be less than 1.0x10-4/year. The NEI evaluation guidance states that the 1.0x10-4/year total CDF value bounds the population of PWRs. The staff accepts that this may be true. However, if a licensee's total CDF is significantly greater than 1.0x10-4/year, considering all modes and initiators, then that licensee should provide additional justification and meet an appropriately higher TR.

The value for the LBLOCA:IEF from NUREG-1150 is 5.0x10-4/reactor-year. The staff recognizes that this value represents a generic bounding value of the LBLOCA frequency and is considerably greater (and thus conservative) than the value used in plant-specific PRAs.

Substituting the above values into the equation results in a TR for the sump mitigation capability of 0.98 per demand (i.e., SMC:FP equals 2.0x10-2/demand).

The staff understands that the reliability of the sump mitigation capability will be determined on a plant-specific basis and ensured with reasonable confidence to be equal to or greater than the above established target reliability. This determination will include evaluations of associated plant modifications, as well as credited operator actions, including those modifications and actions credited in Section 6.4 that represent a change from current operations (e.g., crediting operator action to terminate or reduce containment spray flow to assure NPSH of the low-head pumps).

The staff also accepts that passive components do not need to be considered in the reliability determination, as long as these passive components are demonstrated as being functional by design (e.g., enlarged sump-screen areas) or failure is determined to be extremely unlikely (e.g., less than 1.0x10-5/demand), even given the challenges that passive components might see, such as jet forces or blowdown loads. However, if a measurable and inspectable reliability can be ascribed to a passive component (e.g., passive screen cleaning), then the reliability determination should include these features.

Consistent with the RG 1.174 principles of risk-informed decision-making, the impact of the proposed change must be monitored using performance measurement strategies. Therefore, an implementation and monitoring plan must be developed to ensure that the evaluation conducted to examine the impact of the proposed changes continues to reflect the actual reliability and availability of the SSCs and operator actions that have been evaluated. This will ensure that the conclusions that have been drawn from the evaluation remain valid. Thus, the staff requires licensees to propose, in their plant-specific submissions, a monitoring program that is consistent with RG 1.174, Section 2.3, which includes a means to adequately track the performance of equipment that, when degraded, can affect the conclusions of the licensees' evaluations (i.e., demonstration of the sump mitigative capability to meet its reliability target). The program must be capable of trending equipment performance after a change has been implemented to demonstrate that performance is consistent with that assumed in the traditional engineering and probabilistic analyses that were conducted to justify the change. This must include monitoring associated with non-safety-related SSCs, if the analysis identifies those SSCs to be relied upon to meet the sump mitigative capability TR. The program must also be structured such that feedback of information and corrective actions are accomplished in a timely manner and degradation in performance is detected and corrected before plant safety can be compromised. The staff expects that licensees choosing to apply this methodology will comply with the guidance in RG 1.174 or provide justification for the deviation.

In summary, the staff finds this portion of the alternate approach acceptable for use in the NEI evaluation guidance Region II analyses for the following reasons:

- The TR determination includes a number of conservative simplifications.
- It is performed for the entire LBLOCA break spectrum (i.e., all breaks greater than about 6 inches), while the NEI evaluation guidance Region II alternate approach is only used for those break sizes greater than the DGBS, which is only a portion of the LBLOCA break spectrum.
- The base case condition is assumed not to be susceptible to clogging (i.e., the sump is perfect, with a clogging probability of 0).
- The mitigation condition case assumes if the mitigation capability fails, the sump will clog (i.e., the sump always clogs if the mitigation capability fails, with a clogging probability of 1), and that a clogged sump results in core damage (i.e., no credit for potential recovery actions).
- The NUREG-1150 LBLOCA:IEF of 5.0x10-4/reactor-year is expected to be much greater than the LBLOCA value derived from the ongoing RES expert elicitation process.
- The approach is consistent with RG 1.174 since it uses the acceptance guidelines that define an acceptably small CDF increase in determining the TR of the sump mitigation capability.
- Licensees choosing to apply Region II analyses should implement a performance monitoring program, consistent with Section 2.3 of RG 1.174, to ensure that the conclusions of the licensees' evaluations (i.e., demonstrations that the sump mitigative capability meets the established TR) are maintained valid.

In considering the risk-informing aspects of the resolution of GSI-191, the staff recognized that there is the potential that the containment sump may clog, if the mitigation capability credited in the Region II analysis does not function properly. Based on the industry-proposed approach in the Region II analysis, which also uses the conservative NUREG-1150 LBLOCA frequency to calculate the TR of the mitigation capability, and using the related generic study information, the largest LBLOCA CDF would be 1.4x10-5/year. This indicates that at a minimum, the risk associated with LBLOCAs will be reduced from the current condition by nearly an order of magnitude.

7.0 ADDITIONAL DESIGN CONSIDERATIONS

This section of the GR discusses four extenuating design considerations which are related to the broad issue of recirculation sump operability addressed under GSI-191. These topics include (1) structural analysis of the containment sump, (2) upstream effects that limit water flow, (3) downstream effects related to debris penetration of the screen, and (4) potential chemical effects that contribute to head loss either as an additional debris source or by modifying the hydraulic properties of preexisting beds. Staff evaluations of the GR treatment of these topics follow in corresponding subsections of this SE. The NRC agrees that this list is complete when added to the balance of detail provided in the remainder of the GR, as modified by staff recommendations.

7.1 SUMP STRUCTURAL ANALYSIS

This section of the GR provides general guidance for considerations to be used when performing a structural analysis of the containment sump screen. The GR does not provide specific details on how to perform this analysis. General items identified for consideration include (1) verifying maximum differential pressure caused by combined clean screen and maximum debris load at rated flow rates, (2) geometry concerns (mesh and frame vs. perforated plate), (3) sump screen material selection for the post accident environment, and (4) the addition of hydrodynamic loads resulting from a seismic event. The GR specifically states that section 1.1.1.8 of RG 1.82, Revision 3, may need to be referenced for evaluation of hydrodynamic loads on a strainer.

Staff Evaluation of GR Section 7.1: The staff finds the general statements in Section 7.1 pertaining to the analysis of the structural capability of the containment sump strainer to be acceptable. The staff agrees that potential bending and stretching of existing wire mesh may lead to gaps at the points of attachment between wire and framing structures. The staff further agrees that any modifications to existing sump-screen configurations should employ corrosion-resistant materials that will not be affected by post-LOCA containment conditions.

Consideration of sump structural analysis in the GR and in this SE is limited to the debris loads and the hydraulic loads imposed by water in the sump pool. Dynamic loads imposed on the sump structure and screen by break-jet impingement must be addressed in accordance with GDC 4, including provisions for exclusion of certain breaks from the design basis when analyses reviewed and approved by the NRC demonstrate that the probability of fluid system piping rupture is extremely low.

Paragraph 2(d)(vii) of the information request section of GL 2004-02 requests that addressees verify that trash racks and sump screens are capable of withstanding the loads imposed by expanding jets and missiles. The staff requests addressees to verify that the trash racks and sump screens continue to meet the current design-basis requirements under GDC 4, as discussed above.

The GR does not provide detail in its presentation of criteria for sump-screen performance and comparisons to predicted head loss. To clarify this information, the staff offers the following discussion. It is true that structural loads on a sump screen should be computed using the total pressure drop across the screen. The total pressure drop is the sum of the head loss computed or measured across the clean screen at a rated flow in the absence of debris and the debris-induced head loss computed or measured under the same volumetric flow rate. The limiting conditions for sump-screen structural analysis correspond to a break location and debris source term that induces the maximum total head loss at the sump screen after full consideration of transport and degradation mechanisms. Debris-bed head loss should be calculated for each postulated break scenario according to methods outlined in Sections 3.7 and 4.2.5 of the GR, as amended by these SE recommendations.

Licensing-basis calculations of NPSH margin already include the effects of flow resistance through the clean screen, so it is sufficient to examine the debris-bed head loss separately. For a completely submerged sump screen, if the NPSH margin is smaller than the head loss induced by debris from the limiting break, then the licensing basis has been exceeded and some form of mitigation, modification, or exemption is warranted. For a partially submerged sump screen, a potentially more restrictive condition may apply. In order to supply adequate water flow through the debris bed, the pressure drop cannot exceed one-half of the pool depth in feet of water or the NPSH margin, whichever is smaller. This additional criterion arises because the containment pressure is equal on both sides of the debris bed, and the static pressure of the pool is the only way to force water through the bed (RG 1.82-3).

Thus, different criteria may dictate the structural capacity of the sump screen for supporting water flow through a debris bed under recirculation velocities depending on screen geometry. Other considerations such as maximum water velocities during fill up and hydrodynamic loads during a seismic event may impose additional design constraints.

The guidance presented in the GR would require each licensee to perform a plant-specific evaluation of its respective sump screen to determine structural capability under post accident conditions. The staff agrees with the GR reference of RG 1.82 for evaluation of hydrodynamic loads. This plant-specific analysis would be reviewed on a case-by-case basis.

7.2 UPSTREAM EFFECTS

This section of the GR provides guidance on evaluating the flowpaths upstream of the containment sump for holdup of inventory which could reduce flow to and possibly starve the sump. The GR identifies two parameters important to the evaluation of upstream effects: (1) containment design and postulated break location, and (2) postulated break size and insulation materials in the ZOI. The GR states that the above two parameters provide a basis to evaluate holdup or choke points in the flow field within containment upstream of the containment sump. The GR also advises that the containment condition assessment, as described in NEI 02-01, provides guidance on this review.

The GR provides users of the document the following examples of locations to evaluate for holdup of liquid upstream of the sump screen: narrowing of hallways or passages, gates or screens that restrict access to areas of containment such as behind the bioshield or crane wall, and refueling canal drain. The GR then states that these areas of concern generally apply to all containments, but advises licensees to evaluate their containment for possible holdup at unique geometric features and to evaluate any plant-specific insulation installation.

Staff Evaluation of GR Section 7.2: The staff finds that the above-mentioned items of the GR are appropriate as stated and offers the following amplification. Licensees should use the results of their debris assessments to estimate the potential for water inventory holdup. Based on these assessments and the mapping of probable flowpaths, licensees should use methods provided in Section 5 of the GR for the additional purpose of reducing holdup of blowdown inventory upstream of the sump. Licensees should evaluate the effect the placement of curbs and debris racks intended to holdup debris may have on the holdup of water en route to the sump.

Staff Conclusions Regarding Section 7.2: The staff finds that the GR provides adequate direction regarding the evaluation of holdup of inventory from the sump. The staff provides the above additional comments as amplification to the GR.

7.3 DOWNSTREAM EFFECTS

This section of the GR gives licensees guidance on evaluating the flowpaths downstream of the containment sump for blockage from entrained debris. The GR specifies three concerns to be addressed: (1) blockage of flowpaths in equipment, such as containment spray nozzles and tight-clearance valves, (2) wear and abrasion of surfaces, such as pump running surfaces, and heat exchanger tubes and orifices, and (3) blockage of flow clearances through fuel assemblies. The NRC is currently conducting research in the area of debris bypass through sump-screens and flow blockage of HPSI throttle valves; this SE may be supplemented with the results of this research in early 2005. The staff would then expect licensees to consider the supplemental information in evaluating their plants for downstream effects.

The GR identifies the starting point for the evaluation to be the flow clearance through the sump screen and states that the flow clearance through the sump screen determines the maximum size of particulate debris that will pass through it. The GR states that wear and abrasion of surfaces in the ECC and CS should be evaluated based on flow rates to which the surfaces will be subjected and the grittiness or abrasiveness of the ingested debris. The GR recognizes that the abrasiveness of debris is plant-specific. The GR also states that the pump manufacturer may have addressed the wear and abrasion of pumps caused by ingestion of debris, and advises licensees to contact their vendor regarding the ability of the pump to perform with debris in the process fluid.

Staff Evaluation of GR Section 7.3: The GR states, “If passages and channels in the ECC and CS downstream of the sump screen are larger than the flow clearance through the sump screen, blockage of those passages and channels by ingested debris is not a concern.” In addition, the GR states, “Similarly, wear and abrasion of surfaces in the ECC and CS should be evaluated based on flow rates to which the surfaces will be subjected…”. The staff finds that the GR statements do not fully address the potential safety impact of LOCA generated debris on components downstream of the containment sump. The following represents the staff’s expectations on the review of the effects of debris on components and systems downstream of the containment sump following initiation of containment recirculation (NUREG/CP-0152 Vol. 5, TIA 2003-04).

The evaluation of GSI-191 should include a review of the effects of debris on pumps and rotating equipment, piping, valves, and heat exchangers downstream of the containment sump related to the ECCS and CSS. In particular, any throttle valves installed in the ECCS for flow balancing (e.g., HPSI throttle valves) should be evaluated for blockage potential. The evaluation should also address the effects of entrained debris on the reactor vessel and internal core components (GL 04-02, NRCB, 2003).

In general, the downstream review should first define both long-term and short-term system operating lineups, conditions of operation, and mission times. Where more than one ECC or CS configuration is used during long- and short- term operation, each lineup should be evaluated with respect to downstream effects. The definition of the design and license bases' mission times form the premise from which the short- and long-term consequences will be determined and evaluated.

Once condition of operation and mission times are established, downstream process fluid conditions should be defined, including assumed fiber content, hard materials, soft materials, and various sizes of material particulates. The staff has found that particles larger than the sump-screen mesh size will pass through to downstream components. Debris may pass through because of its aspect ratio or because it is "soft" and differential pressure across the screen pulls it through the mesh. No credit may be taken for thin-bed filtering effects (NUREG/CP-0152 Vol. 5, TIA 2003-04).

Evaluations of systems and components are to be based on the flow rates to which the wetted surfaces will be subjected and the grittiness or abrasiveness of the ingested debris. The abrasiveness of the debris is plant specific, as stated in the GR, and depends on the site-specific materials that may become latent or break-jet-generated debris.

Specific to pumps and rotating equipment, an evaluation should be performed to assess the condition and operability of the component during and following its required mission times. Consideration should be given to wear and abrasion of surfaces, (e.g., pump running surfaces, bushings, wear rings). Tight clearance components or components where process water is used either to lubricate or cool should be identified and evaluated.

Dirt, dust, and other materials may combine or interact with fiber and cause a matting effect. This matting effect may significantly increase the rate of wear. Test data and operating experience have shown that hard-faced components will wear under long-term exposure to post accident slurry conditions. Soft-surface materials, such as brass and bronze will wear at much faster rates.

Component rotor dynamics changes and long-term effects on vibrations caused by potential wear should be evaluated in the context of pump and rotating equipment operability and reliability. The evaluation should include the potential impact on pump internal loads to address such concerns as rotor and shaft cracking (NUREG/CP-0152 Vol. 5, TIA 2003-04).

As stated in the GR, pump manufacturers may have addressed wear and abrasion of pumps caused by ingestion of debris. Licensees may consider requesting information and/or test data from the pump vendor regarding the ability of specific pumps to perform with debris in the process fluid. Other sources of information available to licensees include information generated to support the closeout of unresolved safety issue (USI) A-43, "Containment Emergency Sump Performance," such as NUREG/CR-2792, "An Assessment of Residual Heat Removal and Containment Spray Pump Performance Under Air and Debris Ingesting Conditions."

The downstream effects evaluation should also consider system piping, containment spray nozzles, and instrumentation tubing. Settling of dusts and fines in low-flow/low-fluid velocity areas may impact system operating characteristics and should be evaluated. The matting effect may cause blockages and should be addressed. The evaluation should include such tubing connections as provided for differential pressure from flow orifices, elbow taps, and venturis and reactor vessel/RCS leg connections for reactor vessel level, as well as any potential the matting may have on the instrumentation necessary for continued long-term operation.

Valve (IN 96-27) and heat exchanger wetted materials should be evaluated for susceptibility to wear, surface abrasion, and plugging. Wear may alter the system flow distribution by increasing flow down a path (decreasing resistance caused by wear), thus starving another critical path. Or conversely, increased resistance from plugging of a valve opening, orifice, or heat exchanger tube may cause wear to occur at another path that is taking the balance of the flow diverted from the blocked path.

Decreased heat exchanger performance resulting from plugging, blocking, plating of slurry materials, or tube degradation should be evaluated with respect to overall system-required hydraulic and heat removal capability.

An overall ECC or CS system evaluation integrating limiting or worst-case pump, valve, piping, and heat exchanger conditions should be performed and include the potential for reduced pump/system capacity resulting from internal bypass leakage or through external leakage. Internal leakage of pumps may be through inter-stage supply and discharge wear rings, shaft support, and volute bushings (NUREG/CP-1052 Vol. 5, TIA 2003-04). Piping systems design bypass flow may increase as bypass valve openings increase or as flow through a heat exchanger is diverted because of plugging or wear. External leakage may occur as a result of leakage through pump seal leak-off lines, from the failure of shaft sealing or bearing components, from the failure of valve packing or through leaks from instrument connections and any other potential fluid paths leading to fluid inventory loss.

Leakage past seals and rings caused by wear from debris fines to areas outside containment should be evaluated with respect to fluid inventory and overall accident scenario design and license bases environmental and dose consequences.

Fluids present post-LOCA during long- and short-term recirculation may flow through the reactor vessel and its internal components. The downstream effects evaluation should consider flow passage blockages, such as those associated with core grid supports, mixing vanes, and debris filters. The evaluation should also consider component binding, such as reactor vessel vent valves in Babcock and Wilcox designs.

If flowpaths between upper downcomer and upper plenum/upper head (e.g., hot-leg nozzle gaps and upper head cooling passages) have an influence on long-term cooling, then the potential for plugging these paths should be addressed.

Staff Conclusions Regarding GR Section 7.3: The staff finds that the GR is nonconservative with respect to its statement that the flow clearance through the sump screen determines the maximum size of particulate debris that would pass through it. As stated above, the staff has seen evidence that some particles larger than the flow openings in a screen will deform and flow through or orient axially and flow through the mesh (NUREG/CP-0152 Vol. 5, TIA 2003-04). Licensees should determine, based on their debris generation and transport calculations, the percentage of debris that would likely pass through their sump screens and be available for blockage at the downstream locations discussed above.

The evaluation of downstream effects should include consideration of term of operating lineup (long or short), conditions of operation, and mission times, as stated above.

Consideration should be given to wear and abrasion of pumps and rotating equipment, as discussed above (NUREG/CP-0152 Vol. 5, TIA 2003-04). Licensees' downstream effects evaluations should consider system piping, containment spray nozzles, and instrumentation tubing, as well. Valve and heat exchanger wetted surfaces should be evaluated for wear, abrasion, and plugging. Wear should be evaluated with respect to the potential to alter system flow distribution. Heat exchanger performance should be evaluated with respect to the potential for blockage or the plating of slurry materials. The HPSI throttle valves should be specifically evaluated for their potential to plug and/or wear (IN 96-27). The overall performance of the ECCS and CSS should be evaluated with respect to all conditions discussed above.

Flow blockage, such as that associated with core grid supports, mixing vanes, and debris filters should be considered. Flow paths between upper downcomer and upper plenum/upper head should be evaluated for long-term cooling degradation resulting from flow interruption from plugging.

As stated above, the staff concludes that the GR recommendations do not fully address the potential safety impact of LOCA-generated debris on components downstream of the containment sump. Licensees should address the additional considerations detailed above in the staff's evaluation.

In order to effectively evaluate downstream effects, licensees may need to review equipment specifications, operations and maintenance manuals, and station drawings, such as equipment, piping, isometrics, and flow diagrams. Review of previous physical walkdowns of piping and instrument systems may be necessary to verify low points where debris accumulation may occur, and potential choke points or other areas of concern not readily verifiable from document reviews. Also leakage past seals and rings caused by wear from debris fines to areas outside containment should be evaluated with respect to license bases environmental and dose consequences. Previously issued generic communications regarding downstream effects, HPSI throttle valve clogging, wear of the high-pressure injection (HPI) pump, pipeline clogging, and heat exchanger wear from operation under abrasive or debris-laden conditions should also be reviewed.

7.4 CHEMICAL EFFECTS

Section 7.4 of the GR introduces the potential problems of chemical reactions in the post-LOCA environment of PWR containments. The reaction products formed can contribute to blockage of the ECCS sump screens and increase the associated head loss across the screens. The GR notes that a test plan has been developed to study possible interactions among corrosion products and the resultant effects of those products on sump filtration. The GR defers guidance for dealing with these effects until the testing is completed and the data have been appropriately evaluated.

For the purpose of this SE, the issue of chemical effects involves interactions between the post-LOCA PWR containment environment and containment materials that may produce corrosion products, gelatinous material, or other chemical reaction products capable of affecting sump-screen head loss. The ACRS raised a concern that an adequate technical basis should be developed to resolve the issues related to chemical reactions (ACRS letter dated September 30, 2003). A gelatinous material was observed in a water sample taken from the Three Mile Island (TMI) containment following the accident in 1979. (Oak Ridge National Laboratory Report memorandum dated September 14, 1979). The relevance of the gelatinous material collected at TMI to the evaluation of potential post-LOCA chemical effects during the ECCS recirculation phase in plants today is uncertain for several reasons. The water sample containing a gelatinous material was collected from the TMI containment approximately 5 months after the accident, which is longer than the typical projected mission time for ECCS recirculation following a modern-day PWR LOCA. The source of the water sample collected from the TMI containment was also unique in that water from the Susquehanna River was introduced into the TMI containment after the accident.

The LANL conducted a limited-scope study to evaluate potential chemical effects occurring following a LOCA. This study assessed the potential for chemically induced corrosion products to impede ECCS performance. In some of these tests, LANL added metal nitrate salts to the test water in concentrations above their solubility limits to induce chemical precipitants and assess head-loss effects. Although these LANL tests showed that gel formation with a significant accompanying head loss across a fibrous bed was possible, LANL did not perform integrated testing to demonstrate a progression from initial exposure of metal samples to formation of chemical interaction precipitation products (LANL Report LA-UR-03-6415). In addition, the test conditions were not intended to be prototypical of a PWR post-LOCA environment. Therefore, a more comprehensive study has been initiated to address potential chemical effects.

In a collaborative effort, the NRC and the nuclear industry developed an integrated chemical effects test program. The test characterizes any chemical reaction products, including possible gelatinous materials, which may develop in a representative plant post-LOCA PWR environment. Test conditions (e.g., pH, temperature, boron concentration) were selected to simulate representative, but not necessarily bounding plant conditions. The initial sump conditions experienced during an LBLOCA will not be replicated in order to simplify the experimental test setup and equipment. Instead, the chemical reactions from corrosion and leaching products during the initial LOCA conditions were simulated using the OLI Systems, Inc., suite of thermodynamic equilibrium programs (e.g., Environmental Simulation Program, Version 6.6, and Stream Analyzer, Version 1.2). The simulations varied the amount of key components, different pH moderators (i.e., sodium hydroxide versus trisodium phosphate), pH, temperature, and pressure. The results indicated large-scale corrosion tests using a pressurized test loop were not necessary to capture the period immediately following the LOCA. Thermodynamic simulations and sensitivity analyses of key variables, including corrosion products, were developed to rank species that have a potential for causing sump-head loss through formation of precipitates. Validation of the appropriate OLI Systems, Inc., programs will be performed using available borated water literature and by comparing the program’s initial post-LOCA environment species predictions to results obtained in small-scale (e.g., autoclave) corrosion tests in a representative initial post-LOCA environment.

Larger scale corrosion testing will be conducted using facilities at UNM. Corrosion test coupon materials include zinc (galvanized steel and inorganic zinc-based coatings), aluminum, copper, carbon steel, insulation, and concrete. Relative amounts of test materials were scaled according to plant data provided by the industry based on plant surveys. Test coupons will either be fully immersed or placed above the test loop water line, but subjected to a fine spray to simulate exposure to containment spray. The relative distributions of each material were determined based on estimated percentages submerged or subjected to containment sprays following a plant LOCA. If gelatinous material is observed to develop, alternative courses of action will be considered (e.g., head-loss tests). Initial testing is expected to begin in fall 2004.

In order to address chemical effects on a plant-specific basis, licensees will initially need to evaluate whether the chemical effects test parameters are sufficiently bounding for their plant-specific conditions. If the chemical effects test parameters do not bound the plant-specific materials, licensees must provide technical justification to use any results from the chemical effects tests in their plant-specific evaluation. If chemical effects are observed during these tests, licensees will need to evaluate the sump-screen head loss consequences of this effect in an integrated manner with other postulated post-LOCA effects. In addition, a licensee choosing to modify its plant sump screens before the completion of chemical effects testing and analysis of the test results should consider the potential chemical effects to ensure that a second plant modification is not necessary in the event that deleterious chemical effects are observed during testing.

8.0 CONDITIONS AND LIMITATIONS

The guidance in the GR and in this SE is offered for all licensees of domestic PWRs for the evaluation of ECCS sump performance. However, the following conditions and limitations apply to its use:

Debris Generation

1. The destruction pressures cited in the GR for determining ZOI radii are based on air jet data and could underestimate debris quantities for a two-phase jet, as discussed in Section 3.4.2.2 of this SE. Therefore, destruction pressures based on air jet testing should be lowered by 40 percent to account for two-phase jet effects.
2. Table 3-1 of the GR provides calculated and recommended values for ZOI radii for common PWR insulation and coatings materials. The staff determined that the calculated values are nonconservative at higher destruction pressures, but the recommended values are conservative. Therefore, licensees should only use the recommended values.
3. The staff agrees with the characterization of debris in GR Section 3.4.3; however, licensees should apply insulation-specific debris size information, if possible.

Protective Coatings

1. Characterization of failed coatings with the value of 1000 psi as a destruction pressure, with a corresponding ZOI of 1 pipe diameter, is not sufficiently justified and may be nonconservative, as discussed in Section 3.4.2. Therefore, licensees should use a spherical coatings ZOI equivalent determined by plant-specific analysis, based on experimental data that correlate to plant materials over the range of temperatures and pressures of concern, or 10D.
2. The alternative offered to plant-specific data in Section 3.4.3.4 for the determination of coatings thicknesses (i.e., 3 mil equivalent of 10Z) may not be conservative and is therefore not acceptable without adequate plant-specific justification.
3. For those plants that substantiate no formation of a fibrous thin bed, the assumptions and guidance provided in the GR for coatings may be nonconservative. Therefore, for any such plant, assumptions related to coatings characterization must be conservative with regard to sump blockage. Consideration should be based upon the plant-specific susceptibility to thin-bed formation identified by the licensee. Specifically, this includes the plant-specific consideration of larger sized chips, flakes, or other form of breakdown which is realistically conservative, or use of a default area equivalent to the area of the sump-screen openings for coatings size.

Latent Debris

1. Periodic surveys that monitor changes in latent debris inventory are needed to monitor the effectiveness of cleanliness programs for supporting the overall sump-screen blockage vulnerability. The staff considers the steps presented in the GR for direct assessment of dust thickness to be impractical and unreliable, and thereby unacceptable. To provide more accurate results, statistical surface sampling should be performed in accordance with the guidance provided in this SE.

2. If a licensee chooses to take credit for a cleanliness program to account for a fractional surface area for debris accumulation, documentation should be available to verify proper implementation.

3. In addition to the three categories of miscellaneous debris discussed in the GR, the licensee should note the quantity, characteristics, and location of any failed coatings in the survey to the extent available during plant-specific walkdowns.

Transport

1. Those plants with configurations conducive to fast pool velocities should include large piece debris transport in their evaluations. The GR baseline methodology that assumes no transport of large debris to the sump screens is not adequate. A comparison of the characteristic transport velocities to typical debris transport velocities is needed to determine whether or not large piece debris transport is important.

2. Because (1) the method recommended for determining the quantity of fine debris trapped in inactive pools is oversimplified, (2) a survey of the fractions of inactive pool volumes to total sump pool water volumes is not available to better judge the potential industry-wide impact of this assumption, and (3) the comparison of the baseline methodology and a detailed analysis for the volunteer plants differed considerably; a limit on this fraction is needed to control the impact of this non-conservative methodology assumption. Therefore, the staff concludes that an upper limit on this ratio of 15 percent should be assumed, unless analyses or experimental data adequately support a higher fraction.

3. The baseline assumption that all debris in the containment bottom floor is uniformly distributed throughout the entire volume of water in containment is also not conservative. The baseline guidance made this assumption as justification for the inactive pool volume ratio, but otherwise it does not directly affect the acceptance of the baseline guidance because of the 100 percent recirculation pool transport assumption. However, should a plant subsequently perform a pool transport refinement, then this assumption would not apply and alternative approaches, such as those detailed in Appendix III to this SE, would be required.

Head Loss

1. The licensees should ensure the validity of the NUREG/CR-6224 correlation for their application of specific types of insulations and the range of parameters using the guidance provided in Appendix V to this SE.

Alternate Evaluation

1. Consistent with the principles of risk-informed decision-making in RG 1.174, the impact of the proposed change should be monitored using performance measurement strategies. Therefore, licensees should develop an implementation and monitoring plan to ensure that the evaluation conducted to examine the impact of the proposed changes continues to reflect the actual reliability and availability of the SSCs and operator actions that have been evaluated.

   This plan should include a means to do the following:

   a. Track the performance of equipment that when degraded can affect the conclusions of the licensee's evaluation (i.e., demonstration of the sump mitigative capability to meet its reliability target).

   b. Trend equipment performance after a change has been implemented to demonstrate that performance is consistent with that assumed in the traditional engineering and probabilistic analyses that were conducted to justify the change.

   c. Monitor nonsafety-related SSCs if the analyses determine those SSCs to be relied upon to meet the sump mitigative capability target reliability.

   The program should also be structured such that feedback of information and corrective actions are accomplished in a timely manner and degradation in performance is detected and corrected before plant safety can be compromised.

Downstream Effects

1. Licensees should consider that some particles larger than the flow openings in a sump screen will deform and flow through or orient axially and flow through the screen, and determine what percentage of debris would likely pass through the sump screen and be available for blockage at downstream locations.
2. Licensees should consider term of system operating lineup (short or long), conditions of operation, and mission times.
3. Licensees should consider wear and abrasion of pumps and rotating equipment, piping, spray nozzles, instrumentation tubing, and HPSI throttle valves. The potential for wear to alter system flow distribution and/or form plating of slurry materials (in heat exchangers) should be included.

4. An overall ECC or CS system evaluation should be performed considering the potential for reduced pump/system capacity resulting from internal bypass leakage or through external leakage.
5. Licensees should consider flow blockage associated with core grid supports, mixing vanes, and debris filter, and its effect on fuel rod temperature.

Chemical Effects

1. The staff has considered NEI's response and finds that licensees should address chemical effects on a plant-specific basis. Initially, licensees should evaluate whether the current chemical test parameters, which are available in the test plan for the joint NRC/Industry Integrated Chemical Effects Tests, are sufficiently bounding for their plant-specific conditions. If they are not, then licensees should provide a technical justification to use any of the results from the tests in their plant-specific evaluations. If chemical effects are observed during these tests, then licensees should evaluate the sump-screen head loss consequences of this effect. A licensee that chooses to modify its sump screen before tests are complete should consider potential chemical effects to avoid additional screen modification, should deleterious chemical effects be observed during testing.

Overall

Any analytical refinement(s) proposed in its plant-specific analysis of sump performance that is not addressed in this SE should be presented to the staff for approval.

9.0 CONCLUSION

The GR provides the PWR industry with an important tool for estimating the head loss across the licensees' ECCS sump screens based on the generation, transport, and accumulation of debris in containment and on the sump screens. The NEI approach is to provide guidance and leave certain areas to be resolved on a plant-specific basis, as opposed to providing a detailed methodology that applies to all PWRs as a standalone document (as was done for BWRs with the URG), based on the argument of variability among PWRs. NEI did little testing to support and justify assumptions made in the GR (as opposed to the approach by the BWROG to generate data that support the URG). However, the NEI guidance provides historical data, considerations, and engineering judgments that the industry can use to develop those areas not fully addressed in the GR.

The iterative process used by NEI in this GR also creates some challenges in the overall review. Although NEI has characterized this guidance as extremely conservative, the iterative process allows for the reduction of conservatisms in various areas (identified in each affected section of this evaluation) that could affect other areas of the analysis to produce larger reductions in overall conservatism than would be expected.

The staff evaluated each area of the GR, and for those areas where there was a lack of supporting data or where conservatism is questioned, the staff provides alternative guidance based on its engineering judgment and/or additional data generated in testing done mainly at LANL. These data result from testing specifically contracted by the NRC over the last 5 years as part of the GSI-191 resolution effort and involve sump performance research which was completed, but in a few cases not published, and is referenced and/or included as appendices in this document. This additional information is also intended to provide valuable insight to the industry in its effort toward evaluating plant-specific vulnerability to sump blockage and related issues.

The staff concludes that the guidance proposed by NEI, as approved in accordance with this SE, provides an acceptable evaluation methodology that establishes the necessary basis and provides the realistic conservatism for an acceptable PWR guidance document. The paragraphs below document key conclusions in each area of the analysis.

Pipe Break Characterization: The staff finds that the GR guidance is acceptable provided that each licensee adequately addresses the following two outstanding issues:

1. The GR does not provide guidance for those plants that can substantiate no thin-bed effect, which may impact head-loss results and limiting break location.
2. For plants needing to evaluate secondary-side piping, such as main steam and feedwater pipe breaks, break locations should be postulated in a manner consistent with the guidance in Section 3.3 of this SE.

To address these issues, the staff provides enhanced guidance in the appropriate sections of this SE. When the guidance provided in the GR is supplemented with the enhanced guidance offered in the SE, the staff finds this section to be acceptable.

<u>Debris Generation/Zone-Of-Influence</u>: The staff has reviewed the use of a spherical model sized in accordance with the ANSI/ANS standard and finds this approach acceptable. The spherical geometry proposed encompasses a zone which considers multiple jet reflections at targets, offset between broken ends of a guillotine break, and pipe whip.

With regard to the destruction pressures cited for determining ZOI radii, data are referenced from the BWROG URG which were determined using an air jet. However, a LOCA jet is a two-phase steam/water jet. Based on staff study of this difference and because of experimental evidence from two-phase jets, the destruction pressures based on air jets could be too high leading to an underestimation of debris quantities. Therefore, the staff maintains that destruction pressures based on air jet testing should be lowered by 40 percent to account for two-phase jet effects.

The staff's confirmatory analysis (see Appendix I to this SE) verifies the applicability of the ANSI/ANS standard for determining the size of this zone. Use of a ZOI model is identified as an acceptable approach for analyzing debris generation in accordance with RG 1.82, Revision 3. (The staff also used and reviewed this approach in the BWR sump performance SE.)

The staff finds the refinement offered in the GR which allows the application of spherical ZOIs that correspond to material-specific destruction pressures for each material that may be affected in the vicinity of a break to be acceptable.

The staff concurs with the characterization of debris in GR Section 3.4.3. Confirmatory analyses provided in Appendix II to this SE verify the acceptability of the size distributions recommended in the GR. However, the staff urges application of insulation-specific debris size information, if possible.

<u>Protective Coatings</u>: The GR treats coating debris generation separately from other debris types. The GR assumes that coating debris is generated from postulated failure (destruction) of both "DBA-qualified" and "unqualified" coatings within the ZOI, and from postulated failure of all "unqualified" coatings outside the ZOI. For coatings, the GR recommends a ZOI destruction pressure of 1000 psi, with a corresponding ZOI radius of 1 pipe diameter. The GR assumes that all coating debris will fail to a particulate size equivalent to the basic material constituent.

The staff agrees with the approach taken with regard to characterization of coatings; however, the staff considers there to be insufficient technical justification to support a value of 1000 psi as a destruction pressure with corresponding ZOI of 1 pipe diameter. The staff finds that licensees should use a coatings ZOI spherical equivalent, determined by plant-specific analysis and based on experimental data that correlate to plant materials over the range of temperatures and pressures of concern, or 10D.

With regard to the characterization of coatings in Section 3.4.3.4 of the GR, an alternative offered to plant-specific data for the determination of coatings thicknesses is an equivalent IOZ thickness of 3 mils. Because this recommended value may be nonconservative and is unsubstantiated as described in Section 3.4.3.4, the staff finds this value of 3 mils unacceptable without adequate plant-specific justification for any coatings thicknesses used. The performance of a plant-specific evaluation of the "unqualified" coatings within containment is recommended to determine realistically-conservative coating properties, including thicknesses. Further, the staff recommends that licensees incorporate into the methodology the means to periodically assess the amount of "unqualified" coating identified and used in the sump analysis to ensure the quantity remains bounding, and if nonconservative changes in the amount of "unqualified" coating occur, to evaluate the impact of this change.

In addition, for those plants that substantiate no formation of a fibrous thin bed, the assumptions and guidance provided in the GR for coatings may be nonconservative. Therefore, for any such plant, assumptions related to coatings characterization must be conservative with regard to sump blockage. Consideration must be based upon the plant-specific susceptibility to thin-bed formation identified by the licensee. Specifically, this includes the plant-specific consideration of larger sized chips, flakes, or other form of breakdown which is realistically conservative, or the use of a default area equivalent to the area of the sump-screen openings, for coatings size.

Latent Debris: The staff has reviewed the guidance provided for estimating the impact of latent debris and agrees that it is necessary to determine the types, quantities, and locations of latent debris. The staff also agrees that it is not appropriate for licensees to claim that their existing FME programs have entirely eliminated miscellaneous debris. Results from plant-specific walkdowns should be used to determine a conservative amount of latent debris in containment and to monitor cleanliness programs for compliance to committed estimates.

The staff further concludes that the guidance provided in the GR for consideration of the effects of latent debris is informative and prescriptive, but treats certain attributes in an inconsistent manner, lacks consideration of a number of surfaces and unique phenomena that enhance dust collection, and relies on an impractical and imprecise method for estimating the volume of latent debris on surfaces. This section of the SE provides alternate guidance for statistical sampling and sample analysis to allow licensees to more accurately determine the impact of latent debris on sump-screen performance. This revised approach is based on generic characterization of actual PWR debris samples. If desired, a licensee could pursue plant-specific characterization as a refinement.

Debris Transport: The staff finds that the transport guidance for small fines is conservative and acceptable; however, neglect of the large pieces and the neglect of variability and uncertainties because of a lack of data are nonconservative. Therefore, for those plants with configurations conducive to fast pool velocities, consideration of large pieces of debris is necessary. In addition, the method recommended for determining the quantity of fine debris trapped in inactive pools is oversimplified, and therefore, the acceptability of this method will be determined on a plant-specific basis, depending on whether this portion of the analysis maintains overall realistic conservatism.

Head Loss: Computation of head loss in the GR involves input of design characteristics and reflection of thermal-hydraulic conditions into a head-loss correlation (NUREG/CR-6224) that is acceptable to the staff. The licensees should ensure the validity of the NUREG/CR-6224 correlation for their application of specific types of insulations and the range of parameters using the guidance provided in Appendix V of this SE.

However, the staff finds that licensees should consider the following guidance on fibrous thin-bed formation:

- use of the appropriate density in the determination of the quantity of debris needed to form a thin bed (i.e., the as-manufactured density)
- careful evaluation of the limiting porosity for the particular particulate or mixture of particulates in the debris bed
- consideration of uncertainties in specifying a 1/8-in. bed thickness criteria (e.g., the indication that calcium silicate can form a debris bed without supporting fibers)
- consideration of other uncertainties (e.g., uncertainties associated with mixing of constituents, or uncertainties associated with latent debris data collection)

Before using the NUREG/CR-6224 correlation recommended in the GR or any other head-loss correlation, the licensees should ensure that it is applicable for the type of insulation and the range of parameters. If the correlation has been validated for the type of insulation and the range of parameters, the licensees may use it without further validation. If the correlation has not been validated for the type of insulation and the range of parameters, the licensees should validate it using head-loss data from tests performed for the particular type of insulation.

Analytical Refinements: The GR identifies three analytical topics to be included in this section debris generation, debris transport, and head loss. Section 6.0 of the GR addresses a fourth topic, break selection.

For debris generation, the GR proposes use of debris-specific ZOIs versus use of the most conservative debris type applied to all. In addition, the GR proposes use of two freely-expanding jets emanating from each broken pipe section versus use of a spherical ZOI. The staff finds both debris generation refinements to be acceptable.

For debris transport, the analytical refinements section of the GR provides two methods for computing flow velocities in a sump pool, the network method and the computational fluid dynamics (CFD) method. The staff finds both methods to be acceptable for predicting sump pool flow velocities provided the models are properly applied.

For head loss, the only refinement cited by the GR is in GR Section 3.7.2.3.2.3, “Thin Fibrous Beds,” which addresses the need for consideration of fibrous thin-bed formation, and the alternative consideration of latent debris as the primary contributor to this thin bed for all-RMI plants. However, the staff addresses consideration of thin fibrous beds in Section 3.4, “Debris Generation,” of this SE as related to the baseline, rather than as a refinement.

Therefore, the staff finds no specific refinement offered for the head-loss analysis.

Physical Refinements To Plant: Section 5.0 of the GR provides guidance for refinements in the areas of debris source term, debris transport obstructions, and screen modifications.

The staff has reviewed the debris source term refinements involving primarily enhanced housekeeping programs, insulation and/or coatings modifications, and equipment modifications, and finds them to be acceptable. However, with regard to insulation change-out or modification, the staff emphasizes that although this refinement may address maximum debris loadings on the screen, it may not address minimum loadings required to form a thin-bed effect. In addition, with regard to coatings, the statement that DBA-qualified coatings have very high destruction pressures has not been proven (see Sections 3.4.2, 3.4.2, and 4.2.2.2.3 of this SE).

The staff agrees that debris consistent with the materials listed can be effectively trapped with the use of a debris transport obstructions in optimized locations where the local velocities are less than the test results presented. The staff finds the general statements in parts of this section to provide little specific information regarding the methods for determining proper debris transport obstruction design. The lack of specific implementation strategies and simplified concepts presented would require each plant to perform a plant-specific evaluation of its proposed debris obstruction to determine it's effectiveness and structural capability under post accident conditions. To credit debris transport obstructions for trapping debris, plant-specific documentation will also be required to demonstrate an appropriate correlation to the test results in terms of debris type and velocity limits.

With regard to screen modification, the staff finds those discussed in the GR to be acceptable; however, licensees are not limited to those identified in the GR.

Alternate Evaluation: NEI has proposed an alternative evaluation approach which incorporates realistic and risk-informed elements to the PWR sump analysis, as described in Section 6.0. In considering risk-informing aspects of the resolution of GSI-191, the staff recognized that the containment sump may clog if the mitigation capability credited in the Region II analysis does not function properly. Based on the industry proposed approach in the Region II analysis, which also uses the conservative NUREG-1150 LBLOCA frequency to calculate the target reliability of the mitigation capability, and using the related generic study information, the largest LBLOCA CDF would be 1.4x10-5/year. This indicates that at a minimum the risk associated with LBLOCAs will be reduced from the current condition by nearly an order of magnitude. The staff concludes that GR Section 6.0 provides an acceptable approach for evaluating PWR sump performance. Application of more realistic and risk-informed elements is technically justified based on the low likelihood of such breaks occurring.

Sump Structural Analysis: The GR is not detailed in its presentation of criteria for sump screen performance and comparisons to predicted head loss. Therefore, the staff provides additional guidance for assurance that the ECCS sump can accommodate both the clean-screen-head loss and the debris-induced head loss associated with the limiting break, while providing adequate flow through both the ECCS injection pumps, and the CS pumps if needed. For those structural design considerations mentioned in the GR, each should be assessed for applicability on a plant-specific basis.

Upstream Effects: The GR identifies certain holdup or choke points which could reduce flow and possibly cause blockage upstream of the sump. The staff finds the guidance with respect to upstream blockage to be acceptable.

Downstream Effects: This section provides guidance on the evaluation of entrained debris downstream of the sump causing downstream blockage. Because the GR provides limited guidance on how downstream effects should be evaluated, the staff provides the following alternative guidance with regard to downstream blockage:

- Licensees should consider that some particles larger than the flow openings in a sump screen will deform and flow through or orient axially and flow through the screen, and determine what percentage of debris would likely pass through their sump screen and be available for blockage at downstream locations.
- Licensees should consider the term of system operating line-up (short or long), conditions of operation, and mission times.
- Licensees should consider wear and abrasion of pumps and rotating equipment, piping, spray nozzles, instrumentation tubing, and HPSI throttle valves. The potential for wear to alter system flow distribution and/or form plating of slurry materials (in heat exchangers) should be included.
- An overall ECC or CS system evaluation should be performed considering the potential for reduced pump/system capacity resulting from internal bypass leakage or through external leakage.
- Licensees should consider flow blockage associated with core grid supports, mixing vanes, and debris filter, and their effects on fuel rod temperature.

Chemical Effects: The staff has considered NEI's response and finds that chemical effects should be addressed on a plant-specific basis. Initially, licensees should evaluate whether the current chemical test parameters, which are available in the test plan for the joint NRC/industry integrated chemical effects tests, are sufficiently bounding for their plant specific conditions. If they are not, then licensees should provide a technical justification for the use of any results from the tests in their plant-specific evaluation. If chemical effects are observed during these tests, then licensees should evaluate the sump-screen head-loss consequences of this effect. A licensee that chooses to modify its sump screen before tests are complete should consider potential chemical effects to avoid additional screen modification, should deleterious chemical effects be observed during testing.

Overall Conclusions: The staff has reviewed the GR and finds portions of the proposed guidance to be acceptable. For those areas found to need additional justification and/or modification because of inadequate detail, lack of supporting data, or lack of analysis to support the technical basis, the staff has provided identified conditions and limitations and required modifications, including alternative guidance, to supplement the guidance in the NEI submission. The resultant combination of the NEI submission and staff safety evaluation provide an acceptable overall guidance methodology for the plant-specific evaluation of ECCS or CSS sump performance following all postulated accidents for which ECCS or CSS recirculation is required, with specific attention given to the potential for debris accumulation that could impede or prevent the ECCS or CSS from performing its intended safety functions.

10.0 REFERENCES

1 NEI, 2004a Letter from A. R. Pietrangelo, NEI to J. H. Hannon, USNRC, "Pressurized Water Reactor Sump Performance Evaluation Methodology," Nuclear Energy Institute, (proposed document number NEI 04-07) dated May 28, 2004

2 GL-04-02 NRC Generic Letter 2004-02, "Potential Impact of Debris Blockage on Emergency Recirculation During Design Basis Accidents at Pressurized-Water Reactors," dated September 13, 2004.

3 NEI, 2004b Letter from A. R. Pietrangelo, NEI to J. N. Hannon, USNRC, Transmittal of Baseline Evaluation Method, Nuclear Energy Institute, dated April 19, 2004

4 NEI, 2003 Letter from A. R. Pietrangelo, NEI to J. N. Hannon, USNRC, Transmittal of "Draft PWR Containment Sump Evaluation Methodology," Nuclear Energy Institute, dated October 31, 2003.

5 NRC, 2004a Letter from S. C. Black, USNRC to A. R. Pietrangelo, NEI, Transmittal of NRC Preliminary Review of NEI Submittal of October 31, 2003, dated February 9, 2004.

6 Mtg, 2004a Summary of Public Meeting Held March 23 and 24, 2004, Nuclear Regulatory Commission and Nuclear Energy Institute, to discuss PWR Containment Sump Evaluation Methodology and Requests for Additional Information, by Memorandum from J. G. Lamb, USNRC to L. Raghavan, USNRC, dated April 22, 2004

7 NEI, 2004c Letter from A. R. Pietrangelo, NEI to J. N. Hannon, USNRC, Nuclear Energy Institute Transmittal of Responses to Request for Additional Information of March 10, 2004, dated June 10, 2004.

8 NEI, 2004d Letter from A. R. Pietrangelo, NEI to J. N. Hannon, USNRC, Nuclear Energy Institute Transmittal of Responses to Request for Additional Information of June 28, 2004, dated July 8, 2004.

9 NEI, 2004e Letter from A. R. Pietrangelo, NEI to J. N. Hannon, USNRC, Nuclear Energy Institute Transmittal of Section 6 Revision, "Risk Informed Evaluation" of "PWR Containment Sump Evaluation Methodology," dated July 13, 2004.

10 NUREG-0897 NUREG-0897, "Containment Emergency Sump Performance," US Nuclear Regulatory Commission, dated October 1985.

11 DG-1107 Draft Regulatory Guide DG-1107, "Water Sources for Long-Term Recirculation Cooling Following a Loss-of-Coolant Accident," U. S. Nuclear Regulatory Commission, Office of Nuclear Regulatory Research, transmitted December 2002.

12 NRCB, 1994 Bulletin 93-02, Supplement 1, "Debris Plugging of Emergency Core Cooling Suction Strainers," dated February 18, 1994

13 NRCB, 1995 Bulletin 95-02, "Unexpected Clogging of a Residual Heat Removal (RHR) Pump Strainer While Operating in Suppression Pool Cooling Mode," dated October 17, 1995;

14 NRCB, 1996 Bulletin 96-03, "Potential Plugging of Emergency Core Cooling Suction Strainers by Debris in Boiling-Water Reactors," dated May 6, 1996

15 GL 85-22 NRC Generic Letter GL 85-22, "Potential for Loss of Post-LOCA Recirculation Capability Due to Insulation Debris Blockage," dated December 3, 1985

16	GSI 191	GSI-191, "Assessment of Debris Accumulation on PWR Sump Performance," prioritized September, 1996.
17	NRCB, 2003	NRC Bulletin 2003-01, "Potential Impact of Debris Blockage on Emergency Recirculation During Design-Basis Accidents at Pressurized-Water Reactors," dated June 9, 2003.
18	NUREG/CR-6762-1	NUREG/CR-6762, "GSI-191 Technical Assessment: Parametric Evaluations for Pressurized Water Reactor Recirculation Sump Performance," Vol. 1, dated August 2002.
19	NUREG/CR-6770	NUREG/CR-6770, "GSI-191: Thermal-Hydraulic Response of PWR Reactor Coolant System and Containments to Selected Accident Sequences," dated August 2002.
20	NUREG/CR-6762-3	NUREG/CR-6762, Vol. 3, "GSI-191 Technical Assessment: Development of Debris Generation Quantities in Support of the Parametric Evaluation," dated August 2002.
21	NUREG/CR-6762-4	NUREG/CR-6762, "GSI-191 Technical Assessment: Development of Debris Transport Fractions in Support of the Parametric Evaluation," Vol. 4, dated August 2002.
22	NUREG/CR-6224	NUREG/CR-6224, "Parametric Study of the Potential for BWR ECCS Strainer Blockage Due to LOCA Generated Debris," dated October 1995.
23	RG 1.82-3	Regulatory Guide (RG), Revision 3, "Water Sources for Long-Term Recirculation Cooling Following a Loss-of-Coolant Accident," dated November 2003
24	ANSI/ANS 58.2-1988	ANSI/ANS 58.2-1988, "American National Standard Design Basis for Protection of Light Water Nuclear Power Plants Against the Effects of Postulated Pipe Rupture," 1988.
25	NUREG/CR-6808	NUREG/CR-6808, "Knowledge Base for the Effect of Debris on Pressurized Water Reactor Emergency Core Cooling Sump Performance," U.S. Nuclear Regulatory Commission, February 2003.
26	URG SE	Safety Evaluation by the Office of Nuclear Reactor Regulation Related to NRC Bulletin 96-03, Boiling Water Reactor Owners Group topical Report NEDO-32686, "Utility Resolution Guidance for ECCS Suction Strainer Blockage" (Docket No. Proj0691), dated August 20, 1998.
27	URG	GE Nuclear Energy, "Utility Resolution Guide for ECCS Suction Strainer Blockage," by BWR Owners' Group, NEDO-32686-A, October 1998.
28	NUREG/CR-6369	NUREG/CR-6369, Vol 1: Drywall Debris Transport Study-Final Report; Vol 2: Drywell Debris Transport Study: Experimental Work-Final Report, February 1998.
29	NUREG/CR-6773	NUREG/CR-6773 (LA-UR-02-6786), "GSI-191: Integrated Debris-Transport Tests in Water Using Simulated Containment Floor Geometries," Los Alamos National Laboratory, December 2002.
30	CS, 2004a	C. J. Shaffer, M. T. Leonard, B. C. Letellier, J. D. Madrid, A. K. Maji, K. Howe, A. Ghosh, and J. Garcia, "GSI-191: Experimental Studies of Loss-of-Coolant-Accident-Generated Debris Accumulation and Head Loss with Emphasis on the Effects of Calcium Silicate Insulation," Los Alamos National Laboratory report LA-UR-04-1227 (April 2004).

31	MD, 2004	Mei Ding, Amr Abdel-Fattah, Stewart Fischer, Bruce Letellier, Kerry Howe, Janet Garcia, and Clint Shaffer, "Characterization of Latent Debris from Pressurized-Water-Reactor Containment Buildings," Los Alamos National Laboratory report LA-UR-04-3970 (June 2004).
32	CS, 2004b	Clinton J. Shaffer and Bruce C. Letellier, "GSI-191 Technical Study: Detailed Blowdown/Washdown Transport Analysis for Pressurized-Water-Reactor Volunteer Plant," Los Alamos National Laboratory report LA-UR-04-4338 (June 2004).
33	LA-UR-03-6415	Los Alamos National Laboratory, ADAMS Accession No. ML033230260.
34	GL-87-11	NRC Generic Letter 87-11, "Relaxation in Arbitrary Intermediate Pipe Rupture Requirements," dated June 19, 1987.
35	SRP	NUREG-0800, "Standard Review Plan," U.S. Nuclear Regulatory Commission
36	SECY-04-0037	Memorandum from A. L. Vietti-Cook, to L. A. Reyes, "Staff Requirements - SECY-04-0037 - Issues Related to Proposed Rulemaking to Risk-Inform Requirements Related to Large Break Loss-of-Coolant Accident (LOCA) Break Size and Plans for Rulemaking on LOCA With Coincident Loss-of-Offsite Power," dated July 1, 2004.
37	Mtg, 2003e	Summary of Public Meeting Held September 10, 2003, Nuclear Regulatory Commission and Stakeholders Concerning Generic Safety Issue 191, "Assessment of Debris Accumulation on PWR Sump Performance," (TAC No. MA6454) dated October 16, 2003.
38	Mtg, 2003d	Summary of Public Meeting Held July 1, 2003, Nuclear Regulatory Commission and Stakeholders Concerning Generic Safety Issue 191, "Assessment of Debris Accumulation on PWR Sump Performance," (TAC No. MA6454) dated August 11, 2003.
39	Mtg, 2003c	Summary of Public Meeting Held June 30, 2003, Nuclear Regulatory Commission and Stakeholders Concerning NRC Bulletin 2003-01, "Potential Impact of Debris Blockage on Emergency Sump Recirculation at Pressurized-Water Reactors," (TAC No. MA6454) dated August 12, 2003.
40	Mtg, 2003b	Summary of Public Meeting Held April 29, 2003, Nuclear Regulatory Commission and Stakeholders Concerning Generic Safety Issue 191, "Assessment of Debris Accumulation on PWR Sump Performance," (TAC No. MA6454) dated May 15, 2003.
41	Mtg, 2003a	Summary of Public Meeting Held March 5, 2003, Nuclear Regulatory Commission and Stakeholders Concerning Generic Safety Issue 191, "Assessment of Debris Accumulation on PWR Sump Performance," (TAC No. MA6454) dated April 24, 2003. Attachments: "Current Status and Plans Resolution of GSI-191," Accession Number ML031180084 "Update of PWR Industry Plan to Address GSI-191," Accession Number ML031180102 "NRC Comments on NEI Draft Evaluation Methodology Ground Rules," Accession Number ML031180095. "GSI-191: Analysis of Recovery Options," Accession Number ML031180119.

		"Debris Accumulation & CalSil Head Loss Testing – Findings & Preliminary Conclusions," Accession Number ML031180127. "Volunteer Plant Containment Pool Flow Analysis," Accession Number ML031180140. "Volunteer Plant (VP) ECCS Vulnerability Assessment," Accession Number ML031180154.
42	Mtg, 2003f	Summary of Public Meeting Held December 12, 2003, Nuclear Regulatory Commission and Stakeholders Concerning Generic Safety Issue 191, "Assessment of Debris Accumulation on PWR Sump Performance," (TAC No. MA6454) dated December 12, 2003.
43	Mtg, 2002a	Summary of Public Meeting Held March 28, 2002, Nuclear Regulatory Commission and Interested Stakeholders Concerning Generic Safety Issue 191, "Assessment of Debris Accumulation on PWR Sump Performance," (TAC No. MA6454), dated April 16, 2002.
44	Mtg, 2002b	Summary of Public Meeting Held May 30, 2002, Nuclear Regulatory Commission and Interested Stakeholders Concerning Generic Safety Issue 191, "Assessment of Debris Accumulation on PWR Sump Performance," (TAC No. MA6454) dated June 6, 2002.
45	Mtg, 2002c	Summary of Public Meeting Held July 2, 2002, Nuclear Regulatory Commission and Interested Stakeholders Concerning Generic Safety Issue 191, "Assessment of Debris Accumulation on PWR Sump Performance," (TAC No. MA6454) dated July 31, 2002.
46	Mtg, 2002d	Summary of Public Meeting Held August 29, 2002, Nuclear Regulatory Commission and Stakeholders Concerning Generic Safety Issue 191, "Assessment of Debris Accumulation on PWR Sump Performance," (TAC No. MA6454) dated September 5, 2002.
47	Mtg, 2002e	Summary of Public Meeting Held October 24, 2002, Nuclear Regulatory Commission, the Nuclear Energy Institute, and Interested Stakeholders Concerning Generic Safety Issue 191, "Assessment of Debris Accumulation on PWR Sump Performance," (TAC No. MA6454) dated October 31, 2002.
48	Mtg, 2002f	Summary of Public Meeting Held December 12, 2002, Nuclear Regulatory Commission and Interested Stakeholders Concerning Generic Safety Issue 191, "Assessment of Debris Accumulation on PWR Sump Performance," (TAC No. MA6454) dated December 31, 2002.
49	Mtg, 2001	Summary of July 26-27, 2001, Meeting with Nuclear Energy Institute and Industry on ECCS Strainer Blockage in PWRs, dated August 14, 2001.
50	Rao, 2001	D. V. Rao, B. Letellier, C. Shaffer, S. Ashbaugh, and L. Bartlein, "GSI-191: Parametric Evaluations for Pressurized Water Reactor Recirculation Sump Performance," Draft Technical Letter Report, Los Alamos National Laboratory, July 2001.
51	NUREG/CR-6371	Shaffer, C., W. Bernahl, J. Brideau and D. V. Rao, BLOCKAGE 2.5 Reference Manual, NUREG/CR-6371, U.S. Nuclear Regulatory Commission, December 1996.

52	NEI, 2002a	NEI 02-01, "Condition Assessment Guidelines: Debris Sources Inside PWR Containments," dated April 19, 2002.
53	NEI, 2002b	"NEI Draft Evaluation Methodology Ground Rules" dated December 12, 2002.
54	Wkshp, 2003	NRC Presentations at NEI-Sponsored Public Workshop on Debris Impact on ECCS Recirculation, July 30-31, 2003, Baltimore, MD. [NRC ADAMS Accession No. ML032230372]
55	10 CFR	Code of Federal Regulations, Title 10 "Energy"
56	SB, 2004	Letter from S. C. Black, USNRC, to A. Pietrangelo, NEI, "Nuclear Energy Institute's Proposals for Determining Limiting Pipe Break Size Used in Assessing Debris Generation Following a Design Basis LOCA (TAC NO. MC1154)," dated March 4, 2004.
57	RG 1.174	Regulatory Guide 1.174, "An Approach for Using Probabilistic Risk Assessment in Risk-Informed Decisions On Plant-Specific Changes to the Licensing Basis," dated July 1998.
58	MEB 3-1	Branch Technical Position MEB 3-1, "Postulated Rupture Locations in Fluid System Piping Inside and Outside Containment," included in NUREG-0800, "Standard Review Plan (SRP)," (Reference 2), Section 3.6.2, "Determination of Rupture Locations and Dynamic Effects Associated with the Postulated Rupture of Piping."
59	NUREG-0588	NUREG-0588, "Interim Staff Position on Environmental Qualification of Safety-Related Electrical Equipment," Revision 1, July 1981.
60	RG 1.1	Regulatory Guide 1.1, "Net Positive Suction Head for Emergency Core Cooling and Containment Heat Removal System Pumps," November 2, 1970.
61	RG 1.82-3	Regulatory Guide 1.82, "Water Sources for Long-Term Recirculation Cooling Following a Loss-of-Coolant Accident," Revision 3, November 2003.
62	GL 91-18	Generic Letter 91-18, "Information to Licensees Regarding NRC Inspection Manual on Resolution of Degraded and Non-Conforming Conditions," Revision 1, October 8, 1997.
63	ANSI/HI 1.1-1.5	ANSI/HI 1.1-1.5 - 1994, "American National Standard for Centrifugal Pumps for Nomenclature, Definitions, Application and Operation."
64	OPG, 2001	Ontario Power Generation, "Jet Impact Tests—Preliminary Results and Their Applications," N-REP-34320-10000-R00, April 2001.
65	NIS96	National Institute of Standards and Technology, standard reference database 10, version 2.11, 1996.
66	WEI83	Weigand, G. G., et al., "Two-Phase Jet Loads," NUREG/CR-2913, Sandia National Laboratory (prepared for the U.S. Nuclear Regulatory Commission) January 1983.
67	DIN04	Ding, M., et al., "Characterization and Head-Loss Testing of Latent Debris from Pressurized-Water-Reactor Containment Buildings," prepared for the U.S. Nuclear Regulatory Commission by Los Alamos National Laboratory, LA-UR-04-3970, August 2004.

68	NUREG/CP-0152 Vol. 5	Proceedings of the Eighth NRC/ASME Symposium on Valve and Pump Testing, paper titled "Design, Testing and Implementation of Modifications to the Davis-Besse HPI Pumps for Debris Laden Water Operation" by Robert Coward and Stephen Kinsey, July 12, 2004, MPR Associates and Robert Schrauder, John O'Neill and Stephen Osting, First Energy Nuclear Operating Company.
69	TIA 2003-04	Task Interface Agreement (TIA) No. 2003-04, Tac No. MC0584, "Evaluation of Davis-Besse Modifications to the High Pressure Injection Pump and Associated Mock-up Testing," dated February 11, 2004.
70	IN 96 – 27	NRC Information Notice 96-27, "Potential Clogging of High Pressure Safety Injection Throttle Valves During Recirculation," dated May 1, 1966.
71	IN 93 – 34	NRC Information Notice 93-34, "Potential for Loss of Emergency Cooling Function Due to a Combination of Operational and Post-LOCA Debris in Containment," dated April 26, 1993.
72	IN 93-34S1	NRC Information Notice 93-34, Supplement 1, "Potential for Loss of Emergency Cooling Function Due to a Combination of Operational and Post-LOCA Debris in Containment," dated May 6, 1993.

REVIEW OF NEI GUIDANCE APPENDICES

Review of Appendix A, "Defining Coating Destruction Pressures and Coating Debris Sizes for DBA-Qualified and Acceptable Coatings in Pressurized Water Reactor (PWR) Containments"

The Appendix A test program outlined the industry's effort to determine the minimum coating destruction pressure and provide information relative to coating debris sizes generated from within the zone of influence (ZOI). Testing used high-pressure water to determine the jet effect on qualified coatings. A 3500-psig high-pressure washer with a heated reservoir was used to simulate the loss-of-coolant accident (LOCA) jet. The test lasted 60 seconds. A 15-degree waterjet tip and angles of attack directing the waterjet normal to the surface and at 45 degrees to the surface were used from multiples distances. Surface temperatures were measured during testing and ranged from 80 °F to 150 °F. Coatings were applied to both steel and concrete substrates. The coating systems are characterized as untopcoated inorganic zinc (steel substrate only), inorganic zinc primer with epoxy topcoat (steel substrate only), and a self-priming epoxy, all of which are representative of coating systems currently employed as qualified systems in power plants.

Testing concluded that erosion was the primary mode of coating degradation from interaction with the waterjet in all test cases. The untopcoated inorganic zinc coating failed at a distance up to 3 times greater than the epoxy. The industry concluded that a damage pressure of 333 psig for untopcoated inorganic zinc and 1000 psig for epoxy systems should be used as the corresponding coating destruction pressures. Testing showed that an elevated surface temperature impacted the amount of coating degradation and increased fluid jet temperature resulted in coating degradation at lower jet pressures.

The test program was a good first attempt to define the destruction pressure and debris characteristics associated with LOCA jet interaction with qualified coatings. There appears to be few, if any, other test data available which attempt to define the impingement effects of a LOCA jet on coatings. The guidance report (GR) identifies this lack of data. The test protocols used in the past and as currently specified in American Society for Testing and Materials D3911 to design-basis accident (DBA)-qualify coatings for nuclear service specifically prohibits fluid impingement onto the coated sample surface. The staff believes that the Appendix A test did provide valuable information by identifying erosion as a destruction mechanism for coatings and that the debris size would be characteristic of the basic material constituent under the conditions modeled during the test. The staff also believes that the test illustrated the effect that temperature plays in coating degradation. However, the staff's position is that the test did not provide sufficient justification supporting the destruction pressures and corresponding ZOI identified in the GR. No method was provided which could be used to correlate the waterjet test conditions with LOCA jet conditions. No test data were offered combining both the effects of mechanical insult and elevated temperatures (LOCA initial conditions), nor were data provided on the effects of rapid thermal transients or pressure shock on the performance of qualified coatings. Therefore, the staff found the waterjet testing to be inconclusive.

The staff believes that a test program should be considered which will accurately estimate the coating ZOI based upon a representative LOCA jet (pressure and temperature) interacting with surfaces covered by qualified coatings. Such a test should combine the erosion effects of a water-laden steam jet with the combined thermal and pressure transients associated with a LOCA. Testing should use coatings that can be correlated to qualified plant coatings, includingcoating aged to account for the effects of normal plant operation and the effects of radiation exposure. Provisions should also be established for characterization of coating debris and assessment of the failure mechanism. Such testing could lead to an understanding that debris may be generated in forms other than small particulate from erosion, which may ultimately lead to a more realistic assessment of the coating debris contribution.

Review of Appendix B, "Example of a Latent Debris Survey"

Appendix B to the GR provides a simplified example of a method for determining the amount of latent debris on containment surfaces. Appendix B does not contain new or unique information and is not totally consistent with Section 3.5 of the GR, which contains the detailed guidance for evaluating Latent Debris. In the evaluation of Section 3.5, the staff provides a more comprehensive and accurate method for evaluation of Latent Debris. As such, a separate evaluation of this appendix is not required.

Review of Appendix C, “Comparison of Nodal Network and CFD Analysis”

The staff has reviewed the Appendix C comparison between the nodal network and computational fluid dynamics (CFD) methods.

The staff agrees with the GR statement that the network method does not attempt to analyze the movement of debris during filling operations. The staff recommends CFD simulation to characterize the hydraulic flow conditions of the sump pool formation needed to estimate debris transport due to sheeting flow across the sump floor, which has been observed to effectively transport debris.

The staff agrees with the GR statement that the network method does not calculate turbulent effects or vertical velocities. The GR offers discussion of vertical and horizontal turbulent velocities to support debris transport estimates. The GR also offers a cone-of-influence model emanating from a point source for estimating transport velocities from the point source. The staff recommends CFD simulations to characterize sump pool turbulence, which affects debris suspension and potential debris erosion, and for estimating velocities from the various water entrance locations. Turbulence is a general term representing turbulent velocity fluctuations that are not adequately represented by bulk flow velocities as described in the GR. Typical CFD codes have models to describe turbulence that address localized complex flow interactions, e.g., inertial effects. The cone-of-influence model assumes uniform spreading of the flow from a source point, which does not represent the complex flows illustrated in GR Figure 4-4.

and finds that the conclusion of a “good comparison” is not supported by independent analysis and evaluations. The error values reported are computed by subtracting flow rates of the nodal network from the CFD and dividing by the total flow in the containment pool. The flows computed for the network sections are approximately 1000 gpm (order of magnitude). The total flow is 21,000 gpm, more than an order of magnitude larger than the individual flow rates, and almost two orders of magnitude larger than the flow difference between the two methods. The staff does not consider this approach a valid method for comparing nodal network results to those achieved with CFD analysis.

The staff finds that normalizing the flow error between the two methods by the total recirculation flow rate is incorrect and minimizes the significance of the errors between the two methods. Particles/debris respond to local velocities, not normalized values. Comparison of the nodal values to the CFD values shows that there is quite a discrepancy in the associated local velocity values and that discrepancies can also exist with respect to flow direction.

In addition, in the information presented in the GR, it is not clear how the flow channels were selected. In Figure 4-4 of the GR, the flow channels were determined by using the CFD analysis and essentially encapsulating the high-velocity regions. Where the velocities are uniform across the channel, the comparison is fairly good in absolute terms, but not their “error” terms. When there is a gradient of velocity across the channel, the difference in the CFD versus nodal network velocity is quite large. Without the CFD analysis, the GR does not provide guidance for selecting the channel network. Even when the CFD results are known, the nodal network does not give a reasonable answer. The staff finds that relying on such a method for general use, where the flows are not known *a priori*, is a difficult method to implement.

Appendix C does not provide a reference for the nodal analysis method used, nor does the document explicitly define the method. It does discuss friction factors, choosing a velocity for the Reynolds number assumed for the flow, and iterating to arrive at the correct velocity, but it does not provide any equations or methodology to follow. The appendix should include these conditions and cite appropriate references for both the methodology and previously published applications to this type of flow problem.

Other issues the staff identified in Appendix C include the following:

- Figure 4-4 shows the nodal sections, but no description of how the CFD flow rates were calculated.

- Figure 4-4 is not a "composite" of the CFD results; it is exactly the case for a large LOCA break in the lower-right quadrant, not a composite of all break locations and flows.

-

Review of Appendix D, "Isobar Maps for Zone of Influence Determination"

The staff evaluation of GR Section 3.4.2.2 compared the ZOI isobars set forth in Appendix D of the GR with isobars independently calculated using the methodology of American National Standards Institute/American Nuclear Society (ANSI/ANS) 58.2-1988. The comparison showed good agreement between the calculations for downrange behavior (Zone 3), but discrepancies exist in Zones 1 and 2. As indicated in Figure 3-1 of this safety evaluation report (SER), it appears that contour termination points on the centerline are not accurate and that the quadratic behavior of the Zone 2 isobar equations is not implemented correctly. These differences will have a negligible effect on volume integrals for jet pressures less than 20 psig but may become more of a concern for higher pressures near the break. To quantify the magnitude of the difference, Table D-1 presents a comparison of ZOI radii computed from both methods. In particular, the GR approach may not have preserved the system stagnation pressure throughout the volume of the liquid core region as specified by the standard. However, in application of the calculated values as documented in Table 3-1 of the GR, the recommended value of 1.0 is provided for both the 1000 and 333 psig destruction pressures. The staff considers that using the recommended value of 1.0 is necessary for these pressures for a conservative treatment.

Table D-1 Comparison of Computed Spherical ZOI Radii from Independent Evaluations of the ANSI Jet Model

Impingement Pressure (psig)	ZOI Radius/Break Diameter	
	Guidance Report	SER Appendix I
1000	0.24	0.89[a]
333	0.55	0.90
190	1.11	1.05
150	1.51	1.46
40	3.73	4.00
24	5.45	5.40
17	7.72	7.49
10	12.07	11.92
6	16.97	16.95
4	21.53	21.60

[a] The core volume at stagnation pressure P0 gives a minimum possible ZOI radius of 0.88 diameters.

Review of Appendix E, "Additional Information Regarding Debris Head Loss"

The GR Appendix E contains additional information regarding the estimation of head loss associated with debris beds. The supporting Appendix E repeats the text found in Section 4.2.5 and provides tables that summarize available domestic and international head-loss testing and results. No head-loss refinements are offered other than those given in Section 3.7.2.3.2.3. (See SER Section 3.7.2.3.2.3, "Thin Fibrous Beds," for the staff evaluation of that section.)

Confirmatory Appendices

APPENDIX I

ANSI/ANS JET MODEL

I.1 Introduction

Debris generation is the first chronological step in the accident sequence for a postulated high-energy line break. In the idealized case of a double-ended guillotine break (DEGB), high-temperature, high-pressure reactor-cooling fluid may be ejected (from both sides of the broken pipe) that impinges on structures, equipment, piping, insulation, and coatings in the vicinity of the break. The degree of damage induced by the break jets is specific to the materials and structures involved, but the size and shape of the expanding jets and the forces imparted to surrounding objects depend on the thermodynamic conditions of the reactor at the location of the rupture. To maximize the volume of the damage zone (i.e., the zone of influence [ZOI]), it is conservative to consider free expansion of the break jet to ambient conditions with no perturbation, reflection, or truncation by adjacent structures. Spatial volumes of damage potential, as defined by empirical correlations of local jet pressure and observed damage, for example, can then be integrated over the free-jet conditions and remapped into convenient geometries, such as spheres or cones, which approximate the effects of congested reflection without crediting the associated shadowing, jet dispersion, and energy dissipation.

Appendices B, C, and D to the American National Standards Institute (ANSI) guidance for the protection of nuclear power plants against the effects of pipe rupture (ANS88) present one reasonably accessible model for computing pressure contours in an expanding jet. The ANSI model was used for the evaluation of potential damage volumes in the resolution of the boiling-water reactor (BWR) strainer-blockage study (URG96, NRC98). A similar approach suggested for this analysis by ANS88 is a jet model developed at Sandia National Laboratories (WEI83). Both the ANSI and the Sandia models were developed specifically for assessing structural loadings on relatively large targets near the jet centerline, so neither offers a true estimate of local pressures within a freely expanding jet. However, these models can be used with appropriate caution to learn a great deal about the spatial extent of and the thermodynamic conditions present within a high-energy jet.

This appendix presents the equation set needed to evaluate the ANSI model describing two-phase expansion of a jet from a broken high-energy line in a pressurized-water reactor (PWR). To ensure a conservative review of the guidance report (GR), only the conditions related to full separation and full radial offset of a DEGB are developed. The standard presents alternative equations for partial offsets and for longitudinal tears. This discussion is offered to resolve some of the confusion present in the notation of the standard and to provide a self-consistent basis for interpreting computational results relevant to PWR-break conditions. The complexity of the jet model is somewhat beyond the scope of manual evaluation, but several investigators have performed successful spreadsheet calculations for discrete conditions. This appendix used routines (available in ADAMS document ML042640274) developed in MATLAB and FORTRAN for evaluating the jet model as a further guide to implementation and for critical review;

however, this appendix does not provide routines obtained from the National Institute of Standards and Technology (NIST) for evaluating thermodynamic state points.

I.2 Jet-Model Features and Applicability

Despite the apparent complexity of the equation set needed to evaluate the ANSI jet model, it is based on relatively few thermodynamic assumptions and limited comparisons with experimental observation. The bulk of the analytic detail supplies a geometric framework for interpolating jet pressures between assumed or observed transition points. Figure I-1 presents a sample calculation of jet pressure contours for a cold-leg DEGB. Although this calculation represents a relevant bound for evaluation of the GR, to be discussed later, the figure will be used first to introduce geometric features of the model.

The ANSI jet model subdivides the expanding jet into three zones that are delineated by dashed lines in Figure I-1. Zone 1 contains the core region, where it is assumed that liquid extrudes from the pipe under the same stagnation conditions as the upstream reservoir (interior red triangle). Zone 2 represents a zone of continued isentropic expansion, and Zone 3 represents a region of significant mixing with the environment, where the jet boundary is assumed to expand at a fixed, 10-degree, half angle. One group of equations from Appendix C to the standard defines the geometry of the jet envelope, and another group from Appendix D defines the behavior of internal pressure contours. Key geometry features that are determined by the thermodynamic conditions of the break include the length of the core region, the distance to the asymptotic plane between Zones 2 and 3, and the radii of the jet envelope at the transition planes between zones. At the asymptotic plane, the centerline static pressure is assumed to approach the absolute ambient pressure outside of the jet.

Jet pressures provided by the ANSI model must be interpreted as local impingement gauge pressures. This is a property of the pressure field that is relevant to the interpretation of debris generation data; however, a subtle discrepancy exists between the ANSI model predictions and the desired local pressures. Because target materials may reside anywhere within the jet, fluid impingement can occur from a range of angles. Thus, idealized measurements or calculations of free-field impingement pressure should assume that the fluid stagnates (comes to rest) nonisentropically and parallel to the local flow direction. Note that a further subtlety appears here in the distinction between the classical definition of stagnation pressure that is related to the isentropic deceleration of flow along a streamline and the impingement pressure that includes entropy losses resulting from the impact of a fluid on a physical test object. In general, impingement pressures will be higher than stagnation pressures, but the two terms may be used synonymously at times in this appendix.

In contrast to the desired local impingement pressure, the ANSI model appears to be concerned with total force loadings across relatively large objects placed near the jet centerline. Appendix D to the standard states that the pressure recovered on a target is related to the component of the flow perpendicular to the target and, because of the diverging flow in an expanding jet, the pressure distribution on a large flat target will decrease in the radial direction. The pressure equations in the standard produce exactly this effect, and a brief allusion is made to a comparison of the predicted pressures with data taken across the face of large targets placed perpendicular to the jet. The standard gives further cautionary notes against applying the pressure equations to predict forces on small objects near the edges of the jet where flow velocities are clearly not parallel to the centerline.

These attributes of the model suggest that calculated pressures represent jet impingement conditions that would be experienced in a direction parallel to the midline only. Actual streamlines in a rapidly expanding jet must have a significant radial velocity component to create the characteristic envelope shown in Figure I-1; in a sense, the predicted pressures represent only the longitudinal component of the local, momentum-dominated, total jet pressure. The implication of this interpretation is that true local impingement pressures, as measured normal to realistic flow directions in the jet, may be underestimated, particularly in Zones 1 and 2, where radial expansion is greatest.

Although a computed pressure isobar may be smaller in radius than that of the corresponding local impingement pressure that is desired for debris generation estimates, it may also be longer in the downstream direction. Comparative elongation of isobars from the jet model occurs because the entire mass flux ejected from the break is assumed to pass through the jet cross section at the asymptotic plane. Thus, the forward momentum of the jet is maximized in a manner that would be considered conservative for structural loading calculations. Unrealistic isobar elongation may also be predicted because the jet centerline pressure equation for Zone 3 is inherently unbounded; the centerline gauge pressure only falls to zero as the jet diameter grows infinitely large at infinite distance. The net effect on isobar volume of these disparities between the ANSI model and the desired free-expansion impingement pressures is impossible to quantify without a complete understanding of the experimental measurements on which the model is based; however, the mathematical properties of the pressure equations are certain to exaggerate the length, and hence the volume, of low-pressure isobars.

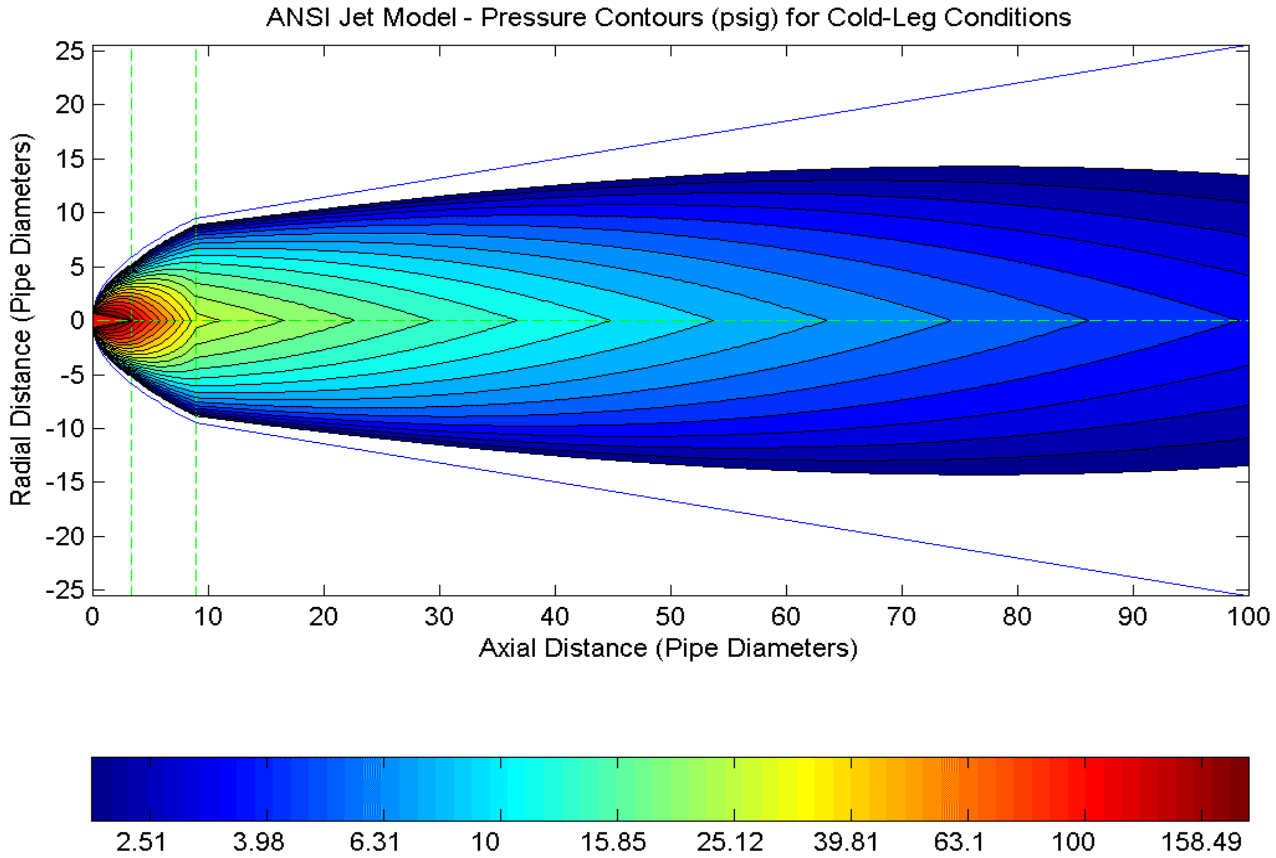

Figure I-1. ANSI Jet-Model Stagnation Pressures for PWR Cold-Leg Break Conditions (530 °F, 2250 psia)

I.3 Jet-Model Equation Set

I.3.1 Fundamentals

Equations developed in the standard frequently refer to four distinct thermodynamic state points:

(1) stagnation conditions of the fluid in the upstream reservoir denoted by subscript "0" (zero)

(2) conditions at the exit plane of the pipe denoted by subscript "e"

(3) conditions at any point in the jet denoted either with subscript "j" or with no subscript at all

(4) conditions at the asymptotic plane denoted by subscript "a"

These conventions are rigidly applied in the following development to resolve some notation inconsistencies found in the standard. Unless otherwise noted, pressures will refer to the absolute thermodynamic static pressure of the fluid. The first exception to this rule has already been mentioned—that is, the jet-pressure equations that define the local, gauge, longitudinal, and impingement pressure.

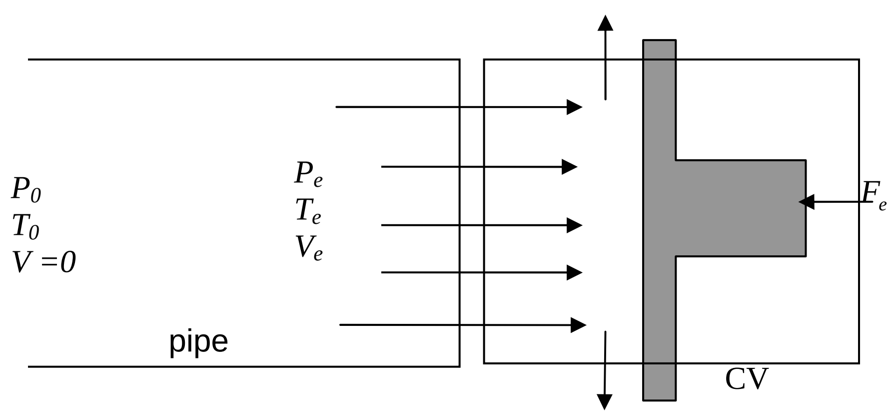

Figure I-2. Control-Volume Force Balance on a Rigid Plate near the Outlet

One of the more fundamental relations in the model is actually presented near the end of the standard in Appendix D; it defines the total thrust (force) of the jet at the outlet. If a rigid plate were placed near the outlet, as shown in Figure I-2, the force balance on a control volume (CV) must consider both the static pressures and the rate of change of momentum acting on the boundary. If mass exits the control volume in a symmetric pattern at uniform velocity, the only possible force imbalance is in the x direction. The force on a plate near the exit is then

$$F_e = P_e A_e - P_{amb} A_e + \frac{1}{g_c}\frac{d}{dt}(m_e v_e) = (P_e - P_{amb})A_e + \frac{1}{g_c}\left[\left(\frac{d}{dt}m_e\right)v_e + m_e\left(\frac{d}{dt}v_e\right)\right] \qquad \text{(I-1)}$$

where

P_e = the fluid pressure at the exit plane,

P_{amb} = the ambient pressure in containment,

A_e = the area of the break, and

m_e = the mass entering the control volume at velocity v_e.

The force-to-mass conversion factor, g_c, equals 32.2 lbm·ft/lbf·s^2 in English units. Mass enters the control volume at constant velocity $\left(\frac{d}{dt}v_e = 0\right)$ at a rate of $\frac{d}{dt}m_e = \rho_e v_e A_e$, where ρ_e is the fluid density at the exit. Thus, the total thrust generated at the exit plane is

$$F_e = (P_e - P_{amb})A_e + \frac{1}{g_c}\rho_e v_e^2 A_e \qquad \text{(I-2)}$$

Substitution of $G_e = \rho_e v_e$ for the critical mass flux crossing the exit plane yields

$$F_e = \left[(P_e - P_{amb}) + \frac{G_e^2}{g_c \rho_e}\right]A_e \qquad \text{(I-3)}$$

where the first term represents force applied by the static pressure of the fluid and the second term represents force imparted by the momentum of the fluid. The ambient pressure is often assumed to be zero to maximize the available jet thrust conservatively.

Division of equation (I-2) or (I-3) by the exit area suggests an effective, or area-averaged, jet pressure of $\overline{P}_e = F_e / A_e$. This effective pressure will be greater than the classical stagnation pressure at the exit, which is defined by Bernoulli's equation as $P_e^{stag} = P_e^{static} + \frac{1}{2g_c}\rho_e v_e^2$ because the derivation of Bernoulli's law requires that the fluid be brought to rest in an idealized, reversible manner. Jet impingement on a body is a highly anisentropic process. For an incompressible fluid, the static pressure at the exit equals the ambient pressure, and if friction losses in piping between the reservoir and the break can be neglected, the stagnation pressure at the exit equals the initial pressure. Under these conditions, Bernoulli's equation can be written as

$$\frac{1}{g_c}\rho_e v_e^2 = 2(P_0 - P_{amb}) \qquad \text{(I-4)}$$

Equations (I-2) and (I-3) are often simplified as $F_e = C_T P_0 A_e$, where P_0 is the upstream stagnation pressure and C_T is the thrust coefficient defined by comparison to be

$$C_T = \frac{1}{P_0}\left[\frac{1}{g_c}\rho_e v_e^2 + \left(P_e - P_{amb}\right)\right] = \frac{1}{P_0}\left[\frac{G_e^2}{g_c \rho_e} + \left(P_e - P_{amb}\right)\right] \quad \text{(I-5)}$$

Equation (I-5) emphasizes that the fluid properties that exist at the exit plane determine the correlation between upstream stagnation pressure and the thrust coefficient. Several alternative models are available to describe the thermodynamic transitions occurring in a high-energy fluid that is expanding and accelerating, which, in turn, determine the exit density and the critical mass flux. It is very important that the specification of C_T be consistent with the models used to evaluate G_e and ρ_e. It should be noted that the standard uses inconsistent notation for the thrust coefficient (e.g., C_T, C_{T_e}, $C^*_{T_e}$). All forms must refer to a single numeric value, if the pressure equations are to be piecewise continuous between jet zones.

Under the conditions of zero friction loss and incompressible flow (solid liquid with no vapor fraction where $P_e = P_{amb}$), equation (I-4) can be substituted into equation (I-5) to obtain a theoretical maximum value of $C_T = 2.0$ when ambient pressure is neglected. By treating steam as a perfect gas under isentropic flow to obtain the exit velocity, Shapiro (SHA53) derives a lower theoretical limit of $C_T = 1.26$. Any numeric evaluation of equation (I-5) using water property tables to derive G_e and ρ_e should be compared to these limits. Although it is clearly most conservative to apply the liquid limit for all state points, numerical evaluation of equation (I-5) using water tables is sufficiently robust to permit this refinement. Section I.4 of this appendix discusses recommendations for computing the thrust coefficient and provides convenient reference figures.

I.3.2 Jet-Envelope Geometry

The thermodynamic conditions upstream of the break dictate the shape and size of the jet envelope predicted by the ANSI model. Except where noted, spatial distances are represented in dimensionless multiples of the broken-pipe inside diameter, D_e. Jet boundaries (and pressure contours) can be scaled in this manner because the equation set is linear with respect to pipe diameter. Linearity can be proven rigorously by factoring and eliminating terms of D_e in every equation. In general, because of potential nonlinearities, it is not sufficient to evaluate a complicated dimensional equation set at a unit value of a candidate scaling parameter and then to assume that the unit result can be multiplied by any desired value of that parameter. To recover physical quantities for a particular pipe size, dimensionless distances must be multiplied by D_e, dimensionless areas must be multiplied by D_e^2, etc.

The distance of extrusion by the jet core is

$$L_c = 0.26\sqrt{\Delta T_{sub}} + 0.5 \quad \text{(I-6)}$$

where ΔT_{sub} is the degree of subcooling (°F) upstream of the break location (i.e., the difference between the saturation temperature T_{sat} at the system pressure P_0 and the system temperature T_0). The interior red triangle in Figure I-1 shows the jet core. Note that L_c takes on a value of 0.5 for saturated or superheated conditions. In addition, if $L_c > L_a$, then the distance to the asymptotic plane defined below, L_c should be set to zero and the jet pressure should be assumed to be uniform across the break area at a value of $\overline{P}_j = \left(F_e / A_e\right)/C_T$, where the ratio F_e / A_e is computed from equation (I-2) or (I-3). This can occur for low-pressure nonexpanding jets. A jet can be treated as nonexpanding when the initial temperature of a liquid reservoir is less than the saturation temperature at P_{amb} or the initial pressure of a gas reservoir is equal to ambient pressure, $P_0 = P_{amb}$.

The diameter of the jet at the exit plane is defined to be

$$D_{je} = \sqrt{C_T} \tag{I-7}$$

which is slightly larger than the diameter of the pipe because $1.26 \le C_T \le 2.0$.

The diameter of the jet at the asymptotic plane (Zone 2 to Zone 3 boundary) is defined by the relation

$$D_a^2 = \frac{G_e^2}{g_c \rho_a C_T P_0} \tag{I-8}$$

where ρ_a is the homogeneous fluid density at the centerline distance to this plane, which is given by

$$L_a = \frac{1}{2}\left(D_a - 1\right) \tag{I-9}$$

Note that some care must be taken to keep pressure and mass flux dimensionally consistent in equation (I-8). The density ρ_a is to be evaluated at a state point defined by the system enthalpy h_0 and an asymptotic-plane static pressure defined by

$$P_a = \left\{1 - 0.5\left(1 - \frac{2P_{amb}}{P_o}\right) f\left(h_o\right)\right\} P_{amb} \tag{I-10}$$

where

$$f\left(h_0\right)=\sqrt{0.1+\frac{h_o-h_f}{h_{fg}}} \text{ for } \frac{h_o-h_f}{h_{fg}}>-0.1, \text{ and } f\left(h_0\right)=0 \text{ otherwise.} \tag{I-11}$$

Within the condition stated by equation (I-11), h_f and h_g are the saturated fluid enthalpy and saturated vapor enthalpy at P_0, respectively, and $h_{fg} = h_g - h_f$ is the heat of vaporization. Further conditions on equation (I-10) are that if the ratio $P_{amb} / P_0 > 1/2$, then it should be set equal to 1/2 and that, as a static pressure, $P_a \geq 0$.

The first criterion on $f\left(h_0\right)$ simply checks whether the initial quality $x_0 = \dfrac{h_o - h_f}{h_{fg}}$ is greater than negative 10 percent. When considered as a whole, these conditions imply that $0 \leq P_a \leq P_{amb}$. If the initial fluid is more than 10 percent subcooled, the jet static pressure equals ambient pressure at the asymptotic plane. If the jet is less than 10 percent subcooled, the jet static pressure at the asymptotic plane can be lower than ambient pressure. Equation (I-10) suggests that the asymptotic plane is placed at the distance where the jet static pressure approaches ambient pressure. The distance to this plane given by equation (I-9) may simply have been chosen by geometric comparison with observed jets.

The state point defined by the asymptotic pressure P_a and the system enthalpy h_0 may be a two-phase condition. In this case, it is necessary to evaluate the asymptotic density ρ_a using the quality $x_a = \dfrac{h_o - h_{fa}}{h_{ga} - h_{fa}}$, where h_{fa} and h_{ga} are the saturated fluid and vapor enthalpies at P_a, respectively. Then, $\rho_a = \left[\dfrac{x_a}{\rho_{ga}} + \dfrac{1-x_a}{\rho_{fa}}\right]^{-1}$, where ρ_{fa} and ρ_{ga} are the saturated fluid and vapor densities at P_a, respectively. Automated steam tables generally give mixture densities directly for a two-phase state point, so this complication may be unnecessary.

The similarity of terms in equation (I-8) to the force-balance equations derived in the previous section suggests a different interpretation for the asymptotic plane. For convenient reference, the jet diameter at the asymptotic plane is again given by

$$D_a^2 = \frac{G_e^2}{g_c \rho_a C_T P_0} \tag{I-12}$$

Given the discussion following equation (I-3) and the definition of the thrust coefficient, the factors $C_T P_0$ in equation (I-12) are immediately recognized as $\overline{P}_e = F_e / A_e$, the average total jet pressure at the exit. If a relation similar to equation (I-3) is written to describe the area-averaged pressure across the jet cross section at the asymptotic plane,

$$\overline{P}_a = \frac{F_a}{A_a} = \left[\left(P_a - P_{amb} \right) + \frac{G_e^2}{g_c \rho_a} \right] \tag{I-13}$$

then the term $G_e^2 / g_c \rho_a$ in equation (I-12) is recognized to be $\overline{P}_a - \left(P_a - P_{amb} \right)$. If the static pressure at the asymptotic plane P_a is not much different than the ambient pressure P_{amb}, then equation (I-12) reduces to the ratio of average pressures computed over the jet cross section at the asymptotic plane and over the jet cross section at the exit,

$$D_a^2 = \frac{F_a / A_a}{F_e / A_e} = \frac{\overline{P}_a}{\overline{P}_e} \tag{I-14}$$

Writing explicitly the definition of the dimensionless asymptotic-plane area as $D_a^2 = \frac{A_a}{A_e}$ illustrates that the diameter of the jet given by equation (I-8) has been chosen at the point where the ratio of average pressures approaches the ratio of cross sectional areas, and for this to be true, the total force across each area must be the same. Hence, the ANSI model implicitly assumes that the jet force available at the outlet is conserved across the jet cross section at the asymptotic plane. At this distance, the jet is presumed to begin interacting with the environment.* This development also shows that the ANSI model projects the entire mass flux across the asymptotic plane rather than following more realistic streamlines across the jet boundary in Zones 1 and 2. Section I.4 derives equation (I-8) more rigorously to further emphasize these points.

The remainder of the jet envelope is simply interpolated as a function of centerline distance *L* between the transition diameters discussed above. Within Zone 1, the diameter of the jet core is given by

$$D_c = \sqrt{C_T} \left(1 - \frac{L}{L_c} \right) \tag{I-15}$$

For Zones 1 and 2 $\left(0 < L \le L_a \right)$, the jet diameter is given by

$$D_j^2 = \left[1 + \frac{L}{L_a} \left(\frac{D_a^2}{D_{je}^2} - 1 \right) \right] D_{je}^2 \tag{I-16}$$

* This observation was derived from the jet equations and is not expounded as part of any derivation in the standard. It is simply an implication of the definitions.

In Zone 3 $(L > L_a)$, the jet diameter expands at a 10-degree half angle beginning from the diameter at the asymptotic plane. The Zone-3 diameter is specified by

$$D_j^2 = \left[1 + \frac{2(L - L_a)}{D_a}\tan(10°)\right]^2 D_a^2 \quad . \tag{I-17}$$

I.3.3 Jet Pressures

Pressure contours also appear to be interpolated from a limited number of geometric reference points, but the basis for this interpolation is not evident from the standard. It can be shown that all equations are piecewise continuous at the separation planes between zones; however, no effort was made to match first-derivative slopes. This deficiency admits the possibility of “kinks” in the contours, as observed in Figure I-1 across the boundary between Zones 2 and 3. Pressure contours in Zone 1 $(0 \le L \le L_c)$ depend on the following discriminant. If

$$D_j^2 + 2D_j D_c + 3D_c^2 \le 6C_T \, , \tag{I-18}$$

then the jet pressures are given as a function of radius $(r_c < r \le r_j)$ for jet diameters $D_j = 2r_j$ as

$$P_j = \left(\frac{D_j - 2r}{D_j - D_c}\right)\left[1 - \frac{2\left(D_j^2 + D_j D_c + D_c^2 - 3C_T\right)}{D_j^2 - D_c^2}\left(\frac{2r - D_c}{D_j - D_c}\right)\right]P_0 \, . \tag{I-19}$$

Otherwise,

$$P_j = \left(\frac{D_j - 2r}{D_j - D_c}\right)^2\left[\frac{6\left(C_T - D_c^2\right)}{\left(D_j - D_c\right)\left(D_j + 3D_c\right)}\right]P_0 \, . \tag{I-20}$$

It is important to note that the leading term $(D_j - 2r)$ vanishes in both equations (I-19) and (I-20) as the radius approaches the jet envelope where the absolute pressure equals P_{amb}. Therefore, evaluations of P_j must be interpreted as gauge pressures. In equation (I-19), the term $\left(\frac{2r - D_c}{D_j - D_c}\right)$ ensures that the jet pressure matches P_0 on the boundary of the core. Equation (I-20) provides no similar constraint, so there will be a sharp discontinuity in pressure at the boundary of the jet core when this condition is invoked, as shown in Figure I-1. Equations (I-19) and (I-20) were not intended to be evaluated inside of the core region. Within the core, the system stagnation conditions are presumed to hold.

In Zones 2 and 3, jet pressures are parameterized in terms of the jet centerline pressure P_{jc}. In Zone 2 $\left(L_c < L \le L_a\right)$,

$$P_{jc} = \left\{ F_c - \left(F_c - \frac{3C_T}{D_a^2} \right) \frac{L_a}{L} \frac{\left(L - L_c\right)}{\left(L_a - L_c\right)} \right\} P_0 , \tag{I-21}$$

where the parameter $F_c = 1.0$, if $D_j^2 \le 6C_T$ at distance L_c, and $F_c = 6C_T / D_j^2$ otherwise. When $L = L_c$, equation (I-21) reduces to $P_{jc} = F_c P_0$. If $F_c = 1.0$, the centerline pressure will match the assumed pressure in the core region, but otherwise, there will again be a discontinuity. Given the centerline pressure, jet pressures in Zone 2 are specified by

$$P_j = \left(1 - \frac{2r}{D_j}\right) \left\{ 1 - 2\left(\frac{2r}{Dj}\right) \left[1 - \frac{3C_T}{D_j^2} \frac{P_0}{P_{jc}} \right] \right\} P_{jc} . \tag{I-22}$$

It can be shown by integration that equation (I-22) is essentially a geometric rather than physical condition—it leads to full recovery of the jet force anywhere in Zone 2 regardless of the value assigned to the jet diameter. In Zone 3, centerline pressures are given by

$$P_{jc} = \frac{3C_T P_0}{D_a^2 \left[1 + \frac{2\left(L - L_a\right)}{D_a} \tan\left(10^\circ\right) \right]^2} \tag{I-23}$$

and jet pressures are given by

$$P_j = \left(\frac{D_j - 2r}{D_j} \right) P_{jc} . \tag{I-24}$$

Pressures on the transition between Zones 2 and 3 are piecewise continuous, including on the centerline.

I.3.4 Pressure-Contour Characteristic Equations

Equations presented in the previous section can be used to evaluate longitudinal impingement pressures at any location in the jet. However, in the present forms, they are not particularly convenient for identifying geometric characteristics, such as isobar boundaries. Similarly, when numerically computing volumes under a given isobar, it is convenient to know the downstream range of the contour, which always begins at $L = 0$ and terminates in a cusp on the centerline at some distance, $L = L_t\left(P_j\right)$. The ANSI standard does not develop the relationships presented in this section; they are offered to facilitate some of the many practical details involved with implementing the standard.

Figure I-1 illustrates the typical behavior of jet-pressure isobars generated by the ANSI model. The isobars outlined in black represent lines of constant pressure that can be found by solving the pressure equations (I-19), (I-20), (I-22), and (I-24) for the radii at a constant pressure, P_j. The jet diameter, D_j, implicitly specifies the downstream distance L. Each pressure equation can be reduced to a general quadratic expression for the radius of the form $Ar^2 + Br + C = 0$.

The coefficients from equation (I-19) for Zone 1 are

$$A = 4H\ ,\quad B = -2\left[1 + H\left(D_j + D_c\right)\right], \text{ and } C = D_j + HD_jD_c + \left(D_c - D_j\right)\frac{P_j}{P_0}\,, \qquad \text{(I-25)}$$

where

$$H = 2\frac{\left(D_j^2 + D_jD_c + D_c^2 - 3C_T\right)}{\left(D_j^2 - D_c^2\right)\left(D_j - D_c\right)}. \qquad \text{(I-26)}$$

The coefficients from equation (I-20) for Zone 1 are

$$A = 4\,,\ B = -4D_j\,, \text{ and } C = D_j^2 - \left(D_j - D_c\right)^2\frac{P_j}{P_0}I\,, \qquad \text{(I-27)}$$

where

$$I = \frac{6\left(C_T - D_c^2\right)}{\left(D_j - D_c\right)\left(D_j + 3D_c\right)}. \qquad \text{(I-28)}$$

A special case occurs in Zone 1 at $L = 0$, where $D_j = D_c$ and $r = D_j/2 = D_c/2$ for all P_j.

Equation (I-22) yields the following coefficients for Zone 2:

$$A = 8\frac{J}{D_j^2}\,,\ B = -\left(\frac{2}{D_j} + \frac{4J}{D_j}\right), \text{ and } C = 1 - \frac{P_j}{P_{jc}}\,, \text{ where } J = \left(1 - \frac{3C_T}{D_j^2}\frac{P_0}{P_{jc}}\right). \qquad \text{(I-29)}$$

Finally, equation (I-24) yields the following coefficients for Zone 3:

$$A = 0\,,\ B = -2/D_j\,, \text{ and } C = 1 - \frac{P_j}{P_{jc}}. \qquad \text{(I-30)}$$

The analytic solution for the radius in Zone 3 is

$$r = \frac{1}{2} D_j \left(1 - \frac{P_j}{P_{jc}} \right). \tag{I-31}$$

The sharp tip of each contour shown in Figure I-1 is another nonphysical feature of the ANSI model that arises from a lack of attention to matching spatial first derivatives. It might be expected that each isobar is smoothly bounded and has infinite slope at the terminal point, especially at very low pressures where the jet returns to ambient conditions. It is helpful to know the distance to the terminal point of each contour for iterative integration of spatial volumes. These points can be found by solving the centerline pressure equations (I-21) and (I-23) for distances L_t corresponding to the desired pressure. Note that Zone 1 has no terminal points except for the jet core.

For Zone 2, equation (I-21) yields the relation

$$L_t = \frac{L_c}{1 - \frac{L_a - L_c}{R L_a} \left(F_c - \frac{P_j}{P_0} \right)}, \tag{I-32}$$

where

$$R = F_c - \frac{3 C_T}{D_a^2}, \tag{I-33}$$

and for Zone 3, equation (I-23) yields the relation

$$L_t = \frac{1}{2} \left[\left(\frac{3 C_T P_0}{D_a^2 P_j} \right)^{1/2} - 1 \right] \frac{D_a}{\tan(10°)} + L_a. \tag{I-34}$$

One remaining practicality is the numerical integration of pressure isobars defined by equations (25), (27), (29), and (31). If these equations are evaluated at a set of discrete distances, L_i, the corresponding radii, r_i, define adjacent conical frusta with unique slopes, as shown in Figure I-3. The analytic formula for the frustum of a cone is given by

$$V_i = \pi \left[\frac{1}{3} m_i^2 L^3 + m_i \left(r_{i+1} - m_i L_{i+1} \right) L^2 + \left(m_i^2 L_{i+1}^2 - 2 r_{i+1} m_i L_{i+1} + r_{i+1}^2 \right) L \right]_{L_i}^{L_{i+1}} \tag{I-35}$$

where the linear slope of the sides of the conical segment is $m = \frac{r_{i+1} - r_i}{L_{i+1} - L_i}$. The total volume under the isobar is approximated by the sum $V_{isobar} = \sum V_i$ and can be refined to any desired accuracy by evaluating the pressure-isobar equations at finer resolution.

The total volume of an isobar should be multiplied by a factor of 2 when double-ended breaks of equivalent upstream pressure are considered and, finally, converted to a volume-equivalent sphere by the formula

$$R_{sphere} = \left(\frac{3}{4\pi} V_{isobar} \right)^{1/3} . \tag{I-36}$$

I.4 Derivation of Asymptotic-Plane Area

To obtain equation (I-8) for the jet diameter D_a at the asymptotic plane, a force balance is applied to the control volume shown in

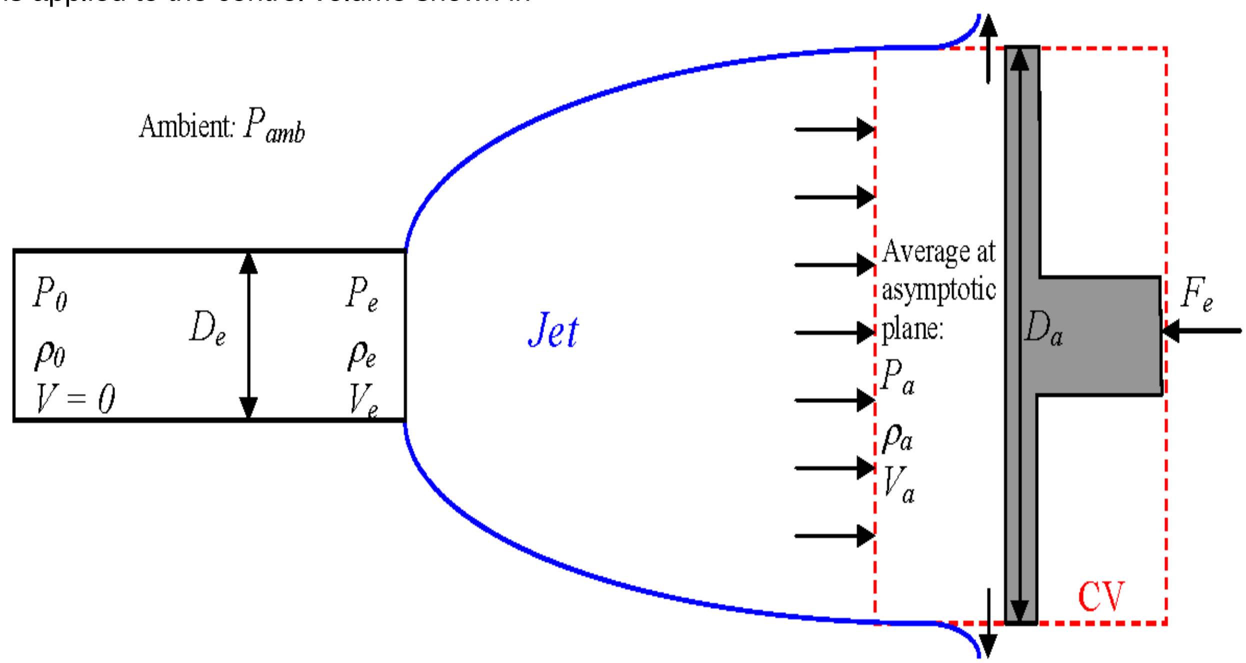

Figure I-4 in a manner analogous to the derivation of the thrust force given by equation (I-2). In the figure, a plate is positioned normal to the flow at the asymptotic plane. The force required to hold the plate in static equilibrium is notated F_e. The fluid deflected by the plate is assumed to exit the control volume isotropically in a plane oriented parallel to the face of the plate.

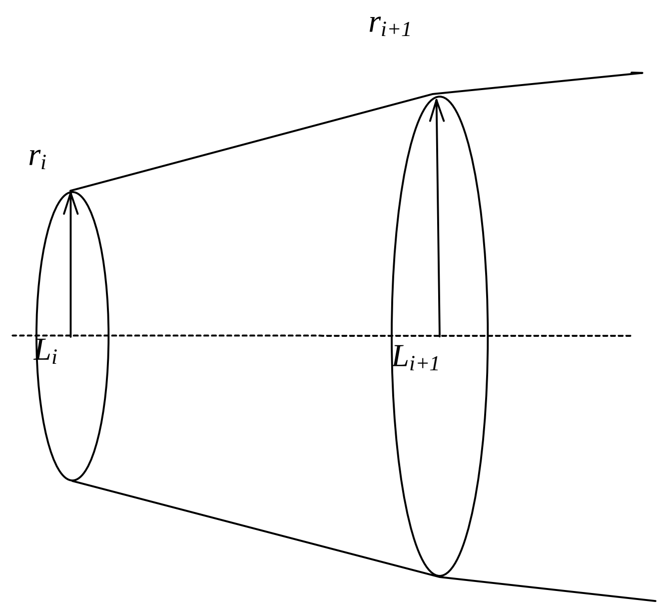

Figure I-3. Linear Segmentation of Jet Cross Sections for Numerical Volume Integration

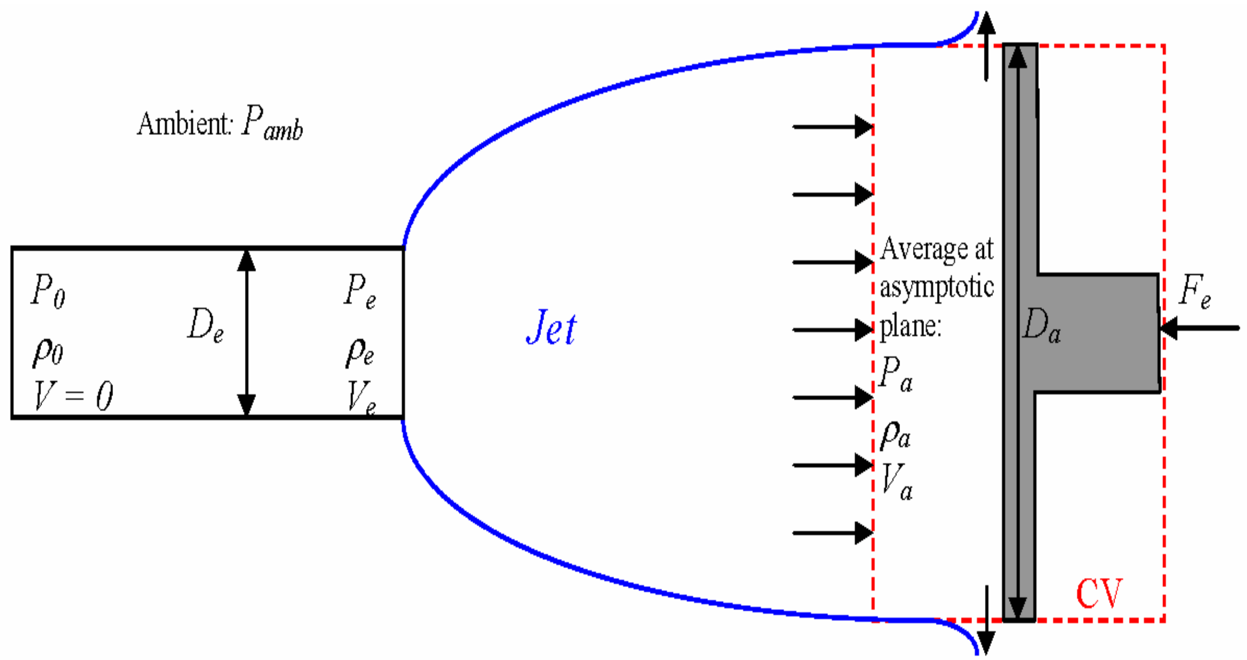

Figure I-4. Control-Volume Force Balance on a Rigid Plate at the Asymptotic Plane Used to Derive Equation (C-3) in the ANSI Standard

It is assumed in Appendix C to the ANSI standard (p. 52) that the fluid does not begin to interact with the surrounding environment until after it crosses the asymptotic plane. Hence, no energy is supplied to or removed from the jet in the region upstream of the control volume in

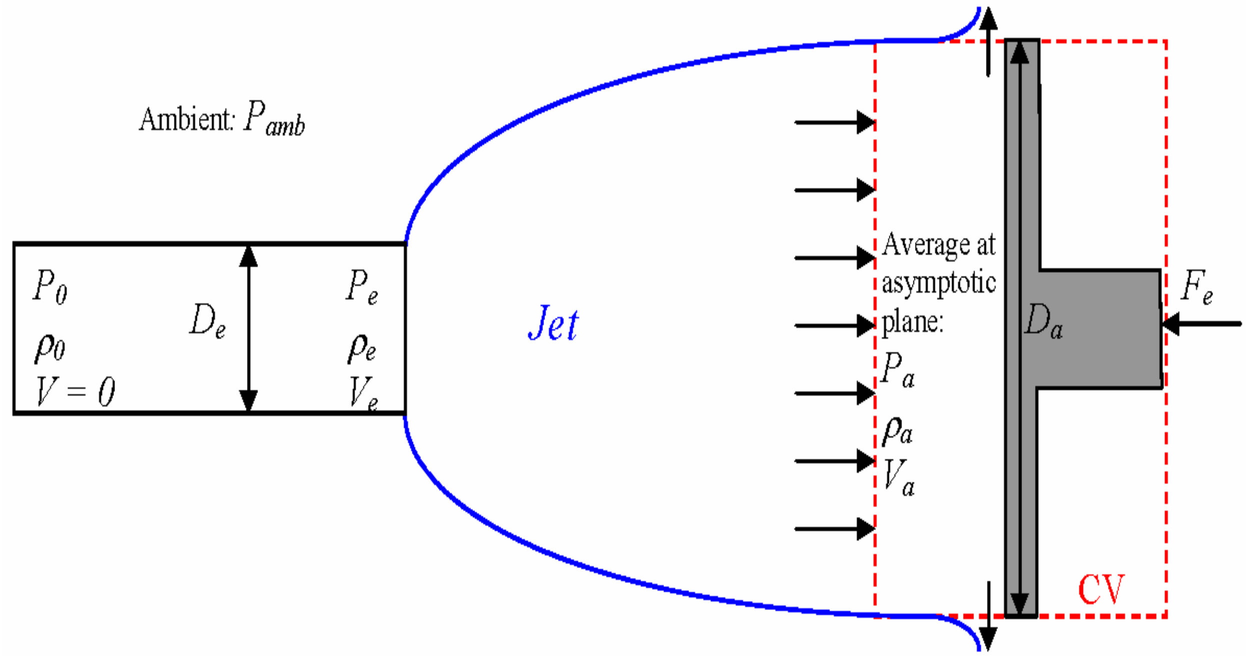

Figure I-4. Therefore, the entire jet force will be recovered on a target at this distance.

The jet characteristics at the asymptotic plane—fluid density ρ_a, velocity v_a, and static pressure P_a—are not expected to be uniform, so to render the force balance for the control volume tractable, these properties are averaged over the jet cross section. The force balance in the direction of the jet flow may hence be written as

$$F_e = (P_a - P_{amb})A_a + \frac{1}{g_c}\left(v_a \frac{d}{dt} m_a + m_a \frac{d}{dt} v_a\right), \qquad \text{(I-37)}$$

where $A_a = \pi D_a^2 / 4$ is the jet area at the asymptotic plane and m_a is the mass of the fluid located within the control volume.

For steady flow, $dv_a/dt = 0$. The rate at which mass enters the control volume, dm_a/dt, is simply the total mass flow crossing the asymptotic plane and is given by

$$\frac{dm_a}{dt} = \rho_a v_a A_a. \qquad \text{(I-38)}$$

Hence, the force balance simplifies to

$$F_e = (P_a - P_{amb})A_a + \frac{1}{g_c}\rho_a v_a^2 A_a. \tag{I-39}$$

Because no mass escapes the jet between the break location and the asymptotic plane, the mass flow rates at the break and at the asymptotic plane must be equal, that is,

$$\rho_a v_a A_a = \rho_e v_e A_e. \tag{I-40}$$

This relation may be employed to eliminate v_a in the force balance.

As mentioned in the discussion following equation (I-11), the static pressure at the asymptotic plane is generally taken to be equal to P_{amb}. Setting P_a equal to P_{amb} yields

$$F_e = \frac{1}{g_c}\frac{\rho_e^2 v_e^2 A_e^2}{\rho_a A_a}. \tag{I-41}$$

Because the full jet thrust force is recovered, this evaluation of F_e may be set equal to that obtained in equation (I-2) to give the result

$$\frac{A_a}{A_e} = \frac{\rho_e^2 v_e^2}{g_c \rho_a} \cdot \frac{1}{(P_e - P_{amb}) + \frac{1}{g_c}\rho_e v_e^2}. \tag{I-42}$$

The second fraction in this equation is recognized by comparison with equation (I-5) as equal to $1/(C_T P_0)$. Making use of the mass flux definition, $G_e = \rho_e v_e$, leads to the expression for the jet area at the asymptotic plane given in the standard,

$$\frac{A_a}{A_e} = \frac{G_e^2}{g_c \rho_a C_T P_0}. \tag{I-43}$$

The standard recommends evaluation of the density ρ_a at the asymptotic plane using the local static pressure P_a and the system stagnation enthalpy h_0, rather than the local static enthalpy h_a. Therefore, it is implicitly assumed that the dynamic enthalpy at the asymptotic plane, $v_a^2/2$, is small. This assumption is questionable given that v_a is generally not small, even for the large asymptotic area obtained by the method of calculation of the standard. For the sample case considered earlier (P_0 = 2250 psia, T_0 = 530°F, h_0 = 522 Btu/lbm upstream stagnation conditions), following the recommendations of the standard, the plane-averaged fluid density at the asymptotic plane is 0.106 lbm/ft^3 and the averaged fluid velocity is 670 ft/s. One would then compute $v_a^2/2 \approx$ 9.0 Btu/lbm, a nonnegligible fraction of the initial enthalpy. The calculational simplicity achieved by use of upstream stagnation conditions, rather than the local static conditions for thermodynamic evaluations, is therefore of doubtful value.

A further inconsistency is noted in the development of the asymptotic plane area because P_a in the ANSI jet model, as governed by equation (I-10), is not always equal to P_{amb}, yet the asymptotic plane area is always computed as if this were the case. For slightly subcooled, saturated, or two-phase upstream conditions, application of equation (I-10) leads to a value for P_a that is less than P_{amb}. Although the standard does not document the physical reasoning behind equation (I-10), it appears to correct for cases in which the dynamic enthalpy is nonnegligible. This development further confirms that only longitudinal pressures are computed for P_{jet}, at least at the asymptotic plane, and probably everywhere within the jet envelope.

I.5 Critical Flow Models

I.5.1 Discharge Mass Flux

Results produced by the jet model are sensitive to the value assigned to the mass flux discharged from the break plane, G_e (lbm/ft^2/s). The area of the jet at the asymptotic plane A_a (ft^2) (i.e., the cross sectional area reached by the jet following free (isentropic) expansion), is proportional to G_e^2. Thus, Figures C-4 and C-5 in the standard indirectly specify G_e and plot the ratio of the asymptotic area to the break plane area A_a/A_e for upstream conditions ranging from 50 °F subcooled liquid to saturated vapor. Aside from difficulties inherent in recovering numerical values from coarsely resolved plots, use of these figures is not recommended for the following two reasons:

(1) The range of upstream stagnation conditions covered by the plot—extending only to 50°F subcooling—is insufficient. Typical cold-leg conditions in a PWR might entail subcooling of 100°F or more.

(2) The origin of the results is unclear. Which model was used to evaluate the relevant mass fluxes and thrust coefficients? Without this information, there can be no confidence that the rest of the model will be applied in a self-consistent manner.

Therefore, this analysis strongly concurs with the recommendation given in the ANSI standard (p. 57) that a two-phase critical flow model be employed to evaluate G_e. The standard cites two models that are in widespread use, the homogeneous equilibrium model (HEM)[†] and the Henry-Fauske model (HEN71). The standard provides a loose recommendation regarding the applicability of the models as a function of upstream stagnation properties—the HEM for saturated or two-phase and Henry-Fauske for subcooled conditions.

[†] For a discussion of practical considerations surrounding implementation of the HEM, as well as a tabulation of results for a wide range of upstream conditions, see HAL80.

Several pitfalls await a naïve application of this guidance. To facilitate the exposition of these pitfalls, it is useful first to provide a simplified description of the physics inherent in each of the models.

The HEM assumes the phases to be in thermodynamic equilibrium and to remain well mixed. The relative velocity between the phases is therefore assumed to be zero. External heat transfer, wall roughness, and other interactions with the environment are neglected so that the expansion is isentropic.

Given these assumptions, the first law of thermodynamics is applied to the homogenized fluid. Combined with the definition of the mass flux, the first law yields an expression for G_e in terms of the mixture's static properties at the choked point. The critical mass flux is defined as the value of G_e that maximizes this expression. Numerical solution of the HEM is thus an iterative process, entailing a search over the space of static state points that preserve the upstream stagnation entropy.

The Henry-Fauske model preserves some of the assumptions made under the HEM, namely that the mass flux may be expressed as a function of the thermodynamic state at the throat, that the critical mass flux can be obtained by maximizing this function, and that the expansion is isentropic. However, Henry and Fauske argue that the assumptions of homogeneous mixing and thermodynamic equilibrium during the expansion are unrealistic given the short time scales involved. Rather, interphase mass transfer is constrained such that the quality, x_t, at the throat is equal to the upstream stagnation quality, x_0. Heat transfer during the expansion is also assumed negligible; the liquid-phase temperature T_{ft} at the throat is held fixed at the upstream liquid temperature, T_{f0}. The temperature of the vapor phase, if it is present, is allowed to vary. The heat- and mass-transfer rates at the throat are treated as significant, and expressions for these are developed assuming polytropic vapor behavior.

In practice, the Henry-Fauske model is implemented by solving a transcendental equation for the static pressure at the throat that maximizes mass flux. Both Henry-Fauske and the HEM are evaluated through iterative procedures, with thermodynamic properties queried upon each iteration. Therefore, the models were coded as a series of FORTRAN subroutines, driven by a MATLAB control function, that directly couple with the FORTRAN implementation of the NIST/American Society of Mechanical Engineers (ASME) steam tables (HAR96) when fluid properties are required. The results obtained from the software were successfully validated against those presented in HAL80 and HEN71**.** These programmed routines allow a thorough assessment of the practical ramifications of using each model within the ANSI jet-modeling framework.

The standard does not provide guidance with regard to critical flow modeling for superheated conditions. The simplest approach would be to treat the steam as an ideal gas and apply the appropriate equation of state. This treatment was attempted and found to be highly inadvisable for the slightly superheated states that are of most relevance to the present application. Two qualitative observations support this conclusion. First, when the upstream superheat is small, the flow at the choked location is in fact two phase; second, slightly superheated, high-pressure steam does not exhibit the typically assumed idealized properties (e.g., a specific heat ratio of 1.3), so that transitions evaluated using the ideal gas law would not preserve entropy. These considerations lead to the recommendation that the HEM be used treat the superheated state points that may arise in this application.

As mentioned above, the standard does provide guidance for two-phase and single-phase liquid stagnation state points. Specifically, it recommends the use of HEM for saturated and Henry-Fauske for subcooled upstream conditions. This appendix recommends using the Henry-Fauske model for both regimes. This recommendation stems from several considerations, as outlined below.

Critical mass fluxes predicted by the HEM and Henry-Fauske models exhibit their most significant disagreement at precisely the transition point recommended in the standard (i.e., for saturated-liquid upstream conditions). **Error! Reference source not found.** and Figure I-6 provide contour plots of G_e, as obtained from the two models for subcooled vessel stagnation conditions. In figures showing flow properties for subcooled state points, the stagnation temperature is varied on the x axis and pressure on the y axis. The regions between contour lines of constant G_e are shaded for ease of delineation. Because the domain of validity of the flow models does not extend to superheated conditions, pressure and temperature combinations that lie within this regime are blanked out on the plots. Figure I-7 and Figure I-8 show mass fluxes for saturated upstream conditions. In these plots, G_e is calculated at several saturated (temperature, pressure) state points as a function of the vessel quality.

Figure I-9 and Figure I-10 display the variation between the HEM and Henry-Fauske mass fluxes. It can be seen from these figures that discrepancies of 50 percent or more exist for saturated liquid upstream conditions and that significant variations persist for slightly subcooled and low-quality, two-phase stagnation conditions. This disagreement follows from a variation in the assumptions regarding interphase mass transfer. Because the quality is held fixed under the Henry-Fauske model, the discharge is almost entirely in the liquid phase. Under the HEM, however, heat and mass transfer between the phases is allowed and the discharge has a quality that is significantly greater than zero. This discharge possesses a lower density and higher velocity than that predicted by Henry-Fauske. It can be shown numerically that the HEM mass flux prediction will be lower than that of Henry-Fauske for the slightly subcooled, saturated liquid, and low-quality upstream conditions in which the HEM prediction of discharge quality is markedly higher than that of Henry-Fauske.

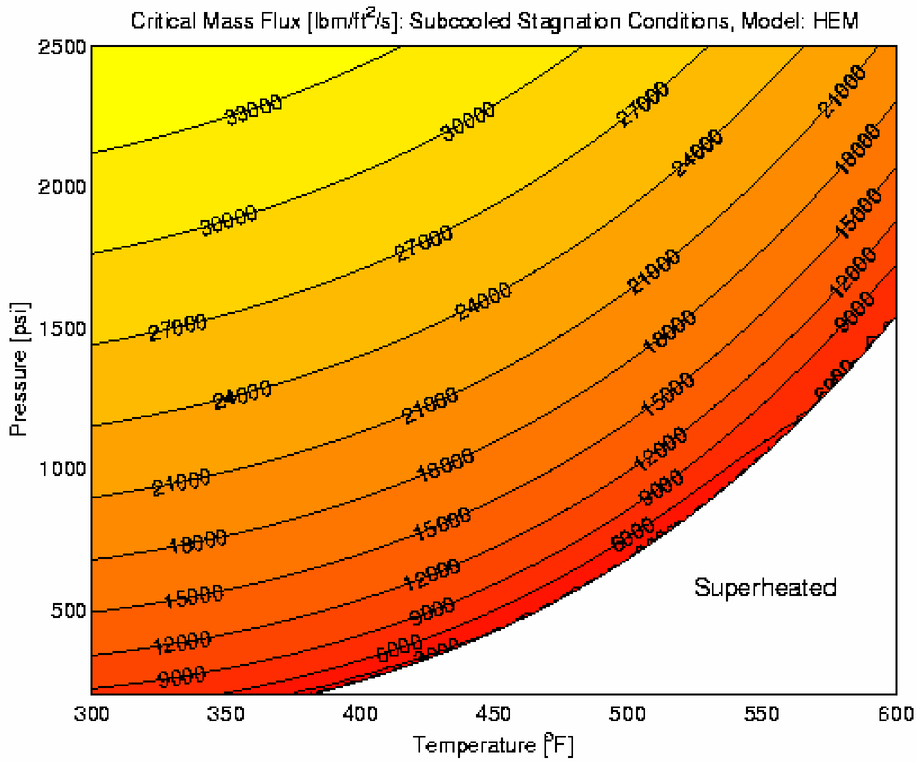

Figure I-5. HEM Critical Mass Flux, Subcooled Stagnation

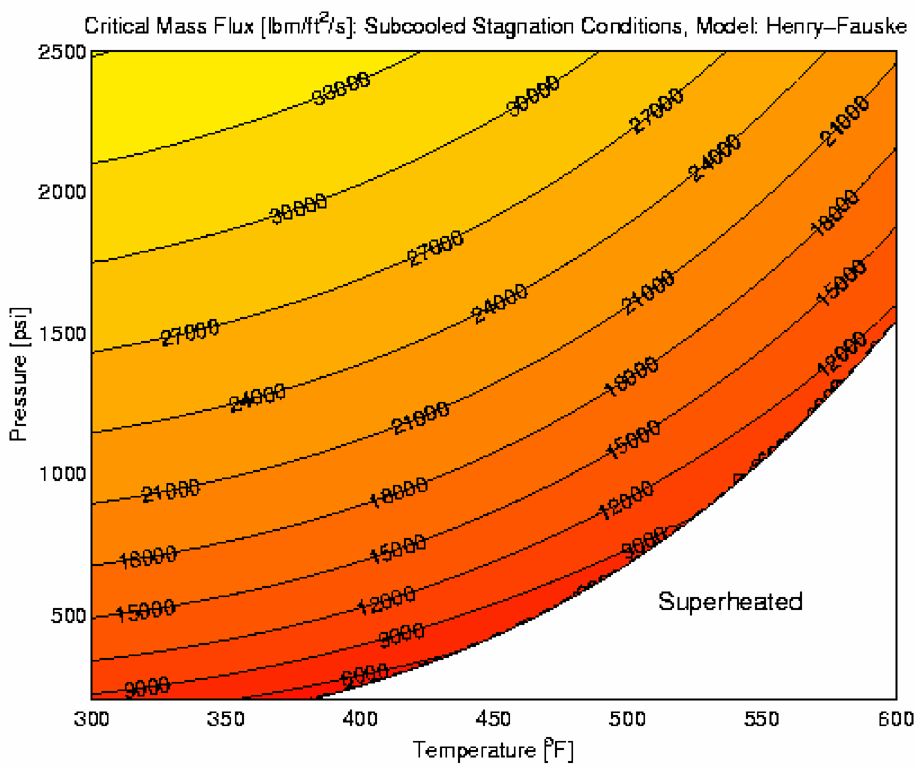

Figure I-6. Henry-Fauske Critical Mass Flux, Subcooled Stagnation

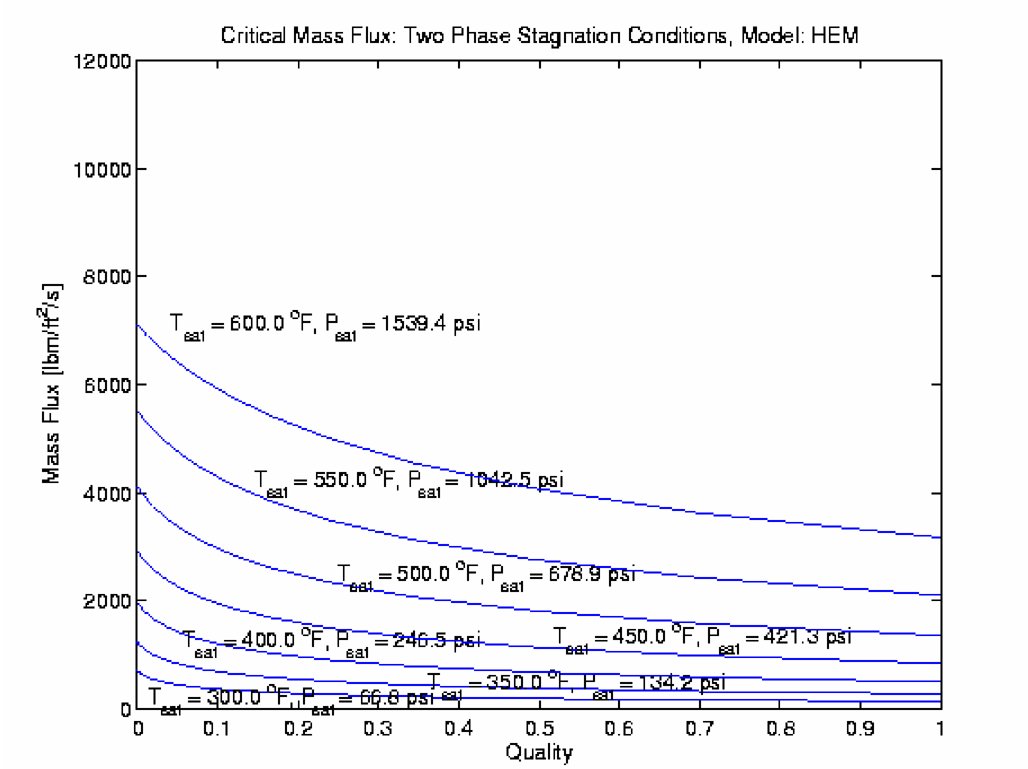

Figure I-7. HEM Critical Mass Flux, Saturated Stagnation

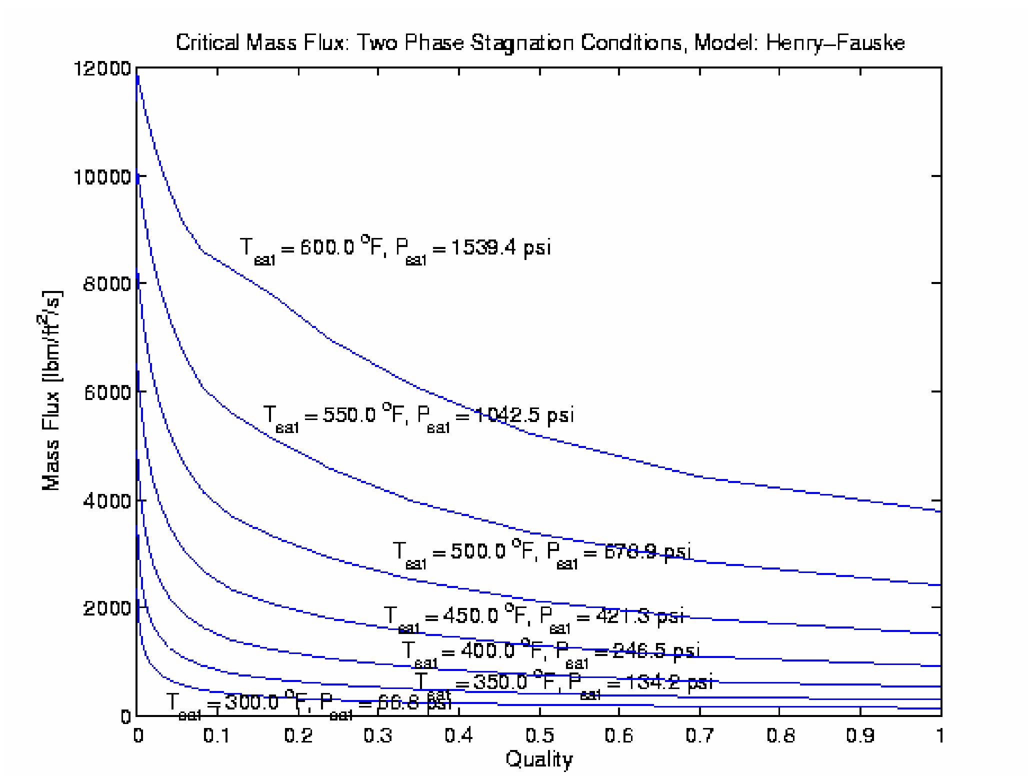

Figure I-8. Henry-Fauske Critical Mass Flux, Saturated Stagnation

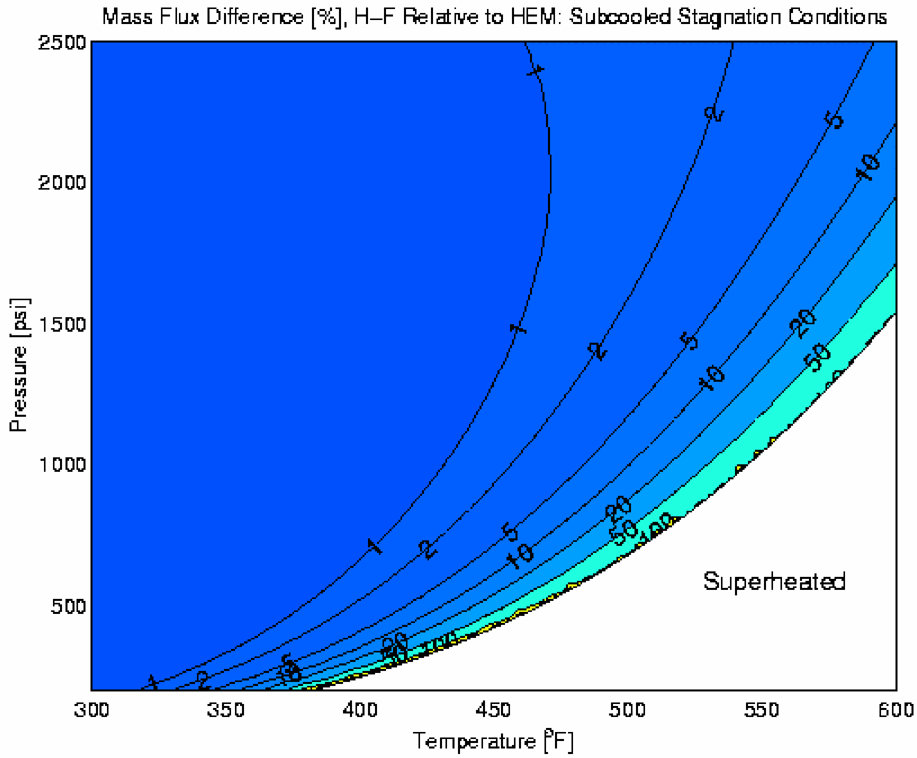

Figure I-9. Mass Flux Difference, Subcooled Stagnation

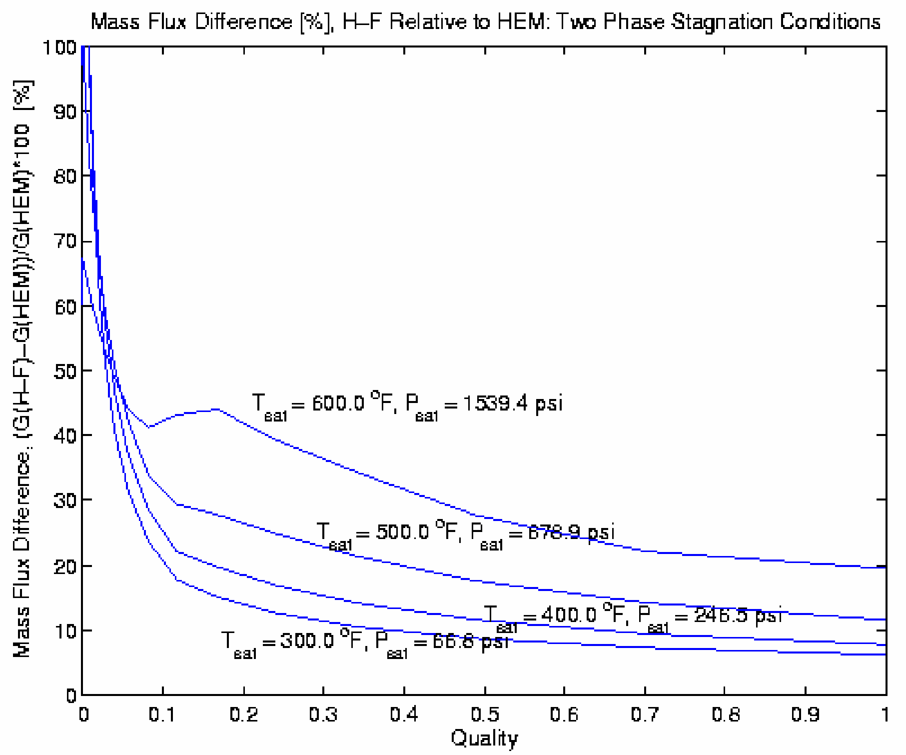

Figure I-10. Mass Flux Difference, Saturated Stagnation

If the advice of the standard is followed, then a significant discontinuity would be observed when the critical flow model transitions from the HEM to Henry-Fauske. The nature and magnitude of this discontinuity is explored further below. Although users of the jet model are in practice unlikely to observe this discontinuity, because during a blowdown, the transition might only occur after significant pressure drops, there is no compelling reason to preserve it. The issue then becomes one of selecting the model that offers the best fidelity to available data. The figures show that the HEM and Henry-Fauske offer comparable predictions for highly subcooled, as well as high-quality two-phase conditions. This is to be expected because under these conditions, both models predict essentially monophasic fluid properties at the throat and the detailed treatment of the interphase heat- and mass-transfer rates offered by Henry-Fauske does not come into play. The benchmarking results reported in HEN71 lead to the conclusion that the Henry-Fauske model exhibits superior agreement to the data under low-quality two-phase and saturated liquid conditions. This alone is sufficient reason to adopt Henry-Fauske; an examination of a second major input to the ANSI jet model, the thrust coefficient, may provide further evidence.

I.5.2 Direct Evaluation of Thrust Coefficients

The thrust coefficient, C_T, acts as a surrogate for the jet thrust force, which the ANSI model does not explicitly call for as an input. This discussion will address only the steady-state thrust coefficient for frictionless, unrestricted flow, but its conclusions can be generalized to include those cases as well. Regardless of upstream conditions, the thrust coefficient is used to correlate the thrust force T, upstream stagnation absolute pressure P_0, ambient pressure P_{amb}, and break area A_e by the expression

$$T = C_T(P_o - P_{amb})A_e. \tag{I-44}$$

Calculation of the thrust coefficient requires knowledge of local flow conditions at the break. Because these are unknown, unless a critical flow model such as the HEM or Henry-Fauske is used to compute them, pp. 35–45 of the standard provide a series of correlations and figures that may be used as surrogates. Because both Henry-Fauske and the HEM were implemented for the current review, the results obtained from these models will be compared with the recommendations provided in the standard.

The thrust force may be computed by calculating the force that must be exerted to hold in static equilibrium a plate positioned normal to the flow directly at the break point. This thrust is given by

$$T = (P_e - P_{amb})A_e + \frac{1}{g_c}\rho_e v_e^2 A_e, \tag{I-45}$$

where the static pressure P_e, fluid density ρ_e, and flow velocity v_e are evaluated at the exit. Combining the above equations yields an expression for the thrust coefficient,

$$C_T = \frac{1}{P_0 - P_{amb}}\left(\frac{1}{g_c}\rho_e v_e^2 + \left(P_e - P_{amb}\right)\right). \tag{I-46}$$

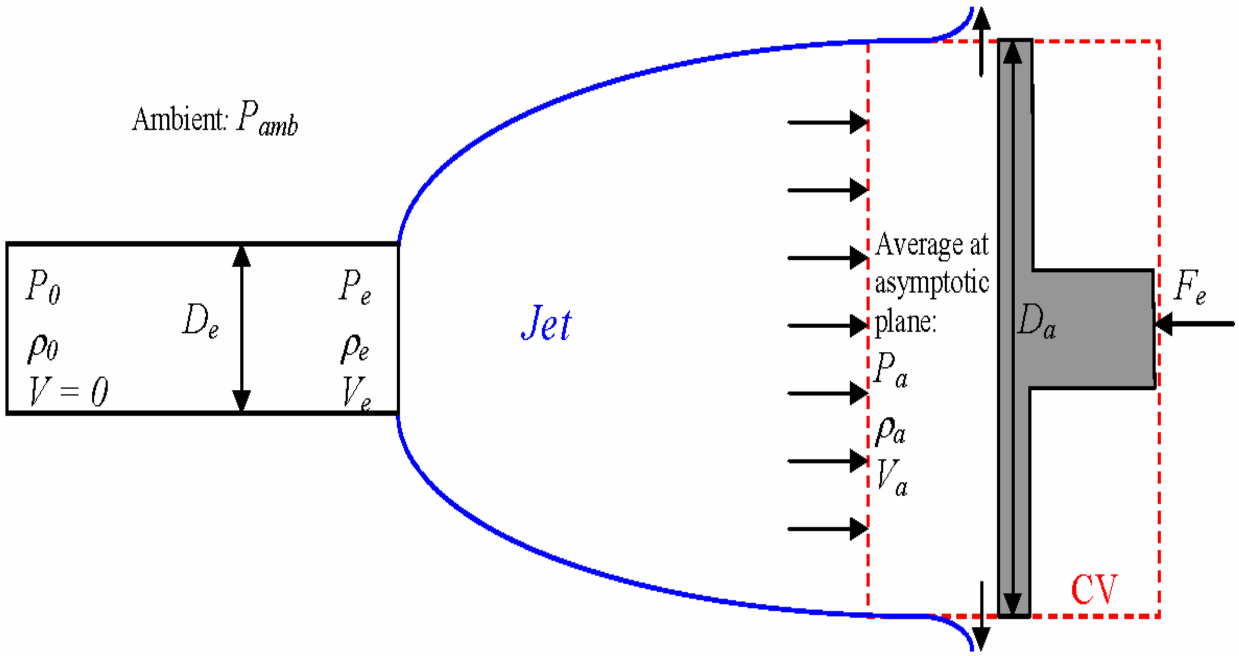

Figure I-4 through Figure I-7 show thrust coefficients computed using pressures and fluid properties evaluated from the HEM and Henry-Fauske models. Regardless of the model, the value of C_T approaches 2.0 for incompressible, highly subcooled liquid and approximately 1.26 for saturated steam. These results agree with theory and are recommended for use in the standard.

For subcooled flashing upstream conditions, p. 42 of the standard recommends use of the curve fits presented by Webb (WEB76). Based on an enthalpy normalization factor

$$h^* = \frac{h_0 - 180}{h_{sat} - 180}, \tag{I-47}$$

where h_0 (Btu/lbm) is the upstream stagnation enthalpy and h_{sat} (Btu/lbm) is the saturated water enthalpy at the stagnation pressure, the correlation is evaluated as

$$C_T = 2.0 - 0.861 h^{*2} \text{ for } 0 \le h^* < 0.75 \tag{I-48}$$

and

$$C_T = 3.22 - 3.0 h^* + 0.97 h^{*2} \text{ for } 0.75 \le h^* \le 1.0. \tag{I-49}$$

For saturated or superheated steam, the standard recommends a thrust coefficient of

$$C_T = 1.26 - P_{amb}/P_0. \tag{I-50}$$

For two-phase steam-water mixtures, the standard provides only a figure that does not address relevant PWR break conditions, and for nonflashing water jets with temperatures less than the saturation temperature at ambient pressure and pressures greater than ambient, the standard recommends that

$$C_T = \frac{2}{1 + fL/D}, \tag{I-51}$$

where the Fanning friction factor f is normally assumed to be zero for conservatism. The ratio L/D represents a dimensionless flowpath length based on the characteristic length and diameter of the piping between the assumed thermodynamic reservoir and the break location.

Webb claims, and calculations performed for this appendix verify, that his correlations agree with values computed from the Henry-Fauske model to within 3 percent for upstream stagnation pressures ranging from 300 to 2400 psia. The standard does not clearly state this range of applicability. Webb's correlation is recommended when a computational implementation of a critical flow model is unavailable, but two inconsistencies require clarification.

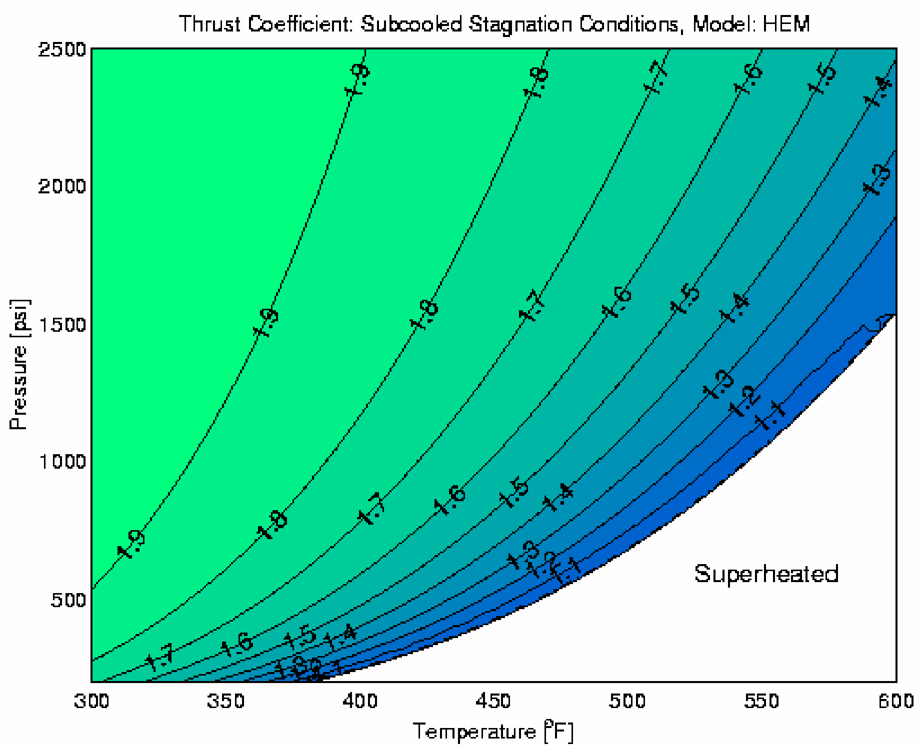

Figure I-11. HEM Thrust Coefficient, Subcooled Stagnation

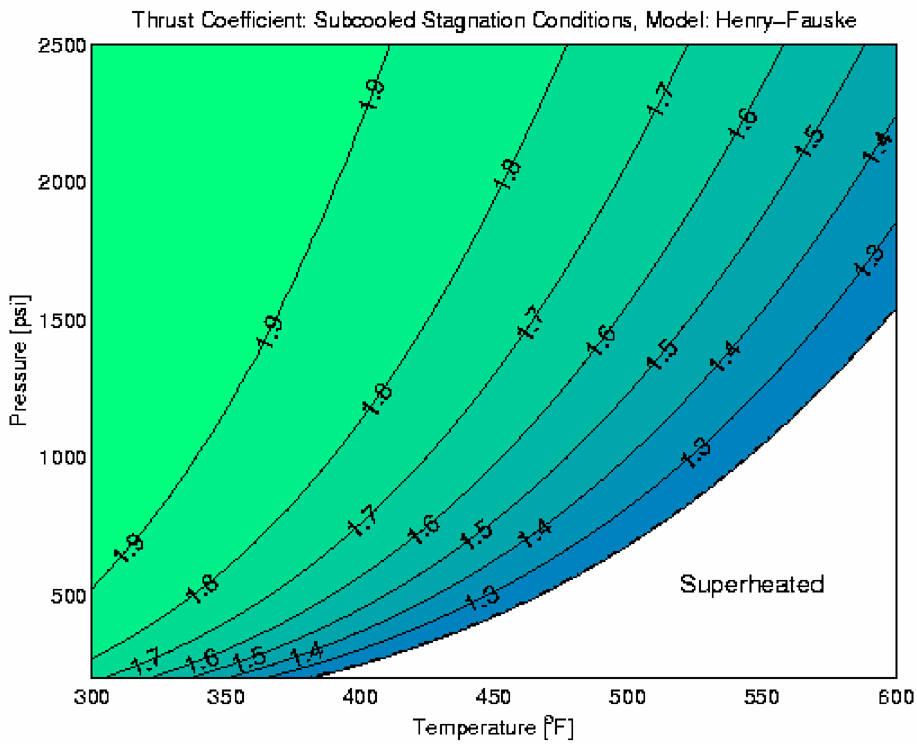

Figure I-12. Henry-Fauske Thrust Coefficient, Subcooled Stagnation

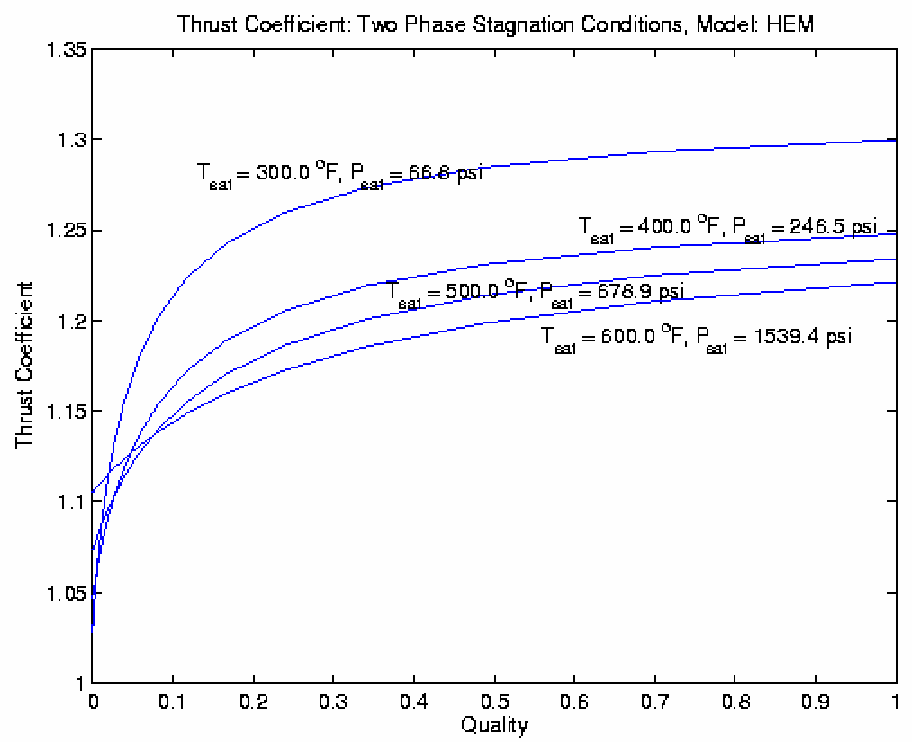

Figure I-13. HEM Thrust Coefficient, Saturated Stagnation

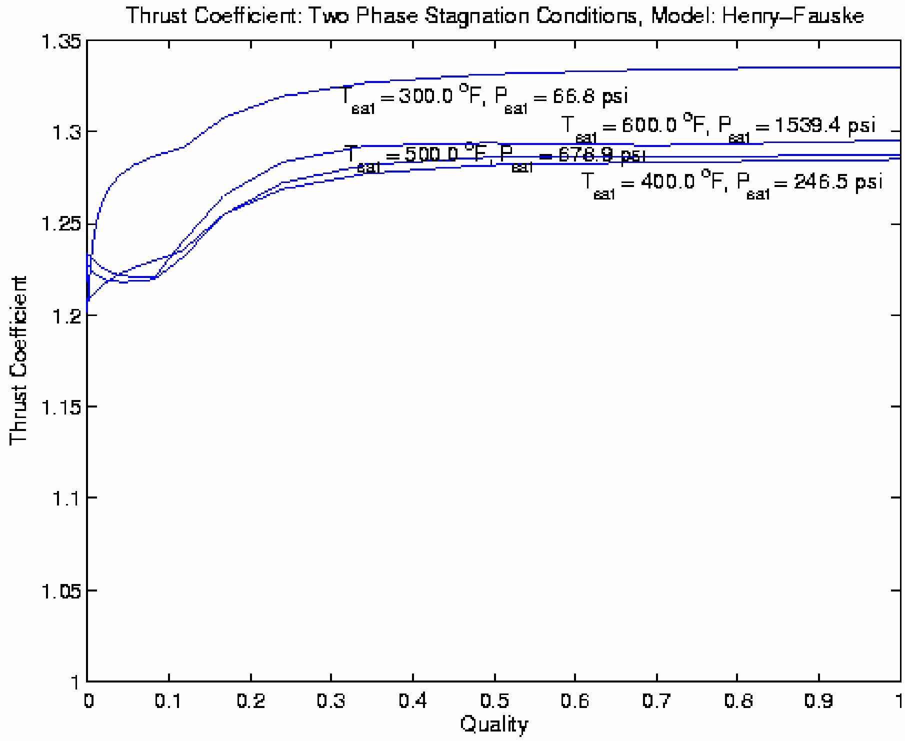

Figure I-14. Henry-Fauske Thrust Coefficient, Saturated Stagnation

In presenting Webb's model, the standard neglects to clarify the "180" figure against which the enthalpy is nondimensionalized. This is, in fact, the enthalpy of saturated water at atmospheric pressure, 14.7 psi. It may be justifiably claimed that during a blowdown, the ambient containment pressure might vary from below atmospheric to significantly above atmospheric. Changes in P_{amb} cannot be accounted for by Webb's model; however, C_T evaluated from the force balance varies weakly with P_{amb}. This effect is not large; even for highly subcooled conditions at the lower end of the range of validity of Webb's correlation, $P_0 = 300$ psia, neglecting P_{amb} altogether changes the thrust coefficient evaluated from the force balance by less than 5 percent.

The standard also places insufficient emphasis on the fact that Webb's correlation is obtained from calculations using the Henry-Fauske model. Because this is the case, employing HEM-derived mass fluxes with thrust coefficients obtained from this correlation propagates a significant inconsistency. Figure I-8 shows that significant deviation exists between thrust coefficients computed from the outlet conditions provided by the two critical flow models. The use of Henry-Fauske-derived thrust coefficients with HEM mass fluxes will result in overprediction of damage radii. This follows because the larger Henry-Fauske thrust coefficient implicitly imposes a higher flow density, velocity, and/or static pressure at the break plane.

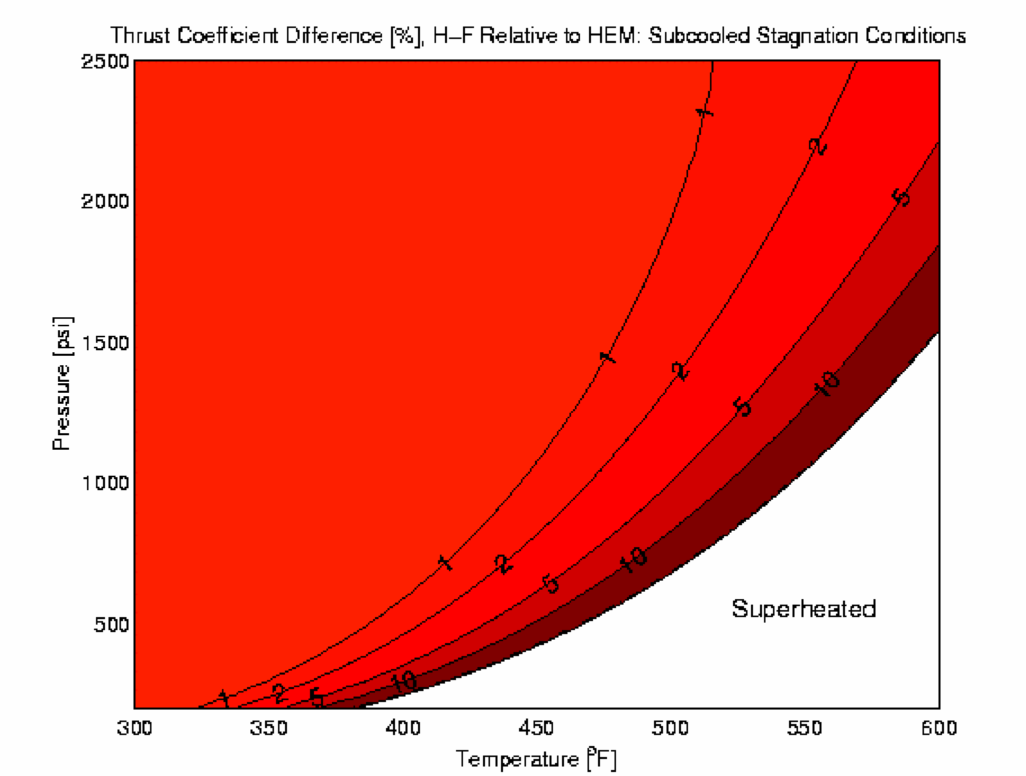

Figure I-15. Thrust Coefficient Difference, Subcooled Stagnation

I.5.3 Effects of Flow Models on Jet Behavior

While the sensitivity of the jet pressure contour map in its entirety to variations in C_T is too complicated to permit analytic treatment, the effect of variation of C_T on conditions at the asymptotic plane can be used for illustration. Equation (I-43) shows that the jet area A_a at the asymptotic plane is inversely proportional to C_T. However, from conservation of mass, equation (I-40), the average flow velocity at the asymptotic plane v_a is inversely proportional to A_a and, thus, directly proportional to C_T. This conclusion can be drawn because the average fluid density, ρ_a, at the asymptotic plane depends, in the ANSI formulation, only upon upstream stagnation conditions. The dynamic pressure of the fluid, which is proportional to the square of its velocity, thus varies as C_T^2. The results of decreased jet cross-sectional area and increased velocity from the larger Henry-Fauske thrust coefficient will be a narrower, more penetrating jet and larger volume-equivalent radii at a given damage pressure.

In fact, it can be seen from Figure I-16 that the thrust coefficient for upstream conditions at or near saturation as derived from the HEM is significantly lower than the value of 1.26 recommended in Figure B-5 of the standard. The inconsistency inherent in use of the 1.26 value with the HEM mass flux would again result in overprediction of volume-equivalent radii. This additional consideration strengthens the recommendation that the Henry-Fauske method be employed for all flow regimes when performing the calculations outlined in the standard.

As mentioned above, the critical mass flux G_e derived from the HEM will be smaller, significantly so for stagnation conditions lying near the liquid saturation line in (P, h) space, than that obtained from Henry-Fauske. Because this is the case, it is also useful to address the behavior at the asymptotic plane when G_e is varied, with C_T held constant. Following the same reasoning pursued above when the thrust coefficient was varied, the jet area at the asymptotic plane varies as G_e^2. The average jet velocity at that location, v_a, on the other hand, behaves as $v_a = k G_e / A_a$ so that $v_a \sim 1/G_e$. Thus, a seemingly paradoxical conclusion is reached, namely that reducing the mass flux while holding the thrust coefficient constant increases the velocity at the asymptotic plane and might *increase* the volume-equivalent radii.

Although this thought experiment is not conclusive or comprehensive—the location of the asymptotic plane, for instance, also depends on G_e and C_T and has not been taken into account—numerical computations verify its conclusions. Table I-1 shows critical flow model results for five of the upstream conditions given in Table I-2. The conditions selected from that table are #8, PWR Hot-Leg Initial; #1, PWR Cold-Leg Initial; #2, PWR Cold-Leg Blowdown; #9, BWR Hot Leg; and #11, Main Steamline. All three PWR stagnation states are subcooled; the BWR state is two phase with a quality of 0.15 and the steamline case is superheated by 35 °F. In addition to the mass flux, G_e, thrust coefficient, C_T, and discharge velocity, v_e, obtained, the table also shows the volume-equivalent damage radii for the 10 and 150 psig contours. It might be intuitively expected that the Henry-Fauske model is the more conservative when calculating damage radii because it predicts critical mass fluxes and thrust coefficients that are greater than those of the HEM, but, as shown in the table, particularly for initial conditions nearing saturation, this is not the case.

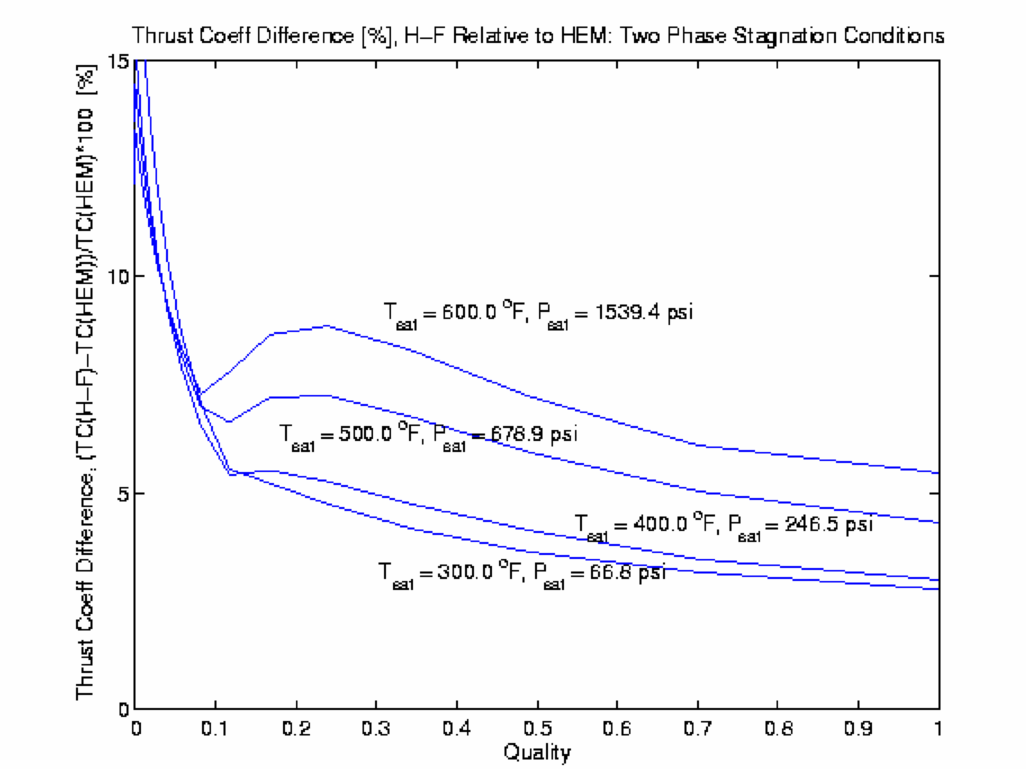

Figure I-16. Thrust Coefficient Difference, Saturated Stagnation

Table I-1. Critical Flow Model Results and Their Effect on Volume-Equivalent Damage Radii

	Critical Mass Flux G_e (lbm/ft^2/s)		Thrust Coefficient C_T (--)			Breakflow Velocity v_e (ft/s)		150-psig* Damage-Pressure Radius (pipe diameters)		10-psig* Damage-Pressure Radius (pipe diameters)	
	HEM	**H-F**	**HEM**	**H-F**	**Webb****	**HEM**	**H-F**	**HEM**	**H-F**	**HEM**	**H-F**
1. Cold-Leg Initial (2250 psia, 530 °F)	**24850**	**25330**	**1.62**	**1.64**	**1.63**	**522**	**527**	**1.48**	**1.48**	**12.00**	**12.04**
2. Cold-Leg Blowdown (393 psia, 291 °F)	**13370**	**13390**	**1.88**	**1.89**	**1.90**	**232**	**232**	**0.96**	**0.96**	**4.42**	**4.43**
8. Hot-Leg Initial (2250 psia, 630 °F)	**11840**	**15400**	**1.17**	**1.28**	**1.28**	**296**	**382**	**1.60**	**1.59**	**11.14**	**11.07**
9. BWR Hot Leg (1040 psia, 550 °F, X = 0.15)	**3920**	**5260**	**1.16**	**1.26**	**N/A**	**178**	**158**	**1.11**	**1.12**	**7.81**	**7.80**
11. Main Steamline (910 psia, 570 °F)	**1800**	**N/A**	**1.24**	**N/A**	**N/A**	**464**	**N/A**	**1.08**	**N/A**	**7.58**	**N/A**

* Damage-pressure radii are given as multiples of the break diameter. They are obtained by constructing spheres with volume equal to the volume enclosed by a given jet stagnation pressure contour. See Section I.3 for further elaboration.

** Shown for purposes of comparison only; not used in damage-pressure-radius calculations given in this table.

I.6 Sample Calculations

A MATLAB routine called ANSIJet (see Attachment 1 ADAMS document ML042640274) implemented the ANSI model presented in the previous sections for predicting stagnation pressures in an expanding jet. This programming language was selected for convenient interface with steam-table routines available from NIST. Several cases relevant to both PWR initial break and blowdown conditions were evaluated. Two generic BWR state points were also evaluated, as were three cases applicable to steamline flow in secondary loops. Two of these relate to a single-pass Babcock & Wilcox steam generator discharging superheated (by ca. 35°F) steam; the third applies to a Combustion Engineering U-tube heat exchanger and is assumed to yield saturated steam. Table I-2 defines these conditions for later reference by case number. Note that Figure I-1 corresponds to the cold-leg initial break condition defined as Case #1.

Table I-2. Comparative Calculation Set Using ANSI Jet Model

Case #	Description	System Stagnation Conditions		
		P_0 (psia)	T_0 (°F)	Quality
1	cold-leg initial[1]	2250	530	Subcooled
2	cold-leg blowdown[1]	393	291	Subcooled
3	cold-leg blowdown[1]	857	351	Subcooled
4	cold-leg blowdown[1]	1321	411	Subcooled
5	cold-leg blowdown[1]	1786	471	Subcooled
6	10% greater pressure than Case 1	2475	530	Subcooled
7	cold-leg initial[2]	2250	540	Subcooled
8	hot-leg initial[3]	2250	630	Subcooled
9	BWR hot leg[4]	1040	550	0.15
10	BWR cold leg[4]	1040	420	Subcooled
11	main steamline (MSL)—Babcock & Wilcox (B&W)[4]—full power	910	570	Superheated
12	B&W MSL—design conditions[4]	1075	603	Superheated
13	MSL—Combustion Engr. Calvert Cliffs[5]	846	525	1.0

[1] From RAO0
[2] From NEI04
[3] From DUD76
[4] From RAH92
[5] From LOB90

Jet-pressure isobars for Cases 1 through 6 were integrated over a wide range of values and converted to equivalent spherical diameters. Figure I-17 presents these results. Recall that the ANSI-model stagnation pressure is used as a correlation parameter that corresponds to observed damage in debris generation tests. The Figure I-17 abscissa is labeled as “Damage Pressure” because of the use of this correlation. Case 1 represents a previously studied hydraulic condition (RAO02) that will be used as the reference case. Reading from the figure, a damage pressure of 10 psig corresponds to an equivalent jet radius of approximately 12 pipe diameters. Note that equivalent radii climb sharply for damage pressures below 20 psig.

This set of calculations suggests that the state-point pressure of the jet dominates the determination of isobar volumes. Case 1 bounded other cases that are not shown in Figure I-17. Case 7, the nominal PWR cold-leg condition recommended in the GR, was almost indistinguishable from Case 1. The reference case also bounded Case 8, a nominal hot-leg break condition, except at damage pressures greater than 120 psig. Hot-leg conditions are much closer to saturation (630°F vs. 653°F); therefore, the shapes of the pressure contours change near the core. Case 6 was run as a perturbation check for plants that may at times have higher operating pressures than the nominal value of 2250 psig. Although the pressure increase was 10 percent higher than the reference, the maximum deviation in spherical volume was only 8 percent; therefore, a linear adjustment for higher pressure would be conservative in the absence of a full jet-model analysis.

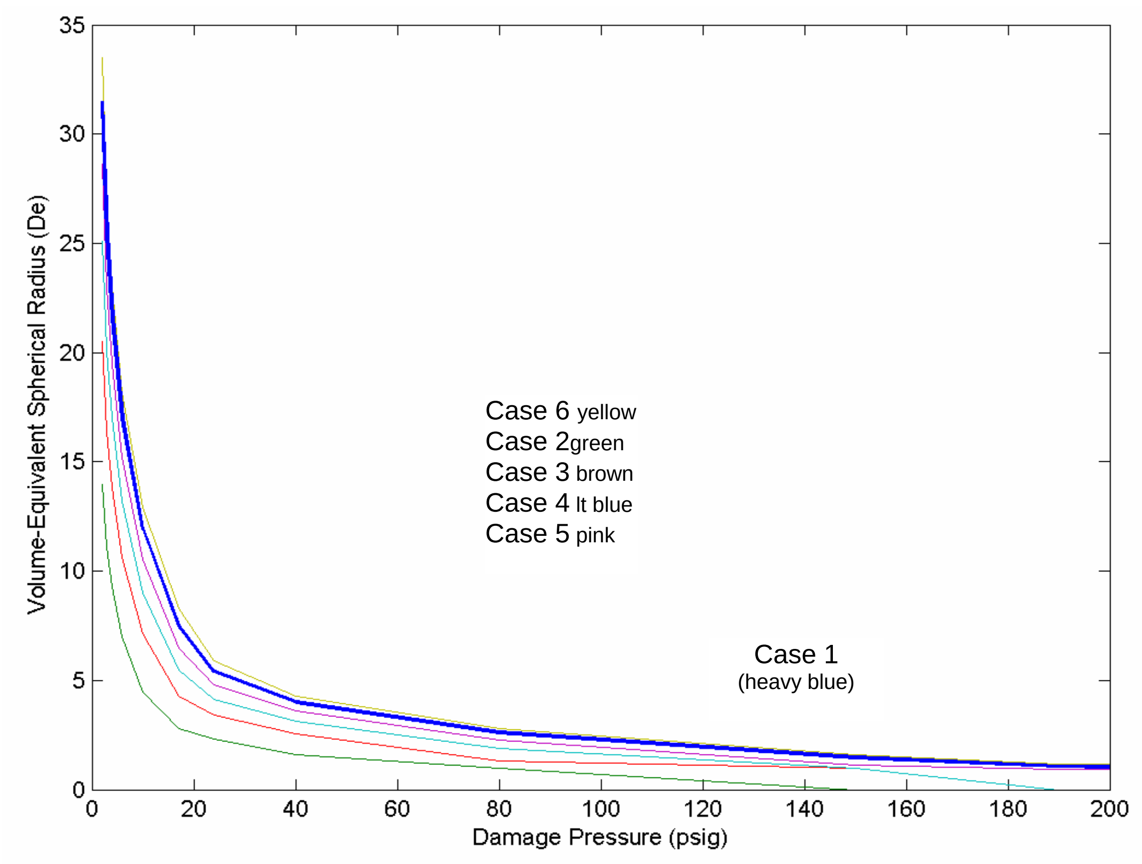

Figure I-17. Comparison of ANSI Jet-Model Equivalent Spherical Radii for Six Initial Break Conditions

Figure I-18 depicts the damage radii associated with the BWR hot-leg and cold-leg conditions of Cases 9 and 10. Given the lower stagnation pressures pertinent to BWR coolant, the equivalent radii are, as expected, smaller than was the case for PWR conditions at comparable values of damage pressure. Figure I-19 provides the radii obtained for the three steamline cases. Two of these, Cases 11 and 13, represent full-power operating conditions. The third, Case 12, is a design specification included to serve as a conservative bounding scenario. Given that the thrust coefficient is nearly invariant at a value near 1.26 for high-quality two-phase and superheated upstream conditions, it appears reasonable to expect damage radii in such regimes to respond linearly to variation in the stagnation pressure. Figure I-20 provides a pressure contour plot for the steamline break condition. This figure compares to Figure I-1 for PWR cold-leg stagnation conditions. One of the subtle differences between these figures is the higher centerline pressure exhibited by the MSL case to axial distances of about 30 pipe diameters. The steamflow exhibits a narrower jet that is higher velocity at the centerline, leading to a greater dynamic contribution to the stagnation pressure. Differences in the initial pressure should also be considered when visually comparing Figure I-1 and Figure I-20.

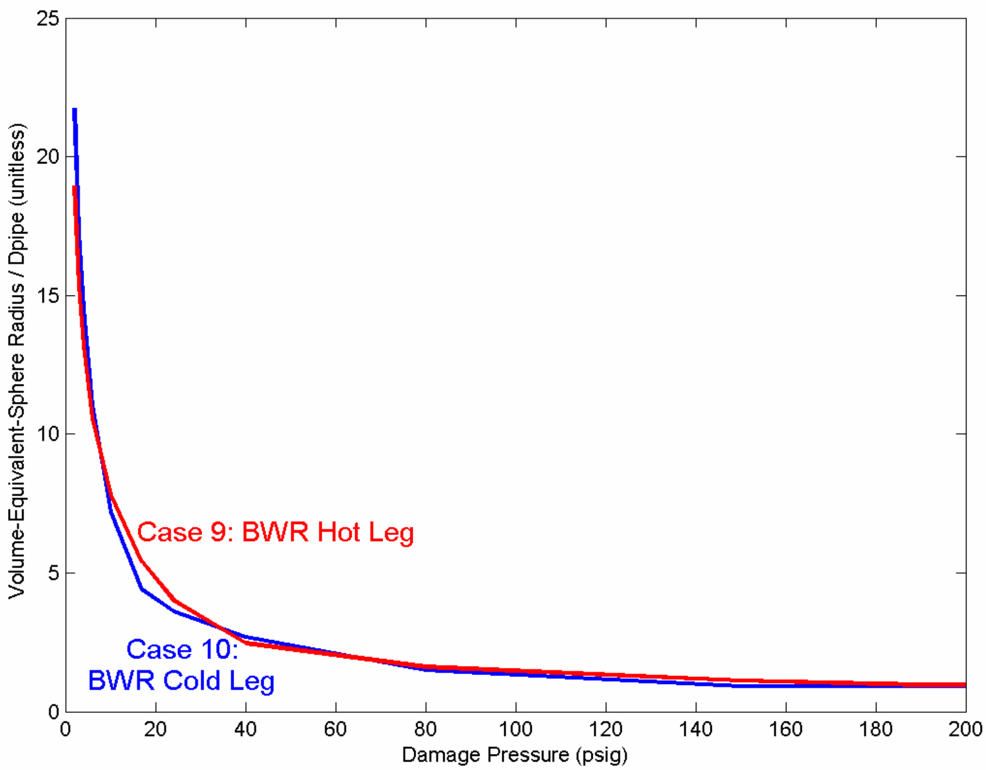

Figure I-18. Comparison of ANSI Jet-Model Equivalent Spherical Radii for BWR Break Conditions

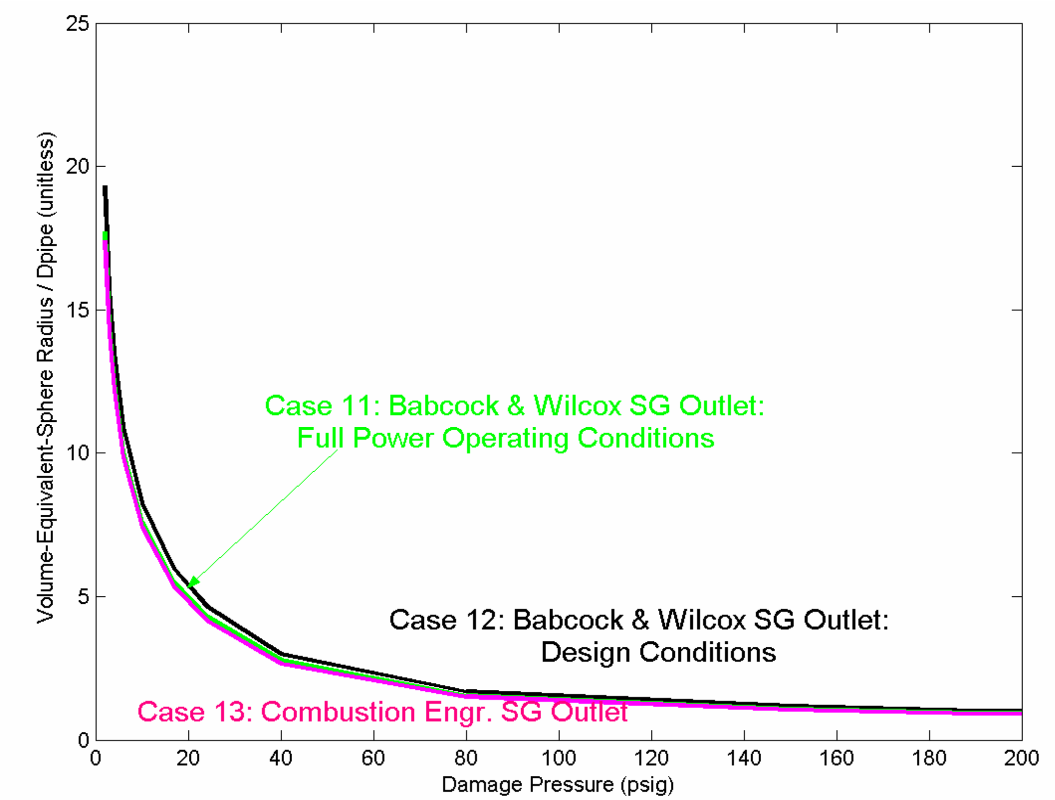

Figure I-19. Comparison of ANSI Jet-Model Equivalent Spherical Radii for MSL Break Conditions

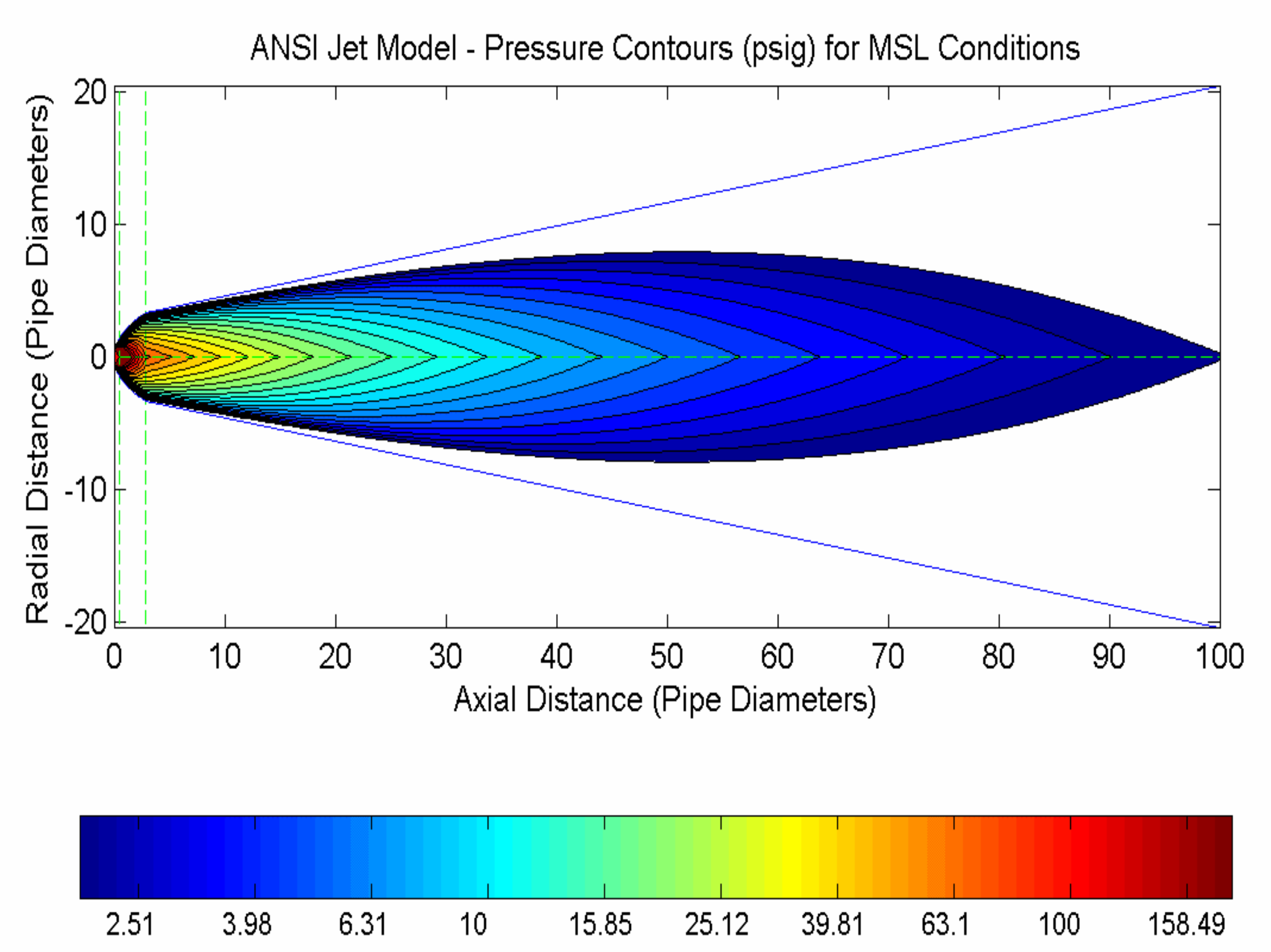

Figure I-20. ANSI Jet-Model Stagnation Pressures for MSL Break Conditions (570°F, 910 psia)

Other useful information can be extracted from the jet model in addition to equivalent spherical diameters derived from spatial volume integrals. Appendix D to the ANSI standard suggests estimating target temperatures by evaluating a thermodynamic state point using the jet pressures P_j and the initial enthalpy h_0. Presuming that the model supplies realistic, nonisentropic impingement pressures (at least in the longitudinal direction), this approach will give the temperature of the stationary fluid striking the surface of a large target. Actual target temperatures might vary with internal heat conduction properties and external drag coefficients that affect aerodynamic heating, but it is instructive to compute this approximation nonetheless. Figure I-21 illustrates the isotherm plot corresponding to Case 1 for the reference cold-leg break.

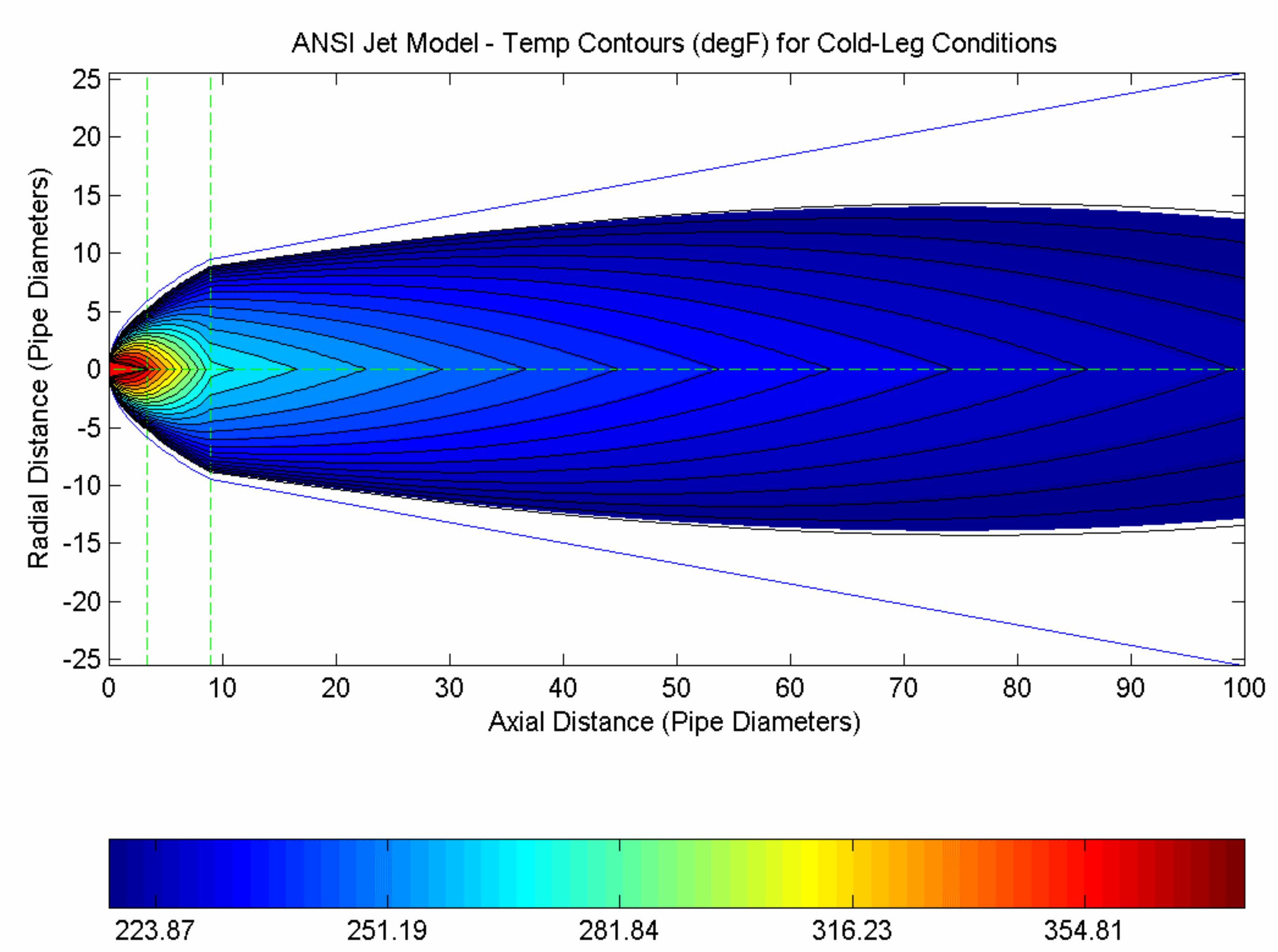

Figure I-21. Isotherm Contours for the Reference Cold-Leg Break at 2250 psia and 530°F

The somewhat surprising attribute of the isotherm map is how slowly the impingement temperature changes beyond the range of 10 to 15 pipe diameters downstream of the break. For potential debris-generation mechanisms that are suspected to have important thermal responses, this information can directly benefit both the specification of relevant test parameters and the interpretation of existing test data. For example, a test performed at 280°F that exhibits good damage resistance demonstrates substantially less spatial vulnerability to high-temperature jets than a test performed at 220°F. As with pressure contours, isotherm volumes can also be mapped to equivalent spherical volumes, and because the ANSI model exhibits spatial monotonicity (uniformly increasing or decreasing in every direction) in all physical jet properties, there is a unique correspondence between pressure, temperature, and contour volume.

Another impingement-state parameter of interest is the fluid quality. There has been a long-standing debate regarding the potential for enhanced debris generation in the presence of entrained water droplets compared with that observed for high-quality steam and for air-jet surrogates. While the ANSI model cannot answer this concern, it may offer information on the spatial extent of the phenomena. Subject to the same interpretations and approximations as those discussed for impingement temperature, the jet quality can also be evaluated at P_0 and h_0. Figure I-22 illustrates contours of equal two-phase steam quality for the reference cold-leg break. Similar to temperature, the fluid quality changes slowly beyond a range of 10 to 15 pipe diameters and maintains a nominal value between 0.25 and 0.35. This range would be considered low-quality steam for turbine generator applications and might be viewed with concern for its potential erosion effects on stainless steel rotor blades. Certainly, the time regimes of jet impact and in-service steam components are drastically different, but the potential damage mechanisms are the same.

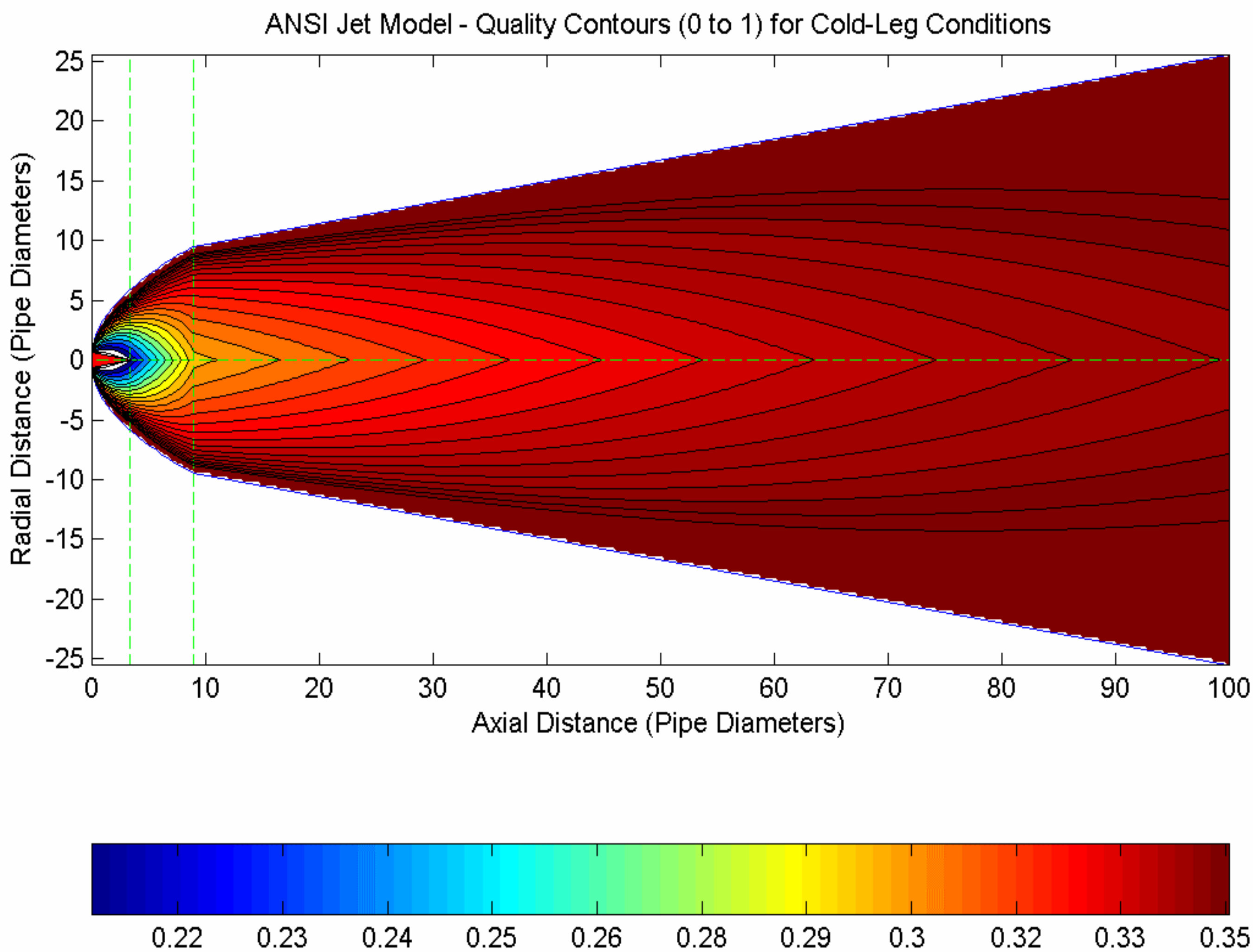

Figure I-22. Contours of Equivalent Steam Quality for the Reference Cold-Leg Break at 2250 psia and 530°F

The thermodynamic treatment of two-phase saturated conditions in the ANSI standard is inherently a homogeneous mass-mixture model. That is, the two-phase mixture is considered to be a single fluid with equivalent mass-weighted thermodynamic properties.

This assumption, along with that of equal phase velocities in the jet, is justified by Lahey and Moody (LAH84). Therefore, void fractions could be estimated from the local pressures and qualities. Under this assumption, it was found that the qualities shown in Figure I-19 would correspond to void fractions greater than 0.95 for all regions of the jet apart from the core. While Figure I-19 could be separated into the fluid and vapor mass fractions using the saturation properties and the definition of quality, the real issue of momentum transfer to a target could not be addressed with convincing accuracy. Theoretical treatments of two-phase transport introduce concepts of condensate nucleation, interphase velocities, droplet drag coefficients, and void fraction (space between droplets) that are difficult to measure experimentally. Pursuing this analysis with the present ANSI model would exceed the scope of its purpose and fidelity.

In summary, Table I-3 presents a set of concomitant values for pressure, temperature, quality, and equivalent spherical radius that characterize the approximate impingement conditions in an expanding jet generated by a cold-leg break at 2250 psia and 530°F. With respect to equivalent spherical diameter, this reference case is observed to bound all break conditions of interest for a PWR accident analysis. Table I-4 lists intermediate parameter values computed by ANSIJet for the reference break conditions. This information may be useful for comparisons of independent implementations of the jet model.

Table I-3. Summary of Jet Properties for the Reference Cold-Leg Break

P_{jet} (psig)	T_{jet} (°F)	Q_{jet}	R_{sphere}
2	218.7	0.35	31.5
3	221.8	0.34	25.4
4	224.6	0.34	21.6
6	230.0	0.34	17.0
10	239.6	0.33	11.9
17	253.7	0.32	7.5
24	265.5	0.31	5.4
40	287.0	0.29	4.0
80	324.2	0.26	2.6
150	366.1	0.21	1.5
190	384.0	0.20	1.1
2250	530.0	0.00	0.9

Table I-4. Intermediate Parameters Computed by the ANSI Jet Routine for the Reference Cold-Leg Break Conditions

Vessel Pressure	P_0	[psia]	2250
Vessel Temp	T_0	[deg F]	530
Vessel Quality	X_0	[-]	-0.430084
Vessel Density	r_0	[lbm/ft^3]	48.0879
Vessel Enthalpy	h_0	[Btu/lbm]	522.455
Sat Temp at P_0	T_{sat}	[deg F]	653.014
Liq Sat Enth at P_0	h_f	[Btu/lbm]	700.946
Vap Sat Enth at P_0	h_g	[Btu/lbm]	1115.96
Ambient Pressure	P_{amb}	[psia]	14.7
Pres at Asym Plane	P_a	[psia]	14.7
Dens at P_a, h_0	rma	[lbm/ft^3]	0.105653
Computed Thrust Coeff	TC	[-]	1.64413
Crit Mass Flux	G_e	[lbm/ft^2/s]	25329.2
T_{sat} at P_{amb}	T_{satamb}	[deg F]	212.238
Liq Sat Enth at P_{amb}	h_{famb}	[Btu/lbm]	180.176
Vap Sat Enth at P_{amb}	h_{gamb}	[Btu/lbm]	1150.28
Degrees Subcooling	$delT_{sub}$	[deg F]	123.014

I.7 Comparison of ANSI Model to Empirical Model of Kastner

Kastner et al. (KAS88) has generated a substantial body of experimental jet force and pressure distribution data. This work was carried out for upstream pressures ranging from 5 to 100 bar, temperatures from 20 to 310°C, and orifice diameters from 1 to 6.5 cm. A large plate was positioned at locations downstream of the orifice; the location of this plate along the jet axis was varied from 0.25 to 10 orifice diameters. Impingement pressures were recovered through a series of pressure taps located upon the plate. From this data, Kastner prepared empirical models for jet behavior given subcooled and saturated upstream stagnation conditions. Because the Kastner model has been formulated through regression analyses upon the data, it offers a convenient avenue for comparison of the ANSI model to experiment-based results.

Kastner's reference presented only the subcooled stagnation model in usable form. Therefore, two state points that fall within the range of validity of this model are selected for this comparative assessment. These are both relevant to BWR conditions—Case 10 from Table I-2 (420°F, 1044 psi) and a less-subcooled condition at the same pressure (516°F, 1044 psi). The quantities to be compared are jet centerline pressure, recovered jet thrust force, and radial pressure distribution. Given the conditions for which Kastner's model was derived, the comparison can only be considered valid for axial distances of less than 10 orifice diameters.

Figure I-23 compares the jet centerline pressure predicted by each model. The discontinuity predicted by the ANSI model when transitioning from the core to the freely expanding region where a high-quality, two-phase mixture flashes off of the core is clearly evident. Kastner's correlations, although they do include the core region, do not preserve this feature. Agreement for the more highly-subcooled upstream condition is poor, with the higher pressure predicted by Kastner implying that, near the jet centerline, a monophasic liquid region might persist farther downstream of the break location.

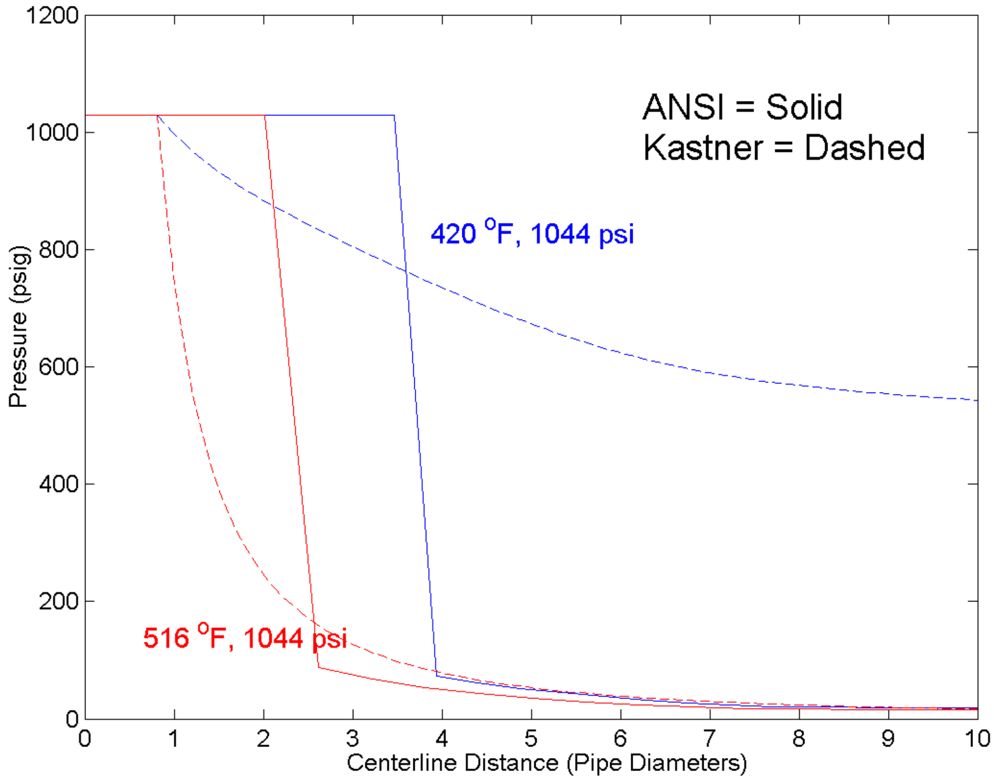

Figure I-23. Comparison of Jet Centerline Pressure Predictions

The radial pressure distributions adopted by the two models present strongly divergent functional forms. Under the ANSI model, the distribution takes on a triangular form. Hence the pressure behaves as an almost-linear function of radial position (exactly linear in Jet Region III of the standard), taking on its maximum value at the centerline and going to zero at the jet boundary. (See Section I.3.2 for further discussion.) Kastner observed that a Gaussian distribution closely approximates the radial impingement pressure. For a given subcooled upstream stagnation condition, Kastner's fit to the data results in a Gaussian radial pressure profile with a half-width independent of axial (downstream) position.

The ANSI model also preserves the concept of an asymptotic plane from classical jet theory as presented in LAH84. Recall that this plane is located at the downstream location at which the jet static gauge pressure is assumed to vanish. Under the ANSI model, downstream of the asymptotic plane mixing with the environment is assumed to take place and the location of the jet boundary is correlated differently. Therefore, it is somewhat misleading to compare radial pressure distributions at only a single axial location. Nonetheless, even one such isolated example will serve to illustrate the significant divergence between the predictions of the two models. Figure I-24 displays the radial pressure distributions at axial distances corresponding to the location of the respective asymptotic planes predicted by the ANSI model. For the more highly subcooled condition, this location is 7.5 break diameters; for the less subcooled state, it occurs at 7.25 break diameters. Although Kastner predicts higher jet centerline pressures, it can be seen that the ANSI model yields a more divergent jet. This follows from two critical physical assumptions inherent in the ANSI model.

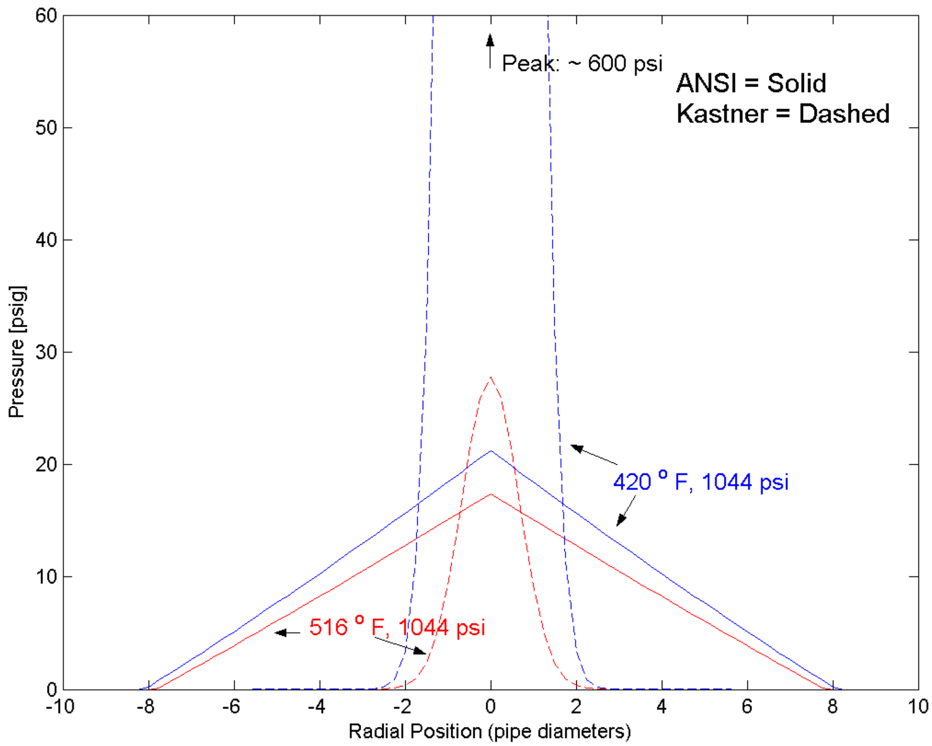

Figure I-24. Radial Impingement Pressure Distribution on a Plate Positioned at the ANSI Model Asymptotic Plane

First, the ANSI model is constrained to preserve the jet mass flow rate (kilogram per second [kg/s]). One might expect some mass to escape from the jet, such that the mass flow rate across a normally oriented plane downstream of the break would be less than the initial flow rate. However, the ANSI model does not allow mass to escape from the jet. Second, the model preserves the initial jet force at all downstream locations; the full force is always recovered on any large normally oriented plate. In fact, four mechanisms leading to downstream recovery of less than the initial force can be identified:

(1) If one envisions a control volume such as that drawn in

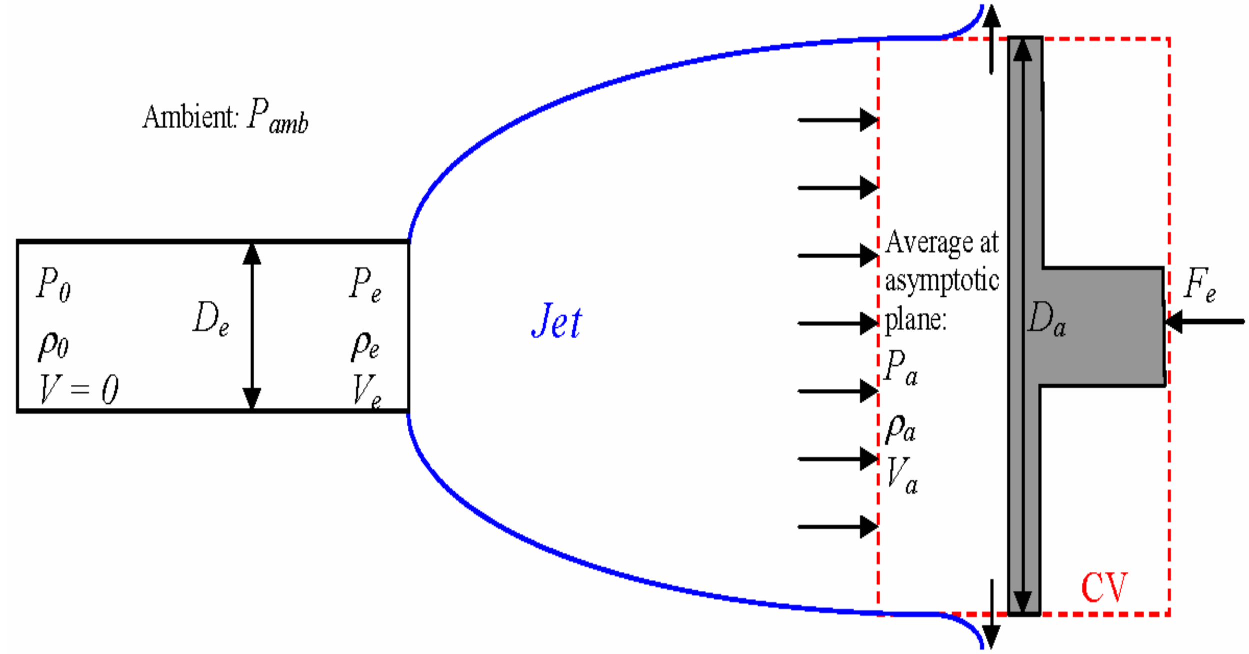

Figure I-4, mass may have departed from the forward-traveling jet and crossed the sides of the control volume before impacting the plate.

(2) Fluid impinging on the plate may have a tangential velocity component that will not contribute to the measured thrust.

(3) Energy transfer via mixing with the environment may occur to some extent dependent on the distance to the target.

(4) Dissipative losses across standing shock boundaries near the targets may be important.

The issue of downstream force recovery may be divided into two components, fraction of initial force recovered and magnitude of initial force. This discussion addressed each separately, with the recovery fraction treated first. Figure I-25 shows the fractional jet thrust force recovery as the downstream location varies from 0 to 10 break diameters. Kastner's correlation implies that significantly less than the full jet force is recovered downstream of the break. These results can be obtained by either numerically or analytically integrating the respective radial pressure profiles for the two models and normalizing by the mass flux present at the break plane. Comparison between the two thermodynamic cases shows that the portion of the initial force that is lost increases as the initial subcooling decreases. The smaller fractional recovery given by the Kastner model may be counterintuitive given that its jet centerline pressure predictions as shown in Figure I-23 and Figure I-24 are greater than that of the ANSI model. However, it must be borne in mind that the recovered force is obtained by computing an integral over the jet impingement area. The ANSI jet, being significantly more dispersed, impinges upon a much larger area; in fact, the area is designed to yield full force recovery and only the definition of the geometric envelope defines the radial extent of the jet cross section.

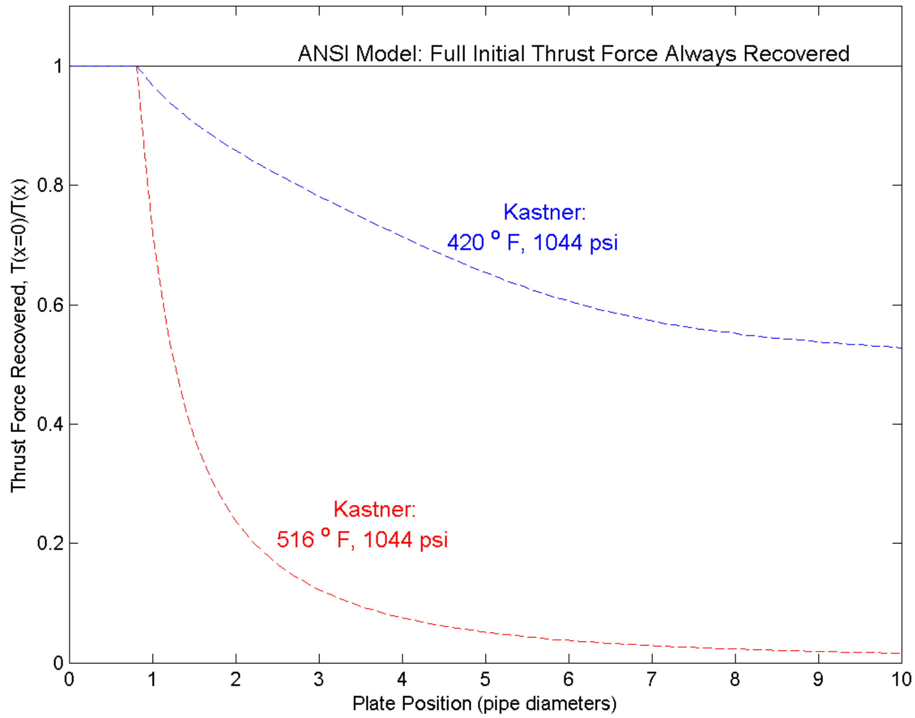

Figure I-25. Fraction of Initial Jet Thrust Force Recovered on Large Normally Oriented Plate, as a Function of Plate Location

The initial thrust force predicted by the ANSI model depends on the method used to compute the discharge mass flow rate (Henry-Fauske was employed here), while the actual flow rate is already embedded in Kastner's experimental results. Hence, the models' initial thrust forces are also different, even for comparable initial conditions. In fact, assuming no resistance in the nozzle, the ANSI model using Henry-Fauske critical flow parameters predicts larger initial thrust forces than the Kastner model. Specifically, the ANSI/Henry-Fauske initial force is 46 percent larger for the less-subcooled condition and 121 percent larger for the more-subcooled state.

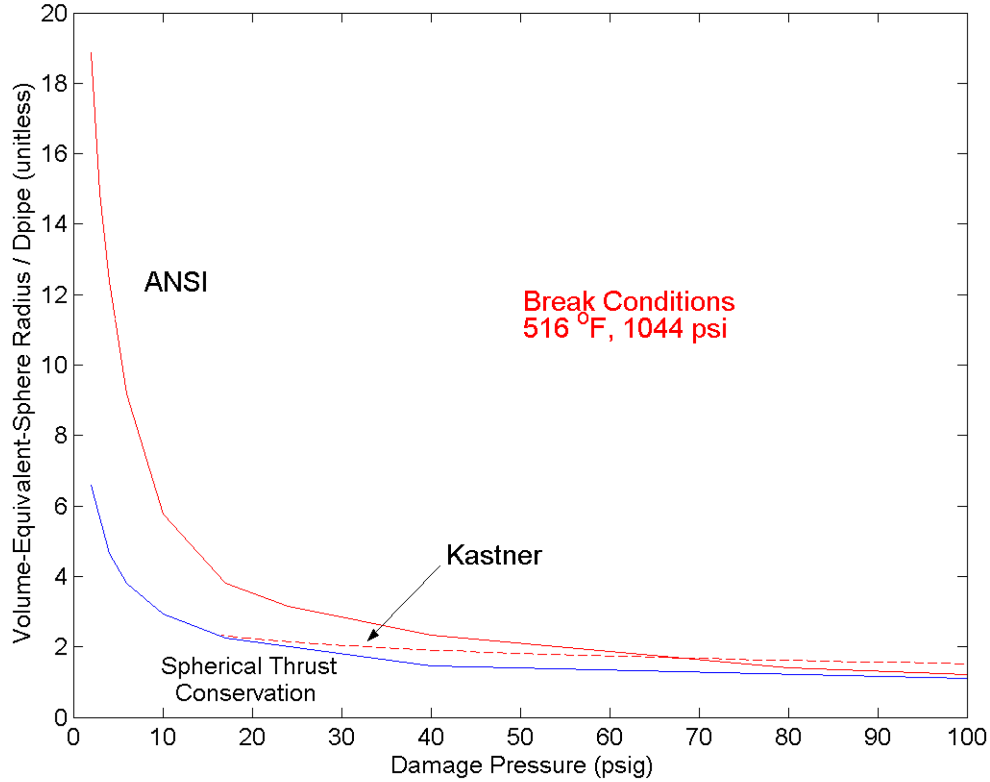

Figure I-26. Comparison of Equivalent Spherical Damage Radii

Figure I-26 presents one comparative metric of great interest for this application, the radius of the volume-equivalent sphere obtained for any given damage pressure. The narrower jet geometry given by the Kastner model leads to smaller radii for all but very high damage pressures. At the highest pressures, differences in the treatment of the area immediately surrounding the core become important. The ANSI model exhibits a large and discontinuous pressure drop as one crosses the core boundary; hence, Kastner's continuous model results in locally higher pressures in this region. The authors of the Kastner model recognize this as a shortcoming of the methodology; however, the correction proposed in KAS88 is only relevant to rectangular orifice geometries and will not be considered here. Also, Kastner's correlation is only fully validated out to a centerline range of 10 pipe diameters, beyond which the pressures fall below 15 psig. Therefore, the dashed line in Figure I-26 is truncated.
The key physical assumption that drives the development of the ANSI model is the conservation of momentum flux across the area of the asymptotic plane. Other considerations define the location and size of this plane, as discussed previously. However, an abstract point source that dissipates energy by geometric attenuation only as it expands isotropically can represent the geometric limit of the momentum conservation approach. The blue line in Figure I-26 illustrates the $1/R^2$ relationship between spherical radius and surface-averaged pressure inherent to the spherical momentum-conservation limit. Physical models based on energy conservation should not yield results below this limit for a given break condition, but empirical data such as Kastner and numerical models that incorporate physical energy losses may yield trends

below the limit. This case is presented to help judge the magnitude of marginal returns that might be realized with respect to ZOI volume by selecting a more realistic jet model.

Generally, the ANSI model, regardless of whether the Henry-Fauske or homogeneous equilibrium critical flow relation is used, yields conservative results when compared to Kastner's correlations—initial thrust forces and downstream force recovery are both larger. Even if the Kastner model is the more accurate, these conservatisms are not entirely unjustified for the present application. First, Kastner's experimental results were universally obtained with nonidealized discharge conditions (i.e., a nonzero hydraulic coefficient of resistance). Although the Kastner model may be compared to the idealized conditions studied here, this represents an extrapolation rather than an interpolation of the experimental results. Furthermore, the present application is not merely concerned with jet impingement on normally oriented structures or on targets located near the jet centerline. For the complicated target geometries that might be encountered within a containment building, volume-equivalent spheres computed using the ANSI model corresponding to a range of impingement pressures provide a conservative approach for computing potential ZOI damage volumes. Hence, pending experimental and/or theoretical investigation of jet stagnation pressures and velocity fields at locations away from the centerline, it seems prudent to impose full jet mass flow and force recovery as preserved by the ANSI model.

I.8 Summary of Examination of the ANSI Jet Model

Appendix I provides an exposition of the ANSI model and addresses several points where the model may be insufficiently clear or may suffer from an inconsistency. The following summarizes the major issues raised in the appendix and provides recommendations for remediation where applicable:

- The pressure distribution produced by the model exhibits a discontinuity across the boundary of the core. Within the core, the stagnation pressure is assumed to equal the upstream pressure P_0; the discontinuity has been observed to reach an order of magnitude for certain upstream conditions.
- Although not explicitly stated in the model, the jet pressure distribution, which falls to zero in the far field, must be interpreted as representative of local impingement gauge pressures.
- The jet pressure at the centerline, however, remains nonzero for any finite value of the axial penetration distance. This exaggerates pressure isobar volumes and causes volume-equivalent spherical damage radii to approach infinity as the damage pressure goes to zero.
- The pressure distribution has evidently been formulated such that the thrust force is correctly recovered only for targets oriented normal to the flow direction at the orifice. Therefore, the model may not be a good approximation to free-field expansion; it may not accurately predict local conditions at points away from the jet centerline, where the flow velocity on such a normally oriented plate would exhibit a significant tangential component. This concern is not addressed by the application of a shape factor, as outlined in Appendix D to the ANSI report.

- The above point has further ramifications for the applicability of the model to small targets. Because the stagnation pressure field produced by the model was developed to reproduce loadings on large flat targets, it is inaccurate to apply the stagnation pressures to small and/or nonflat objects. One could bound the true conditions by computing local static pressures, as well; however, knowledge of the local velocity field and of the characteristics of the two-phase jet flow that are beyond the scope of the ANSI model would be required.
- A discontinuity in the slope of the isobars exists between Zones 2 and 3. Figure I-1 clearly shows this discontinuity. The sharp terminal points of pressure isobars at the axial centerline also suggest that more attention could be given to the behavior of first spatial derivatives.
- The assumption of isentropic and/or isenthalpic expansion should be made with caution. For instance, stagnation conditions at the asymptotic plane are evaluated assuming isenthalpic behavior, implying no energy loss to the environment. In general, however, the isentropic assumption appears to be applied to the expanding jet. For a discussion of the limitations of these assumptions, see WIT02.
- Although it was analytically confirmed that all characteristic lengths in the problem scale linearly with the break diameter, D_e, it is recommended that users implement the formulation of the model presented herein, as it has been nondimensionalized with respect to this quantity.
- The notation adopted by the standard for the thrust coefficient is evidently inconsistent; C_T, C_{Te}, and C^*_{Te} all appear in the equations describing the pressure distribution for the various jet zones. These forms must all refer to a single numeric value if the pressure equations are to be piecewise continuous between zones.
- The ANSI model presents an expression for the jet area at the asymptotic plane that rests upon the assumption that the average flow static pressure at that location equals the ambient pressure, P_{amb}. Elsewhere in the ANSI model, however, the asymptotic plane static pressure is assigned a value that may be less than P_{amb}.
- The standard advises users to implement a critical flow model, either the homogeneous equilibrium model (HEM) or the Henry-Fauske model, to obtain the jet mass flux G_e. Users not having such a model available may estimate G_e from Figure C-4 of the ANSI report; however, this figure only covers stagnation conditions extending to 2000 psi and 50°F of subcooling, leaving certain states (e.g., cold-leg conditions in many PWRs) unaddressed. Given the additional inaccuracies that reading from the figure may introduce, it is strongly recommended that a critical flow model be implemented for use with the jet model.
- The standard recommends that the Henry-Fauske critical flow model be used for subcooled vessel conditions and the HEM for saturated conditions. This would introduce a strong discontinuity as the liquid saturation point is crossed. Therefore, because Henry-Fauske is evidently in better agreement with the

data for both subcooled and two-phase conditions, exclusive use of this model is recommended.

- An implied discontinuity exists across the break plane, as the ANSI model assumes that fluid in the core is in equilibrium at the upstream stagnation pressure and quality. This assumption contradicts aspects of both the HEM and the Henry-Fauske models.

- The correlation recommended by the standard for use in calculating the thrust coefficient, C_T, for subcooled conditions applies only to Henry-Fauske derived mass fluxes. The standard does not make this clear. In addition, it left unclear the assumption inherent in the correlation that ambient conditions are at standard pressure. Therefore, this correlation should not be used in conjunction with HEM mass fluxes, and users of the standard should bear in mind that the correlation is not strictly validated for ambient conditions deviating from those of the standard atmosphere. The error is small, though, for most upstream pressures of interest in the present analysis.

- The standard provides no analytic correlation for the thrust coefficient relevant to saturated steam-water mixtures. Within the standard, users may only consult Figure B-5 to visually gauge an approximate value. Another recourse would be to consult the thrust coefficient contour plots presented in this appendix or, better, implement a critical mass flux model to enable direct calculation of mass flux and thrust coefficient via the Henry-Fauske model.

- Users should be aware that one desired result of the model, volume-equivalent spherical damage-pressure radii, can behave nonintuitively as certain upstream conditions are varied. For instance, the PWR hot-leg and cold-leg results presented in Table I-1 of this appendix show that the flow from the hot-leg break exhibits a lower mass flux and thrust coefficient than that from the cold leg. Nonetheless, the damage radii are roughly comparable, with radii for the hot-leg break exceeding those of the cold leg for higher damage pressures and smaller for lower damage pressures. These results, which follow from variations in the flow velocity and density at the break, reinforce the importance of not eliminating lower energy break points *a priori* when conducting ZOI analyses.

I.9 References

ANS88 "American National Standard: Design Basis for Protection of Light Water Nuclear Power Plants Against the Effects of Postulated Pipe Rupture," American Nuclear Society, ANSI/ANS-58.2-1988, October 1988.

DUD76 Duderstadt, J.J. and L.J. Hamilton, *Nuclear Reactor Analysis*, Wiley and Sons, New York, New York, 1976.

HAL80 Hall, D.G. and L.S. Czapary, "Tables of Homogeneous Equilibrium Critical Flow Parameters for Water in SI Units," EG&G Idaho Report EGG-2056, 1980.

HAR96 Harvey, A.H., A.P. Peskin, and S.A. Klein, "NIST/ASME Steam Properties: Formulation for General and Scientific Use," Version 2.11, 1996.

HEN71 Henry, R.E. and H.K. Fauske, "The Two Phase Critical Flow of One-Component Mixtures in Nozzles, Orifices, and Short Tubes," *J. Heat Transfer*, p. 179, May 1971.

KAS88 Kastner, W. and R. Rippel, "The Two Phase Critical Flow of One-Component Mixtures in Nozzles, Orifices, and Short Tubes," *Nucl. Engr. and Design*, 105, p. 269, 1988.

LAH84 Lahey, R.T. and F.J. Moody, *The Thermal-Hydraulics of a Boiling Water Nuclear Reactor*, 3rd ed., La Grande Park, IL: ANS Press, p. 381, 1984.

LOB90 Lobner, P., C. Donahoe, and C. Cavallin, "Overview and Comparison of U.S. Commercial Nuclear Power Plants," prepared for the U.S. Nuclear Regulatory Commission by Science Applications International Corporation, NUREG/CR-5640, SAIC-89/1541, September 1990.

NEI04 "Pressurized-Water-Reactor Sump Performance Evaluation Methodology," Nuclear Energy Institute, May 28, 2004.

NRC98 "Safety Evaluation by the Office of Nuclear Reactor Regulation Related to NRC Bulletin 96-03, Boiling Water Reactor Owners Group Topical Report NEDO-32686," U.S. Nuclear Regulatory Commission, August 1998.

NRC03 Regulatory Guide 1.82, Rev. 3, "Water Sources for Long-Term Recirculation Cooling Following a Loss-of-Coolant Accident," U.S. Nuclear Regulatory Commission, Office of Nuclear Regulatory Research, August 2003.

RAH92 Rahn, F.J., et al., *Guide to Nuclear Power Technology: A Resource for Decision Making*, Krieger, Malabar, FL, 1992.

RAO02 Rao, D.V., K.W. Ross, and S.G. Ashbaugh, "GSI-191: Thermal-Hydraulic Response of PWR Reactor Coolant System and Containments to Selected Accident Sequences," prepared for the U.S. Nuclear Regulatory Commission by Los Alamos National Laboratory, NUREG/CR-6770, LA-UR-01-5561, August 2002.

URG96 NEDO-32686, Rev. 0, "Utility Resolution Guidance for ECCS Strainer Blockage," General Electric Nuclear Energy Company, Class 1, November 1996.

WEB76 Webb, S.W., "Evaluation of Subcooled Water Thrust Forces," *Nucl. Technology*, Vol. 31, p. 48, October 1976.

WEI83 Weigand, G.G., et al., "Two-Phase Jet Loads," NUREG/CR-2913, prepared for the U.S. Nuclear Regulatory Commission by Sandia National Laboratory, January 1983.

WIT02 Witlox, H.W. and P.J. Bowen, "Flashing Liquid Jets and Two-Phase Dispersion: A Review," United Kingdom Health and Safety Executive Contract Research Report 403/2002, p. 37, 2002.

Appendix II

Confirmatory Debris Generation Analyses

The Nuclear Energy Institute (NEI) guidance contains recommendations that will determine the quantities of insulation debris generated with the zone of influence (ZOI). These recommendations include the size of the ZOI based on the insulation destruction pressure and the fraction of the insulation located within the ZOI that subsequently is damaged into the small-fine-debris category. Confirmatory research ascertained whether the NEI recommendation would reliably result in conservative estimates for the volumes of debris generated within the ZOI. This appendix documents the confirmatory research estimates for the volumes of small fine debris. Appendix I covers the confirmatory research for determining the size of the ZOI. Both the NEI guidance and the confirmatory research used the American National Standards Institute (ANSI)/American Nuclear Society (ANS)-58.2-1988 standard to calculate the jet isobar volumes with very similar results. The confirmatory research issues addressed herein include the following:

- The NEI guidance recommends the assumption that 60 percent of the fibrous and 75 percent of the reflective metal insulation (RMI) volume contained within the ZOI become small fine debris. The confirmatory research integrated the insulation damage versus jet pressures over the ZOI volume to determine the fraction of the insulation within the ZOI that would become small fine debris based on available debris generation data.
- The NEI guidance recommends adapting the debris-size distribution for NUKON™ to other types of fibrous insulation that have a destruction pressure higher than that of NUKON™. The size distribution confirmatory research provides partial justification that supports that NEI recommendation.
- The applicability of air-jet-determined destruction pressures to two-phase pressurized water reactor (PWR) loss of coolant accident (LOCA) jets has been questioned. Volume 3 of NUREG/CR-6762 noted that data from the Ontario Power Generation (OPG) two-phase debris generation tests indicate that the destruction pressure could be lower for a two-phase jet than for an air jet and that the resultant debris could be finer. Therefore, it may be prudent to apply a safety factor to accommodate the uncertainty. This confirmatory analysis estimates the volume fractions for small fine debris if an alternate lower destruction pressure were used than those in the NEI guidance.

II.1 Comparison of Jet Isobar Volume Calculations

Three calculations of the jet isobar volumes were available for comparison:*

* The volumes are actually presented in terms of the break diameter cubed (D^3) corresponding to an equivalent spherical radius in terms of r/D (i.e., $4\pi/3\ r^3/D^3$).

(1) the volumes determined from the NEI guidance recommended values for ZOI radii versus the destruction pressures in Table 3-1 of the NEI baseline guidance, where the destruction pressure represents the jet isobar pressure for each particular ZOI radii,

(2) the volumes determined from the confirmatory research (Appendix I) for the ZOI radii versus the jet pressure,

(3) the volumes determined from the Boiling Water Reactor Owners Group (BWROG) recommendation documented in their utility resolution guidance (URG).

Although the volumes in item (3) above apply to a BWR steam jet rather than a PWR two-phase jet, the volumes are compared here to demonstrate the differences between PWR and BWR LOCA jets.

Both the NEI guidance and the confirmatory research volume calculations used the ANSI/ANS-58.2-1988 standard method, whereas the BWROG URG method used the computational fluid dynamics (CFD) code, NPARC, to evaluate the volumes. Figure II-1 compares the equivalent spherical radii for these three methods.

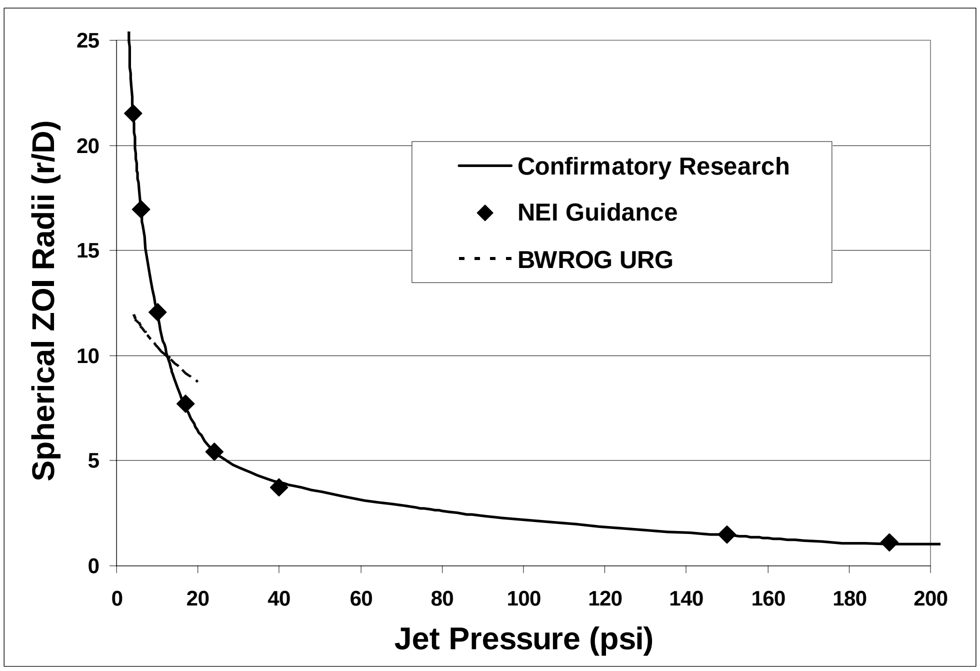

Figure II-1. Comparison of Jet Isobar Volumes

As shown, at the lower jet pressures, the pressure isobar volumes are much larger for the PWR two-phase LOCA jet than for the BWR steam jet. A principal reason for this difference is the higher energy associated with the higher pressure of a PWR reactor coolant system (RCS) than with a BWR RCS; however, another consideration is the accuracy of the ANSI/ANS-58.2-1988 standard at the lower pressures. For example, the validity of the assumption in the ANSI/ANS-58.2-1988 standard that the jet expands at a half angle of 10 degrees once the jet expansion has reached the asymptotic plane becomes more important at the lower expansion pressures. The accuracy of the debris volumes of insulations that damage significantly at the lower jet pressures is subject to the accuracy of this assumption. Note that the confirmatory research and NEI-recommended-equivalent spherical ZOI radii are in good agreement.

II.2 Method of Determining ZOI Debris-Size Distributions

The volume of debris generated within a ZOI depends on (1) the size of the ZOI defined by the spherical radius, (2) the concentration of a particular insulation within the ZOI, and (3) the fraction of the ZOI insulation that is damaged into a particular debris-size classification. The size distribution and spherical ZOI radius are interdependent. The threshold damage pressure and the jet volumes determine the size of the ZOI (Appendix I). Plant-specific information (i.e., the volume of a particular insulation within the ZOI divided by the volume of the ZOI) determines the insulation concentration within a ZOI.

Integration of experimental debris generation data is required to determine the fraction of the ZOI insulation that is damaged into a particular debris-size classification (e.g., NEI small fine debris). For this integration, NUREG/CR-6808 offered a generalized equation. A slightly expanded version of this equation is

$$F_{ZOI} = \frac{3}{r_{ZOI}^3} \int_0^{r_{ZOI}} f_d \left(P_{jet}(r) \right) r^2 \, dr \quad ,$$

where

F_{ZOI} = the fraction of the ZOI insulation type i that is damaged into a particular debris-size classification,

f_d = the fraction of debris damaged into a particular debris size as a function of the jet pressure P_{jet}, which is a function of the spherical radius, *r*, within the ZOI, and

r_{ZOI} = the outer radius of the ZOI.

Implicit in this integration is the assumption that the insulation is uniformly distributed within the ZOI, which may not be realistic. Because the functional information needed for this integration is not available in an equation form simple enough for a formal integration to proceed, the following simplification is used,

$$F_{ZOI} = \frac{1}{r_{ZOI}^3} \sum_j \left[\frac{f_{fines}\left(P_{jet}(r_j)\right) + f_{fines}\left(P_{jet}(r_{j-1})\right)}{2} \left(r_j^3 - r_{j-1}^3 \right) \right] \quad ,$$

where

f_{fines} = the fraction of debris damaged into a particular debris size as a function of the jet pressure P_{jet} at a radius of r_j.

The spherical ZOI is first subdivided into numerous spherical shells (j). The precision of the integration increases with the number of subdivisions. In a spreadsheet, the jet pressure is listed in increasing values and then the spherical radii are determined, followed by the damage fraction evaluated at each r_j. For the intervals, the average damage across the interval and the volume of the interval are determined. Multiplying the average interval damage by the interval volume, summing, and dividing by the total ZOI volume results in the debris fraction for the ZOI.

II.3 Evaluation of Debris-Specific Damage Fractions and Potential Debris Volume

Potential debris volumes were calculated for fibrous, RMI, and particulate debris types and compared with the NEI baseline model to determine whether the baseline is conservative. The potential volume of debris is defined as the fraction of the ZOI debris damaged into a particular debris size multiplied by the total volume of the sphere, as

$$V_{Potential} = F_{ZOI}\left(\frac{4}{3}\pi\right)r_{ZOI}^{3} \quad .$$

Note that to calculate the volume of small fine debris generated, the potential volume must be multiplied by the concentration of insulation ($C_{insulation}$) (i.e., the fraction of the ZOI actually occupied by the insulation) and by the pipe break diameter cubed. Again, it is assumed that the insulation type in question is uniformly distributed over the ZOI, regardless of the size of the ZOI, as

$$V_{Fines} = C_{Insulation}\,V_{Potential}\,D^{3} \quad .$$

II.3.1 Fibrous Debris

The fibrous insulation types evaluated include NUKON™, Transco (Transco Products, Inc., or TPI), Temp-Mat, K-wool, and Knauf. Table II-1 shows the destruction pressures recommended in the NEI guidance and an alternate set of values used herein to test the sensitivity of the potential debris volumes to the destruction pressures.

Table II-1. Fibrous Insulation Destruction Pressures

Insulation	NEI Recommendation	Alternate Lower Pressure
NUKON™	10 psi	6 psi
TPI	10 psi*	6 psi
Knauf	10 psi	6 psi
Temp-Mat	17 psi	10 psi
K-wool	40 psi	17 psi

* NEI guidance considers TPI fiber blankets to behave similarly to NUKON™ blankets.

II.3.1.1 Low-Density Fiberglass Debris

A review of the air jet testing debris generation data, both the BWROG air jet impact testing (AJIT) data (BWROG URG) and the drywell debris transport study (DDTS) data (NUREG/CR-6369, 1999), demonstrates that NUKON™, TPI, and Knauf fiberglass insulations underwent similar damage. These insulations have approximately the same as-manufactured density (approximately 2.4 lb/ft^3), and their recommended minimum pressures for destruction are usually taken to be the same pressure. Therefore, these insulations have been grouped together as low-density fiberglass (LDFG) insulation.

Figure II-2 plots the fractions for the small fines from the AJIT debris generation test data as a function of the jet centerline pressure for these three types of LDFG insulations. A curve drawn through the data represents the damage as a function of jet pressure for use in the damage integration over the ZOI. One set of seven data points was from tests (in the DDTS) that used a 4-in. nozzle, whereas the remainder used a 3-in. nozzle. The 4-in. nozzle data from the DDTS generally shows more damage than do the 3-in. nozzle tests. In general, the higher damage occurred because the larger diameter jet exposed more of the target insulation blanket to higher pressures. Note that the data were correlated by the estimated jet centerline pressure, but the pressure on the blanket decreased outward from the centerline. When the blanket was placed close to the jet, the ends of the blanket were hit with substantially less force of flow than the centerline for which the data were correlated. For example, the 3-in. nozzle data point for NUKON™ at a jet pressure of 20 psi damaged only approximately 7 percent of the insulation into small fine debris, whereas this pressure totally destroyed the TPI blankets in the 4-in. nozzle. Apparently, testing blanket destruction for insulations requiring a pressure higher than approximately 17 psi requires a jet nozzle larger than 3 in. For LDFG, any jet pressure larger than 17 psi will totally destroy the blanket into small fine debris, whereas the NEI guidance cited an OPG two-phase jet test with 52 percent of the insulation damaged into small fine debris as its basis of conservatism.

Another significant point of discussion is that the threshold of damage for LDFG insulation has been specified as 10 psi, where Figure II-2 clearly shows damage at jet pressures less than 10 psi. Apparently, neglecting the tail of the damage curve was considered acceptable for the BWR strainer resolution because of the lesser BWR jet volumes at lower pressures, as shown in Figure II-1. However, the much larger jet volumes below 10 psi for the Confirmatory Research/NEI Guidance PWR jet shown in Figure II-1 make the neglect of the tail less acceptable.

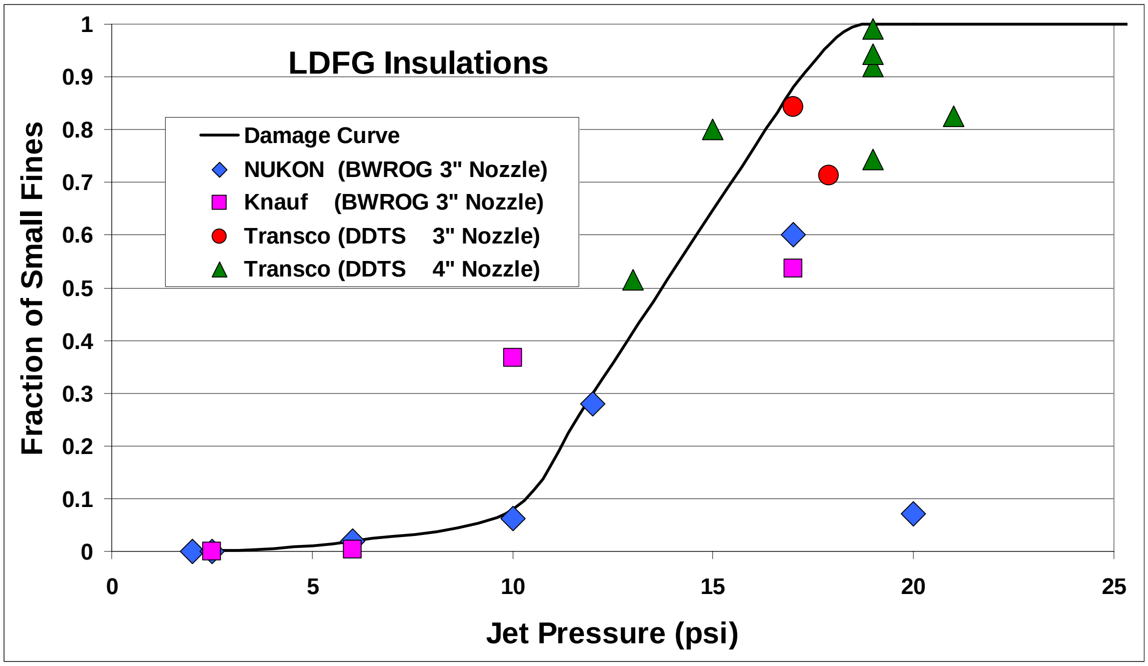

Figure II-2. LDFG Damage Curve for Small Fine Debris

Table II-2 provides the results of debris-size distribution integration over the ZOI. A lower alternate damage pressure results in a larger equivalent spherical ZOI; however, a lesser fraction of the debris is damaged into small fine debris. The use of the alternate damage pressures over the NEI-recommended damage pressures for PWR analyses would result in approximately 16 percent more small fine debris. Figure II-3 compares the potential debris volumes and provides an estimate using the baseline guidance. The baseline estimate is simply 60 percent of $4\pi/3\ (12.1/D)^3$. As shown, the baseline guidance appears to be conservative, but not overly so.

Table II-2. Results of Debris-Size Distribution Integration for LDFG Insulations

Jet Pressure Isobar Volume Calculation	Radius of Sphere (r/D)	Fraction Small Fines	Potential Debris Volumes (V/D^3)
NEI-Recommended Damage Pressures			
BWROG Steam Jet	10.4	0.83	3910
PWR Two-Phase Jet (Confirmatory)	11.9	0.53	3790
Alternate Damage Pressures			
BWROG Steam Jet	11.4	0.65	3980
PWR Two-Phase Jet (Confirmatory)	17.0	0.22	4410

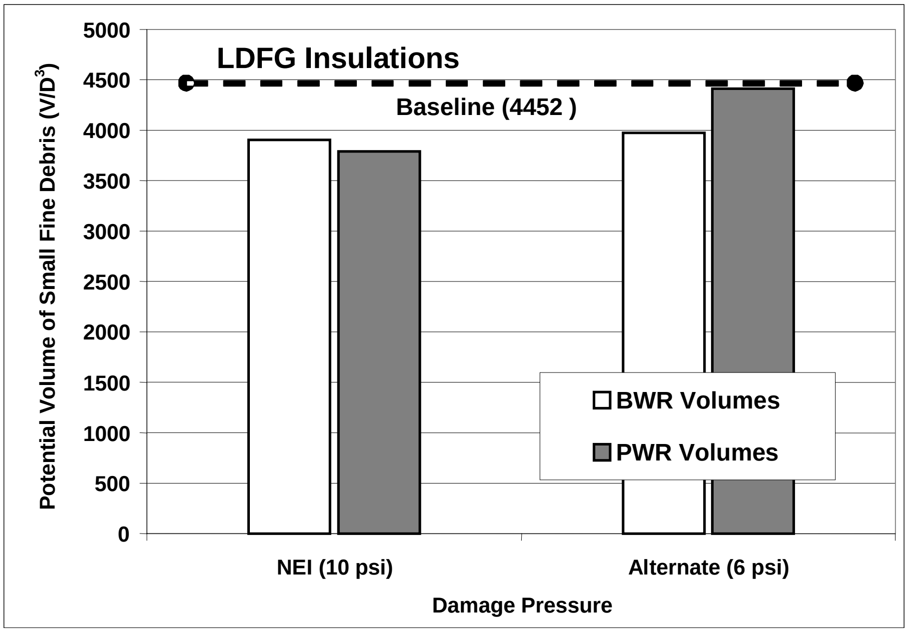

Figure II-3. Potential Volumes of Small Fine LDFG Debris

The NEI baseline guidance completely neglects the transport of large debris to the sump screen; however, some plants will likely need to consider large debris transport as part of a more realistic evaluation. Therefore, the following equation estimates the volume of large debris generated within the ZOI:

$$V_{Large} = C_{Insulation}\,(1 - F_{ZOI})\left(\frac{4}{3}\pi\right) r_{ZOI}^3\ D^3 \quad .$$

In addition, plants that must perform more realistic evaluations may need to subdivide the baseline small-fine-debris class into fines and small-piece debris, where the fines (e.g., individual fibers) remain suspended in the pool and the small-piece debris sinks to the pool floor, where the debris may or may not transport to the sump screen. The baseline guidance has the inherent assumption that all of its small fine debris essentially remains suspended.

In the debris generation tests conducted during the DDTS, 15 to 25 percent of the debris from a completely disintegrated TPI fiberglass blanket was classified as nonrecoverable. The nonrecoverable debris either exited the test chamber through a fine-mesh catch screen or deposited onto surfaces in such a fine form that it could not be collected by hand (it was collected by hosing off the surfaces). Therefore, it would be reasonable to assume that 25 percent of the baseline small fine debris (i.e., F_{ZOI}) is in the form of individual fibers and that the other 75 percent is in the form of small-piece debris.

II.3.1.2 Temp-Mat Debris

Temp-Mat is much higher density insulation (approximately 11.8 lb/ft^3) than the LDFG insulation and requires a significantly higher jet pressure to damage the insulation.

Figure II-4 shows the Temp-Mat insulation debris fractions for the small fine debris from the AJIT tests. This figure shows six data points for Temp-Mat, two of which represent tests where no significant damage was noted. The test with the maximum damage had approximately 36 percent of the insulation damaged into small fine debris, with the remainder of the insulation forming large-piece debris. Unfortunately, no tests were conducted with jet pressures high enough to complete the damage curve to total destruction into small fine debris, as was done for the LDFG insulations. Therefore, a conservative extrapolation of the data is required to perform the debris generation integration over the equivalent ZOI sphere. Figure II-4 shows the extrapolation used herein as a dashed line. Figure II-4 also illustrates the selection of the NEI-guidance damage pressure of 17 psi, where it is seen that significant small fine debris is generated at jet pressures below 17 psi.

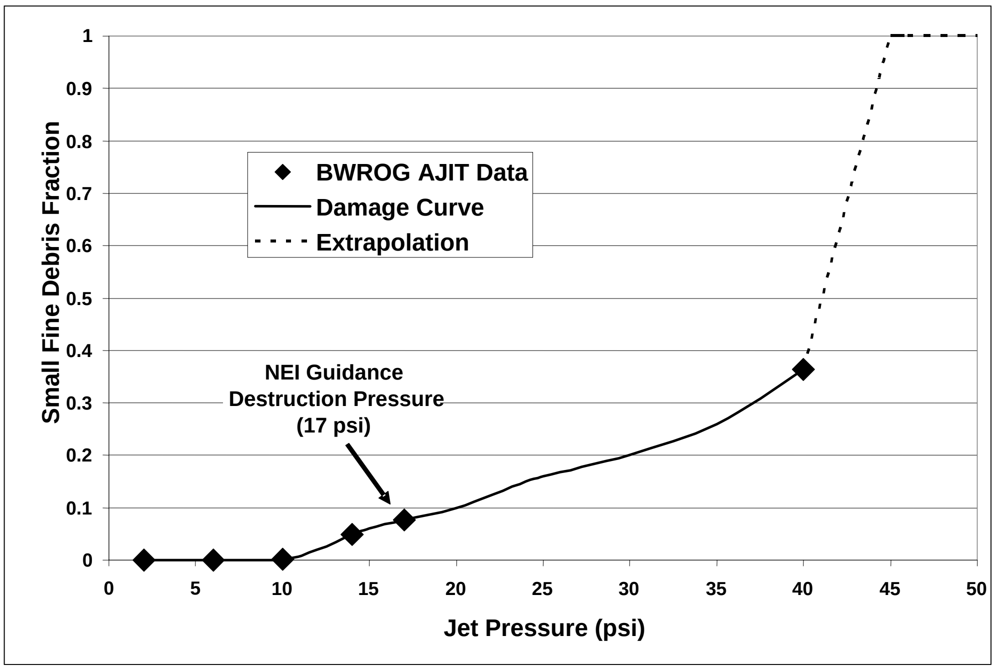

Figure II-4. Temp-Mat Damage Curve for Small Fine Debris

Table II-3 provides the results of the Temp-Mat debris-size distribution integration over the ZOI. Figure II-5 compares the potential debris volumes and provides an estimate using the baseline guidance (60 percent of $4\pi/3\ (7.8/D)^3$). A lower alternate damage pressure results in a larger equivalent spherical ZOI; however, a lesser fraction of the debris is damaged into small fine debris. The use of the alternate damage pressures over the NEI-recommended damage pressures for PWR analyses would result in approximately 36 percent more estimated small fine debris. For Temp-Mat insulation, the baseline is conservative with respect to both the NEI-guidance damage pressure of 17 psi and the alternate pressure of 10 psi.

The debris-size estimate for Temp-Mat has more uncertainty associated with the estimate than does the similar calculation for LDFG, primarily because of more limited data. The negative uncertainties include the neglect of the damage curve tail by the

NEI-recommended damage pressure (quantified using the alternate damage pressure) and the fact that the BWROG AJIT tests used the small 3-in. nozzle, which makes it difficult to subject the entire target blanket to the characteristic jet pressure (near the centerline pressure) when the blanket is located close to the nozzle. The positive uncertainty is the sharp extrapolation of the damage curve to 100 percent destruction at 45 psi. In this case, it is possible that the positive uncertainty overshadows the negative uncertainties.

Table II-3. Results of Debris-Size Distribution Integration for Temp-Mat Insulation

Jet Pressure Isobar Volume Calculation	Radius of Sphere (r/D)	Fraction Small Fines	Potential Debris Volumes (V/D^3)
NEI Recommended Damage Pressures			
PWR Two-Phase Jet (Confirmatory)	7.5	0.25	448
Alternate Damage Pressures			
PWR Two-Phase Jet (Confirmatory)	11.9	0.086	608

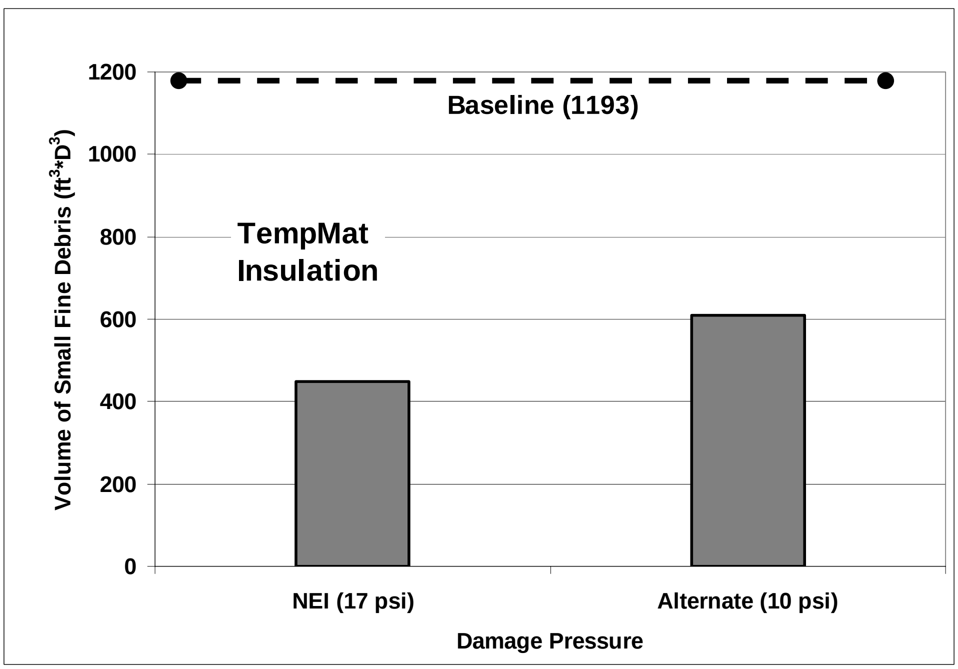

Figure II-5. Potential Volumes of Small Fine Temp-Mat Debris

II.3.1.3 K-Wool Debris

K-wool is also higher density insulation (approximately 10 lb/ft^3) than the LDFG insulation and requires an even higher jet pressure to damage the insulation. The NEI-recommended damage pressure for K-wool is 40 psi. Figure II-6 shows the K-wool insulation debris fractions for the small fine debris from the AJIT tests. This figure shows only four data points for K-wool, two of which represent tests where no significant damage was noted. The test with the maximum damage had approximately 7.1 percent of the insulation damaged into small fine debris, with much of the remainder of the insulation still contained in the blanket cover and still attached to the target mount. As with the Temp-Mat data, the K-wool damage curve is incomplete because the highest jet pressure tested was that of the NEI-recommended damage pressure. To perform the debris generation integration over the equivalent ZOI sphere, the test data were conservatively extrapolated, as shown in Figure II-6.

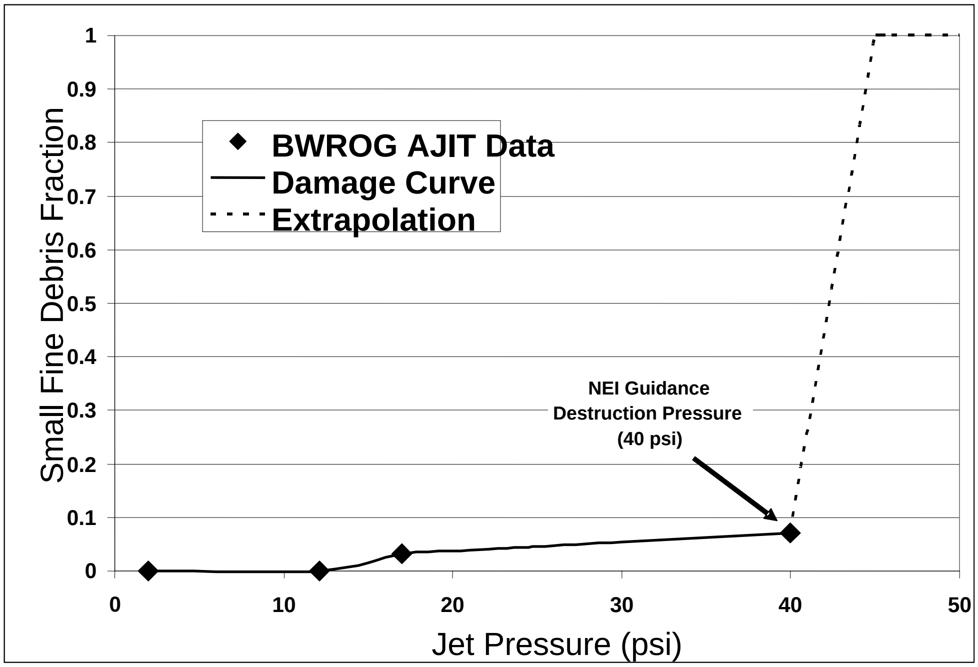

Figure II-6. K-Wool Damage Curve for Small Fine Debris

Table II-4 provides the results of the K-wool debris-size distribution integration over the ZOI. Figure II-7 compares the potential debris volumes and provides an estimate using the baseline guidance (60 percent of $4\pi/3\ (3.8/D)^3$). The lack of debris generation data for a jet pressure higher than the NEI-recommended destruction pressure of 40 psi makes K-wool integration difficult. Therefore, to ensure conservative debris-size integration, it must be assumed that the insulation is completely destroyed at a pressure higher than 40 psi (i.e., the integration herein assumed to be 100 percent at 45 psi). However, this assumption may be overly conservative. For K-wool insulation, the baseline is not conservative with respect to either the NEI guidance damage pressure of 40 psi or the alternate pressure of 17 psi.

Table II-4. Results of Debris-Size Distribution Integration for K-Wool Insulation

Jet Pressure Isobar Volume Calculation	Radius of Sphere (r/D)	Fraction Small Fines	Potential Debris Volumes (V/D^3)
NEI-Recommended Damage Pressures			
PWR Two-Phase Jet (Confirmatory)	4.0	0.92	246
Alternate Damage Pressures			
PWR Two-Phase Jet (Confirmatory)	7.5	0.17	307

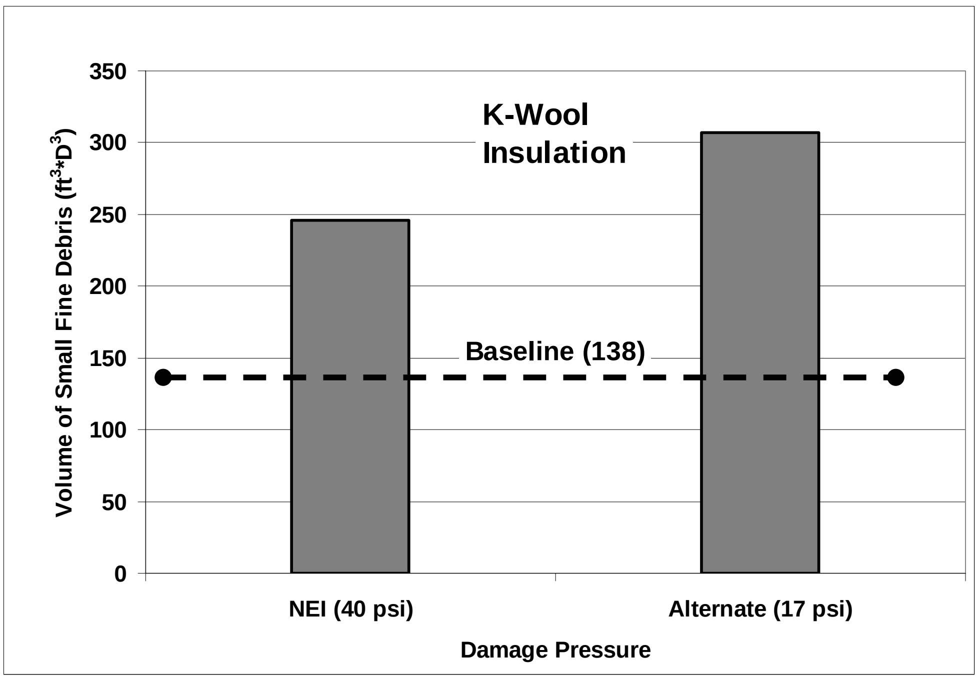

Figure II-7. Potential Volumes of Small Fine K-Wool Debris

II.3.1.4 Correlation between Debris Size and Destruction Pressure

The NEI guidance assumes that it is conservative to adapt the debris-size distribution for NUKON™ to other types of insulations that have a higher destruction pressure than NUKON™ (e.g., Temp-Mat and K-wool). Figure II-8 examines this assumption by comparing the debris generation data for LDFG, Temp-Mat, and K-wool.

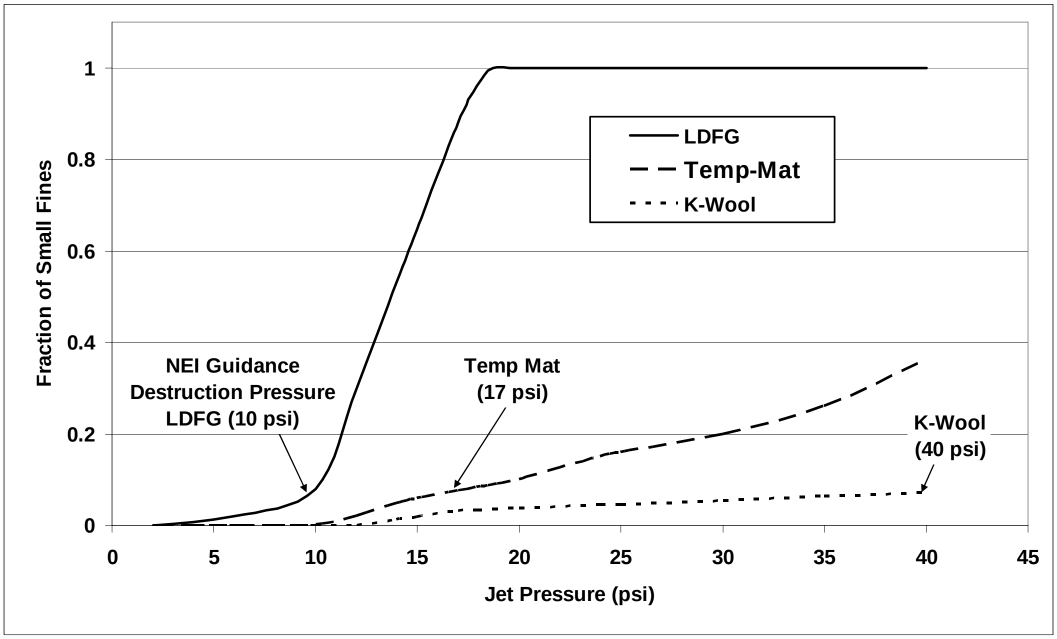

Figure II-8. Comparison of Fibrous Insulation Damage Curves

This damage curve comparison for LDFG, Temp-Mat, and K-wool does seem to support the concept that a higher destruction pressure results in the fractions of small fines becoming increasingly smaller as the destruction pressure increases. Certainly this is the case for Temp-Mat, where the baseline guidance is conservative relative to the integration herein and both the fractions of small fine debris and the potential debris volumes are smaller than the baseline guidance. Although this case is likely true for K-wool as well, it cannot be proven conclusively because of the complete lack of data beyond the NEI-recommended destruction pressure.

II.3.2 RMI Debris

The NEI guidance contains recommendations for three types of RMI insulation:

(1) DARMET®, manufactured by Darchem Engineering, Ltd.

(2) RMI, manufactured by TPI

(3) Mirror®, marketed by Diamond Power Specialty Company (DPSC)

The NEI recommends an assumption that 75 percent of the RMI insulation contained in the equivalent spherical ZOI will be turned into small fine debris. Table II-5 shows the NEI-recommended destruction pressures and the corresponding NEI-recommended radii for those pressures. Note that the ZOI for DARMET® and TPI are quite small compared with the ZOI for DPSC Mirror®.

Table II-5. NEI-Recommended RMI Insulation Destruction Pressures and ZOI Radii

RMI Insulation	Destruction Pressures (psi)	ZOI Radius (r/D)
DARMET®	190 psi	1.3
TPI	190 psi	1.3
DPSC Mirror®	4 psi	21.6

Nearly all the debris generation data used to justify the NEI recommendations came from the BWROG AJIT data (BWROG URG); therefore, the NEI recommendations must be anchored to the insulation types as tested. Besides the BWROG AJIT tests, the U.S. Nuclear Regulatory Commission (NRC) sponsored a single test* using a stainless-steel DPSC Mirror® RMI cassette at the Siemens AG Power Generation Group (KWU) test facility in Karlstein am Main, Germany, in 1994 and 1995 (SEA-95-970-01-A:2, 1996). Table II-6 provides the cassettes and their closures, as tested in the AJIT tests with the cassettes mounted perpendicular to the jet centerline.† All of the cassettes tested had stainless-steel sheaths.

A review of the data indicates that the air jet did not directly penetrate the stainless-steel sheaths; rather, the sheaths disassembled at the seams, such as with rivet failures. Those cassettes secured by stainless-steel bands in addition to latches and strikes generally remained relatively intact. The severity of the damage, in terms of the generation of small fine debris, depends on the degree or ease of disassembling the cassette. However, when considering large-piece debris, all detached cassettes, disassembled or not, become large-piece debris.

Table II-6. BWROG AJIT RMI Insulations Tested

Insulation	RMI Foils Tested	Cassette Closures
DARMET®	Stainless-Steel Foils	Darchem Stainless-Steel Bands and CamLoc® Latches and Strikes
TPI	Aluminum Foils	Latch and Strike Closures
TPI	Stainless-Steel Foils	Latch and Strike Closures
DPSC Mirror®	Aluminum Foils	Latch and Strike Closures
DPSC Mirror®	Stainless-Steel Foils	Latch and Strike Closures
DPSC Mirror®	Stainless-Steel Foils	Latch and Strike Closures and Sure-Hold Band Closures

*The NRC-sponsored test involved a stainless-steel Mirror® cassette mounted directly on a device designed to simulate a double-ended guillotine break, such that the discharge impinged on the inner surface of the RMI target as it would an insulation cassette surrounding a postulated pipe break. This NRC-sponsored test was performed with a high-pressure blast of two-phase water/steamflow from a pressurized vessel connected to a target mount by a blowdown line with a double-rupture disk. This test completely destroyed the cassette into debris that can be considered small fine debris.

†Two tests were conducted, with the cassette mounted parallel to the jet centerline.

II.3.2.1 DARMET®, Manufactured by Darchem Engineering, Ltd.

The NEI-recommended destruction pressure of 190 psi for stainless-steel DARMET®, manufactured by Darchem Engineering, Ltd. and held in place by Darchem stainless-steel bands and CamLoc® latches and strikes, is based on two AJIT tests, Tests 25-1 and 25-2, with jet centerline pressures on target of 190 and 590 psi, respectively. In both of these tests, the cassettes, although deformed, remained intact and attached to the target mount. In effect, the tests did not generate any debris. This result indicates that debris generation requires a pressure greater than 590 psi, with the exception of a cassette mounted over the break, where the jet would enter the inside of the cassette. This scenario would almost certainly result in complete destruction of that cassette. Another possible exception could be a jet approximately parallel to the cassette sheath that could penetrate through the ends—a configuration that has not been tested. It is apparent that the baseline recommendation of assuming that 75 percent of this insulation within a 1.3/D spherical radius becomes small fine debris is conservative.

II.3.2.2 RMI, Manufactured by Transco Products, Inc.

TPI manufactures stainless-steel and aluminum RMI insulation. The NEI guidance recommends a destruction pressure of 190 psi for the TPI RMI. The TPI cassettes tested included both aluminum and stainless-steel foils encased in stainless-steel sheaths secured with latches and strikes (no bands were used). Although the recommended destruction pressure is 190 psi, a small amount of fine debris was noted for jet pressures as low as 10 psi (Test 21-3). On the other hand, only small quantities of fine debris (i.e., less than 0.5 percent) were found for tests with jet pressures as high as 600 psi. Figure II-9 shows the debris generation fractions for TPI stainless-steel RMI small fine debris.

Table II-7 compares potential debris volumes when estimated using the NEI baseline guidance and when acknowledging debris generation at jet pressures as low as 10 psi. As stated above, to obtain actual volumes of debris, the potential volumes must be multiplied by the insulation concentration and again by D^3. For the baseline estimate, the volume associated with a ZOI radius of 1.3/D is multiplied by 75 percent to obtain the baseline potential volume. For the alternate estimate, the ZOI volume out to a jet pressure of 10 psi was multiplied by 0.5 percent to obtain the alternate potential volumes. The application of the alternate pressure results in approximately three times as much small fine debris as using the baseline guidance. However, even these quantities are not very large compared with such insulations as LDFG.

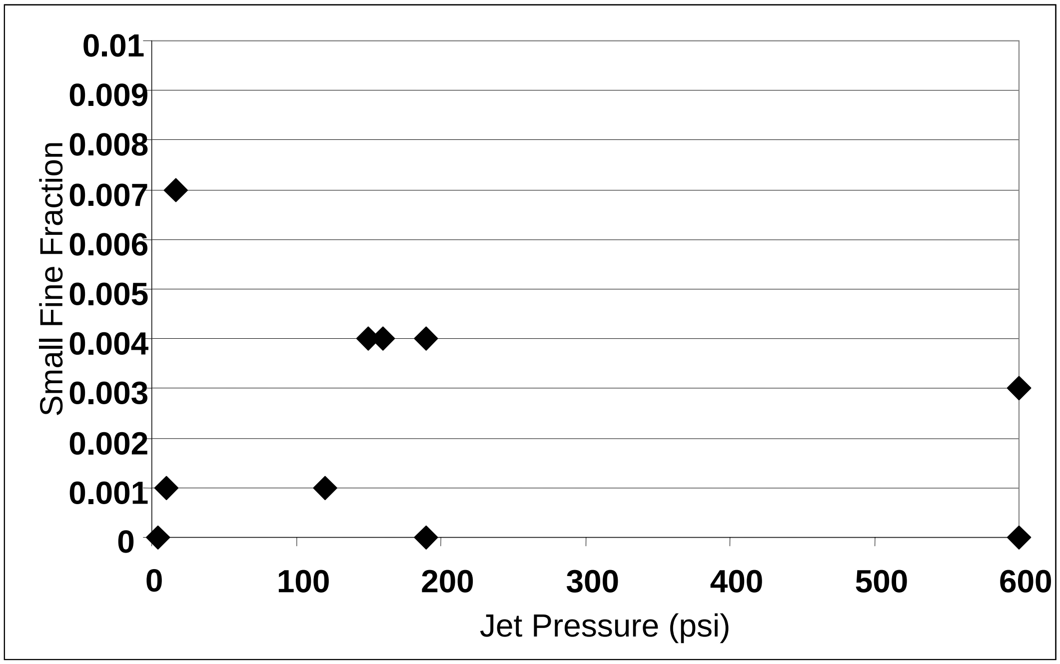

Figure II-9. TPI Stainless-Steel RMI Small-Fine-Debris Fractions

Table II-7. Comparison of TPI Potential Debris Volumes

Guidance	Damage Pressure (psi)	Radius of ZOI (r/D)	Damage Fraction	Potential Volume of Debris (V/D^3)
Confirmatory Recommended Jet Isobar Volumes				
NEI Guidance	190	1.5	0.75	10.6
Alternate	10	11.9	0.005	35.3

However, if the transport of large-piece TPI RMI debris becomes necessary to the strainer blockage evaluation, the use of 190 psi to define the ZOI is totally inadequate. Although the TPI stainless-steel sheaths may effectively contain the foils, their latches and strikes do not effectively keep the cassettes attached to the mounts (or pipes). AJIT Test 21-2, with a jet pressure of only 4 psi, shows the two cassette half sections detached from the target mount (i.e., the cassettes become large-piece debris). At 4 psi, the ZOI radius would be approximately 21.6/D; therefore, numerous cassettes in various degrees of damage would be expected on the breakroom floor. If the transport flow velocities were sufficient to move cassettes, then these cassettes could become a significant problem.

II.3.2.3 DPSC Mirror®, Manufactured by Diamond Power Specialty Company

DPSC manufactures stainless-steel and aluminum RMI insulations marketed as Mirror® insulations. The Mirror® cassettes tested included both aluminum and stainless-steel foils encased in stainless-steel sheaths secured with latches and strikes with or without

Sure-Hold bands. The NEI guidance recommends a destruction pressure of 4 psi for the DPSC Mirror® insulations. The apparent reason that Mirror® cassettes form debris at much lower pressures than does the TPI RMI is the construction of the sheaths (i.e., the cassette integrity depends on strength of the seams).

Figure II-10 shows the debris fractions for the small fine debris from the AJIT tests. In the figure, the small fine debris was correlated as pieces less than 6 in., although the NEI guidance specified RMI small fines as less than 4 in.; therefore, a small measure of conservatism was added to the comparison. Figure II-10 shows six data points for Mirror®, with two of those tests generating very minor quantities of small fines. Note that with the lower pressure test, where the RMI cassette was exposed to a jet pressure of only 2 psi (AJIT Test 18-3), the cassette was still detached from the target mount, leaving two half cassettes on the chamber floor. The test with the largest quantity of small fine debris (AJIT Test 17-1) had only 10.6 percent of the foils turned into pieces less than 6 in., with the remaining foils becoming large-piece debris. The conservative extrapolation shown in Figure II-10 to complete the spherical ZOI debris fraction integration assumes complete destruction at a jet pressure of 130 psi. Note that in the single NRC-sponsored Mirror® debris generation test conducted at the KWU test facility, the test article was completely destroyed.

Table II-8 provides the results of the Mirror® debris-size distribution integration over the ZOI. The potential debris volume of $661/D^3$ is quite low compared with an estimate using the baseline guidance (i.e., 75 percent of $4\pi/3\ (21.6/D)^3$) of $31660/D^3$. Although this insulation is damaged at jet pressures as low as 4 psi, a relatively small amount of small debris is formed at pressures less than approximately 120 psi, and when the debris damage data are applied to the larger ZOI radius of 21.6/D, only a small fraction of the insulation in that sphere becomes small fine debris. For DPSC Mirror® RMI insulation, the assumption in the NEI baseline guidance that 75 percent of the insulation within a 21.6/D ZOI sphere would become debris less than 4 in. in size (i.e., $31,660/D^3$) is overly conservative. However, the quantities of large-piece debris, including nearly intact cassettes, could be very large because even 2 psi can detach the cassettes, which could become very important in containments where the transport velocities are high enough to move this heavier debris significantly.

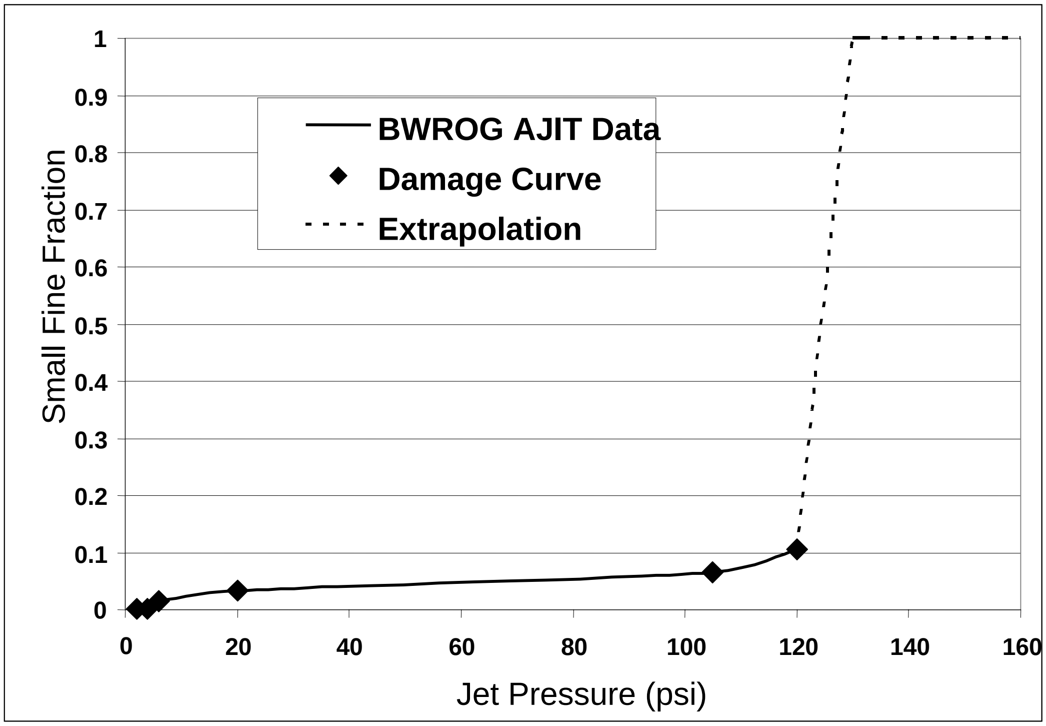

Figure II-10. DPSC Mirror Damage Curve for Small Fine Debris

Table II-8. Results of Debris-Size Distribution Integration for DPSC Mirror® Insulation

Jet Pressure Isobar Volume Calculation	Radius of Sphere (r/D)	Fraction Small Fines	Potential Debris Volumes (V/D^3)
NEI-Recommended Damage Pressures			
PWR Two-Phase Jet (Confirmatory)	21.6	0.016	658

II.3.3 Particulate Insulation Debris

II.3.3.1 Min-K Debris

The NEI baseline guidance recommends the assumption that 100 percent of the Min-K insulation located inside a ZOI defined by the destruction pressure of 4 psi, corresponding to a radius of 21.6/D, becomes small fine debris. The basis for this recommendation is apparently the single Min-K BWROG AJIT debris generation test, Test 9-1. In this test, approximately 70 percent of the Min-K insulation became small fine debris. In fact, most of this debris was not recovered, apparently because it was too fine.* Based on the extensive damage to this Min-K blanket at 4 psi, it does not seem reasonable to assume that the threshold of damage is 4 psi.

At jet pressures substantially higher than 4 psi, it seems likely that the Min-K would be totally destroyed. At jet pressures less than 4 psi, the damage to Min-K would continue but would decrease in severity until the pressure became insufficient to cause damage. However, that pressure is not known. It is unlikely that the NEI baseline guidance is conservative with respect to the Min-K blanket tested. On the other hand, Min-K insulation protected by a metal jacket secured with steel bands would most likely be substantially less damaged than the unjacketed blanket tested.

II.3.3.2 Calcium Silicate Debris

The NEI baseline guidance recommends the assumption that 100 percent of the calcium silicate insulation located inside a ZOI defined by the destruction pressure of 24 psi (corresponding to a radius of 5.5/D) becomes small fine debris. The OPG debris generation tests (N-REP-34320-10000-R00) were cited to justify the 24-psi destruction pressure. The OPG tests involved impacting aluminum-jacketed calcium silicate insulation targets with a two-phase water/steam jet. The jacketing was secured with stainless-steel bands, and the jacketing seams were typically oriented at 45 degrees from the jet centerline—an orientation that appeared to maximize damage. The OPG data, illustrated in Figure II-11, only cover a limited range of damage pressures (approximately 24 to 65 psi).

The damage curve shown in Figure II-12 was generated by summing all four debris categories in Figure II-11 to obtain the OPG debris fractions shown and then constructing a plausible curve through the data that was conservatively extrapolated at both ends. Table II-9 provides the results of the calcium silicate debris-size distribution integration over the ZOI. Figure II-13 compares the potential debris volumes and provides an estimate using the baseline guidance (100 percent of $4\pi/3\ (5.45/D)^3$). A lower alternate damage pressure results in a larger equivalent spherical ZOI, but a lesser fraction of the debris is damaged into small fine debris. The use of the alternate damage pressures over the NEI-recommended damage pressures for PWR analyses would result in approximately 43 percent more estimated small fine debris. For calcium silicate insulation, the baseline is conservative with respect to both the NEI guidance damage pressure of 24 psi and the alternate pressure of 20 psi.

---

*It was noted that a cloud of debris was observed to exit the test chamber through the exhaust screen and that the venting of the chamber to clear the dust required more than 15 minutes.

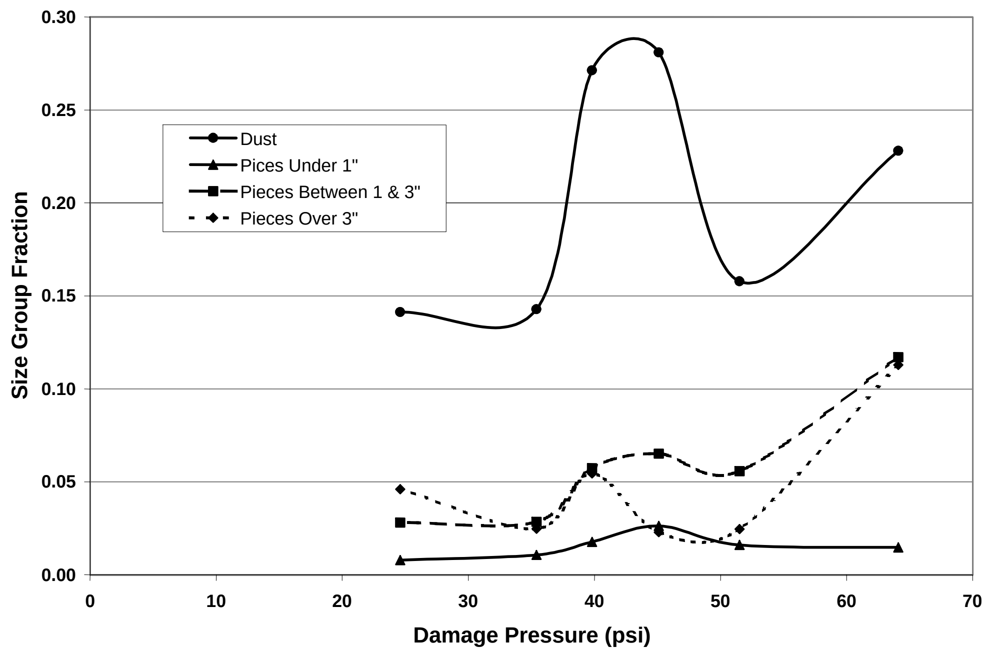

Figure II-11. Debris-Size Distributions for OPG Calcium Silicate Tests

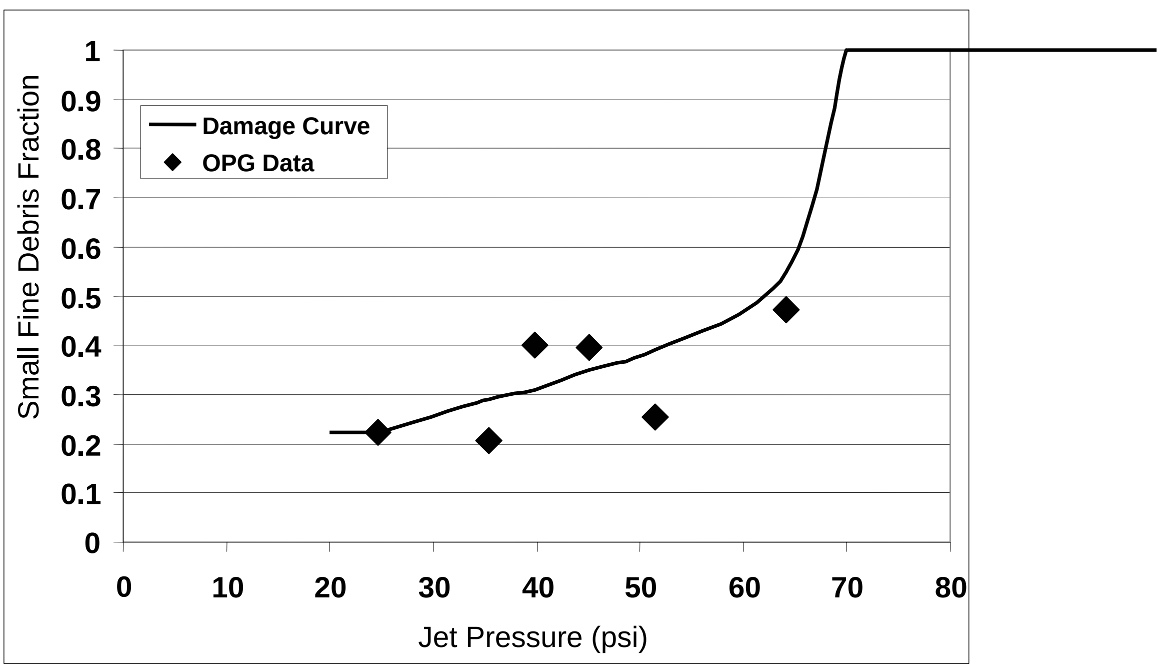

Figure II-12. Calcium Silicate Damage Curve for Small Fine Debris

Table II-9. Results of Debris-Size Distribution Integration for Calcium Silicate Insulation

Jet Pressure Isobar Volume Calculation	Radius of Sphere (r/D)	Fraction Small Fines	Potential Debris Volumes (V/D^3)
NEI-Recommended Damage Pressures			
PWR Two-Phase Jet (Confirmatory)	5.4	0.42	273
Alternate Damage Pressures			
PWR Two-Phase Jet (Confirmatory)	6.4	0.34	372

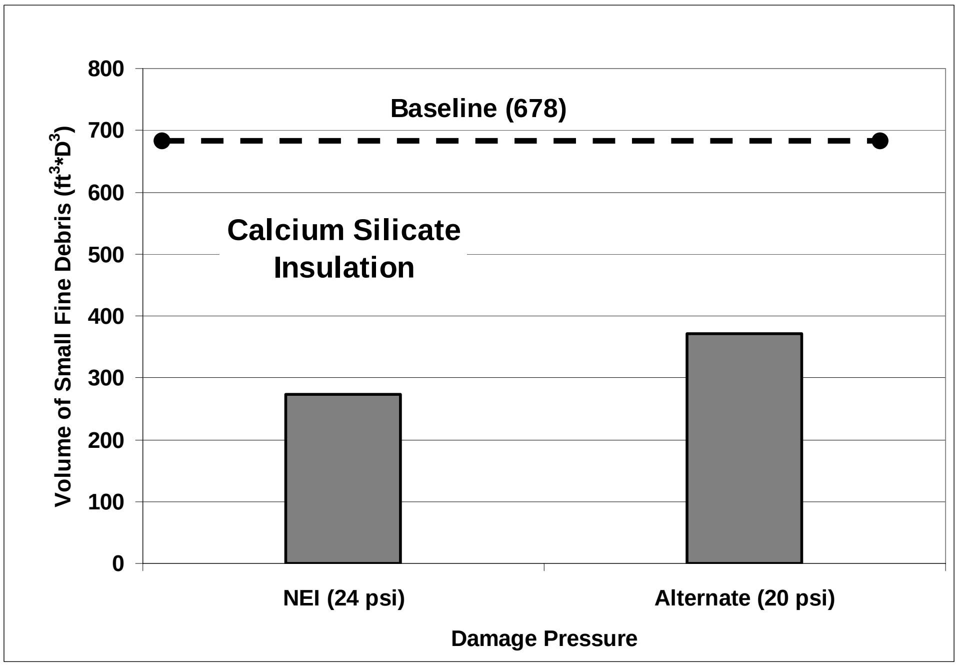

Figure II-13. Potential Volumes of Small Fine Calcium Silicate Debris

The BWROG AJIT tests also contain four tests of calcium silicate with aluminum jacketing secured by four 3/4-in. stainless steel bands; however, these tests indicated that a jet of 150 psi was needed to cause significant damage. The reason that a much higher pressure was needed to cause significant damage in the AJIT calcium tests than in the OPG tests has not been determined, but it likely results from the differences in jacketing thickness, seam orientation, and strength of the bands. Here the destruction pressure depends more on the pressure needed to remove the jacket and expose the insulation than on the pressure required to erode the calcium silicate.

II.4 Summary and Conclusions

Confirmatory research was performed to ascertain whether the NEI recommendations for ZOI destruction pressures and debris fractions would reliably result in conservative estimates for the volumes of debris generated within the ZOI. Specifically, the NEI guidance recommends the assumption that 60 percent of the fibrous and 75 percent of the RMI insulation volume contained within the ZOI become small fine debris for ZOI radii defined by their recommended destruction pressures. The NEI guidance recommends adapting the debris-size distribution for NUKON™ to other types of fibrous insulation that have a destruction pressure higher than that of NUKON™.

Available debris generation data were used to define debris fractions versus jet pressure curves for the insulations examined. Difficulties encountered when correlating these data include aspects of protective jacketing and banding, as well as the variability in insulations. Before the insulation is subjected directly to jet flow forces, the flow must penetrate the protective coverings. Steel bands securing a metal jacket can require a rather high jet pressure to open the jacket before insulation debris is generated. The seam orientation affects the ease with which an edge of the jacket can be peeled back; it appeared that a seam orientation of approximately 45 degrees from the oncoming jet maximizes the potential for jacket opening. The size of the jet nozzle relative to the insulation destruction pressure also affected the quality of debris generation data. If the target insulation had to be placed close to the nozzle to get the required destruction pressure, then the jet pressure became uneven along the length of the target; in fact, in some tests the target ends were likely located outside the influence of the jet. To test insulations with a higher destruction pressure, either larger nozzles or shorter targets are required. The evaluation of debris fractions considers all of these factors.

The ZOI debris fractions and insulation destruction pressures are interdependent; that is, the larger the ZOI, the smaller the fraction of the insulation within the ZOI that becomes small fine debris. Therefore, when the lower alternate pressure is used in the integration process, the resultant debris fraction will be less than that corresponding to the NEI-recommended destruction pressure.

Table II-10 summarizes the results and conclusions regarding relative conservatism of this confirmatory debris generation analyses for the insulations examined. These results are relative to the NEI baseline guidance for the small fine debris size category.

Table II-10. Summary Comparison of Confirmatory and Baseline Potential Debris Volumes

Insulation	Confirmatory Research Result	Relative Conservatism of Baseline Guidance
Fibrous Insulations		
NUKON™	Baseline guidance results compare well with confirmatory results.	Baseline guidance for NUKON™ provides realistic results that are only slightly conservative.
Temp-Mat	Baseline results are approximately twice the confirmatory results (based on limited data).	Baseline guidance is conservative for Temp-Mat insulation.
K-wool	Baseline results are only about half that of the confirmatory results (based on limited data).	Baseline guidance is likely conservative for K-wool, despite the nonconservative comparison with confirmatory analysis. The poor nonconservative comparison results from the extreme extrapolation of data required by the lack of data for pressures greater than the NEI destruction pressure. Still, conservatism cannot be proven with existing data.
RMI Insulations		
DARMET®	No confirmatory analysis for this insulation. Rather, a review of the debris generation data illustrated substantially less small fine debris than would be estimated using the baseline guidance methodology.	Baseline guidance is conservative for DARMET® insulation.
TPI	Baseline results account for only one-third of the confirmatory debris estimate, which includes the small quantities of debris generated at lower pressures but that are neglected when the baseline destruction pressure is used.	Baseline guidance is not conservative, but the quantities of this debris are relatively low; therefore, this nonconservative estimate is not a major issue.
DPSC Mirror®	Baseline results were almost 50 times that of the confirmatory result. The baseline minimum destruction pressure of 4 psi results is a very large ZOI volume, but the damage to the insulation is relatively minor at the lower pressures, thus the large differences in results.	Baseline guidance is conservative for Mirror® insulation.
Particulate Insulations		
Min-K	No confirmatory analysis for this insulation. Rather, the data from the single Min-K debris generation test were examined (i.e., approximately two-thirds of the insulation was turned into fine dust debris at a jet pressure of only 4 psi).	Baseline guidance is not conservative because the one test indicated that substantial damage would occur to Min-K insulation at significantly lower pressures than the destruction pressure of 4 psi and that the damage at 4 psi was extreme.
Calcium Silicate	Baseline results are approximately twice the confirmatory results, even when the lower jet pressure of 20 psi (recommended in NUREG/CR-6808) is considered instead of the baseline destruction pressure of 24 psi.	Baseline guidance appears to be conservative for calcium silicate insulation, but the debris generation data are not sufficient to determine the threshold jet pressure for generating small fine debris (i.e., the threshold destruction pressure could actually be less than the 20 psi alternate pressure used in the confirmatory analysis).

Note the following additional comments:

- The use of the alternate destruction pressure provides some quantification of the uncertainty associated with the selection of the destruction pressures. These uncertainties include the neglect of the tails of the debris damage curves and the uncertainty associated with the potential two-phase effect on debris generation relative to the available air-jet-generated data.
- A comparison of the NUKON™ results with the BWROG URG steam jet model illustrates that the neglect of the tails of the debris damage curve has a larger impact for PWRs than for BWRs (see Figure II-3).
- The NEI guidance recommendation that adapts the debris-size distribution for NUKON™ to other types of fibrous insulation that have a destruction pressure higher than that of NUKON™ has been partially supported (see Figure II-8), although it cannot be conclusively ensured.
- The ZOI for large debris generation in some cases does not correlate with the ZOI for small-fine-debris generation. A case in point is the analysis for TPI RMI, where most of the small fine debris would be generated inside jet pressures of 190 psi, but large debris was generated (in the form of detached cassettes) at pressures as low as 4 psi. Therefore, rather larger quantities of large debris could be formed than were predicted using the baseline guidance ZOI sizes.
- It should be emphasized that the typical debris generation analyses were performed for insulations where the debris generation data were very limited. The data for the LDFG insulations (see Figure II-2) illustrate the potential variability in such data. Therefore, the limited debris generation data cause substantial uncertainty with debris generation estimations.

II.5 References

(NUREG/CR-6762, Volume 3, 2002) C.J. Shaffer, D.V. Rao, and S.G. Ashbaugh, "GSI-191 Technical Assessment: Development of Debris-Generation Quantities in Support of the Parametric Evaluation," LA-UR-01-6640, NUREG/CR-6762, Volume 3, 2002.

(NUREG/CR-6369, 1999) Rao, et al., "Drywell Debris Transport Study: Experimental Work," SEA97-3501-A:15, NUREG/CR-6369, Volume 2, September 1999.

[NEDO-32686, Rev. 0, 1996] "Utility Resolution Guidance for ECCS Suction Strainer Blockage," BWROG, NEDO-32686, Rev. 0, November 1996.

(SEA-95-970-01-A:2, 1996) Zigler, G., et al., "Experimental Investigation of Head Loss and Sedimentation Characteristics of Reflective Metallic Insulation Debris," draft letter report prepared for the U.S. Nuclear Regulatory Commission, SEA No. 95-970-01-A:2, May 1996.

(N-REP-34320-10000-R00, 2001) Ontario Power Generation, "Jet Impact Tests—Preliminary Results and Their Applications," N-REP-34320-10000-R00, April 2001.

(ANSI/ANS-58.2, 1988) American National Standard/American Nuclear Society: “Design Basis for Protection of Light Water Nuclear Power Plants Against the Effects of Postulated Pipe Rupture,” ANSI/ANS-58.2-1988, October 1988.

Appendix III

Volunteer-Plant Containment Pool Computational Fluid Dynamics Analysis

III.1 Introduction

A three-dimensional computational fluid dynamics (CFD) model was developed to analyze the flow patterns developed in the U.S. Nuclear Regulatory Commission (NRC) volunteer-plant reactor containment during loss-of-coolant accidents (LOCAs). The CFD modeling assessed the water velocities and flow patterns developed during sump pump operation to support estimates of subsequent LOCA-generated sump pool debris transport. Water sources to the sump pool included effluents from the LOCA break and containment spray drainage. The locations and flow rates of each of these water sources and the recirculation pumping rates determined the characteristics of the sump pool that subsequently determined whether, and what fraction of, the debris deposited into the pool could transport to the recirculation sump screens. Experiments conducted at the University of New Mexico determined threshold transport velocities for debris from pressurized-water reactor (PWR) insulating materials (NUREG/CR-6772, 2001). These threshold velocities were used to set the velocity contours of the CFD flow diagrams to facilitate the determination of whether debris would likely transport. Section III.2 discusses the CFD simulations.

A logic chart debris-transport model was developed to supplement the CFD analyses so that information from the CFD simulations can be used with the blowdown/washdown transport analyses documented in Appendix VI to determine estimates of debris transport to the recirculation sump screens. The pool velocity and turbulence characteristics determine areas of the pool where debris entrapment may occur. The flow streamlines can be used to determine whether debris entering the pool at a discrete location would likely pass through one of the potential entrapment locations. The debris transport process was decomposed using a logic chart approach to facilitate the individual transport steps—steps that could be determined analytically or experimentally, or simply judged. The subsequent quantification of the chart then provided an estimate of the overall sump pool debris transport. Section III.3 discusses the debris transport estimates.

III.2 Analysis of the CFD Simulation

III.2.1 Modeling Methodology, Assumptions, and Conditions Simulated

The commercial CFD program Fluent™ was used to compute the volunteer-plant containment pool flows for large and small LOCA breaks. The containment geometry was available in Autocad™ format and was imported into the Fluent™ preprocessor and grid generator. As shown in Figure III-1, the model geometry included all of the structures, stairwells, and sumps, but the containment pool was modeled only to a depth of 6 ft. This is the maximum anticipated depth of water during steady-state operation of the spray system and sump pump operating in the recirculation mode.

Figure III-2 shows the splash locations, which can be seen as the extruded volumes above the containment pool in Figure III-1. Appendix VI explains in detail the splash locations and flow rates shown in Figure III-2. The CFD model included the following modifications to the splash locations and flow rates:

- One of the four "yellow" floor drains from Level 832, with a total flow rate of 397 gpm in Figure III-2, is located on top of a wall. Thus, the adjacent yellow splash located in the corridor had double the individual flow rate. (For all the Level 832 floor drains, the total mass flow was evenly distributed to all locations, with the exceptions noted here.)
- The liner film flow of 700 gpm was uniformly distributed.
- The Level 808 sprays of 1080 gpm were neglected entirely.

Thirteen LOCA break conditions were simulated. These included eight large LOCA conditions (four break locations, each considered with and without the spray flows) and five small LOCA conditions (four break locations without spray flows and one location with spray flows). The analysis considered both large and small LOCA breaks because each can cause the sump screens to become clogged in a different way. The large LOCA break and spray flows will result in a large pool depth and the wetting of all of the screen surface area. The large LOCA break will likely generate more debris that can migrate to the sump screens, causing an unacceptable head loss because of the amount of debris collected. The small LOCA break may not cause the spray systems to activate and could result in a water depth that wets only the lower portion of the sump screens. This has the potential of forming a thin bed debris mat over a small portion of the screen area resulting in an unacceptable head loss. If the spray flow systems do not activate, depending on break location, a larger portion of the pool flows do not have velocities in excess of the debris threshold velocities and do not participate in the recirculation flow. Therefore, the debris generated in those regions does not migrate to the sump screens.

The four break locations considered correspond to a break occurring in one of the four quadrants (steam generator (SG) compartments) in Figure III-2. The total break flow was assumed to be 7400 and 1611 gpm for the large and small LOCA break flows, respectively. It was assumed that the upper two SG compartments were physically separate from the lower two compartments. Thus, if the break were postulated to occur in the upper left quadrant, 75 percent of the break flow would be partitioned to the upper left and 25 percent to the upper right quadrants; none of the break flow would be in the lower two quadrants. The 75/25-percent partitioning was determined arbitrarily, but it seemed to be a realistic assumption. Additionally, a transient pool fillup simulation was initiated for a large LOCA break in the upper-left quadrant. Only the break flows were simulated in the upper half of the SG compartments with the break flow partitioned as described above. The above apportionment of the flow represents an estimate of the volunteer-plant break resulting from the SG compartment configuration. The SGs are raised above the pool floor level and do not participate in the recirculation flow. Thus, the break flow enters the pool by flowing down the SG stairwells, and the water sheets across the SG compartment and does not pool to any significant depth. Although the 75/25-percent apportionment was assumed, a thorough analysis of how the break flow would enter the pool is needed. Each plant would require such an analysis, which would benefit from the plant personnel's expert knowledge of the containment configuration. The above apportionment merely illustrates the types of flows that would enter the pool.

The simulation used three boundary condition types. All hard surfaces (walls, floors, etc.) were specified to be a no-slip wall condition. The spray system splash and LOCA break flows were specified as a mass flow inlet condition, and the sumps were set to a pressure outflow boundary condition. Because the break flow sheeting described previously was not included, the break and spray flows present in the SG compartment were applied as a mass inflow boundary on a vertical surface at the exit of the SG entrance steps of each quadrant (i.e., a mass flow boundary condition located at the "door" of the SG entrance steps, for instance). The spray/splash mass flow boundary conditions were placed on the "top" of each extruded spray location, as shown in Figure III-1. This extruded volume was found to be easier to handle in Fluent™ rather than trying to set the boundary condition on the "top" of the pool surface.

The combination of mass inflow and pressure outflow satisfies the mass continuity condition without unnecessary complications from numeric and other boundary condition errors. In theory, a mass outflow condition at the bottom of the sump could be specified, but that condition results in numerical instabilities when prescribed. By using a pressure outflow condition at the sumps, the pressure is allowed to "float" to satisfy the incompressible continuity equation. In other words, the code adjusts the pressure at the bottom of the sump to balance the mass flow entering and exiting the pool. This method avoids the introduction of artificial pressure waves in the solution which can be created by specifying mass inflow and outflow conditions.

A second-order-accurate numerical method was used to solve the incompressible Navier-Stokes equations, in conjunction with a renormalized group-theory turbulent-kinetic-energy (TKE) and dissipation turbulence closure (RNG κ-ε). This closure was chosen because of its ability to treat swirling flows, but in practice, little difference was found between the RNG κ-ε and the more traditional κ-ε closure for these simulations. The pressure equation was solved using a pressure-implicit split-operator (PISO) numerical method, as described in the Fluent™ documentation. For the steady-state pool flow analyses, the pool volume was assumed to be completely full of liquid water and initialized to zero velocity. The inflow boundary conditions were flowing from the start, and the solution was allowed to proceed until a steady-state condition was achieved. The normalized residuals of the continuity, momentum, and κ and ε equations were monitored until convergence was achieved, typically after about 400 iterations. For the steady-state pool flow analysis, an additional convergence criterion was to integrate the mass flow rate at the two sump pressure outflow boundaries and compare it with the mass inflow. Achievement of a mass balance, in addition to a drop in the normalized residuals, was necessary for the simulation to be deemed converged.

III.2.2 Results and Discussion

This section contains the results of the CFD simulations. These simulations illustrate what can be achieved with a CFD analysis of the containment pool flows. Application to a particular plant containment would require a more rigorous set of simulations to be performed, including grid convergence tests (e.g., does doubling the number of grid points change the results significantly).

One figure of merit was to determine the fraction of the pool flow volume that produced velocities in excess of the debris migration threshold velocities. Based on the experimental measurements reported in NUREG/CR-6772, the reflective metal insulation (RMI) and fiber flock transport threshold velocities were determined to be 0.085 and 0.037 m/s, respectively. The following analyses use only one debris transport threshold velocity for fiber and one for small RMI.

III.2.2.1 Transient Containment Pool Fillup

This simulation used a volume-of-fluid (VOF) method. The containment pool was initially filled with air, and water was allowed to enter the pool from the SG entrance stairs. The simulation included only the break flows for a large LOCA break, located in the upper-left quadrant. As noted in Section III.2.1, the break flow is partitioned such that 75 percent of the water leaves the upper-left SG compartment stairwell and 25 percent leaves the upper-right SG compartment stairwell. This condition corresponds to the time immediately after a break occurs and before the spray system is activated. All walls were treated as no-slip surfaces, and because the fillup phase was simulated, the sumps were also treated with no-slip surfaces instead of pressure outflow boundary conditions. The top boundary of the simulated pool was prescribed as a pressure outflow boundary condition instead of as a no-slip wall. This treatment allows the air to leave the domain as the water displaces it. The containment pressurization that occurs during a LOCA was not modeled because it has minimal effect on pool transport.

Figure III-4 through Figure III-12 show the volume fraction of water, at a height of 0.01 m above the containment floor, as the containment pool fills at 0.34, 0.94, 11.4, 21.4, 31.4, 41.4, 51.4, 71.4, and 111.4 seconds after the water leaves the SG compartment stairwells. The color scheme shown corresponds to a red color for 100-percent water in the computational cell and blue for 100-percent air in the cell. Other colors indicate that the computational cell has both air and water partially filling the cell. Figure III-4 through Figure III-12 show the areas that are first swept by the water, as well as how the containment pool fills. This simulation shows the areas that fill first and thus provides information needed to design systems to divert debris to areas of the pool that do not participate in recirculation flow. In general, the water leaves the SG compartment, flows out the doorway, and hits the circular outer wall. Then, the water flows circumferentially around the containment until the two water streams meet near the sumps. The water then starts to enter the areas between the upper and lower SG compartments. For this plant configuration, these two areas between the upper and lower SG compartments are the only “quiet” zones (i.e., they have flow velocities much lower than the debris threshold) in the pool when all break locations are considered in the subsequent steady-state pool flow analysis.

Figure III-13 through Figure III-21 show the fluid velocity during the fillup at the same set of time increments previously discussed for volume fractions. Note that when the water volume fraction and fluid velocity plots are compared, there is motion ahead of the water. This motion is the air moving in response to the approaching front of water. During fillup, the water velocity near the front is in the range of 2–3 m/s, well in excess of the debris transport threshold velocities of 0.037 and 0.085 m/s for fiber and RMI, respectively.

III.2.2.2 Steady-State-Flow Analysis

To study the containment pool’s steady-state-flow dynamics, the simulated volume was considered to be completely full of water. In the case of a small LOCA break, the simulations did not include the spray flows; however, for the large LOCA break, they did include spray flows. With the simulated pool full of water, the break and spray flows were introduced as mass inflow boundary conditions, and the sumps were set to a pressure outflow boundary condition. These simulations produced a stimulated steady-state-flow condition for further debris transport analysis, discussed in Section III.3.

Figure III-22 through Figure III-29 show the steady-state-flow pattern developed for a small LOCA break condition, without spray flows, and Figure III-30 to Figure III-37 show large LOCA break conditions, including spray flows. These figures show contours of water velocity at a height of 0.01 m above the containment floor and show a velocity range from 0 m/s up to the threshold velocity for fiber or RMI, 0.037 and 0.085 m/s, respectively. From these plots, the area enclosed by the threshold velocity contour can be computed, and by dividing by the entire available flow area in the containment, a percentage of area in excess of the threshold velocity may be calculated. Table III-1 summarizes these percentages, or fractional areas in excess of the threshold velocity, for both large and small LOCA break conditions.

Figure III-38 through Figure III-47 show streamlines for origins near the splash locations for a large LOCA break at two different locations, an upper-left break and a lower-right break. A rake of particles was released from ($-15 < X < -5$, $Y=10$) and also from ($0 < X < 5$, $Y=15$) and allowed to follow the flow. From these streamlines, debris trajectories can be determined and their fate postulated. Figure III-38 and Figure III-39 show the streamlines superimposed on the background velocity map that were color coded using the fiber (0.037 m/s) and RMI (0.085 m/s) threshold velocity, respectively. Figure III-41 and Figure III-42, color coded according to the flow speed, using the fiber and RMI threshold velocity, respectively, show an oblique view of the three-dimensionality of the streamlines. Thus, it can be deduced that if the velocity (speed) along a particular streamline became smaller than the debris type threshold velocity, the debris would not be so likely to migrate to the sump screen. By using rakes and streamline analysis at potential debris entry locations, a method for determining whether the debris will transport to the sump screens could be developed.

Figure III-42 through Figure III-45 show a similar set of plots for the large LOCA break located in the lower-right quadrant. The streamline patterns are quite different for the lower-right break location when compared to the upper-left break location.

Figure III-46 shows a vortex induced by the splash located in the upper-right quadrant in Figure III-42. Here the streamlines are color coded by velocity using the fiber velocity threshold. Because the water enters the pool from above and penetrates to the containment floor, a vortex with significant vertical motion is created. Figure III-47 shows the streamlines color coded by TKE. This type of information would be useful in determining debris degradation mechanisms, particularly for fibrous debris. In Figure III-46 to Figure III-47, the streamlines show the type of rotation that debris can encounter near the entry of a splash into the pool. The water flow produces vortices around the splash entry and could potentially shred debris into finer particles and pieces than those generated by the break itself.

Table III-1. Percentage of Containment Pool Flow Area in Excess of the Debris Transport Threshold Velocity (Total Pool Area = 767.7 m^2)

Break Location	Break Size	RMI (%)	Fiber Flocks (%)
Upper Right	Large	35	60

Break Location	Break Size	RMI (%)	Fiber Flocks (%)
Upper Left	Large	30	54
Lower Left	Large	22	43
Lower Right	Large	22	41
Upper Right	Small	5	31
Upper Left	Small	2	25
Lower Left	Small	5	14
Lower Right	Small	5	19

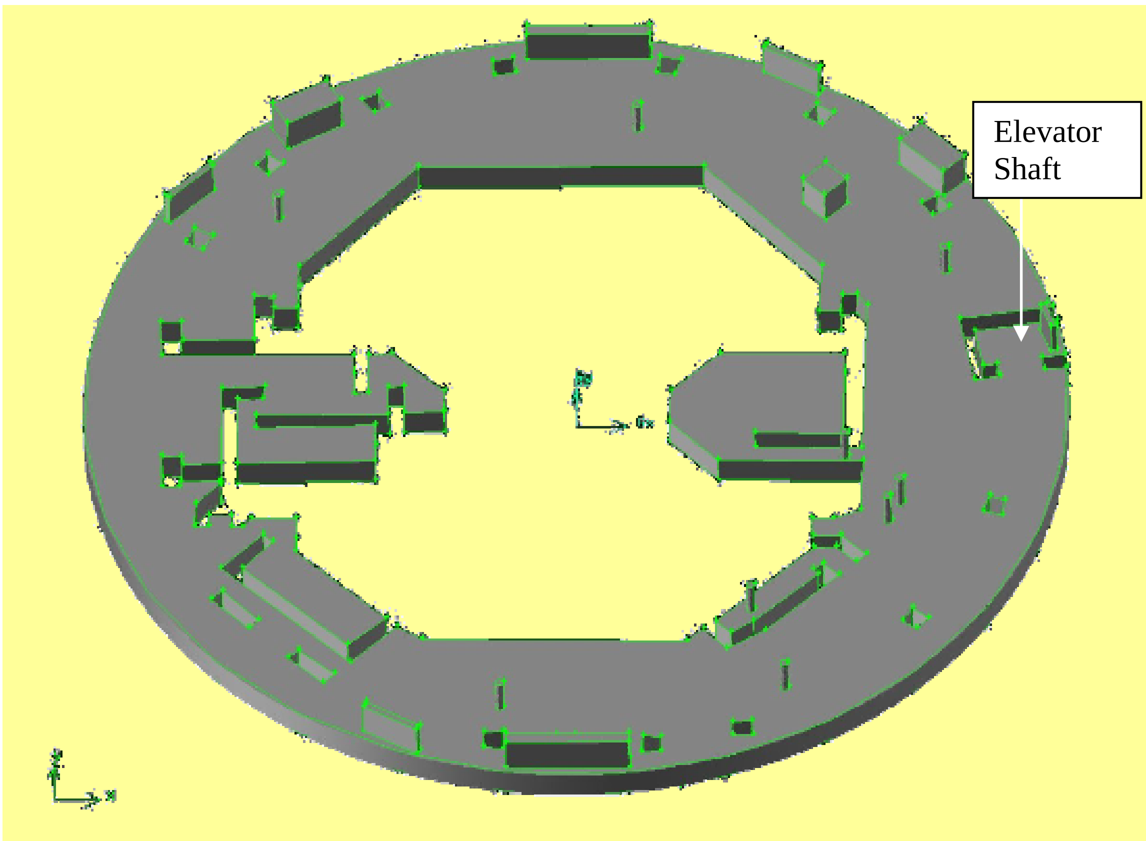

Figure III-1. Volunteer-Plant Geometry and Flow Region Modeled
(Note: Splash Locations Are Shown Extruded above the Nominal Pool Depth)

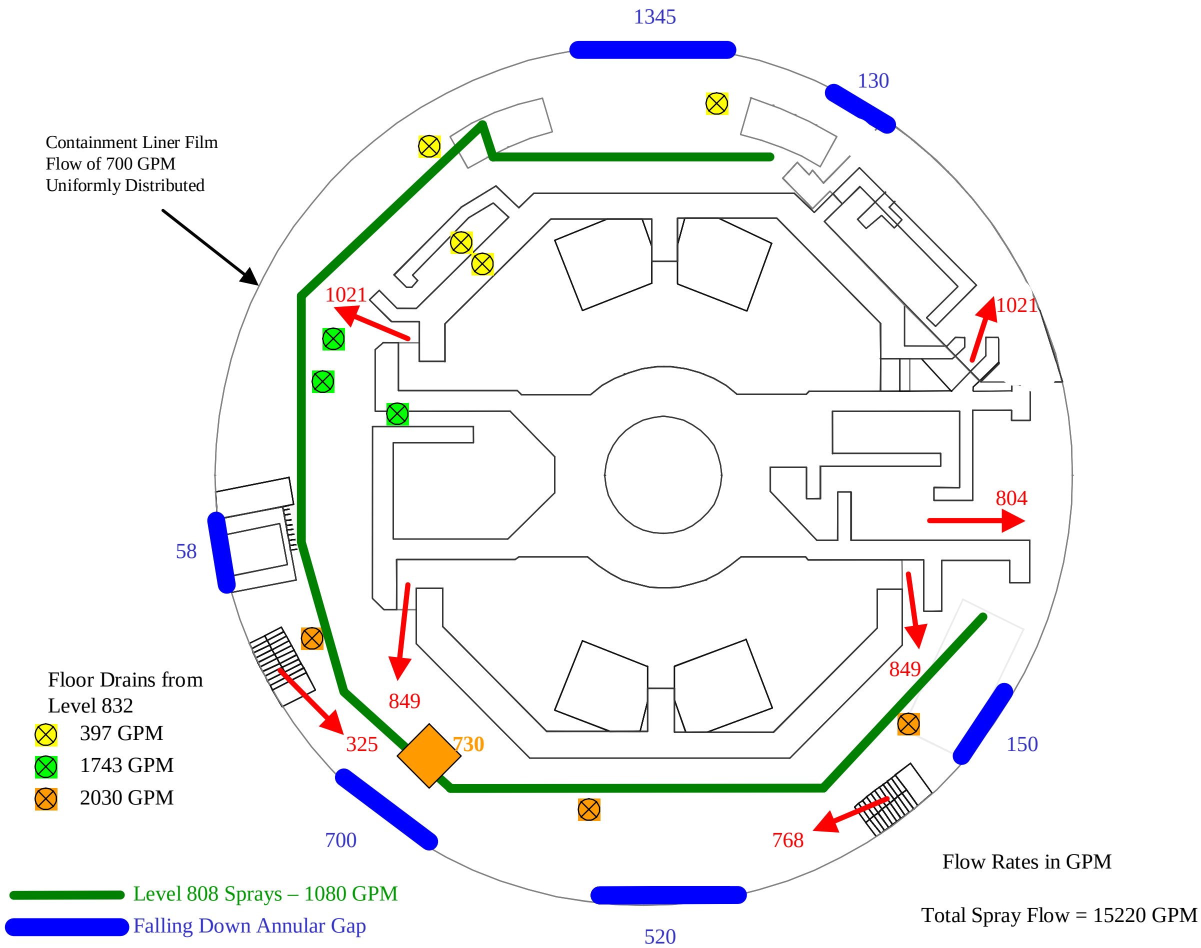

Figure III-2. Spray Flow Rates (gpm) and Locations for the Volunteer-Plant Pool Flow Calculations

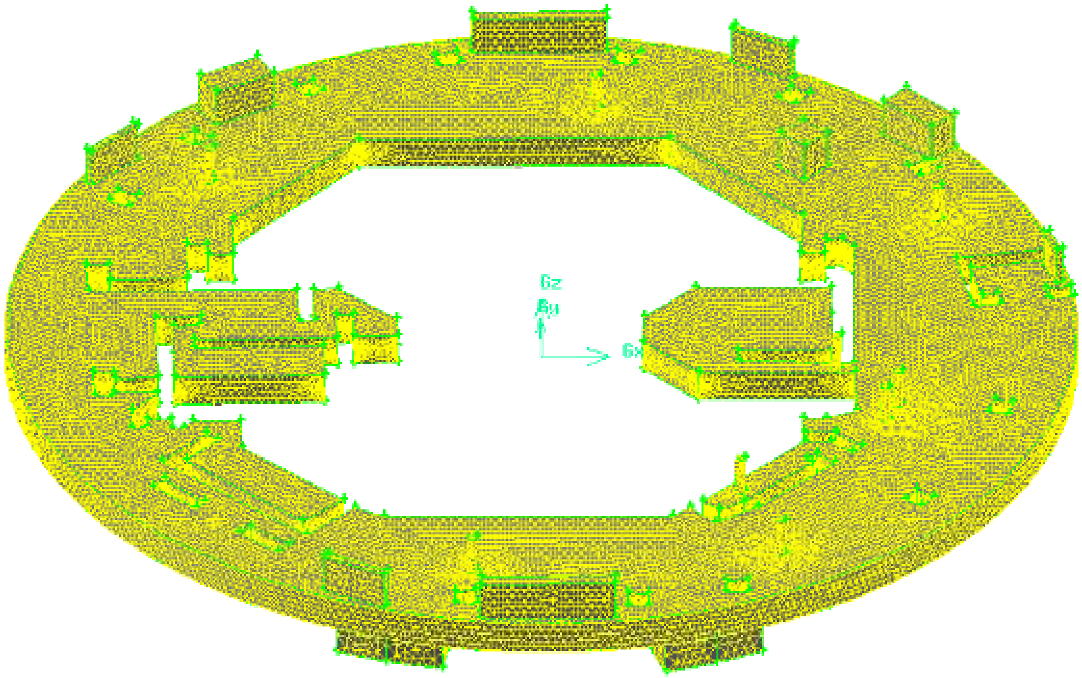

Figure III-3. Unstructured Mesh Created for Containment Pool Flow Calculations

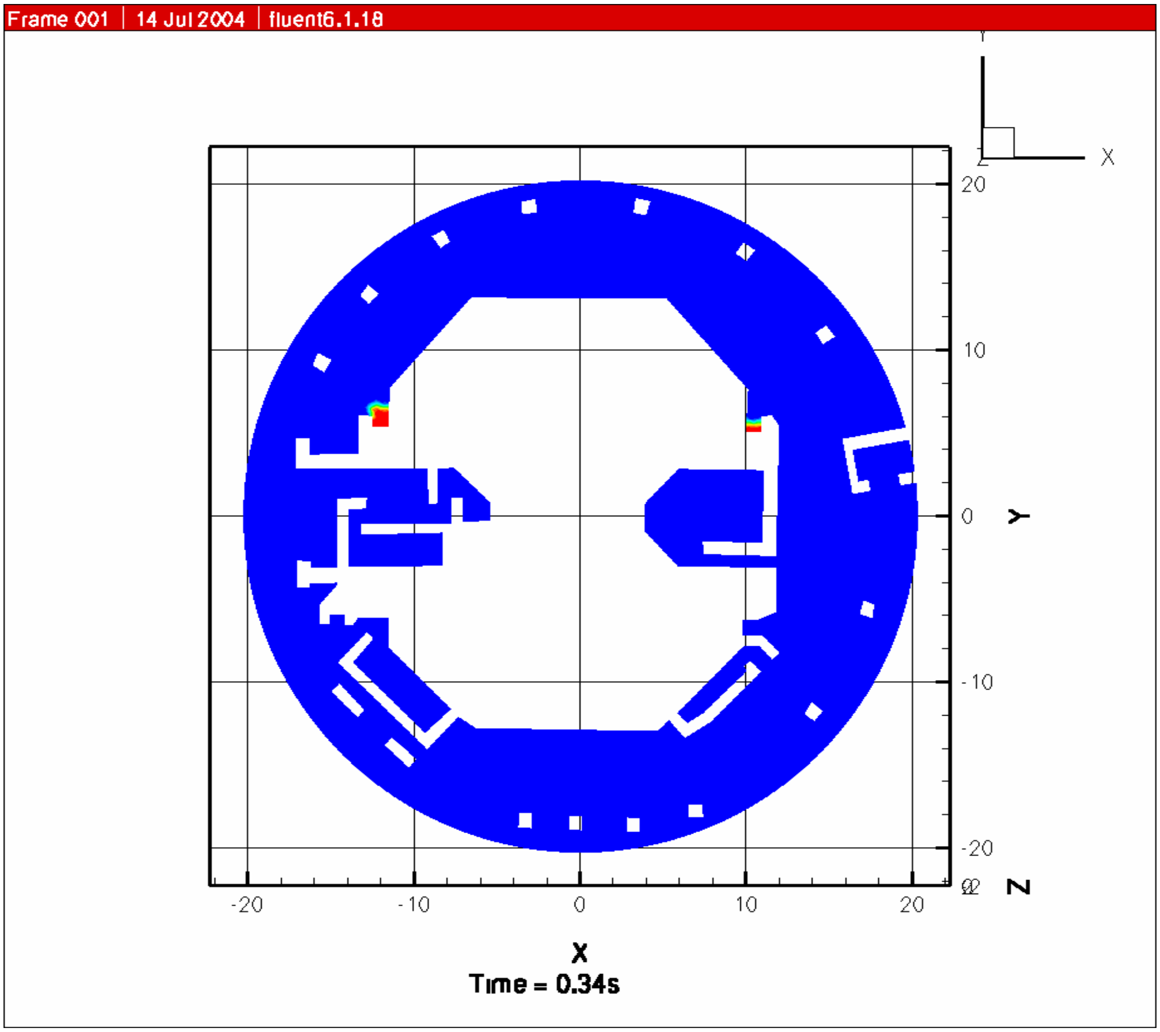

Figure III-4. Transient Volume of Fluid during the Simulation of Containment Pool Fillup

Figure III-4 shows the computational cell volume fraction of Water at a height of 0.01 m above the containment floor. The red color represents 100-percent water (0-percent air), while blue represents 0-percent water (100-percent air). The bottom of the figure shows the time of the snapshot in seconds after the breakflow is initiated.

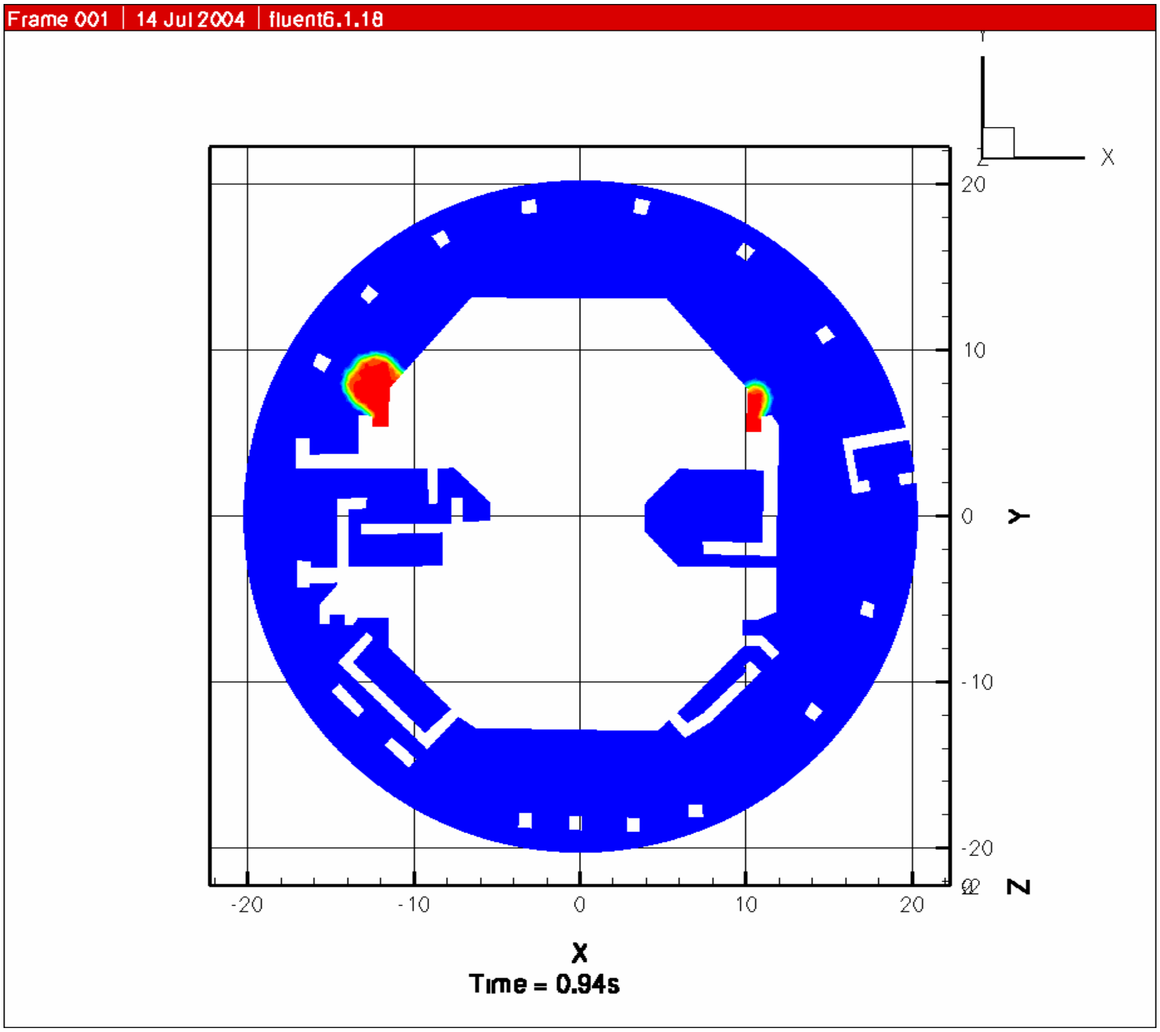

Figure III-5. Same as Figure III-4 for t = 0.94 Seconds

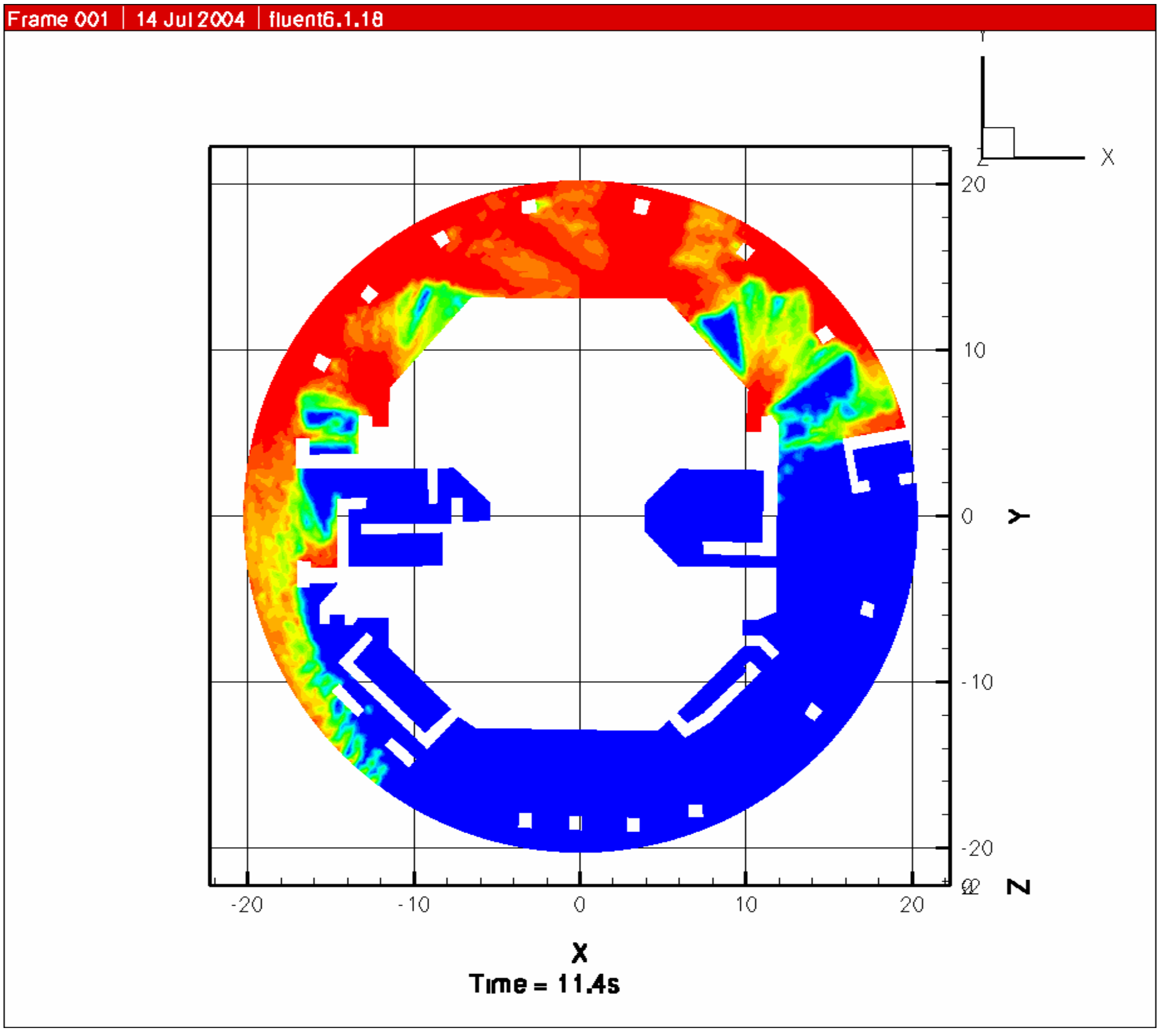

Figure III-6. Same as Figure III-4 for t = 11.4 Seconds

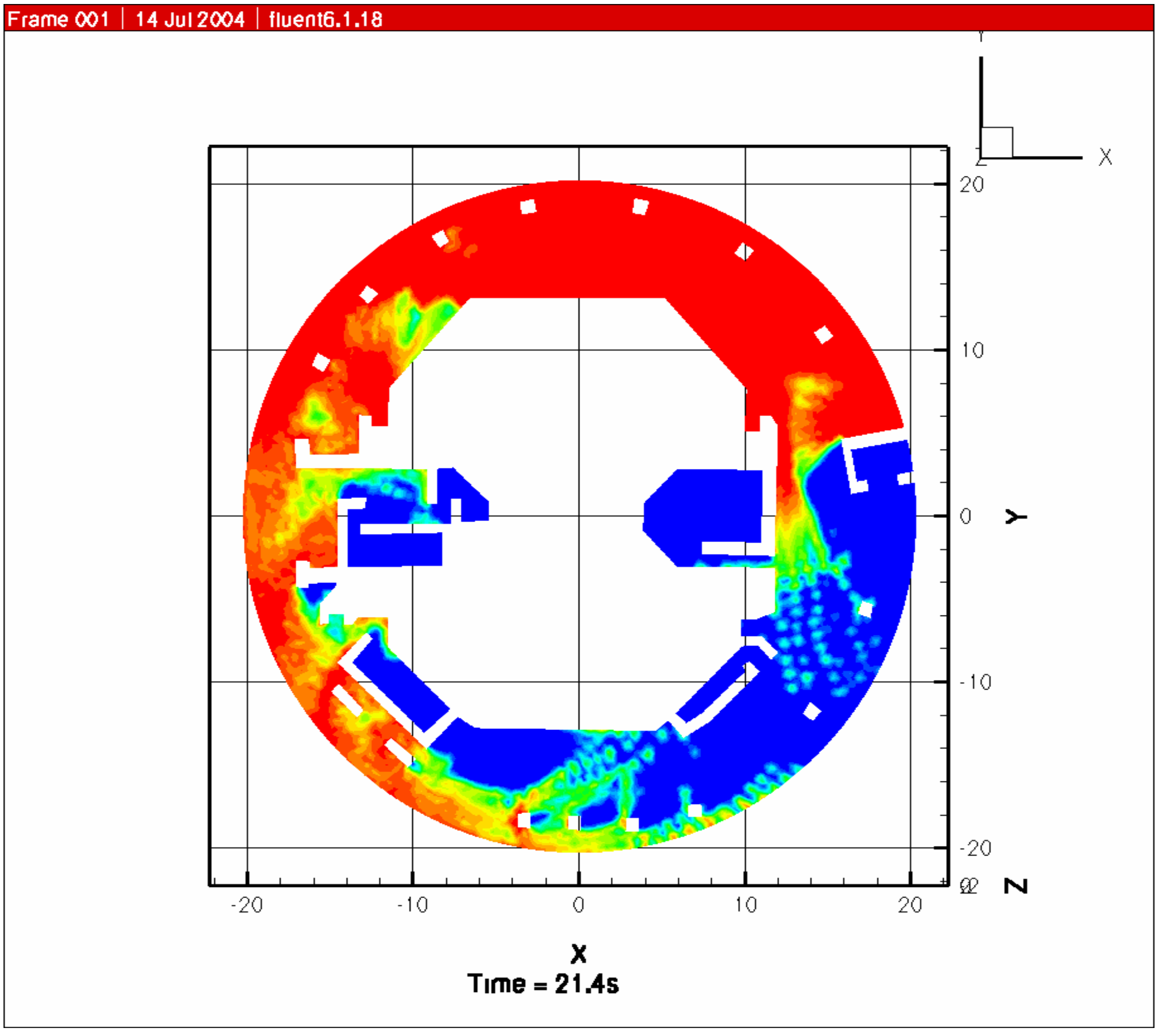

Figure III-7. Same as Figure III-4 for t = 21.4 Seconds

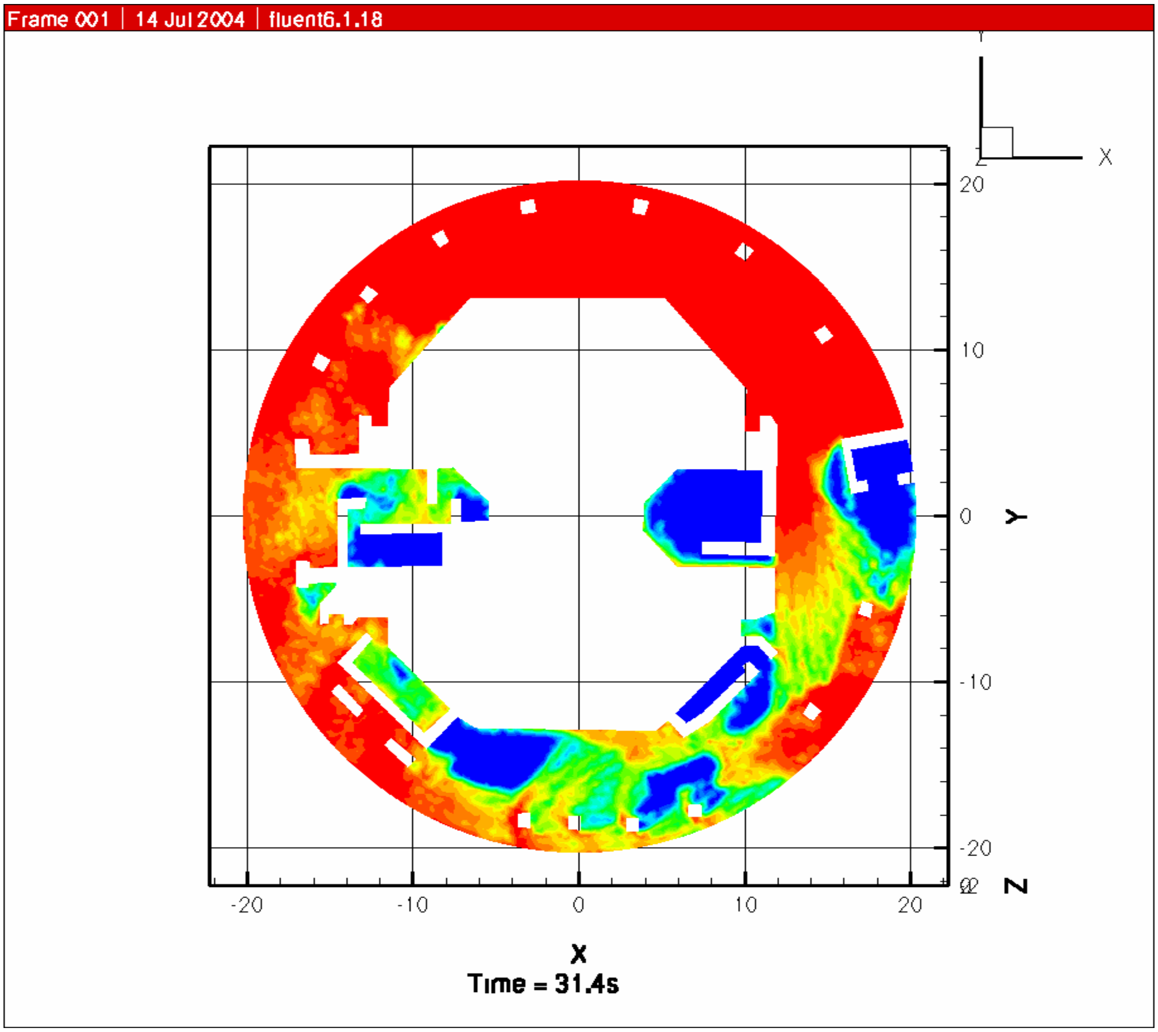

Figure III-8. Same as Figure III-4 for t = 31.4 Seconds

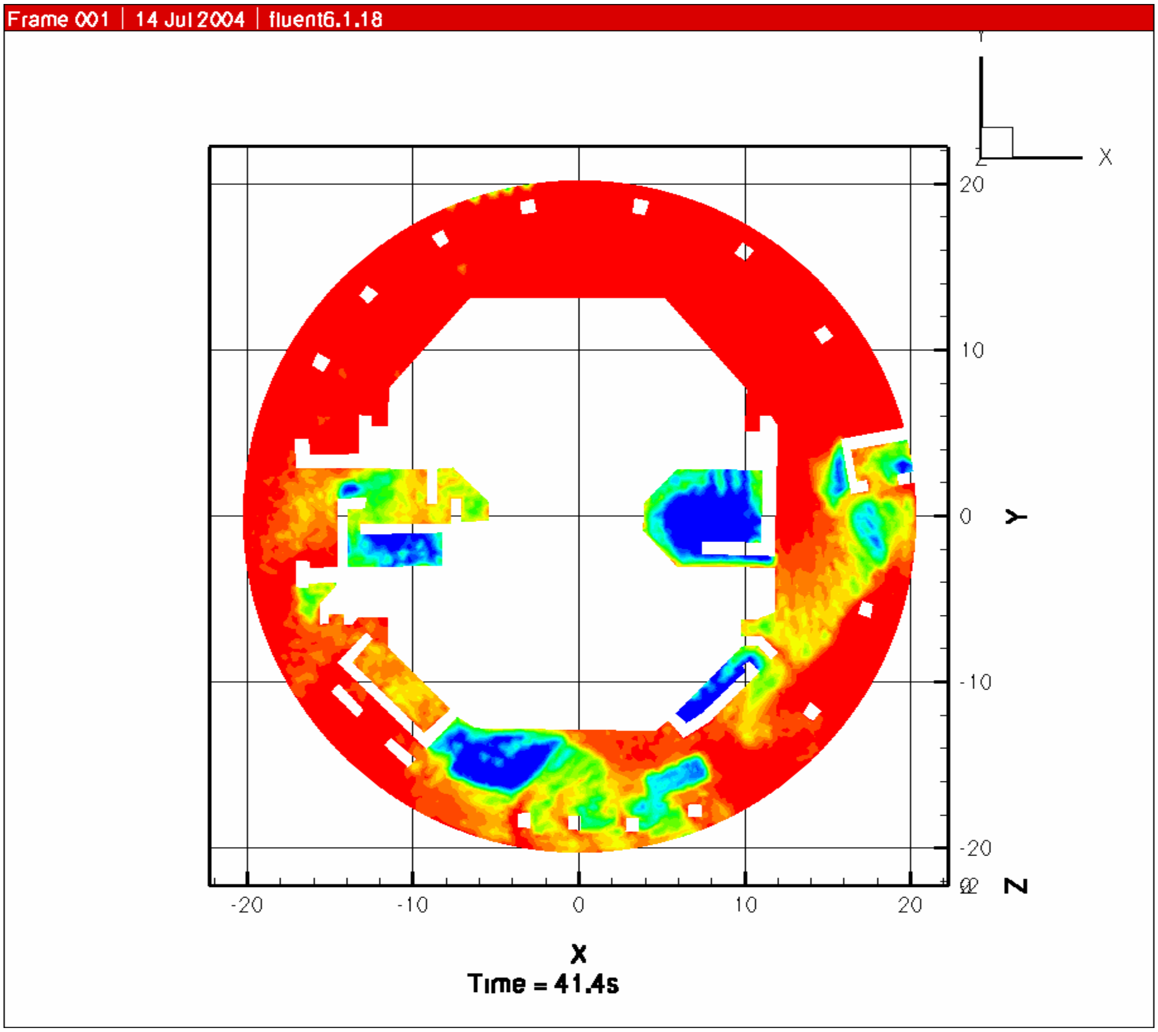

Figure III-9. Same as Figure III-4 for t = 41.4 Seconds

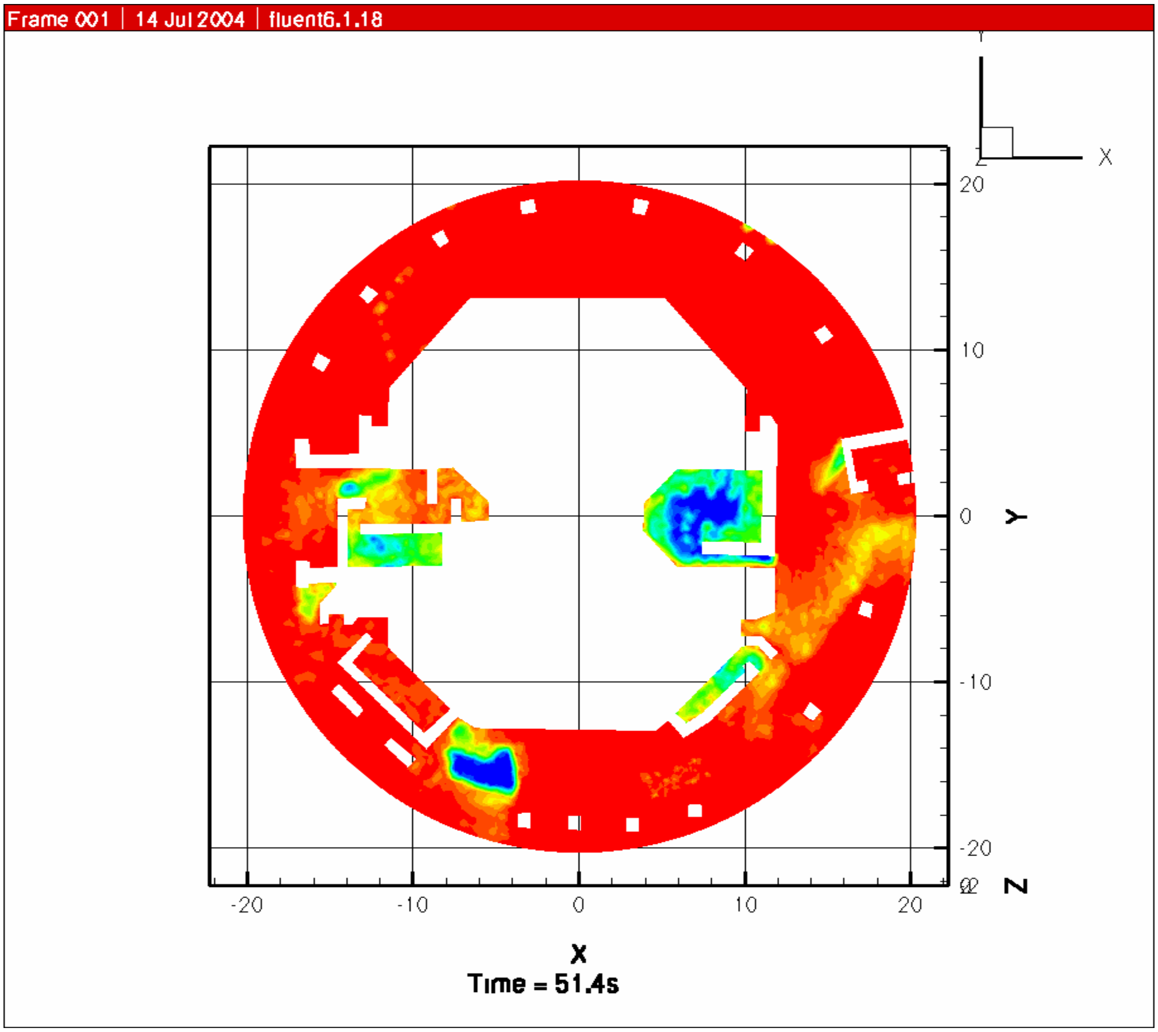

Figure III-10. Same as Figure III-4 for t = 51.4 Seconds

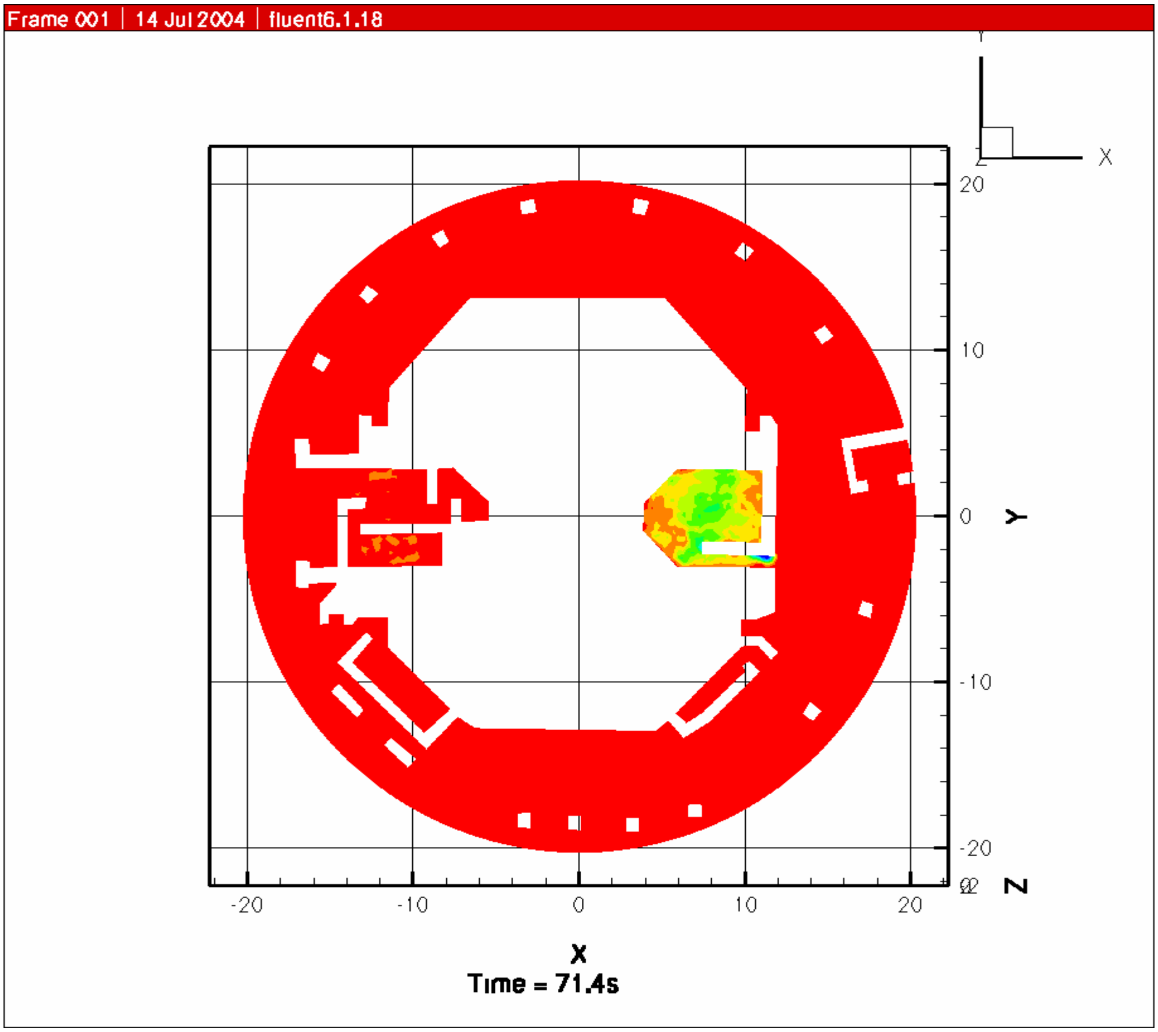

Figure III-11. Same as Figure III-4 for t = 71.4 Seconds

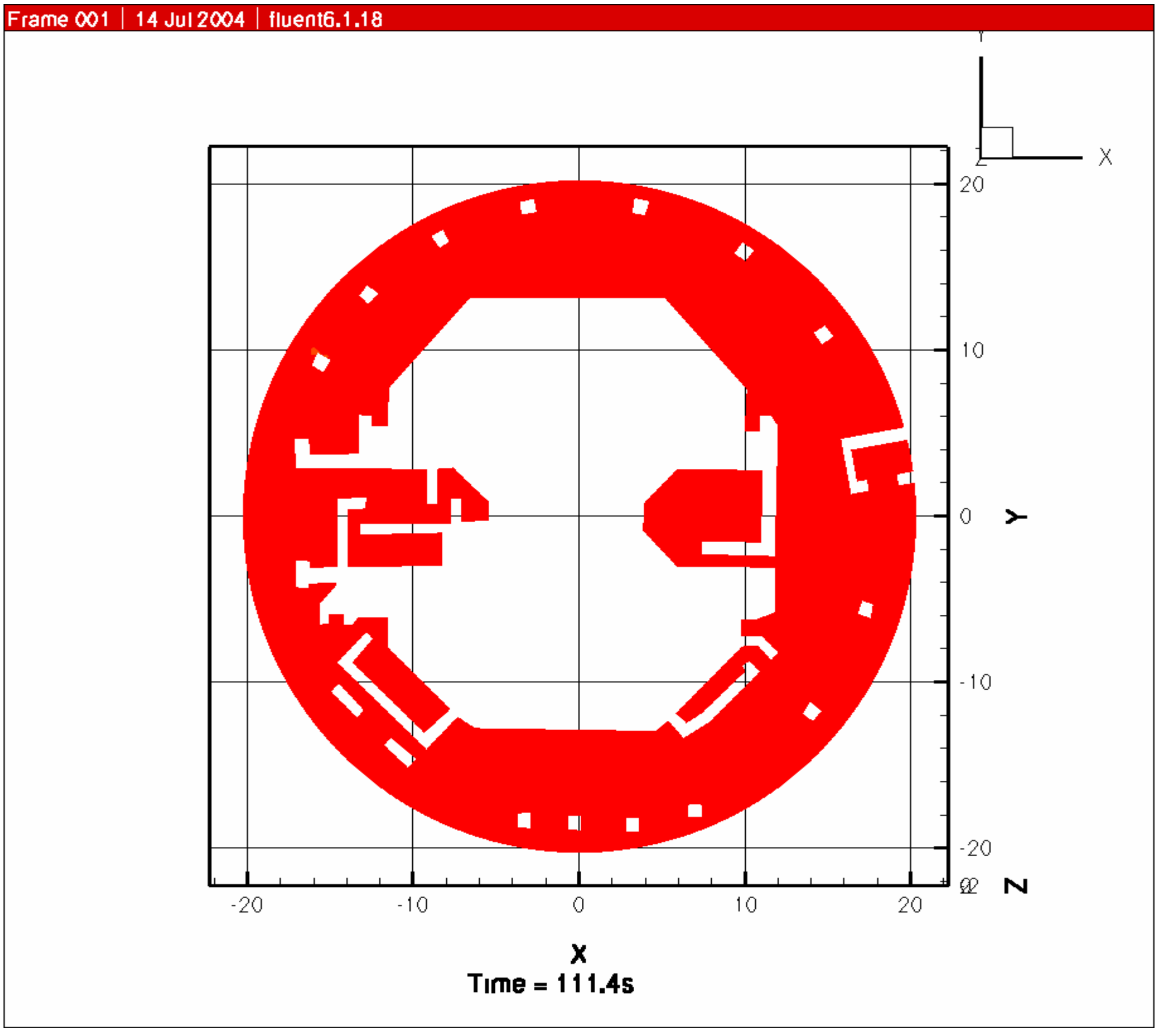

Figure III-12. Same as Figure III-4 for t = 111.4 Seconds

In Figure III-12, the solid red color indicates that the cells adjacent to the floor are full of water, not that the entire pool is full of water.

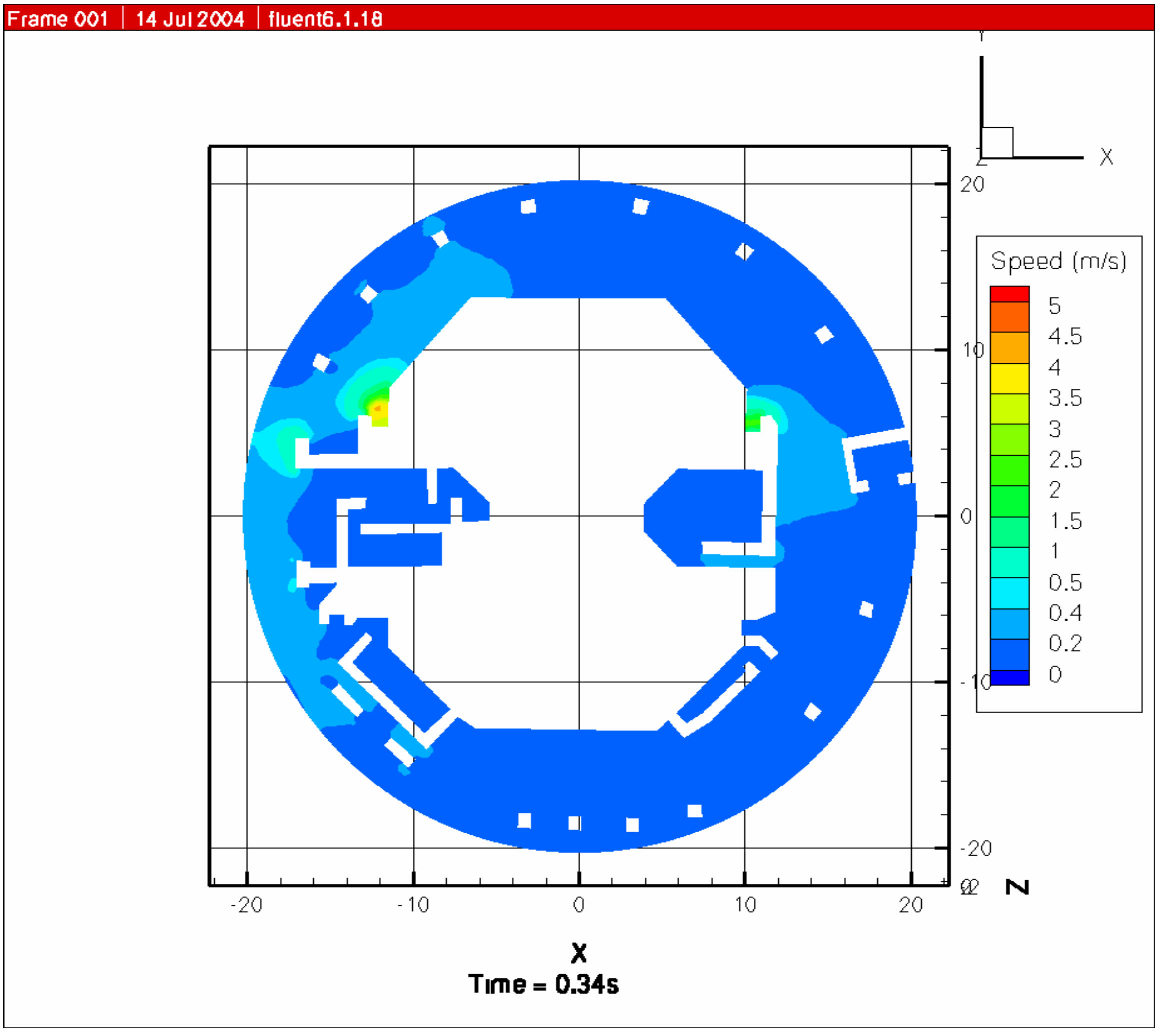

Figure III-13. Transient VOF Simulation of Containment Pool Fillup

Figure III-13 shows the contours of fluid velocity. The time snapshot shown in the figure is seconds after the breakflow is initiated. Note that the fluid velocity may be water or air; Figure III-4 to Figure III-12, showing the volume fraction of water, should be used to determine the actual water velocity.

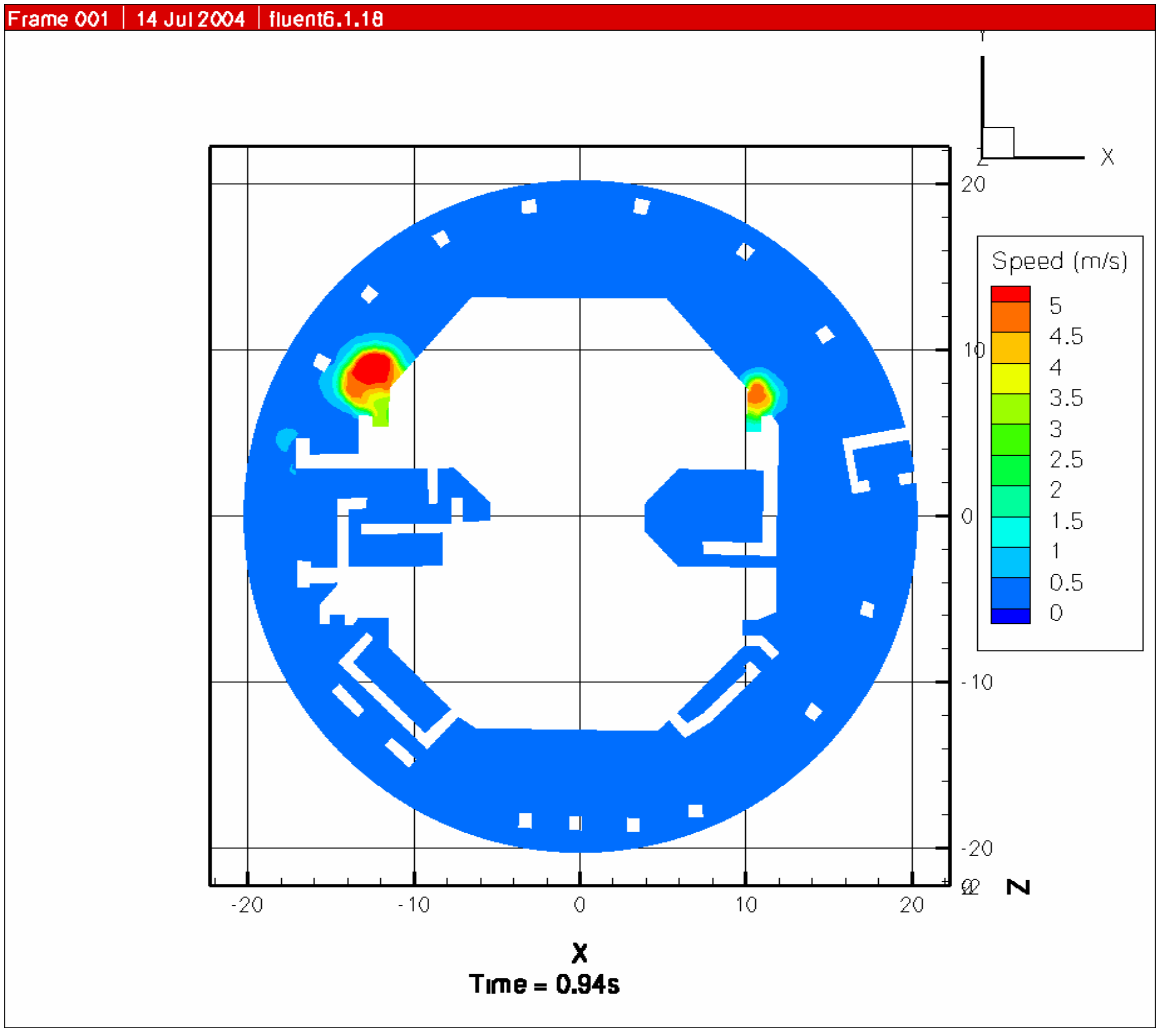

Figure III-14. Same as Figure III-13 for t = 0.94 Seconds

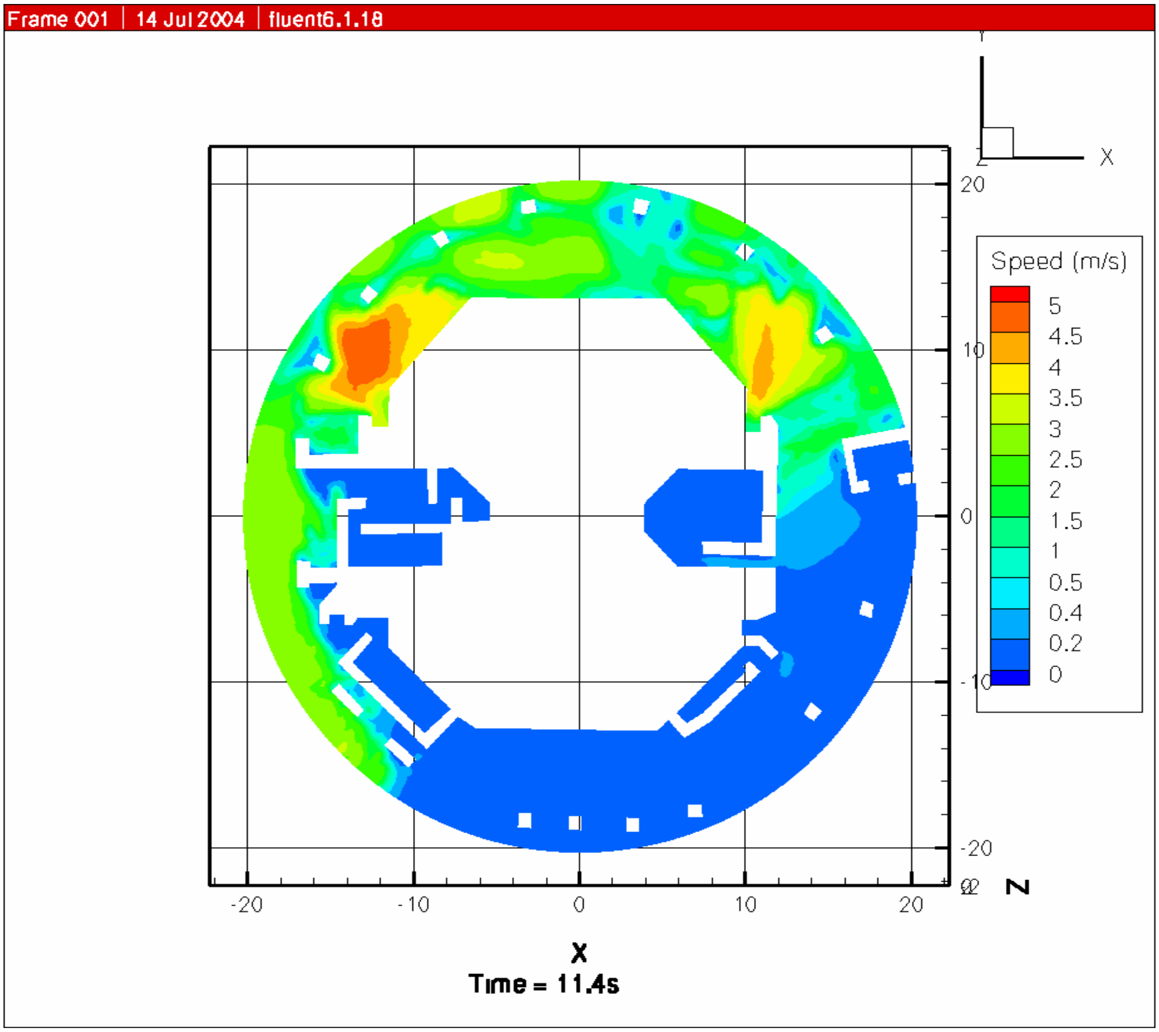

Figure III-15. Same as Figure III-13 for t = 11.4 Seconds

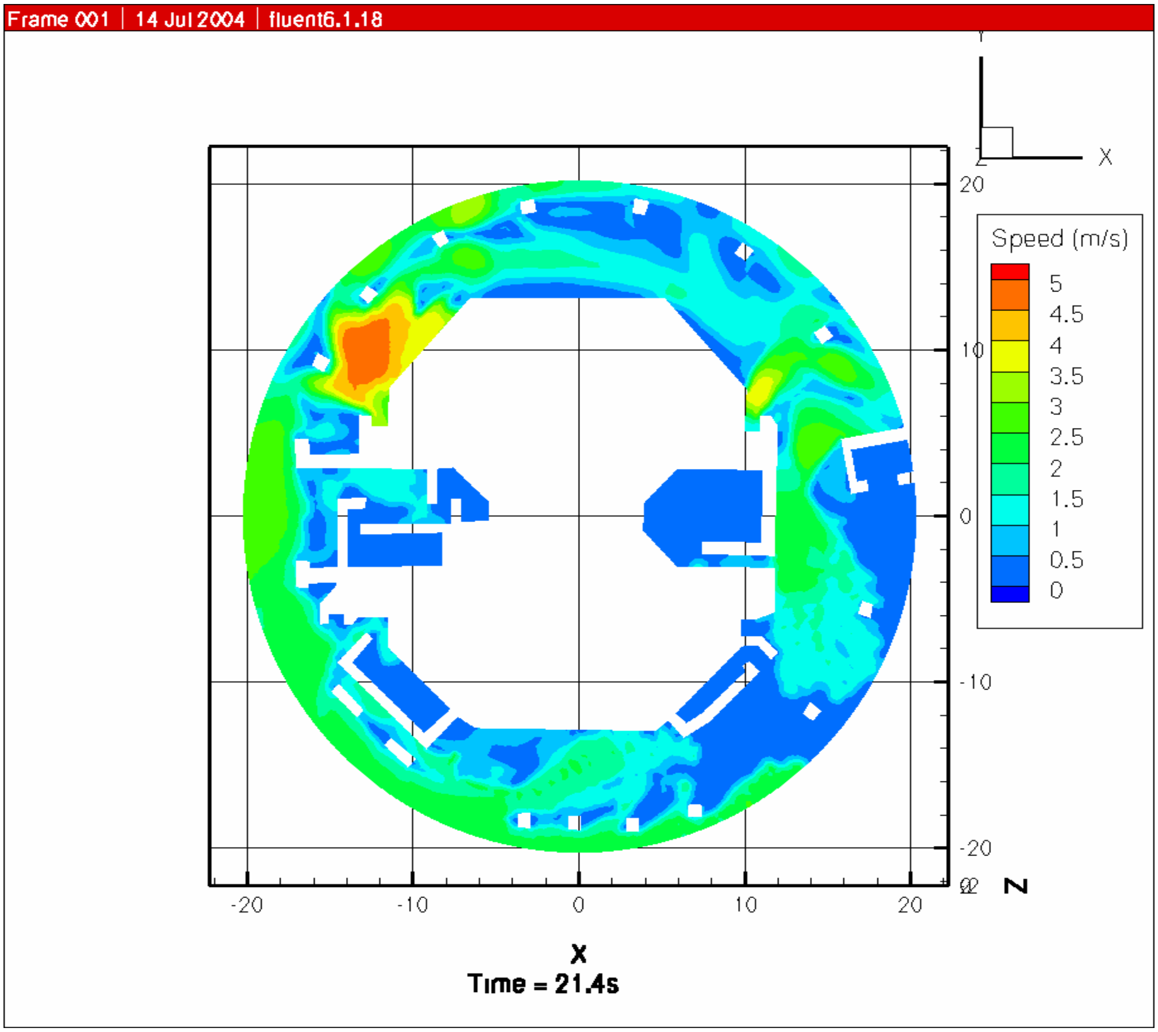

Figure III-16. Same as Figure III-13 for t = 21.4 Seconds

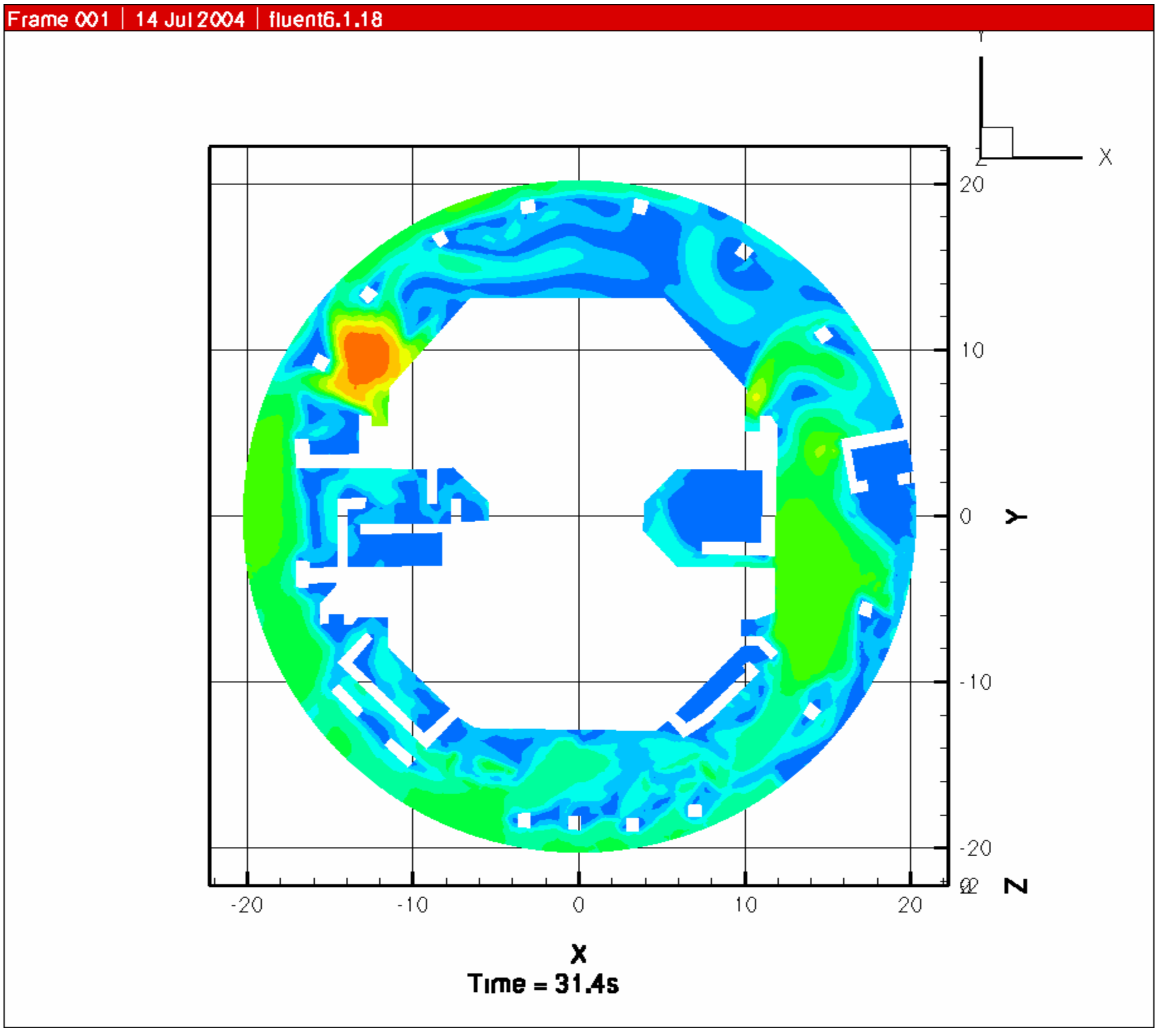

Figure III-17. Same as Figure III-13 for t = 31.4 Seconds

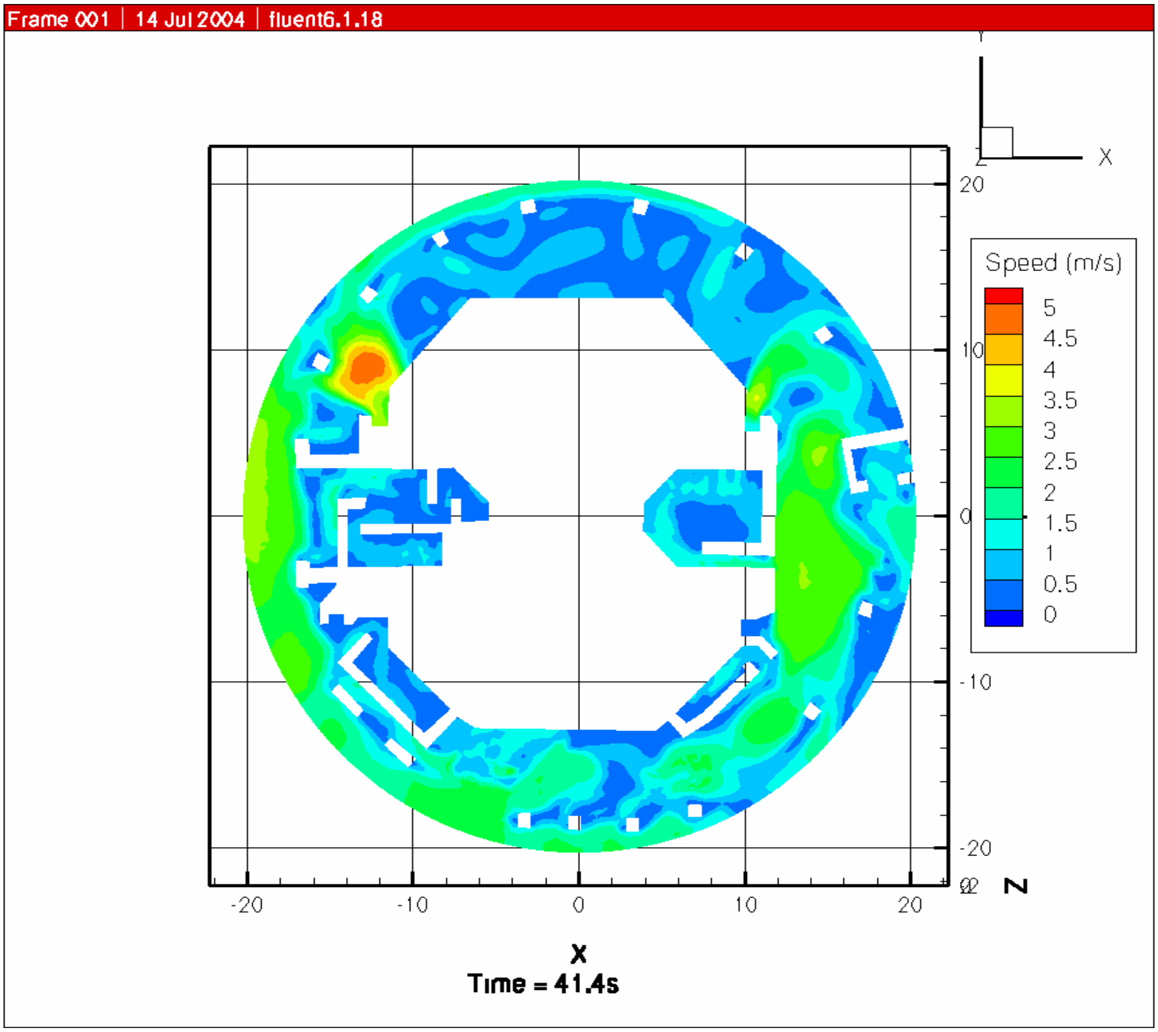

Figure III-18. Same as Figure III-13 for t = 41.4 Seconds

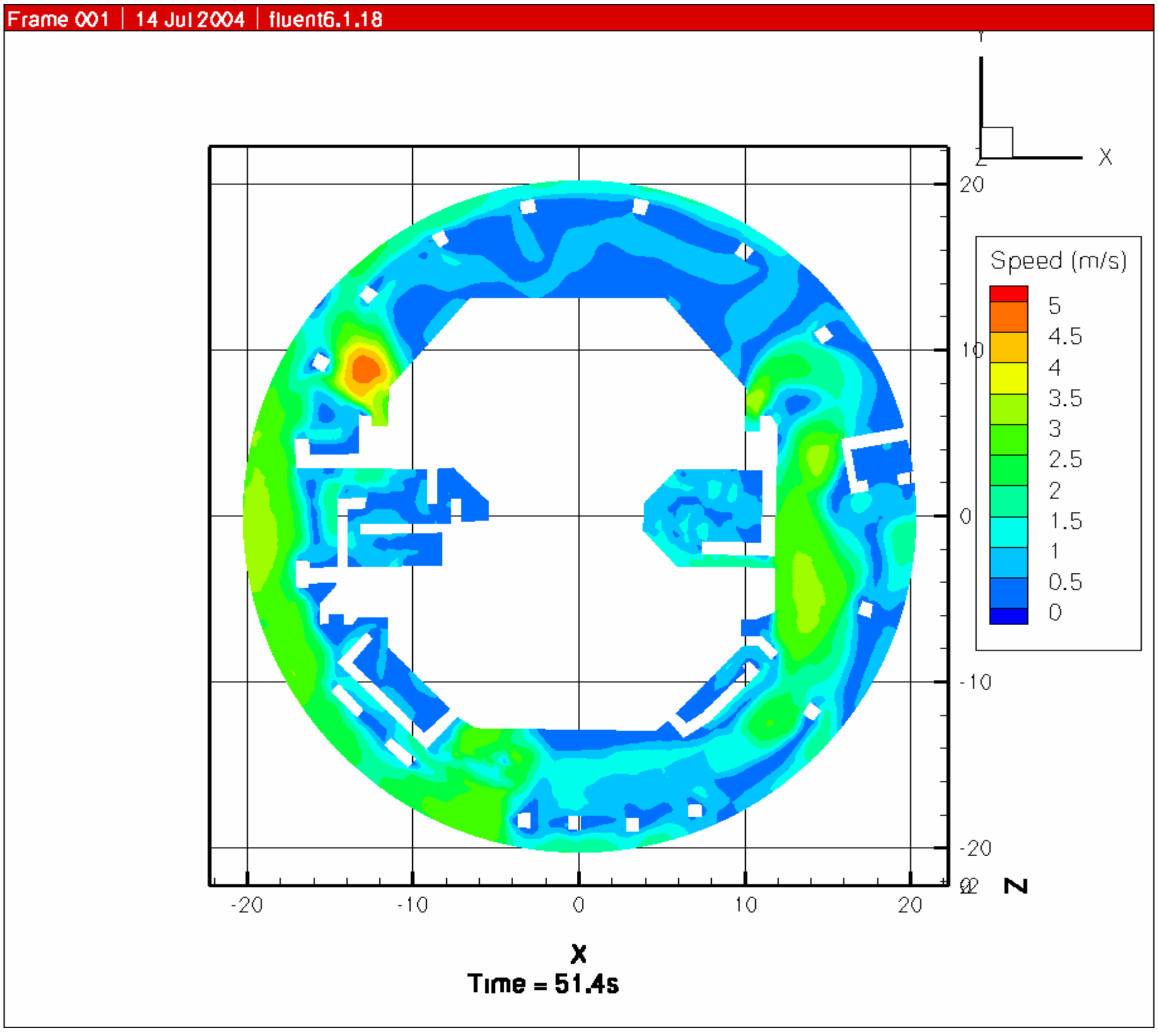

Figure III-19. Same as Figure III-13 for t = 51.4 Seconds

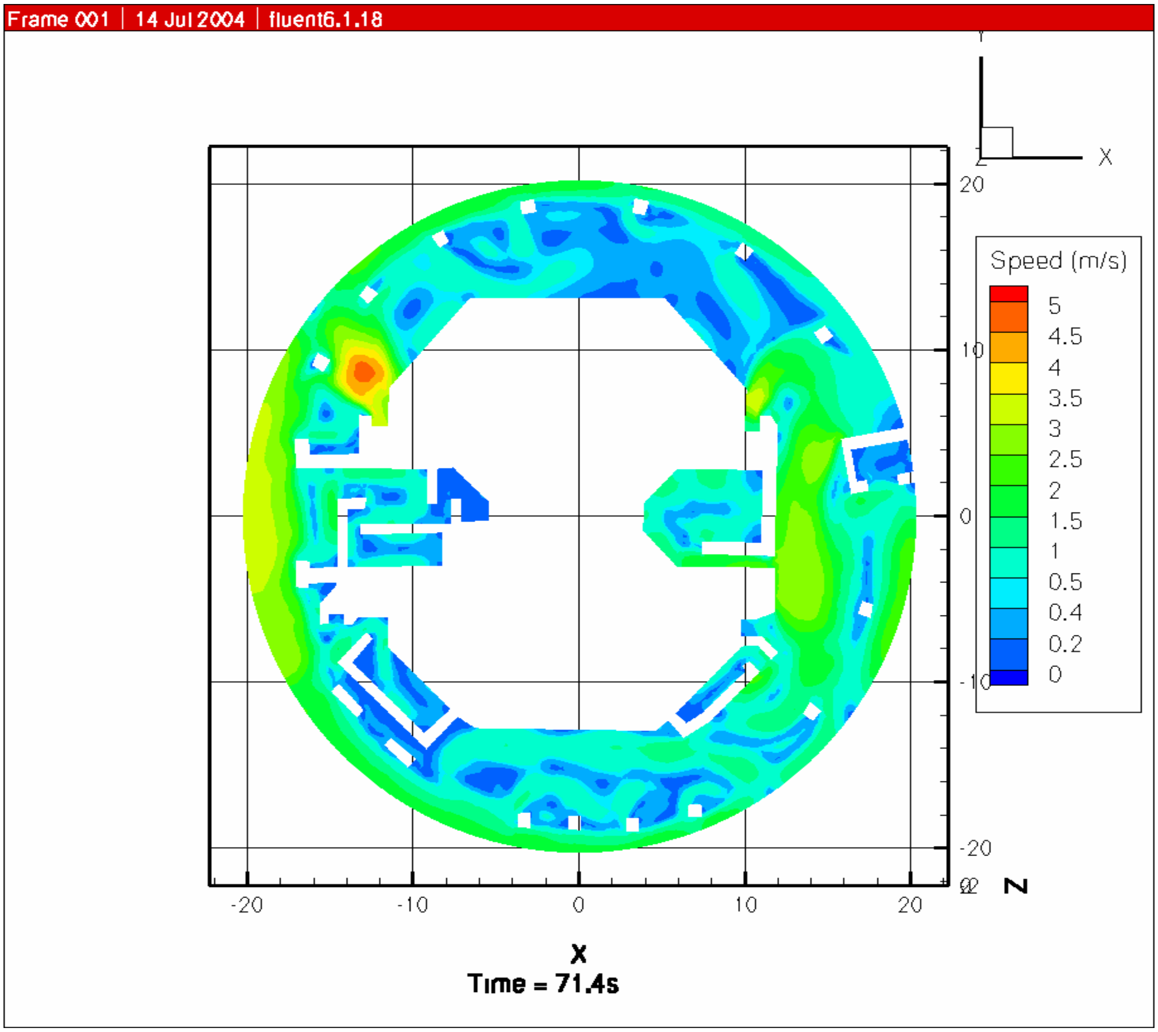

Figure III-20. Same as Figure III-13 for t = 71.4 Seconds

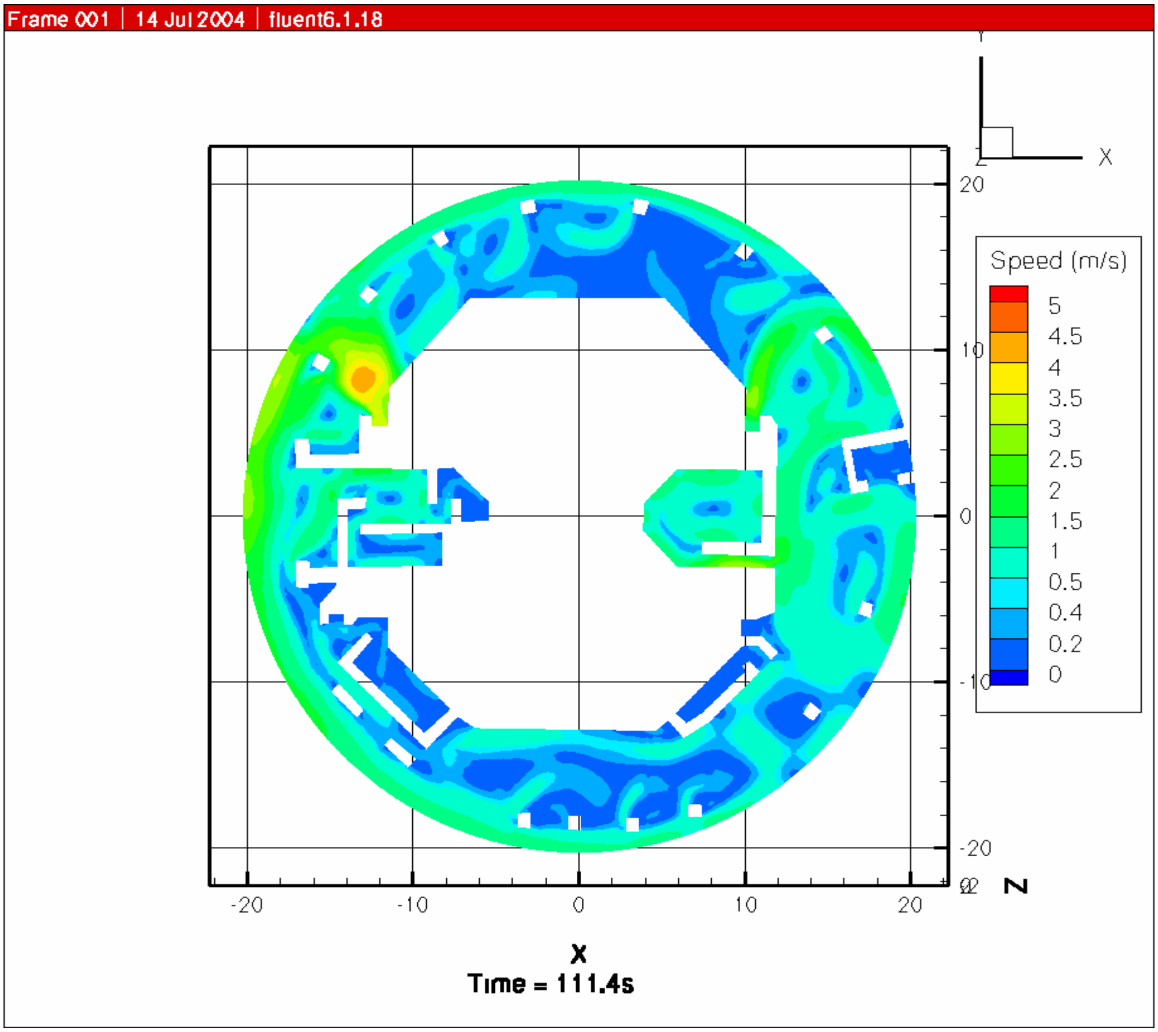

Figure III-21. Same as Figure III-13 for t = 111.4 Seconds

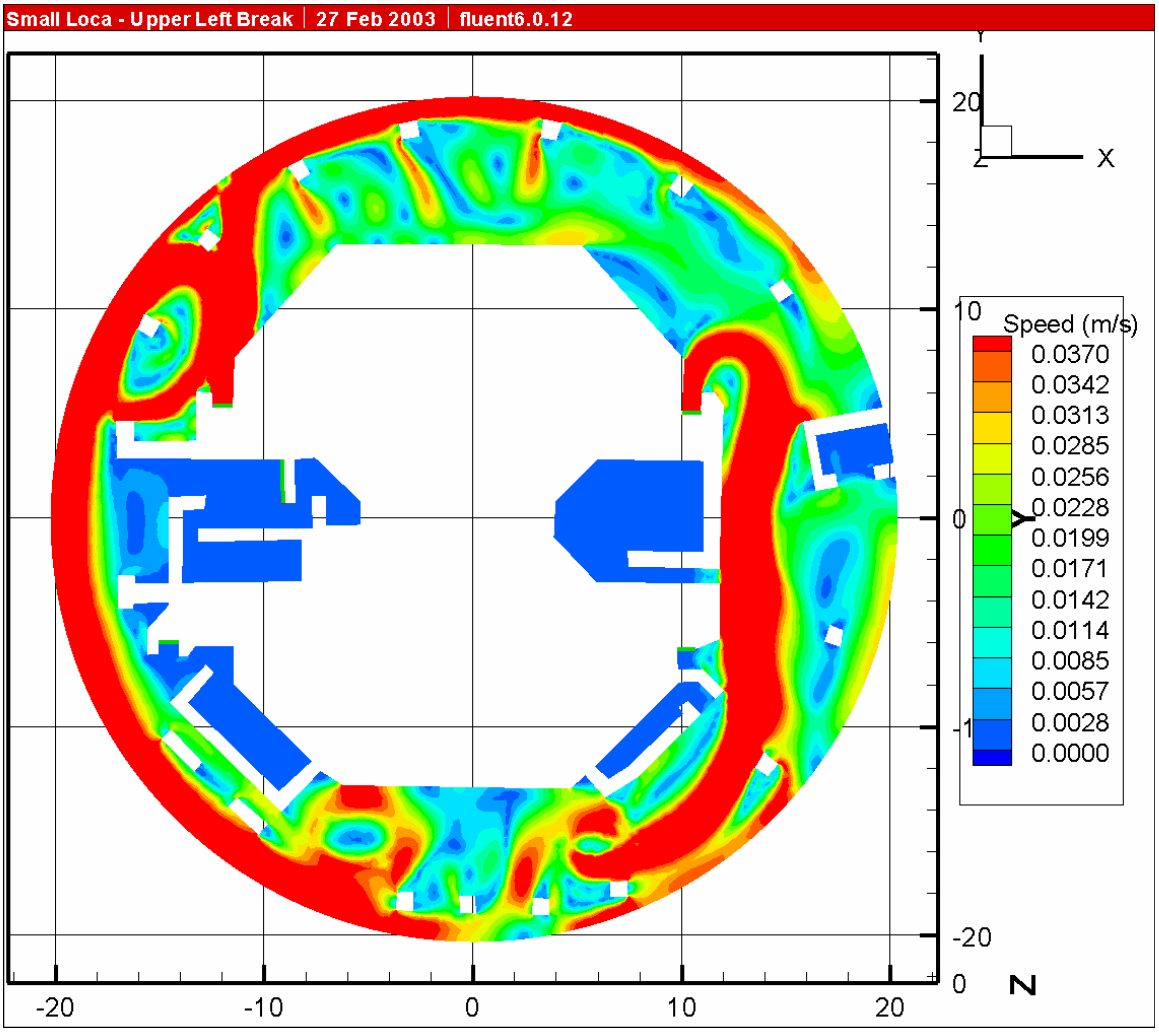

Figure III-22. Small LOCA Break Located in the Upper-Left Quadrant

In Figure III-22, speeds greater than or equal to the fiber threshold (0.037 m/s) are colored red.

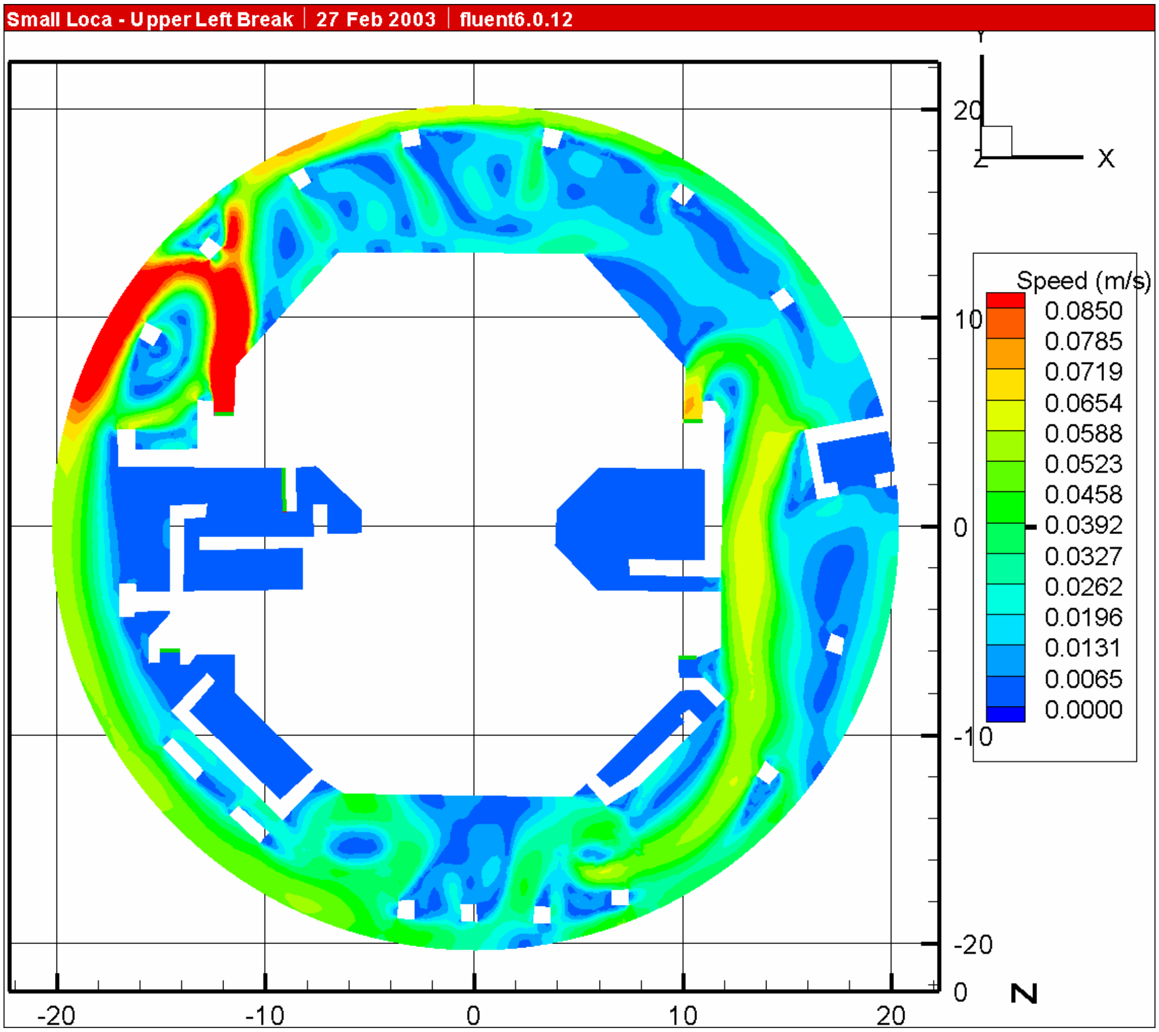

Figure III-23. Small LOCA Break Located in the Upper-Left Quadrant

In Figure III-23, speeds greater than or equal to the RMI threshold (0.085 m/s) are colored red.

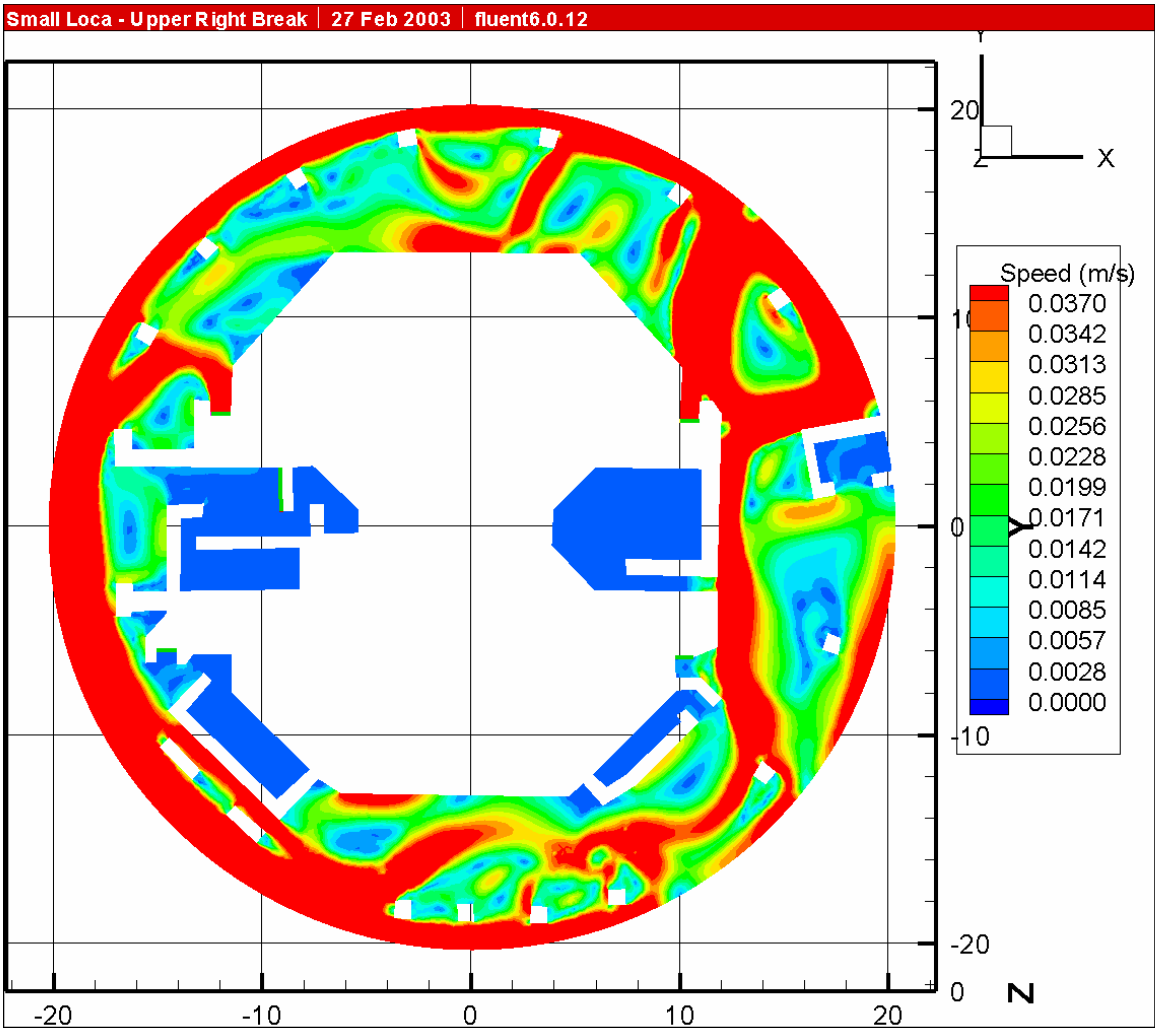

Figure III-24. Small LOCA Break Located in the Upper-Right Quadrant

In Figure III-24, speeds greater than or equal to the fiber threshold (0.037 m/s) are colored red.

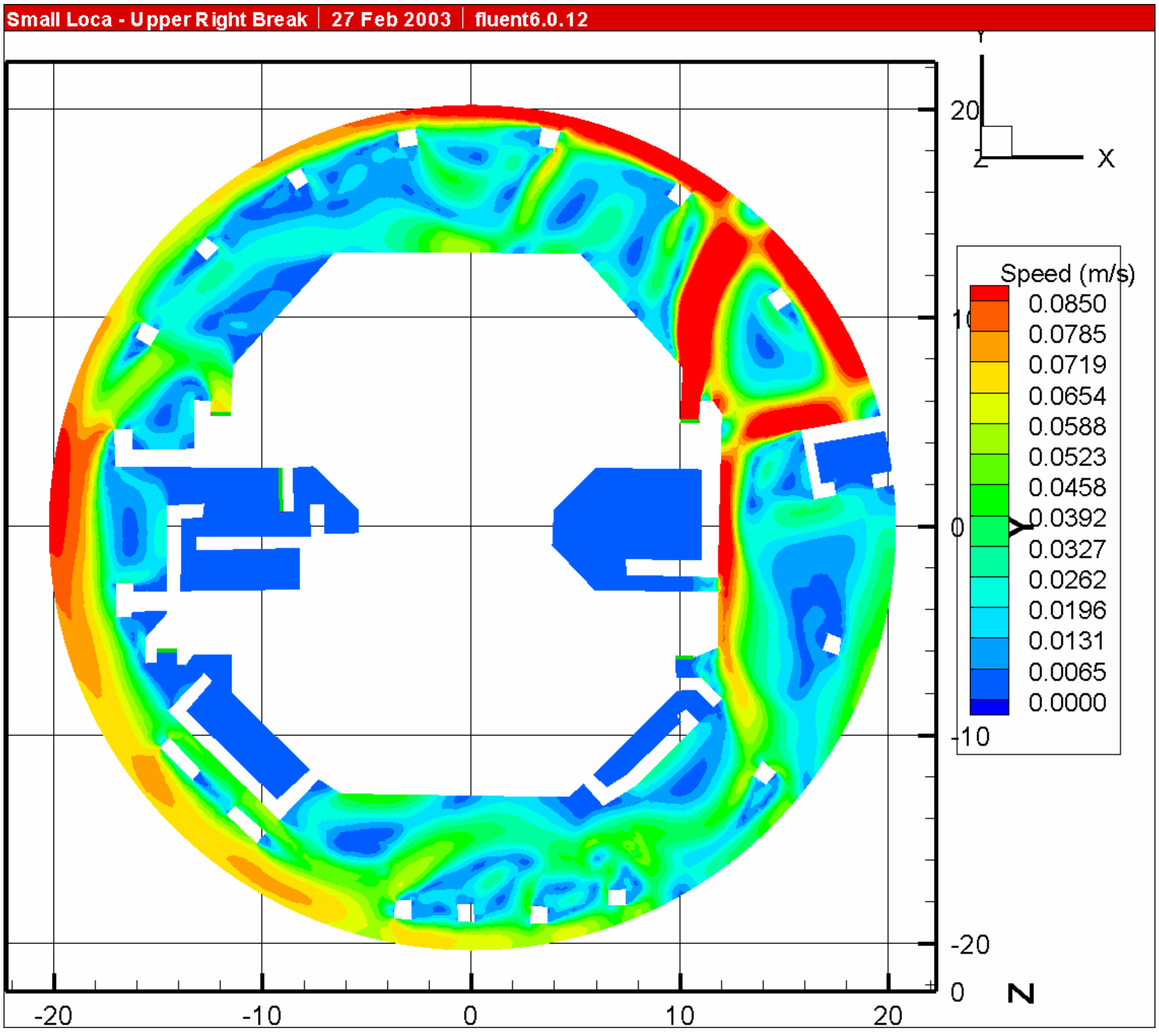

Figure III-25. Small LOCA Break Located in the Upper-Right Quadrant

In Figure III-25, speeds greater than or equal to the RMI threshold (0.085 m/s) are colored red.

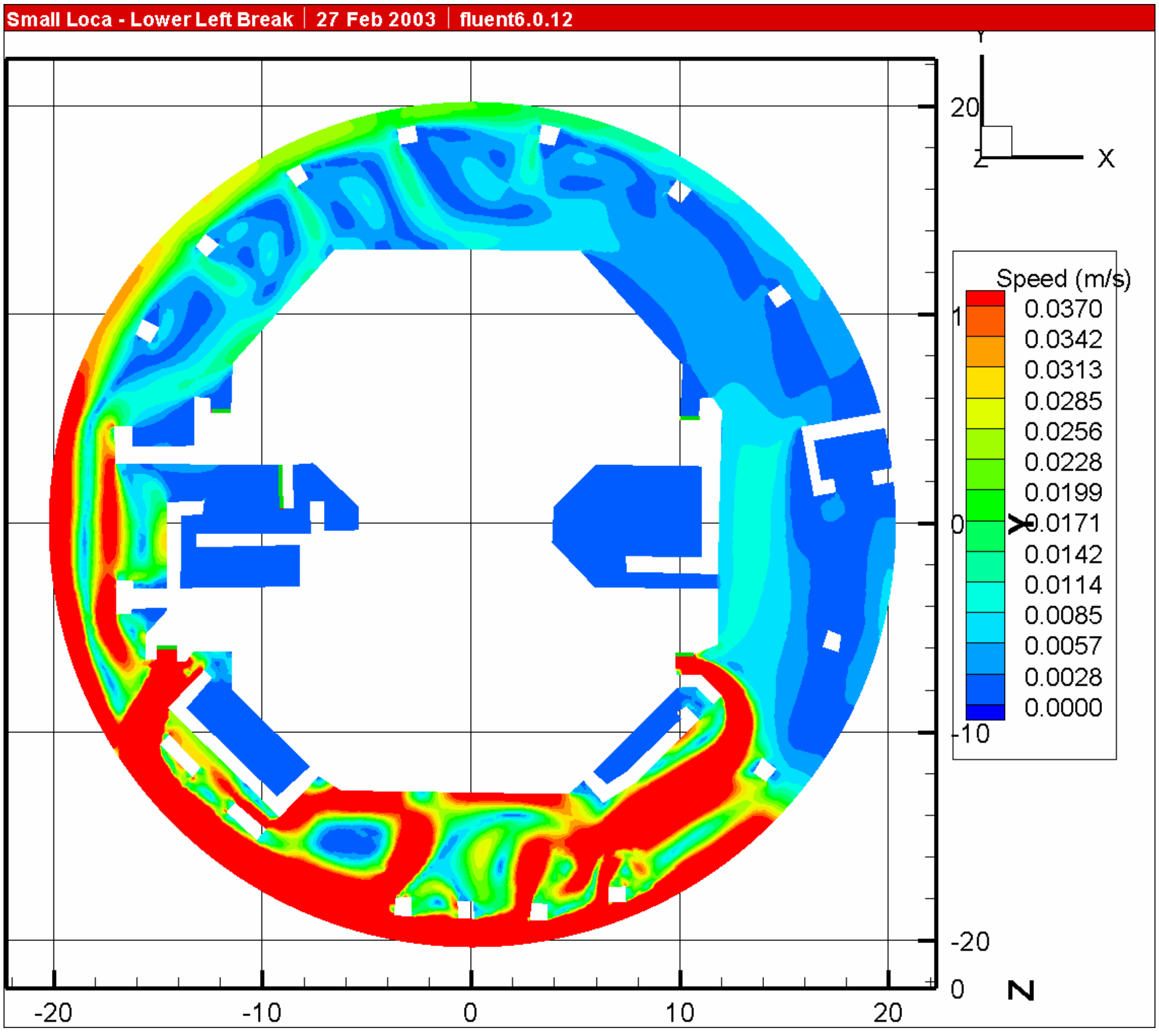

Figure III-26. Small LOCA Break Located in the Lower-Left Quadrant

In Figure III-26, speeds greater than or equal to the fiber threshold (0.037 m/s) are colored red.

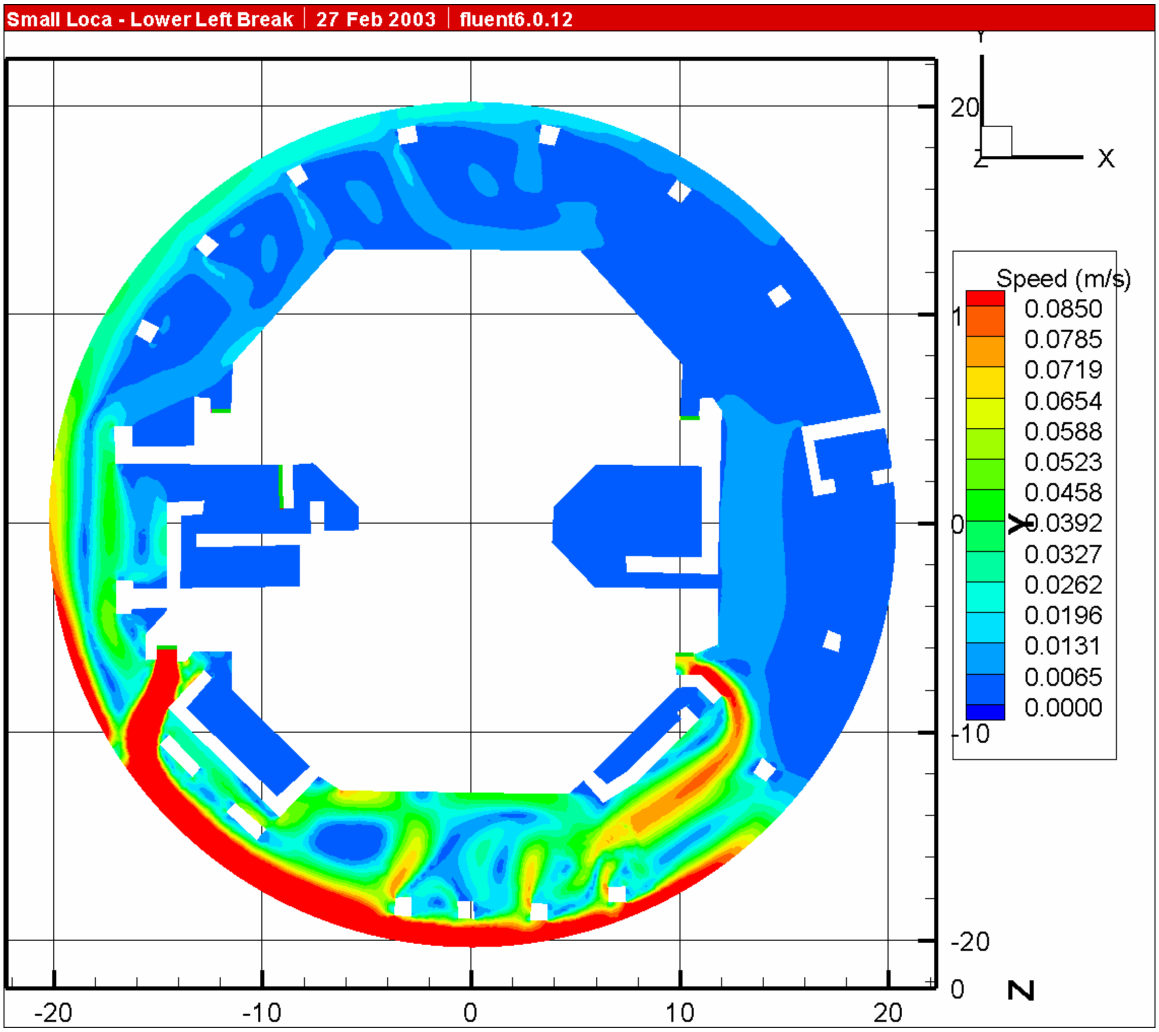

Figure III-27. Small LOCA Break Located in the Lower-Left Quadrant

In Figure III-27, speeds greater than or equal to the RMI threshold (0.085 m/s) are colored red.

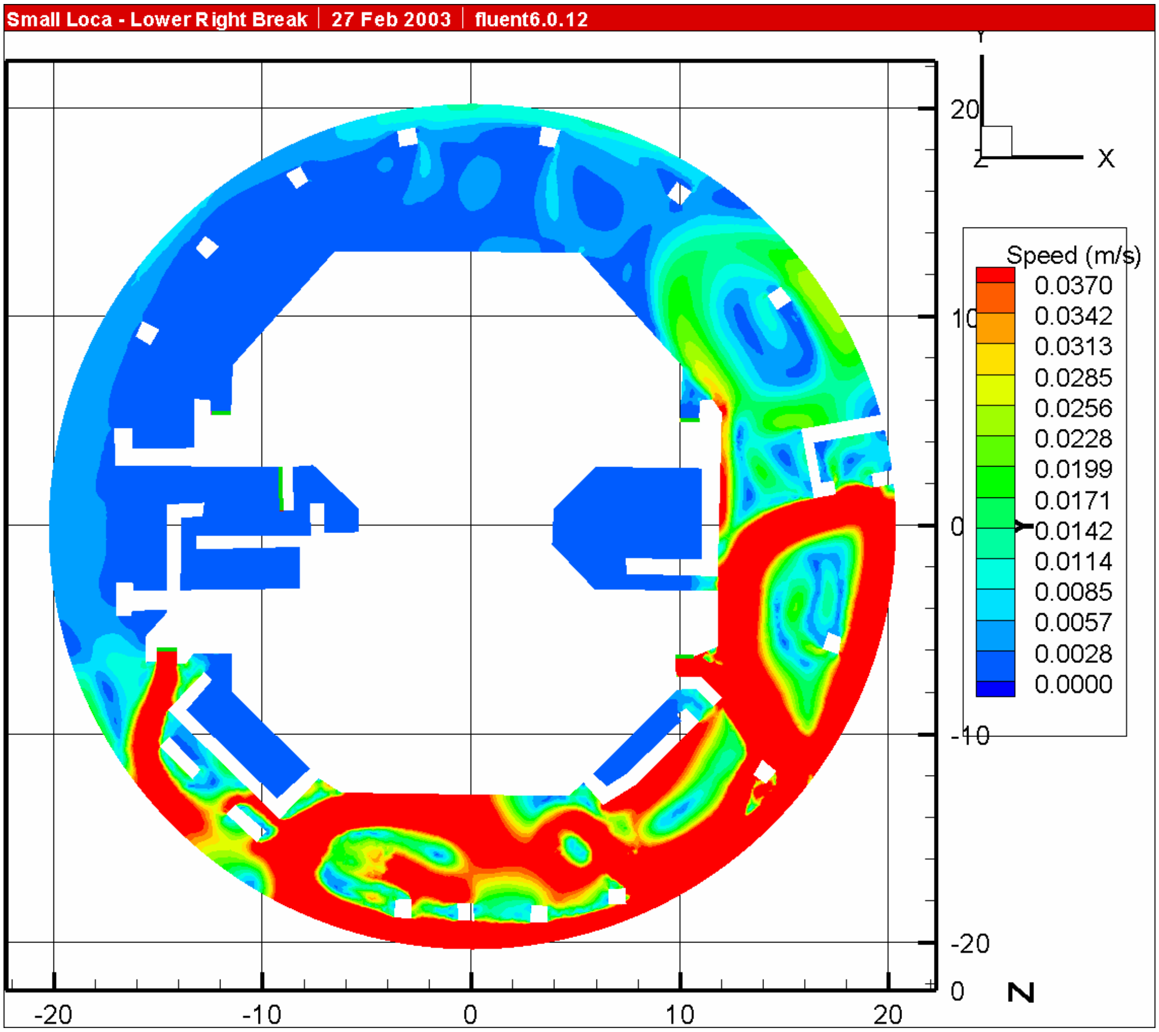

Figure III-28. Small LOCA Break Located in the Lower-Right Quadrant

In Figure III-28, speeds greater than or equal to the fiber threshold (0.037 m/s) are colored red.

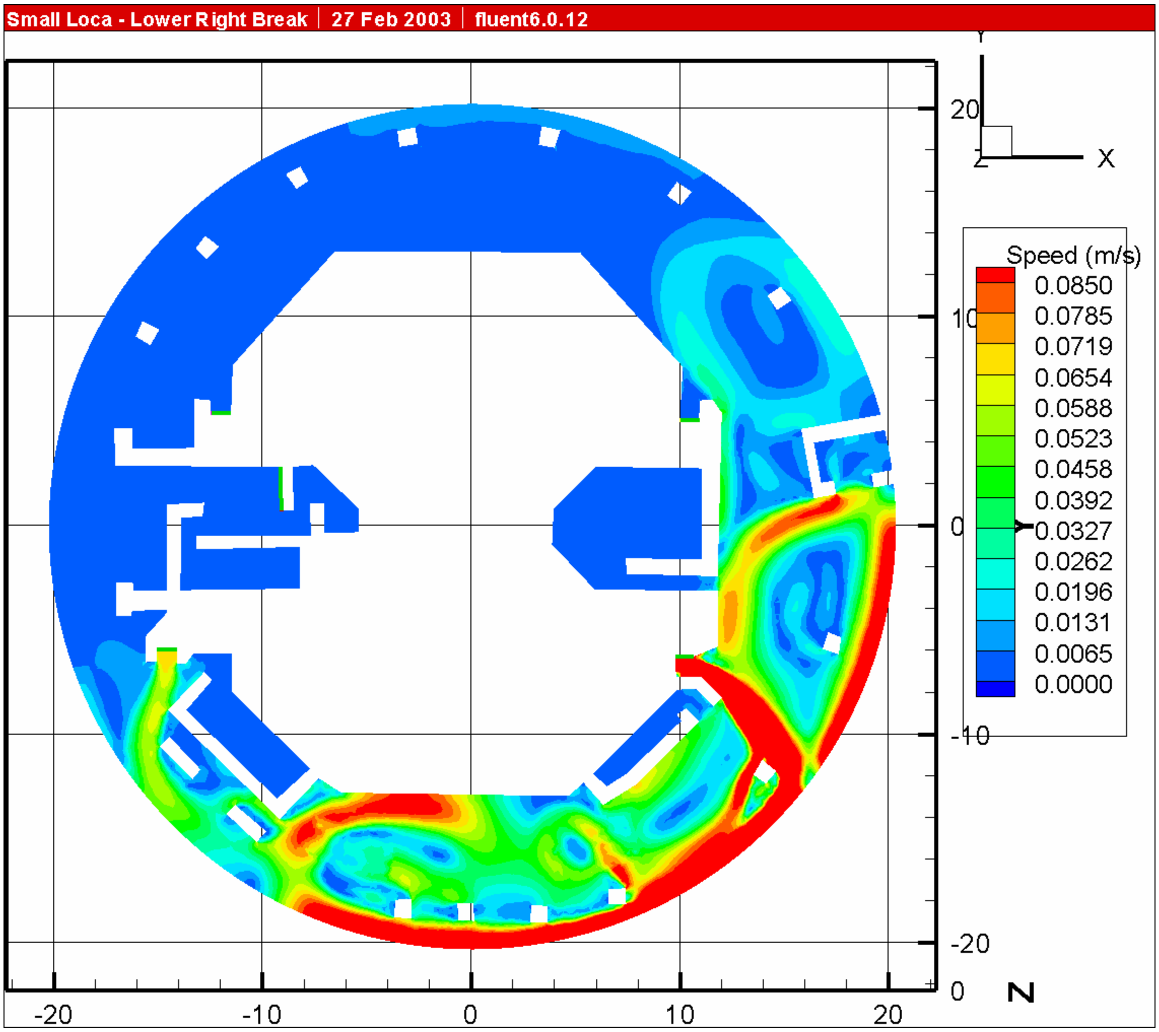

Figure III-29. Small LOCA Break Located in the Lower-Right Quadrant

In Figure III-29, speeds greater than or equal to the RMI threshold (0.085 m/s) are colored red.

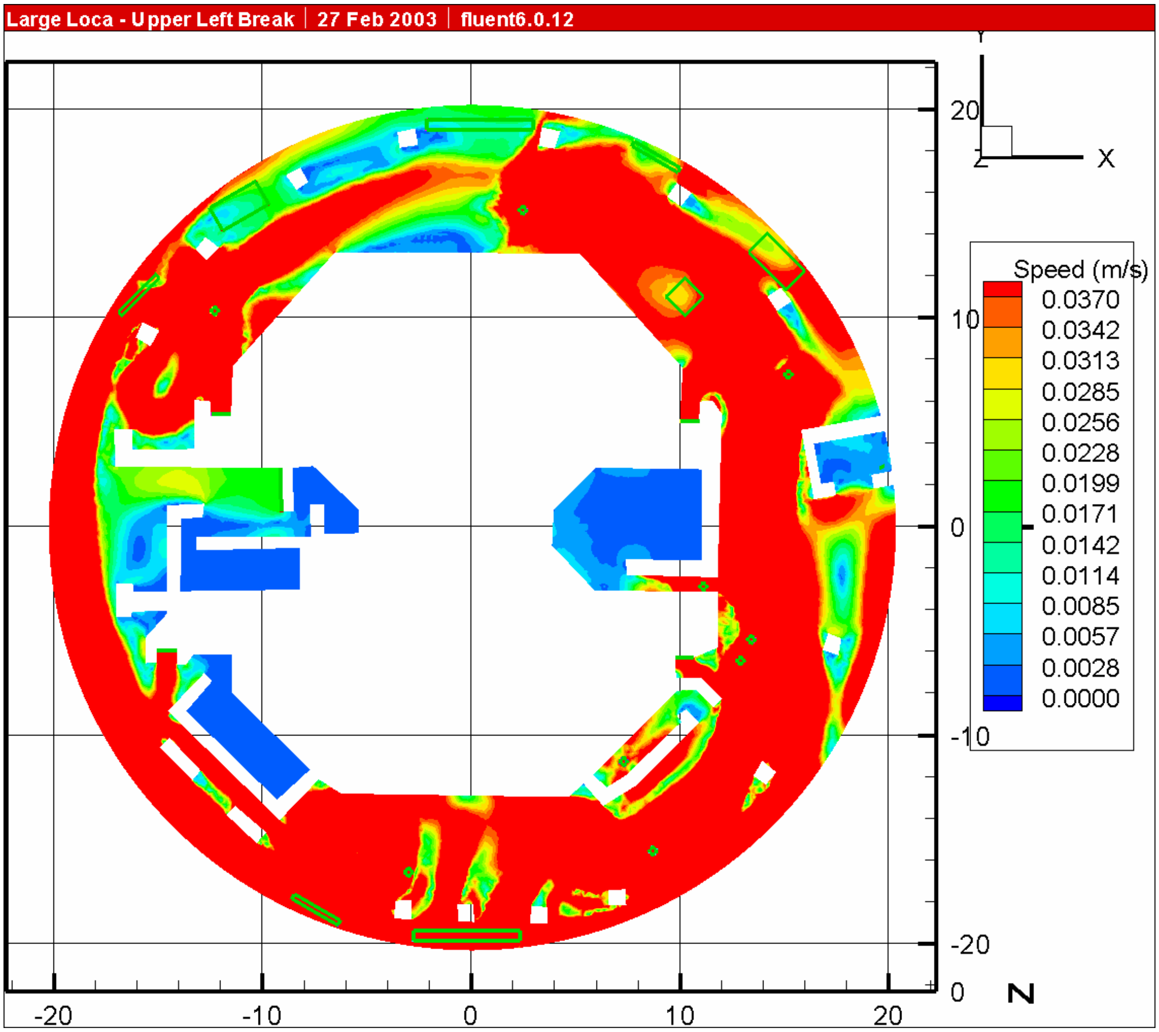

Figure III-30. Large LOCA Break Located in the Upper-Left Quadrant

In Figure III-30, speeds greater than or equal to the fiber threshold (0.037 m/s) are colored red.

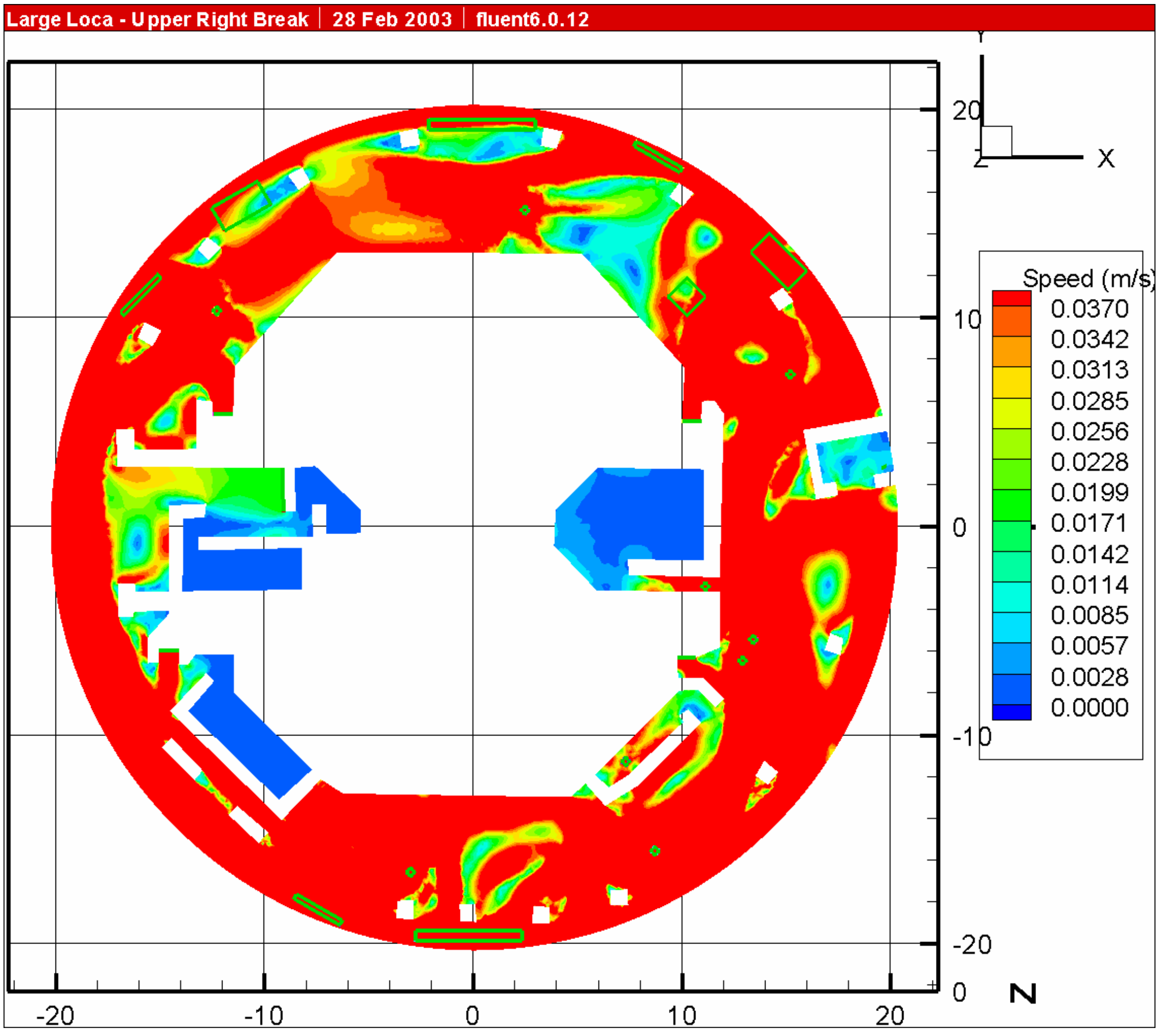

Figure III-31. Large LOCA Break Located in the Upper-Right Quadrant

In Figure III-31, speeds greater than or equal to the fiber threshold (0.037 m/s) are colored red.

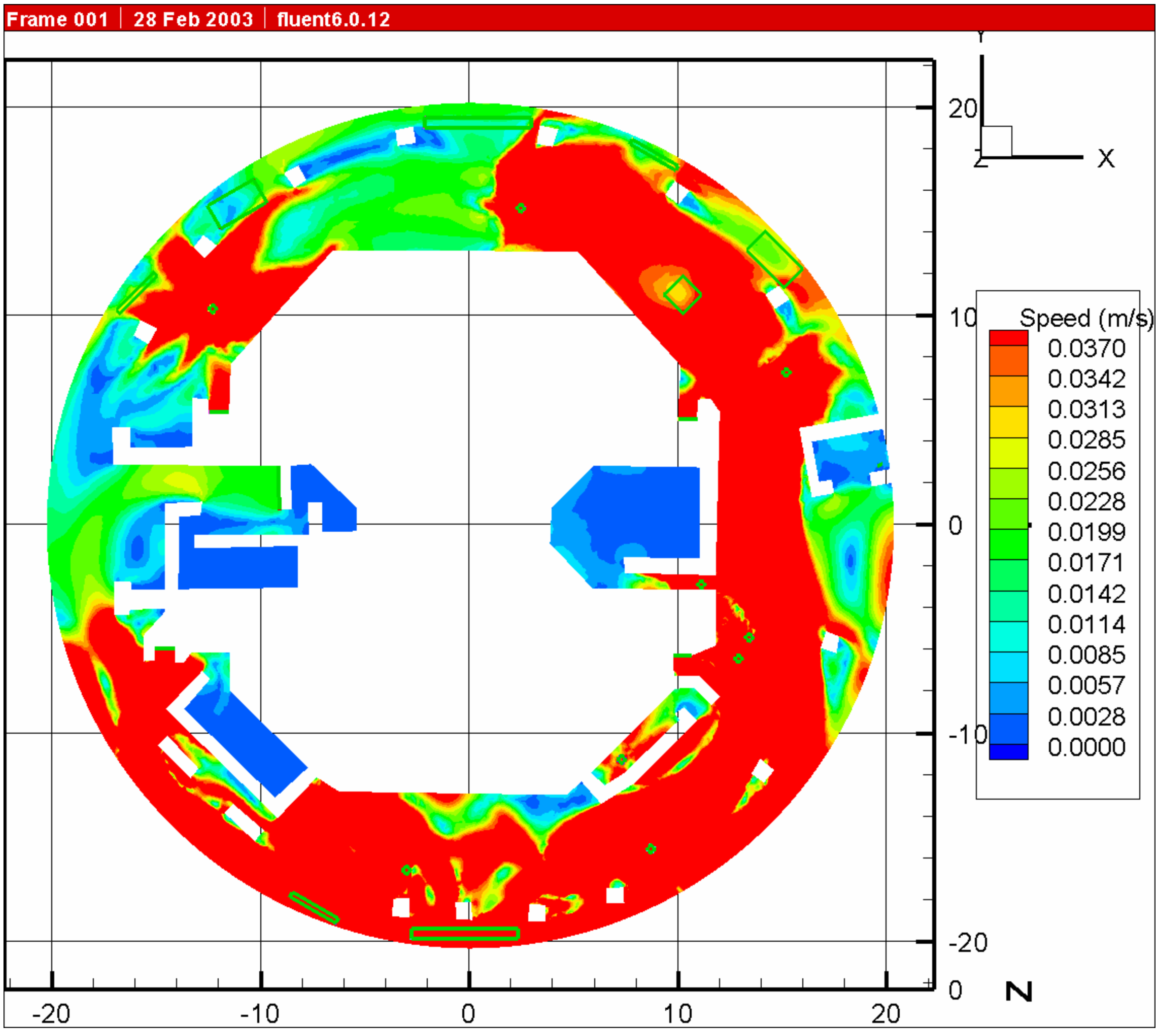

Figure III-32. Large LOCA Break Located in the Lower-Left Quadrant

In Figure III-32, speeds greater than or equal to the fiber threshold (0.037 m/s) are colored red.

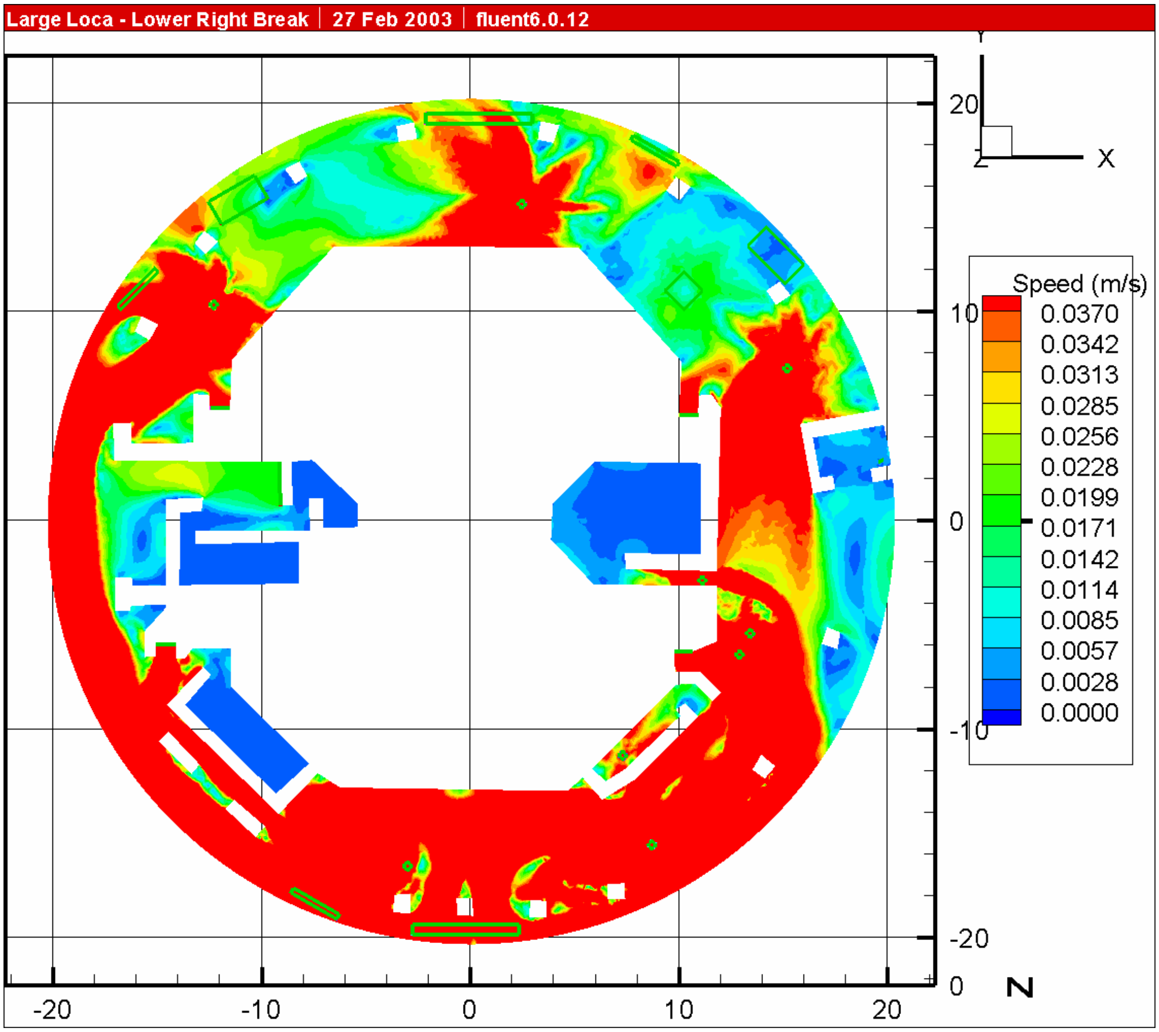

Figure III-33. Large LOCA Break Located in the Lower-Right Quadrant

In Figure III-33, speeds greater than or equal to the fiber threshold (0.037 m/s) are colored red.

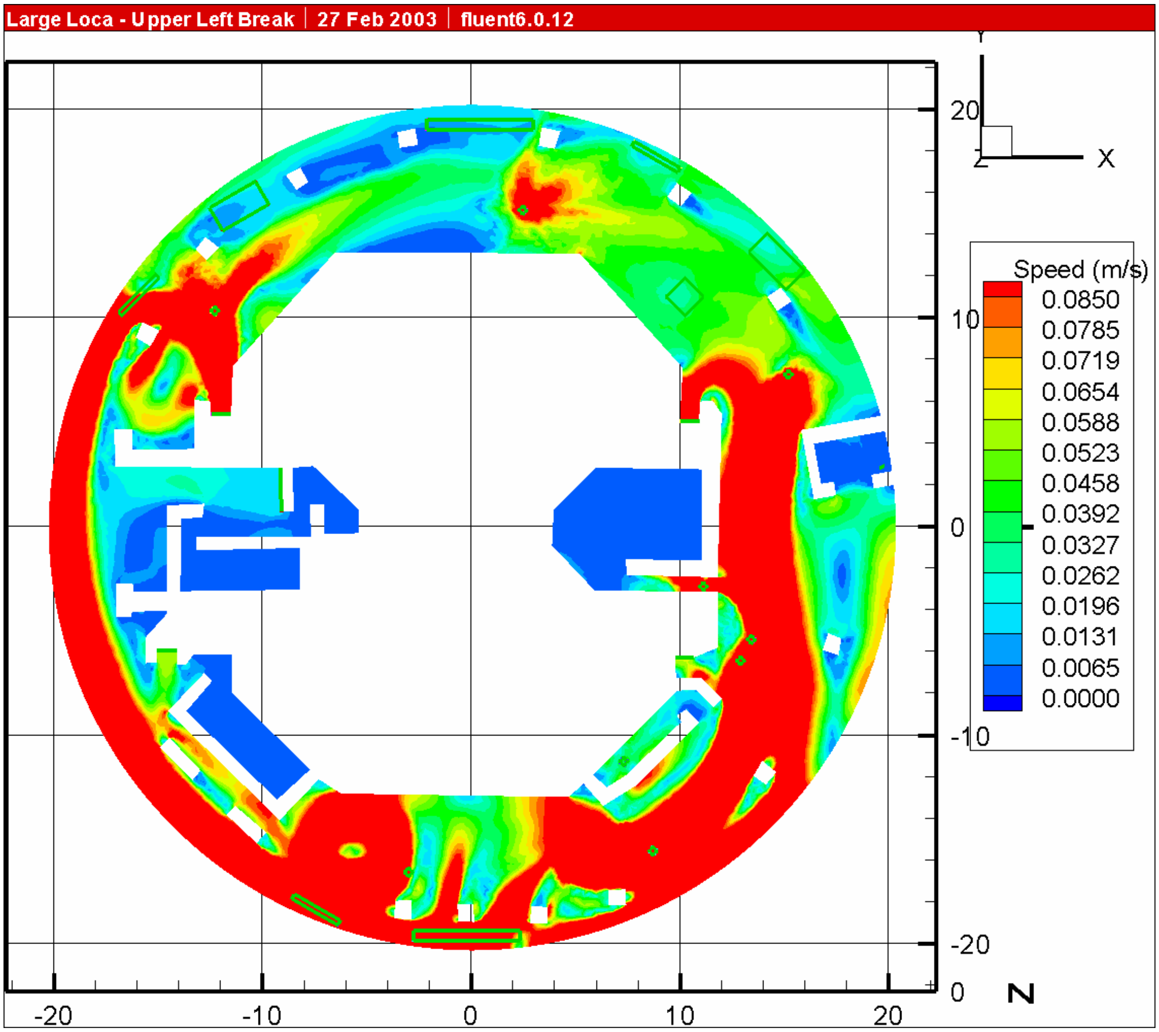

Figure III-34. Large LOCA Break Located in the Upper-Left Quadrant

In Figure III-34, speeds greater than or equal to the RMI threshold (0.085 m/s) are colored red.

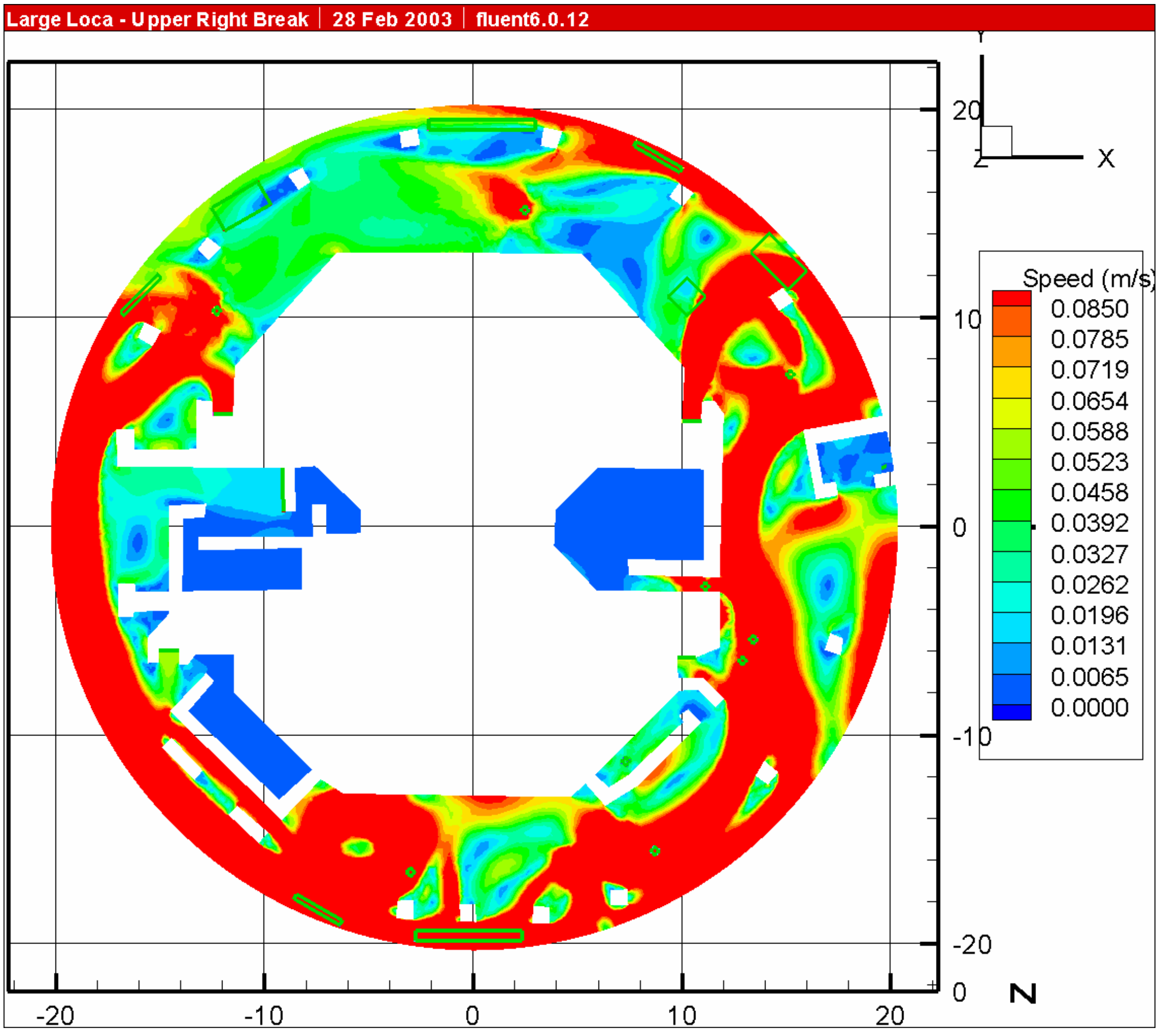

Figure III-35. Large LOCA Break Located in the Upper-Right Quadrant

In Figure III-35, speeds greater than or equal to the RMI threshold (0.085 m/s) are colored red.

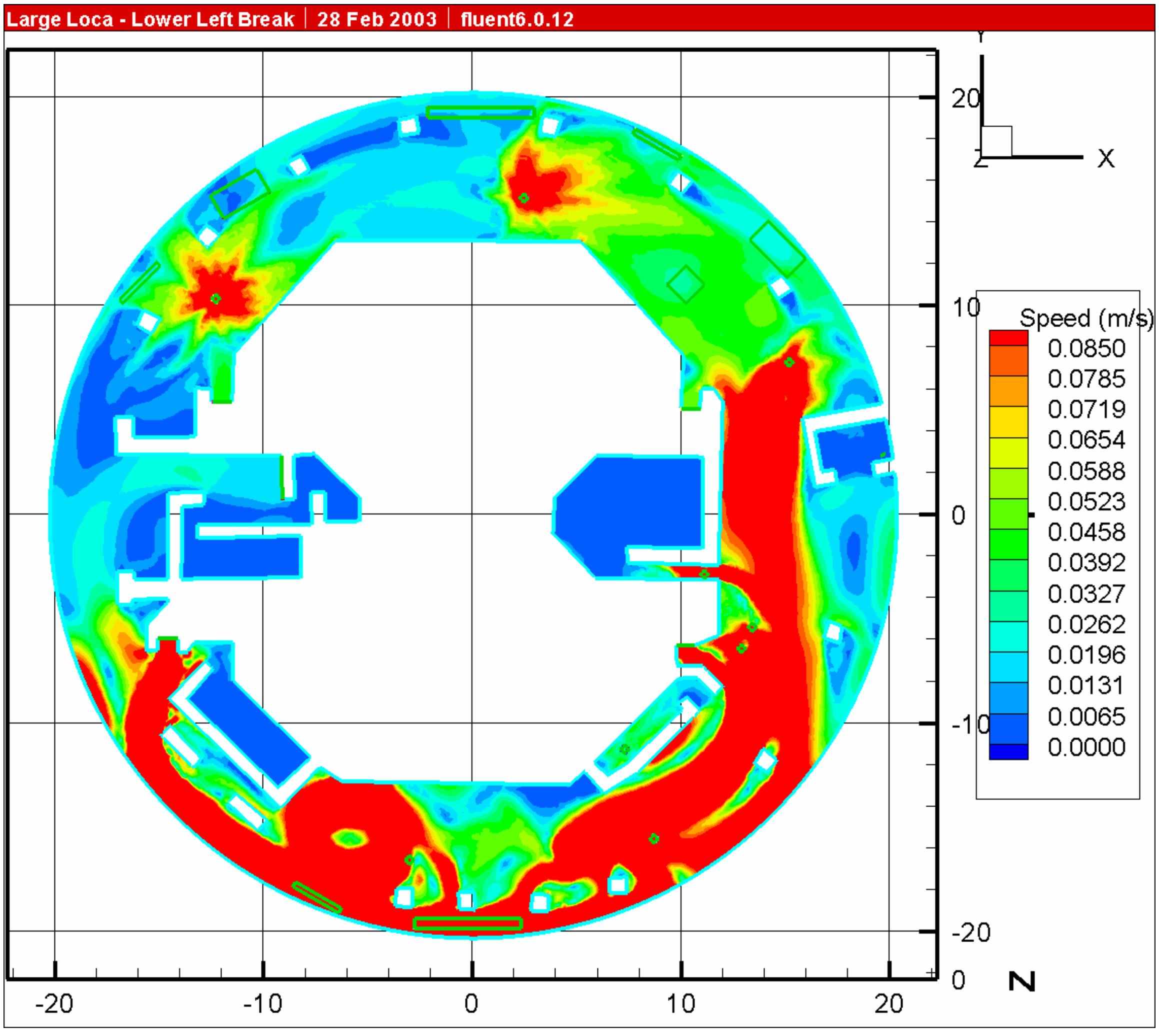

Figure III-36. Large LOCA Break Located in the Lower-Left Quadrant

In Figure III-36, speeds greater than or equal to the RMI threshold (0.085 m/s) are colored red.

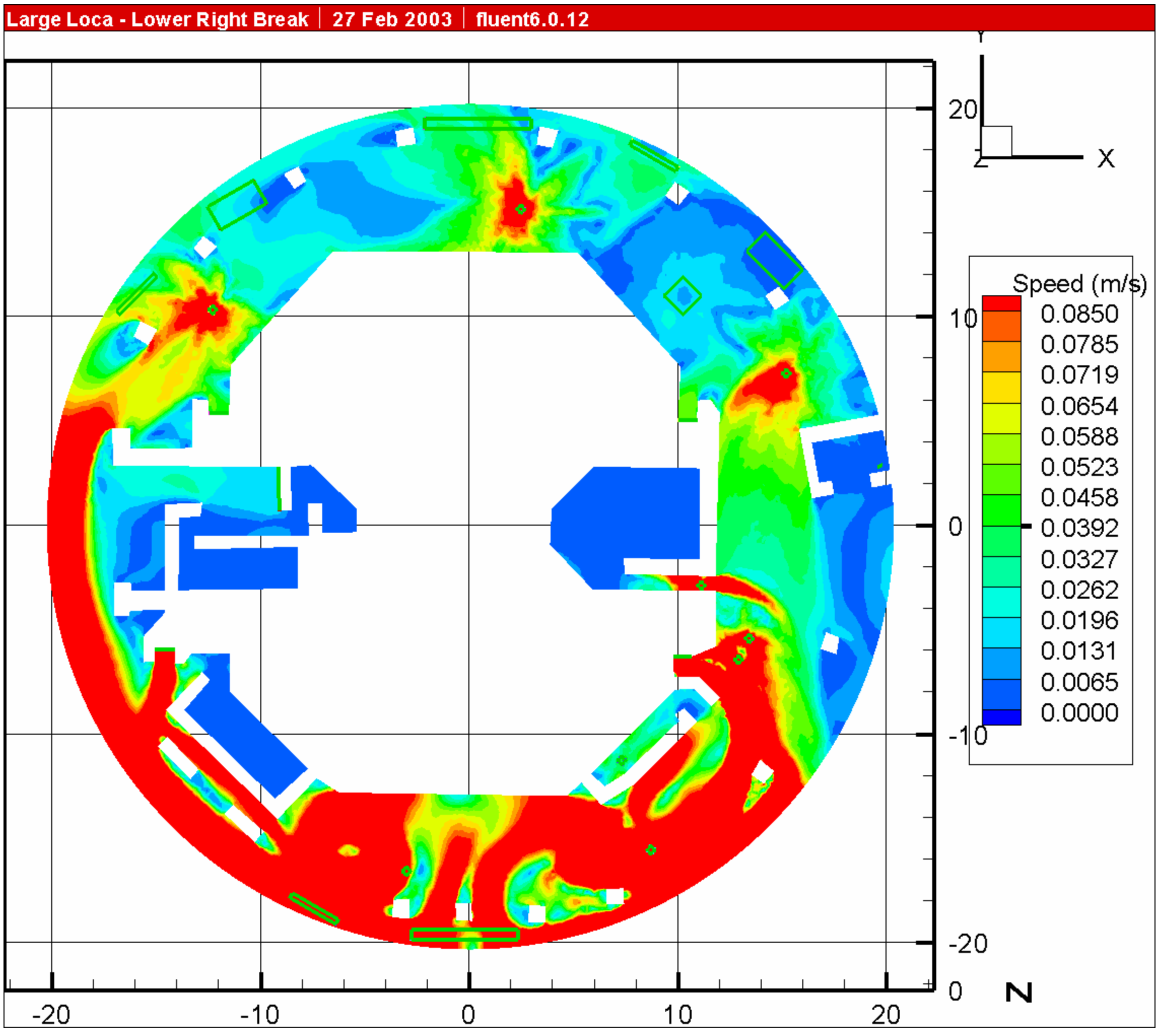

Figure III-37. Large LOCA Break Located in the Lower-Right Quadrant

In Figure III-37, speeds greater than or equal to the RMI threshold (0.085 m/s) are colored red.

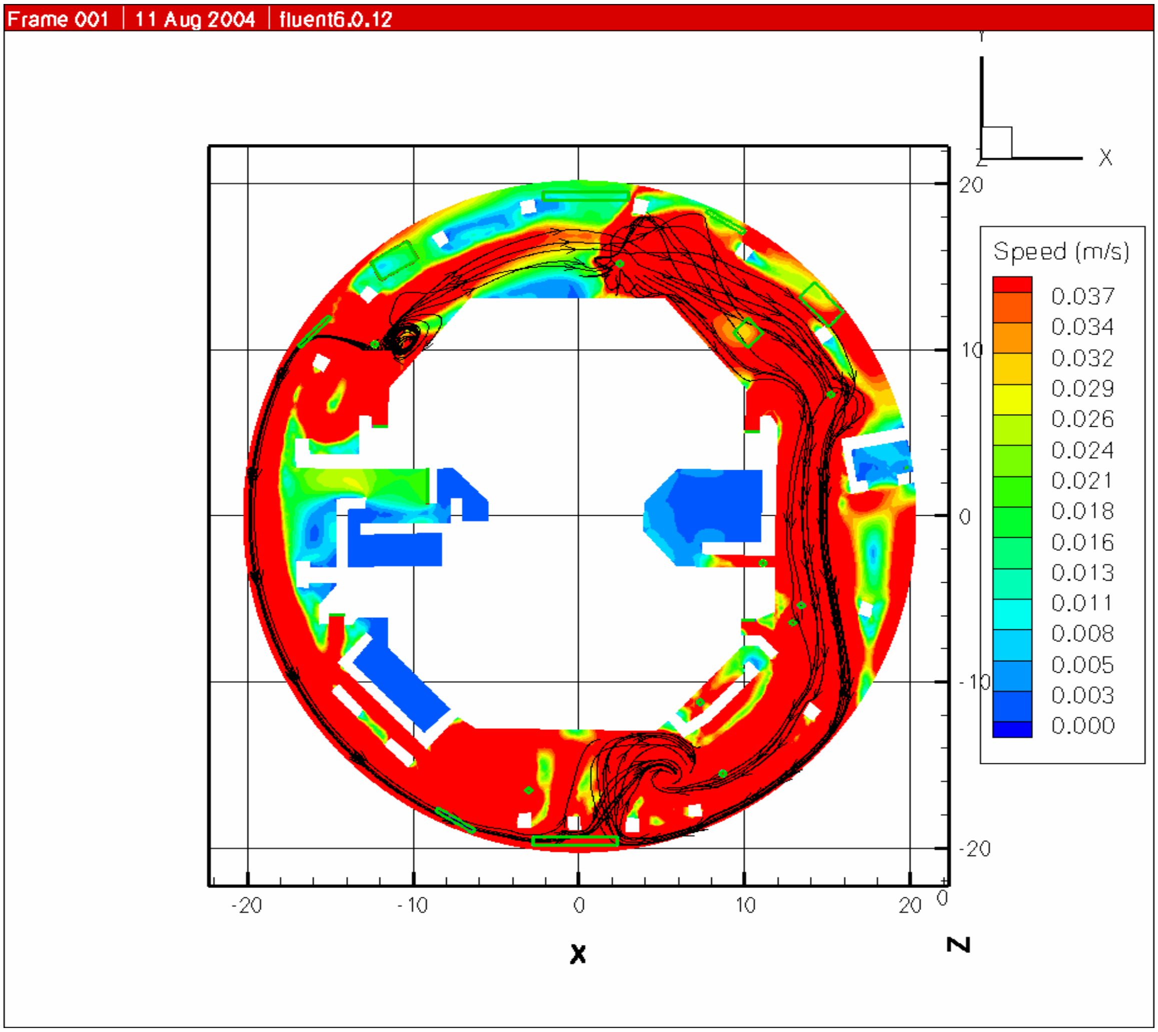

Figure III-38. Streamtraces across Two Splash Locations, Coordinates (-12,10) and (5,15), as Shown in the Figure, for a Large LOCA Break Located in the Upper-Left Quadrant

In Figure III-38, speeds greater than or equal to the fiber threshold (0.037 m/s) are colored red.

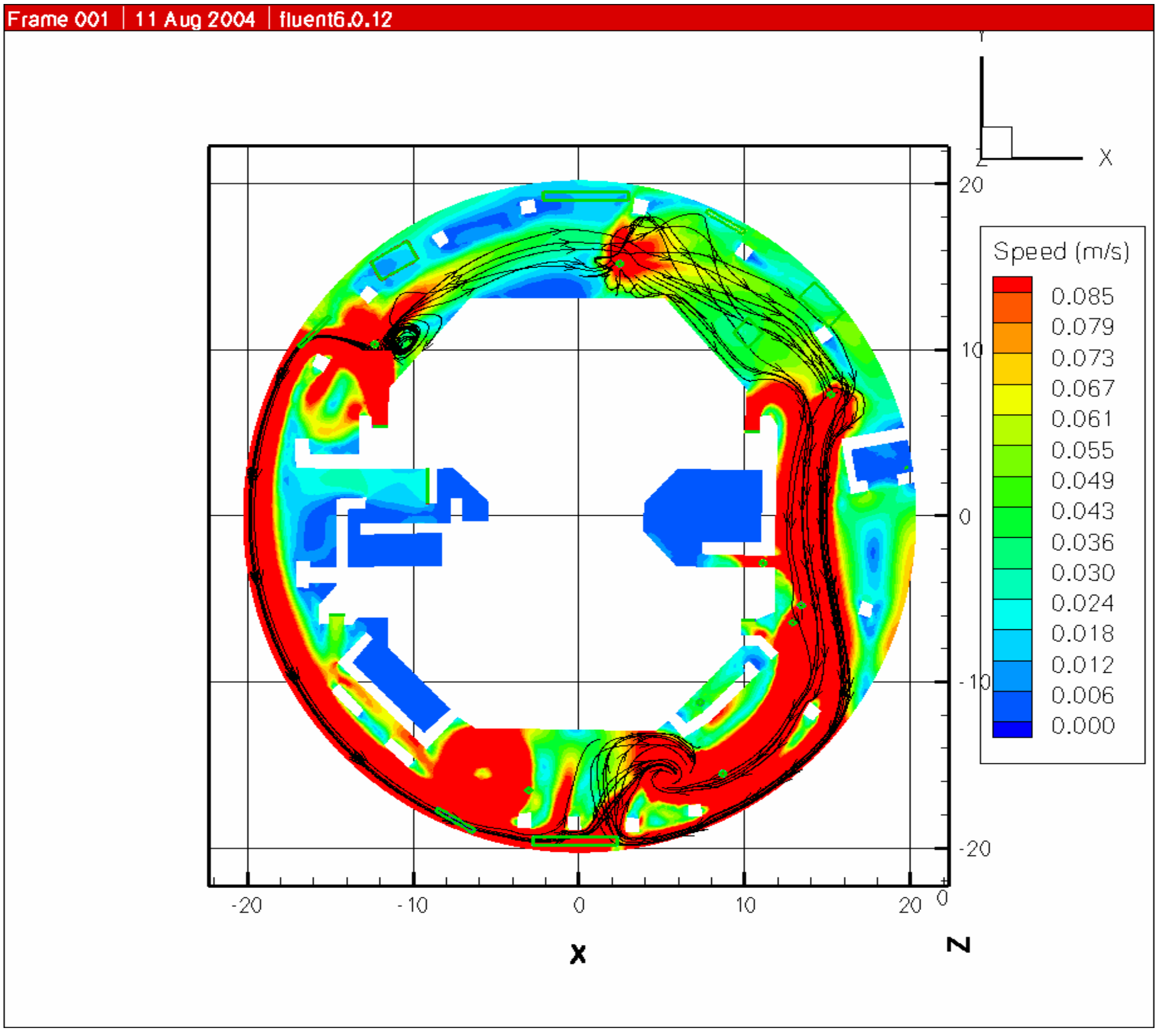

Figure III-39. Streamtraces across Two Splash Locations, Coordinates (-12,10) and (5,15), as Shown in the Figure, for a Large LOCA Break Located in the Upper-Left Quadrant

In Figure III-39, speeds greater than or equal to the RMI threshold (0.085 m/s) are colored red.

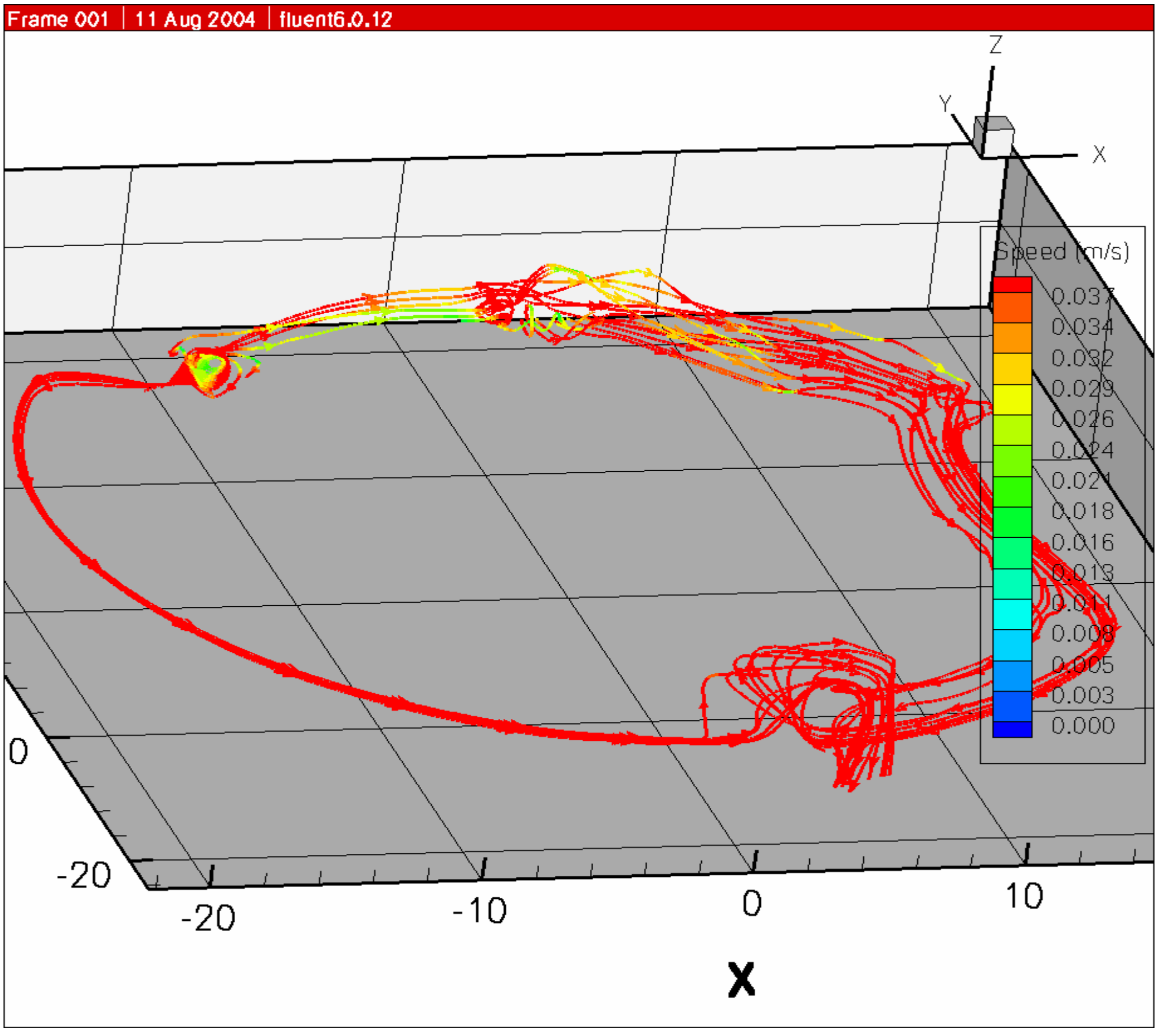

Figure III-40. Oblique View of the Streamtraces, as Shown in Figure III-38 for the Fiber Threshold Velocity

In Figure III-40, the traces are color coded to the local fluid velocity. Speeds greater than or equal to the fiber threshold (0.037 m/s) are colored red.

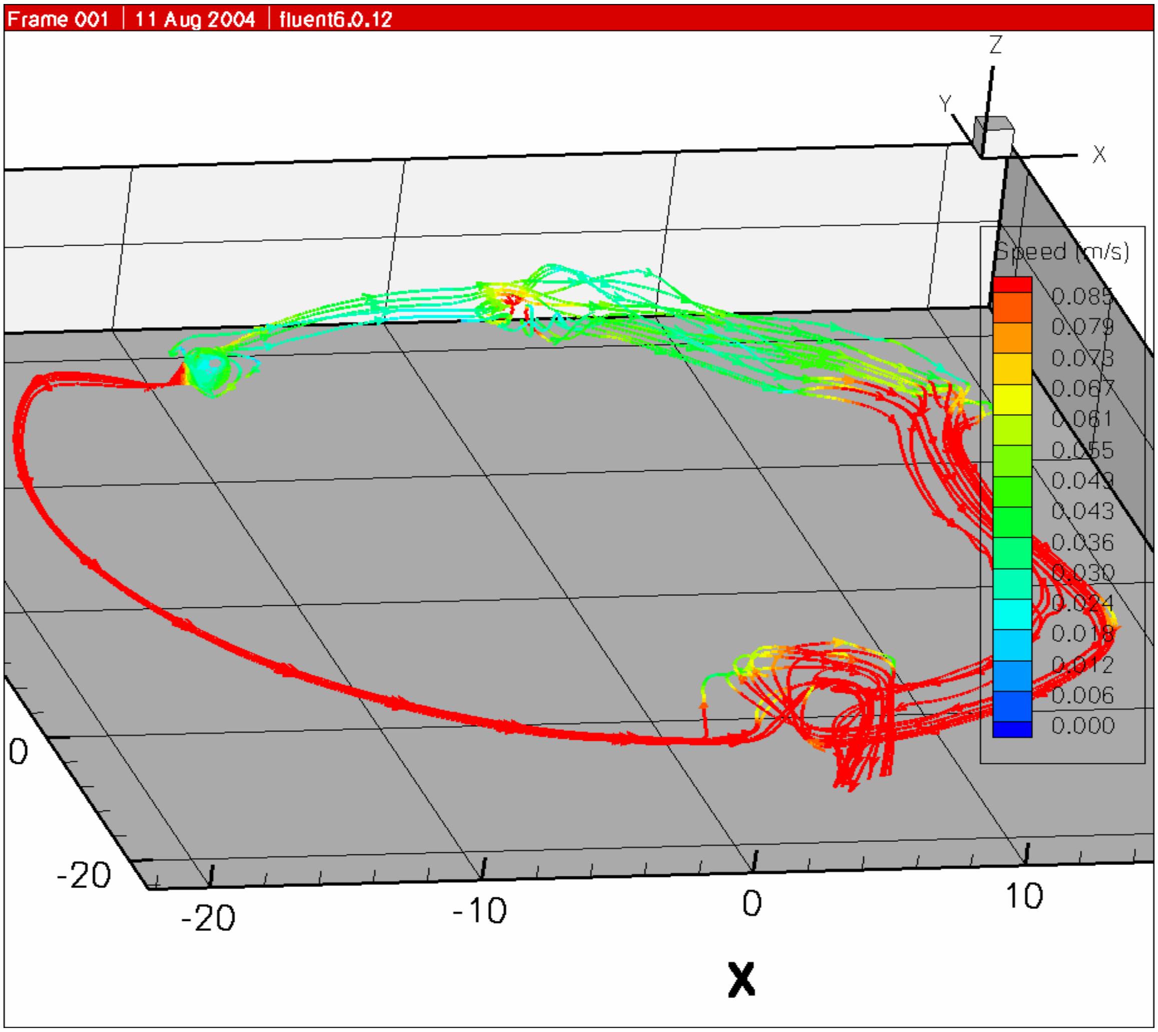

Figure III-41. Oblique View of the Streamtraces Shown in Figure III-39 for the RMI Threshold Velocity

In Figure III-41, the traces are color coded to the local fluid velocity. Speeds greater than or equal to the RMI threshold (0.085 m/s) are colored red.

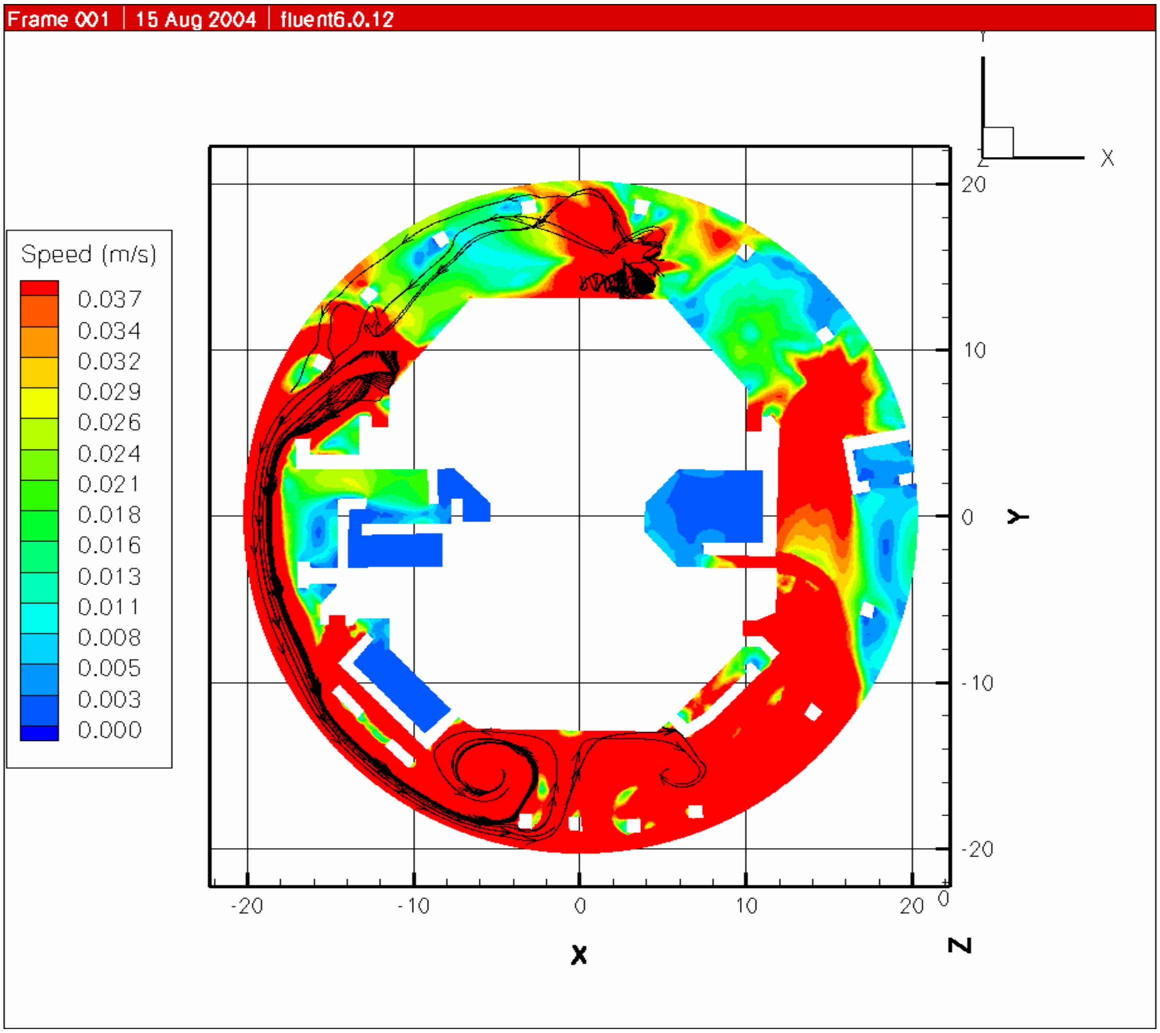

Figure III-42. Streamtraces across Two Splash Locations, Coordinates (-12,10) and (5,15) as Shown in the Figure, for a Large LOCA Break Located in the Lower-Right Quadrant

In Figure III-42, speeds greater than or equal to the fiber threshold (0.037 m/s) are colored red.

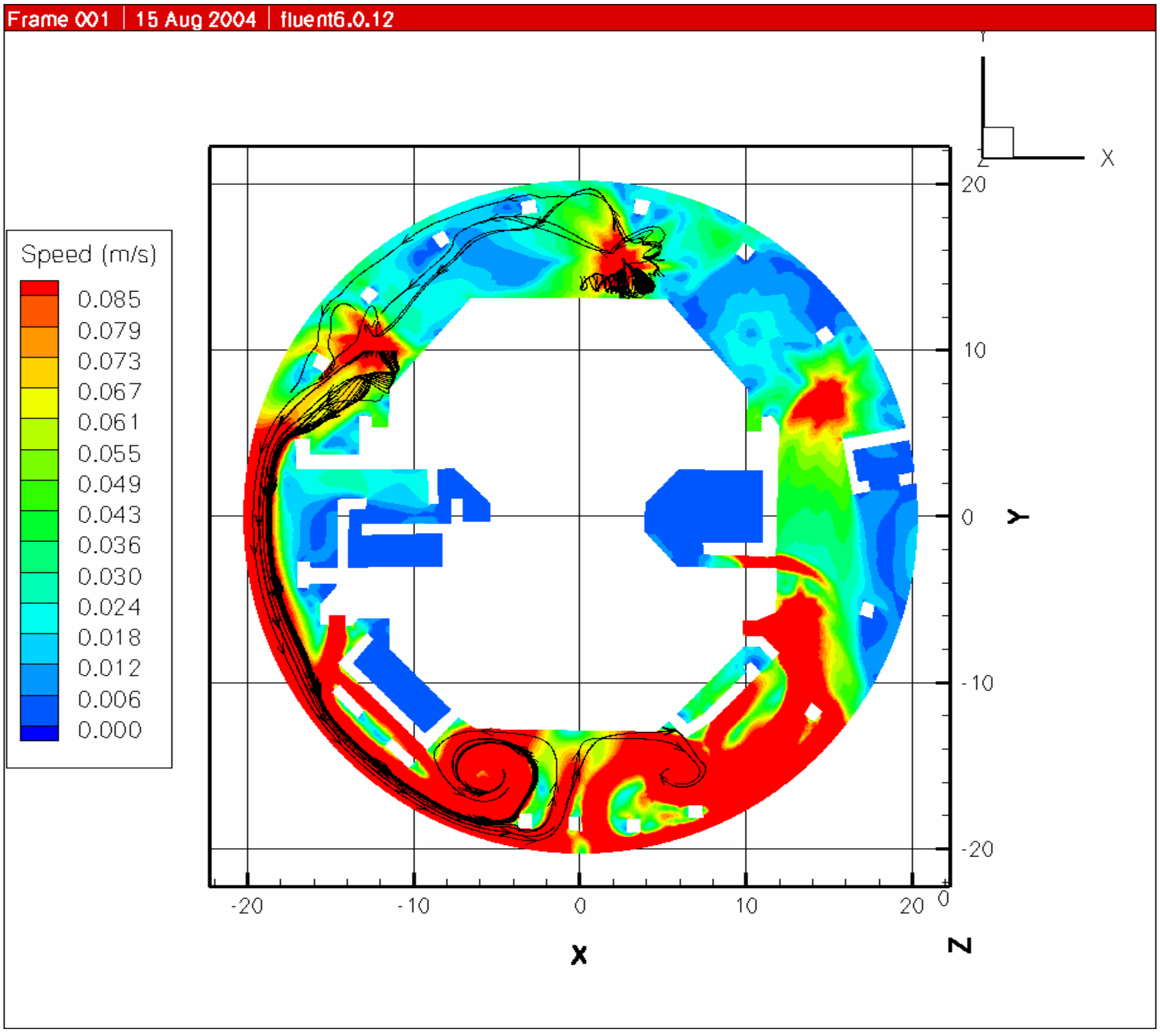

Figure III-43. Streamtraces across Two Splash Locations, Coordinates (-12,10) and (5,15), as Shown in the Figure, for a Large LOCA Break Located in the Lower-Right Quadrant

In Figure III-43, speeds greater than or equal to the RMI threshold (0.085 m/s) are colored red.

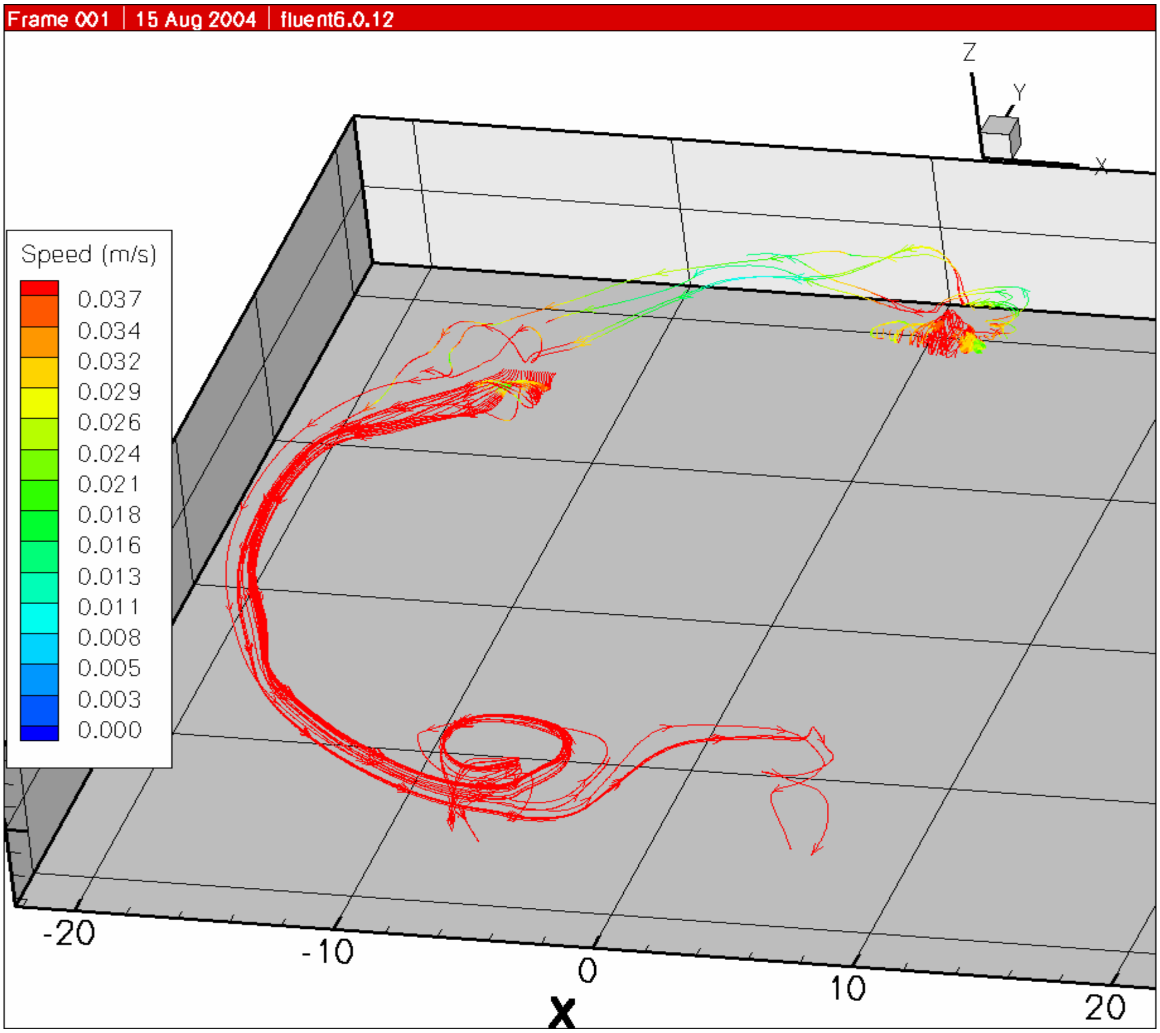

Figure III-44. Oblique View of the Streamtraces Shown in Figure III-42 for the Fiber Threshold Velocity

In Figure III-44, the traces are color coded to the local fluid velocity. Speeds greater than or equal to the fiber threshold (0.037 m/s) are colored red.

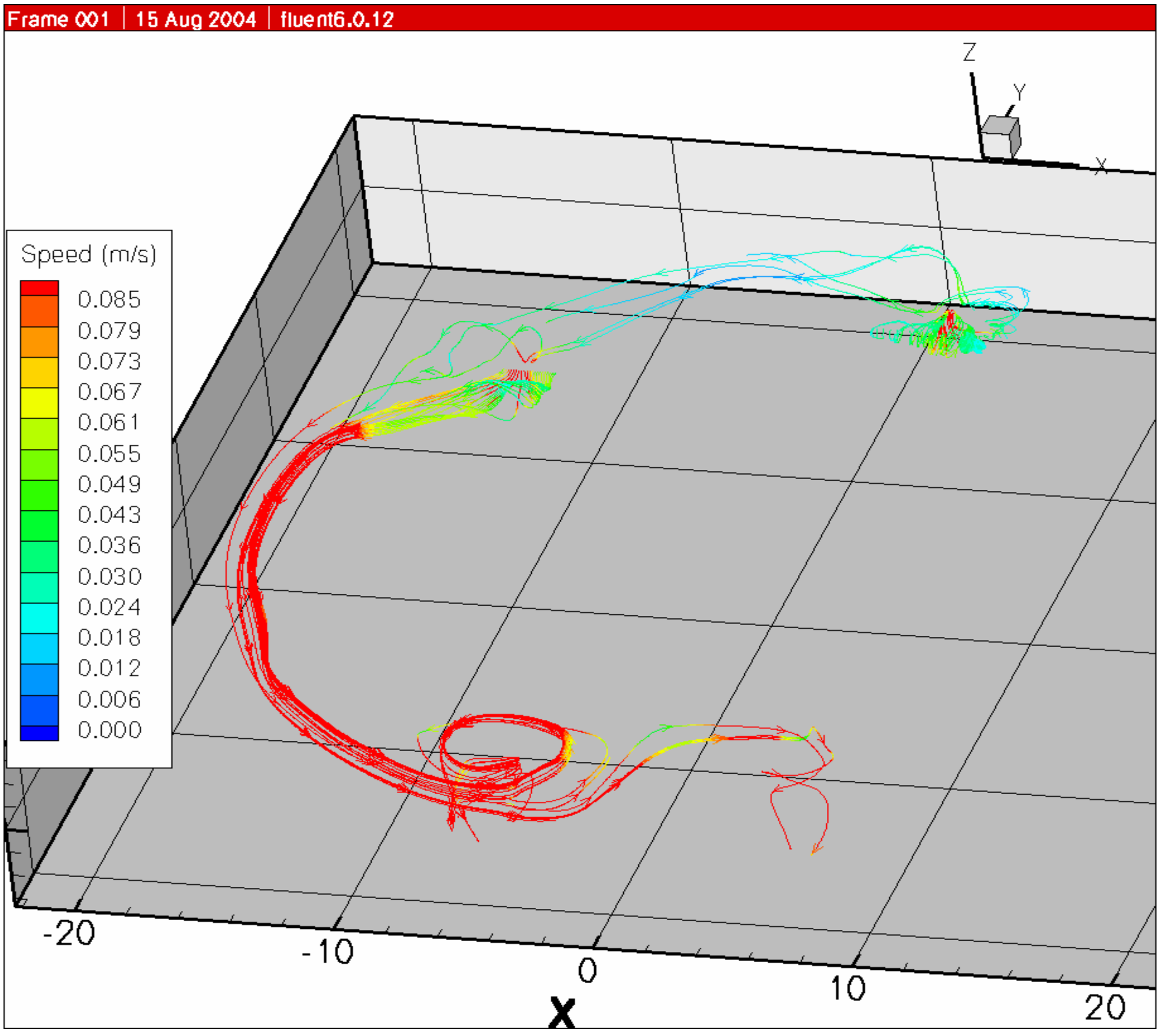

Figure III-45. Oblique View of the Streamtraces Shown in Figure III-43 for the Fiber Threshold Velocity

In Figure III-45, the traces are color coded to the local fluid velocity. Speeds greater than or equal to the RMI threshold (0.085 m/s) are colored red.

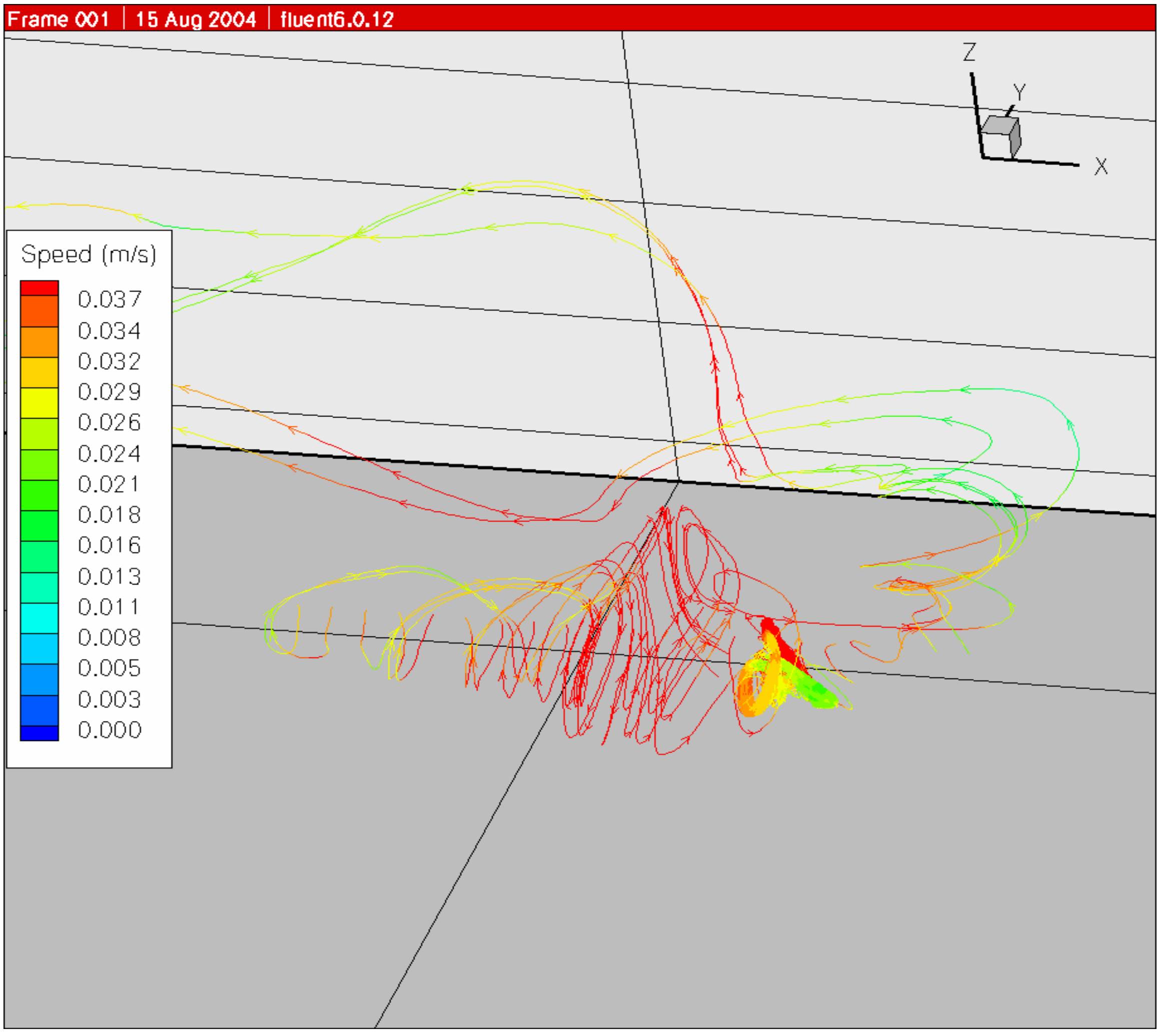

Figure III-46. Large LOCA Lower-Right Break, Zoom in at Upper-Right Splash Location Shown in Figure III-42 and Figure III-43

In Figure III-46, the traces are color coded to the local fluid velocity. Speeds greater than or equal to the fiber threshold (0.037 m/s) are colored red.

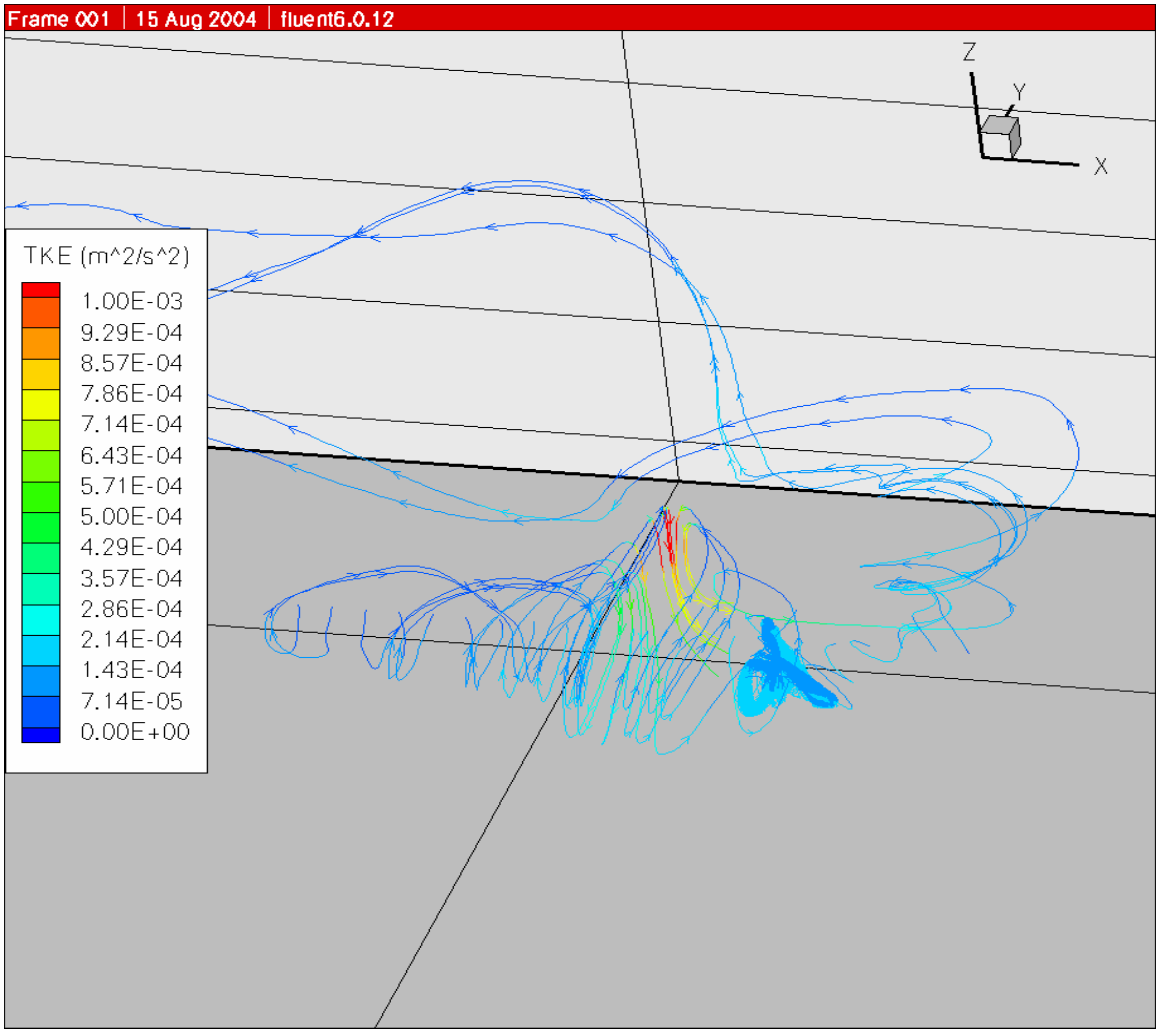

Figure III-47. Same as Figure III-46, with Streamlines Color Coded by TKE

III.3 <u>Sump Pool Debris Transport</u>

The CFD analyses characterized the flow conditions in the sump for a selection of LOCA accident scenarios. These conditions include flow velocity patterns, pool turbulence, and flow streamlines. The pool velocity and turbulence characteristics determine areas of the pool where debris entrapment may occur. The flow streamlines can be used to determine whether debris entering the pool at a discrete location would be likely to pass through one of the potential entrapment locations. The debris transport process was broken down using a logic chart approach to facilitate the individual transport steps—steps that could be determined analytically or experimentally, or simply judged. The subsequent quantification of the chart then provided an estimate of the overall sump pool debris transport.

III.3.1 Debris Transport Logic Chart Methodology

When and where the debris enters the pool is key to the evaluation of sump pool debris transport. The debris enters the pool either when directly deposited onto the sump floor during the blowdown phase or with the subsequent drainage of the containment sprays. To put the timing in perspective, the reactor cavity would likely fill in less than 12 minutes (e.g., a large LOCA break flow rate of 7,400 gpm would fill the reactor cavity volume, estimated by the plant to be less than 12,000 ft^3, in less than 12 minutes neglecting the contribution from the containment sprays), and the sump pool should reach a reasonable steady state in about 30 minutes. The entrance location for blowdown-deposited debris is a debris distribution on the floor that likely favors deposition nearer the location of the break.

Where the debris enters the pool depends on whether the debris is blown onto the break room floor (SG compartment housing the break) or the remainder of the sump floor, which is the lower level annulus floor. Debris transported into the pool via the spray drainage would enter at the primary drainage locations. The debris transport analysis requires a distribution for where the washdown debris enters the sump pool. The spray drainage analysis in Appendix VI provides a distribution for drainage flows entering the sump pool. These analyses assume that the distribution of washdown debris entering the pool mimics that of the spray water distribution for debris deposited outside the break compartment. The blowdown deposition analyses determined substantial debris deposition within the break compartment that would subsequently wash directly to the break compartment floor; this deposition was considered in the debris introduction to the pool. The drainage from the containment sprays entered into the sump pool at many locations, including floor drains, stairwells, an equipment hatch, the containment liner, refueling pool drains, and containment spray trains located at the sump level. The drainage flowed over from upper levels into the annular gap, or spray fell directly into the SG compartments. To simplify the analysis, the multiple drainage entrance locations into the sump pool were grouped into seven groups around the sump annulus. Figure III-48 shows this distribution in an event chart format. One of these charts applies to each size category of each type of insulation. The chart includes the following distributions (moving from left to right):

- the blowdown transport deposition distribution that splits the total debris among debris deposited in the upper level floors, the break compartment floor, and the remainder of the lower level (sump) floor
- the washdown transport distributions of whether the debris deposited in the upper levels would likely transport to the sump pool or remain in the upper levels
- the distribution of the locations where debris entrained in the containment spray drainage would enter the sump pool
- the distributions associated with sump pool formation debris transport
- the distributions associated with pool recirculation debris transport
- the distributions associated with potential debris erosion

Each transport path is assumed to transport debris to one of three destinations, which include (1) accumulation on the sump screens, (2) entrapment within the inactive pools, and (3) entrapment at other locations along the transport pathways. The fraction of the debris predicted to accumulate on the screens is then the transport fraction for the size and type of debris. The overall transport fraction by insulation type is obtained by applying the debris-size distributions to the size-specific transport fractions.

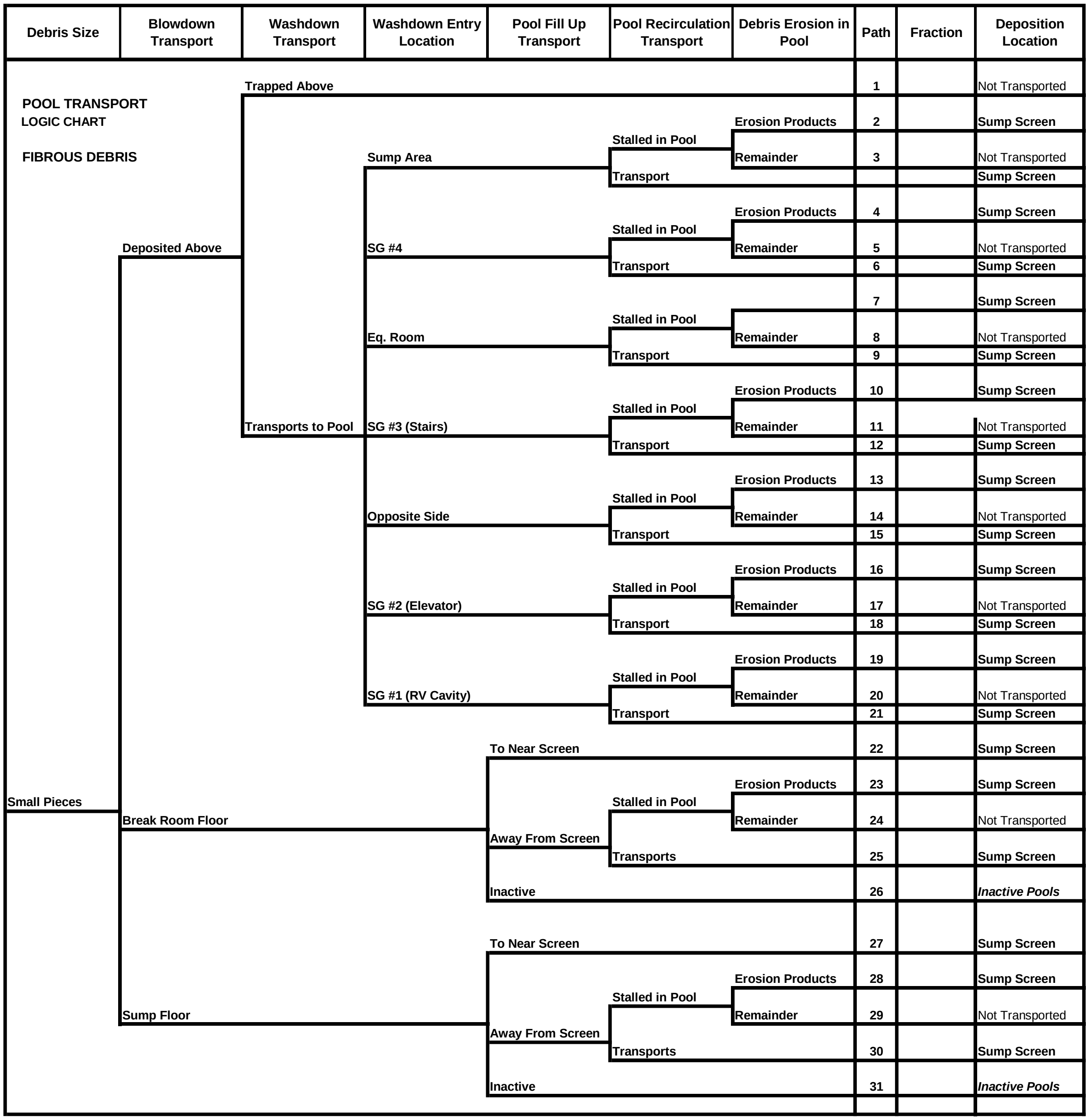

Figure III-48. Sump Pool Debris Transport Chart

III.3.2 Blowdown/Washdown Debris Entry into the Sump Pool

The details of the volunteer-plant blowdown/washdown debris transport analyses documented in Appendix VI provided the distributions for the blowdown and washdown phases of the transport analysis. Table III-2 shows these distributions.

The volunteer-plant fibrous debris was categorized as (1) fines, (2) small pieces, (3) large pieces, and (4) intact pieces. The fines and small pieces represent debris capable of passing through a typical grating during blowdown. The fines are generally the individual fibers that remain suspended in the sump pool, whereas the small-piece fibrous debris typically would readily sink to the pool floor in hot water. Thus, the fines and small pieces must be evaluated differently. The large-piece and intact-piece debris represents debris too large to pass through a grating, which is a process fundamental to blowdown debris transport evaluations. The difference between the large- and intact-piece debris is whether the fibrous insulation continues to be protected by covering material. With large-piece debris, the fibrous insulation is subject to erosion, whereas the intact-piece debris insulation is not. Another distinction is that the covering materials on the intact debris, which include nearly intact blankets, are more likely to snag onto structures, including gratings, during blowdown transport such that the debris is less likely to fall back to a floor or wash off with the sprays. The guidance report (GR) baseline small-fines category corresponds to the combination of the fines and small-piece debris in the volunteer-plant analyses, and the GR large-piece debris corresponds to the large- and intact-piece debris in the volunteer-plant analyses.

Table III-2. Blowdown/Washdown Debris Transport Fractions

Debris Size and Type	Debris Transport Fractions				
	Blowdown Transport			Washdown Transport	
	Deposited in Upper Levels	Deposited on Break Room Floor	Deposited on Sump Floor	Remains Trapped Above	Transports to Sump Pool
Fibrous Debris					
Fines	0.92	0.05	0.03	0.07	0.93
Small Pieces	0.92	0.05	0.03	0.37	0.63
Large Pieces	0.57	0.39	0.04	0.81	0.19
Intact Pieces	0.69	0.30	0.01	0.78	0.22
RMI Debris					
< 2 in.	0.47	0.50	0.03	0.38	0.62
2 to 6 in.	0.35	0.61	0.04	0.69	0.31
> 6 in.	0.22	0.77	0.01	0.68	0.32

The volunteer-plant RMI debris was categorized as (1) debris pieces smaller than 2 in., (2) pieces between 2 and 6 in., and (3) pieces larger than 6 in. The GR RMI size groups were subdivided at 4 in. rather than the 2 and 6 in. used for the volunteer-plant analysis. However, the combination of the volunteer-plant analysis categories less than 6 in. is a reasonable representation of the GR small-fines category, leaving the pieces larger than 6 in. to represent the large-piece debris.

The debris washing down from the upper levels was assumed to enter the sump pool with the same distribution as the spray drainage. However, blowdown debris that was preferentially deposited in the SG compartment where the break occurred (SG1) and its adjacent SG compartment (SG4) would wash directly to the floors of these compartments, regardless of the spray drainage fractions. For the volunteer plant, the spray drainage analysis documented in Appendix VI provided the spray drainage distribution, as shown in Table III-3. Table III-4 and Table III-5 provide the location distributions for debris washing down from the upper levels by debris size category for fibrous and RMI debris, respectively. Because the larger debris was preferentially trapped in SG1 and SG4, these washdown location fractions are larger.

Table III-3. Spray Drainage Distribution into the Sump Pool

No.	Location in Annular Sump	Spray Drainage Water Sources	Drainage Fraction
1	Annulus Section Containing Recirculation Sumps	Floor drains and annular gap sources.	0.14
2	Vicinity of SG4 Access (SG Adjoining Break Room)	SG4 personnel access doorway and liner flow. Includes flow from a 6-in. refueling pool drain.	0.08
3	Vicinity of Interior Equipment Room Access (~90° from Sumps)	Refueling pool water drains into equipment room below refueling pools, then exits doorway into sump and liner flow.	0.06
4	Vicinity of SG3 Access	SG3 personnel access doorway, annular gap sources, and stairwell. Includes flow from a 6-in. refueling pool drain.	0.18
5	Annulus Section Directly Opposite Recirculation Sumps	Floor drains and annular gap sources.	0.09
6	Vicinity of SG2 Access	SG2 personnel access doorway, floor drains, upper level equipment hatch, annular gap sources, and stairwell. Includes flow from a 6-in. refueling pool drain.	0.25
7	Vicinity of SG1 Access (Compartment with Break)	SG1 personnel access doorway, floor drains, and annular gap sources. Includes flow from a 6-in. refueling pool drain.	0.20

Table III-4. Fibrous Debris Entrance Distributions to Sump Pool

No.	Location in Annular Sump	Drainage Fraction	Fines Debris	Small-Piece Debris	Large-Piece Debris	Intact-Piece Debris
1	Sumps	0.14	0.09	0.09	0.01	0.01
2	SG4	0.08	0.17	0.17	0.28	0.22
3	Eq. Room	0.06	0.04	0.04	0	0
4	SG3	0.18	0.12	0.12	0.07	0.07
5	Opposite	0.09	0.06	0.06	0.01	0.01
6	SG2	0.25	0.16	0.16	0.07	0.07
7	SG1	0.20	0.36	0.36	0.56	0.62

Table III-5. RMI Debris Entrance Distributions to Sump Pool

No.	Location in Annular Sump	Drainage Fraction	<2-in. Debris	2- to 6-in. Debris	>6-in. Debris
1	Sumps	0.14	0.06	0.01	0.01
2	SG4	0.08	0.24	0.28	0.22
3	Eq. Room	0.06	0.02	0	0
4	SG3	0.18	0.06	0.07	0.07
5	Opposite	0.09	0.04	0.01	0.01
6	SG2	0.25	0.09	0.07	0.07
7	SG1	0.20	0.49	0.56	0.62

III.3.3 Sump Pool Debris Transport Estimates

The following three phases represent debris transport in the sump pool:

(1) transport of floor-deposited debris during the formation (fillup) of the sump pool

(2) debris transport in an established sump during recirculation mode

(3) long-term erosion of exposed fibrous debris in the sump pool

III.3.3.1 Pool Formation Debris Transport

As observed during the integrated debris transport tests (NUREG/CR-6773, 2002), the primary driver for moving debris during pool formation, especially for the large debris, is the sheeting flow as the initial water from the break spreads across the sump floor. Debris initially deposited on the floor is pushed along with the wave front. Thus, the movement of the debris has significant momentum that can carry the debris past the openings into interior spaces. Once the water depth becomes significant, further transport occurs because of the drag forces of the flow of water, and for larger debris, that transport becomes substantially less dynamic than the sheeting flow transport. Individual fibers will move as suspended debris following the waterflow.

In the volunteer plant, most of the debris initially deposited on the floor of the compartment containing the break (SG compartment 1 in this evaluation) would likely transport from that compartment onto the annular sump floor through either the personnel access door for SG1 or the door for SG4. Because the break is in SG1, considerably more flow would exit the door to SG1 than to SG4. In the scenario evaluated here, the larger portion of the break room flow and therefore the debris (perhaps 75 percent) would flow through the personnel access door into the annulus on the side nearer the access for the reactor cavity (Section III.2.1 discusses the flow distribution assumption). A smaller portion of the debris would exit the SG compartment through the access door into SG compartment 2. In the volunteer plant, nearly all of the essentially inactive pool is the water below the sump floor in the reactor cavity. All other quiescent regions would have sufficient water circulation so that suspended fibers over time would circulate from those regions. When debris exits an SG compartment through a personnel access door because of the initial sheeting flow, the flow splits, with part going toward the recirculation sumps and part going in the opposite direction. In the scenario analyzed, the part going away from the sump screens flowed past the narrow passageway into the room leading to the reactor cavity access hatch. For debris to follow water into this passageway, it must essentially make a 90-degree bend in a short distance. Therefore, the conclusion is that only a small fraction of debris moving with the dynamic wave front, especially larger debris, will make the 90-degree turn into the reactor cavity passageway.

With these concepts as a basis, the pool transport distributions were judged as shown in Table III-6. Starting with the fines, it is assumed that 75 percent of the flow exits the SG1 compartment on the reactor cavity side; then, 60 percent of that flows in the direction of the reactor cavity; then, 50 percent of the flow makes the turn into the reactor cavity passageway. Thus, perhaps 25 percent of the fines initially on the break room floor go into the reactor cavity on initial formation of the pool. Because these fibers are suspended, the remaining pool formation could increase this number to, for example, a conservative 40 percent. Then, the remaining amount is split 50 percent–50 percent toward the recirculation sump and away from the sump. With each fibrous debris category of increasing size, the fraction entering the reactor cavity decreases somewhat, with the even split maintained between the flow toward and the flow away from the screen. With the heavier metallic debris, even the smaller pieces would transport less readily than the fiber pieces.

Of the debris initially deposited on the annular sump floor, a significant fraction could be located such that flow from the break compartment to the reactor cavity would not greatly affect it because the exit from the break compartment is near the entrance to the reactor cavity. However, larger debris deposition would also be more likely near the break compartment door. For lack of a better justification, the same distributions judged for debris initially deposited on the break room floor are assumed for debris initially deposited on the annular sump floor. In any case, only a few percent of the total debris is estimated to be deposited on the annular sump floor because of the relatively small doorway areas as compared with the upward area of the SG compartments.

Table III-6. Pool Formation Debris Transport Distributions

Debris Size and Type	Pool Formation Debris Transport Distributions					
	Floor of Break Room			Floor of Sump Pool		
	Toward Screen	Away from Screen	Into Inactive Pools	Toward Screen	Away from Screen	Into Inactive Pools
Fibrous Debris						
Fines	0.30	0.30	0.40	0.30	0.30	0.40
Small Pieces	0.35	0.35	0.30	0.35	0.35	0.30
Large Pieces	0.40	0.40	0.20	0.40	0.40	0.20
Intact Pieces	0.40	0.40	0.20	0.40	0.40	0.20
RMI Debris						
<2 in.	0.35	0.35	0.30	0.35	0.35	0.30
2 to 6 in.	0.40	0.40	0.20	0.40	0.40	0.20
>6 in.	0.50	0.50	0.00	0.50	0.50	0.00

III.3.3.2 Recirculation Pool Debris Transport

Important aspects of the transport of sump pool debris were observed during the integrated debris transport tests (NUREG/CR-6773, 2002). For low-density fiberglass debris, the fines (e.g., individual fibers) remain suspended and move with the flow of water, whereas larger debris pieces readily saturate with water at the water temperatures typical of LOCA accidents and then sink to the pool floor, where further transport depends on the flow velocity and turbulence near the floor. All RMI debris sinks to the floor of the pool, with the occasional exception of a piece of debris that encapsulates an air pocket, keeping that piece buoyant.

The CFD analyses provide realistic descriptions of the floor-level flow conditions, which Section III.2 describes as contours established so that the velocities higher than the experimental measured threshold are clearly indicated. The velocity contours illustrate the portion of the pool where debris would most likely move readily with the flow. In addition to velocity contours, the streamline plots provide a reasonable connecting pathway whereby a piece of debris would likely travel from its original location in the pool to the recirculation sumps. If a transport pathway passes through a slower portion of the pool, then debris moving along that pathway could stall and not transport to the recirculation sump. Otherwise, the transport is very likely.

The effects of pool turbulence are more difficult to quantify. Test observations have shown the occasional reentrainment of debris once stalled in relatively quiescent water. Water within quiescent regions typically tends to rotate, sending debris into the center of the vortex, where it becomes semi-trapped. However, an occasional pulsation can kick a piece of debris out of the vortex and back into the main stream. Although this behavior cannot be reasonably quantified, transport estimates should be enhanced to consider these effects.

A detailed transport analysis using the CFD predicted flow contours and flow streamlines would subdivide the sump pool floor into relatively fine subdivisions, with each subdivision having a source term for debris depositing onto the pool floor at that location. Then, the transport of the debris from each specific subdivision would be evaluated independently using a streamline generated from that subdivision to the recirculation sumps to illustrate where that debris would likely reside after movement ceases. Quantification of all the subdivision transport results would provide an overall sump pool transport fraction for each debris category. The transport results should then be adjusted to account for pool turbulence effects on debris (i.e., the threshold transport tumbling velocities reported in NUREG/CR-6772 were measured in very uniform and turbulence-dampened flows, but turbulence is capable of moving debris where bulk flow will not). One method of accounting for turbulence effects would be to decrease the threshold velocities for transport.

This analysis simplified the preceding detailed model description to include only seven subdivisions for the sump floor. Even then, the available CFD streamlines did not form a complete set. Thus, the individual pool transport fractions used to populate the transport charts were basically engineering judgments based on the velocity profiles. Table III-7 provides the individual transport estimates. Figure III-33 and Figure III-37 show the CFD flow velocity contour maps used to make these judgments for fibrous and RMI debris, respectively. Figure III-42 and Figure III-43 show a sampling of corresponding flow streamline plots for fibrous and RMI debris, respectively. The transport fractions range from 100-percent transport for the suspended fibers and debris located nearer the recirculation sumps to 0-percent transport for the largest debris located on the opposite side of the containment.

Table III-7. Recirculation Pool (Steady-State) Debris Transport Fractions

Location Where Debris Enters Sump Pool	Fraction of Debris Transported to Sump Screen						
	Fibrous Debris				RMI Debris		
	Fines	Small Pieces	Large Pieces	Intact Pieces	<2 in.	2 to 6 in.	>6 in.
Debris Entering Annular Sump Pool by Containment Spray Drainage (Debris Assumed to Enter Established Sump Pool)							
Annulus Section Containing Recirculation Sumps	1	1	1	1	1	1	1
Vicinity of SG4 Access (SG Adjoining Break Room)	1	1	1	1	1	1	1
Vicinity of Interior Equipment Room Access (~90° from Sumps)	1	1	1	1	1	1	1
Vicinity of SG3 Access (Includes Inter-Level Stairwell)	1	0.5	0.4	0.3	0.3	0.2	0.1
Annulus Section Directly Opposite Recirculation Sumps	1	0.2	0.1	0	0.1	0	0
Vicinity of SG2 Access (Includes Inter-Level Stairwell and Hatch)	1	0.5	0.4	0.3	0.3	0.2	0.1
Vicinity of SG1 Access (Compartment with Break, Includes Multiple Floor Drains)	1	0.7	0.6	0.5	0.5	0.4	0.3
Debris Directly Blowdown Deposited onto Sump Floor but Subsequently Relocated Away from Recirculation Sumps during Pool Formation (Section III.3.3.1)							
Initially on Break Room Floor, Relocated Away from Recirculation Sumps	1	0.3	0.2	0.1	0.2	0.1	0
Initially Spread Around Annular Sump Floor, Relocated Away from Recirculation Sumps	1	0.3	0.2	0.1	0.2	0.1	0

III.3.3.3 Sump Pool Debris Erosion

The only source of data for the erosion of fibrous debris in a sump pool was the integrated debris transport tests documented in NUREG/CR-6773. This test program included four longer term tests (3- to 5-hour durations) where debris accumulation on the simulated sump screen was collected every 30 minutes.

The three sources of fibrous debris contributing to this accumulation are (1) small-piece debris tumbling or sliding along the floor, (2) suspended fibers initially introduced into the tank, and (3) fibers that had eroded from the small-piece debris residing on the floor of the tank. Late in these tests, most of the small-piece debris had already either been transported to the screen or had come to relative rest in some quiescent location on the tank floor; therefore, the contribution of the small-piece debris should have been minimal near the end of the tests. Also late in the tests, water recirculation should have substantially reduced the initially suspended fibers so that continued accumulation would fall off quite noticeably. Sufficient time had elapsed in each test for the water in the tank to be replaced (tank water volume divided by the simulated break flow) from 19 to 46 times during the course of the test. Because the continued accumulation tended to hold at a somewhat sustainable rate, it is likely that continued erosion was supporting the continued debris accumulation.

Table III-8 shows the end of test debris accumulation rates for these longer term tests. Although these tests ran for several hours, as indicated in the table, the tests were of short duration compared with LOCA long-term recirculation times. One of the four tests was conducted with a shallower pool of 9-in. depth compared with the usual depth of 16 in The accumulation was about eight times more rapid for the shallow pool test than for the deeper tests. In addition, during the shallow pool test, the water recirculation in terms of water replacements (46) was significantly more frequent for the 9-in. test than for the 16-in. tests; thus, the initial suspended debris would have been more readily filtered from the tank. Therefore, most of the longer term debris accumulation should have resulted from the continued erosion of fibrous debris in the tank. Further, the erosion rate was greater in the shallow depth pool, most likely because of the greater turbulence in the shallow pool relative to the deeper pools.

Table III-8. Late-Term Debris Accumulation in Integrated Debris Transport Tests

Test ID	Pool Depth (in.)	Test Duration (Hours)	Accumulation Rate near the End of the Test (Percent of Debris in Tank/hr)	Approximate Number of Water Replacements During the Test
LT1	16	4	0.4	26
LT2	9	4	2	46
LT3	16	3	0.3	19
LT4	16	5	0.3	32

In conclusion, the only applicable test data for long-term debris erosion in a sump pool strongly indicate a sustainable rate of erosion that is affected by the relative turbulence in the pool. The small-piece debris residing on the floor of the pool, late term, was generally found in quiescent locations, not necessarily directly under the simulated break flow. The turbulence associated with the spray drainage was not simulated. Because the 16-in. depth more closely resembles the fully established volunteer-plant pool, this analysis adopts the erosion rate of 0.3 percent of the current tank debris/hour.

In the debris transport charts, the overall fraction of debris on the sump floor that erodes into fines is required. Using the long-term recirculation mission time of 30 days, analysis indicates that nearly 90 percent of the initial debris mass would become eroded if this erosion rate remained constant throughout the 30 days. This calculation took into account the steadily decreasing mass of debris in the pool using the following equation:

$$f_{eroded} = 1 - (1 - rate)^{\substack{Number \\ ofHours}} .$$

Therefore, in the debris transport charts, 90 percent of the small- and large-piece debris predicted to reside on the sump floor is assumed to erode into suspended fibers unless the debris is still enclosed in a protective cover.

This calculation has the following substantial sources of uncertainty:

- The integral debris transport tests lasted 3 to 5 hours. Therefore, the question remains whether the erosion rate tapers off with time. In addition, it is not certain that all of the end-of-test debris accumulation was the result of erosion products.
- The test results include the usual variances in test data, such as flow and depth control and debris collection.
- Although the test series was designed to approximate the flow and turbulence characteristics of the volunteer-plant sump pool, the tank characteristics may have been significantly different than those at the plant. The difference in the erosion rates between the 9-in. and 16-in. pool depths in the integrated tests clearly illustrates the effect of pool turbulence on fibrous debris erosion.
- The geometry of the volunteer-plant sump pool is larger and more complex than that of the test tank used in the integrated tests.
- The long-term tests did not study large-piece debris.

The 90-percent debris eroded value is used for both the small- and large-piece debris, despite the uncertainties. With such limited data, the use of the 90-percent value is necessary to ensure conservatism in the overall transport results. This number can possibly be reduced, once better erosion data are available.

III.3.4 Quantification Results

The blowdown/washdown/pool transport estimates presented in Sections III.3.2 and III.3.3 were entered into debris transport charts (shown generically in Figure III-48) and quantified to obtain overall transport fractions. A separate chart was created for each size category and for each type of debris. Figure III-49, Figure III-50, Figure III-51, and Figure III-52 illustrate the transport processes for the fibrous debris categories of fines, small pieces, large pieces, and intact pieces, respectively. Figure III-53, Figure III-54, and Figure III-55 illustrate the transport processes for RMI debris categories of pieces less than 2 in., 2 to 6 in., and greater than 6 in., respectively.

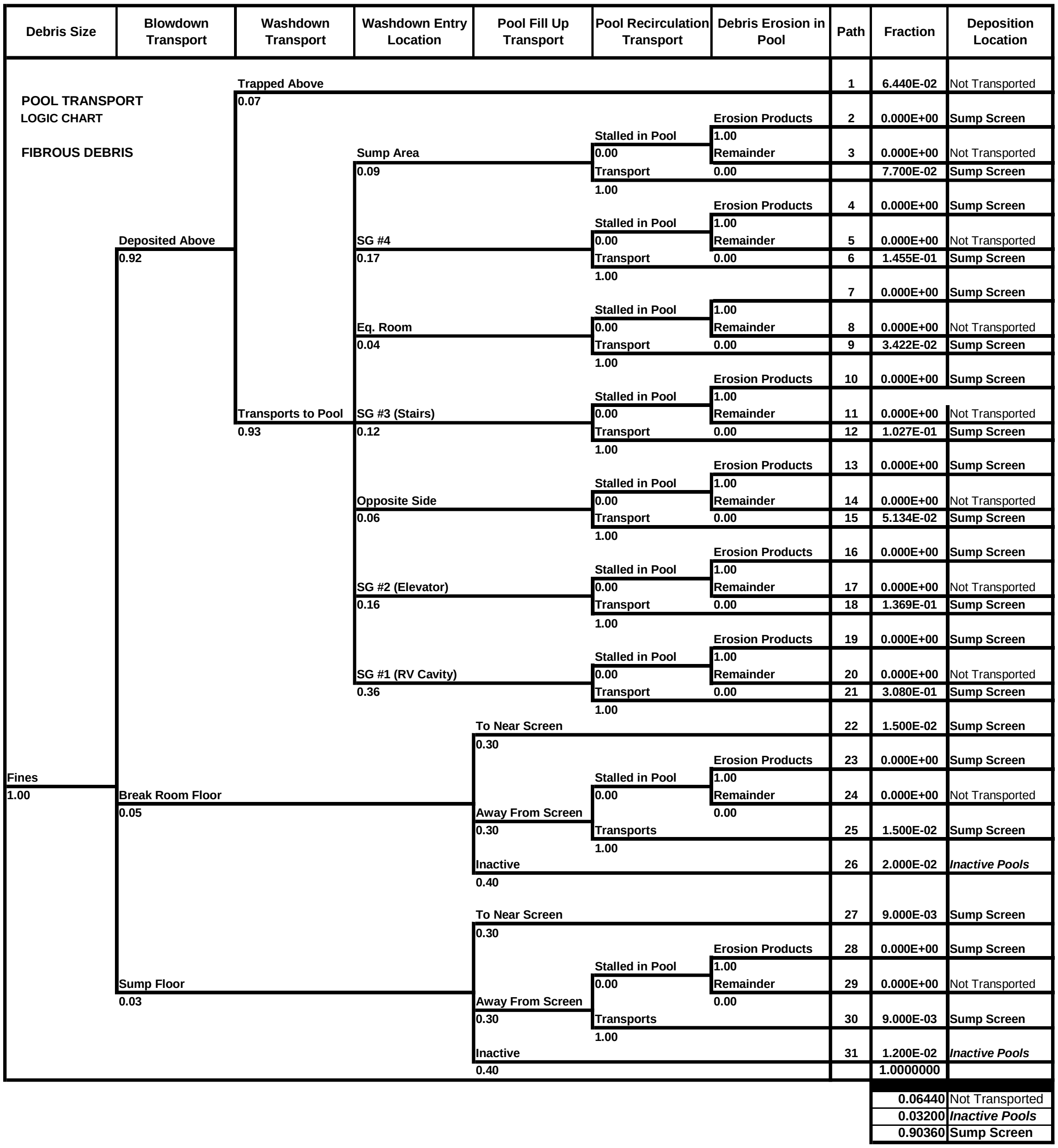

Figure III-49. Sump Pool Debris Transport Chart for Fine Fibrous Debris

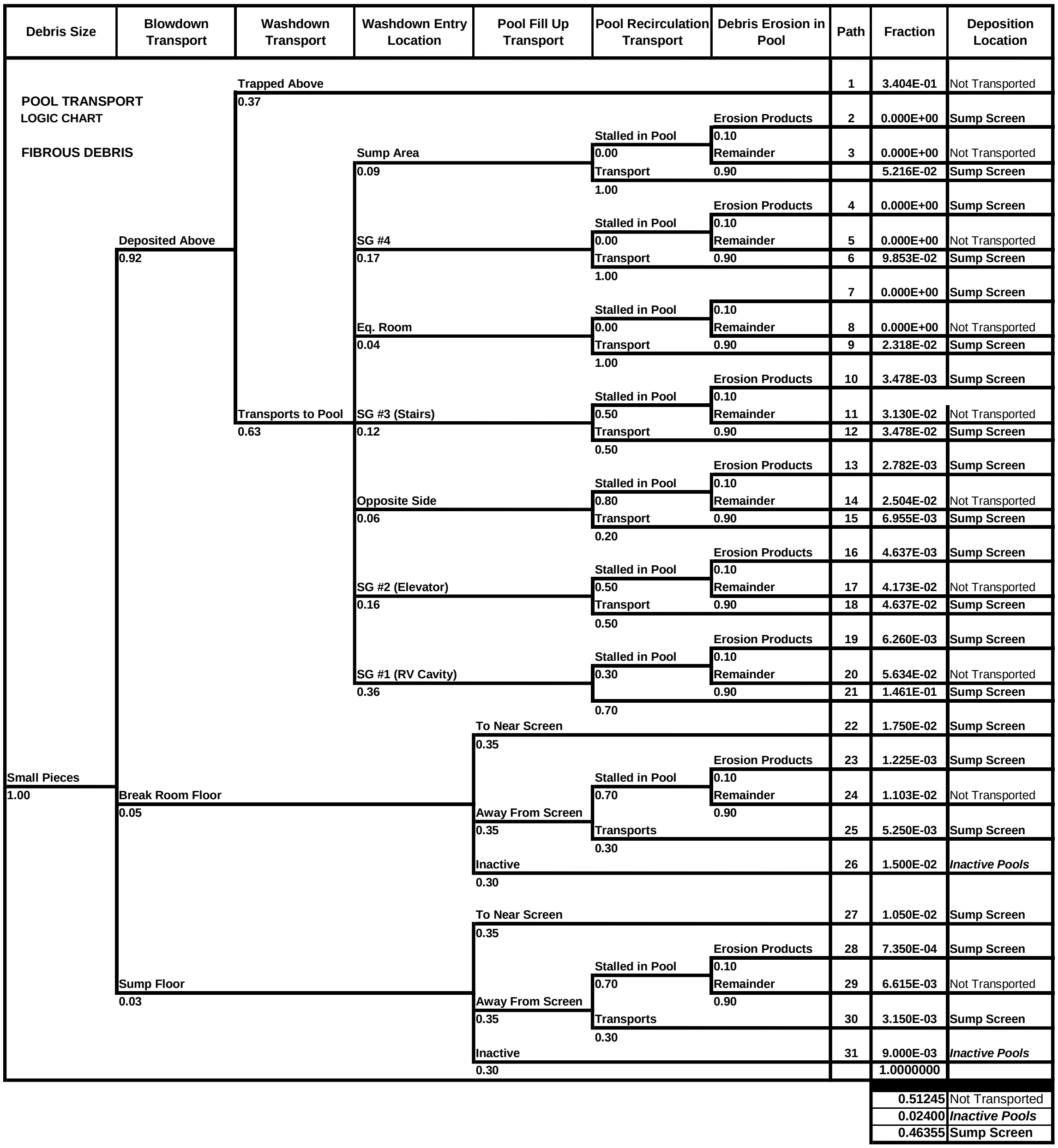

Figure III-50. Sump Pool Debris Transport Chart for Small-Piece Fibrous Debris

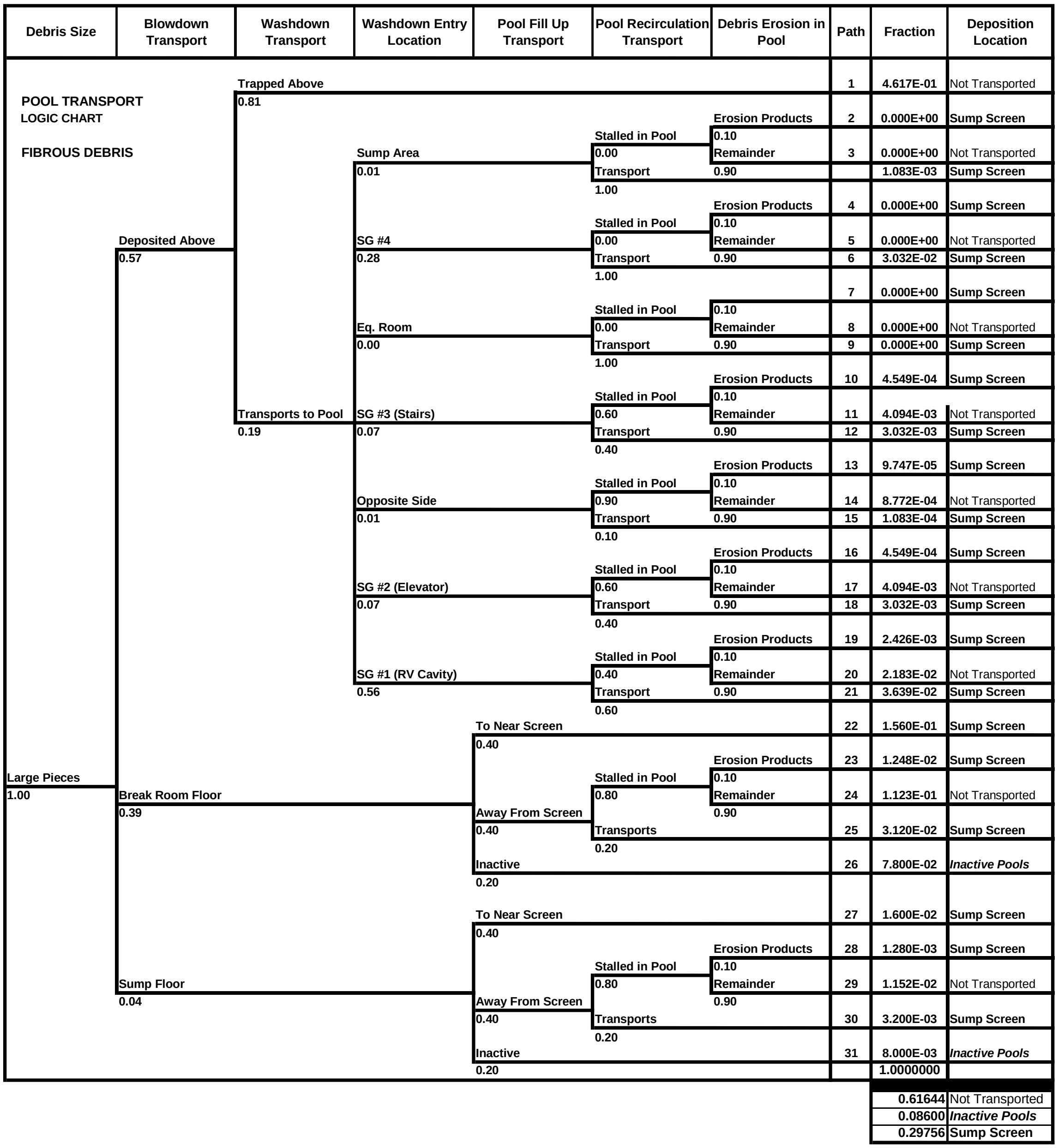

Figure III-51. Sump-Pool-Debris Transport Chart for Large-Piece Fibrous Debris

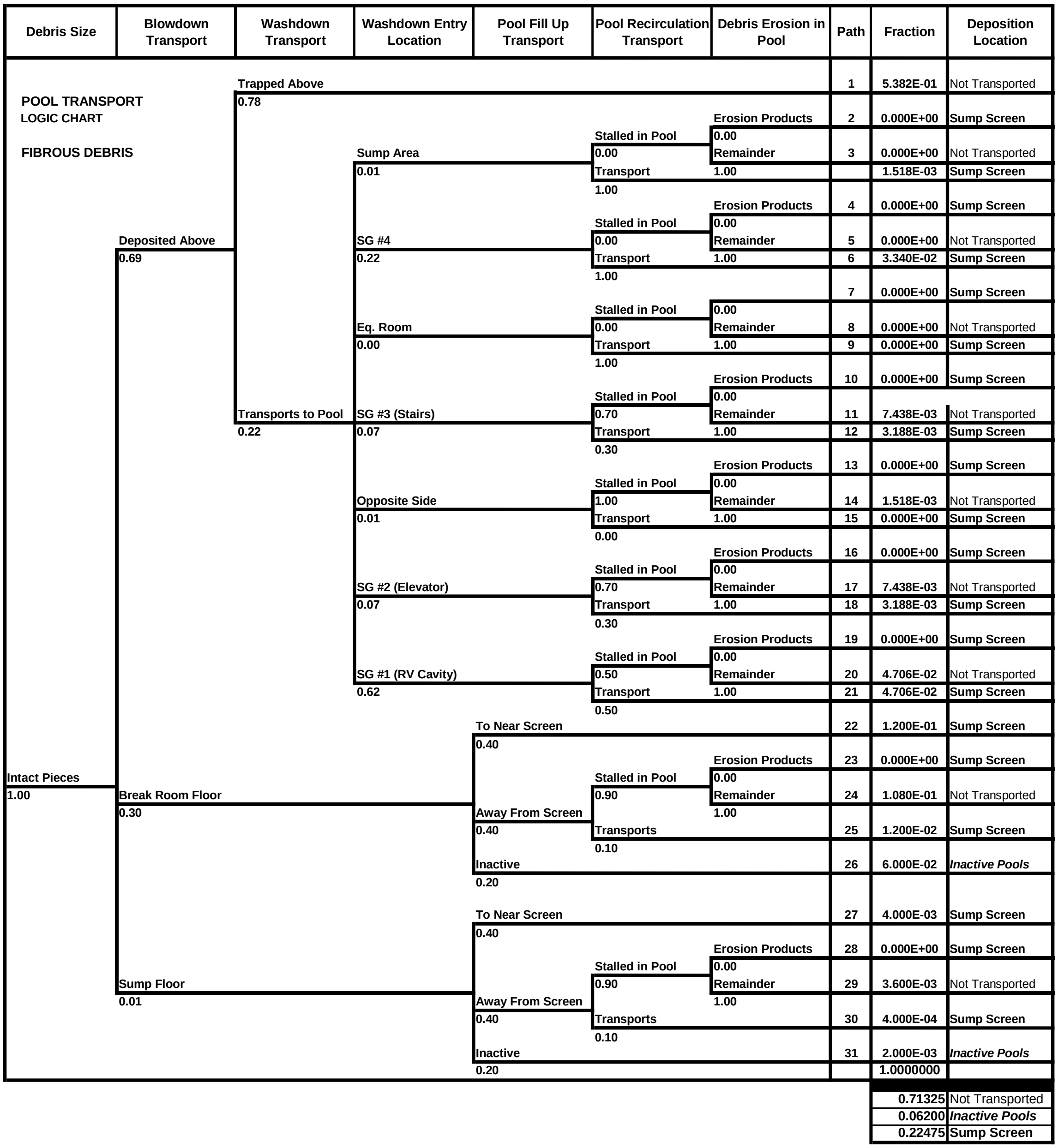

Figure III-52. Sump-Pool-Debris Transport Chart for Intact-Piece Fibrous Debris

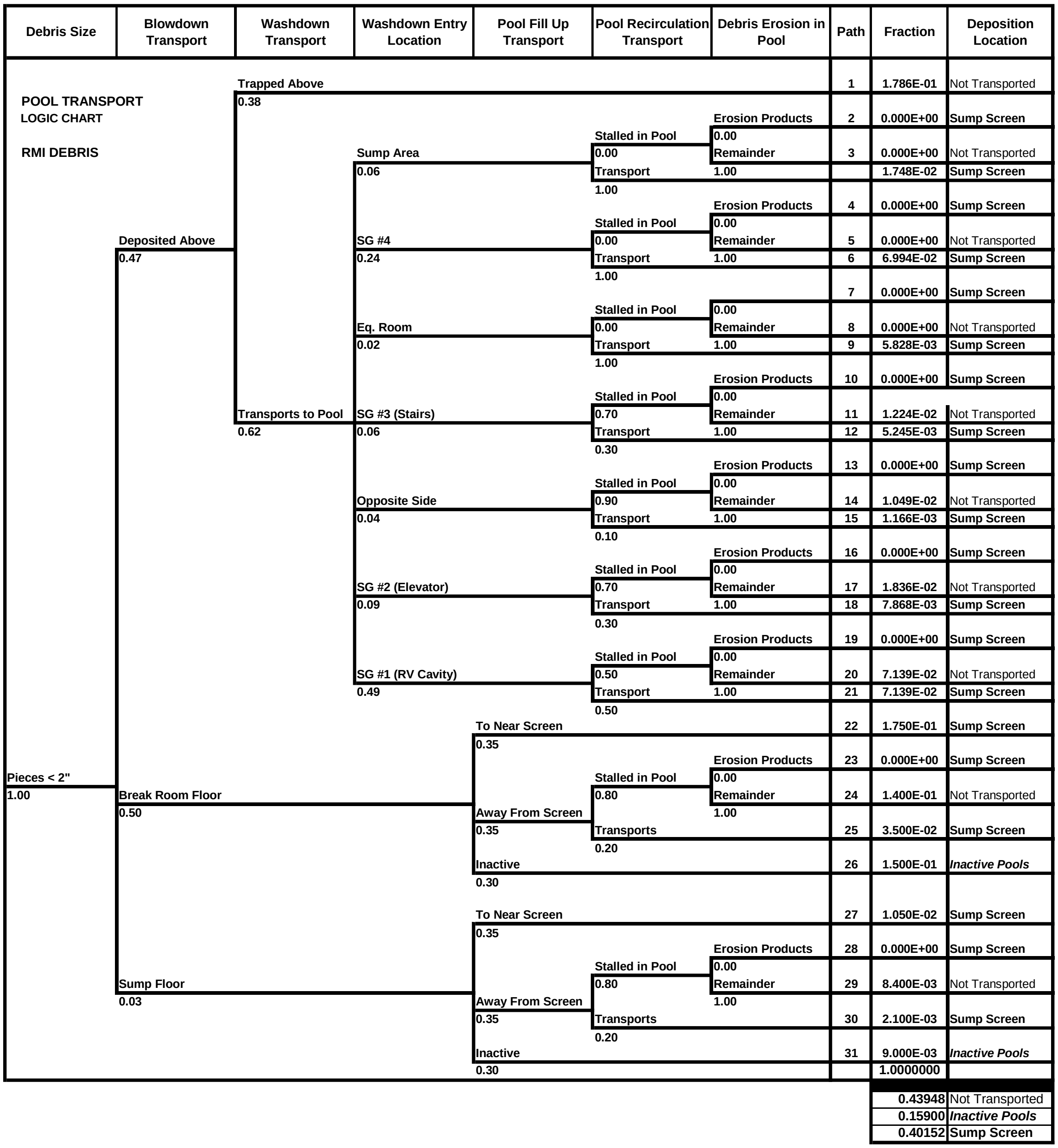

Figure III-53. Sump-Pool-Debris Transport Chart for <2-in. RMI Debris

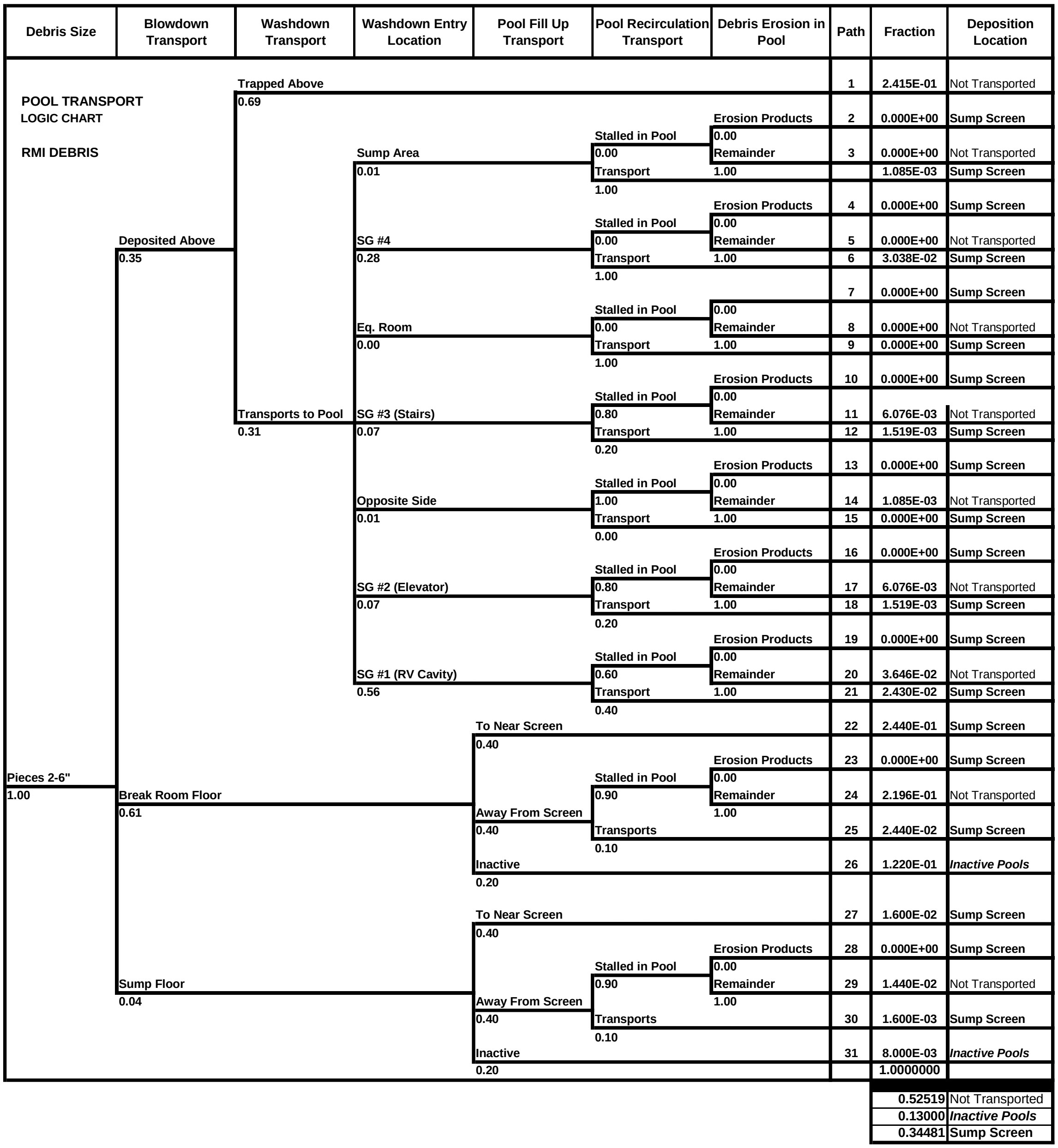

Figure III-54. Sump-Pool-Debris Transport Chart for 2- to 6-in. RMI Debris

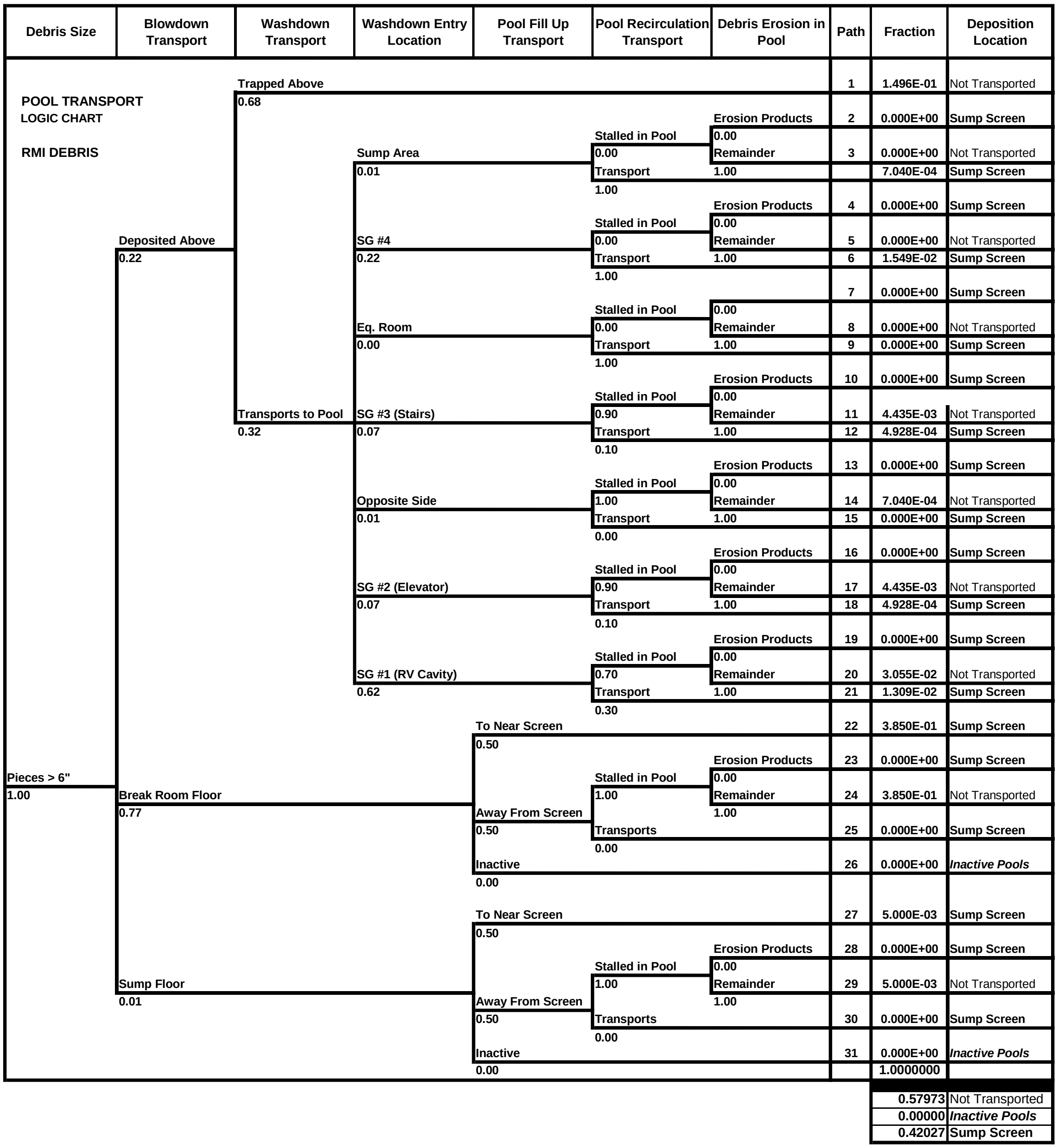

Figure III-55. Sump-Pool-Debris Transport Chart for >6-in. RMI Debris

Table III-9 shows the quantified results by debris category and insulation type, and Table III-10 shows the same results combined for each insulation type. The analysis indicates that about 52 percent of the fibrous and about 42 percent of the RMI debris would accumulate on the recirculation screens for a large LOCA in SG1. The sump pool transport fractions for the small- and large-piece debris are quite high, 97 and 96 percent, respectively. The high fraction for debris eroded contributed substantially to these numbers. However, to put this assumption into perspective, if only 10 percent had been assumed for the erosion, the pool transport fractions would still be 73 and 66 percent, respectively.

The large (greater than 6 in.) debris dominated the RMI debris transport fractions since 98.4 percent of the RMI was predicted to be in this category. This category includes quite large pieces including intact or nearly intact cassettes, which would require a faster flow to move the debris than the 0.28 ft/s used in the CFD analyses.

Table III-9. Quantified Category-Specific Sump-Pool-Debris Transport Results

Debris Category	Category-Specific Debris Transport Fractions				
	Size Distribution	Entering Pool	Into Inactive Pools	Sump Pool Transport	Overall Transport
Fibrous Debris					
Fines	0.133	0.90	0.032	1	0.90
Small Pieces	0.397	0.64	0.024	0.97	0.62
Large Pieces	0.235	0.45	0.086	0.96	0.44
Intact Pieces	0.235	0.40	0.062	0.56	0.23
RMI Debris					
<2 in.	0.011	0.66	0.15	0.61	0.40
2 to 6 in.	0.005	0.63	0.13	0.55	0.35
>6 in.	0.984	0.85	0	0.49	0.42

Table III-10. Quantified Insulation-Specific Sump-Pool-Debris Transport Results

Debris Category	Insulation-Specific Debris Transport Fractions			
	Entering Pool	Into Inactive Pools	Sump Pool Transport	Overall Transport
Fibrous	0.57	0.05	0.88	0.52
RMI	0.85	0.0024	0.50	0.42

The fractions of the sump pool floor where the floor-level flow velocity was slower than the threshold velocities for debris (0.12 and 0.28 ft/s for fibrous and RMI debris, respectively) were calculated from the CFD results presented in Section III.2. The floor fractions corresponding to a large break in SG1 (lower-right quadrant in the CFD results) are 0.41 and 0.22 for fibrous and RMI debris, respectively. Figure III-56 compares these floor area fractions with the sump pool transport fractions by insulation type and size categories. In this scenario, if the debris was uniformly introduced into the pool across the pool cross-sectional area and erosion was not significant, then the area fractions might be a reasonable indicator of the pool debris transport fractions. However, as shown, the area fractions are a poor indicator of debris transport when the debris is introduced into the pool in a more realistic and nonuniform manner and erosion is substantial. A uniform area fraction model can easily underpredict the pool debris transport by a factor of 2 or more.

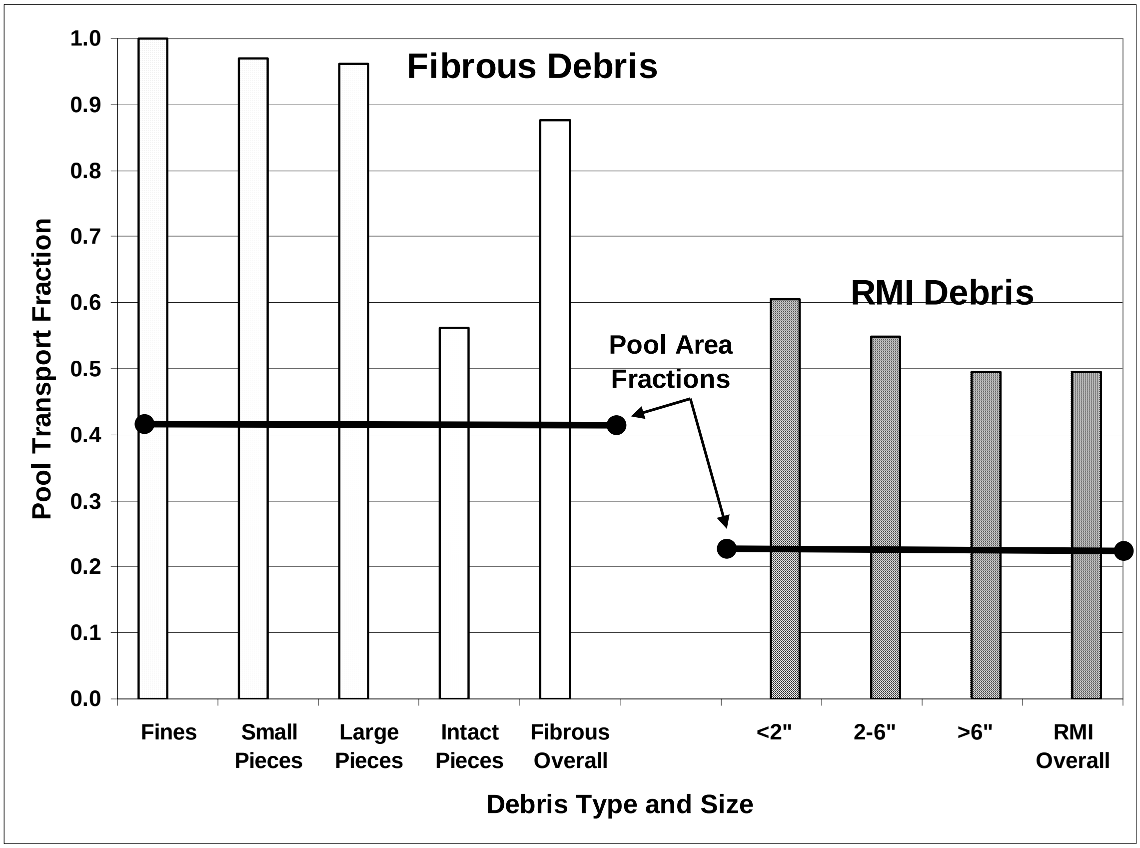

Figure III-56. Comparison of Sump Pool Transport Fraction with Velocity Area Fractions

The transport of debris from its generation in the zone of influence (ZOI) throughout the containment during the reactor coolant system (RCS) depressurization phase, then the washdown transport by the containment sprays, and then its transport through the sump pool to the recirculation sump screens is a rather intractable problem. A logic chart method was used to decompose the overall transport problem into many smaller problems that were subsequently either evaluated by analysis or simply conservatively judged. As such, the results of the volunteer analyses contain many sources of uncertainties; however, these uncertain results are plausible and offer insight into many aspects of debris transport that should be useful to subsequent evaluations. These sources of uncertainty regarding sump pool transport include (1) the timing and locations where debris enters the pool, (2) concerns regarding the effects of local pool turbulence that can move debris even when the bulk flow does not, (3) lack of data regarding erosion rates for debris that can decompose within the pool (e.g., fibrous debris), (4) the simplification of the analysis, and (5) the limited scenario space that can be realistically evaluated.

The debris transport results in this section pertain to a large LOCA in SG1. The same LOCA in another compartment could easily result in different transport results, which could be higher or lower than the scenario evaluated here. In addition, the transport of debris through the sump pool was evaluated here using simplified nodalization, as discussed above. A more detailed evaluation would likely refine these transport results significantly; however, this analysis has demonstrated the transport methodology.

III.4 <u>Conclusions and Recommendations</u>

Section III.2 outlined a method for performing reactor containment pool flow dynamic analysis. A commercial CFD code was used to perform the simulations and assess the flow properties relevant to debris transport. The simulations obtained flow area fractions in excess of transport threshold velocities of debris. Transient containment pool fillup simulations were performed that could potentially be used to design debris diversion systems to sequester debris into zones that do not participate in the flow when sump pumps are engaged.

Recommendations for future simulations include performing grid-mesh convergence studies, further analysis of debris degradation mechanisms, and flow diversion. The grid-mesh convergence studies are required to have a defensible CFD analysis. Additional constraints on the grid mesh, not used or presented in this document, should include clustering grid points near the mass flow injection locations (break and splash locations) and development of a proper boundary layer grid near the no-slip walls, particularly on the containment floor. With additional grid points near the floor, a near-wall velocity profile will be established. The grid refinement study should thoroughly investigate this near-wall velocity gradient and drag forces which could have an impact on debris transport. The debris degradation mechanisms should also be further studied. This document shows examples of degradation, but no attempt to quantify the dynamics has been made at this time.

The transport of debris from its generation in the ZOI throughout the containment during the RCS depressurization phase, then the washdown transport by the containment sprays, and then its transport through the sump pool to the recirculation sump screens is a rather intractable problem. A logic chart method was used to separate the overall transport problem into many smaller problems that were subsequently either evaluated by analysis or by engineering judgment. As such, the results of the volunteer analyses contain many sources of uncertainty; however, these uncertain results are plausible and offer insight into the many aspects of debris transport that should be useful to subsequent evaluations. These sources of uncertainty regarding sump pool transport include (1) the timing and locations where debris enters the pool, (2) concerns regarding the effects of local pool turbulence that can move debris even when the bulk flow does not, (3) lack of data regarding erosion rates for debris that can decompose within the pool (e.g., fibrous debris), (4) the simplification of the analysis, and (5) the limited scenario space that can be realistically evaluated.

The debris transport results in this appendix pertain to one LOCA scenario (a large LOCA in SG1). The same LOCA in another compartment could easily result in different transport results that could be higher or lower than the scenario evaluated here. In addition, the transport of debris through the sump pool was evaluated here using simplified nodalization, as discussed above. A more detailed evaluation would likely refine these transport results significantly; however, the transport methodology has been demonstrated.

III.5 III.5 References

(NUREG/CR-6772, 2001) Rao, D. V., B. C. Letellier, A. K. Maji, and B. Marshall, "GSI-191: Separate-Effects Characterization of Debris Transport in Water," NUREG/CR-6772, LA-UR-01-6882, 2001.

(NUREG/CR-6773, 2002) Rao, D. V., et al., "GSI-191: Integrated Debris-Transport Tests in Water Using Simulated Containment Floor Geometries," NUREG/CR-6773, LA-UR-02-6786, December 2002.

Appendix IV

Debris Transport Comparison

The Nuclear Energy Institute (NEI) guidance report (GR) baseline debris transport recommendations contain both conservative and nonconservative assumptions which were used to simplify the transport evaluation. To assess the effect of the nonconservative assumptions used in the baseline model, the baseline model was applied to the pressurized-water reactor (PWR) volunteer plant, whereby those baseline results could be compared with the detailed debris transport evaluation performed for the volunteer plant. The comparison supported the review and acceptance of the NEI baseline evaluation methodology by illustrating that the baseline predicted conservative debris transport results for the volunteer plant. Insights gained from this comparison regarding debris entrapment in the inactive pool and the transport of large debris support staff-imposed limitations on the acceptance of the baseline methodology.

Because the volunteer plant contains substantial quantities of both fibrous and reflective metal insulation (RMI), the baseline model was applied to both types of insulation debris. Appendix III documents the detailed sump pool debris transport analyses that were performed for the volunteer plant containment. Appendix VI documents the detailed blowdown and washdown debris transport analyses that were performed for the volunteer plant containment. Appendix IV compares the GR baseline analysis to the detailed analyses for the volunteer plant as documented in Appendices III and VI.

The comparison is based on the GR baseline two-group debris-size distributions (i.e., small fines and large-piece debris). The detailed analyses used a four-group distribution of fine debris, small pieces, large pieces, and intact pieces. The detailed four-group results were reduced to two groups by combining the fine and small-piece debris into the NEI small fine debris group and combining the large-piece and the intact-piece groups into the NEI large-piece group. This approach enabled a direct comparison.

The size distributions for both the NEI baseline results and the detailed analyses results were based on destruction pressures of 10 psi for the fibrous debris and 4 psi for the RMI debris. Appendix II documents the research used for the respective size distributions. The radii of the fibrous and RMI zone of influence (ZOI) for these pressures are 11.9D and 21.6D, where D is the diameter of the pipe that breaks (see Appendix I). In applying the baseline model to the volunteer plant, the comparison assumed that the containment was highly compartmentalized.

Table IV-1 and Table IV-2 compared the baseline and detailed analyses results by debris size for fibrous and RMI debris, respectively. Table IV-3 compares the overall transport fractions, which combine the small fine debris and the large-piece debris to obtain the total estimated screen accumulation. The respective debris-size distributions shown in Table IV-1 were used to calculate the overall transport results shown in Table IV-3. Note that the transport fractions in Table IV-1 and Table IV-2 pertain only to the respective size categories.

Table IV-1. Baseline Comparison with Detailed Volunteer-Plant Fibrous Transport Results

Transport Phase	Debris Transport Fractions			
	Small Fine Debris		Large-Piece Debris	
	Baseline	Detailed	Baseline	Detailed
Fraction of Debris Generated	0.60	0.53	0.40	0.47
Fraction of Debris Generated that Transports into Upward Levels by Blowdown	0.25	0.92	0	0.63
Fraction of Debris Generated that Transports Directly to Sump Pool Floor by Blowdown	0.75	0.08	1	0.37
Fraction of Debris Generated that Blows into Upper Levels and Washes Down into Sump Pool	1	0.71	0	0.21
Fraction of Debris Generated that Enters Sump Pool	1	0.73	1	0.50
Fraction of Debris Generated that Enters Inactive Sump Pool	0.14	0.03	N/A	0.07
Fraction of Debris Generated that Enters Active Sump Pool	0.86	0.70	1	0.43
Fraction of Debris that Enters Sump Pool that Transports to Sump Screens	1	0.98	0	0.76
Fraction of Debris Generated that Accumulates on Sump Screens	0.86	0.69	0	0.33

Table IV-2. Baseline Comparison with Detailed Volunteer-Plant RMI Transport Results

Transport Phase	Debris Transport Fractions			
	Small Fine Debris		Large-Piece Debris	
	Baseline	Detailed	Baseline	Detailed
Fraction of Debris Generated	0.75	0.02	0.25	0.98
Fraction of Debris Generated that Transports into Upward Levels by Blowdown	0.25	0.44	0	0.22
Fraction of Debris Generated that Transports Directly to Sump Pool Floor by Blowdown	0.75	0.56	1	0.78
Fraction of Debris Generated that Blows into Upper Levels and Washes Down into Sump Pool	0	0.55	0	0.32
Fraction of Debris Generated that Enters Sump Pool	0.75	0.80	1	0.85
Fraction of Debris Generated that Enters Inactive Pools	0.11	0.15	N/A	0
Fraction of Debris Generated that Enters Active Sump Pool	0.64	0.65	1	0.85
Fraction of Debris that Enters Sump Pool that Transports to Sump Screens	1	0.59	0	0.49
Fraction of Debris Generated that Accumulates on Sump Screens	0.64	0.39	0	0.42

Table IV-3. Comparison of Overall Baseline and Detailed Analysis Transport Fractions

Debris Type	Fraction of ZOI Insulation Debris Accumulated on Sump Screens	
	Baseline	Detailed
Fibrous Debris	0.52	0.52
RMI Debris	0.48	0.42

Substantial uncertainty exists in various aspects of the volunteer plant analyses that affect this comparison, including the following:

- uncertainties in determining the debris generation size distributions
- uncertainties in specifying various aspects of the blowdown and washdown debris transport and deposition processes
- uncertainties in estimating the locations where debris enters the sump pool and when the debris enters with respect to the formation of the pool
- uncertainties in estimating the quantities of debris transported into the inactive pool regions
- uncertainties in estimating debris transport within an established sump pool

The following four points apply to the comparison of the fibrous debris transport:

(1) The baseline recommendation for the debris-size distribution assumed 60 percent for the small fine debris, which is higher than the 53 percent determined from the integration of the air-jet debris generation data and used for the detailed analysis (Appendix II).

(2) The detailed analysis predicted that most of the smaller fibrous debris would be deposited in the upper levels during blowdown debris transport, rather than directly on the sump floor as proposed in the baseline model. Because the transport of this upper level debris to the sump pool by containment spray drainage (washdown) is delayed by a variable and indeterminate period of time, it must be postulated that relatively little of the debris reaches the sump floor in time to be entrained in the water flow filling the inactive pools (primarily the reactor cavity in the volunteer plant), which occurs relatively early in the accident sequence (less than 12 minutes). The detailed analyses predicted that, at the end of the blowdown/washdown transport, a significantly less amount of debris, compared to the baseline analyses, would enter the active sump pool.

(3) The baseline model sump pool transport onto the sump screen was 100 percent of debris entering the sump pool for small fine debris and 0 percent for large-piece debris. The baseline model predicted more small fine debris accumulation on the sump screens than did the detailed analyses. However, the detailed analyses predicted substantial accumulation of large-piece debris on the screens, whereas the baseline predicted none.

(4) The baseline and detailed analyses both predicted that approximately 52 percent of the fibrous debris generated within the ZOI would accumulate on the sump screens.

The following four points apply to the comparison of the RMI debris transport:

(1) The baseline recommends using more small fine RMI debris (75 percent of debris generated) than that was determined from the integration of the air-jet debris generation data and used for the detailed analysis (2 percent) (Appendix II). The primary reason for the large difference is the large increase in ZOI

volume predicted by the American National Standards Institute (ANSI)/American Nuclear Society (ANS)-58.2-1988 standard. When that standard is applied to jet impingement pressures as low as 4 psi, only a small amount of small fine debris is generated over much of the ZOI volume. Most of the ZOI debris is large-piece debris.

(2) The detailed analyses predicted lesser quantities of small fine RMI debris than fibrous debris would deposit in the upper levels of the containment (44 percent versus 92 percent of debris generated), although it was substantially more than the baseline model recommendation of 25 percent. A primary reason for this result was that so little blowdown debris transport data exist for RMI debris, and thus the blowdown analyses conservatively assumed a large fraction of debris depositing directly on the sump floor. Both the detailed and baseline analyses predicted that approximately the same amount of debris would enter the active sump pool at the end of the blowdown/washdown transport (65 percent versus 64 percent of debris generated).

(3) The baseline model sump pool transport was 100 percent for small fines and 0 percent for large-piece debris. The baseline model predicted more small fine debris accumulation on the sump screens than did the detailed analyses (64 percent versus 39 percent of debris generated). However, the detailed analyses predicted substantial accumulation of large-piece debris on the screens (42 percent of debris generated), whereas the baseline predicted none.

(4) The baseline method predicted slightly more RMI debris accumulation on the sump screens than did the detailed analyses (i.e., 48 percent as compared with 42 percent of the debris generated).

In conclusion, the application of the baseline methodology to the volunteer plant predicted approximately the same accumulation of fibrous debris and conservatively more RMI on the sump screen than did the detailed transport analyses. Although this comparison does not explicitly demonstrate that the baseline methodology is conservative relative to fibrous debris transport in the detailed volunteer plant evaluation, detail-specific conservatisms built into various aspects of the blowdown/washdown and pool debris transport analyses still support the overall conclusion that the baseline methodology is conservative with respect to its application to the volunteer plant. Even though the baseline and detailed evaluation arrived at the same fractions for sump screen debris accumulation, the intermediate steps disagreed. Because of the diversity among the PWR containment designs, this analysis does not conclusively demonstrate that the baseline methodology will be conservative for debris transport in all of the PWRs. In addition, the detailed volunteer plant analyses contained substantial sources of uncertainty.

Insights gained from this comparison regarding debris entrapment in the inactive pool and the transport of large debris support staff-imposed limitations on the acceptance of the baseline methodology to prevent an outlier plant from demonstrating adequate net positive suction head (NPSH) margin using the baseline methodology where adequate NPSH margin might not exist in reality. The limitations resulted from the following two concerns that should be addressed before accepting baseline method results for plant-specific analyses.

First, if a plant baseline analysis estimates a relatively large fraction of the debris trapped in the inactive pools, as could be the case with a large reactor cavity volume and a shallow sump pool, then the baseline inactive pool fraction should be more limited than the current baseline model. Note that the detailed analyses reported herein predicted that only approximately 3 percent of the small fibrous debris generated would trap in the inactive pool, as compared with 14 percent that was predicted using the baseline model. Based on this comparison, the staff limits the fraction of debris assumed to be trapped in the inactive pool to no more than approximately 15 percent, unless a higher fraction is adequately supported by analyses or experimental data. The 15-percent upper limit on the debris transport into the inactive pools does not make the inactive pool model conservative but serves to ensure that the baseline methodology, as a package, is conservative. If analytical refinements are made for debris transport, then the debris transport into the inactive pools must be evaluated in a conservative manner using models that describe the actual transport processes but not the model described in the baseline guidance.

Second, if the characteristic sump pool transport velocities are relatively high, such that large transport fractions for large debris are indicated, then the baseline method should be modified to include the transport of large debris. In the volunteer plant, for example, the detailed analysis predicted that approximately 98 percent of the RMI debris generated in the ZOI (based on a destruction pressure of 4 psi) were large pieces greater than 6 in. in size, of which about 42 percent would be transported to the sump screens. The characteristic transport velocities must be compared with typical debris transport velocities to determine whether the baseline method should be modified to include the transport of large debris. Characteristic transport velocities can be sufficiently estimated using recirculation flow rates and nominal sump dimensions to determine if a potential exists that substantial portions of the large debris will transport. If substantial transport of large debris is reasonably possible and if such transport can alter the outcome of the sump performance evaluation, the licensees should evaluate large debris transport.

REFERENCES

(ANSI/ANS-58.2, 1988) American National Standard/American Nuclear Society: "Design Basis for Protection of Light Water Nuclear Power Plants Against the Effects of Postulated Pipe Rupture," ANSI/ANS-58.2-1988, October 1988.

Appendix V

Confirmatory Head-Loss Analyses

V

Confirmatory research was performed to determine whether specific parameter assumptions made in the Nuclear Energy Institute (NEI) guidance report (GR) are conservative with respect to more realistic parameters. This research also provided additional insights into the estimation of head-loss parameters for the NUREG/CR-6224 head-loss correlation. Additional guidance is provided for determining appropriate parameters for a mix of multiple fiber and particulate components. This appendix also provides procedures for applying the NUREG/CR-6224 head loss correlation.

V.1 Fibrous Debris Head-Loss Parameters

A comparison of specific surface areas (*Sv*) deduced from head-loss test data and the simple geometric correlation of four divided by the characteristic fiber diameter (4/d) is presented for NUKON™ and Kaowool™ insulation debris. The Boiling Water Reactor Owners Group (BWROG) head-loss tests documented in Volume 1 of the BWROG Utility Resolution Guidance (URG) provide the test data used in both of these deductions.

V.1.1 NUKON™ Fibrous Debris

The URG has three head-loss tests that used only NUKON™ insulation debris and used a type of strainer that behaved similarly to that of a flat-plate screen (i.e., a truncated cone strainer). These tests were numbered 2, 4, and 5 and used 8, 8, and 16 lb of NUKON™, respectively, and no particulate. The flow velocities through the bed varied from approximately 0.15 to 0.75 ft/s, resulting in a total of 15 head-loss data points. A specific surface area was deduced for each data point using the NUREG/CR-6224 head-loss correlation and using an as-manufactured density of 2.4 lb/ft^3 and a fiberglass material density of 175 lb/ft^3 (NUREG/CR-6224 study recommendations). Figure V-1 compares the resultant *Sv* values.

The comparison was based on the debris bed compression as determined by the NUREG/CR-6224 correlation (the ratio of the compressed thickness divided by the uncompressed thickness), which is directly affected by the flow pressure (i.e., flow velocity). The average value for *Sv* was approximately 170,600 ft^{-1}. The nominal diameter for NUKON™ fibers has been specified as 7.1 µm, which translates into an *Sv* of 171,710 ft^{-1}. The NUREG/CR-6224 study recommended an *Sv* of 171,420 ft^{-1}. For NUKON™ insulation debris, the *Sv* determined using 4/d is in excellent agreement with the experimentally deduced value.

The NEI guidance has recommended using a material density of 159 lb/ft^3 rather the NUREG/CR-6224 study value of 175 lb/ft^3. Confirmatory analysis using the NUREG/CR-6224 correlation verified that it is conservative to use 159 lb/ft^3 rather than 175 lb/ft^3, provided that the remaining head-loss parameters of 2.4 lb/ft^3 for the as-manufactured density and 171,000 ft^{-1} for the specific surface area are maintained. The lower value for the material density estimates a slightly higher head loss than does the larger value.

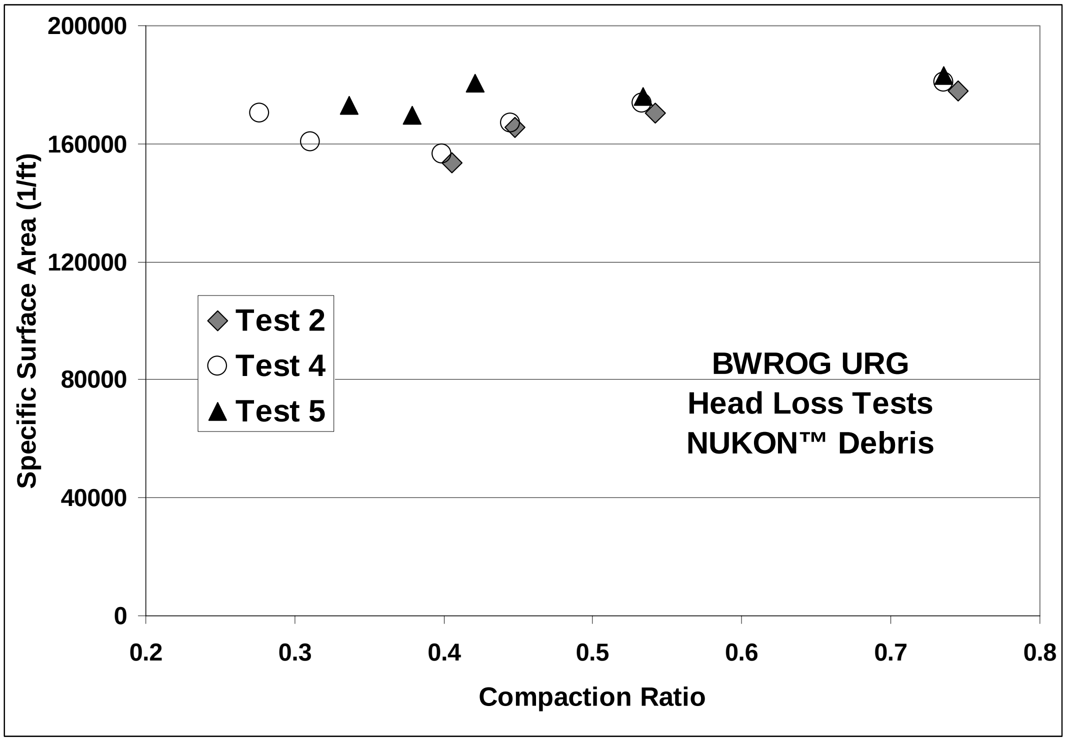

Figure V-1. NUKON™ Specific Surface Area

Similarly, the NEI guidance recommended using 1.0 g/cm^3 (62.4-lb/ft^3) for material density of latent fibers to enhance transport (neutral buoyancy). The latent debris characteristics test results (LA-UR-04-3970, 2004a) that analyzed latent debris collected in the containments of several volunteer plants show that the latent debris fibers had material densities ranging from 1.3 to 1.9 g/cm^3. Again, confirmatory analyses verified that it is conservative from a head-loss prediction perspective to assume that the latent fiber material density is 1.0 g/cm^3 rather than 1.3 to 1.9 g/cm^3, provided that the remaining head-loss parameters are appropriately specified.

V.1.2 Kaowool™ Fibrous Debris

The URG has one valid head-loss test that used Kaowool™ insulation debris and used a type of strainer that behaved similarly to that of a flat-plate screen (i.e., a truncated cone strainer). Test J13 initially had added 12 lb of Kaowool™, then later added 5 lb of iron oxide corrosion products (CPs), and subsequently added another 5 lb of CP. The flow velocities through the bed varied from approximately 0.31 to 0.62 ft/s, resulting in a total of nine head-loss data points (three data points without particulate). A specific surface area was deduced for each data point using the NUREG/CR-6224 head-loss correlation, with the NUREG/CR-6224 study-recommended parameters for the corrosion products used as input.[*] The recommended fiber material density for Kaowool™ is 160 lb/ft^3.

[*] The NUREG/CR-6224-recommended parameters are 183,000 ft^{-1} for the specific surface area, 324 lb/ft^3 for the particulate material density, and 65 lb/ft^3 for the granular packing-limit density.

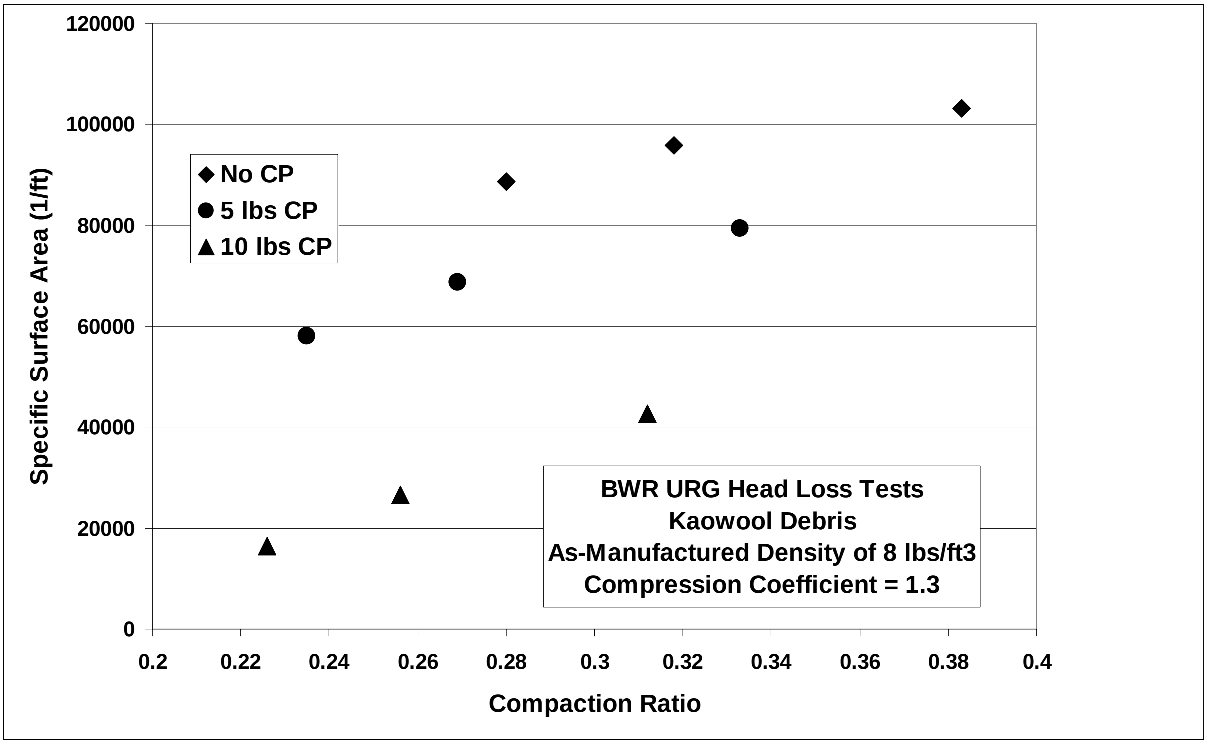

Figure V-2. Kaowool Specific Surface Area Assuming Base Parameters

The NEI guidance recommends an as-manufactured density of Kaowool™ ranging from 3 to 12 lb/ft^3, whereas the URG recommended a value of 8 lb/ft^3, apparently a mid-range value. First, the *Sv* values were deduced from Test J13 data by assuming an as-manufactured density of 8 lb/ft^3 and the same bed compression correlation that was so successful for NUKON™. Figure V-2 compares these resultant *Sv* values. The values of *Sv*, as shown, are very scattered, ranging from 16,000 to 103,000 ft^{-1}. All in all, the NUREG/CR-6224 correlation does not work well with these input parameters. Noting that the as-manufactured density cited in the GR ranged from 3 to 12 lb/ft^3, it was subsequently determined that a smaller value of the density would reduce the scatter in the resultant *Sv* values. Further, it was discovered that stiffening the compression function also reduced the scatter. Figure V-3 shows the results from a second comparison of the deduced *Sv* values that was developed assuming an as-manufactured density of 4 lb/ft^3 and a leading compression coefficient of 0.5 (rather than the standard 1.3). The comparison in Table V-3 has the deduced values in good agreement, with an average value of 165,500 ft^{-1}.

The NEI guidance specified 2.7 to 3.0 µm as the nominal diameter for Kaowool™ fibers, which translates into an *Sv* of 406,400 to 451,500 ft^{-1} using the 4/d formula. Although using such high values for *Sv* is conservative, the simple formula is not even close to the experimentally deduced value of 165,500. The application of an *Sv* of 406,400 ft^{-1} would substantially overpredict the results of Test J13.

The coefficient of the NUREG/CR-6224 compression correlation is an important issue. The standard coefficient of 1.3 was developed and validated essentially using NUKON™; therefore, the validation of other fibrous insulation must assess the validity of this value for the insulation under consideration. It is noted that the baseline guidance in the GR considers this point by including the constant K (Equation 3.7.2-4 in Section 3.7.2.3.1.1 of the baseline guidance with a default value of 1 for K). For Kaowool™, a K = 0.385 and a Sv of 165,500 ft^{-1} in the NUREG/CR-6224 correlation predict URG Test J13 results reasonably well.

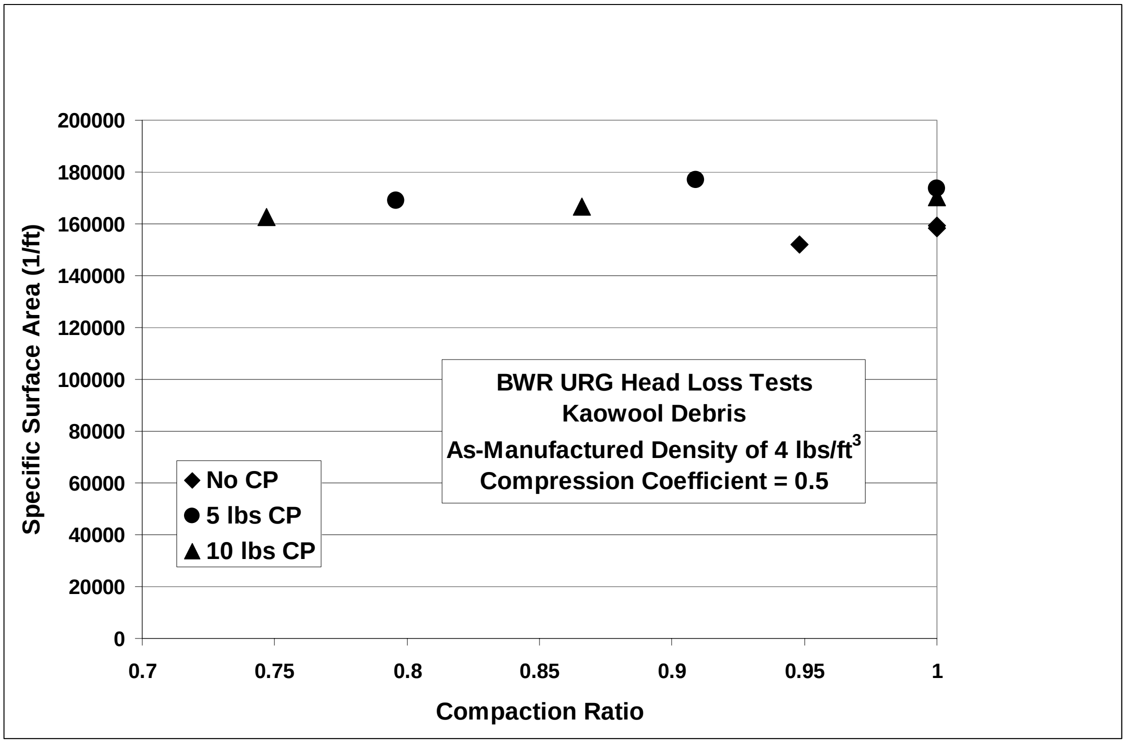

Figure V-3. Kaowool™ Specific Surface Area Using Modified Parameters

V.1.3 Comparison of Fibrous Debris

Figure V-4 compares the specific surface areas for areas determined using the 4/d formula and the two experimentally deduced values presented herein for NUKON™ and Kaowool™. The figure illustrates the following three points:

(1) The coefficient(s) for the compression correlation also have a role in the application of the NUREG/CR-6224 correlation to the various types of fibrous debris.

(2) The 4/d formula was formerly validated using NUKON™, but not necessarily for other types of fibrous insulations.

(3) The 4/d formula is not reliable and should not be applied indiscriminately. It should not be assumed that because this formula overpredicts Kaowool™ head-losses that it will be conservative for untested types of fibrous debris. The only reliable method of determining the specific surface area of a particular insulation material is deduction from applicable test data.

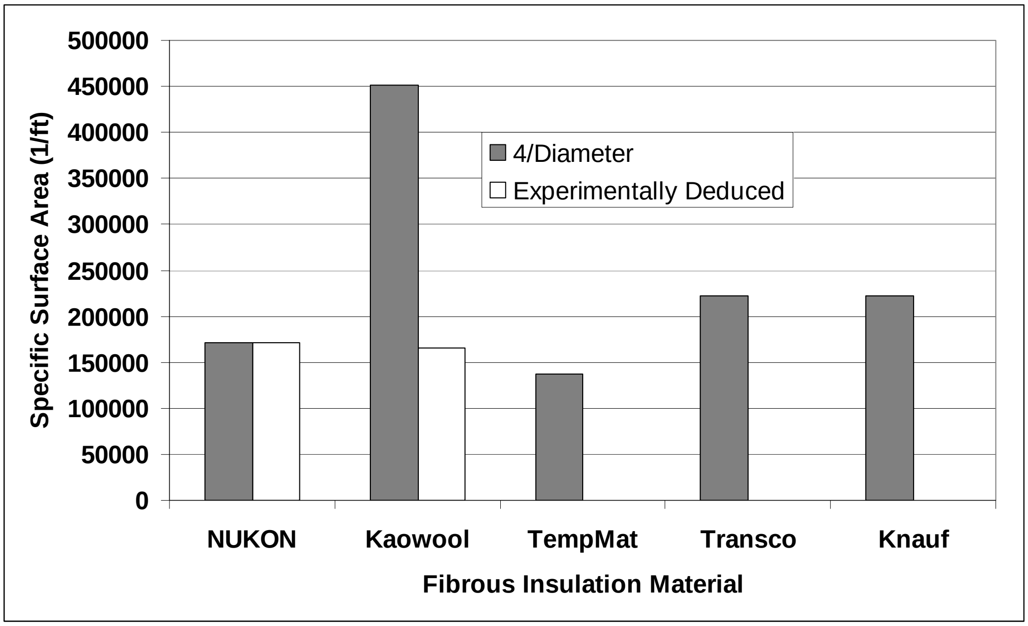

Figure V-4. Comparison of Fibrous Insulation Specific Surface Areas

V.2 <u>Particulate Debris Head-Loss Parameters</u>

In Section 3.7.2.3.1.1 of the GR, the NEI recommends using the simple formula of six divided by the characteristic particle diameter (6/d) to determine the specific surface areas for particulate debris. The following confirmatory analyses provide insights into this relationship and experimentally deduced values for particulate *Sv.*

V.2.1 Iron Oxide Corrosion Products

During the resolution of the boiling-water reactor (BWR) strainer blockage issue, the iron oxide CPs that accumulate in a BWR suppression pool were the primary particulate in the head-loss calculations. The size distribution shown in **Error! Reference source not found.** characterizes the BWR sludge CP.

The NUREG/CR-6224 correlation recommends a specific surface area of 183,000 ft^{-1} for head-loss estimates with CP, which has been validated by comparison with test data. Using the mid-range diameters from **Error! Reference source not found.** to estimate the *Sv* for the CP distribution using the 6/d formula, the *Sv* estimate becomes 48,400 ft^{-1} (almost a factor of four less than the NUREG/CR-6224 recommendation). Note that an error of a factor of 4 in the *Sv* can result in an error of a factor as large as 16 in the head loss at low-flow velocities.

If the minimum value of the range is used (assuming a minimum particle size of 2 µm for the 0- to 5-µm size group), then an *Sv* of approximately 290,000 ft^{-1} is calculated (approximately 58 percent higher than the recommended validated area). The smaller particles have more effect on the particulate *Sv* than do the larger particles, which is why the mid-range diameters are not a valid representation of the distribution. Using the smallest diameters of each group is conservative but can result in large estimates of *Sv*.

Further, these examples illustrate that it is difficult to determine where in a size range is an appropriate diameter for the *Sv* determination using 6/d.

Table V-1. Size Distribution of BWR Suppression Pool Iron Oxide Corrosion Products

Size Range (µm)	Percent by Number of Particles	Percent by Weight
0–5	81%	0.3%
5–10	14%	1.5%
10–75	5%	98.2%

Figure V-5 illustrates an example of how the 6/d formula works over a particle-size grouping, where 6/d is plotted for particle diameters ranging from 5 to 75 µm (typical distribution grouping). If it is assumed that particles are uniformly distributed (by weight) across this size range (which is not necessarily a valid assumption), then the average 6/d corresponds to a diameter of 25.8 µm, whereas the mid-range diameter is 40 µm. Because this simple arithmetic relationship arrives at differing conclusions, depending on the range specification, this method cannot be used reliably in a general sense, even if the uniform distribution assumption is valid.

In summary, the only reliable method of determining the *Sv* for a particulate, unless the particulate-size distribution is known in much greater detail than has been typically specified to date, is to deduce *Sv* from valid head-loss test data. It is conservative to use the lower diameter of each size group but this can lead to large estimates of the *Sv*. However, this method is valid when applicable head-loss data are lacking. Another difficulty is the determination of the smallest particles in the distribution. Although most particulates will have submicron particles in the distribution, fiber debris beds may not filter such small particles; certainly, the efficiency of filtration could be rather low and is difficult to determine.

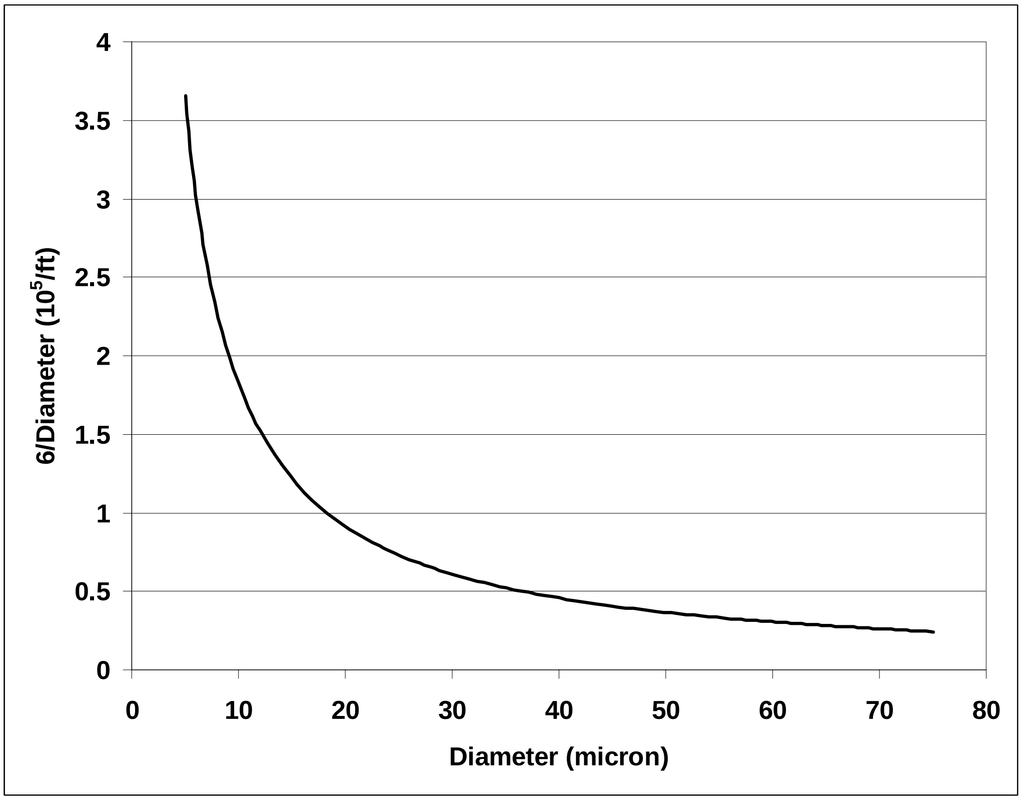

Figure V-5. Example of *Sv* Variation with Particle Diameter

V.2.2 Latent Debris

Los Alamos National Laboratory (LANL) (LA-UR-04-3970, 2004a) determined the characteristics of latent debris collected from inside containments of several nuclear plants. These characteristics included properties of material composition and hydraulic flow properties (e.g., specific gravities and characteristic dimensions). Based on these characteristic properties, surrogate latent particulate debris* was formulated for testing in the closed-circulation head-loss simulation loop operated by the Civil Engineering Department at the University of New Mexico (UNM).† Applying the NUREG/CR-6224 head-loss correlation to the test data for the surrogate latent debris resulted in parameter recommendations for the application of the correlation to plant latent debris. Summaries of those recommendations follow, together with insights gained from the surrogate latent debris data reduction. The calcium silicate debris test report (LA-UR-04-1227, 2004b) describes the test apparatus and base test procedures in detail.

The plant debris characteristics pertinent to the specification of a recipe to create a suitable latent particulate surrogate include the particulate specific gravity and the particulate-size distribution. Table V-2 shows the particulate-size distribution that was

* A surrogate was required to provide the quantities of debris needed for head-loss testing. The latent debris collected in containment required the special handling associated with radioactive materials.

† NUKON™ insulation debris was selected to form the fiber bed to filter the surrogate particulate from the flow because of its well-established head-loss properties.

used as a recipe for the particulate. The surrogate particulate debris tested at UNM was constructed from common sand and soil (referred to as dirt), with the sand used for the two larger size groups and the dirt for the less than 75-µm-size group. The specific gravity of the latent debris characterized at LANL varied but is well represented as a specific gravity of 2.7, and both the sand and dirt used to formulate the surrogate were found to have a specific gravity near 2.7. The dirt had a clay component that tended to disintegrate, in part, in water, thereby adding substantial particulate less than 10 µm to accommodate the LANL, finding that the filters collected substantial very fine debris. Both granular (thin-bed) and nongranular debris beds were tested.

Table V-2. Surrogate Particulate Size Distribution

Size Range (µm)	Fraction
500 to 2000	0.277
75 to 500	0.352
<75	0.371

Tests were conducted using the individual size groupings for the 75- to 500-µm sand and the less than 75-µm dirt (without the other groups present) to determine specifically the head-loss characteristics of these individual size groupings; then the latent debris recipe was tested with all three size groups represented according to the recipe. The largest size group (500 µm to 2 mm) was not individually tested because of its relatively minor impact on the recipe head loss; its small specific surface area was estimated using the 6/d equation. For the other two size groups, the specific surface area was deduced from the head-loss data. The bulk densities of the three components were estimated by measuring the bulk volume in a calibrated beaker for a weighted mass of particulate. Given the particle specific gravity and the bulk densities, the granular debris bed porosities were estimated. Table V-3 summarizes the test results for the surrogate latent particulate debris.

Table V-3. Summary of Test Results

Particulate (µm)	Bulk Density (lbm/ft^3)	Limiting Granular Porosity	Limiting Granular Solidity	Specific Surface Area (ft^{-1})
500 to 2000 (Sand)	104	0.38	0.62	2,000
75 to 500 (Sand)	99	0.41	0.59	10,800
<75 (Dirt)	39	0.77	0.23	285,000
Recipe	63 to 75	0.62 to 0.55	0.38 to 0.45	106,000

The table shows a range of numbers for the bulk density and limiting granular porosity and solidity because of the uncertainty associated with filtration of the very fine dirt from the water flow (i.e., how much of the dirt introduced into the test loop actually resided in the debris bed). Test-loop water turbidity measurements clearly showed that the fibrous bed did not filter significant, sometimes substantial quantities of the fine dirt from the flow. If there is a minimum particle size for effective filtration, it is most certainly significantly less than 10 µm and likely less than a few microns. Table V-3 presents nominal estimates for the specific surface area for each component; however, there is significant uncertainty in determining these numbers. The primary uncertainty associated with the less than 75µm particulate was the filtration efficiency of the finer particles. Assessing the uncertainties in the turbidity resulted in the conclusion that between 30 and 45 percent of the particulate remained in solution, which corresponded to a range of about 250,000 ft^{-1} to 340,000 ft^{-1} in the specific surface area when the correlation was applied. For the two larger particulate size groups (75 to 500 µm and 500 to 2000 µm), the uncertainties were analytically estimated using the 6/d formula where the diameter was ranged from the smallest diameter particles up to 25 percent of the range. Figure V-6 compares these estimated uncertainties.

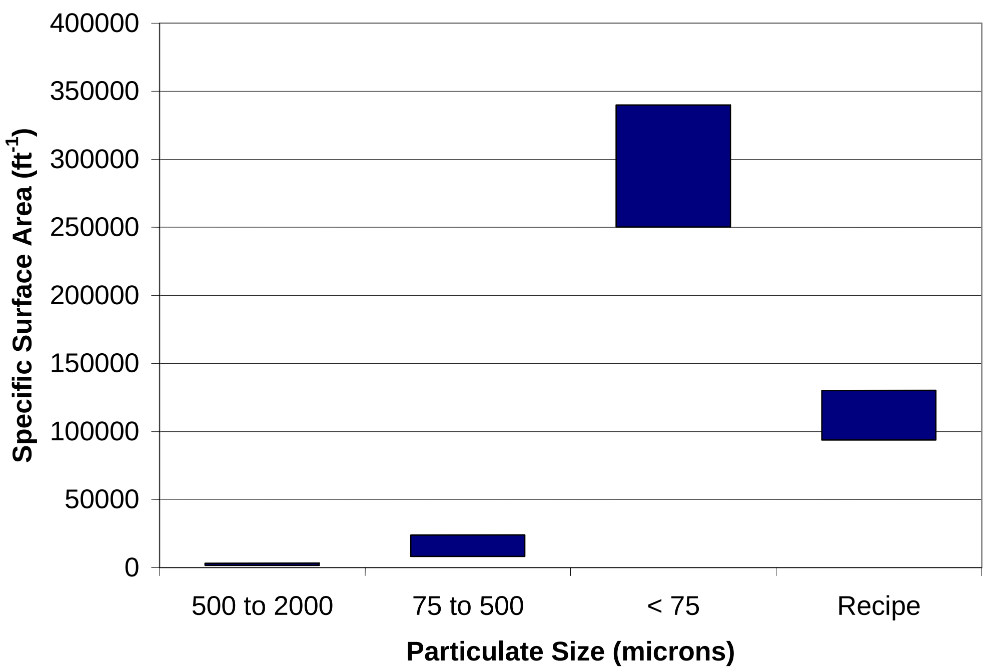

Figure V-6. Comparison of Component and Recipe Specific-Surface-Area Ranges

The following eight key points can be deduced from the foregoing discussions relative to latent debris:

(1) The limiting porosity (solidity), which depends on the composition of the debris, controls the head loss through granular (thin-bed) debris. Solidity certainly is not a fixed number, as is indicated in the presentation of the NEI guidance as a solidity of 0.2. Handbooks on soils show many materials with limiting porosity less than 0.8 (e.g., common sand is approximately 0.40 to 0.43 and was experimentally verified in the LANL tests).

(2) The major contributors to the head loss are the increasingly smaller particles (less than 75 µm), as illustrated by the 6/d formula, until the particles become

too small for filtration. However, it is difficult to determine some limiting particle diameter that will not filter.

(3) It is difficult to formulate specific recommendations for the appropriate parameters to use in the NUREG/CR-6224 correlation for pressurized-water reactor (PWR) containment latent particulate because the latent debris composition will vary from plant to plant and because the latent debris transported to the sump screen will also be plant-specific because of such differences as flow velocities. In addition, the uncertainties associated with whether the surrogate recipe suitably represents actual containment latent debris further compound the problem of developing recommended characteristics for latent debris. More important than specific recommendations are the methods for ascertaining appropriate head-loss parameters once the plant has assessed latent debris accumulation on the sump screen.

(4) The surrogate latent particulate debris head-loss tests effectively demonstrate the necessity of characterizing the latent particulate so that appropriate parameters can be estimated. For example, if deposition of the entire mass of the latent debris onto the sump screen is assumed, then a lower specific surface area, such as the recipe in these tests, can be applied. However, if transport analyses are used to limit the transport of latent particulate to only the fine particulate, then the appropriate specific surface area would be more like that of the fine dirt in these tests. The same consideration also applies to the limiting packing density.

(5) It is recommended that plant latent debris estimates be separated into as many particle size groupings as reasonably possible and then that subsequent transport analysis be applied to each group to determine the particulate makeup on the sump screen.

(6) Wherever possible, specific surface areas should be determined for each size group based on test data. When the areas must be estimated from the particle diameters, the appropriate diameter is clearly not the mean or average diameter of the size group but a diameter closer to the minimum diameter of the group. The minimum diameter should normally result in a conservative specific surface area.

(7) The use of the simple geometric relationship of 6/d to estimate the specific surface areas for particulate is not reliable because the appropriate diameter within the range is not known. Table V-4 illustrates this point, where values for *Sv* are estimated using both the mid-range and minimum diameters for each size group in the surrogate latent particulate recipe. These values are compared to the *Sv* deduced from the experimental head loss and the particle diameters that correspond to the experimental *Sv*. This minimum diameter in the size range estimates a conservative *Sv*; however, that number could be unacceptably large if the minimum size for the smallest particles is not well known. The use of mid-range diameters is unacceptable because this approach excessively underpredicts *Sv* values for plant-specific evaluations. If the specific surface areas corresponding to the minimum particle diameters in each size grouping range are unacceptable, then head-loss test data are required to determine a specific surface area for the particulate size distribution in question.

(8) The NEI guidance recommends the use of 100 lb/ft^3 for the material density of latent particulate, whereas LA-UR-04-3970 indicates a density of approximately 168 lb/ft^3 (specific gravity of approximately 2.7). The use of the lighter density of 100 lb/ft^3 is conservative relative to a heavier density of 168 lb/ft^3, for example, if the other head-loss parameters are appropriately specified.

Table V-4. Comparison of Specific Surface Area Estimation Methods

Particulate Size (µm)	Analysis			Experimental *Sv*	
	Mid-Range Diameter (µm)	*Sv* = 6/d Mid-Range *Sv* (ft^{-1})	*Sv* = 6/d Mid-Range *Sv* (ft^{-1})	*Sv* Deduced from Experimental Head-Loss Data (ft^{-1})	6/*Sv* Experiment (µm)
500 to 2000 (Sand)	1250	1,460	3,660	2,000	914
75 to 500 (Sand)	287.5	6,360	24,380	10,800	169
<75 (Dirt)	37.5	48,770	914,000*	285,000	6.4
Recipe	88.2	20,740	349,000	106,000	17.3

* Assuming a 2-µm minimum particle size.

V.3 <u>Formulas for Mixing Multiple Fiber and Particulate Components</u>

Most head-loss testing has been performed with a single type of fibrous debris (e.g., NUKON™) and particulates such as CPs. However, plant-specific analyses may well postulate debris beds containing more than one type of fiber and several types of particulate. The application of the NUREG/CR-6224 correlation requires the head-loss properties for the mixture to be estimated from the individual species properties.

V.3.1 Mixture of Specific Surface Areas

The equation for the mixture of the specific surface areas simply multiplies each area by the species volume and sums these products to calculate the total surface area, which is then divided by the total volume to obtain the mixture-average specific surface area. Such an equation was recommended in NUREG/CR-6371. Section 3.7.2.3.1.1 of the NEI guidance on the mixing equation recommends using the square of the specific surface area rather than the linear relationship. The following equation for the mixing is set up to accommodate the linear (n = 1), the square (n = 2), or any other exponent. Performing example-mixing evaluations demonstrated that using the square results in larger values for the mixture of specific surface areas than does using the linear relationship; therefore, it is conservative to use the square of the specific surface area in the mixing rather than the linear

$$Sv_{Mixture} = \left[\frac{\sum_i \frac{m_i}{\rho_i} Sv_i^n}{\sum_i \frac{m_i}{\rho_i}} \right]^{\frac{1}{n}} ,$$

where

Sv = the specific surface area for component *i* or for the mixture,

m_i = the mass of component *I*,

ρ_i = the material (solid) density of the particles in component *I*, and

n = the weighting exponent.

For the surrogate latent particulate debris, mixing the three constituents to get the recipe test result seemed to work best using an n = 4/3 (assuming that approximately 40 percent of the fine dirt did not filter from the flow). Because of the substantial uncertainties associated with head-loss predictions, it is prudent to include a safety factor; therefore, the NEI recommendation of using the square of the specific surface area in the mixing equation is a good recommendation.

V.3.2 Mixture Densities

The equation for the mixture of densities (bulk, material, or granular) simply adds all of the species masses and then divides by the total of the species volumes as

$$\rho_{Mixture} = \frac{\sum_i m_i}{\sum_i \frac{m_i}{\rho_i}} ,$$

where

ρ_i = the density of the particles in component *I* and

m_i = the mass of component *i*.

This density mixing equation can be reduced to the following, even simpler form:

$$\frac{1}{\rho_{Mixture}} = \sum_i \frac{f_i}{\rho_i} ,$$

where

f_i = the mass fraction of component *i*.

V.4 Procedures for Applying the NUREG/CR6224 Correlation

The application of the NUREG/CR-6224 head-loss correlation requires several input parameters that must be conservatively specified to ensure bounding head-loss predictions. The most reliable method of determining these input parameters is the application of the correlation to appropriate head-loss test data. Analytical determinations are suitable under some conditions if sufficient conservatism is used throughout the determination. Although the correlation was developed for flat screen geometries, the correlation has been successfully applied to other strainer geometries, such as the stacked-disk strainers.

V.4.1 Experimental Determination of Correlation Parameters

The proper application of the NUREG/CR-6224 correlation to applicable head-loss test data leads to input parameters that ensure bounding head-loss prediction when the correlation is applied to postulated plant conditions that would form debris beds similar to those in the tests. The closer the test data is to the postulated debris beds the more certain the determination of the input parameters. Appropriate conservatism is required whenever the test data are dissimilar to the postulated conditions.

V.4.1.1 Success Criteria for Applicable Test Data

The assumptions associated with the development of the NUREG/CR-6224 correlation included the following:

- The debris bed consists of fibrous debris with or without particulate debris.
- The debris bed has a uniform thickness.
- The debris bed is homogeneous.
- The flow approach velocity is perpendicular to the debris bed.
- The flow and debris accumulation on the screen are relatively quasi-steady-state.

Therefore, the success criteria for applicable test data to determine applicable correlation input parameters include the following:

- The test debris bed consists of some mixture of fibrous debris with or without particulate debris.
- The debris bed must be relatively uniform.
- The debris bed must be relatively homogenous.
- The approach velocity must be perpendicular to the flow.
- The debris accumulation, flow rate through the debris bed, the temperature, and the measured pressure differential across the bed must be relatively steady.
- The quantities of debris in the bed must be known.

When tests are conducted, care must be taken to minimize edge effects where a portion of the flow can leak through an edge gap between the debris bed and the test chamber.

Flow that bypasses the debris bed, such as edge leakage, or holes penetrating the debris bed reduce the debris bed flow velocity below that deduced from the flow instrumentation. A nonuniform bed can have shallow locations where water preferentially flows through the bed, thereby reducing the measured head loss.

Typically, in head-loss testing, debris is introduced into a closed loop test apparatus and then allowed to settle onto the test screen. Some debris, especially the particulate, can penetrate the screen and subsequently return to the screen after transiting the flow loop. The gradual filtration process of the finer particulate causes the pressure differential measurements to be initially transient. Therefore, sufficient time must be allowed to let the filtration become relatively steady-state before recording the test data point. The filtration process is such that the finest of the particulate is the most difficult to filter completely out of the flow, but the finer particulate has a greater impact on head loss on per mass basic than does the coarser particulate. The finest of the particulate might not be filterable under some conditions. All these considerations are taken into account when assessing the quality of the head-loss test data for application to determining correlation input parameters.

V.4.1.2 Parameter Deduction

The input parameters required by the NUREG/CR-6224 correlation include the following:

- debris quantities
  - quantity of fibrous debris expressed as the thickness of the debris on the screen assuming its nominal density before destruction (referred to as as-manufactured density)—equivalent to specifying its mass.
  - mass of particulate debris
- flow approach velocity
- temperature-dependent water properties
  - viscosity
  - density
- material specific surface areas
  - — fibrous debris
  - — particulate debris
- densities
  - material density of fibers in the fibrous debris
  - material density of the particulate
  - as-manufactured density of the fibrous insulation

- sludge density of the particulate (also referred to as the granular density or packing limit density)

- compression function coefficients (e.g., 1.3 and 0.38 for NUKON)

The experimental determination of a set of parameters for a specific debris bed would be performed along the following five steps:

(1) Select the appropriate head-loss test for each particulate parameter determination. When applying the correlation to the data from a particular test, the test parameters specify the approach velocity, the quantities of debris, and the temperature.

(2) Determine a set of densities for the debris bed test data. Manufacturer's data can often supply the densities, but if those data are not readily available, volume displacements for measured masses of debris can determine densities for typical debris. Bulk densities are determined from bulk displacements and material densities from water displacement.

(3) If possible, experimentally evaluate the compression function coefficients from test data where the particular fibrous debris is the only debris in the bed and the bed is thick enough to allow reasonable thickness measurements as a variety of velocities and bed thicknesses. Statistical analysis of the thickness data can determine the coefficients. If applicable thickness test data are not available, initially assume the coefficients validated for NUKON™ (i.e., $\alpha = 1.3$ and $\gamma = 0.38$).

(4) With these other parameters determined, as discussed, the remaining parameters are the specific surface areas for the fibrous and particulate debris. Starting with a fibrous debris bed without any particulate, adjust the specific surface area until the correlation reasonably bounds the data. The resultant specific surface area then applies to that particular fibrous debris. Note that other uncertainties are subsumed into the specific surface area.

(5) With the specific surface area for the fibrous debris determined, another test(s) is selected that uses that fibrous debris but also has the particulate under study. The specific surface area of particulate is adjusted until the correlation reasonably bounds the data. This specific surface then represents the specific surface area for the particulate.

The above procedure has developed a set of parameters from a set of tests. The quality of the recommended parameters is greatly improved by simulating as many tests as reasonably possible because the resultant parameters will vary somewhat from test to test. If the NUKON™ compression coefficients were initially assumed and do not reasonably apply to the fibrous debris in question, then the data analysis may need to vary these parameters. An example is the lead alpha coefficient (as proposed in GR Section 3.7.2.3.1.1) in steps 3, 4, and 5 in an attempt to align the parameter deductions from the specific tests into coherent set of parameters.

The evaluation should include thin-bed head-loss tests as well as mixed bed tests (i.e., the granular packing limit compression was not reached). The filtration efficiency can increase substantially when the flow must pass through a granular bed as opposed to a fibrous bed because of the reduced porosity. The determination of the particulate specific surface area should consider the worst-case particulate filtration.

V.4.1.3 Parameter Recommendations (Bounding)

The recommended correlation input parameters should ensure that the most severe head losses associated with a particulate type of debris bed are conservative enough to provide a bound prediction of the head loss associated with a particular postulated bed of debris. The recommendation should consider the uncertainties associated with head-loss testing (e.g., nonuniformities in the test debris bed could have reduced the measured head loss below that which would have been measured if the bed had been truly uniform). Other considerations include the potential variability in manufacturing processes of the debris. If, for example, parameters are recommended for calcium silicate debris, then it can be expected that those parameters will likely be universally used for any calcium silicate debris calculation. However, the recommendations should include a built-in safety factor because the manufacturing of calcium silicate varies with manufacturer, and even by a single manufacturer from one batch to another.

V.4.1.4 Ranges of Validated Parameters

The NUREG/CR-6224 correlation was developed and initially validated to support the resolution of the BWR strainer blockage issue. This development focused on validation of NUKON™ fibrous debris and iron oxide corrosion products. The insulation in the volunteer plant was NUKON™, hence the validation focused on NUKON™. For all BWRs, the dominant form of particulate was the corrosion products that formed and collected in the suppression pools. Therefore, the baseline validation compared the correlation results to head-loss tests using these two types of debris. In addition to the baseline, other validations were performed using other types of materials. A lesser amount of corrosion products is expected in a PWR containment than in a BWR containment. Therefore, the more likely particulates in a PWR containment will be latent particulate, coatings debris, and particulate insulation debris (e.g., calcium silicate).

Over the years, many analyses have applied the correlation to head-loss test data over various ranges of test data. These test programs typically explored the head loss until a judgment was made that the test encompassed the parameter space needed for a particular application. The maximum head loss tested was typically not larger than approximately 25 ft of water, primarily resulting from the limits of the test apparatus, which is generally sufficient for most applications.

Because most test apparatus were constructed of materials that were not able to reliably withstand the higher temperatures expected in a post-loss-of-coolant accident (LOCA) sump pool, the available test data does not extend the range of postulated sump temperatures. However, because the data on the effect of temperature-dependent water viscosity and density are available, it has been deemed acceptable to test at lower temperatures and then analytically extend calculations into the higher temperatures. However, this recommendation does not necessarily include the potential for debris decomposition at higher temperatures, which in some tests was factored into the tests by pre-aging the debris using techniques such as boiling the debris for a period to break down the binder. For other parameters, the correlation is not validated beyond the ranges of the test parameters tested. Care must be taken, in reviewing the data, to ensure that a significant gap in data does not exist within the validation range at a parameter that significantly affects the current application.

Table V-5 and Table V-6 list the specific validations for screens that function effectively as flat plates for fibrous and particulate debris, respectively. Section V.4.2 discusses validations that involved special geometries.

Table V-5. Validation Ranges for Fibrous Insulation Debris

Debris Type	Velocity (fps)	Temperature (˚F)	Debris Bed Thickness (in.)	Comments	References
NUKON™	0.15 to 1.5	60 to 125	1/8 to 4		NUREG/CR-6224 NUREG/CR-6367 NEA/CSNI/R (95)11 LA-UR-04-1227 SER Appendix V
Kaowool	0.3 to 0.62	~85	2		SER Appendix V
Transco Thermal-Wrap	0 to 0.5	129			NEA/CSNI/R (95)11
Mineral Wool	0 to 0.23	55 to 131	1.6 to 4		NEA/CSNI/R (95)11

Table V-6. Validation Ranges for Particulate Insulation Debris

Debris Type	Velocity (fps)	Temperature (˚F)	Particulate to Fiber Mass Ratio	Comments	References
Iron Oxide Corrosion Products	0.15 to 1.5	60 to 125	0 to 30	With 0 to 2-in. bed of NUKON™ or Kaowool	NUREG/CR-6224 NUREG/CR-6367 NEA/CSNI/R (95)11 SER Appendix V
Calcium Silicate	0.1 to 0.8	70 to 140	0.5	With NUKON™ 0.1 to 1.6 in. Few test to mass ratio up to 2	LA-UR-04-1227
Latent Particulate (surrogate)	0.1 to 0.5	70 to 140	1 to 40	With NUKON™ 0.2 to 2.3 in.	LA-UR-04-3970 SER Appendix V

The staff extended the applicable temperature range of the NUREG/CR-6224 head loss correlation as summarized below and described in detail in Attachment V-1. The acceptable operating conditions for flow through a sump screen are bounded by the operating containment pressure, the sump water temperature, and the pressure drop through the sump screen. The acceptable operating conditions require that no significant two-phase flow conditions exist in the region downstream of the sump screen. Consequently, the pressure downstream of the sump screen cannot fall below the saturation pressure at the sump water temperature, and no significant amount of noncondensible gas dissolved in the sump water can come out of solution. It is generally accepted that a pump will experience cavitation problems when its inlet void fraction exceeds about 0.03 (3%). Using 3% void fraction as the upper limit for acceptable conditions downstream of the sump screen, Figure 1 can be used to determine the maximum acceptable temperature for flow through a sump screen. This figure is used in the following fashion.

1. Identify the actual sump water temperature.
2. Identify the containment pressure.
3. Calculate the pressure drop through the sump screen.
4. Using the containment pressure and calculated sump screen pressure drop, read the maximum allowable sump water temperature off Figure 1.

5a If the actual sump water temperature is lower than the maximum allowable temperature, acceptable pump inlet conditions exist and the sump screen pressure drop calculation is acceptable.

5b If the actual sump water temperature is higher than the maximum allowable temperature, the void fraction at the sump screen exit exceeds 3% which indicates that pump cavitation is possible. This condition indicates that the sump screen pressure drop calculation in inapplicable.

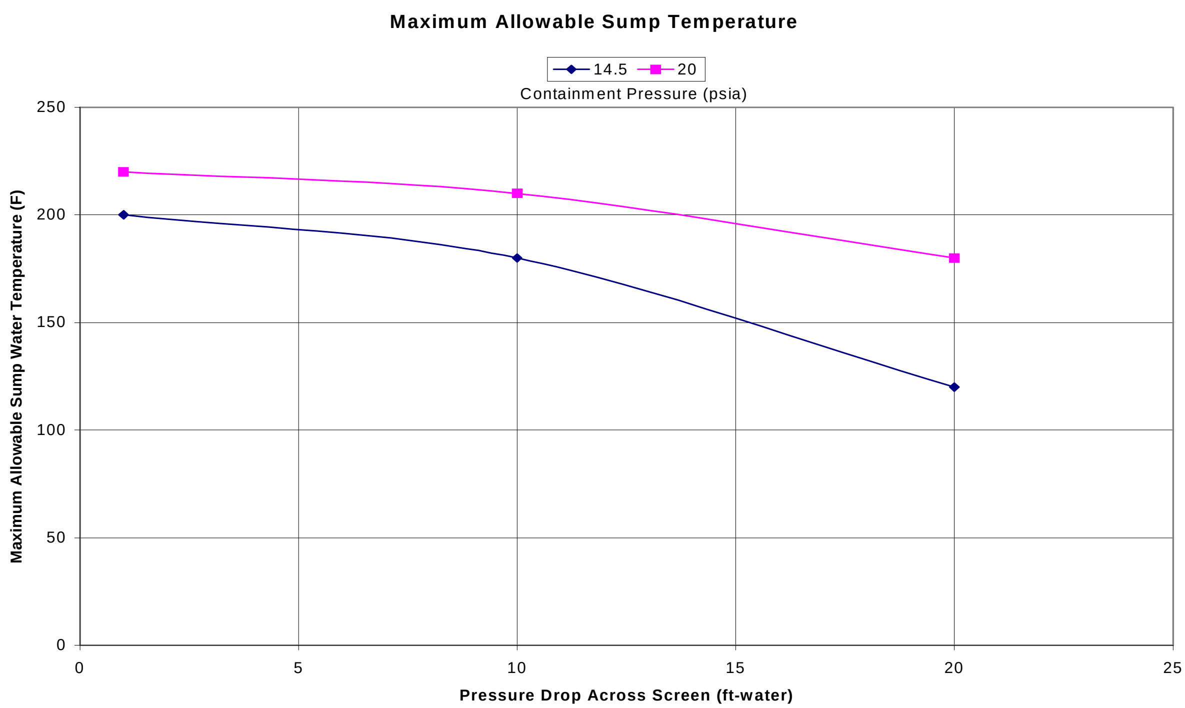

Figure V-7. Sump screen pressure drop versus maximum allowable sump water temperature for downstream void fraction < 3%.

V.4.2 Analytical Determination of Correlation Parameters

When test data are not available, the specific surface area may be calculated for some materials. For fibrous debris of low-density fiberglass in which the fibers have relatively uniform cross sections (e.g., NUKON™), the specific surface area can be reasonably estimated using the 4/d calculation. The extension of this relationship to fibrous insulations with fine fibers such as mineral wool has not been documented. Some evaluation is needed to generally accept the specific surface area of fiber as equivalent to 4/d. Until such a demonstration is documented, a significant safety factor should be factored into the specific surface area estimate to compensate the uncertainties.

The specific surface area particulate can be calculated using 6/d. For the NEI guidance assumption that coatings debris forms 10µm particulate, the use of 6/d is appropriate because the particles all have the same diameter. However, for a realistic particulate, the particle sizes vary over a wide range, typically from sub-micron to a few millimeters. If the size distribution is known in fine detail, a reasonable specific surface area can be estimated, but typically, the size distribution is specified by mass fractions associated with only three or foursize groups. The latent debris discussed in Section V.2.2 of this report is an example of coarse size distributions. Because the smaller particles contribute substantially more to the specific surface area than the coarser particles, using the mid-range size of each grouping results in estimates of specific area which is significantly smaller than the actual. Using the smaller diameter of each size group to calculate the specific surface area would result in a conservative estimate. However, the smallest diameter of the smallest size group, which corresponds to the finest particulate that can be filtered by the debris bed, depends upon several other factors. If too small a minimum particle size is estimated, the resultant specific surface area can become significantly larger than actual, leading to overly conservative head-loss estimates.

When applying the specific surface areas for the latent debris specific surface areas given in Section V.2.2, the value of 106,000 ft^{-1} applies to the entire recipe. If analytical refinement in a plant-specific analysis seeks to reduce the transport such that the larger particulate is assumed not to transport to the sump screens, thereby reducing the particulate mass in the debris bed, the 106,000 ft^{-1} specific area no longer applies. If, for example, only the particulate of diameter less than 75 µm is assumed to reach the screens, the appropriate specific surface area would be 285,000 ft^{-1}.

The above discussion on using 6/d to calculate the specific surface area of particulate applies to hardened particulate that does not change shape under debris bed pressures. For particulate consisting of materials that can deform (e.g., calcium silicate), special care must be taken because the 6/d specific area may not adequately represent the particulate behavior that has been demonstrated that causes the high head loss associated with calcium silicate.

V.4.3 Application to Special Strainer Geometries

Section 7.3.2.2 of NUREG/CR-6808 provides the application of the NUREG/CR-6224 correlation to a special strainer geometry of the stacked disk strainer. Several full scale or prototype scale test programs have been performed where the application has been validated.

V.4.3.1 Beginning and Ending Strainer Conditions

The correlation can be applied to the initial debris loading on these strainer designs by using the total screen area and the appropriate input parameter determined from flat screen head-loss testing or other means as discussed above. Then the correlation can be applied to the fully engulfed debris loading by assuming what has been referred to as the circumscribed screen area, which neglects the screen area within the gaps that has been completely filled with debris. In between, many analyses have assumed a linear extrapolation between the end conditions. Section V.4.3.2 discusses another alternative.

V.4.3.2 Experimentally Determined Effective Strainer Areas

The NUREG/CR-6224 correlation is applied to the head-loss test data using appropriate input parameters determined from flat screen head-loss testing or other means as discussed above. Developing the correlation to fit the data, which have a range of debris loading (from a clean screen to a fully engulfed screen), involves plotting the effective screen area versus debris loading. This plot can then be used to determine head losses for the design as a function of debris loading.

V.4.3.3 Special Strainer Geometries Testing and Validation

The NUREG/CR-6224 correlation was applied to Performance Contracting Inc. (PCI) stacked disk strainers and General Electric (GE) stacked disk strainers.

V.4.3.3.1 PCI Stacked Disk Strainer

Performance Contracting Inc. (PCI) designed, developed, and supplied advanced passive stacked-disk strainers to the nuclear industry that accommodated large volumes of insulation debris without substantial increases in the head loss. The PCI strainer concept, referred to commercially under the trademark Sure-Flow strainer, consists of a stack of coaxial, perforated metal plate disks that are welded to a common perforated internal core tube. The design maximizes the surface area of the perforated plate while keeping the size of the strainer to a minimum. The Sure-Flow strainer is not a standardized strainer i.e., one size fits all. Instead, the concept promoted by PCI is to use similarly designed strainer modules of various sizes and quantities as necessary for each plant.

PCI fabricated and tested prototypes to evaluate the head loss performance of the Sure-Flow strainers. The hydraulic performance testing was conducted at the EPRI NDE Center. One prototype, referred to as Stacked-Disk #1 in the URG, was a 40%-scale prototype with six disks, five troughs, between the disks, a 13-inch core tube, a 30-inch outside diameter, and was a 2.5-ft long. A larger prototype, referred to as Stacked-Disk #2, was a 4-ft long strainer with a core tube diameter of 26-inches and a stack outer diameter of 40-inches. For generic calculations of head loss performance, PCI team member, the Innovative Technology Solutions (ITS) Corporation, programmed the NUREG/CR-6224 resulting in a proprietary computer code named HLOSS whereby the correlation was extended to the stacked-disk strainer geometry.

The PCI head loss data is documented in the PCI report "Summary Report on Performance of Performance Contracting, Inc.'s Sure-Flow™ Suction Strainer with

Various Mixes of Simulate Post-LOCA Debris," dated September 1997. At the request of the NRC, LANL reviewed the PCI test data and evaluated the adequacy of the head loss models. The results of that review are summarized in LANL TER LA-UR-00-5159, entitled "Technical Review of Selected Reports on Performance Contracting, Inc. Sure-Flow Strainer™ Test Data,' dated April 27, 2000. The head loss testing used NUKON™ fibrous debris, with and without sludge, and RMI debris.

LANL applied the NUREG/CR-6224 correlation to the PCI strainer design and its head loss test data. The application involved varying the strainer screen area (as input to the correlation) until the correlation predicted the test head loss, thereby determining an effective screen area for the strainer at varying debris loadings (volumes of fiber). The resultant effective area varied between the total perforated plate area and the strainer projected area (referred to as the circumscribed area). At the beginning of debris accumulation, the entire strainer screen area would be used. When debris accumulation covers the entire strainer such that the spaces between the strainer disks are filled, the circumscribed area would be appropriate. The effective strainer screen area varies between these two limiting areas depending upon debris volumes accumulated. The effective screen area is essentially an equivalent flat plate area that results in the same head loss at a particular volume of debris accumulation when applying the NUREG/CR-6224 correlation to that particular strainer.

V.4.3.3.2 GE Stacked Disk Strainer

General Electric (GE) designed, developed, and supplied advanced passive stacked-disk strainers (proprietary) to the nuclear industry that accommodated large volumes of insulation debris without substantial increases in the head loss and where each GE strainer could be designed specifically to suit a particular plant application. The GE provided it application methodology in the Licensing Topical Report (LTP) [NEDC-32721P], "Application Methodology for GE Stacked-Disk ECCS Suction Strainer," dated December 23, 1998 (Proprietary). The NRC staff reviewed this methodology as documented in LANL Technical Evaluation Report LA-CP-99-7, "Technical Review of GE LTR NEDC-32721P: Application Methodology for GE Stacked-Disk ECCS Suction Strainer," dated December 23, 1998 (Proprietary). The GE application methodology included: 1) hydraulic performance design methodology and 2) procedures for calculating hydrodynamic loads for new strainer installations that can be used in the structural analysis of the torus penetration, the strainer supports, and the strainer itself. GE fabricated a prototype strainer and tested its hydraulic performance at the EPRI NDE Center using both NUKON™ fibrous debris and RMI debris. GE developed an empirical correlation for NUKON™ fiber and corrosion products mixtures applicable within a limited range of tested parameters. The NRC staff examined the application of the NUREG/CR-6224 correlation to the GE strainer design whereby the strainer area was varied with debris loading.

V.4.4 Procedures for Determining Correlation Parameters for Mixtures

Plant-specific debris beds will likely contain a mixture of debris types including multiple types of fibers and multiple types of particulate (e.g., NUKON™ and latent fibers and calcium silicate insulation debris and latent particulates) whereas most head loss testing has involved one type of fibrous debris combined with one type of particulate. Formulas were presented in Section V.3 for estimating effective parameters for mixtures. The effective parameters that need to be estimated for mixtures include the specific surface area, the bulk and material densities, and the coefficients for the compression function.

V.4.4.1 Mixture Specific Surface Areas

An equation was provided in Section V.3.1 to calculate the effective specific surface area for a mixture of debris. This equation can be applied to a mixture of fibrous debris, to a mixture of particulate debris, or to a mixture of fibrous and particulate debris combined. This equation simply performs a solid-volume averaging of the specific surface areas of each component of the mixture. Such an equation was recommended in NUREG/CR-6371. NEI GR Section 3.7.2.3.1.1 provides guidance for estimating specific surface area for mixtures that is based on volume averaging the square of the specific surface areas[*].

An exponent (n) was incorporated into the equation to accommodate both the NUREG/CR-6371 and the GR recommendations (i.e., n=1 for NUREG/CR-6371 and n=2 for the GR). Performing example-mixing evaluations demonstrated that using the square results in larger values for the mixture of specific surface areas than does using the linear relationship; therefore, it is conservative to use the square of the specific surface area in the mixing rather than the linear.

The staff recommends following the GR guidance of using the square (n=2) unless experimental data has established a value less than two but in no circumstances will the exponent be less than one. Note that the analysis of the surrogate latent debris testing (Section V.2.2) demonstrated that an exponent of 4/3 correlated (Section V.3.1) the data taken for the mixture with the data taken for the components.

V.4.4.2 Mixture Densities

Four densities are required in the application of the NUREG/CR-6224 correlation to a fiber/particulate debris bed. These include the bulk (as-manufactured) and material densities for fibrous debris and the bulk (sludge) and material densities for the particulate debris. Effective mixture densities must be determined for each of these four densities for debris containing more than type of fiber and/or more than one type of particulate. An equation is provided in Section V.3.2 that applies to each of these four densities. The NUREG/CR-6224 does not apply to coating debris in the form of significantly-sized paint chips. Inclusion of relatively minor quantities of paint chips can be performed by assuming the chips are decomposed into fine particulate (as recommended in the GR baseline methodology).

V.4.4.3 Compression Function Coefficients

The coefficients in the compression function that determines debris-specific compressibility of the debris bed may differ from one type of fiber to another. The coefficients documented in NUREG/CR-6224 were determined for NUKON™ and may or may not be valid for another type of fibrous debris. If the debris bed contains a

---

[*] The GR rationale for using the square was not provided. The GR reference points to NUREG/CR-6371 but this report does not recommend using the square of the specific surface area.

mixture of fibrous debris types (e.g., NUKON™ and mineral wool) then the compressibility may be based on a mix of two sets of coefficients. However, the correlation as now established does not accommodate multiple sets of coefficients and no guidance has been developed to facilitate such a determination.

The staff recommendation is to apply each set of coefficients to the head loss calculation individually and then used the worst case head loss as conservative. If however, the fibrous debris bed is clearly dominated by one type of fibrous debris (e.g., 99% NUKON™ and 1% latent) then it is acceptable to use the NUKON™ coefficients rather than the coefficients for the other 1% latent.

V.5 APPLICATION LIMITS OF NUREG/CR 6224 CORRELATION

The following three tier approach has been used to define the application limits of the NUREG/CR-6224 correlation.

1. Application limits inherent in the correlation due to assumptions and/or approximations implemented in the development of the correlation.
2. Application limits established by validating the correlation against head loss data applicable to specific test conditions (e.g., debris type, approach velocity, temperature, and bed thickness).
3. Application limits established by engineering judgment extensions of specific validations to more general parameter ranges.

The development of the correlation and supporting constitutive equations was based on previous correlation development work and basic assumptions. Therefore, the correlation does not apply for conditions beyond the conditions established during correlation development unless notable exceptions can be properly justified and validated. The developmental application limits are discussed in Section V.5.1. The most reliable method of establishing correlation applicability is to apply the correlation to head loss test data that was conducted with test parameter ranges that match the application parameter ranges. Validation for specific application-matching test conditions provides the reliability needed to support the relaxation of safety-related conservatisms required to ensure long-term recirculation. Existing validation studies are discussed in Section V.5.1.4.

The framework of NUREG/CR-6224 correlation was developed for a much wider application range than what the correlation is currently been validated. Therefore, additional validations can legitimately expand the current validation parameter ranges as needed, which is the responsibility of the licensees to perform. Validations for the complete range of each correlation input parameter would require extensive head loss testing due to the wide range of possible debris materials and quantities and mixture compositions for those types of debris, the variations in flow approach velocities, and water temperatures. The water temperature is a an example of a engineering judgment extension of existing validations. Difficulties associated with testing at the higher temperatures associated with postulated LOCA scenarios have kept the performance of head loss testing in temperature range of about 60 to 140 ^{o}F, whereas postulated temperatures in some scenarios approach the boiling point of water. Because the water temperature affects the head loss primarily due to the changing viscosity and density of the water, it has been considered through the years of testing that testing at practical temperatures could be applied to postulated scenario temperatures. Such engineering judgment extensions to specific validations are the subject of Section V.5.2.

V.5.1 Application Limitations Inherent in the NUREG/CR-6224 Correlation

The semi-theoretical/semi-empirical NUREG/CR-6224 head loss correlation combines hydraulic concepts with experimental data for flow through fibrous media. In addition to the primary equation of the correlation, constitutive equations for porosity, fiber bed compression, and compaction limiting are required to close the solution [NUREG/CR-6224 and NUREG/CR-6371]. The application of the correlation is limited to conditions that satisfy the assumptions inherent in the development of the correlation. Therefore, these assumptions place limitations on the application of the correlation. Special case exceptions to these limitations must be properly supported and validated.

First of all, the primary correlation and the constitutive compression equation were specifically developed for flow through a fibrous media and the constitutive equations for porosity and the compaction limiting provides the capability of simulating particulate embedded within the fiber matrix. Therefore, the correlation is not applicable to debris types that effectively behave like sheet material that partially block a portion of the screen, such as metallic foils, tags, tape, or large paint chips. The correlation is generally applicable to any type of fibrous debris typically in use in PWR and BWR containment provided the correlation input parameters for that type of fiber material have been determined and properly validated. These parameters include the bulk and material densities, the specific surface area, and the coefficients for the fiber compression function that determines fibrous bed compaction due to flow-driven pressure gradient on the bed. The compression coefficients documented in NUREG/CR-6224 were validated for debris formed from the destruction of a low-density fiberglass insulation known as NUKON™ debris with beds thicknesses less than 4-inches thick. (For NUKON fiber material?)

The porosity and compaction limiting equations that integrate the effects of the particulate with the effects of the fibrous debris are based on hardened particles that do not deform under pressure. As such the particulate bulk and material densities and specific surface area are constants. The same constancy is also assumed for the fibers. Particulate, such as pieces of soft rubber debris, could deform under pressure and therefore not behave as was assumed in the development of these constitutive equations and therefore are not generally suitable for the application of this correlation. Further, the development of the constitutive equations assumed the particles to be small enough to fit between the fibers without significantly impacting the behavior of the fiber matrix and the particles have generally been assumed to be somewhat spherical in nature. Coatings debris in the form of fine particles is acceptable to the correlation but significant quantities of larger paint chips are outside the limitations of the correlation unless applicable testing is performed that demonstrates otherwise. The use of the GR recommended postulated 10-micron coating particles are within the correlation limitations. Applicable test data is required to determine the boundaries on paint chip dimensions that fit within the applicability of the correlation.

Because the correlation was developed for a one-dimensional flow through the debris bed, the correlation applies to debris beds of uniform thickness with the flow entering perpendicular to the surface of the bed. However, from the standpoint of predicting conservative head losses across the debris bed, applying the correlation to a nonuniform bed will overpredict the head loss for the non-uniform bed. Hence, for safety evaluations, it is acceptable to apply the correlation to a non-uniform debris bed. As an example, at high pressure differentials, channeling has been observed where 'bore holes' have formed in the bed such that substantial flow effectively bypasses the debris. In such cases, the measured head losses are substantially less than those predicted assuming a uniform bed, i.e., the predictions are conservative but may not be realistic.

The NUREG/CR-6224 correlation was developed for a homogenous debris bed, i.e., the mixture concentrations are constant throughout the depth in the debris bed. Therefore, the correlation cannot typically be directly applied to a stratified debris bed. In a thin-bed debris bed (discussed in detail in Appendix VIII), the mass of the particulate for most particulates (e.g., latent particulate typically consisting of sand and dirt) is much larger than the fiber mass. Therefore, a thin-bed can be a stratification that occurs with a modest quantity of fibrous material supporting a layer of particulate and it has been successfully simulated with the correlation. Analytically, in such a bed, the effects of the fiber are minor relative to the effects of the particulate; therefore the particulate layer dominates in the correlation. The debris bed in a thin-bed starts to approach the behavior of a layer of particulate. The correlation in that mode predicts a porosity that approaches that of the particulate in its bulk or sludge form; predicts a bed thickness that approaches that of the sludge without fiber, and the specific surface area approaches that of the particulate. Noting that the primary correlation was based on fibrous media but now being applied to a particulate media, it is even more important that the correlation be properly validated for the thin-bed based on each specific particulate, which has been done for a few particulates (e.g., surrogate latent particulate, see Sections V.2.2 and VIII.4).

For debris stratification within a mixed debris bed (with substantial quantities of fibers), the application of the correlation requires special handling. Assuming the stratification can be treated as stacked uniform layers, the head loss across each layer can be evaluated separately and then the head loss contributions summed to get the total head loss. For the upper layer, the correlation can be directly applied assuming this layer is compatible with the other noted limitations. For a layer of particulate, the application can be applied in the same manner as the thin-bed where the layer in based on the particulate sludge density (i.e., compression is not an issue for this layer). However, the correlation cannot be applied to a fibrous layer that has been compressed by the forces from an upper layer. The constitutive compression equation does not have a term to represent the externally applied force; hence the compression for this layer and the associated head loss would be underpredicted. The evaluation of a stratified debris bed in a plant-specific evaluation will require either the analytical application of a demonstrated-conservative compression ratio for this layer or appropriate experimental data.

The NUREG/CR-6224 correlation does not simulate the filtration of particulate from the flow. It is assumed that the particulate mass specified as an input parameter is embedded in the debris bed in a homogeneous manner. Filtration is a complicated process that depends upon the particle sizes, interfiber spacing, and number of passes that the particles may take through the bed in a recirculating system and has not been successfully modeled analytically. It is conservative to assume complete filtration even though some of the finest particulate may continue to pass through the bed.

The NUREG/CR-6224 correlation was developed for single phase incompressible flow; either laminar or turbulent flow. Although the form of the primary correlation may well be appropriate for compressible flow, as well, the sump screen blockage issue does not involve compressible flow, therefore no attempt has been made to make the correlation applicable to compressible flow. The correlation is only applicable to single phase flow (water being the only application for the sump screen blockage issue) due to the basic hydraulics and single phase experimental data used to develop the correlation.

At higher sump blockage application temperatures, it may possible that voiding could occur in the debris bed as the pressure drops across the bed. Based on analyses presented in Attachment V-1 "NUREG/CR-6224 Head Loss Calculation Temperature Assessment," it was reasoned that an exit void fraction of 3% or less is acceptable for the application of the correlation. If a head loss evaluation determines a debris bed pressure drop high enough that the flow exiting the debris bed has a void fraction that exceeds 3%, then the correlation is not applicable to that evaluation.

The NUREG/CR-6224 correlation was developed for steady state flow conditions, i.e., transient behavior is not simulated. If a flow rate or sudden change in debris bed composition occurs, the correlation is not valid again until a relatively quasi-steady-state in again achieved. For example, the compression behavior following a substantial addition to the debris bed would lag behind the transient accumulation. The use of 'quasi' reflects on the fact that a debris bed may be slowly changing or there may be small pulsations in the flow that change slowly enough that effectively there is no significant transient behavior. A transient estimate of head loss would occur on a time scale such that the head loss at any given time would correspond to quasi-steady-state.

Most head loss testing has been performed using one type of fiber and one type of particulate in a given test. In reality, a sump screen debris bed is likely to contain multiple types of debris. For example, NUKON™ insulation debris combined with latent fibers and latent particulate combined with calcium silicate particulate. Simple supporting equations are used to volume or mass average correlation input parameters (as appropriate) to obtain parameters applicable to the mixture (see Section V.3). Note application limitations apply to mixtures, as well as, individual constituents.

The SER recommendations for applying the NUREG/CR-6224 correlation to thin-bed debris beds with calcium silicate contain exceptions to the application limits to the correlation that are based on experimental test data. First, there is microscopic experimental evidence that calcium silicate particles are not hardened (due to voiding internal to the particles) in that under pressure the particulate may deform somewhat such that the constituent porosity equation is not entirely accurate for this material. For mixed debris beds, it is apparent that the particulate would not deform but in thin beds where the particles interact under pressure, deformation may occur. The approach used in the SER thin-bed guidance for calcium silicate was established as a bounding approach rather than a realistic simulation of the calcium silicate behavior. This application limitation exception was based on applicable test data.

In the second calcium silicate exception, there is a possibility that calcium silicate could accumulate on a sump screen without any supporting fibrous debris, other than the fibers inherent to calcium silicate. That is, the fibers in the calcium silicate could be sufficient to support its particulate. Note that it has been the practice to assume that all of the calcium silicate was particulate rather than attempt to separate the components.

In an unlikely scenario where a plant can justify that no significant quantities of fiber are in containment (either latent or insulation) but the plant has significant calcium silicate, then a calculation of calcium silicate only on the sump screen may be needed (see Appendix VIII.7 for more detail). In this case, the NUREG/CR-6224 primary correlation is applied without fiber by specifying calcium silicate parameters for specific surface area and porosity and a non-compactable debris bed of calcium silicate with a thickness based on the bulk density of the calcium silicate. The success of this second exception is again based on experimentally determined recommendations designed for bounding calculations and that included a safety factor.

The application of the correlation to special geometry strainers (e.g., the stacked disk strainers) has been accommodated by deducing an effective screen area by applying the correlation to appropriate test data. As such, the debris-specific effective area varied from the total screen area down to a circumscribed area depending upon the loading of debris on the strainer. Once this area curve is determined, it can subsequently be applied to that particular strainer design to estimate plant-specific head losses as a function of the evaluated debris loading, as well as, the other parameters (discussed in Section V.54.3). In this manner, the effects of non-uniform debris accumulation are subsumed into an effective curve that represents a specific strainer design for a specific type of debris based on strainer-specific testing.

Perhaps,The greatest challenge with regards to the application of the NUREG/CR-6224 correlation to the resolution of the PWR sump screen blockage issue is the variety of debris materials available in the fleet of PWR containments. Existing head loss testing has focused on a relatively few of these materials and there is little if any head loss data for several materials. Filling in the gaps will requiresd additional applicable head loss testing to determine the appropriate parameters for these materials where data does not exist. An example is MinK, which is a particulate insulation material similar to calcium silicate, perhaps with even more severe head loss behavior. Head loss data does not currently exist to evaluate thin-bed behavior for Min-K debris.

In summary, the NUREG/CR-6224 correlation applies to one-dimensional single-phase incompressible quasi-steady-state flow through debris beds consisting of fibrous material with or without embedded particulate (no sheet type materials) that has accumulated uniformly and homogenously. An applicable particulate consists of hardened materials (non-deformable particles) that fit embedded among the fibers without significantly impacting the behavior of the fiber matrix. Complete filtration of the particulate from the flow is assumed. Certain applications beyond these conditions are known to predict conservative head losses, which may be satisfactory for safety analyses but may not be realistic (e.g., applying the correlation to a non-uniform debris bed). In certain plant-specific conditions, the correlation may be applied layer-by-layer to a stratified bed using special handling with the primary difficulty being the application to a compressible inner fiber layer where an external force is applied to that layer. Based on supporting analyses, it has been reasoned that voiding in the flow exiting the debris bed is acceptable provided that voiding does not exceed 3%. Other exceptions to the inherent limitations of the correlation must be properly validated to demonstrate that the head loss predictions are suitably conservative (or bounding) to that application, e.g., the application to thin-bed debris beds containing calcium silicate where there is microscopic experimental evidence that calcium silicate particles are not hardened (due to voiding internal to the particles).

V.5.2 NUREG/CR-6224 Correlation Application Limitations Based on Validation

This section describes the establishment of application limits by engineering judgment extensions of specific validations to more general parameter ranges. Section V.5.1 describes the application limitations inherent in the NUREG/CR-6224 correlation due to the constitutive correlations and assumptions used in the development of the NUREG/CR-6224 correlation. Within these inherent limitations, the application of the correlation is necessarily limited to the validation of the correlation against applicable test data to ensure conservative head loss predictions. Parameters ranges associated with current validations are discussed in Section 5.1.4. The NUREG/CR-6224 correlation was developed for a much wider application range than has currently been validated. Therefore, additional validations can legitimately expand the current validation parameter ranges as needed. It is the responsibility of the licensee to provide necessary validation when applying the correlation using parameters beyond the parameter ranges of the current validations.

The parameters that are required to apply the correlation to a particular debris bed scenario include:

1. The water temperature that determines the viscosity and water density,
2. The approach velocity,
3. The area of the sump screen or strainer,
4. The quantities of fiber and particulate debris by debris type,
5. The bulk density for each type of fiber (as-manufactured) and each type of particulate (sludge) debris,
6. The material density for each type of fiber and each type particulate debris,
7. The specific surface area for each type of fiber and each type of particulate debris, and
8. The coefficients for the fiber bed compression function for fibrous debris that controls the bed compression.

The sump screen or strainer area is not an independent variable, i.e., it is used to calculate the flow velocity when the flow rate is specified and to calculate the debris bed thickness from the specified debris quantities. Therefore no application limits are applied to the screen area other than it cannot be zero. Rather, the application limits are applied to the flow velocity and the debris bed thickness. Several of these parameters (i.e., bulk and material densities, specific surface areas, and compression function coefficients) are associated with the particular type of debris. Therefore, the application limits are discussed in relation to debris types and no specific limits are applied to these specific parameters.

<u>Application Limits on Types of debris</u> The most severe limitation to the application of the NUREG/CR-6224 is the limited head loss test data for many of the debris types associated with PWR containment. Some engineering judgment extensions of existing validation are reasonably based on similarities with debris types where substantial testing and validation are available. For example, Transco fibrous insulation is very much like NUKON™, which has been tested and validated extensively with noted parameter application limits. Therefore, it is reasonable to extend the validation for NUKON™ fibrous insulation debris to Transco fibrous insulation debris. These two insulations are so similar that their associated densities and specific surface areas have been treated identically. This same engineering judgment extension cannot be applied

to dissimilar debris such as mineral wool, which is very different than NUKON™. However, a lesser engineering judgment extension may be reasonably applied where the bed thickness for a dissimilar material is extended to 4-inches provided existing head loss data has been validated for this dissimilar material over a reasonable portion of this thickness range. It is specifically noted that the compression function coefficients for the correlation (i.e., $\alpha = 1.3$ and $\gamma = 0.38$) were established for NUKON™ and may therefore not be applicable for another type of fibrous debris. For example, confirmatory research in Section V.1.2 indicated that α of 0.5 is more appropriate for Kaowool than a value of 1.3. The application of the correlation compression function requires the validation of the compression function to types of fibrous debris grouped by similar characteristics over the applicable range of bed thicknesses. This validation optimally would apply the compression function directly to bed thickness data taken at various bed compressions or less optimally, the application of the entire correlation including its constitutive equations to applicable head loss data.

CalSil debris has its own unique behavior during the compression process due to its compressible particulate content. The confirmatory tests performed so far only provides reasonable assurance that the NUREG/CR-6224 can be used as a scoping tool to calculate the pressure drop across a CalSil debris bed. Therefore, the correlation and the applicable application procedures can not be used to design a sump involving CalSil debris. Licensees will have to use other verifiable methods to calculate the pressure drop across a CalSil debris bed.

<u>Application Limits on Water Temperature</u> Head loss testing has been performed in the range of about 60 to 140 ^{o}F but sump pool temperatures in postulated LOCA scenarios may approach the boiling point of water at atmospheric pressure or possibly higher if over-pressure credits are granted. Testing at higher temperatures would require more costly high-temperature equipment than has been typically used in head loss testing and pump cavitation would occur at relatively low head losses. Because the water temperature affects the head loss primarily due to the changing viscosity and density of the water, it has been consider through the years of testing that testing at practical temperatures could be applied to postulated scenario temperatures. It is a engineering judgment extension that the correlation is applicable to a temperature range that allows the water to remain liquid provided one of the following two qualifiers is not encountered. The correlation was specifically developed for single-phase liquid water flow; therefore the correlation cannot be applied if significant vaporization occurs. It was reasoned (Attachment V-1) that an exit void fraction of 3% or less is acceptable for the application of the correlation. The correlation is also not applicable if the higher temperatures cause the debris bed to destruct or deform due to heating of the debris, as opposed to simple pressure-driven compression. Because insulations typical of PWR containment are subjected to operational temperatures for long periods that exceed the sump pool water temperatures, it is reasonable to assume fibrous debris from such insulations can be subjected to sump pool water temperatures without undergoing significant temperature-driven deformation. With the structural properties of the fibrous debris being the primary concern with this qualifier, it is unlikely that the fibers would be significantly deformed due to the water temperature (note that temperature enhancement of potential chemical deformation of the fiber is not addressed here). However, before the high temperature application limit is used, the licensee should access the potential temperature effect for each plant-specific debris type.

Application Limits on Approach Velocity Head loss testing has been typically performed in the 0.1 to 1.5 ft/sec range. Many PWR plants currently have approach velocities less than 0.1 ft/sec and sump screen blockage resolutions will most likely result in many more plant justifying an approach velocity less then 0.1 ft/sec. At these low velocities, the first term in the correlation that is strictly a function of the velocity is expected to be as valid at 0.01 ft/sec as it is at 0.1 ft/sec. Therefore, the NUREG/CR-6224 correlation is expected to be valid at velocities approaching zero if it has been validated at a velocity of 0.1 ft/sec. At the other end of the range, if the correlation is validated at 1.5 ft/sec, it is expected that it is still valid at 2 ft/sec, which is as high as the maximum current plant approach velocities [computed using plant-specific data documented in NUREG/CR-6762]. In conclusion, if the correlation has been validated over a reasonable portion of the velocity range for each particular debris type, then it is considered valid for velocities ranging from 0 to 2 ft/s.

Application Limits on Debris Bed Thickness The thickness of a bed of debris depends upon the quantities of fibrous debris and the area of the sump screen. For thin-bed formations with large quantities of particulate, the bed thickness may be determined by the mass of the particulate, its bulk (sludge) density, and the screen area in combination with the fibrous debris. The thickness of debris beds that have been validated range from approximately 1/8 to 4 inches and these validations focused on NUKON™ insulation debris. For other types of fibrous debris, the testing and validation range has been in some cases substantially less than that of NUKON™. A engineering judgment extension is that if particular fibrous debris has been validated over a reasonable portion of the 1/8 to 4-inch range, then the correlation can be applied to this entire range. The validation of the bed thickness is interrelated to the validation of the compression function coefficients discussed above. The application limit of 4-inches may well increase should subsequent head loss testing with thicker debris beds justify the increase. An exception to the 1/8-inch minimum bed thickness is debris beds containing significant particulate insulation debris (e.g. calcium silicate) where the correlation is applied to debris beds less than 1/8-inch (refer to Section VIII.7).

Application Limits on Head Loss The NUREG/CR-6224 correlation does not have any inherent head loss limits on its application, therefore it head loss application limits depends upon validation against specific head loss data. Typical valid head loss data does not exceed approximately 20 ft-water because debris beds tend to disrupt whenever the head loss become excessive, e.g., bore-holes may form in the bed to relieve pressure. Establishing an upper application limit on the head loss of 20 ft-water is somewhat arbitrary but it does provide a boundary for validations to avoid unnecessary validation efforts since realistic NPSH availabilities at PWR will not allow debris bed head losses exceeding this value. Related to the maximum head loss is whether or not a maximum application limit on the particulate to fiber mass ratio should be established. Valid head loss testing has been performed at ratios up to about 40 and other testing has been performed at even higher ratios where bed disruption occurred due to excessive head losses. The difficulty with establishing some sort of ratio limitation is that the limit is so dependent upon the type of particulate (the ratio would be much lower for calcium silicate than it would be for latent particulates) and would be based on when head losses caused bed disruption. Hence, an application limit on head loss also effectively limits the mass ratio.

The application limits discussed in this section are summarized in Table V-7.

Table V-7. Application Parameter Limits and Ranges

Parameter		Current Correlation Validation Limits	Validation Limits Extensions Based On Engineering Judgment	Extension Qualifiers
Types of Debris	Fiber	NUKON TRANSCO	Similar to Types of Debris with Substantial Validation	Must be either very similar or a significant validation subset is available.
	Particulate	Iron Oxide Corrosion Products		
		Latent Particulate	NUREG/CR-6224 is only good for scoping analysis. Licensees will have to use other verifiable methods to calculate the pressure drop across a CalSil /Latent debris bed.	
		CalSil		
Water Temperature		60 to 140 ^{o}F	32 to 212 ^{o}F	Exit voiding less than 3%. No significant structural deformation to debris bed.
Approach Velocity		0.1 to 1.5 ft/sec	0 to 2 ft/sec	Correlation must be validated over a reasonable portion of this velocity range for each particular debris type.
Fibrous Debris Bed Thickness		1/8 to 4 inches for limited fibrous debris types	1/8 to 4 inches for all type of fibrous debris	Correlation must be validated over a reasonable portion of this bed thickness range for each particular debris type.
Head Loss		0 to ~20 ft-water	No Extensions	

Table V-7 covers the applicable parameter ranges of the correlation. Any extensions beyond its defined ranges require further validations and justifications. If a licensee decides to perform more validation tests, 10CFR50 Appendix B requirements need to be followed.

V.6 References for Appendix V

(LA-UR-04-1227, 2004b) Shaffer, C. J., et al., “GSI-191: Experimental Studies of Loss-of-Coolant-Accident-Generated Debris Accumulation and Head Loss with Emphasis on the Effects of Calcium Silicate Insulation,” Los Alamos National Laboratory, LA-UR-04-1227, April 2004.

(LA-UR-04-3970, 2004a) Ding, M., et al., “Characterization of Latent Debris from Pressurized-Water-Reactor Containment Buildings,” Los Alamos National Laboratory, LA-UR-04-3970, June 2004.

(NUREG/CR-6224, 1995) NUREG/CR-6224, “Parametric Study of the Potential for BWR ECCS Strainer Blockage due to LOCA Generated Debris,” October 1995.

(NUREG/CR-6371, 1996) Shaffer, C., W. Bernahl, J. Brideau, and D. V. Rao, *BLOCKAGE 2.5 Reference Manual*, NUREG/CR-6371, U.S. Nuclear Regulatory Commission, December 1996.

ATTACHMENT V-1. NUREG/CR-6224 HEAD LOSS CALCULATION TEMPERATURE ASSESSMENT

In support of General Safety Issue (GSI)-191, "Potential Impact of Debris Blockage on Emergency Recirculation During Design-Basis Accidents at PWRs", a sensitivity study has been performed to determine the appropriate range of temperatures for applying the pressure drop correlation obtained from NUREG/CR-6224 across a debris blocked sump screen of a pressurized water reactor (PWR) containment. The sensitivity study is intended to address operating and calculational conditions which are beyond the range of testing. Specifically, the objective of this study is to recommend an acceptable application range for pool water temperature.

Testing to measure the pressure drop across a debris blocked sump screen was performed at temperatures between ~70 and ~140ºF. The conditions for sump pump operation should correspond to the containment pressure and water temperature that exist at and after the start of the recirculation phase. The following tables, which were obtained from NUREG/CR-6808, provide a more realistic picture of containment and sump conditions for typical PWR large dry and ice condenser containments at the start of the post-LOCA recirculation phase. It should be noted that the actual plant requirements exceed the tested temperature conditions.

Table 1: Typical PWR Large Dry Containment Conditions After Start of Recirculation

	Large Break LOCA			Medium Break LOCA			Small Break LOCA		
	recirc start			recirc start			recirc start		
Time after start of LOCA	27 min	2 hr	24 hr	57 min	2 hr	24 hr	3 hr	12 hr	24 hr
Containment pressure (psig)	7	1.5	0	3	4.2	1.5	3	1	0.75
Containment temperature (°F)	163	115	95	140	148	120	140	115	110
Pool temperature(°F)	187	125	100	145	147	125	150	125	118

Table 2: Typical PWR Ice Condenser Containment Conditions After Recirculation Start

	Large Break LOCA			Medium Break LOCA			Small Break LOCA		
	recirc start			recirc start			recirc start		
Time after start of LOCA	17 min	2 hr	24 hr	57 min	2 hr	24 hr	35 min	5 hr	24 hr
Containment pressure (psig)	4.5	3	2	4	1.8	1.4	4.2	2.25	1.8
Containment temperature (°F)	105	98	100	110	87	90	110	92	95
Pool temperature(°F)	159	148	126	146	117	104	137	120	114

The NUREG/CR-6224 head loss correlation is an empirically derived equation which is dependent on water properties, flow velocity, and debris properties. Only the water properties exhibit large changes in value as a function of temperature. Using the recommended bounding calculational debris properties from LA-UR-04-1227, pressure drop calculations across a clogged screen with varying amounts of Nukon and

Nukon/CalSil were performed for different approach velocities and water temperatures. It can be concluded that the calculated pressure drop decreases with increasing temperature. The pressure drop decrease is primarily attributed to the reduction in water viscosity with increases in temperature. Therefore, assuming that the head loss relation correctly accounts for the fluid properties and that the debris properties and characteristics do not change with temperature, the head loss calculation should be able to be applied to a wide range of water temperatures as long as the appropriate fluid properties are used.

The NUREG/CR-6224 pressure drop correlation was developed to calculate one-phase pressure drop, and has not been validated and cannot be applied to two-phase flow conditions. Pressure drop can significantly increase with two-phase flow. Two-phase condition can result from two causes. As pressure decreases downstream of the screen, noncondensible gas dissolved in the water can come out of solution and/or hot water can flash into steam. Either or a combination of these two phenomena can result in two-phase flow with increased pressure drop.

In order to prevent water flashing, the pressure downstream of the sump screen must always remain above the saturation pressure at the sump water temperature. Calculations have been performed to estimate the point at which significant void fraction is created downstream of the sump screen as a result of air coming out of solution or as a result of liquid flashing. The release of air from solution can produce nucleation sites which can increase the possibility of steam formation and flashing. A sensitivity analysis was performed during which the water upstream of the sump screen is assumed to contain the maximum amount of dissolved air for a range of water temperatures and containment pressures. The maximum dissolved air mass in subcooled water is determined from the information on air equilibrium concentration contained in reference 4. Assuming homogeneous conditions, the void fraction downstream of the screen is calculated for different sump screen pressure drops, and upstream temperature and pressure conditions. Figures 1 and 2 plot the downstream void fraction as a function of water temperature for two containment pressures and three assumed sump screen pressure drops. It is assumed that the excess air above the saturated air condition downstream of the sump screen is immediately released as gas. This study reflects the requirement that the pressure downstream of the screen remain above the saturation pressure at the sump water temperature.

The study results indicate that the condition at which a significant void fraction occurs downstream of the sump screens is dependent on containment pressure and sump water temperature. It should be stated that the NUREG/CR-6224 head loss equation is not appropriate for calculating pressure drops which result in large downstream void fractions. However, the void fraction which can result in pump cavitation problems is very low and within the range of application of the correlation and testing. It is generally accepted that a pump will experience cavitation problems when its inlet void fraction exceeds about 0.03 (3%) (Reference 5). Using a 3% void fraction limit for conditions downstream of the sump screens, the sensitivity study identified the acceptable sump pool temperature operating range. Table 3 and Figure 3 illustrate the relationship between the maximum allowable sump pool temperature, containment pressure and sump screen pressure drop. The recommended temperature value reflects the inclusion of a conservative margin of at least 5ºF. Because the void fraction assessment was performed for a range of assumed sump screen pressure drops, the results provided can be applied to any sump screen pressure drop calculational method including the NUREG/CR-6224 correlation.

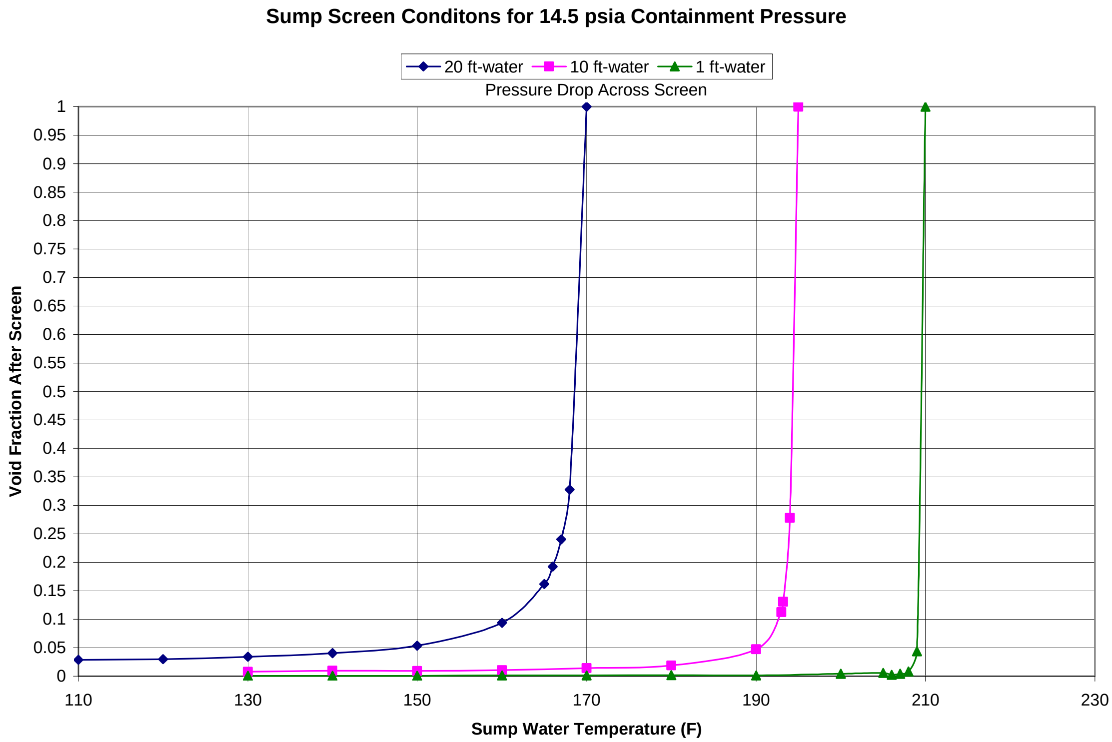

Figure 1: Downstream Void Fraction Versus Water Temperature at 14.5 psia

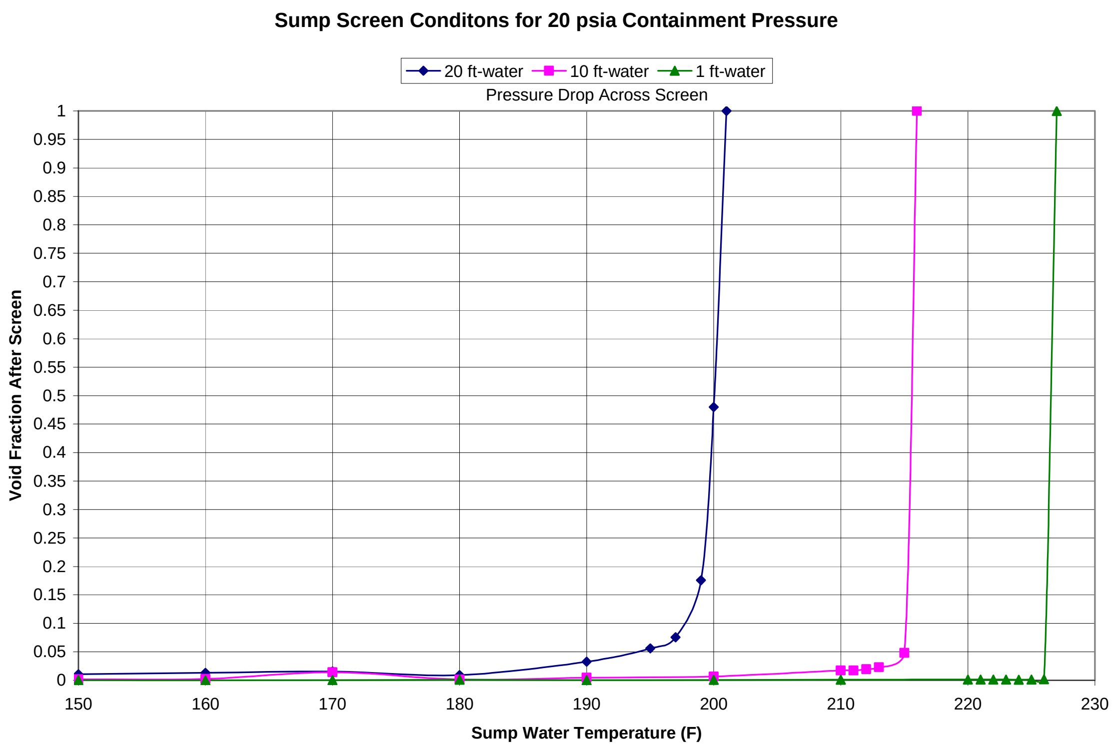

Figure 2: Downstream Void Fraction Versus Water Temperature at 20 psia

Table 3: Acceptable Range of Sump Pool Water Temperature

Containment Pressure (psia)	Pressure Drop Across Sump Screen (ft-water)	Acceptable Sump Pool Water Temperature (ºF) for Void Fraction < 0.03
14.5	1	< 200
14.5	10	< 180
14.5	20	< 120
20	1	< 220
20	10	< 210
20	20	< 180

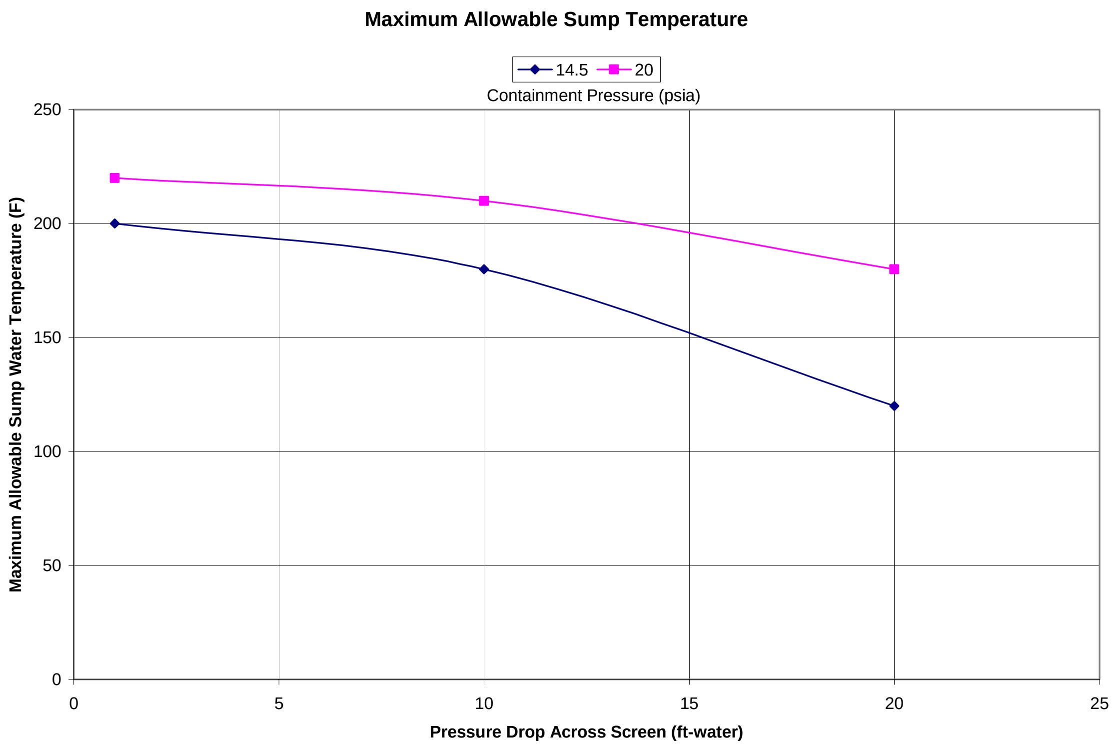

Figure 3: Screen Pressure Drop Versus Maximum Allowable Sump Water Temperature for Downstream Void Fraction < 0.03

References

1. “Parametric Study of the Potential for BWR ECCS Strainer Blockage Due to LOCA Generated Debris,” U. S. Nuclear Regulatory Commission, NUREG/CR-6224, October 1995.
2. “GSI-191: Experimental Studies of Loss-of-Coolant-Accident-Generated Debris Accumulation and Head Loss with Emphasis on the Effects of Calcium Silicate Insulation,” Los Alamos National Laboratory, LA-UR-04-1227, April 2004.

3. “Knowledge Base for the Effect of Debris on Pressurized Water Reactor Emergency Core Cooling Sump Performance,” U. S. Nuclear Regulatory Commission, NUREG/CR-6808, February 2003.
4. “Contribution to the Theory of Two-Phase Blowdown Phenomenon,” Hutcherson, M. N., Argonne National Laboratory, ANL-75-82, December 1975.
5. *Centrifugal Pumps – Design and Application*, Lobanoff, V. S. and Ross, R. R., Gulf Publishing Company, 1992.

Appendix VI

Detailed Blowdown/Washdown Transport Analysis for Pressurized-Water Reactor Volunteer Plant

VI.1 Introduction

In the event of a loss-of-coolant accident (LOCA) within the containment of a pressurized-water reactor (PWR), break-jet impingement will dislodge piping thermal insulation and other materials in the vicinity of the break. The steam/water flows induced by the break and containment sprays (CSs) will transport a fraction of this fragmented and dislodged insulation and other materials, such as chips of paint, paint particulates, and concrete dust, to the containment floor. Some of this debris eventually will transport to and will accumulate on the recirculation sump suction screens. Debris accumulation on the sump screen may challenge the sump's ability to provide adequate, long-term cooling water to the emergency core cooling system (ECCS) and to the CS pumps. The Generic Safety Issue (GSI)-191 study, "Assessment of Debris Accumulation on PWR Sump Performance," addresses the issue of debris generation, transport, and accumulation on the PWR sump screen and its subsequent impact on ECCS performance. The GSI-191 study examined whether debris accumulation in containment following a postulated LOCA would prevent or impede the performance of the ECCS. Los Alamos National Laboratory has been supporting the U.S. Nuclear Regulatory Commission (NRC) in the resolution of GSI-191.

Analytical studies were performed and small-scale experimental programs (NUREG/CR-6772, 2002; NUREG/CR-6773, 2002) were conducted to support the resolution of GSI-191. A parametric evaluation of the U.S. PWR plants demonstrated that potential sump-screen blockage was a plausible concern for operating PWRs (NUREG/CR-6762, Vol. 2, 2002). As part of the GSI-191 study, a U.S. PWR plant was volunteered and selected for a detailed analysis to develop and demonstrate a methodology for estimating the debris-transport fractions within PWR containments using plant-specific data. This report documents the blowdown and washdown transport portion of the study, describes the methodology, and provides an estimate for the transport of debris from its points of origin to the sump pool. The transport analysis consisted of (1) blowdown debris transport, where the effluences from a high-energy pipe break would destroy insulation near the break and then transport that debris throughout the containment, and (2) washdown debris transport caused by the operation of the CSs. Along the debris-transport pathways, substantial quantities of debris came into contact with containment structures and equipment where that debris could be retained, thereby preventing further transport. The blowdown/washdown debris-transport analysis provides the source term for the subsequent sump-pool debris-transport analysis.

The volunteer plant has a large, dry, cylindrical containment with a hemispherical dome constructed of steel-lined reinforced concrete and having a free volume of approximately 3 million ft^3. The nuclear steam supply system is a Westinghouse reactor with four steam generators (SGs). Each of the SGs is housed in a separate compartment that vents upward into the dome. Approximately two-thirds of the free space within the containment is located in the upper dome region, which is relatively free of equipment. The lower part of the containment is compartmentalized. The internal structures are supported independently so that a circumferential gap exists between the internal structures and the steel containment liner. Numerous pathways, including the circumferential gap, interconnect the lower compartments. The CS system has spray train headers at four different levels; however, approximately 70 percent of the spray nozzles are located in the upper dome. The spray system does not spray some spaces in the lower levels; therefore, areas of significant size exist where debris washdown by the sprays would not occur. The sprays activate when the containment pressure exceeds 18.2 psig. If the sprays do not activate, debris washdown likely would be minimal. The insulation composition for the volunteer plant is approximately 13 percent fiberglass, 86 percent reflective metal insulation (RMI), and 1 percent Min-K insulation. For the purposes of this study, it was assumed that the fiberglass insulation was one of the low-density fiberglass (LDFG) types. For plant-specific analyses, these transport results for fibrous debris may have to be adjusted to compensate if the fiberglass insulation makeup is determined to be significantly different.

The effluences from a high-energy pipe break not only would destroy insulation near the break but also would transport that debris throughout the containment (i.e., blowdown debris transport). Substantial amounts of this airborne* debris would come into contact with containment structures and equipment and would be deposited onto these surfaces. As depressurization flows slow, debris would settle gravitationally onto equipment and floors. If pressurization of the containment were to occur, the CSs would activate to suppress pressurization. These sprays would tend to wash out remaining airborne debris (except in areas not covered by the sprays), and the impact of these sprays onto surfaces and the subsequent drainage of the accumulated water would wash deposited debris downward toward the sump pool (i.e., washdown debris transport). In addition, CSs could degrade certain types of insulation debris further through the process of erosion, thereby creating even more of the fine transportable debris.

An assessment of the likelihood of blocking the recirculation sump screens requires an estimate of the debris transport from the containment to the sump pool.† The debris transport within the sump pool is analyzed separately from this analysis, but the sump pool analysis requires the quantities of debris and the entry locations and timing as input to that analysis. This analysis sought to develop and demonstrate an effective methodology for estimating the transport of debris from the debris point of origin in the containment down to the sump pool, thereby providing the source term to the sump-pool debris-transport analysis. Applying the methodology to the volunteer plant generated plausible debris-transport fractions for that plant.

The analyses herein considered only one break location—a LOCA located in one of the SG compartments, which is a probable location for that plant because most of the primary system piping is located in these compartments.

Neither the debris-size distributions nor the overall transport fractions in this report are valid for plant-specific evaluations because these fractions were calculated using LOCA-generated debris-size distributions that did not account properly for PWR jet

---

* The terms "airborne" and "airflow" are used loosely with regard to gas flows, which actually consist of both air and steam.

† The simplest and most conservative assessment would be to assume 100-percent transport to the sump pool.

characteristics. Boiling-water reactor (BWR) jet characteristics were substituted for PWR jet characteristics because the PWR jet analyses had not yet been performed. When the PWR jet characteristics do become available, the overall transport fractions can be recalculated easily using PWR LOCA-generated debris-size characteristics.

The basic concepts of this methodology apply to the assessment of the debris transport within other PWR plants as well; however, that application depends on the plant-specific aspects of each plant. The complexity of a plant-specific methodology could vary significantly from one plant to the next.

VI.2 Debris-Transport Phenomenology

Both the spectrum of physical processes and phenomena and the features of a particular containment design would influence the transport of debris within a PWR. Because of the violent nature of flows following a LOCA, insulation destruction and subsequent debris transport are rather chaotic processes. For example, a piece of debris could be deposited directly near the sump screen or it could take a much more tortuous path, first going to the dome and then being washed back down to the sump by the sprays. Conversely, a piece of debris could be trapped in any number of locations. Aspects of debris-transport analysis include the characterization of the accident, the design and configuration of the plant, the generation of debris by the break flows, and both air- and water-borne debris dynamics.

Long-term recirculation cooling must operate according to the range of possible accident scenarios. A comprehensive debris-transport study should consider an appropriate selection of these scenarios, as well as all engineered safety features and plant-operating procedures. A small subset of accident scenarios will likely determine the maximum debris transport to the screen, but this scenario subset should be determined systematically. Many important debris-transport parameters will be dependent on the accident scenarios. These parameters include the timing of specific phases of the accident (i.e., blowdown, injection, and recirculation phases) and pumping flow rates. The blowdown phase refers to primary-system depressurization. The injection phase corresponds to ECCS injection into the primary system, a process that subsequently establishes the sump pool. The recirculation phase refers to long-term ECCS recirculation.

Many features in nuclear power plant containments significantly affect the transport of insulation debris. The dominant break flows will move from the break location toward the pressure suppression system (i.e., the suppression pool in BWR plants and the upper regions of the compartment in PWR plants). Structures such as gratings are placed in the paths of these dominant flows and likely would capture substantial quantities of debris. The lower compartment geometry (e.g., the open floor area, ledges, structures, and obstacles) defines the shape and depth of the sump pool and is important in determining the potential for debris to settle in the pool. Furthermore, the relative locations of the sump, LOCA break, and drainage paths from the upper regions to the sump pool are important in determining pool turbulence, which in turn determines whether debris can settle in the pool.

Transport of debris depends strongly on the characteristics of the debris that has formed. These characteristics include the types of debris (e.g., insulation type, coatings, and dust) and the size distribution and form of the debris. Each type of debris has its own set of physical properties, such as densities, specific surface areas, buoyancy (including dry, wet, or partially wet), and settling velocities in water. The PWR plants use several distinct types of insulation (NUREG/CR-6762, Vol. 2, 2002). The size and form of the debris, in turn, depends on the method of debris formation (e.g., jet impingement, erosion, aging, and latent accumulation). The size and form of the debris affect whether the debris passes through a screen, as well as the transport of the debris to the screen. For example, fibrous debris may consist of individual fibers or of large sections of an insulation blanket and all sizes within these two extremes.

The complete range of thermal-hydraulic processes affects the transport of insulation debris, and the containment thermal-hydraulic response to a LOCA includes most forms of thermal-hydraulic processes. Debris transport is affected by a full spectrum of physical processes, including particle deposition and resuspension for airborne transport and both settling and resuspension within calm and turbulent water pools for both buoyant and nonbuoyant debris. The dominant debris-capture mechanism in a rapidly moving flow likely would be inertial capture; however, in slower flows, the dominant process likely would be gravitational settling. The CSs or possibly condensate drainage would likely wash off much of the debris deposited onto structures. Other debris on structures could be subject to erosion.

A panel of experts sought to identify and rank the important phenomena, processes, and systems with regard to PWR debris transport (LA-UR-99-3371, 1999). The analysis methodology incorporated the insights gained from the work of this panel. Additionally, this analysis accessed all of the experimental and analytical research performed to resolve the BWR strainer-blockage issue (LA-UR-01-1595, 2001; NUREG/CR-6369-1, 1999; NUREG/CR-6369-2, 1999; NUREG/CR-6369-3, 1999). The NRC published a summary on the base of knowledge for the effect of debris on PWR ECC sump performance (NUREG/CR-6808, 2003).

VI.3 <u>Methodology</u>

VI.3.1 Overall Description

Transport of LOCA-generated debris from its point of origin to the PWR sump pool is a multifaceted procedure involving many physical processes and complex plant-specific geometry. To evaluate the blowdown and washdown debris transport within the drywell of a BWR plant, the NRC developed a methodology that accomplished the objectives of the drywell debris-transport study (DDTS) (NUREG/CR-6369-1, 1999; NUREG/CR-6369-2, 1999; NUREG/CR-6369-3, 1999). The BWR methodology provided the basis for the methodology used herein.

The BWR methodology separated the overall transport problem into many smaller problems that were either amenable to the solution or that could be judged conservatively. The breakdown of the problem was organized using logic charts that were similar to well-known event-tree analyses. For some solution steps, sufficient data were available to solve that step reasonably. For other steps, insufficient data were available; therefore, the solution required the use of engineering judgment that was applied after review of the available knowledge base. Judgments were tempered to the desired level of conservatism called for in that particular analysis (sometimes assuming the worst case for a particular step). The result of each specific analysis was a transport fraction, defined as the fraction of insulation contained within the pipe-break destructive zone of influence (ZOI) that subsequently was damaged or destroyed by a LOCA and was eventually transported to the suppression pool. Certainly, the degree of refinement that is feasible depends on available resources and time restraints. In addition, the conservatism in the estimates for each step in the divided problem may be compounded when the final transport fraction is quantified.

The PWR debris-transport methodology necessarily will differ from the BWR transport methodology because of differences in plant designs. These differences include the basic transport pathways, dominant capture mechanisms, and the timing of the accident sequence events. The dominant transport pathway for a PWR is different from the dominant pathway for a BWR. In a BWR, where pressure suppression would be caused by steam condensation in the suppression pool, the debris initially would be transported directly to the suppression pool, where the ECCS strainers operate. In PWR containments, which are designed to suppress pressurization by channeling break effluences* to the relatively large free volume of PWR containments, debris likely would be blown away from the sump area initially. Because one-half to three-quarters of the containment free volume typically is located in the upper regions of the containment, including the dome, it is justified to assume that a significant fraction of the small debris is blown directly into the upper regions, where the debris will settle onto floor surfaces or structures. Although the CSs could then wash the debris blown into the upper regions back down to the compartment sump area, the washdown pathway can be tortuous and could certainly result in substantial debris entrapment.

The dominant debris-capture locations are different in a PWR than in a BWR. In many typical PWRs, the likely dominant locations are the upper regions of the containment, the ice condensers in an ice-condenser plant, the refueling pool, an outer annulus pool, and the sump pool. In the volunteer-plant containments, dominant locations for debris capture may not exist; rather, the debris likely would be blown throughout the entire containment. Gratings in a PWR could play a substantially different role versus the gratings played in the BWR methodology because the debris likely would be blown up through a grating as opposed to down through a grating. Debris trapped underneath a grating would be less likely to remain there than debris trapped on top of a grating.

The water drainages of break recirculation overflow, the CSs, and condensate would cause debris transport during the washdown phase. The drainage of the activated CSs would be the most important of these drainages because the sprays usually cover a majority of the containment free volume, whereas the break overflow would wash only surfaces directly below the break. In a PWR, the break overflow could impinge on piping and equipment before reaching the containment sump floor, thereby washing debris from these surfaces, as well as potentially dispersing the flow. In a BWR, the break overflow for a majority of postulated breaks would pass down through at least one grating, where the flows would erode larger debris trapped on the gratings directly below the break—a situation less likely in a PWR. Although condensate drainage could transport debris from surfaces, the quantities of debris transported would likely be much less than the quantities transported by spray drainage.

The following methodology was designed specifically to analyze debris transport within the volunteer-plant containments; however, it also applies directly to several other

* In an ice-condenser plant, the break effluences would be channeled through the ice banks to condense steam.

containment designs, and it can be modified to tailor the methodology to any other PWR design. The best method for a particular plant will depend on the complexity of the containment design. If the containment has definitive upper and lower compartments that are separated by relatively few and narrow pathways, the analysis may be used to track debris transports in a manner similar to the DDTS analysis. Using an ice-condenser plant as an example, the containments were designed specifically to channel break flow through the ice banks to the dome region. This generally means that the connecting flow pathways between the lower and upper containments include the ice banks, small air-circulation return pathways (needed to establish postblowdown air circulation through the ice banks), and refueling-pool drains. Debris capture through the ice banks could be substantial. In addition, a large fraction of the small and fine debris would be blown into the dome region, where substantial quantities could be retained, even with the CSs operating.

The analysis here would focus on debris capture in the ice banks during blowdown and on debris retention in the upper compartment during the spray washdown process to identify debris transported from the lower containment and not likely to return there. Some plants would have a flooded outer annulus in which debris deposited in that pool would be less likely to transport from that pool to the sump pool. A conservative estimate of the maximum debris quantities that would be expected to transport to the sump pool can be made by subtracting masses of debris retained at various locations from the generation totals.

The design of the volunteer-plant containments is more complex than an ice-condenser design, from a debris-transport perspective; that is, the lower and upper regions of the containment are less well defined and are connected by several different pathways, thereby making it difficult to determine the motion of air and steam flows and the transport of debris. Certainly, system-level codes such as MELCOR can model the progression of break flows throughout the containment; however, the input model for the volunteer plant would have to be rather detailed to follow the flows through all of the lower levels in the containment. The modeling detail must include all of the levels and rooms and separate sprayed areas from nonsprayed areas. The model would need to simulate all of the connecting flow pathways, such as stairwells, equipment hatches, and doorways. The volunteer-plant analysis did <u>not</u> include a detailed thermal-hydraulics analysis.

The transport and deposition of insulation debris cannot be simulated realistically using a thermal-hydraulics computer code that incorporates aerosol transport models. Inertial capture serves as the primary mode of debris capture during the violent primary-system depressurization. The available models for inertial capture are based on data taken for rather simple geometries (e.g., a bend in a pipe). Current codes cannot reasonably model inertial capture in the complex geometry of containments. However, inertial capture can be determined in specific parts of the containment. For example, at the volunteer plant, the personnel access doors between an SG compartment and the sump annulus have at least one 90-degree bend. A LOCA, particularly a large LOCA, in an SG compartment would result in depressurization flows that would carry insulation debris through these doors with the flow. As the flow moved through the sharp bend, inertia would cause the deposition of some types of debris on the wall at the bend. The tests conducted at the Colorado Engineering Experiment Station, Inc. (CEESI) demonstrated an average inertial capture fraction for fibrous debris of 17 percent at such a bend if the surface were wetted, and analysis has shown that surfaces within the containment likely would build a filmy layer of condensation rapidly. Because the CSs do not impinge on these wall surfaces, the debris would remain attached to those surfaces. In this situation, small amounts of debris can be removed from the equation, thereby lowering the transport fraction. Perhaps many of these types of definable captures can add up to a significant reduction in the transport fraction. Again, the size of that reduction would depend somewhat on both the geometry/conditions and the depth of the analysis.

The mechanics of this methodology basically involve looking for such reductions systematically. The demonstration of this methodology in this volunteer-plant analysis assumed a large LOCA occurred inside SG compartment number 1 (SG1) of the containment. Figure VI-1 illustrates this methodology in the general sense. First, the blowdown dispersal of the debris is estimated until all of the debris is associated with some surface area. Then the likelihood of debris remaining on each of these surfaces during washdown is estimated or judged. For example, debris deposited onto a surface that has been impacted by the CSs is much more likely to transport than debris deposited onto surfaces that have been wetted only by condensate.

As with the DDTS, the debris for transport must first be categorized according to type and size according to transport properties so that the transport of each type of debris can be analyzed independently. Some damage is assumed for all insulation located within the break-region ZOI. Section VI.3.2 discusses these categories and their properties.

The containment free volume in the volunteer plant was subdivided into many regions based on geometry and the locations of the CSs. The volume region containing the postulated LOCA was analyzed first. For SG1, a MELCOR simulation of only the break compartment determined the distribution of flows exiting that compartment (i.e., the fraction of flow going upward into the dome as opposed to the fraction entering the lower levels through personnel access doors). Debris capture within SG1 was based on such considerations as flows through gratings and flows making sharp bends (see Section VI.3.3.1). In each region, debris capture would deposit debris onto the floor or other surfaces, based on surface areas and judgment regarding whether debris was deposited by settling or by another mechanism. The analysis treated floor surfaces separately because these surfaces would collect and drain spray water differently from vertical surfaces, for example, and because debris that gravitationally settles would deposit onto horizontal surfaces. These surfaces were divided further according to their exposure to spray and condensate moisture. All surfaces would collect condensate. The sprays would impact some surfaces directly, and others simply would be washed by the process of spray drainage. Debris entrained by spray-drainage water could become captured a second time as the drainage fell from one level to another.
Because the chart illustrated in Figure VI-1 would become unreasonably large if it were developed for the entire volunteer-plant containment, another approach was used. The process was handled using an equation-format model (described in Figure VI-1), with the input entered into data arrays.

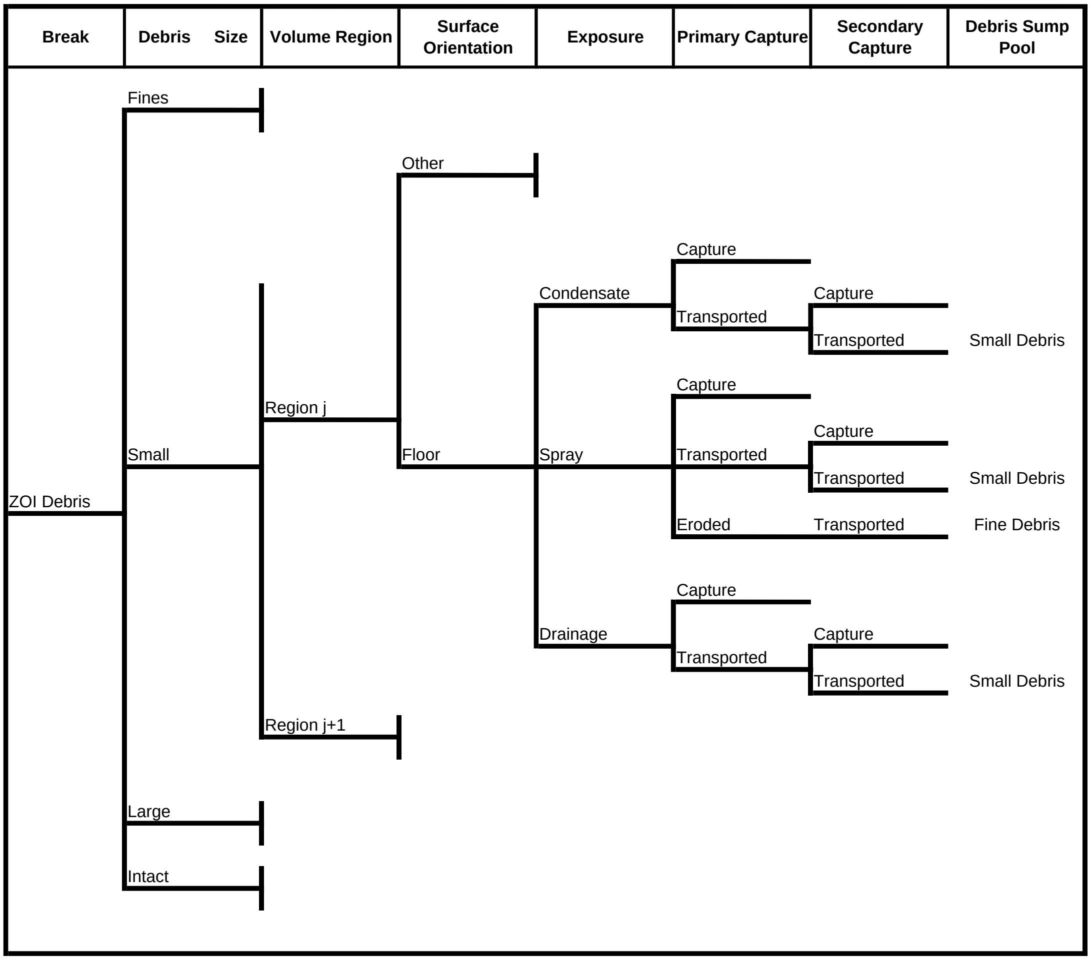

Figure VI-1. Example of a Section of a Debris-Transport Chart

VI.3.2 Debris-Size Categorization

The types of insulation used inside the volunteer-plant containments include fiberglass insulation,* RMI, and stainless-steel-encapsulated Min-K insulation at approximately 13.4 percent, 85.7 percent, and 0.9 percent, respectively (NUREG/CR-6762, Vol. 2, 2002). Although RMI comprises a majority of the insulation within these containments, the fibrous insulation more likely would cause blockage of the sump. First, the RMI debris would transport less easily than the fibrous debris (i.e., it takes a faster flow of water to move RMI debris than it does for fibrous debris). In addition, it takes substantially more RMI debris than fibrous debris on the sump screens to block the flow effectively through the screens. Although the Min-K debris, in combination with the fibrous debris, could create substantial head losses on the screen, the inventory of the Min-K in the containments is relatively low. Therefore, this analysis focused primarily on the transport of fibrous debris, with the transport of RMI and Min-K estimated more crudely.

* The type (or types) of fiberglass insulation used in the volunteer-plant containments has yet to be determined. This analysis assumes that the fiberglass is LDFG.

The difficulties associated with determining debris-size distributions to represent the LOCA-generated debris are (1) the limited debris-generation data and (2) the need to determine the characteristics of the LOCA jet (i.e., the size of the ZOI and volumes within specific pressure isobars). The limitations in the debris-generation data must be handled by skewing the integration of size fractions conservatively over the ZOI toward the smaller debris sizes—the more limited the data, the more conservative the integration. The determination of the jet characteristics for a PWR jet is a relatively straightforward analysis, but those characteristics unfortunately were not yet available for use in this report. Because debris-size distributions are necessary to determine estimates for the overall transport of debris to the sump pool, assumptions were made to provide distributions that were suitable to illustrate the transport methodology.

Therefore, <u>neither</u> the debris-size distributions <u>nor</u> the overall transport fractions in this report are valid for plant-specific evaluations.

However, the transport fractions for specific debris-size classes are considered to be valid for the volunteer plant.

VI.3.2.1 Fibrous Insulation Debris-Size Categorization

The analysis assumed some damage to all insulation located within the break-region ZOI. The damage could range from slight damage (insulation erosion occurring through a rip in the blanket cover) that leaves the blanket attached to its piping to the total destruction of a blanket (with its insulation reduced to small or very fine debris). This analysis considered all of the insulation within the ZOI to be debris. The fibrous debris was categorized into one of four categories based on transport properties so that the transport of each type of debris could be analyzed independently. Table VI-1 shows these categories and their properties.

The two smaller and two larger categories differed primarily as to whether the debris was likely to pass through a grating that is typical of those found in nuclear power plants. The DDTS analysis also used this criterion. Thus, fines and small pieces pass through gratings but large and intact pieces do not. The fines and small pieces are much more transportable than the large debris. The fines were then distinguished from the small pieces because the fines would tend to remain in suspension in the sump pool, even under relatively quiescent conditions, whereas the small pieces would tend to sink. Furthermore, the fines tended to transport slightly more as an aerosol in the containment-air/steam flows and were slower to settle than the small pieces when airflow turbulence decreased. The CEESI tests illustrated that when an LDFG blanket was completely destroyed, 15 to 25 percent of the insulation was in the form of very fine debris (i.e., debris too fine to collect readily by hand).

Table VI-1. Debris-Size Categories and Their Capture and Retention Properties

Fraction Variable	Size	Description	Airborne Behavior	Waterborne Behavior	Debris-Capture Mechanisms	Requirements for Crediting Retention
D_F	Fines	Individual fibers or small groups of fibers.	Readily moves with airflows and slow to settle out of air, even after completion of blowdown.	Easily remains suspended in water, even relatively quiescent water.	Inertial impaction Diffusiophoresis Diffusion Gravitational settling Spray washout	Must be deposited onto surface that is not subsequently subjected to CSs or to spray drainage. Natural-circulation airflow likely will transport residual airborne debris into a sprayed region. Retention in quiescent pools without significant flow through the pool may be possible.
D_S	Small Pieces	Pieces of debris that easily pass through gratings.	Readily moves with depressurization airflows and tends to settle out when airflows slow.	Readily sinks in hot water, then transports along the floor when flow velocities and pool turbulence are sufficient. Subject to subsequent erosion by flow water and by turbulent pool agitation.	Inertial impaction Gravitational settling Spray washout	Must be deposited onto surface that is not subsequently subjected to high rates of CSs or to substantial drainage of spray water. Retention in quiescent pools (e.g., reactor cavity). Subject to subsequent erosion.

Fraction Variable	**Size**	**Description**	**Airborne Behavior**	**Waterborne Behavior**	**Debris-Capture Mechanisms**	**Requirements for Crediting Retention**
D_L	Large Pieces	Pieces of debris that do not easily pass through gratings.	Transports with dynamic depressurization flows but generally is stopped by gratings.	Readily sinks in hot water and can transport along the floor at faster flow velocities. Subject to subsequent erosion by flow water and by turbulent pool agitation.	Trapped by structures (e.g., gratings) Gravitational settling	Must be either firmly captured by structure or on a floor where spray drainage and/or pool flow velocities are not sufficient to move the object. Subject to subsequent erosion.
D_I	Intact	Damaged but relatively intact pillows.	Transports with dynamic depressurization flows, stopped by a grating, or may even remain attached to its piping.	Readily sinks in hot water and can transport along the floor at faster flow velocities. Assumed to remain encased in its cover, thereby not subject to significant subsequent erosion by flow water and by turbulent pool agitation.	Trapped by structures (e.g., gratings) Gravitational settling Not detached from piping	Must be either firmly captured by structure or on a floor where spray drainage and/or pool flow velocities are not sufficient to move the object. Intact debris subsequently would not erode because of its encasement.

The distinguishing difference between the large and intact debris was whether the blanket covering still protected the fibrous insulation, and therefore whether the CSs could further erode the insulation material.

The analysis first estimated the volume (or mass) distribution, D_i, of the four categories of insulation debris. This estimate assumed that the fibrous insulation within the ZOI was uniformly distributed and that the distribution must add up to one, as

$$\sum_{i=1}^{N_{types}} D_i = 1 \quad ,$$

where

D_i = the fraction of total debris that is type *i*.

The volume of each category of debris is simply the distribution fraction multiplied by the total volume of insulation within the ZOI. Debris-transport analysis has used volumes of fibrous debris interchangeably with mass on the basis that the density is that of the undamaged (as fabricated) insulation. Certainly the density would be altered by the destruction of the insulation and again when the debris became water saturated. For example, the physical volume of debris on the screen must include the actual density of the debris on the screen as

$$V_i = D_i V_{ZOI} \quad ,$$

where

V_i = the volume of debris of type *i* and

V_{ZOI} = the total volume of insulation contained within the ZOI.

The estimation of the debris-size distribution must be based on experimental data. When sufficient data are available, the following analytical model illustrates how the fraction of fine and small debris can be estimated from that data. Using the spherical ZOI destruction model, the fraction of the ZOI insulation that becomes type-*i* debris is given by

$$F_i = \frac{3}{r_{ZOI}^3} \int_0^{r_{ZOI}} g_i(r)\, r^2 \; dr \quad ,$$

where

F_i = the fraction of debris of type *I*,

$g_i(r)$ = the radial destruction distribution for debris of type *I*,

r = the radius from the break in the spherical ZOI model, and

r_{ZOI} = the outer radius of the ZOI.

Typical test data provide an estimate of the damage to insulation samples at selected distances from the test jet nozzle (i.e., the size distribution of the resultant debris). The jet pressure at the target is determined from test pressure measurements, suitable analytical models, or both. Thus, the size distribution as a function of the jet pressure is obtained. The volume associated with a particular level of destruction is determined by estimating the volume within a particular pressure isobar within the jet (i.e., any insulation located within this pressure isobar would be damaged to the extent (or greater) associated with that pressure). The isobar volumes then are converted to the equivalent spherical volumes; thus, the debris-size distribution is associated with the spherical radius (i.e., $g_i(r)$). The distribution would be specific to a particular kind of insulation, jacketing, jacketing seam orientation, and banding.

To demonstrate the transport methodology completely, the analysis assumed that the volunteer-plant containments used LDFG insulation as the fibrous insulation, since significant data on LDFG insulation are available to predict the LOCA-generated size distribution. The most extensive debris-generation data for LDFG insulation are the data from the BWR Owners Group (BWROG) air-jet impact tests (AJITs) (NEDO-32686, 1996). These data, combined with the jet characteristics of a PWR LOCA, could result in a realistic LOCA size distribution; however, the PWR jet characteristics were not available at the time of this writing.

The development of a suitable size distribution for the purposes of demonstrating this methodology follows. For fibrous debris, the BWROG correlated the fraction of the original insulation that became fine debris with the distance from the jet nozzle and then crudely estimated the ZOI destruction fractions for specific types of insulation. The fine debris in the BWROG analysis correlates with the combined fine and small debris of Table VI-1.

For the NUKON™ insulation debris—both jacketed and unjacketed insulation—the BWROG recommended in its utility resolution guidance (URG) the assumption that 23 percent of the insulation within the ZOI be considered in the strainer head-loss evaluations during the resolution of the BWR strainer-blockage issue. Applying this recommendation to this analysis means that 23 percent of the ZOI would be distributed between the fine and small debris and that the remaining 77 percent would be distributed between the large and intact debris. The NRC reviewed the BWROG recommendations and documented its findings in a safety evaluation report (SER) (NRC-SER-URG, 1998). Although the NRC had some reservations regarding the BWROG's method for determining the debris fractions, the NRC believed the debris fractions to be conservative primarily because the blanket seams were arranged in the AJITs to maximize the destruction of the blankets.

Whereas the BWROG based its recommendations on AJITs, more recent testing using two-phase jet impact testing indicated the need for somewhat higher small-debris fractions than did the AJIT data (refer to Section 3.4.2.2 in this SER for the evaluation of the two-phase jet concern). Ontario Power Generation (OPG) of Canada conducted these debris-generation tests (OPG, 2001). A report (NUREG/CR-6762, Vol. 3, 2002) supporting the PWR parametric evaluation (NUREG/CR-6762, Vol. 1, 2002) compared the AJIT and the OPG tests. This comparison illustrated the potential for a two-phase jet to generate more small debris than the AJIT data indicated. The parametric evaluation concluded when comparing these two sets of test data the small debris fraction should be increased from the BWROG recommendation. The evaluation used engineering judgment to increase the recommended destruction fraction for small debris from 23 percent to 33 percent. The remaining 67 percent of the insulation would be assumed to be large debris either exposed or enclosed in its covering material.

This analysis split the small-debris fraction of 33 percent that was used in the parametric evaluation to accommodate the fine- and small-debris categories of this analysis. The analysis of the AJIT testing performed at CEESI to support the DDTS determined that whenever entire blankets were completely destroyed, 15 to 25 percent of the insulation was too fine to collect by hand.* In this case, complete destruction means that nearly all of the insulation was either fine or small pieces. In any case, 15 to 25 percent of the blanket (an average of 20 percent) can be considered fine debris for the purposes of this analysis. This analysis assumed that 20 percent of the 33-percent small-debris fraction was fine debris (i.e., $0.2 \times 0.33 = 0.066$). Therefore, the analysis estimated the destruction of 7 percent of the ZOI insulation into fine debris, leaving 26 percent for the small-piece debris.

In a similar manner, this analysis split the parametric evaluation of the 67-percent large-debris fraction to accommodate the large- and intact-debris categories. The DDTS analysis, based on the AJIT data, assumed that 40 percent of the blanket insulation remained covered. This analysis accepted the DDTS assumption of 40 percent for the covered (intact) debris fraction. However, that number had to be adjusted downward to account for the increase in the small-debris fraction from 23 to 33 percent (i.e., $0.67/0.77 \times 0.4 = 0.35$). Therefore, 35 percent of the ZOI insulation was considered to be intact debris, leaving 32 percent for the exposed large-piece debris. Table VI-2 summarizes the debris category distribution for fibrous debris assumed in this analysis.

Table VI-2. Fibrous-Debris Category Distribution

Category	Category Percentage
Fines	7%
Small Pieces	26%
Large Pieces	32%
Intact	35%

* This debris either was blown through the fine-mesh screen at the end of the test chamber and lost from the facility or was deposited onto surfaces inside the chamber in such a dispersed manner that it could be collected only by hosing down the walls and structures.

VI.3.2.2 RMI Insulation Debris-Size Categorization

In the volunteer-plant containments, the RMI insulation is made of stainless steel. Transco Products, Inc., manufactured the insulation around the reactor vessel. Diamond Power Specialty Company (DPSC) manufactured all of the other RMI inside the containments and marketed it as DPSC MIRROR™ insulation. Furthermore, the insulation panels generally are held in place simply by buckling the panels together (i.e., an absence of bands on most panels). Because the reactor vessel insulation is shielded from a postulated jet impingement for the most part, LOCA-generated RMI debris would consist primarily of the DPSC type. The BWROG (NEDO-32686, 1996) estimated, and the NRC accepted (NRC-SER-URG, 1998), the threshold jet-impingement pressure required to damage DPSC MIRROR™ insulation with standard bands as 4 psi; these data should be applicable to the volunteer-plant RMI. Therefore, some debris could be formed from any insulation subjected to a differential of 4 psi or greater, but the extent of damage would depend on the magnitude of the pressure. Insulation that is closer to the break would be destroyed completely and form small pieces of debris, whereas insulation farther from the break may remain nearly intact. The transport analysis requires a size distribution. Data from two experimental programs provide limited information on the extent of destruction that would occur in this type of RMI insulation. These programs are (1) the Siemens Karlstein tests (SEA-95-970-01-A:2, 1996) and (2) the BWROG AJIT (NEDO-32686, 1996).

Swedish Nuclear Utilities conducted metallic insulation jet impact tests at the Siemens AG Power Generation Group (KWU) test facility in Karlstein am Main, Germany, in 1994 and 1995. During this test program, the NRC conducted a single RMI debris-generation test to obtain debris-generation data and debris samples that are representative of RMI used in U.S. plants. The DPSC provided the NRC test sample. The NRC-sponsored test was performed with a high-pressure blast of two-phase water/steam flow from a pressurized vessel connected to a target mount by a blowdown line with a double-rupture disk. The target was mounted directly on a device designed to simulate a double-ended guillotine break (DEGB) such that the discharge impinged the inner surface of the RMI target as it would an insulation cassette surrounding a postulated pipe break. Most of the RMI debris was recovered and analyzed with respect to size distribution. Figure VI-2 shows the overall size distribution for the total recovered debris mass, and Figure VI-3 shows a photograph of the recovered RMI debris. This debris sample is likely typical of debris formed from the RMI cassettes nearest the break.

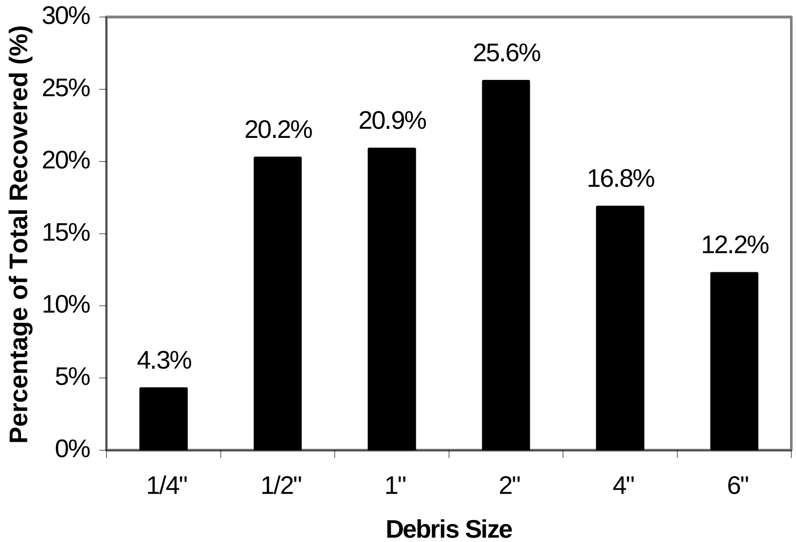

Figure VI-2. Size Distribution of Recovered RMI Debris

Figure VI-3. RMI Debris Observed in Siemens Steam-Jet Impact Tests

The BWROG-sponsored tests conducted at CEESI examined the failure characteristics of various types of insulation materials when subjected to jet impingement forces. The CEESI has compressed-air facilities that provided choked nozzle airflow. The tests directed this airflow at insulation samples mounted inside a test chamber that did not pressurize significantly but retained most of the insulation debris for subsequent analysis. The variety of insulation materials tested included samples of the stainless-steel DPSC MIRROR™ insulation. The test samples were mounted at various distances from the nozzle, thereby subjecting similar samples to varying damage pressures. In this manner, the test data were used to estimate the threshold pressure required to damage this type of insulation. The data also provided information regarding the size distribution of the resulting debris. The formation of debris depended on the separation of the outer sheath, which in turn depended on the type, number, and placement of the supporting bands. The data used herein were for stainless-steel DPSC MIRROR™ cassettes mounted either with standard bands or without bands; therefore, these data are conservative with respect to data for cassettes mounted with even stronger banding. The recorded debris-generation data separated the quantities of debris into several distinct size groupings. For this transport analysis, the debris was grouped into three size groups: (1) debris generally smaller than 2 in., (2) debris larger than 2 in. but smaller than 6 in., and (3) all RMI pieces larger than 6 in. (including both debris and relatively intact insulation cassettes). Figure VI-4 shows the fractions of the collected debris for the two finer groups as a function of the damage pressure on the cassette; all other insulation either remained relatively intact or formed debris larger than approximately 6 in.

The BWROG data describe the damage to stainless-steel DPSC MIRROR™ insulation (standard banding) when subjected to jet pressures of up to 120 psi. The NRC-sponsored Siemens test demonstrates the complete destruction of stainless-steel DPSC MIRROR™ insulation when impacted by the highest jet pressure near the break. A gap exists in the data between 120 psi and the higher pressure near the jet. The damage to the RMI within the ZOI was estimated using the spherical equivalent volume method in conjunction with BWR-specific data (i.e., volumes with specific pressure isobars). The BWROG analysis that was provided to the utilities (NEDO-32686, 1996) was used to convert jet isobar volumes to equivalent spherical volumes. Furthermore, the outer radius of the equivalent sphere was assumed to be 12D (i.e., 12 times the diameter of the pipe break), which corresponds to an insulation destruction pressure of 4 psi for a BWR radial offset DEGB. **The resultant size distribution can demonstrate the overall transport methodology fully but is not suitable for PWR plant-specific analyses.** The BWROG data were applied when the impact pressure was less than 120 psi; the Siemens data were conservatively applied when the impact pressure was greater than 130 psi (insulation totally destroyed), and a linear extrapolation was applied between 120 and 130 psi. The data shown in Figure VI-4indicate that when the insulation is totally destroyed, approximately 70 percent of the debris would be less than approximately 2 in. in size and the remaining 30 percent would be between 2 and 6 in. in size.

Because of variability and uncertainty in debris-generation estimates, as well as the use of BWR-specific jet characteristics, it is prudent to enhance the fractions for the finer groups of debris, noting that the smaller debris would transport more easily than would the larger debris. One uncertainty is the fact that the BWROG data were generated using an air jet, whereas the postulated accident would involve a two-phase steam/water jet; the comparison of two-phase and air test data has indicated that a two-phase jet could generate finer debris than could an air jet. To make the debris-generation estimates more conservative to compensate for variability and uncertainty in the estimates, the fractions for the two fines size groups were increased by 50 percent. Table VI-3 shows the spherical volume damage estimates with and without the 50-percent increase.

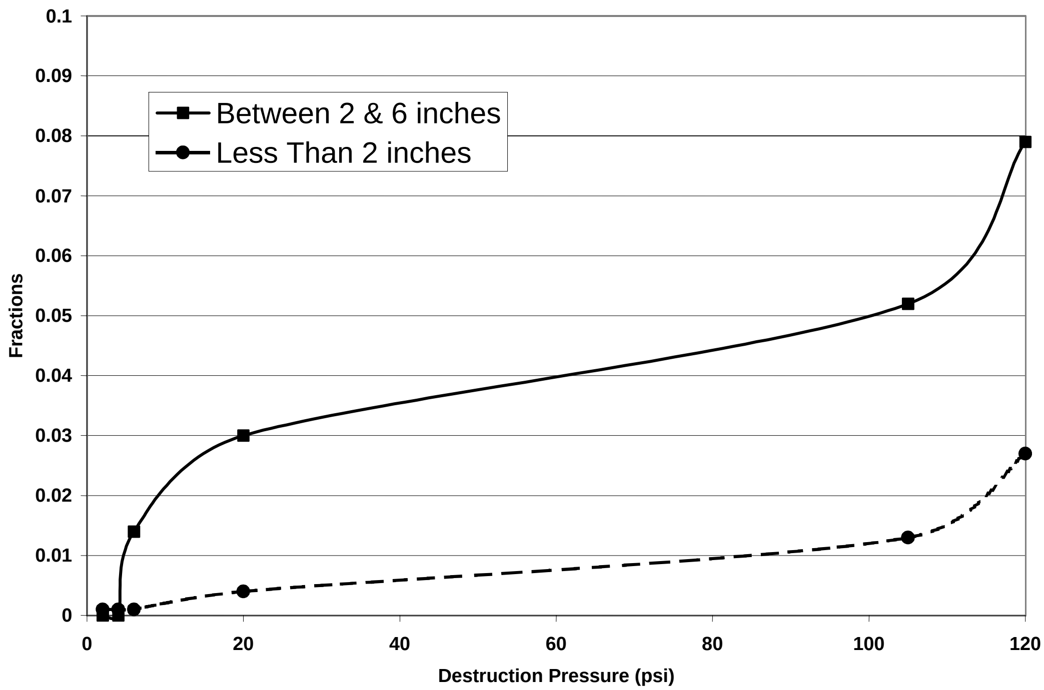

Figure VI-4. Relative Damage of Stainless-Steel DPSC MIRROR™ Insulation

Table VI-3. RMI Debris Category Distribution

Category	Category Percentage	
	Integration Result	Conservative Estimate
Less than 2 in.	14 percent	21 percent
Between 2 and 6 in.	8 percent	12 percent
Greater than 6 in.	78 percent	67 percent

VI.3.2.3 Min-K Insulation Debris-Size Categorization

In locations where insulation thickness was a specific concern, such as pipe-whip-restraint locations, fully encapsulated Min-K insulation was used instead of the usual RMI insulation. Containment-wide, approximately 0.9 percent of the insulation is Min-K. Although the potential quantities of Min-K debris would be substantially smaller than corresponding quantities of fibrous or RMI debris, a small amount of Min-K particulate debris could contribute more significantly than RMI debris to sump-screen head loss. In particular, Min-K debris dust would contribute to the particulate load in the debris bed when combined with the fibrous debris on the screens. Min-K is a thermo-ceramic insulation (also referred to as a particulate insulation) that is made of microporous material. The particulate insulations include calcium silicate, asbestos, Unibestos, Microtherm, and gypsum board. Test data have demonstrated that microporous particulate, combined with fibrous debris, creates a debris bed that can cause relatively high head losses across that bed. This head loss is over and above the corresponding head loss associated with more ordinary particulate, such as corrosion products. The most notable of the particulate insulation types has been calcium silicate.

Limited debris-generation data exist for the microporous insulations, and most of the available data were obtained for calcium silicate. No debris-generation data were available for Min-K insulation. Data from tests conducted by the OPG (NUREG/CR-6762, Vol. 3, 2002) serve as the primary source of calcium silicate debris-generation data. These tests involved impacting aluminum-jacketed calcium silicate insulation targets with a two-phase water/steam jet. Figure VI-4 shows the size distribution data.

Even if it is assumed that Min-K behaves similarly to calcium silicate with regard to debris generation, the OPG data cover only a limited range of damage pressures. Integrating the damage over the spherical ZOI requires a conservative extrapolation to a full range of pressures. The ZOI for Min-K corresponds to a destruction pressure of 4 psi, based on the BWROG guidance to utilities. At high pressures, the conservative extrapolation should assume that complete destruction of the insulation occurs (i.e., all of the insulation is pulverized to dust). At lower pressures, the damage fractions of the lowest pressures tested would extend out to the ZOI boundary. This crude conservative extrapolation indicates that about half of the insulation should be considered dust. In addition to the conservative extrapolation, the debris-generation fraction is conservative with respect to the jacket seam angle relative to the jet. The seams in the test data shown in Figure VI-5 were oriented toward maximum damage. In reality, the seams within the ZOI likely would be distributed more randomly with respect to the jet; therefore, many of the jackets would provide more protection for the Min-K than the OPG data indicate. On the other hand, applying data for calcium silicate to Min-K insulation introduces substantial uncertainty.

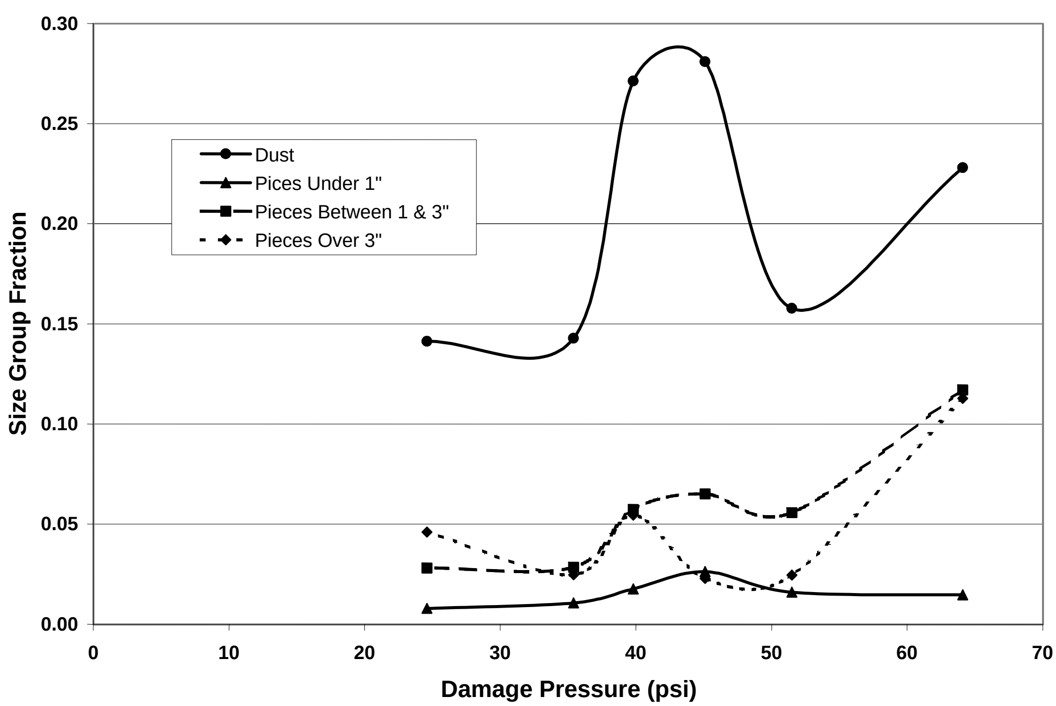

Figure VI-5. Debris-Size Distributions for OPG Calcium Silicate Tests

Another source of uncertainty is the location of the minimal quantities of Min-K insulation with respect to the break. A key assumption of the ZOI integration is a uniform distribution of insulation within the ZOI. However, with so little Min-K insulation inside the volunteer-plant containments, all damaged Min-K insulation could be located preferentially near or far from the break. Therefore, all Min-K insulation could be destroyed totally or only slightly damaged. Another source of uncertainty that has not been assessed experimentally is the subsequent erosion of the Min-K debris by the CSs. In light of these uncertainties, it is conservative and prudent to assume that all of the Min-K insulation inside a ZOI would be pulverized to dust.

VI.3.3 Blowdown Debris Transport

The break region, SG1, would be the source of all insulation debris and would be subject to the most violent of the containment flows, and the primary debris capture mechanism in this region would be inertial capture. For these reasons, the transport of debris within the region of the pipe break should be solved separately from that of the rest of the containment. The methodology is described for fibrous-debris transport but also was applied to RMI debris in a similar manner.

VI.3.3.1 Break-Region Dispersion and Capture

The first step in determining the dispersal of debris near the debris-generation source was to determine the distribution of the break flow from the region—specifically, the fractions of the flow directed to the dome versus other locations. This determination was accomplished using the containment thermal-hydraulics code MELCOR. The containment was designed to force reactor coolant system break effluents upward through the open tops of the SG compartments and into the dome. Figure VI-6 shows the nodalization diagram for the break-region MELCOR calculation.

The LOCA-generated debris that was not captured within the region of the break would be carried away from the break region by the break flows. The primary capture mechanism near the break would be inertial capture or entrapment by a structure such as a grating. The break-region flow that occurred immediately after the initiation of the break would be much too violent to allow debris simply to settle to the floor of the region.

The inertial capture of fine and small debris occurs when a flow changes directions, such as flows through the doorways from the SG compartments into the sump-level annular space. These flows must make at least one 90-degree bend through these doorways, and steam condensation as well as the liquid portion of the break effluence would wet these surfaces. Debris-transport experiments conducted at CEESI (NUREG/CR-6369-2, 1999) demonstrated an average capture fraction of 17 percent for fine debris and small debris that make a 90-degree bend at a wetted surface. Other bends in the flow would occur as the break effluents interacted with equipment and walls.

The platform gratings within the SG compartments would capture substantial debris, even though the gratings do not extend across the entire compartment. The CEESI debris-transport tests demonstrated that an average of 28 percent of the fine and small debris was captured when the airflow passed through the first wetted grating that it encountered and that an average of 24 percent was captured at the second grating. A grating would completely trap the large and intact debris. In addition, equipment such as beams and pipes was shown to capture fine and small debris. In the CEESI tests, the structural maze in the test section captured an average of 9 percent of the debris passing through the maze.

To evaluate the transport and capture within the break region, the evaluation must be separated into many smaller problems that are amenable to resolution. This separation can be accomplished using a logic-chart approach that is similar to the approach developed for the resolution of the BWR-strainer-blockage issue (NUREG/CR-6369-1, 1999). Figure VI-7 shows the chart for a LOCA in the volunteer-plant SG1, which is based on the MELCOR nodalization diagram in Figure VI-6. This chart tracks the progress of small debris from the pipe break (Volume V12) until the debris is assumed to be captured or is transported beyond the compartment. Because SGs 1 and 4 are joined at two locations, the compartments were combined into one model (i.e., a LOCA in SG1 will discharge to the containment through SG4 as well).

The questions across the top of the chart, shown in Figure VI-7, alternate among volume capture, flow split, and junction capture as the debris-transport process progresses through the nodalization scheme. The nodalization scheme was constructed to place the gratings at junction boundaries. The first chart question (header) after the initiator asks how much debris would be captured in Volume V12, where the LOCA was postulated to occur. The evaluation of this question involves simply estimating the fraction of small debris that was deposited by inertia near the pipe break; the remainder of the debris would be assumed to transport beyond this volume. The next question in the chart concerns a flow split (i.e., the distribution of the break flow going upward or downward from the break). The flow split is actually a debris split (i.e., how much debris goes in each direction). For fine- and small-piece debris, it is reasonable to assume that the debris split is approximated by the flow split. For large and intact-piece debris, the debris split may differ from the flow split, depending on the geometry. The third question concerns the amount of the debris captured at the flow junction between two volumes. The two junctions in the third question represent gratings that extend partly across the compartment at two levels. The fourth question starts the cycle over again for the next set of volumes in the sequence.

Once the distributions are inserted into the chart and the results are quantified, the results will indicate the distribution of captured debris within the compartments, as well as the debris transport from the compartments. The chart also will indicate the destination of the debris that is transported from the SG compartments (e.g., the dome or the lower levels through access doorways).

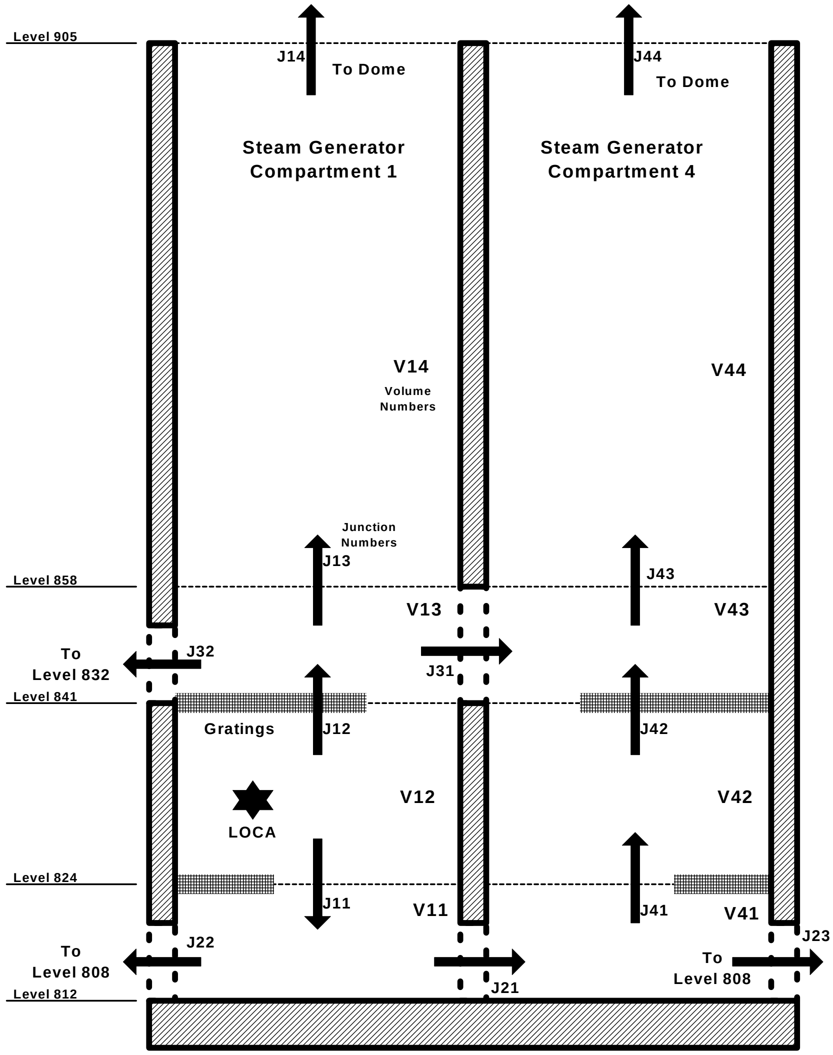

Figure VI-6. Break-Region Nodalization

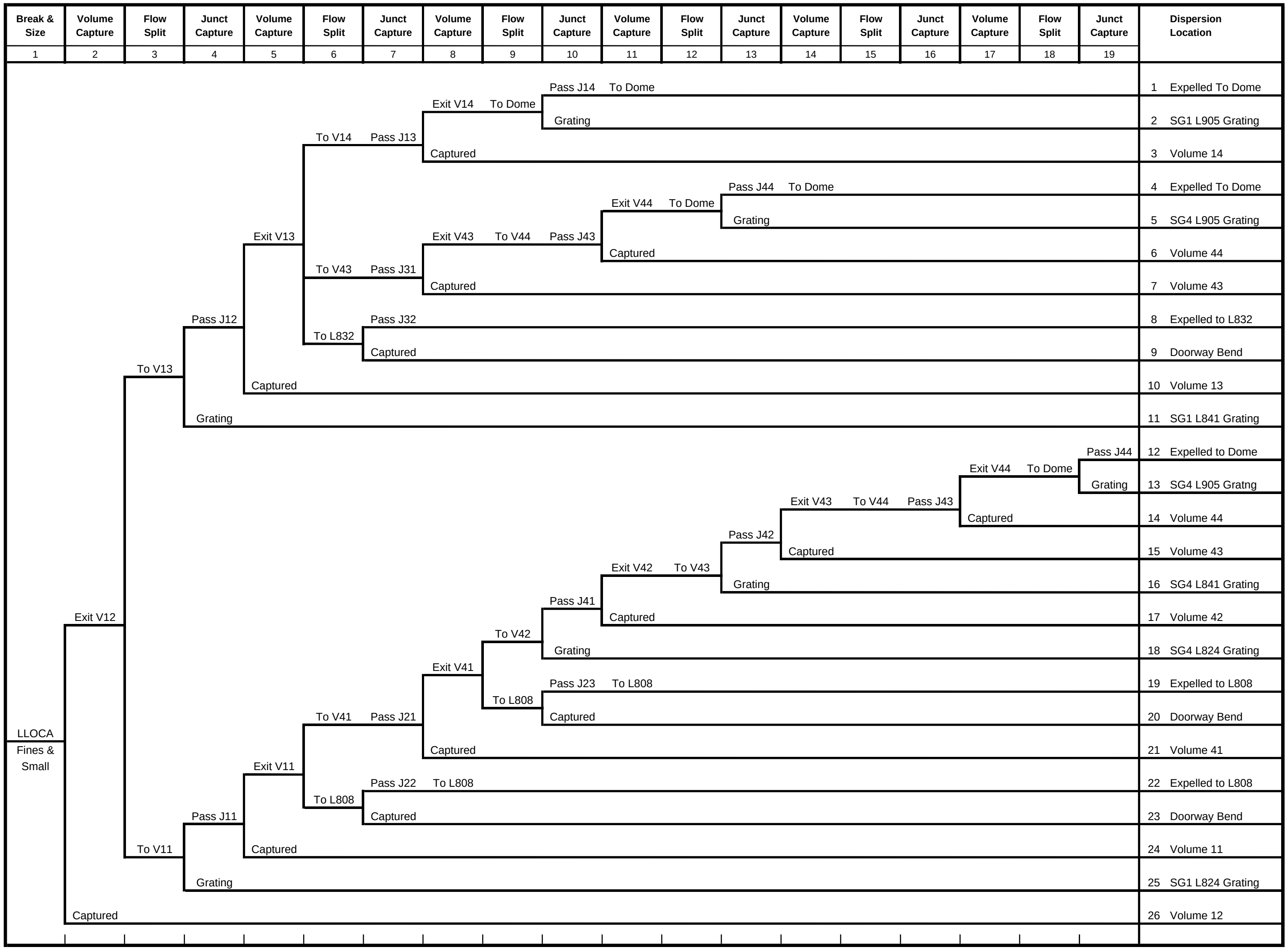

Figure VI-7. Chart for the Structure of Break-Region Debris Transport

VI.3.3.2 Dispersion and Capture throughout the Containment

The debris dispersion model used to evaluate debris transport within the volunteer-plant containments estimated dispersion throughout the containment first by free volume and then by surface orientation within a volume region. The model based the dispersion distributions first on actual volumes and areas and then adjusted them using weighting factors that were based on engineering judgment.

VI.3.3.2.1 Dispersion by Region

As the containment pressurizes following a LOCA, break flows carrying debris would enter all free volume within the containment. Larger debris would tend to settle out of the break flows as the flow slowed down after leaving the break region. However, the fine and smaller debris more likely would remain entrained so that fine and small debris would be distributed more uniformly throughout the containment. Certainly, the distribution would not be completely uniform because of debris being captured along the way, which is the reason for the weighting factors.

First, the containment free volume was subdivided into volume regions. This subdivision was based on geometry (i.e., floor levels and walls) and on the location of CSs. Specifically, areas where the CSs would not likely entrain the deposited debris were separated from areas that were impacted by the sprays. Some areas that were not actually sprayed still could be washed by the drainage of spray water as the water worked its way down through the containment structures. Areas where debris could be deposited without subsequently being washed downward by the sprays and the spray drainage could reduce the estimated transport fractions.

The total free volume of the containment is the sum of the free volumes for all of the volume regions. The volunteer-plant containment free volume was subdivided into a total of 24 volume regions (J = 24) as

$$V_{cont} = \sum_{j=1}^{J} Vc_j \quad ,$$

where

V_{cont} = the total free volume of the containment,

Vc_j = the free volume in containment region *j*, and

J = the number of volume regions.

The following equations define the dispersion model,

$$V_{i,j} = F_{i,j} \; D_i \; V_{ZOI} \quad ,$$

where

$V_{i,j}$ = the volume of debris-type *i* located in region *j*,

$F_{i,j}$ = the fraction of debris-type *i* deposited in region *j* during blowdown,

D_i = the fraction of total debris-type *i*, and

V_{ZOI} = the total volume of insulation contained within the ZOI.

For fibrous debris, the numbering system is *i* = 1, 2, 3, and 4 for fines, small pieces, large pieces, and intact debris, respectively.

The volume dispersion distribution must add up to one, as

$$\sum_{j=1}^{J} F_{i,j} = 1 \text{ (for each } i\text{)} \quad .$$

The break region was designated as Region 1 (i.e., $j = 1$ and $F_{i,1} = F_{i,break}$), and Section VI.3.3.1 of this appendix provides the methodology for the break-region dispersion fraction. The remaining distribution fractions were estimated using the volume and engineering judgment weighted distribution

$$F'_{i,j(j\neq 1)} = (1 - F'_{i,break}) \frac{wc_{i,j}\ Vc_j}{\sum_{j=2}^{J} wc_{i,j}\ Vc_j} \quad ,$$

where

$wc_{i,j}$ = the weighting factor based on engineering judgment.

If all of the $wc_{i,j}$ were set to one, then the distribution would be simply a volume-weighted distribution.

For large and intact pieces, many of these weighting values $wc_{i,j}$ were set to zero to reflect the fact that large and intact debris likely would not transport into many of the lower level volume regions. It is anticipated that most of the large and intact debris would reside in the break-region volume, sump-pool volume, containment-dome volume, or refueling area.

The substantial quantities of debris transported into the dome subsequently would tend to either fall out of the atmosphere or be washed out by the CSs. About half of this debris would be deposited onto the Level 905 floors that are associated with the dome. However, the other half would fall below this level, thereby entering other volume regions. The volume distribution function $F'_{i,j}$ is modified to account for debris fallout between regions as

$$F_{i,j} = F'_{i,j} + T_j \, F'_{i,2} \quad ,$$

where

T_j = the fraction of debris (type independent) located in the dome that subsequently falls or washes to region *j*.

The values of T_j are based on the opening areas into regions below the dome (e.g., the cross-sectional area of the SG compartments divided by the total cross-sectional area of the containment provides the values for debris that is falling into an SG compartment). The value for a region receiving no debris from dome fallout would be zero. Note that the dome volume region was designated Region 2; therefore, the value for Region 2 (i.e., T_2) must be negative to remove debris from Region 2, as

$$T_2 = -\sum_{j=1}^{J} T_{j(j \neq 2)} \quad .$$

VI.3.3.2.2 Dispersion by Surface Orientation and Exposure

Once the debris was dispersed to a volume region, the analysis assumed it to have been deposited within that region. Some residual fine debris could remain airborne in regions that are not impacted by the sprays; however, the total quantity of this residual airborne debris was not expected to be significant.

The surface area within each volume region was subdivided into six subsections. These subsections reflect both the differing surface orientations and their exposure to moisture. The floors were separated from all of the other surfaces because the floors would receive the gravitationally settled debris and the other surfaces could be flooded partially by spray drainage. The spray water would not accumulate on the other surfaces, which include the walls, ceilings, and equipment.

The analysis considered three surface exposures or moisture conditions—surfaces wetted directly by the CSs, surfaces not directly sprayed but washed by spray drainage (most likely floor surfaces), and surfaces wetted only by steam condensation. Condensation would likely wet all surfaces. The surface exposure determined how likely the flow of water would subsequently transport debris that was deposited onto that particular surface.

The following three-dimensional array describes these areas:

$A_{j,k,l}$ = area for volume region *j*, orientation *k*, and exposure *l*.

All of the area within a particular volume region then would be

$$A_j = \sum_{k=1}^{2} \sum_{l=1}^{3} A_{j,k,l} \quad .$$

The numbering system is k = 1 and 2 for floor and other surfaces, respectively, and l = 1, 2, and 3, for condensate, spray, and drainage exposures, respectively.

The surface-area distribution fractions were estimated using the following area and engineering judgment weighted distribution:

$$f_{i,j,k,l} = \frac{w_{i,j,k,l}\ A_{j,k,l}}{\sum_{k=1}^{2} \sum_{l=1}^{3} w_{i,j,k,l}\ A_{j,k,l}} \quad ,$$

where

$f_{i,j,k,l}$ = the fraction of debris-type i deposited within volume region j that was deposited onto surface k, l, and

$w_{i,j,k,l}$ = the weighting factor based on engineering judgment for debris-type i deposited within volume region j that was deposited onto surface k, l.

An equivalent expression for $f_{i,j,k,l}$ is

$$f_{i,j,k,l} = \frac{w_{i,j,k,l}\ g_{j,k,l}}{\sum_{k=1}^{2} \sum_{l=1}^{3} w_{i,j,k,l}\ g_{j,k,l}} \quad ,$$

where

$$g_{j,k,l} = \frac{A_{j,k,l}}{A_j} \quad .$$

The fractions summed within a particular volume region and for a particular debris type must add up to one:

$$\sum_{k=1}^{2} \sum_{l=1}^{3} f_{i,j,k,l} = 1 \quad .$$

If all of the $w_{i,j,k,l}$ were set to one, then the distribution would be simply an area-weighted distribution. If all the $w_{i,j,k,l}$ were set to zero for k = 2 (other surfaces), then all of the debris would be deposited on the floor, as likely would be the case for the large and intact debris. It is anticipated that most of the large and intact debris would reside on the floors in the break-region volume, sump-pool volume, containment-dome volume, or refueling area. In the SG compartment, much of the large debris stopped on the underside of a grating could fall back down after the depressurization flows subsided.

The volume of debris on a particular surface is expressed by

$$V_{i,j,k,l} = f_{i,j,k,l}\ F_{i,j}\ D_i\ V_{ZOI} \quad .$$

VI.3.4 Washdown Debris Transport

Potential washdown by the CSs, the drainage of the spray water to the sump pool, and (to a lesser extent) the drainage of condensate would subsequently affect the debris that is deposited throughout the containment. Debris on surfaces that would be hit directly by CS would be much more likely to transport with the flow of water than would debris on a surface that is wetted merely by condensation. The transport of debris entrained in spray water drainage is less easy to characterize. If the drainage flows were substantial and rapidly moving, the debris likely would transport with the water. However, at some locations, the drainage flow could slow and be shallow enough for the debris to remain in place. As drainage water dropped from one level to another, as it would through the floor drains, the impact of the water on the next lower level could splatter sufficiently to transport debris beyond the main flow of the drainage, thereby essentially capturing the debris a second time. In addition, the flow of water could erode the debris further, generating more of the very fine debris. These considerations must be factored into the analysis. Figure VI-8 illustrates the washdown processes schematically.

The drainage of spray water from the location of the spray heads down to the sump pool was evaluated. This evaluation provided insights for the transport analysis, such as identifying areas that were not impacted by the CSs, the water drainage pathways, likely locations for drainage water to pool, and locations where drainage water plummets from one level to the next.

VI.3.4.1 Debris Erosion during Washdown

Experiments conducted in support of the DDTS analysis demonstrated that the flow of water could further erode insulation debris. The DDTS analysis was primarily concerned with LDFG debris that was deposited directly below the pipe break and therefore was inundated by the break overflow. Debris erosion in this case was substantial (i.e., approximately 9 percent/h at full flow). Debris erosion caused by the impact of the sprays and spray drainage flows was certainly possible but was found to be much less significant. The DDTS study concluded that the CSs caused less than 1 percent of the LDFG to erode. The analysis neglected debris erosion occurring because of condensation and condensate flow. Debris with its insulation still in its cover was not expected to erode further. For RMI debris, erosion was not a consideration. However, for a microporous insulation such as calcium silicate or Min-K, the washdown erosion has not been determined; it would be expected to be substantial and could potentially erode this type of debris completely into fine silt.

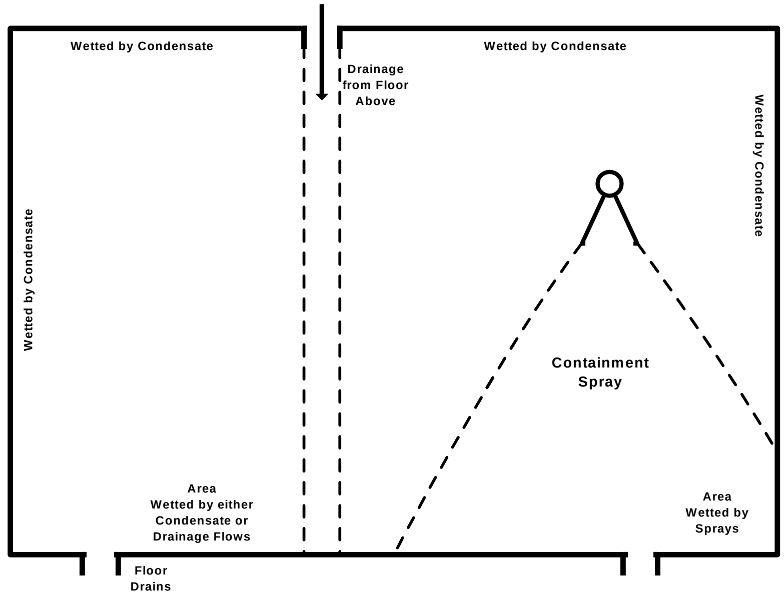

Figure VI-8. Schematic of Debris-Washdown Processes

Because the byproduct of the erosion process is more of the very fine and easily transportable debris, the process must be evaluated. All erosion products were assumed to transport to the sump pool. Because this debris would remain suspended in the sump pool until filtered from the flow at the sump screens, even a small amount of erosion could contribute significantly toward the likelihood of screen blockage.

The only erosion process evaluated herein was the erosion of debris that was impacted directly by the CSs. Erosion caused by break overflow was deferred to the degeneration of debris caused by sump pool turbulence associated with the plummeting of the break flow into the pool. This assumption neglects the erosion of any large debris that is deposited on top of the lower grating in SG1 and impacted directly by the break overflow; however, this quantity of debris was not considered to be substantial. Most of the debris that is located directly below the break likely would be pushed away from the break and into the sump pool. Note that the floors of the SG compartments are 4 ft above the floor of the sump pool. At switchover, the SG floor would not be flooded, but at the maximum pool height, that pool would have a depth of 0.7 ft in the SG compartment.

Table VI-4 summarizes the assumed fractions of fibrous debris that were eroded. It was assumed that condensate drainage would not cause further erosion of debris and that intact or covered debris would not erode further. Erosion does not apply to fine debris because that debris is already fine. About 1 percent of the small- and large-piece debris that the sprays directly impacted was considered to have eroded. This amount of erosion was considered to be conservative because the DDTS concluded that the erosion was less than 1 percent. No erosion of the intact debris was assumed because the canvas cover likely would protect the insulation.

Table VI-4. Total Erosion Fractions for Fibrous Debris

Exposure	Fines	Small	Large	Intact
Condensate	N/A	0	0	0
Sprays	N/A	1%	1%	0

To estimate the volume of debris that was eroded, the volume of debris that was impacted by the sprays first must be estimated. The latter estimate can be made using the data arrays that were already established in this methodology. These volumes for small and large debris, respectively, are estimated using the following two equations:

$$Vspr_2 = \sum_{j=1}^{J} \sum_{k=1}^{2} f_{2,j,k,2}\ F_{2,j}\ D_2\ V_{ZOI}$$

and

$$Vspr_3 = \sum_{j=1}^{J} \sum_{k=1}^{2} f_{3,j,k,2}\ F_{3,j}\ D_3\ V_{ZOI} \quad .$$

The volumes that are eroded (E_2 and E_3 for small and large debris, respectively) are simply 1 percent of the debris volumes impacted by the sprays, given as

$$E_2 = e_{spr} Vspr_2$$

and

$$E_3 = e_{spr} Vspr_3 \quad ,$$

where the spray erosion fraction e_{spr} is 0.01.

VI.3.4.2 Capture Retention during Washdown

The retention of debris during washdown must be estimated for the debris deposited on each surface (i.e., the fraction of debris that remains on each surface). The study assigned these estimates, based on experimental data and engineering judgment, somewhat generically. For surfaces that would be washed only by condensate drainage, nearly all deposited fine and small debris likely would remain there. The DDTS assumed that only 1 percent of the fibrous debris would be washed away in the more realistic central estimate of that study (a value of 10 percent was assumed for the upper bound estimate). When the analysis applied the 1 percent assumption, all of the surfaces that drained only condensate would have a retention fraction of 0.99 with respect to fibrous debris.

For surfaces that were hit directly by sprays, the DDTS assumed 50 percent and 100 percent for the central and upper bound estimates for small fibrous debris. Large and intact debris likely would not be washed down to the sump pool (retention fractions of 1).

For surfaces that were not sprayed directly but subsequently drain accumulated spray water, such as floors close to spray areas, the retention fractions were much less clear. These fractions likely would vary with location and drainage flow rates and therefore must be area location specific, with more retention for small pieces than for fine debris.

The retention fraction for a specific volume region is expressed as

$$R_{i,j} = \sum_{k=1}^{2} \sum_{l=1}^{3} f_{i,j,k,l} \; r_{i,j,k,l} \quad ,$$

where

$R_{i,j}$ = the fraction of debris-type *i* retained in region *j*, and

$r_{i,j,k,l}$ = the fraction of debris-type *i* retained, on surface *k*, *l*, in region *j*.

These volume region retention fractions $R_{i,j}$ do not account for the quantities that are eroded from the captured pieces of debris. To complete the erosion model, the analysis estimated the volumes of eroded debris that came from debris that remained captured versus debris that transported to the sump pool. Therefore, the debris that remained captured during the washdown process is estimated using the following two equations for small- and large-piece debris, respectively:

$$Rspr_2 = \sum_{j=1}^{J} \sum_{k=1}^{2} r_{2,j,k,2} \; f_{2,j,k,2} \; F_{2,j} \; D_2 \; V_{ZOI}$$

and

$$Rspr_3 = \sum_{j=1}^{J} \sum_{k=1}^{2} r_{3,j,k,2} \; f_{3,j,k,2} \; F_{3,j} \; D_3 \; V_{ZOI} \quad .$$

Therefore, the volumes of eroded debris associated with the debris that remained captured are expressed as

$$ER_2 = e_{spr} Rspr_2$$

and

$$ER_3 = e_{spr} Rspr_3 \quad .$$

Debris transported from its original volume region still could be captured at a lower elevation. This analysis neglected this secondary capture.

VI.3.5 Debris Volumes Introduced to the Sump Pool

The blowdown/washdown transport analysis primarily results in the volume that is transported to the sump pool by debris category. The volumes of debris transported to the pool are given by

$$V_{i,pool} = \left[1 - \sum_{j=1}^{J} R_{i,j} F_{i,j}\right] D_i \, V_{ZOI} + Ve_i \quad ,$$

where

$V_{i,pool}$ = the volume of debris-type *i* transported to the sump pool, and

Ve_i = the volumes of eroded debris transferring from small- and large-debris categories to the fine-debris category.

The erosion translation array is given by

$$Ve_i = \begin{bmatrix} +(E_2 + E_3) \\ -(E_2 - ER_2) \\ -(E_3 - ER_3) \\ 0 \end{bmatrix} \quad .$$

This array adds the eroded product ($E_2 + E_3$) to the fine-debris category and subtracts the eroded volume from the noncaptured small- and large-debris categories ($E_i - ER_i$). The total debris that transports to the pool is

$$V_{pool} = \sum_{i=1}^{4} V_{i,pool} \quad .$$

This model does not track debris transport in sufficient detail to determine where the debris would enter the sump pool. It assumed simply that the debris would mix uniformly with flows entering the pool.

VI.3.6 Transport Fractions

The overall debris-transport fraction now can be estimated as

$$TF_{ZOI} = \frac{V_{pool}}{V_{ZOI}} \quad ,$$

where

TF_{ZOI} = the fraction of insulation that is located in the ZOI and subsequently is transported to the sump pool.

The transport fractions for each individual debris category can be estimated as

$$TF_i = \frac{V_{i,pool}}{D_i \, V_{ZOI}} \quad ,$$

where

TF_i = the fraction of debris-type *i* that is generated within the ZOI and subsequently is transported to the sump pool.

Note that the transport fractions incorporate the translation of erosion products from the small- and large-debris categories to the fine-debris category.

VI.4 Debris-Transport Analysis

When the methodology presented in Section VI.3 was used, plausible estimates were developed for the transport of insulation debris within the volunteer-plant containments. Because of the complexity of the analysis and the limited available data, substantial uncertainty exists in these estimates. Engineering judgment that was used to fill gaps in the data was tempered conservatively. Despite the uncertainty, the transport analysis illustrated trends, as well as plausible estimates of the fractions of the debris that was generated and subsequently could transport to the sump pool.

VI.4.1 Fibrous Insulation Debris Transport

As discussed in Section VI.3.2, the insulation that is used in the volunteer-plant containments consists of fibrous, RMI, and Min-K insulation at approximately 13.4 percent, 85.7 percent, and 0.9 percent, respectively. The majority of the available debris-transport data was obtained for LDFG insulation debris, specifically experimental data taken for the DDTS (NUREG/CR-6369-2, 1999). Although a majority of the insulation within these containments is RMI, the fibrous insulation debris, in combination with particulate, is expected to be a larger challenge to the operation of the recirculation sump screens. Therefore, the debris transport for the fibrous debris was analyzed first. Even with the available transport data for LDFG debris, the transport analysis required the application of conservatively tempered engineering judgment.

VI.4.1.1 Fibrous Blowdown Debris Transport

The first consideration in performing the dispersion estimate for the fibrous blowdown insulation debris was the dispersion and deposition within the break region (assumed to be a break in SG1), where deposition likely resulted from inertial impaction. The dispersion through the remainder of the containment was subsequently estimated.

VI.4.1.1.1 Break-Region Blowdown Debris Deposition

The effluences from the break would carry insulation debris with the flows into the upper containment dome through the large opening at the top of the SG compartment and into lower compartments through the compartment access doorways. Along the way, substantial portions of that debris likely would be inertially deposited or otherwise entrapped onto structures. In general, the break-region flow immediately after the initiation of the break would be much too violent to allow debris simply to settle to the floor of the region.

VI.4.1.1.1.1 Characterize Break Flows within Break Region

The thermal-hydraulic MELCOR code was used to determine the distribution of the break effluents from the SG compartment. When a break in SG1 was postulated, it was determined that most of the break effluent would be directed upward toward the large upper dome. Because of the large openings connecting SG1 to SG4, the venting to the dome would occur through both SG compartments. Effluents venting into lower level compartments (surrounding the two SGs) by way of open access doorways would flow at much lower rates than the upward flows to the dome. Figure VI-6 shows the nodalization of the two SG compartments, where the break was postulated to occur in Volume V12. The analysis assumed break effluents that are typical of three break sizes—large-break (LB) LOCA, medium-break (MB) LOCA, and small-break (SB) LOCA. Table VI-5 summarizes the results of the MELCOR simulations and shows the distributions from a particular control volume by the connecting junction. For example, given an LBLOCA scenario, approximately 80 percent of the flow from Volume V12, where the break was postulated, went upward through Junction J12, with the remainder going downward through Junction J11. Note that the flow splits were somewhat transient and that the results in Table VI-5 are reasonable approximations of the transients over the time where most debris transport would occur. The LBLOCA and MBLOCA flows were reasonably steady over the transport period, but SBLOCA flows were not steady because of transition into natural circulation after approximately 6 s.

Inertial debris deposition depends on the flow velocities transporting the debris. The MELCOR calculations predicted transient flow velocities for each flow junction and each size of break. Table VI-6 provides the general ranges of these velocities. The velocities are in the general range as the test velocities for which the DDTS measured the debris-capture data.

Table VI-5. Break Effluent Flow Splits

Break Size	**Flows Exiting Volume V_i through Junction J_j**								
	V12		**V11**		**V41**		**V13**		
	J11	**J12**	**J21**	**J22**	**J23**	**J41**	**J13**	**J31**	**J32**
LBLOCA	20%	80%	70%	30%	5%	95%	62%	33%	5%
MBLOCA	20%	80%	70%	30%	14%	86%	62%	33%	5%
SBLOCA	15%	85%	80%	20%	30%	70%	66%	28%	6%

Table VI-6. Characteristic Velocities in SG1

Postulated Break Size	Characteristic Velocities	
	m/s	ft/s
LBLOCA	25–200	80–660
MBLOCA	5–45	15–150
SBLOCA	1–8	5–25

VI.4.1.1.1.2 Debris-Transport Distributions from Volumes

The very fine debris would transport more like an aerosol in that the particles would disperse within the flow and follow the flow. Portions of this debris would be deposited onto structures along the transport pathways, primarily because of inertial deposition at bends in the flow. However, with larger debris, the tendency would be greater for the debris not to follow the flow through sharp bends in the flow and larger debris would more likely be trapped by a structure such as a grating. In addition, gravitational settling as the flow velocities slow would be more effective for larger debris than smaller debris. For example, following an LBLOCA in an SG compartment, a large, nearly intact insulation pillow could travel upward with the main flow to the containment dome unless an obstacle, such as a grating, impeded that pillow. However, this pillow would be much less likely to follow the flow through a connecting doorway to the next SG compartment.

The solution to this problem required assumptions based on engineering judgments that were tempered by experimental observations. The assumptions provide a reasonable crude approximation of debris transport from a volume when there is a split in the flow. These assumptions include the following:

- The fine and small fibrous debris would be well dispersed within the flow and would transport uniformly with the flow; therefore, the debris-transport junction distributions for fines and small debris are the same as the junction flow distributions in Table VI-7.
- Large and intact debris would not make the turn to exit SG1 at Level 832 (Junctions J31 and J32). In addition to the turn, the gratings that cover approximately 45 percent of the cross-sectional area of the compartment that is nearest those exits would stop most of this debris that was moving towards these exits.
- Large and intact debris entering SG4 at the floor level (Level 812) would be much less likely to follow the flow through the 90-degree bend and subsequently transport upward through SG4. Debris entering Volume V41 that is not captured in Volume V41 would exit by either Junction V23 or V41. For large and intact debris, the flow fractions for Junction V41 were reduced by one-half and two-thirds, respectively, based on engineering judgment.

Applying these assumptions to the transport of the large and intact debris through the node junctions resulted in the junction transport distributions that are shown in Table VI-7 and Table VI-8.

Table VI-7. Large-Debris-Transport Junction Distributions

Break	V12		V11		V41		V13		
	J11	J12	J21	J22	J23	J41	J13	J31	J32
LBLOCA	20%	80%	70%	30%	52%	48%	100%	0%	0%
MBLOCA	20%	80%	70%	30%	57%	43%	100%	0%	0%
SBLOCA	15%	85%	80%	20%	65%	35%	100%	0%	0%

Table VI-8. Intact-Debris-Transport Junction Distributions

Break	V12		V11		V41		V13		
	J11	J12	J21	J22	J23	J41	J13	J31	J32
LBLOCA	20%	80%	70%	30%	68%	32%	100%	0%	0%
MBLOCA	20%	80%	70%	30%	71%	29%	100%	0%	0%
SBLOCA	15%	85%	80%	20%	77%	23%	100%	0%	0%

VI.4.1.1.1.3 Capture Fractions at Junctions

Debris-transport data from the Army Research Laboratory (ARL) and the CEESI tests that were conducted to support the DDTS (NUREG/CR-6369-2, 1999) provide average capture fractions for LDFG debris that is passing though typical gratings and around typical structures, such as piping and beams, and for debris making a 90-degree bend. These structures and the bend were wetted during the tests; the data do not apply to dry structures. These data are assumed to apply in general to the volunteer-plant containments because it is expected that steam condensation,* as well as liquid break effluent, would rapidly wet the containment surface and because the range of predicted flow velocities (Table VI-6) are in general agreement with the flow velocities of the tests. The flow velocities ranged from 25 to 150 ft/s for the ARL tests and from 35 to 60 ft/s for the CEESI tests. The debris capture applied most to MBLOCAs and perhaps least to SBLOCAs.

Fine and small fibrous debris could be captured inertially onto wetted surfaces whenever the break flow changed direction, such as flows through the doorways from the SG compartments into the sump-level annular space. These flows must make at least one 90-degree bend through those entrances. Debris-transport experiments that were conducted at CEESI demonstrated an average capture fraction of 17 percent for fine and small debris that were making a 90-degree bend. These surfaces would be wetted because of steam condensation and the liquid portion of the break effluence. Other flow bends likely would occur within the violent three-dimensional flows near the break. The platform gratings within the SG compartments would capture substantial amounts of debris, even though the gratings do not extend across the entire compartment. The CEESI debris-transport tests demonstrated that an average of 28 percent of the fine and small LDFG debris was captured when the airflow passed through the first wetted grating encountered and that an average of 24 percent was captured at the second grating. A grating would completely trap the large and intact debris. In addition, the tests showed equipment (such as beams and pipes) to capture fine and small debris. In

* Based on analyses performed for the DDTS (NUREG/CR-6369-3, 1999).

the CEESI tests, the structural maze in the test section captured an average of 9 percent of the debris passing through the maze.

In the volunteer plant, partial gratings exist at three levels in each of the SG compartments. The gratings extend over approximately 22 percent, 45 percent, and 15 percent of the SG cross-sectional area at plant elevations 824, 841, and 905 ft, respectively.* If it is assumed that a grating captures 28 percent of small and fine fibrous debris and 100 percent of the large and intact debris from the flow as it passes through the grating, Table VI-9 provides the capture fractions for model junctions that contain a grating.

Table VI-9. Grating Capture Fractions at Model Junctions

Grating Level	Model Junctions	Fine and Small Debris		Large and Intact Debris	
		Unit Area Capture Fraction	Junction Capture Fraction	Unit Area Capture Fraction	Junction Capture Fraction
Level 905	J14 and J44	0.28	0.04	1.0	0.15
Level 841	J12 and J42	0.28	0.13	1.0	0.45
Level 824	J11 and J 41	0.28	0.06	1.0	0.22

Depressurization flows also would exit the SGs by way of the SG access doorways at Levels 808 and 832. Flows traveling through these pathways would carry debris directly into the lower levels of the containment; in fact, some of the debris likely would be deposited near the recirculation sumps. Because these doorways were designed with at least one 90-degree bend, debris would be deposited inertially onto wetted surfaces at each bend in the flow. Furthermore, because the CSs would not impact these vertical surfaces, the debris likely would remain on the surfaces once it was captured there. The CEESI data showed an average of 17 percent debris capture at its 90-degree bend for debris that was small enough to already have passed through a grating (i.e., fines and small debris). The analysis assumed that 17 percent of fine and small debris that was transported from the SG break region through the Level 808 and Level 832 doorways to the bulk containment would be captured at a bend (one bend assumed). No comparable data exist for the large and intact debris; however, the larger debris would be much less likely to stick to a wall once it impacted inertially against the wall. Because of a lack of appropriate data, it was assumed conservatively that these doorways would capture no large or intact debris.

VI.4.1.1.1.4 Capture Fractions within Volumes

As illustrated in Table VI-9, debris would be captured on structures within the model nodes, as well as the node junctions. As the break effluents flowed around and through the structural and equipment congestion within the SG compartment, debris would be

*These fractions were estimated from plant drawings.

driven inertially onto surfaces where some portion of it would remain captured. The structures include the pumps, SGs, and associated piping, beams, equipment stands, cabling, and other items. The chaotic nature of the flows as the break jet is deflected off structures and wall surfaces could create a multitude of bends in the flow that could deposit debris inertially onto wall surfaces and irregular wall features. In the CEESI tests, approximately 9 percent of the fine and small debris was deposited onto wetted structures as the debris passed through a test structural assembly and 17 percent was captured onto a wetted surface at a sharp 90-degree bend in flow. Estimates of the amounts of debris captured within a node volume were based on this CEESI test data and on conservatively tempered engineering judgment. It is likely conservative to capture more debris within the SG than to transport the debris throughout the containment because washdown within the SG should be relatively greater than some other areas of the containment and because debris washed off the SG structures can go directly to the sump pool.

Applying a number of engineering judgments in conjunction with the CEESI data resulted in estimates for the capture of debris within each volume of the break-region debris-transport model. Table VI-10 provides these estimates, along with the associated assumptions.

Table VI-10. Fractions of Debris Captured within Each Volume

SG1					SG4			
Volume	Fines and Small Pieces	Large Pieces	Intact Pieces		Volume	Fines and Small Pieces	Large Pieces	Intact Pieces
V14	1% (A)	2% (A)	5% (A)		V44	1% (A)	2% (A)	5% (A)
V13	1% (A)	2% (A)	5% (A)		V43	1% (A)	2% (A)	5% (A)
V12	14% (C)	30% (E)	50% (F)		V42	9% (B)	15% (E)	30% (G)
V11	26% (D)	40% (E)	80% (H)		V41	14% (C)	25% (E)	80% (H)

Assumptions
A. Volumes contain minimal structures and no significant flow bends; therefore, a minimal amount of capture occurs. It is somewhat more likely that large debris would be captured than small debris and more likely that intact debris would be captured than large debris.
B. Structures are equivalent to one CEESI structural test assembly (9 percent), and no significant flow bends exist.
C. Structures are equivalent to one CEESI structural test assembly (9 percent), and significant flow bending that is less than a sharp 90-degree bend exists (5 percent).
D. Structures are equivalent to one CEESI structural test assembly (9 percent), and significant flow bending that is equivalent to a sharp 90-degree bend exists (17 percent).
E. Large debris is more likely to be captured than small debris, and 50 percent more large debris is captured than small debris.
F. Intact debris is much more likely to snag on equipment than the large debris. In addition, some insulation within the ZOI likely could remain attached to piping.
G. Intact debris is much more likely to snag on equipment than the large debris.
H. The congestion of equipment and cables near the floor is expected to trap most of the intact debris as the flow makes a 90-degree bend near the floor. Intact debris is less likely to follow the distribution of flow than is smaller debris.

VI.4.1.1.1.5 Break-Region Debris-Transport Quantification

The logic chart shown in Figure VI-7 and discussed in Section VI.3.3.1 was used to quantify the various flow splits and capture and to estimate the debris deposition within and from SG1. The chart divides the evaluation into many smaller problems that are amenable to resolution—an approach that was adapted from the resolution of the BWR strainer-blockage issue (NUREG/CR-6369-1, 1999). This chart tracks the progress either of small debris from the pipe break (Volume V12) until the debris is assumed to be captured or until the debris is transported beyond the compartment. Charts were quantified for each of the three LOCA sizes (i.e., small, medium, and large) and for three classifications of fibrous debris (i.e., fines and small pieces, large pieces, and intact pieces). Note that there was no basis to treat the fines and small pieces differently. Sections VI.4.1.1.1.1 through VI.4.1.1.1.4 discuss the data that were used to quantify the charts. As an example, Figure VI-9 shows the chart for the transport of fines and small debris following an LBLOCA.

Table VI-11 shows the overall results of the break-region quantification. The results for the three break sizes were averaged into a single set of results because the differences among the three size groups were substantially less than the substantial uncertainties associated with these analyses. The charts also provided information regarding the distribution of debris captured with the SGs, as well as the debris driven from the SGs.

Table VI-11. Distribution of Debris Captured and Exiting Break Region

Location	Debris Category		
	Fines and Small Pieces	**Large Pieces**	**Intact Pieces**
Captured within SGs 1 and 4	0.36	0.70	0.82
Expelled to Dome	0.58	0.26	0.17
Expelled to Level 832	0.03	0	0
Expelled to Level 808	0.03	0.04	0.01

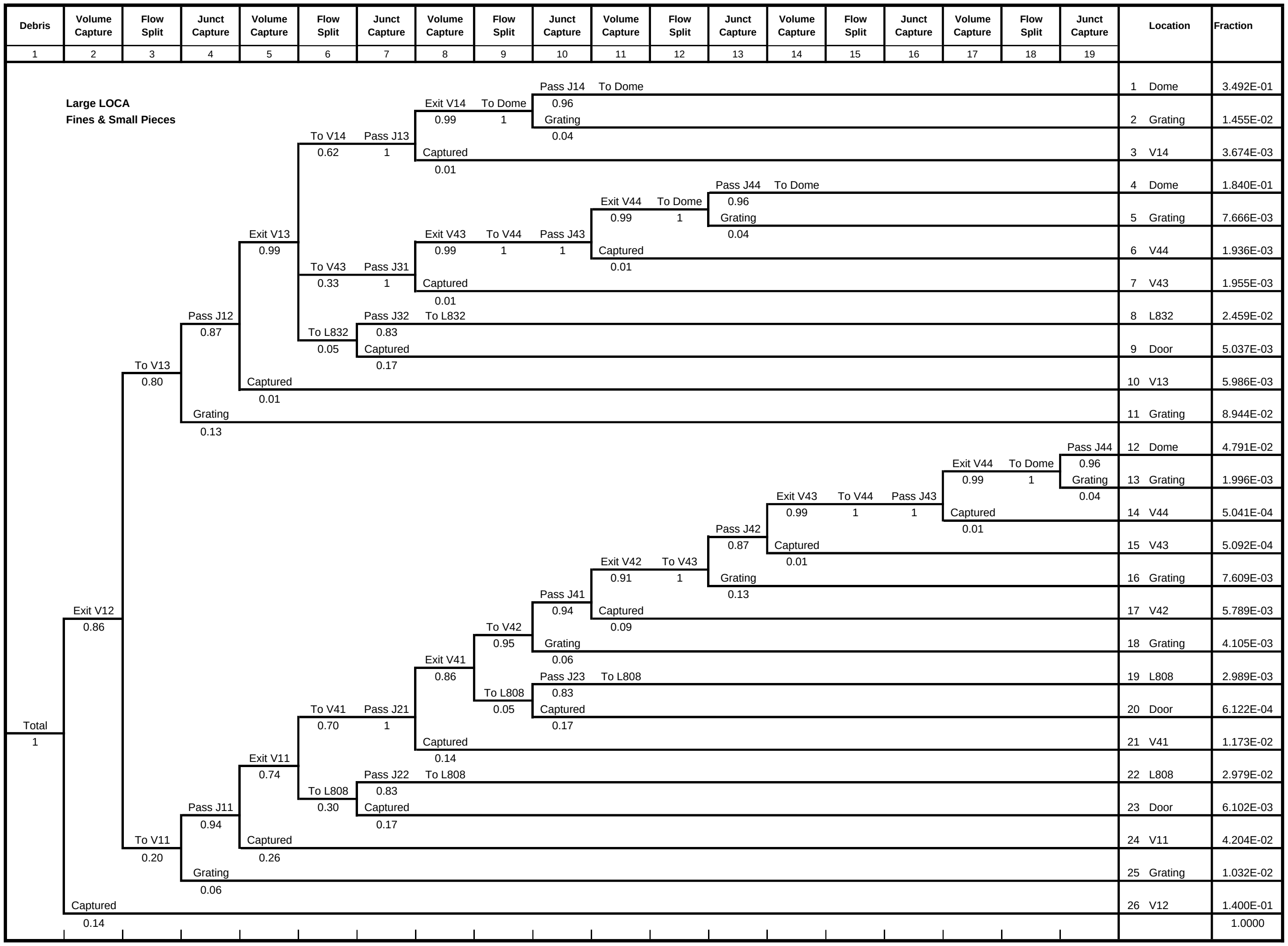

Figure VI-9. Break-Region LBLOCA Transport Chart for Fines and Small Debris

VI.4.1.1.2 Dispersion throughout Remainder of Containment

Section VI.3.3.2 presents the debris dispersion model used to evaluate debris transport within the volunteer-plant containments by estimating dispersion throughout the containment first by free volume and then by surface orientation within a volume region.

VI.4.1.1.2.1 Dispersion by Volume Region

The containment free volume was subdivided into volume regions that were based on geometry, such as floor levels and walls, and on the location of CSs. Specifically, areas where CSs would not likely wash down deposited debris were separated from areas that were impacted by the sprays. The volunteer-plant free volume was subdivided into 24 distinct regions, as shown in Table VI-12. The volumes of each region were estimated from plant drawings.

Table VI-12. Subdivision of Containment Free Volume

No.	Volume Region	Volume (ft^3)	Volume Fraction Vc_j
1	SG1&4	76600	0.02570
2	Dome—Above 905.75-ft	1992060	0.66848
3	L873—MS	39300	0.01319
4	Head Lay-Down—L871.5	17120	0.00574
5	Below Head Platform	5750	0.00193
6	Refueling A	45340	0.01521
7	Refueling B	53860	0.01807
8	Refueling C	48660	0.01633
9	Refueling D	47960	0.01609
10	SG2&3	76600	0.02570
11	Pressurizer	11250	0.00378
12	L860 Annulus—Section 1	34100	0.01144
13	L860 Annulus—Section 2	54580	0.01832
14	L860 Annulus—Section 3	94310	0.03165
15	L851—FW	25800	0.00866
16	Accumulator Section	31500	0.01057
17	L832 Annulus—Section 1	37250	0.01250
18	L832 Annulus—Section 2	33940	0.01139
19	L832 Annulus—Section 3	69890	0.02345
20	L808 Annulus—Section 1	61650	0.02069
21	L808 Annulus—Section 2	30830	0.01035
22	L808 Annulus—Section 3	61650	0.02069
23	Reactor Cavity	25000	0.00839
24	Equipment Room L808	5000	0.00168
	Containment Total	2980000	1.00000

Key aspects of the region subdivision follow. The first region, designated SG1 and 4, is the SG compartment 1 where the break was postulated and its connected neighboring SG compartment, SG4. Section VI.4.1.1.1 predicted debris dispersion and deposition in these SG compartments. The second region represents the free volume above the highest floor (i.e., the dome region), which is approximately two-thirds of the entire containment free volume. As shown in Figure VI-10, the lower floor levels were subdivided azimuthally into three sectors to better distinguish the areas with CSs from areas without the sprays. The refueling pool area was subdivided into four regions to reflect the three different pools and the reactor vessel head area (i.e., (A) storage pool for reactor vessel upper internals, (B) reactor vessel area, (C) storage pool for reactor vessel lower internals, and (D) pool for fuel transfer and storage).

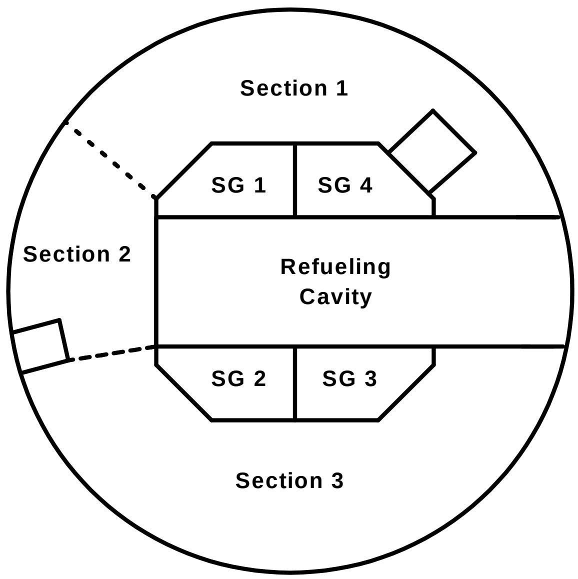

Figure VI-10. Volume Region Sector Model

Debris, particularly the larger debris, would not distribute uniformly throughout the free volume. The methodology presented in Section VI.3.3.2.1 applies weighting factors ($wc_{i,j}$) to the free-volume distribution to estimate the distribution of debris throughout the containment (i.e., the distribution of the debris among the 24 volume regions) by debris type. The very fine debris likely would transport somewhat uniformly with the depressurization flows, which would penetrate all free space within the containment as the containment pressurized. The transient nature of debris generation would also introduce nonuniformities into the dispersion of the fine debris. Because no rationale was found to weight the distribution of the fine and small debris away from that of a uniform free-volume distribution outside the break region, all weighting factors were assumed to be 1 for fine and small fibrous debris.

For the largest debris, specifically the large-piece and intact-piece classifications, the debris that is ejected from the SG compartments into the dome region likely would fall back to the floors and structures of the higher levels. The settling of debris that was ejected into the dome atmosphere was proportioned onto the upper floors according to the distribution of floor area (e.g., the cross-sectional area of a SG compartment divided by the cross-sectional area of the overall containment determined the fraction of settling debris that would fall into that compartment). The largest debris likely would not enter lower compartment volumes, except for debris ejected into the sump-level annulus via personnel access doorways. The assumed weighting factors for the large and intact debris were specified to give preference to the deposition of larger debris onto the uppermost floors and into the sump-level annulus. The large-piece debris was assumed to transport somewhat more easily than the intact-piece debris. Table VI-13 shows the assumed weighting factors and the dome fallout fractions.

Table VI-13. Volume Region Weighting Factors

No.	Volume Region	Dome Fallout Fraction T_j	Volume Weighting Factors			
			Fines $wc_{1,j}$	Small Pieces $wc_{2,j}$	Large Pieces $wc_{3,j}$	Intact Pieces $wc_{4,j}$
1	SG1&4	0.0951	1	1	1	1
2	Dome - Above 905.75-ft	0	1	1	1	1
3	L873 - MS	0.0555	1	1	0.5	0.3
4	Head Lay-Down - L871.5	0.0349	1	1	0.8	0.5
5	Below Head Platform	0	1	1	0.3	0
6	Refueling A	0.0495	1	1	0.8	0.5
7	Refueling B	0.0579	1	1	0.8	0.5
8	Refueling C	0.0505	1	1	0.8	0.5
9	Refueling D	0.0596	1	1	0.8	0.5
10	SG2&3	0.0978	1	1	0.5	0.3
11	Pressurizer	0	1	1	0	0
12	L860 Annulus - Section 1	0.0092	1	1	0.3	0
13	L860 Annulus - Section 2	0.0052	1	1	0.3	0
14	L860 Annulus - Section 3	0.0241	1	1	0.3	0
15	L851 - FW	0	1	1	0	0
16	Accumulator Section	0.0060	1	1	0.8	0.5
17	L832 Annulus - Section 1	0	1	1	0	0
18	L832 Annulus - Section 2	0	1	1	0	0
19	L832 Annulus - Section 3	0	1	1	0	0
20	L808 Annulus - Section 1	0	1	1	1	1
21	L808 Annulus - Section 2	0	1	1	1	1
22	L808 Annulus - Section 3	0	1	1	0.3	0
23	Reactor Cavity	0	1	1	0	0
24	Equipment Room L808	0	1	1	0	0
	Total	0.5453				

Figure VI-11 illustrates the results of the blowdown distribution by groups of volume regions. In this estimate, the largest portion of the debris was deposited inside the SG compartments, where the break was postulated, because of inertial deposition that occurred as the fast-moving flows drove the debris into and through equipment and structures. This was particularly true for the larger debris, which could not pass through the gratings. The upper level floors (871-, 873-, and 905-ft levels) received substantial debris falling or settling out of the dome atmosphere. The regions above the refueling pools received debris that was driven into those volumes, as well as debris falling or settling from the dome atmosphere; this comment also applies to the opposite SG compartments, SGs 2 and 3. The pressurizer compartment received only small amounts of fine and small debris and no larger debris because the compartment has a roof that prevents debris from falling into the compartment and is relatively small. The lower levels received relatively small quantities of mostly large-piece debris because of their remoteness from the dome. Most of the debris entering Levels 832 and 808 was debris that was expelled from the SG compartments by way of the personnel access doorways; therefore, this debris would likely be located near those doors.

The CSs would impact most of the deposited debris; these surface areas include the four SG compartments, the upper floor surfaces, and the refueling area. The sprays did not impact regions such as the pressurizer compartment and certain portions of the lower levels. This observation suggests that a large fraction of the more transportable debris would move to the sump pool.

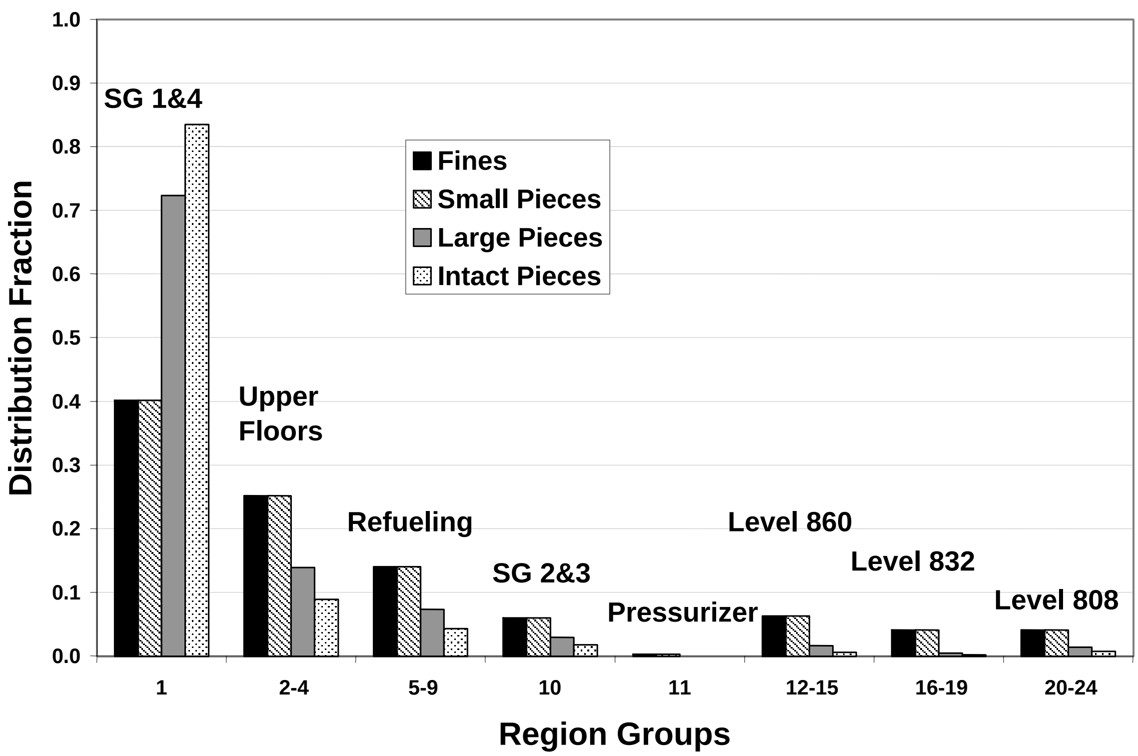

Figure VI-11. Blowdown Distribution by Region Groups

VI.4.1.1.2.2 Dispersion by Surface Orientation and Surface Wetness

Once the debris dispersion prediction placed each type of debris within the 24 volume regions, the debris was dispersed further by surface area classification (i.e., orientation and exposure to moisture). The surface orientation was either floor area or other area, distinguished by the fact that gravitational settling preferentially deposited debris onto the floor. The surface exposure to moisture included surfaces that the CSs impacted directly, surfaces subjected to spray drainage but not sprayed directly, and the remaining surfaces, which would be wetted by condensation. In this manner, the surface area within each volume region was subdivided into six surface groupings. This subdivision was based on both engineering drawings and engineering judgment. The drawings provided basic geometric information such as floor areas; however, engineering judgment, in addition to drawings, was required to estimate fractions of surfaces that were sprayed directly or covered by spray drainage. Table VI-14 shows the estimated area distribution fractions.

The floor fraction is an estimate of the total surface area that would receive gravitationally settling debris. This estimate includes upward-facing equipment, as well as the floor (the equipment and piping was assumed to have the same floor fraction as the wall, floor, and ceiling surfaces). The condensate, spray, and drainage fractions represent the fraction of each orientation with this type of exposure. With these fractions, the surface areas and area ratios (i.e., $A_{j,k,l}$ and $g_{j,k,l}$) are determined. For example, the floor fraction for a given region multiplied by the spray $g_{j,k,l}$ fractions for that region's floor multiplied by the total surface area of the region yields the floor surface area that was sprayed directly by the sprays.

Table VI-14. Regional Areas Fractions

No.	Volume Region	Floor Fraction	Floor Surface Area			Other Surface Area		
			Condensate Fraction	Spray Fraction	Drainage Fraction	Condensate Fraction	Spray Fraction	Drainage Fraction
1	SG1&4	0.07	0	1	0	0.1	0.5	0.4
2	Dome - Above 905.75-ft	0.09	0	1	0	0	1	0
3	L873 - MS	0.17	0.2	0.6	0.2	0.9	0.1	0
4	Head Lay-Down - L871.5	0.61	0	1	0	0	0	1
5	Below Head Platform	0.30	0.6	0.1	0.3	0	0	1
6	Refueling A	0.37	0	1	0	0	0	1
7	Refueling B	0.41	0	1	0	0	0	1
8	Refueling C	0.55	0	1	0	0	0	1
9	Refueling D	0.68	0	1	0	0	0	1
10	SG2&3	0.07	0	1	0	0.1	0.5	0.4
11	Pressurizer	0.04	1	0	0	1	0	0
12	L860 Annulus - Section 1	0.10	0.9	0.1	0	1	0	0
13	L860 Annulus - Section 2	0.19	0.1	0.6	0.3	0.6	0.1	0.3
14	L860 Annulus - Section 3	0.19	0.1	0.6	0.3	0.6	0.1	0.3
15	L851 - FW	0.19	0.8	0	0.2	1	0	0
16	Accumulator Section	0.13	0	0.5	0.5	0.5	0	0.5
17	L832 Annulus - Section 1	0.18	0.9	0	0.1	0.7	0	0.3
18	L832 Annulus - Section 2	0.15	0.4	0	0.6	0.6	0	0.4
19	L832 Annulus - Section 3	0.17	0.3	0.5	0.2	0.6	0	0.4
20	L808 Annulus - Section 1	0.18	0	0	1	0.7	0.3	0
21	L808 Annulus - Section 2	0.18	0	0	1	0.7	0.3	0
22	L808 Annulus - Section 3	0.19	0	0	1	0.7	0.3	0
23	Reactor Cavity	0.13	0	0	1	1	0	0
24	Equipment Room L808	0.21	0	0	1	1	0	0

Next, the area weighting factors ($w_{i,j,k,l}$) were estimated, which preference debris toward one surface over another. The dominant preferential debris deposition (and the only preference that can be estimated realistically) is gravitational debris that settles to the floor surfaces. The weighting factors for the nonfloor surfaces ($k = 2$) were set first to 1 (i.e., $w_{i,j,2,l} = 1$), and then the weighting factors for the floor surfaces within each volume region were estimated for each debris type such that the weighting factors preferentially forced debris deposition onto the floor surfaces. The floor weighting factor estimates used the following equation, where the weighting factor is a function of two physical variables that can be estimated more readily. These variables are the fraction of the surface area that is floor area (a geometric determination) and the fraction of the debris that is deposited onto the floor (an engineering judgment and computational determination):

$$w_{floor} = \left(\frac{d_{floor}}{1-d_{floor}}\right)\left(\frac{1-g_{floor}}{g_{floor}}\right) ,$$

where

w_{floor} = the weighting factor for debris deposited onto the floor inside a volume,

d_{floor} = the fraction of the debris deposited within a volume that was on the floor,

and

g_{floor} = the fraction of the volume surface area that is floor area.

The determination of the floor-area fraction (g_{floor}) is a straightforward estimate of the floor area divided by the total surface area in a volume region (listed in Table VI-14). In actuality, the surface-area estimate includes the areas associated with equipment and piping because debris can settle onto equipment and piping, as well as onto floors. To reduce the complexity of the area estimates, it was assumed that the area fractions for the equipment and piping were the same as the area fractions for the wall, ceiling, and floor surfaces. Because of this assumption and other geometrical assumptions, these area fractions have an inherent uncertainty associated with the estimates; however, this uncertainty should be significantly smaller than some of the other transport uncertainties.

Debris deposition processes other than gravitational settling, such as diffusiophoresis (condensation-driven deposition), do not depend on surface orientation for these processes; the weighting factors all would be set to 1. Driven debris could be deposited inertially onto any surface or could snag on an obstacle. Heavy, inertially deposited debris subsequently may fall to the floor, but substantially smaller debris likely would remain pasted onto the surface. Even heavy debris can remain on a nonhorizontal surface if the piece were physically snagged. Vertically moving debris eventually would settle onto a surface that is sufficiently horizontal to retain the debris. The fraction of debris deposition onto the floor is highly dependent on the size of the debris.

The estimate of the fraction of the debris that was deposited onto the floor depended greatly on conservative judgments; therefore, the fraction introduced substantial uncertainty into the transport estimates. The engineering judgments accounted for the geometry of the region under consideration, including the relative structural congestion. It was conservative to place the debris on the floor as opposed to other surfaces because more of the debris that was deposited on the floor would be subjected to spray washdown on the floor than on other surfaces. For the SG compartments where the pipe break was postulated (SGs 1 and 4), debris deposition data from the logic charts were used to estimate debris on the floor of these compartments. This estimate included larger debris that was trapped on the underside of gratings and that would likely fall back once the depressurization flow subsided. It was assumed that debris that fell or settled from the dome atmosphere into lower level regions would fall or settle onto a floor surface.

A typical judgment estimate for fractions of debris that had been driven into an enclosure and that would subsequently settle to the floor was 0.4, 0.7, 0.99, and 0.99 of the fines, small pieces, large pieces, and intact pieces, respectively. For fine debris, the floor deposition fraction was two to three times the floor area fraction, thereby allowing a substantial settling of the very fine debris, even though diffusion processes would deposit the fine debris onto any surface. The floor fraction for small-piece debris was substantially higher than for the fine debris. Large and intact debris would fall to a horizontal surface unless it snagged on an obstacle. The floor fraction was set to 0.99 to place the large debris on the floor; however, some pieces could have snagged on an obstacle before reaching the floor.

For the far-side SG compartments (SGs 2 and 3) and the pressurizer compartment, the floor-debris deposition fractions acknowledged that the debris would have to travel downward in the compartment and through a variety of structures, including gratings, before reaching the floor; the fractions were reduced for these compartments. For instance, the gratings would catch much of the large debris before it could reach the floor. For open regions, such as the refueling pool regions, where a small amount of equipment and piping is located and the region is not enclosed completely by walls, the floor-debris fractions were increased substantially.

Once the weighting factors were estimated, the final deposition of the debris was determined both as a function of the region and by the surface orientation and its exposure to moisture. Figure VI-12 and Figure VI-13 illustrate the dispersion patterns in the containment according to surface orientation and surface wetness.

In Figure VI-12, all of the LOCA-generated debris is distributed fractionally according to surface orientation (floor surfaces or other surfaces), whether the debris was captured within the break region (SGs 1 and 4), and debris type. This distribution reflects the debris-generation size distribution of Table VI-2 and the break-region capture fractions of Table VI-11. For the fines and small-piece debris, the largest fractions corresponded to floor surfaces outside or beyond the break region; debris preferentially settled onto the floors. Most of the debris that was captured within the break region was located on other structures that correspond to equipment, piping, and gratings within those SG compartments. For the larger debris, the congestion of structures trapped the majority of the debris within the break region. Nearly half of this debris either was deposited onto the floor of the break region or was assumed to fall to the floor after the break flows subsided. Most large debris that was ejected from the break region was predicted to fall out onto floor surfaces; therefore, small amounts of large debris were found on other structures outside of the break region.

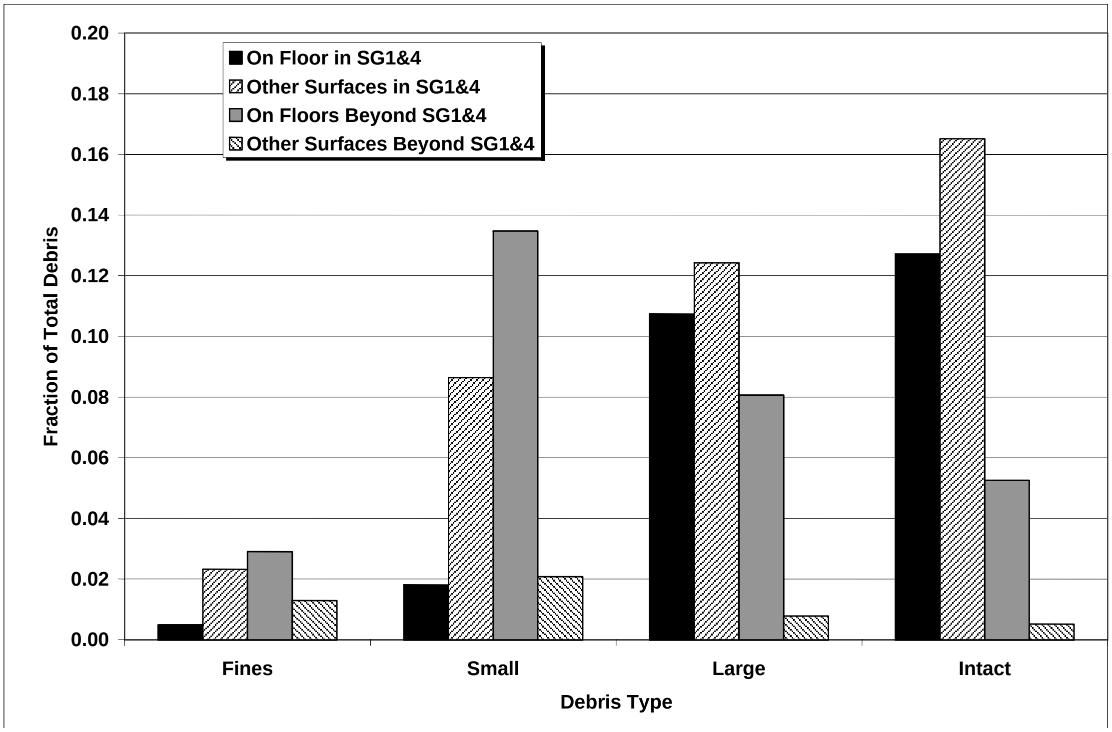

Figure VI-12. Blowdown Debris Dispersion by Surface Orientation

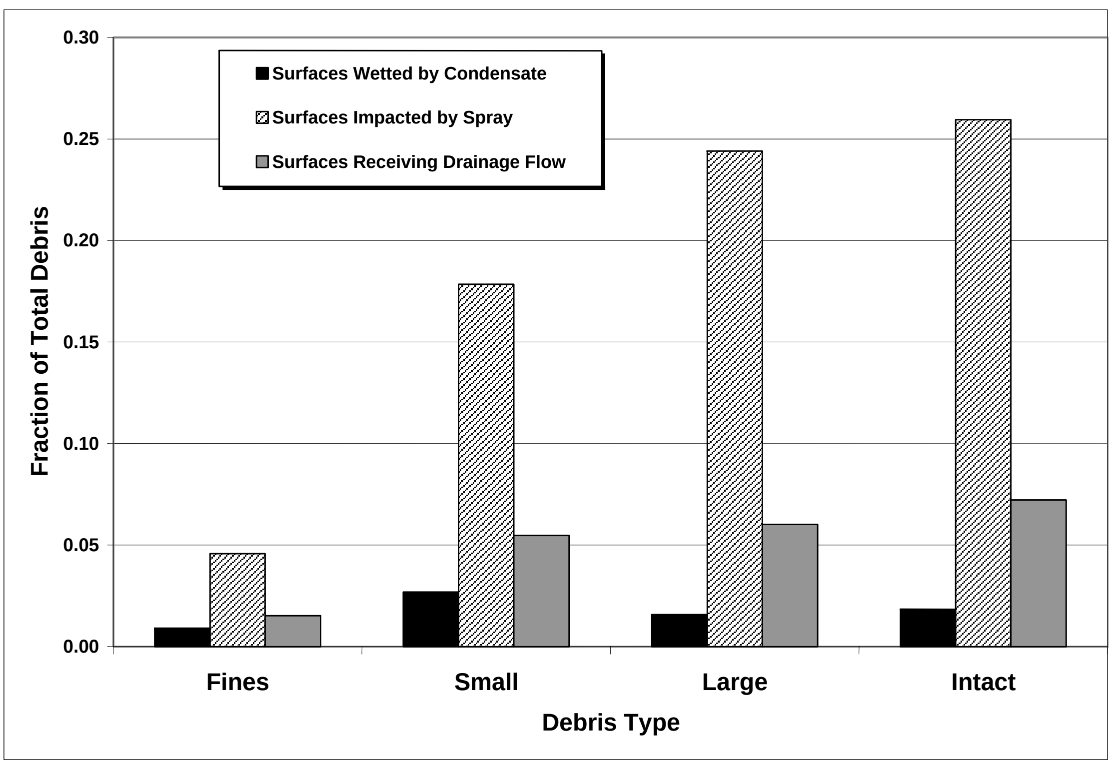

Figure VI-13. Blowdown Debris Dispersion by Surface Wetting

In Figure VI-13, all of the LOCA-generated debris is distributed fractionally according to the surface wetting condition (condensate, sprayed, or spray drainage) and by debris type. Only relatively small quantities of debris were predicted to reside at locations where the CSs or the spray drainage would not wash the debris downward. Conservatively speaking, the sprays falling from the upper dome would wash a majority of the surfaces within the SG compartments, as well as all of the upper floor surfaces and the refueling pool areas.

Although there is a relatively high degree of uncertainty with these blowdown transport results, the trends generally make sense. Because so little debris is protected from the CSs, these trends indicate a relatively high transport of debris to the sump pool.

VI.4.1.2 Fibrous Washdown Debris Transport

The CSs and condensation of steam throughout the containment and subsequent drainage to the sump pool would entrain substantial debris that was deposited onto the various surfaces and would transport the debris to the sump pool. In addition, these processes would degrade the fibrous insulation debris to some extent further, thereby creating more of the very fine, readily transportable debris.

VI.4.1.2.1 Surface Retention of Deposited Debris

The fraction of debris that stays on a specific surface, as opposed to washing away, is referred to as the retention fraction. The fraction transported from a specific surface would then be 1 minus the retention fraction. Estimates of the retention fractions were essentially engineering judgments that were based on experience with small-scale testing during the DDTS. These experiments did not examine specifically the flow requirement needed to remove a piece of debris from a specified type of surface. Most of these tests dealt with either debris generation or airborne debris transport. One set of tests examined the erosion that was associated with fibrous debris inundated by water flow. During the conduct of these tests, experience with the handling of the debris provided some understanding regarding the ease or difficulty of forcing a piece of debris to move. Table VI-15 summarizes these findings. Table VI-16 and Table VI-17 show the estimated transport and corresponding retention fractions, respectively.

Debris transport from condensate drainage would be expected to affect only the smaller debris. As condensation builds on a surface, it forms a thin film that subsequently drains and typically forms small rivulets of flow. This flow usually would move around significantly sized pieces of debris. Individual fibers could be entrained in the flow, or the fiber simply could be pushed to the sides of the rivulets. Some fine and small-piece debris certainly would transport, but the quantities of small debris transporting were estimated to be a small portion of the total. The DDTS's central estimate (realistic yet conservative) assumed that 1 percent of small debris transported (the extreme upper bound was 10 percent) but no large debris. The DDTS did not separate fines from small pieces. For this estimate, increasing the 1 percent to 2 percent for small-piece debris and increasing the 1 percent to 5 percent for the fines increased the level of conservatism. The larger debris was assumed not to transport because of condensate runoff.

Table VI-15. Fibrous-Debris Washdown Transport Trends

Debris Type	Surfaces Wetted by Condensate	Surfaces Either Sprayed or Receiving Drainage Flow	
		Without Intervening Floor Drains	**With Intervening Floor Drains**
Fines	Minority Transport	Nearly Complete Transport	
Small Pieces	Minority Transport	Majority Transport	
Large Pieces	No Significant Transport	Medium Transport	No Significant Transport
Intact Pieces	No Significant Transport	Minority Transport	No Significant Transport

Table VI-16. Estimated Fibrous-Debris Washdown Transport Percentages

Debris Type	Surfaces Wetted by Condensate	Surfaces Either Sprayed or Receiving Drainage Flow	
		Without Intervening Floor Drains	**With Intervening Floor Drains**
Fines	5%	99%	
Small Pieces	2%	70%	
Large Pieces	0%	50%	0%
Intact Pieces	0%	20%	0%

Table VI-17. Estimated Fibrous-Debris Washdown Retention Fractions

Debris Type	Surfaces Wetted by Condensate	Surfaces Either Sprayed or Receiving Drainage Flow	
		Without Intervening Floor Drains	**With Intervening Floor Drains**
Fines	0.95	0.01	
Small Pieces	0.98	0.3	
Large Pieces	1	0.5	1
Intact Pieces	1	0.8	1

Whenever fine and small-piece debris would be subjected to the substantial flows of the impacting CSs or the subsequent drainage of the sprays, the flow likely would entrain nearly all of the fine debris and a majority of the small debris. Test experience indicates that the CSs would wash fines from surfaces easily and carry those fines with the drainage to the sump pool. However, some of this fine debris would be pushed into relatively protected spots, corners, and crevices where the debris would remain. Surfaces that were impacted directly by sprays and drained surfaces were grouped together for washdown transport because of the lack of information that was required to treat these two surface types differently. It was assumed that 99 percent of the fines would be transported from surfaces that were impacted by the sprays or drainage and that the other 1 percent experienced something less than total transport.

The CSs also would wash substantial small-piece debris off structures, walls, and floors. The DDTS's central estimate was 50 percent (realistic yet conservative), with an extreme upper bound of 100 percent. Substantial quantities of debris likely would become trapped at locations that were protected from full spray flow by the complex arrangements of containment equipment and piping. It was assumed that 70 percent of the small debris would transport from surfaces that were impacted directly either by the CSs or by the subsequent drainage. This assumption adds conservatism to the DDTS's central estimate without becoming excessively conservative.

A simple floor-water drainage calculation, in which a uniform spray was applied to a floor area at a rate of flow corresponding to the containment-dome spray trains A and B, further supported the 70-percent estimate. A floor-area estimate indicates that each floor drain would drain approximately 800 ft^2. A plant calculation estimated that the floor-water holdup depth would be approximately 1.5 in. The separate-effect characterization of debris transport in water tests (NUREG/CR-6772, 2002) shows that a turbulent flow velocity as low as approximately 0.06 ft/s can cause a small piece of debris to tumble or slide along the floor. If circular drainage geometry is assumed, the transport estimate indicates that 30 to 40 percent of the floor area would not have sufficient flow velocity to transport small-piece debris. This calculation did not consider the effect of structures on the transport, which would create locations for debris entrapment. Therefore, the 70-percent estimate is a reasonable number for small-debris transport by the CSs.

For the large and intact pieces of debris, the surfaces were split into two additional categories based on whether the transport of the debris would encounter floor drain holes that would prevent further transport. A typical floor drain is approximately 6 1/2 in. in diameter and has a coarse grating that would stop any debris that is larger than approximately 3 in. square. A few floor drains have a relatively fine mesh screen over the hole. Floor surfaces are sloped to channel water to the drains. Large debris deposited onto the upper floors likely would have to pass through more than one of these floor drains to reach the sump. Large debris settling into the refueling pools would also have to pass through drains to reach the sump, some of which have a screen cover. The two largest of the refueling drains are nominal 6-in. drains without any cover or grating and are open during normal operation. Although a piece of large debris could pass through this 6-in. drain, the amount of debris would not be enough to treat these drains separately. It was assumed that these drains would stop further transport of large and intact debris.

Conversely, large and intact debris that is deposited at locations such as the SG compartments would not encounter any drain holes as the debris transports toward the sump pool. The CSs would wash substantial quantities of large-piece debris off structures, walls, and floors. A portion of the large debris would be trapped on top of gratings and would not transport. Other large pieces would snag onto structures such that the sprays would not dislodge them. Substantial quantities of debris likely would become trapped at locations that are protected from full spray flow by the complexities of containment equipment and piping. Because large debris would transport less easily than small debris, it was assumed that 50 percent of the large debris was transported.

The intact debris would be less likely to transport than the large-piece debris. Based on DDTS experience, the intact pieces of debris were significantly more likely to snag on structures than the large pieces, and substantial quantities of intact debris were likely to remain attached to the original piping. It was assumed that 20 percent of the intact debris would transport.

VI.4.1.2.2 Erosion of Debris by CSs

Experiments conducted in support of the DDTS analysis illustrated that the flow of water could further erode insulation debris. Some debris erosion could occur because of the impact of the sprays and spray drainage flows, but the amount of erosion would not be great. The DDTS concluded that less than 1 percent of the fibrous debris eroded as a result of CS operation. The analysis neglected debris erosion caused by condensation and condensate flow. Debris containing insulation that is still in its cover would not be expected to erode further. The sump-pool transport analysis includes the erosion of debris caused by the plummeting of the break flow into the sump pool.

It was assumed that condensate drainage would not cause further erosion of fibrous debris and that intact or covered debris would not erode further. Erosion does not apply to fine debris because the debris is already fine. It was assumed that 1 percent of the small- and large-piece debris that was impacted directly by the sprays would erode, and that intact pieces of debris could not erode because its canvas cover would protect the fibrous materials.

VI.4.1.3 Quantification of Fibrous-Debris Transport

The transport of fibrous debris was quantified using the models presented in Section VI.3 and the input presented in Section VI.4.1. Table VI-18 presents the quantified transport results and shows the transport fractions for each size category, as well as the overall transport fraction. It also shows the fractions of the total ZOI insulation that entered the pool, which were normalized to provide a size distribution for the debris entering the pool. About 57 percent of the ZOI fibrous insulation was predicted to transport to the sump pool, and nearly half of that would be the relatively transportable sizes. The transport fraction for the fines includes the erosion products from the predicted erosion of the small and large pieces of debris. The quantity of erosion products was approximately equal to 6 percent of the original generated fines.

Table VI-18. Fibrous-Debris-Transport Results

Debris Size Category	Category Generation Fraction	Size Category Transport Fraction	Fraction of ZOI Insulation	Distribution Entering Sump Pool
Fines	0.07	0.93	0.07	0.12
Small Pieces	0.26	0.66	0.17	0.30
Large Pieces	0.32	0.54	0.17	0.30
Intact Pieces	0.35	0.46	0.16	0.28
All Debris	1.00	0.57	0.57	1.00

VI.4.2 RMI Debris Transport

Roughly 85.7 percent of the insulation in the volunteer-plant containment is RMI. The debris-transport methodology discussed in Section VI.3 applies to RMI debris, as well as fibrous debris. Unfortunately, unlike the fibrous insulation, very little useful airborne transport data for RMI debris exist. Specifically, the capture fractions for the capture of RMI debris passing through structures such as gratings and of RMI debris inertially impacting surfaces have not been measured. Only secondary experience associated with RMI debris-generation experiments applies in this study. For RMI debris washdown, the pool transport velocities are available. Small-scale experiments suggest that RMI debris transports less easily than the fibrous debris, primarily because the RMI debris is heavier. In addition, it would take substantially more RMI debris on the sump screen than fibrous debris to block flow effectively through the screen.

VI.4.2.1 RMI Blowdown Debris Transport

The capture fractions for RMI debris are likely much different from the corresponding fractions for fibrous debris. For fibrous debris, the capture fractions were very dependent on surface wetting; when the surfaces were dry, debris capture was minimal. For RMI, surface wetting may not be important. For instance, it seems likely that the capture of RMI on a grating depends on the foil folding over a bar in such a manner that it remains in place. Capture may depend on the debris remaining stuck on a structure. The amount of RMI debris that was captured by a grating could be significantly less than the amount of fibrous insulation; conversely, it could be substantially more. Furthermore, the ability of flows to transport large cassette-like RMI debris is not known. Therefore, application of the Section VI.3 methodology required very conservative assumptions to compensate for the nearly complete lack of data.

VI.4.2.1.1 Break-Region Blowdown Debris Transport

It is conservative to overestimate the retention of debris within the SG compartments because subsequent debris washdown is more likely if the debris were in the SGs as opposed to dispersed throughout the containment. Because the capture rates for RMI debris passing through a grating have not been determined, it was conservatively assumed that the grating stopped 100 percent of all RMI debris impacting it from further forward transport. Debris stopped on the underside of a grating likely could fall back once depressurization flows subside. Because the gratings do not extend completely across the SG compartments, substantial debris still could be propelled upward into the containment dome.

Likewise, the inertial capture of RMI debris by miscellaneous structures (e.g., pipes, beams, or vessels) or by inertial impaction whenever the flow makes a sharp bend has not been determined. For instance, it would seem less likely that a piece of RMI debris would stick to a wall than would a small piece of fibrous debris. The fibrous-debris capture fractions for miscellaneous structures and sharp bends were applied to the RMI debris to conservatively overpredict the retention of RMI debris within the SG compartments. Applying these assumptions to the logic charts, which are similar to Figure VI-7, results in the conservative SG capture fractions shown in Table VI-19. The values for 2- to 6-in. and the larger-than-6-in. debris categories in Table VI-19 correspond to the values for the fibrous large- and intact-category values (shown in Table VI-11) a result of similar assumptions. The assumption that the gratings capture all of the RMI debris, even the smallest pieces, predicts substantially more RMI retention within the SG compartments than likely would occur in reality. The lack of RMI transport data necessitated the predicted overconservative retention.

Table VI-19. Fractional Distribution of Debris Captured and Exiting Break Region

Location	RMI Debris Category		
	<2-in. Pieces	2- to 6-in. Pieces	>6-in. Pieces
Captured within SGs 1 and 4	0.64	0.70	0.82
Expelled to Dome	0.32	0.26	0.17
Expelled to Level 832	0.01	0	0
Expelled to Level 808	0.03	0.04	0.01

VI.4.2.1.2 Dispersion throughout the Remainder of Containment

The RMI debris-transport estimate employed the same 24-region subdivision of the containment free volume that was used in the fibrous-debris-transport estimate (Table VI-12). The volume weighting factors that were estimated for fibrous-debris transport (Table VI-13) also were applied to the RMI debris because no rationale was found to weight the distributions otherwise. For RMI debris, no fine debris was postulated (i.e., even the smaller pieces of RMI debris should sink readily in water, as opposed to fibrous fines, which tend to remain in suspension). The predicted dispersion of RMI debris was judged to place more debris into locations where it subsequently would be predicted to transport with the CS drainage to the sump pool. Table VI-14 illustrates the results of the blowdown dispersion by groups of volume regions. As modeled, the break region (SGs 1 and 4) retained a majority of the debris. In reality, it is likely that much more of the smaller debris would be blown free of the break region and into the upper dome region, where subsequent washdown to the sump pool would be substantially less than it would be if the debris were kept within the break region. However, the lack of RMI debris-transport data necessitated the conservative assumptions leading to these results.

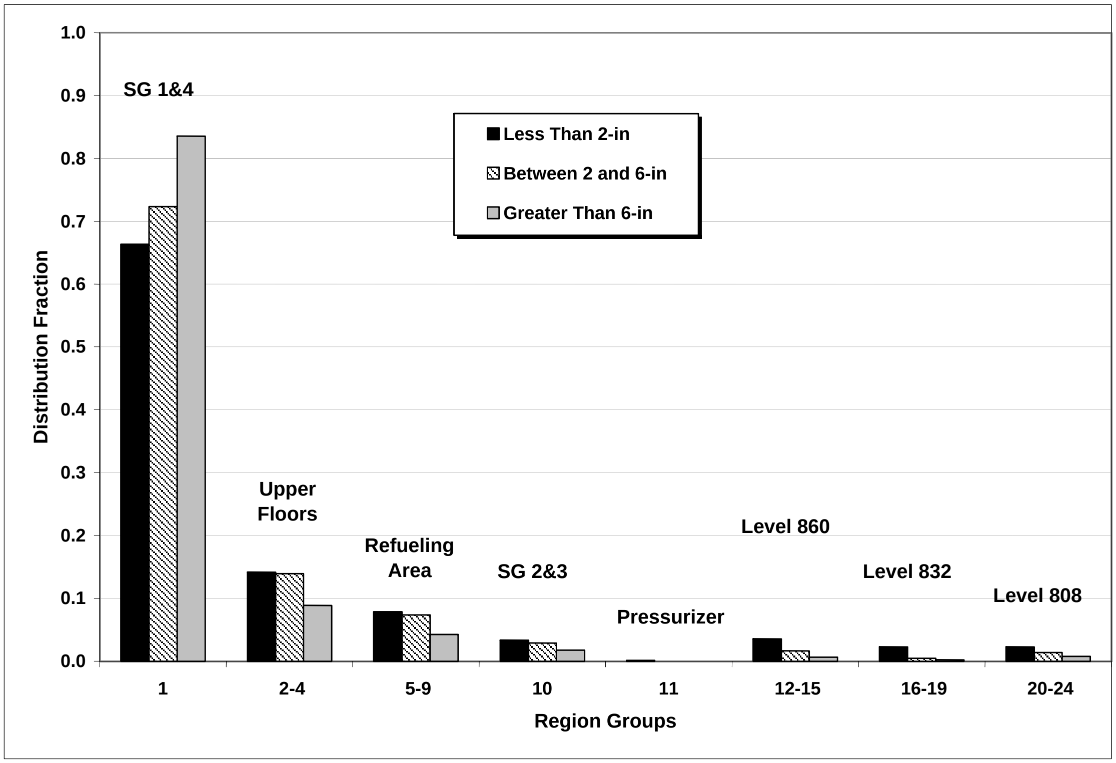

Figure VI-14. RMI Blowdown Distribution by Region Groups

VI.4.2.1.3 Dispersion by Surface Orientation and Surface Wetness

A review of photos that were taken of RMI debris following RMI debris-generation tests indicates that RMI debris would reside preferentially on the floor surfaces (NEDO-32686, 1996; LA-UR-01-1595, 2001), although some RMI debris was caught on structures. However, the structures in these debris-generation tests were dry; therefore, it is not known if surface wetness would cause RMI to stick to wetted surfaces. Still, it is conservative to place the debris on the floors, where the subsequent washdown would be more effective. Therefore, the various surface-area-weighting factors were set to place most of the RMI debris on the volume region floors. It was assumed that 99 percent of the RMI debris would reside on the floor. The surface-area fractions shown in Table VI-14 apply to RMI debris as well as to fibrous debris. In these assumptions, approximately 99 percent of the RMI debris following blowdown was located where it either was impacted directly by the sprays or was located in the path of the spray drainage, leaving only 1 percent on surfaces that were wetted by condensation only.

VI.4.2.2 RMI Washdown Debris Transport

The RMI debris surface-retention fractions (i.e., the fraction that was not washed away) were estimated based primarily on engineering judgments and RMI pool debris-transport data. Small-scale testing of the transport of RMI debris in a pool of water demonstrated the ease or difficulty of forcing a piece of debris to move in a pool of water. Debris transport in a flowing layer of water that resides on a floor is similar to the transport of the debris in an established pool of water. Table VI-20 summarizes perceptions regarding the transport of RMI debris in nonpool situations. Table VI-21 and Table VI-22 show the estimated transport and corresponding retention fractions, respectively.

Table VI-20. RMI-Debris-Washdown Transport Trends

Debris Type	Surfaces Wetted by Condensate	Surfaces Either Sprayed or Receiving Drainage Flow	
		Without Intervening Floor Drains	With Intervening Floor Drains
<2 in.	Minority Transport	Medium Transport	
2 to 6 in.	No Significant Transport	Medium Transport	No Significant Transport
>6 in.	No Significant Transport	Minority Transport	No Significant Transport

Table VI-21. Estimated RMI-Debris-Washdown Transport Percentages

Debris Type	Surfaces Wetted by Condensate	Surfaces Either Sprayed or Receiving Drainage Flow	
		Without Intervening Floor Drains	With Intervening Floor Drains
<2 in.	1%	40%	
2 to 6 in.	0%	30%	0%
>6 in.	0%	10%	0%

Table VI-22. Estimated RMI-Debris-Washdown Retention Percentages

Debris Type	Surfaces Wetted by Condensate	Surfaces Either Sprayed or Receiving Drainage Flow	
		Without Intervening Floor Drains	With Intervening Floor Drains
<2 in.	99%	60%	
2 to 6 in.	1%	70%	1%
>6 in.	1%	90%	1%

All debris that was deposited onto the SG compartment floors and the sump-level floors automatically was assumed to have entered the sump pool; the tables do not indicate this assumption. This assumption primarily affected the debris that was deposited onto the break-region floor during either blowdown or washdown. The falling and spreading break flow would drive the actual movement of this debris from the SG compartment floor into the outer annulus; this would generally be expected to result in a relatively high level of transport.

Debris transport resulting from condensate drainage would be expected to affect only the smaller debris. As condensation builds on a surface, it forms a thin film that subsequently drains and typically forms small rivulets of flow. This flow usually would not move around significantly sized pieces of debris. Significant transport of RMI debris does not seem likely; however, it is possible that some of the smaller debris could move with the condensate flow until the condensate flow linked up with more substantial water drainage. It was assumed that 1 percent of the debris that was less than 2 in. and subjected only to condensate drainage ultimately would transport to the sump pool. Furthermore, it was assumed that none of the debris that was greater than 2 in. would transport to the sump pool.

Whenever pieces of debris less than 2 in. were subjected to substantial flows from the CSs or from the subsequent drainage of the sprays, the flow likely would entrain a substantial portion of that debris. The evaluation of the transport of the smaller RMI debris that was exposed to sprays and/or spray drainage was based on a floor-pool drain velocity estimate and on the pool debris-transport threshold velocities. The drainage-flow velocity calculation assumed that a uniform spray was applied to an upper level floor area corresponding to the containment-dome spray trains A and B. A floor-area estimate indicated that each floor drain would drain approximately 800 ft^2 of floor area. A plant calculation estimated a floor-water holdup depth of approximately 1.5 in. The separate-effect characterization of debris transport in water tests (NUREG/CR-6772, 2002) showed that a turbulent flow velocity of approximately 0.2 ft/s would be required to cause small stainless-steel RMI debris to tumble or slide along the floor. If it is assumed that circular drainage geometry exists, the transport estimate indicates that 60 to 80 percent of the floor area would not have sufficient flow velocity to transport small stainless-steel RMI debris, depending on the assumed thickness of the water layer. This conclusion resulted in the 40-percent transport estimate shown in Table VI-21. Because this calculation did not consider the effect of structures on the transport, which would create locations for debris entrapment, the 40-percent transport estimate is a reasonable number for the transport by the CSs of RMI debris that is less than 2 in.

As was done for fibrous debris, pieces of RMI debris that were greater than 2 in. were assumed not to pass through floor drains or refueling-pool drains. At locations where the larger debris would not encounter floor or refueling drains, 30 percent of the 2- to 6-in. debris and 10 percent of the debris that was greater than 6 in. were assumed to transport. The corresponding fibrous-debris-transport number simply was reduced based on engineering judgment to account for the fact the RMI debris transports less easily than does fibrous debris. In any case, these two estimates affected only a relatively minor portion of the total debris.

Debris erosion of any significance would not happen to stainless-steel RMI debris; therefore, this study did not consider the erosion of the RMI debris by the CSs.

VI.4.2.3 Quantification of RMI Debris Transport

The transport of fibrous debris was quantified using the models presented in Section VI.3 and the input presented in Section VI.4.2. Table VI-23 presents the quantified transport results. The table shows the transport fractions for each size category, as well as the overall transport fraction. It also shows the fractions of the total ZOI insulation that entered the pool. These fractions then were normalized to provide a size distribution for the debris entering the pool. Approximately 83 percent of the ZOI RMI was predicted to transport to the sump pool, but only approximately 20 percent of that amount was pieces less than 2 in.

Table VI-23. Fractional RMI Debris-Transport Results

Debris-Size Category	Category Generation Fraction	Size Category Transport Fraction	Fraction of ZOI Insulation	Distribution Entering Sump Pool
<2 in.	0.21	0.82	0.17	0.21
2 to 6 in.	0.12	0.76	0.09	0.11
>6 in.	0.67	0.85	0.57	0.68
All Debris	1.00	0.83	0.83	1.00

VI.4.3 Min-K Insulation Debris Transport

Less than 1 percent of the insulation in the volunteer-plant containment is Min-K insulation, a form of insulation referred to as microporous or particulate insulation. Although the transport methodology discussed in Section VI.3 also applies to Min-K insulation, a nearly complete lack of airborne transport data for this type of insulation exists, as well as debris-generation data, which were discussed in Section VI.3.2.3. Because of the lack of data for the generation of debris from Min-K insulation, the unknown erosion characteristics of this insulation, and the sparseness of the insulation within the containment (i.e., leads to a potential spatial nonuniform distribution), it was conservatively assumed that all Min-K located within the ZOI would be pulverized into a fine, highly transportable dust. If the CSs inundated the larger pieces of Min-K debris, these pieces simply could dissolve into fine silt and transport with the spray drainage; however, this outcome is yet to be proven. Although less than 1 percent of the containment insulation is Min-K, this type of particulate debris could affect the sump-screen head losses significantly.

A conservative transport fraction for Min-K dust must be relatively high, and it seems likely that this fraction would be similar to the fraction for the transport of fibrous fines without the addition of erosion products, which was approximately 0.87. That is, the transport of fibrous fines generated from the ZOI to the sump pool was approximately 87 percent. (Note that the 93 percent value that was shown in Table VI-18 included erosion products.) Because the bulk of the 13 percent of fine fibers that did not transport was located on surfaces wetted only by condensate, it seems likely that a similar result would occur for the Min-K. This study assumed that 90 percent of the Min-K dust would transport to the sump pool.

VI.5 Blowdown/Washdown Conclusion

A methodology was developed that considers both transport phenomenology and plant features. It divides the overall complex transport problem into many smaller problems that either are amenable to solution by combining experimental data with analysis or that can be judged conservatively based on the foundation of debris-transport knowledge. The quantification of the methodology results in predicted transport fractions that are both conservative and plausible. Table VI-24 shows the overall transport results. These transport fractions represent the fractions of the insulation by type that was initially located within the ZOI and that subsequently would transport to the sump pool. Sections VI.3 and VI.4 discuss the detailed results, including size distribution information.

Table VI-24. Overall Transport Results

Insulation Type	Overall Transport Fraction*	Debris-Size Distribution
Fibrous	57%	Table VI-18
RMI	83%	Table VI-23
Min-K	90%	All Dust

* Overall percentages are for demonstration only.

The overall transport fractions listed in Table VI-24 serve for demonstration purposes but are not valid for plant-specific evaluations because these fractions were calculated using LOCA-generated debris-size distributions that did not account properly for PWR jet characteristics. The BWR jet characteristics were substituted for PWR jet characteristics because the PWR jet analyses had not been performed yet. When the PWR jet characteristics become available, it will be a simple matter to recalculate the overall transport fractions using PWR LOCA-generated debris-size characteristics.

Neither the debris-size distributions nor the overall transport fractions in this report are valid for plant-specific evaluations.

The transport fractions for each debris-size category are considered to be conservative for the LDFG insulation in the volunteer plant (but not necessarily for containments of other design). The fibrous-debris-transport analysis contained herein was based on LDFG insulation and may require adjusting for any high-density fiberglass insulation or mineral wool that may also be in the plant.

For the volunteer plant, a high percentage of the fine LOCA-generated debris most likely would transport to the sump pool via the spray drainage flows. The transport fractions tended to decrease as the debris size increased. A majority of the larger debris that was predicted to transport to the sump pool was stopped in the SG compartments that were associated with the break, where subsequent CS drainage was assumed to be readily capable of moving the debris downward to the pool.

The lack of transport data caused the transport of the RMI and Min-K debris to skew more conservatively toward larger transport fractions than the fibrous debris. Realistically speaking, the RMI might be expected to transport less readily than would the fibrous debris because it is heavier. However, a larger fraction of the RMI debris could be trapped in the break region (SG compartments), where it could be transported subsequently into the sump pool, and thus the need to skew the transport fractions conservatively. A similar discussion applies to the Min-K because of the lack of LOCA debris-generation data, lack of erosion data, and the potential nonuniform placement of Min-K in the ZOI. Therefore, most of the Min-K must be conservatively assumed to transport to the sump pool as a fine dust or silt.

This analysis used conservative engineering judgments at various steps along the way. The degree of conservatism that was associated with these judgments was intended to ensure conservative final results without straying too far from realistic behavior. The judgments were not intended to be upper bounding. For example, the DDTS assessed the erosion of LDFG by CSs as less than 1 percent. In reality, the erosion may be significantly less than 1 percent. The 1 percent value was assumed to be conservative but not far from reality. In addition, many conservative judgments tend to compound as the analysis progresses.

The analyses herein considered only one break location (SG1), although they included a range of break sizes at that location. Plant-specific analyses must consider a range of break locations. For the volunteer plant, LOCAs can occur within an SG compartment, which is likely the most probable location. A break in the same SG but at a different level likely would have a result similar to the one analyzed because most of the break effluent still would flow to the containment dome. A break in an SG compartment different from SG1 most likely would have a similar result, except that the debris would tend to enter the sump pool at different locations. A break outside the SG compartments, such as in a main steamline, would behave differently than a break inside an SG compartment and probably should be analyzed separately. A break in the pressurizer certainly would be different because that compartment does not vent directly to the containment dome as do the SG compartments (i.e., no major upper openings exist). Therefore, a larger fraction of the debris might be driven out of the pressurizer compartment directly into the sump area, but the total quantity of debris might be substantially less than a primary-loop piping break. This discussion does not analyze either a pressurizer-line break or a main steamline break.

In performing blowdown/washdown analyses, it is important to ensure the following:

- The debris-size categories match the characteristics of the debris-transport behavior.
- The break region is analyzed in substantial detail because so much of the debris capture is likely to occur in this region.
- The debris capture along the primary exits from the break region also should be analyzed in substantial detail.
- The CS drainage patterns should be determined to support the washdown analysis and to indicate where the debris would enter the sump pool and how the spray drainage would impact sump pool turbulence.

- Vulnerable spray-drainage pathways, where potential debris blockage might occur, should be identified.

VI.6 References

(LA-UR-99-3371, 1999) Boyack, B.E., et al., “PWR Debris Transport in Dry Ambient Containments—Phenomena Identification and Ranking Tables (PIRTs),” LA-UR-99-3371, Revision 2, December 14, 1999.

(LA-UR-01-1595, 2001) Rao, D.V., C.J. Shaffer, and R. Elliott, “BWR ECCS Strainer Blockage Issue: Summary of Research and Resolution Actions,” prepared for the U.S. Nuclear Regulatory Commission by Los Alamos National Laboratory, LA-UR-01-1595, March 21, 2001.

(NEDO-32686, 1996) “Utility Resolution Guidance for ECCS Suction Strainer Blockage,” BWROG, NEDO-32686, Rev. 0, November 1996.

(NRC-SER-URG, 1998) “Safety Evaluation by the Office of Nuclear Reactor Regulation Related to NRC Bulletin 96-03 Boiling Water Reactor Owners Group Topical Report NEDO-32686, ‘Utility Resolution Guidance for ECCS Suction Strainer Blockage,’” Docket No. PROJ0691, August 20, 1998.

(NUREG/CR-6369-1, 1999) Rao, D.V., C. Shaffer, and E. Haskin, “Drywell Debris Transport Study,” NUREG/CR-6369, Volume 1, SEA97-3501-A:14, September 1999.

(NUREG/CR-6369-2, 1999) Rao, D.V., et al., “Drywell Debris Transport Study: Experimental Work,” NUREG/CR-6369, Volume 2, SEA97-3501-A:15, September 1999.

(NUREG/CR-6369-3, 1999) Shaffer, C.J., D.V. Rao, and J. Brideau, “Drywell Debris Transport Study: Computational Work,” NUREG/CR-6369, Volume 3, SEA97-3501-A:17, September 1999.

(NUREG/CR-6762, Vol. 1, 2002) Rao, D.V., et al., “GSI-191 Technical Assessment: Parametric Evaluations for Pressurized Water Reactor Recirculation Sump Performance,” LA-UR-01-4083, Los Alamos National Laboratory, August 2002.

(NUREG/CR-6762, Vol. 2, 2002) Rao, D.V., et al., “GSI-191 Technical Assessment: Summary and Analysis of U.S. Pressurized Water Reactor Industry Survey Response and Responses to GL 97-04,” Volume 2, LA-UR-01-1800, Los Alamos National Laboratory, August 2002.

(NUREG/CR-6762, Vol. 3, 2002) Rao, D.V., C.J. Shaffer, and S.G. Ashbaugh, “GSI-191 Technical Assessment: Development of Debris-Generation Quantities in Support of the Parametric Evaluation,” LA-UR-01-6640, Los Alamos National Laboratory, August 2002.

(NUREG/CR-6772, 2002) Rao, D.V., B.C. Letellier, A.K. Maji, and B. Marshall, “GSI-191: Separate-Effects Characterization of Debris Transport in Water,” NUREG/CR-6772, LA-UR-01-6882, August 2002.

(NUREG/CR-6773, 2002) Rao, et al., “GSI-191: Integrated Debris-Transport Tests in Water Using Simulated Containment Floor Geometries,” NUREG/CR-6773, LA-UR-02-6786, December 2002.

(NUREG/CR-6808, 2003) Shaffer, C.J., D.V. Rao, M.T. Leonard, and K.W. Ross, “Knowledge Base for the Effect of Debris on Pressurized Water Reactor Emergency Core Cooling Sump Performance,” NUREG/CR-6808, LA-UR-03-0880, February 2003.

(OPG, 2001) Russell, J., “Jet Impact Tests—Preliminary Results and Their Application,” N-REP-34320-10000, Rev. R00, April 18, 2001.

(SEA-95-970-01-A:2, 1996) Zigler, G., et al., “Experimental Investigation of Head Loss and Sedimentation Characteristics of Reflective Metallic Insulation Debris,” draft letter report, prepared for the U.S. Nuclear Regulatory Commission, SEA No. 95-970-01-A:2, May 1996.

ATTACHMENT 1 TO APPENDIX VI

VOLUNTEER-PLANT SPRAY-WATER DRAINAGE ANALYSIS

1. Introduction

A postulated LOCA in the volunteer plant would distribute insulation debris throughout the containment, whereby the subsequent drainage of spray water following the LOCA would transport portions of this insulation debris toward the recirculation sump screens. A best estimate of how the water would drain to the sump was performed to support subsequent debris-transport calculations. The analysis will help to identify spaces and surfaces where sprays or drainage flow would not likely wash away insulation debris (e.g., an area that was not impacted by sprays and has too little drainage flow to transport debris). The analysis will help to determine how the drainage water enters the sump pool, which in turn will affect debris transport within that pool.

2. System Descriptions

The CS systems in the volunteer plant consist of two independent trains (trains A and B), with headers located in four containment regions. Spray nozzles are located in one of four regions of the containment:

- Region A—containment dome spraying down toward Level 905
- Region B—below Level 905 spraying Level 860
- Region C—below Level 860 spraying Level 832
- Region D—below Level 832 spraying Level 808

Table 1 shows the specifications for both trains in Unit 1, combined. Spray train B has one more nozzle in the dome than train A; therefore, the flows that are associated with single train operations constitute essentially half of the flows shown for both trains. Unit 1 has seven more nozzles than Unit 2. The drainage estimate performed for Unit 1 applies also to Unit 2.

Table 1. Unit 1 Spray Nozzle Summary

Spray Region	Number of Nozzles	Nozzle Flow (gpm)	Region Flow (gpm)
A	545	20	10,900
B	134	20	2,680
C	28	20	560
D	54	20	1,080
Total	761	20	15,220

The containment was designed to drain the spray water down to the containment recirculation sumps. Furthermore, the containment apparently was designed to minimize water holdup, thereby maximizing the depth of the sump pool. Several features of the containment, including those described below, determine the primary drainage pathways in the containment.

Floor drains that drain water from one floor directly down to the next floor are a primary means of draining spray water. Figure 1 shows a typical drain, which is approximately 6.5 in. in diameter. At the top of this figure, another type of drain leads directly to the containment sump. Floor surfaces are sloped to channel water into the drains.

Figure 1. Typical Floor Drain

Water barriers (curbs), both concrete and metallic types, control water drainage. These barriers are placed around floor-area perimeters to prevent water from draining from those perimeters. However, these barriers do not cover the entire perimeter of a floor. Gaps exist in the barriers at locations such as the areas around walkways and ladders. In many places, water can flow from a floor perimeter onto another floor, into the gap between the internal structures and the outer wall, into an SG compartment, or into a stairwell. Figure 2 shows a typical curb. Figure 3 shows another curb next to an SG compartment that illustrates a discontinuity in a curb.

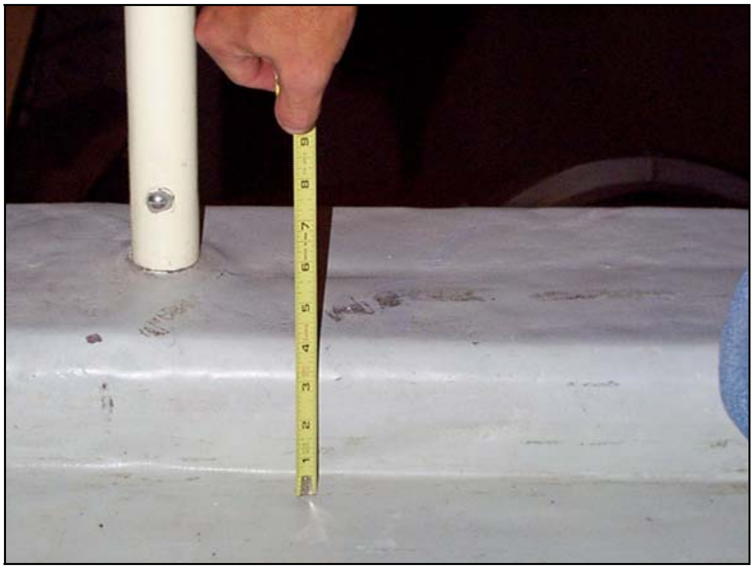

Figure 2. Typical Concrete Curb

Figure 3. Gap in Concrete Curb Surrounding an SG Compartment

A substantial portion of the dome sprays will fall into the refueling cavity and accumulate in the three pool areas of the cavity. During normal operation, the pool drains are open, allowing spray water to drain down to the sump. The pool drains consist of 4-in. and 6-in. sizes. Figure 4 shows the drains in the pool that are used to store the reactor vessel lower internals during refueling. Near the center, the photo shows a 4-in. drain with a cover screen (with holes approximately 1/4 to 1/2 in. in diameter). In the upper-right (cover off) and lower-right corners (cover in place), the photo also shows two 6-in. drains. These 6-in. drains are closed off with blind flanges during refueling and are uncovered during normal operations. The 4-in. drains lead down into the labyrinth of rooms on Level 808, which is located directly below the refueling pools. The two 6-in. drains flow to SGs 3 and 4. A single 4-in. drain draws off the pool that is used to store and transfer fuel to Level 808. The pool that is used to store reactor vessel upper internals during refueling has a single 4-in. drain, which drains into the pool that stores the lower internals.

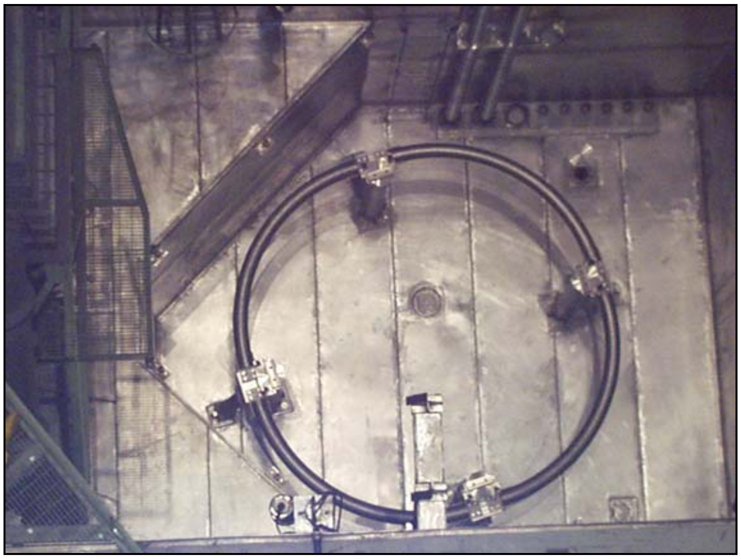

Figure 4. Refueling Pool Drains

Water drainage between floors also occurs through the floor gratings that cover several open areas in the floors (e.g., the equipment-transfer floor hatches).

At several staircases, water can drain through stairwells from one floor to the next. Two primary staircases extend all the way from sump Level 808 up to the top floor at Level 905.

3. Approach

A review of containment drawings and plant documents led to many general observations:*

- Little, if any, water is expected to drain down the elevator shaft by way of the elevator doors. The plant's minimum pool calculation did not treat the elevator shaft as a wetted drain perimeter, and the floors generally slope away from elevator. Furthermore, elevator doors may prevent water entry into the elevator shaft.
- The pressurizer compartment should remain essentially dry. A roof covers the compartment so that sprays do not enter this compartment. Drains and sloping floors generally prevent water flow into this compartment at other entrances.
- Water entering the SG compartments consists of dome-spray droplets falling directly into those compartments. Droplets falling onto the wall-tops and floor that are located between or near the SG compartments likely will flow into the

*The most useful drawings were floor layouts that showed floor slopes, water barriers, and floor drains. The most useful document was a plant calculation of the minimum sump-pool height.

SG compartments. In addition, the two 6-in. refueling-pool drains flow directly into the SG compartments.

- Water entering the stairwells consists of spray droplets falling directly into stairwells and of some water overflowing a floor perimeter.
- Water entering the refueling cavity consists of spray droplets falling directly into the cavity. This water includes droplets that are falling onto walkways surrounding the refueling pool and that subsequently would flow into the pool.
- Water entering the gap between the inner containment structure and the containment outer wall consists of spray droplets impinging the outer containment wall and subsequently flowing down the liner and of water from gaps in the water barriers along the floor perimeters.
- Floor drains between the floors are intended to drain substantial quantities of water from one floor to the next.

Because of the complexity of the water drainage, many simplifying assumptions and engineering judgments were necessary. The primary assumptions include the following:

- All spray systems were active (only one possible spray scenario was evaluated).*
- No blockage of drain flows by debris was postulated.†
- Dome spray droplets fall vertically and distribute uniformly across the containment cross section before encountering any containment structure. Distribution was based on cross-sectional areas.
- Crosswalks on Level 905 that are directly between the refueling cavity and the SG compartments drain into those compartments.
- Refueling cavity walkways on Level 860 drain into pools.
- Levels 873 and 851 do not have floor drains (i.e., floor drains not shown in drawing).
- Water draining onto Level 849 from Level 860 subsequently draws off to Level 832.
- Water drains that lead directly to a containment sump (e.g., the one shown in the upper portion of Figure 1) are neglected. The drawings do not delineate these specialized drains assumed to be substantially fewer in number than the main floor drains.

Engineering judgments were necessary where insufficient data were available to estimate drainage accurately.

---

*The scenario where one train operates and one train is inactive can be estimated by dividing all flows for both trains by a factor of 2.

†Insulation debris could block a floor drain or a refueling pool drain.

The calculational approach included the following steps:

- The locations of all spray nozzles were identified.
- The dome spray impacting and running down the containment liner was estimated.
- The main floor areas on Levels 808, 832, 860, and 905 were nodalized into three sections for each floor.
- The locations where the spray droplets would settle were identified.
- The drainage process was tracked from the uppermost surfaces down to Level 808.

The dome spray nozzles, arranged around four rings for each of the two trains, are aimed in four different directions. Some of the nozzles apparently are aimed to spray the dome liner. A portion of this spray impacting the liner subsequently should drain down the liner itself. The number of nozzles aimed in each of the four directions was tabulated for each ring. Then the spray impact and runoff was judged for each ring location. Of the 10,900-gpm total dome spray flow, 700 gpm was estimated to flow down the liner.

Figure 5 illustrates the subdivision of the main floors. Section 1 includes the side of the containment where the main steam and feedwater lines penetrate the containment. Drainage on this side would be distinctly different from the remainder of the containment. Section 2 includes unique features such as Level 849 and Level 832; sprays do not extend into this section. Section 3 includes the remainder of the floors.

To estimate the distribution of settled dome spray water, the containment cross-sectional area was estimated for each section of floor, refueling cavity, SG compartment, open area, and other areas. It was assumed that the spray droplets would fall uniformly onto these areas. Once the settled flows were determined, the drainage from floor to floor was estimated, starting with the uppermost floor surface. For each floor section, a drainage distribution was estimated, based on floor sloping relative to drainage pathways.

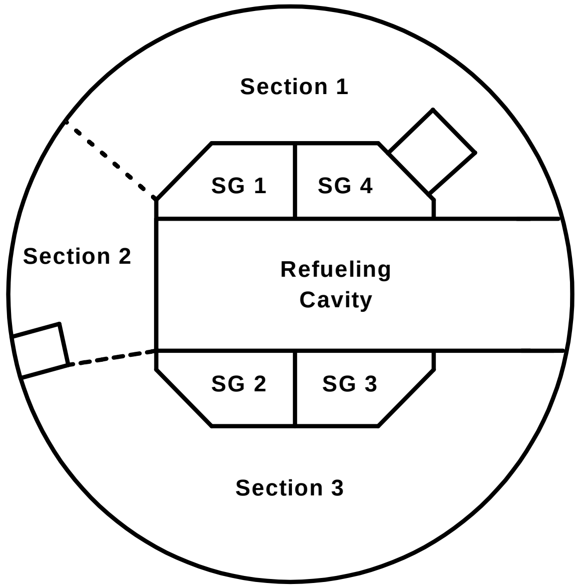

Figure 5. Schematic of Floor Sections

Figure 6 shows the overall spray drainage. The dashed lines represent spray droplets falling onto a surface* (the arrow head indicates the surface receiving the droplets). The numbers indicate flow rates in gallons per minute. The solid lines indicate water draining from one surface to another or water falling into and through a stairwell or the outer wall gap. Figure 7 shows a diagram illustrating where the water enters the Level 808 sump pool.

* The surfaces are not drawn to scale.

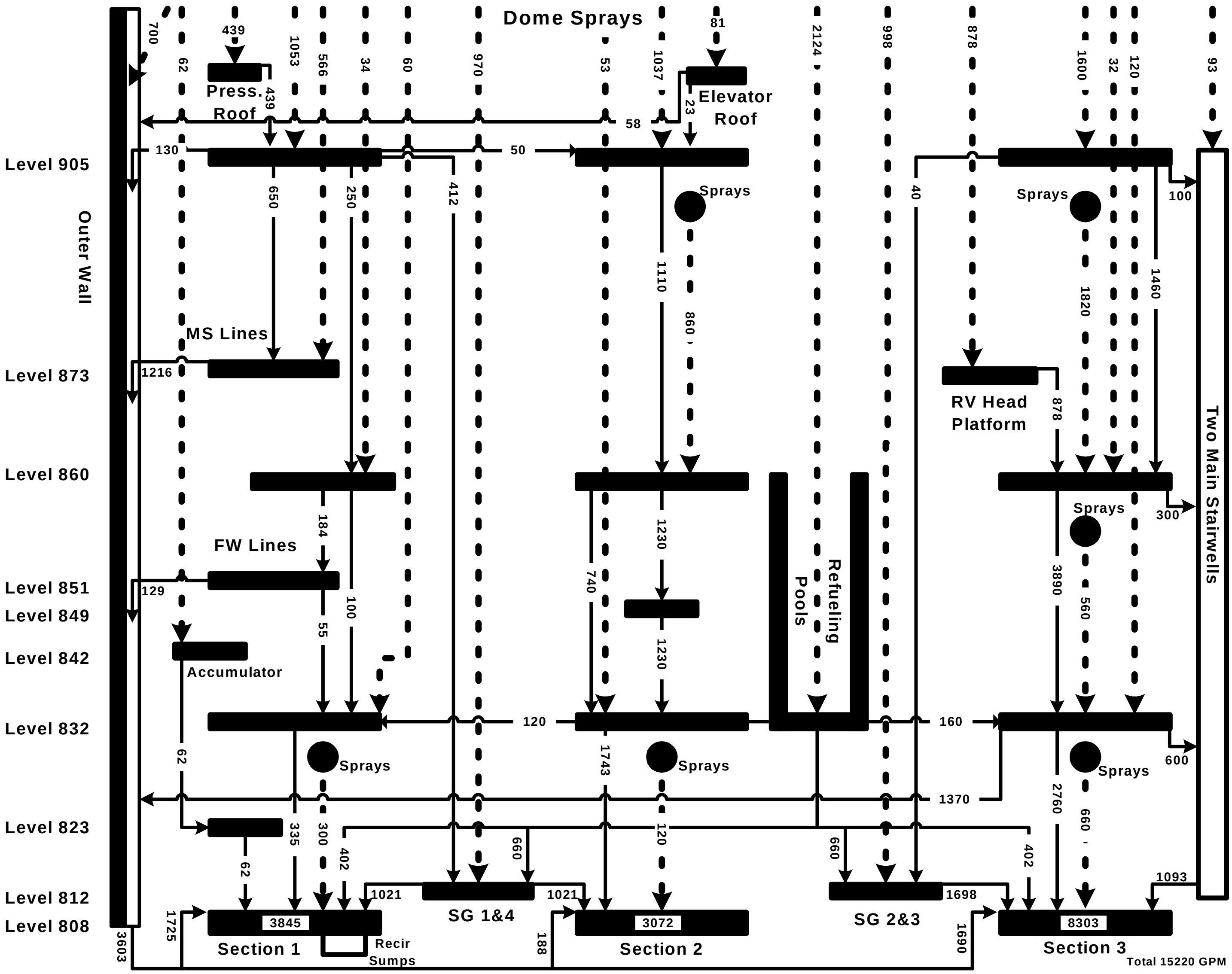

Figure 6. Spray-Water Drainage Schematic

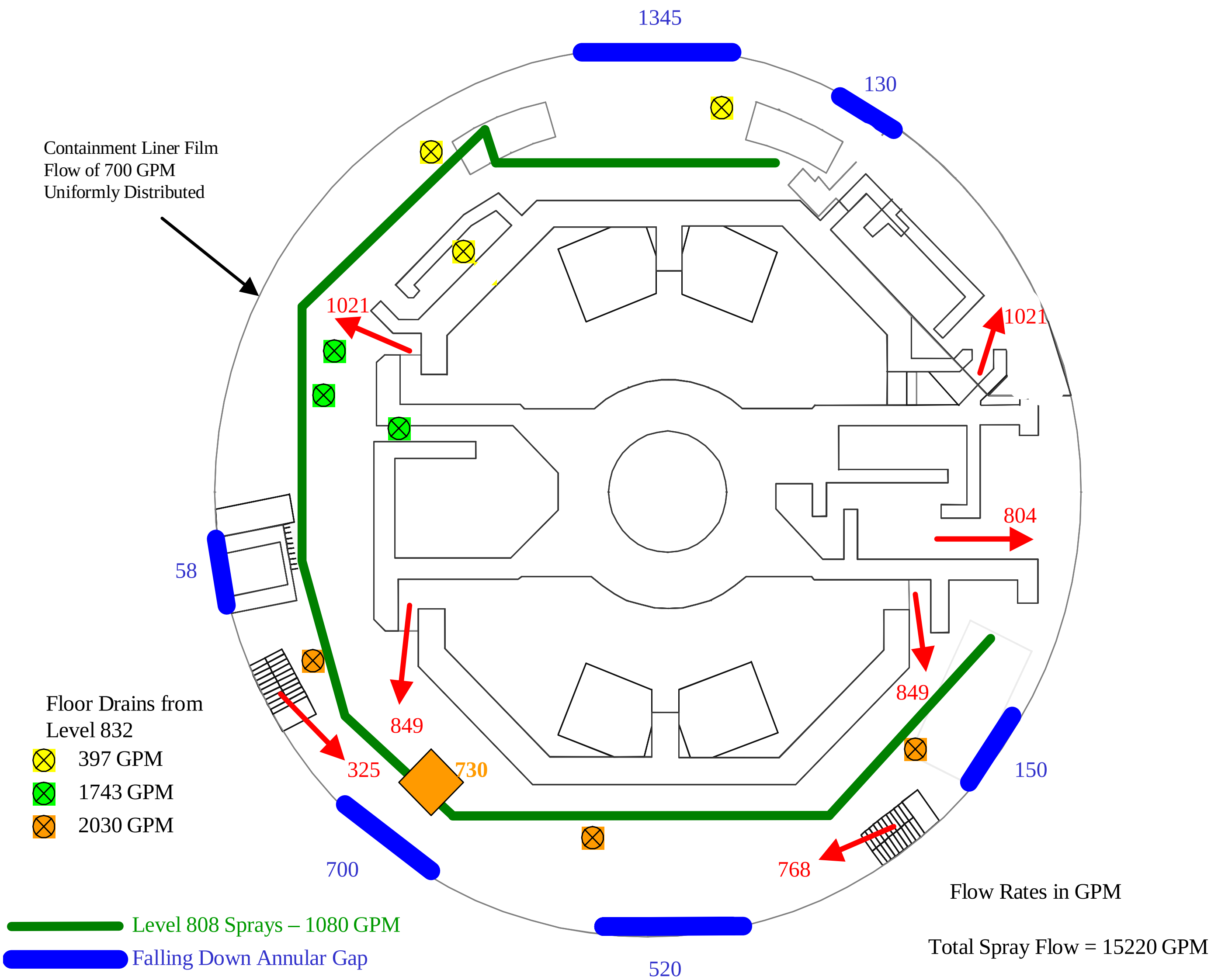

Figure 7. Spray-Water Drainage to Level 808 Sump Pool

Appendix VII

Characterization of Pressurized-Water-Reactor Latent Debris

The U.S. Nuclear Regulatory Commission has recently initiated a study conducted through Los Alamos National Laboratory (LANL) and the University of New Mexico (UNM) to characterize latent debris samples collected at five individual volunteer plants. This work focuses on the physical attributes of dust and dirt, such as particulate-to-fiber mass ratio, size distributions of particulate, material and bulk densities, and hydraulic parameters, including the specific surface area. Because of variations in plant collection methods and sampling schemes, it is not possible to estimate the total latent-debris inventories. This appendix documents preliminary results of that study that are relevant to the supplementary guidance provided by the staff in Section 3.5 of the safety evaluation report.

LANL received a total of five sets of samples, but only totally characterized four. The study did not fully characterize the fifth set because it was dominated by paint chips generated from pressure washing and was therefore deemed to be unrepresentative of pressurized-water reactor containment debris. Material property data collected for the latent-debris samples establish the basis for preparation of a particulate-debris simulant that is suitable for large-scale head-loss testing at UNM. The head-loss testing seeks to quantify the hydraulic properties of latent debris that are needed for the proper application of the NUREG/CR-6224 debris-bed head-loss correlation.

LANL conducted the sample characterization according to the following experimental scope:

- The debris was removed from its shipping container and transferred to plastic laboratory containers for gamma-spectrum counting.
- The fiber and particle fractions were separated from the remaining (or “other“) debris items by manual manipulation, sieving, and water rinsing.
- Particulate size distributions were obtained by graduated sieving.
- The weight of fine particles attached to swiping (Masolin) cloth or filter paper was determined by mass balance and comparisons of clean collection media to soiled collection media.
- The fiber thickness/diameter was determined by scanning electron microscopy (SEM) and microphotographic statistics.
- The material and bulk densities of fibers were estimated by mass measurement combined with volume estimates obtained from water displacement and direct measurement in graduated columns, respectively.
- Particle surface area and density measurements were taken using state-of-the-art nitrogen adsorption techniques.
- Scanning electron microscope/energy-dispersive spectroscopy methods were used to characterize the chemical composition of representative particulate and fiber samples.

Figure VII-1 illustrates a typical variety of composition and proportion between particulate, fiber, and other larger pieces that are assumed to have minimal transport potential. All plants submitted multiple samples ranging from a few grams to several thousand grams that exhibited similar characteristics. For some plants, the samples had to be combined to obtain meaningful measurements; for others, each individual sample could be fully characterized.

Figure VII-1. Representative Latent-Debris Components from a Single Volunteer Plant

Objects larger than a 0.132-in.–mesh size sieve were classified as a debris type other than particulate or fiber. This category of size, composition, and characteristics should be removed from any plant-specific samples that are collected before applying any mass fractions reported in this appendix. Larger latent debris types are not assumed to be transportable at recirculation pool velocities and so do not contribute to long-term increases in sump-screen head loss. Table VII-1 presents the range of particulate and fiber mass fractions that were measured for samples that were characterized after the larger pieces were removed. From these data comes the generic recommendation that 15 percent of the transportable latent debris be assumed to be fiber.

Each volunteer plant used a different collection method and sampling scheme. When separating particulates by wet sieving into fractions (greater than 2 mm, 500 μm to 2 mm, 75 μm to 500 μm, and less than- 75 μm), it became apparent by comparing plants that scraping and bristle-brush collection were not effective at capturing the smaller particulate fractions. The SEM photos of filter papers and cloth swipes that showed significant loadings of particles less than 10 μm in diameter further reinforced this conclusion. High-efficiency particulate air filter vacuuming with the brush attachments or manual swiping with lint-free (Masolin) cloth are recommended collection methods for characterizing plant-specific latent debris loadings.

A suitable surrogate formulation for latent particulate was found using a 28% mass fraction of common sand (ρ=2.6 g/cm^3) sieved between 500 μm and 2 mm, a 35% mass fraction of common sand sieved between 75 μm and 500 μm, and a 37% mass fraction of clay–based soil sieved <75 μm. Clay was used to conservatively incorporate the particulate fraction <10 μm that was observed in the plant samples.

Table VII-1. Particulate and Fiber Mass Fractions for Volunteer Plants A–D

Plant	Particle Weight	Fiber Weight	% Particle	% Fiber
A	5.42	1.04	84	16
B1	214	20	91	9
B2	369	64	85	15
B3	390	37	91	9
B4	592	47	93	7
B5	792	34	96	4
B6	122	50	71	29
B Total	2479	252	91	9
C	13.77	0.76	95	5
D1	2.51	0.47	84	16
D2	0.29	0	100	0
D3	12.45	0.28	97	3
D4	34.34	2.20	94	6
D6	5.56	0.1	98	2
D8	9.15	0.09	99	1
D10	11.98	0.74	94	6
D15	74.92	7.0	91	9
D Total	151.2	10.88	93	7

Sample Range	Total Particulate	71%–100%
	Total Fiber	0%–29%
Plant Range	Particulate	84%–95%
	Fiber	5%–16%

The material density of characterized fibers was found by water displacement measurements of 10 plant samples to range between 1.0 to 1.9 g/cm^3. The mean value of 1.5 g/cm^3 is recommended for use if needed in generic latent-debris assessments. However, a more relevant parameter of fiber is the dry-bed bulk density that can be used to estimate the volume of fiber needed to form a 1/8-in. thick thin bed across the wetted-screen area of a given sump configuration. This property and the suggested application are comparable to the use of the as-manufactured bulk density for fiberglass insulation.

The dry-bed density of latent fiber depends greatly on the amount of compaction applied for the measurement. Several alternatives were tried, but ultimately the staff recommends using the fiberglass density of 2.4 lbm/ft^3 = 38.4 kg/m^3 as a surrogate for dry latent debris. Similarly, fiberglass hydraulic properties should also be used as a surrogate for latent fiber. The following rationale supports these recommendations. First, in cases where fiberglass debris is present on the screen, minor inaccuracies in the latent fiber properties will not affect head-loss calculations. Second, where latent fiber is the dominant fibrous debris source and there is sufficient quantity to form a thin-bed filter, the properties of particulates captured on the fiber bed will dominate maximum head loss. Again, the difference between the actual hydraulic behavior of latent fiber and the presumed properties of fiberglass will not affect head-loss calculations adversely.

Particulate densities for each size fraction and volunteer plant were measured very accurately using the Brunauer-Emmett-Teller nitrogen adsorption method. Densities of particulates in the debris range from 125 to 250 lbm/ft^3 (2 to 4 g/cm^3) with only a few exceptions, and densities for most of the samples range between 156 to 188 lbm/ft^3 (2.5 and 3.0 g/cm^3), regardless of their particle size. These data form the basis of the recommendation for a nominal latent particulate density of 169 lbm/ft^3 (2.7 g/cm^3).

A nominal size distribution of particulates found in the latent debris samples was used as a starting point to develop a formula for surrogate particulate debris that could be tested in a vertical-flow test loop at UNM. This apparatus permits measurement of pressure drop across a debris bed of known composition under a range of water velocities. Hydraulic parameters of the debris bed can then be inferred from differential pressure data by iteratively applying predictive correlations until the model results envelope a range of observed data. Material-specific parameter values, such as the specific surface areas that are inferred in this manner, are only appropriate for use with the particular head-loss formula with which they were derived. In this case, the NUREG/CR-6224 head-loss correlation was applied. Microporous flow-resistance tests were performed on both the latent-debris samples and the surrogate formula to confirm that the surrogate could produce reasonably representative yet conservative hydraulic behavior.

Equivalent mass fractions of common sand and clay-based soil were used to recreate the size distribution of the latent particulate. Over a set of well-conditioned head-loss tests where the surrogate particulate was tested in combination with fiberglass insulation, the specific surface area of the surrogate was estimated to be 106,000 ft^{-1}. The penetration of the debris bed by extremely fine clay silt that continued to circulate in the test loop complicated the analyses of these tests. Within the range of the tests where flow velocities at the screen are less than 0.2 ft/s (uncompressed fiber bed) and the estimated particulate-to-fiber mass ratios cannot exceed 3, the estimated particulate loading on a postulated debris bed can be reduced by 7.5 percent (one-quarter of the less than 75-µm mass fraction) to accommodate realistic debris-bed penetration of latent fine particulates.

The surrogate debris formula was further refined by eliminating the latent-debris fraction with nominal dimensions greater than 2 mm because the particles (sand grains) are not likely to transport at the pool velocities of less than 0.5 ft/s that may exist near the screen under recirculation conditions. This size fraction represents approximately 22 percent of the particulate mass on average that can be discounted from the particulate inventory that is available for long-term transport under recirculation. This size fraction may be subjected to high-velocity transport during fillup, and so the fractional decrease was only recommended for latent-particulate inventories residing above the flood level.

Appendix VIII

Formation and Prediction of Thin-Bed Head Losses and Behavior of Compacted Calcium Silicate

VIII.1 Introduction

Relatively high head losses have occurred across relatively thin layers of debris consisting of fibrous and particulate debris, whereas substantially thicker debris beds have caused lesser head losses. This behavior has been referred to as the "thin-bed effect" where the head loss per unit thickness of debris is relatively high. Such debris beds have caused head losses high enough to threaten boiling-water reactor (BWR) emergency core cooling system (ECCS) sump recirculation pumps with modest quantities of debris on the strainers, and such debris beds can threaten pressurized-water reactor (PWR) sump recirculation sump screens as well. These types of debris beds have occurred operationally at nuclear power plants, have been created during head-loss testing, and have been analytically simulated with the NUREG/CR-6224 head-loss correlation.

VIII.2 Operational Incidents

Two operational strainer clogging events occurred at the Perry Nuclear Power Plant (PNPP) and one event occurred at the Limerick Generating Station, Unit 1, whereby in each event a high head loss occurred with a relatively thin layer of debris present on the strainers.

VIII.2.1 Perry Nuclear Power Plant

On May 22, 1992, during a refueling outage inspection at the PNPP, inspectors found debris on the suppression pool floor and on the residual heat removal (RHR) suction strainers. In addition, the buildup of debris on the strainers caused an excessive differential pressure across the strainers and resulted in deformation of the strainers. PNPP replaced the strainers and cleaned the suppression pool. Then in March 1993, several safety/relief valves (SRV) lifted, and the RHR was used to cool the suppression pool. The U.S. Nuclear Regulatory Commission (NRC) Information Notice (IN) 93-34, "Potential for Loss of Emergency Cooling Function Due to a Combination of Operational and Post-LOCA Debris in Containment," dated April 26, 1993, discusses this issue. PNPP subsequently inspected and found the strainers covered with debris. A test of the strainers in the as-found condition was terminated when the pump suction pressure dropped to zero. The debris on the strainers consisted of glass fibers (from temporary drywell cooling filters inadvertently dropped into the suppression pool), corrosion products, and other materials filtered from the pool water by the glass fibers adhering to the strainer surfaces (IN-93-34, Supplement 1). The suppression pool debris also consisted of general maintenance types of materials and a coating of fine dirt that covered most of the surface of the strainers and the pool floor. Fibrous material acted as a filter for suspended particles, a phenomenon not previously recognized by the NRC or the industry. This event suggested that filtering of small particles, such as suppression pool corrosion products (sludge), by the fibrous debris would result in significantly increased pressure drop across the strainers.

VIII.2.2 Limerick Generating Station, Unit 1

Another event occurred at the Limerick Generating Station, Unit 1 on September 11, 1995. The NRC discusses this event in IN-95-47, "Unexpected Opening of a Safety/Relief Valve and Complications Involving Suppression Pool Cooling Strainer Blockage," dated November 30, 1995. An SRV opened on Unit 1 while at 100-percent power. Before the SRV opened, Limerick was running Loop A of the RHR in suppression pool cooling mode. The operators initiated a manual scram in response to the SRV opening and a second loop (Loop B) of suppression pool cooling. Approximately 30 minutes later, operators observed fluctuating motor current and flow on Loop A. The cause was believed to be cavitation, and Loop A was secured. Following the event, a diver's inspection revealed a thin mat of material covering the Loop A strainer. The mat consisted of fibrous material and sludge. The Loop B strainer had a similar covering but to a lesser extent. Limerick subsequently removed about 635 kg (1400 lb) of debris from the pool. Similar to the PNPP events, the mat of fibers on the strainer surface converted the strainer into a filter, collecting sludge and other material on the strainer surface.

These strainer-clogging events caused substantial loss of pump flow and fluctuating conditions, indicating cavitation, resulting from debris beds consisting primarily of fibers and corrosion products. The debris bed descriptions "coating of fine dirt" and "thin mat of material" describe thin beds of debris. The conclusion is that relatively thin layers of debris caused relatively high head losses. Following these events, the thin-bed effect behavior has been experimentally replicated and analytically simulated, which has resulted in an understanding of how such thin layers caused such high head losses. These types of debris accumulation came to be known as the "thin-bed effect."

VIII.3 <u>Phenomenological Description</u>

The head loss across a bed of debris is directly related to the porosity of that debris bed (i.e., the lower the porosity, the higher the head loss). For fibers similar to low-density fiberglass insulation such as NUKON™, the porosity of a bed of these fibers typically ranges from 90 to 99 percent, depending upon the mechanical compression of the bed by the frictional drag caused by the flow. The porosity decreases with the compression of the debris. The porosity of a bed of particulate (without any fibers), however, is substantially less than the porosity of a fibrous debris bed. The iron oxide corrosion products sludge that is typically formed in BWR suppression pools has a porosity of about 80 percent. In sludge, the particulate cannot be compressed significantly because the particles are hardened, and the particles are already in contact with other particles. The porosity varies with types and size of the particulate. Common sand in soils has porosity in the neighborhood of 40 to 46 percent.

When fibrous and particulate debris are mixed, the porosity of the mixture depends upon the relative quantities of fiber and particulate and the mechanical compression of the fibers. When quantities of particulate are relatively small compared to the quantities of fibrous debris, the individual particles are trapped in the fibers such that the particles do not generally interact. Figure VIII-1 shows an example of a debris bed that has been referred to as a mixed debris bed. The particles contributed to the head loss, but the particles still resist flow individually.

As the quantity of particulate relative to the quantity of fibers increases (typically referred to as the particulate-to-fiber mass ratio), the contribution of particulate increases and head loss increases. As head loss increases, the fibrous bed further compacts thereby reducing the spacing between the fibers, which also increases the ability of the bed to filter finer particulate from the flow. Eventually, further increases in the particulate to fiber mass ratio results in increasing particle interaction. When this interaction reaches its maximum limit, based on the particulate bulk density or sludge density, further compaction becomes difficult. As this maximum limit is approached, the bed porosity approaches that of the particulate sludge, which is substantially less than the fibrous debris, and the head loss increases correspondingly. Once the porosity of the debris bed approaches the porosity of the particulate sludge, high head loss can occur in a thin layer of debris (i.e., the thin-bed effect). A definition of the thin-bed effect follows:

The thin-bed effect refers to the debris bed condition in a fibrous/particulate bed of debris whereby a relatively high head loss can occur because of a relatively thin layer of debris, by itself or embedded as a stratified layer within other debris, because the bed porosity is dominated by the particulate, and the bed porosity approaches that of the corresponding particulate sludge.

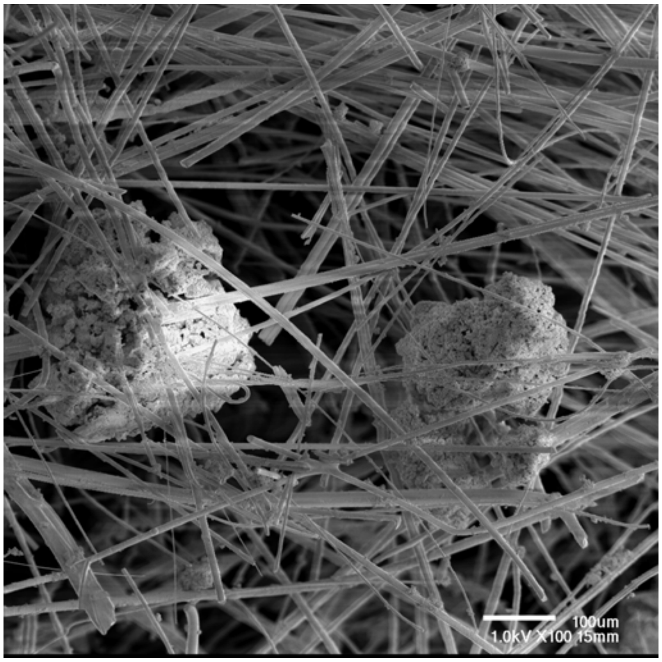

Figure VIII-1. Example of Particulate Embedded in Fibrous Debris[1]

During the PNPP and Limerick events, relatively small quantities of fibrous debris and relatively large quantities of corrosion product particulate debris were discovered in each suppression pool. When the recirculation pumps were operated, both the fiber and particulate would have been drawn to the strainers, but initially the particulate would pass through the strainers whereas the fibers preferentially filtered from the flow. Once

[1] Previously unpublished posttest scanning electron microscope (SEM) photo taken during the conduct of the NRC-sponsored calcium silicate head-loss tests (LA-UR-04-1227).

the screens accumulated sufficient fibers, the fibers filtered the particulate. The particulate would then have dominated subsequent accumulation such that the resultant accumulation would appear to be a layer of iron oxide sludge. As such, the pump had to draw water through this layer of sludge, which had a porosity near 80 percent. Fibers would have been interspersed throughout the bed but likely were concentrated nearer the screen surface, and associated pressures would have tightly compressed those fibers. The bed would have a high particulate-to-fiber mass ratio, which is characteristic of thin beds involving typical hardened particles.

The formation of a thin bed is somewhat variable. In laboratory testing, fibrous debris has been introduced before the particulate, in conjunction with the particulate, and after the particulate. During an actual event, the fibers and particulate debris would arrive in a mixed concentration that would likely vary with time, depending upon such factors as pool turbulence and relative densities. It is highly unlikely that the fiber could all arrive at the screen in advance of the particulate. If the particulate arrived at screen before significant fibers, then it would pass through the screen (i.e., the fibers are required to filter the particulate). Calcium silicate is a possible exception to this rule because this material has its own fiber component, and that fiber component must be on the screen to filter the fine particles. The efficiency of the particle filtration depends upon the thickness of the fibrous debris and on its porosity. Further, the porosity of the fibers depends upon how tightly it is compacted by the flow (e.g., a fibrous bed will filter more efficiently at a flow velocity of 1 ft/s than it will at 0.25 ft/s given the same thickness of fibers).

From a practical standpoint, a certain minimum thickness of fibers is needed to uniformly cover a strainer surface and to subsequently filter the particulate. For NUKON™ fibrous insulation debris, studied extensively during the BWR strainer-clogging resolution, NUREG/CR-6224 recommended an 1/8-in. fibrous debris bed thickness (based on the original bulk density generally referred to in head-loss analyses as the as-manufactured density). The NRC based the 1/8-in. recommendation on experimental observations, which show that typically at lesser thicknesses, the bed does not appear to have the required structure to bridge the strainer holes and filter the sludge particles. During an NRC-sponsored head-loss test program (NUREG/CR-6367), five tests were conducted with 1/8-in. fibrous debris beds (formed with shreds of NUKON™ debris) and iron oxide particulate with mass ratios ranging from 10 to 60. The head losses associated with these tests were minor because of the inability of the fibrous debris to filter sufficient particulate. In addition, Pennsylvania Power and Light Company (Brinkman) sponsored tests that demonstrated low head losses for thin fibrous debris beds (i.e., beds nearly as thin as 1/8 in.).

When the Boiling Water Reactor Owners Group (BWROG) conducted its head-loss tests (URG), in many of the tests it introduced the particulate into the test apparatus before introducing the fibrous debris, then allowed sufficient time for the particulate to become thoroughly dispersed. Once this was accomplished, the fibrous debris was introduced to allow a fibrous debris bed to slowly form, which subsequently filtered particulate from the flow once sufficient fibrous debris collected on the test screen. This type of bed formation created debris beds that were well intermixed, although it cannot be guaranteed that the bed was completely homogeneous. Like the PNPP and Limerick events, it is likely that some fibrous debris was concentrated at the screen to hold onto the particulate. Another aspect of particulate filtration is the particle size. Within any particulate distribution, some particles may be so fine that these particles pass through the fibrous debris bed whereas the larger particles are readily trapped. The in-between sizes could have varied behavior such that some of these particles may be alternately trapped and freed, thereby contributing to homogeneity. The fineness of the particles that become firmly trapped depends upon the tightness of the fiber matrix. When a thin bed is formed, the filtration process becomes more efficient, and more of the fine particulate is filtered from the flow because of its associated reduced porosity. It should be noted that on a per mass basis, the finer particles have a substantially greater impact on the head loss (i.e., the resistance to flow is correlated with surface area, and smaller particles have more surface area per unit volume than do larger particles [specific surface area]).

The method of introducing the particulate debris before the fibrous debris is likely more realistic with respect to actual plant conditions; however, many tests have been conducted where the fibrous debris was introduced before the particulate. When conducting thin-bed debris tests, it is advantageous to establish as uniform a fibrous debris bed as reasonably possible before significant head loss is achieved. This can be achieved more easily when the particulate is not involved with the fibrous bed formation. When the fibrous and particulate debris are introduced at the same time, the debris bed tends towards homogeneity for thicker debris but can lead to lesser head losses for thin-bed formations compared to establishing the fibrous debris bed first at flow velocities sufficient to compact the fiber before the arrival of the particulates.

Establishing a fibrous debris bed first and then introducing the particulate can create a more stratified debris bed (sometimes referred as a sandwich configuration), especially if a higher rate of flow compacts the bed before introducing the particulate. Such stratified beds have been achieved[2]. Such a configuration is analogous to a typical coffee filter, where the filter corresponds to the fibers and the particulate is the coffee grounds. Although a truly stratified bed is not the anticipated plant accident condition debris bed, it is useful for determining specific debris head-loss properties and generally leads to more severe head losses than the truly mixed debris beds.

This discussion has so far focused on particulate that can be characterized as hardened (i.e., the particles do not deform under the pressures encountered in a debris bed and are therefore considered solid). Head-loss testing using calcium silicate insulation debris as the particulate has encountered behavior that is apparently different from the behavior of hardened particulate.

The calcium silicate insulation tested was manufactured primarily from diatomaceous earth (DE) and lime (calcium carbonate) in roughly equal portions (approximately 90 percent of the total mixture). The remaining 10 percent consisted of small quantities of fiberglass fibers and a binder added for strength. The components were mixed, shaped, and baked, whereby the DE and lime reacted to form the calcium silicate in a porous crystal lattice structure that provides good insulation properties. The particulate debris created from the destruction of this insulation was examined under a scanning electron microscopy (SEM), which showed substantial very fine particulate and indicated voiding within the particles. Figure VIII-2 shows an example SEM photo, where a white bar scaled to 20 µm in the upper left corner indicates the magnification.

---

[2] As an example, during the conduct of the surrogate latent particulate head-loss tests documented in LA-UR-04-3970, the fibrous and particulate debris for an intended mixed debris bed test was inadvertently introduced separately instead of the being premixed as intended. Because the particulate was coarse sand (75 to 500 µm), the particulate essentially remained in place above the fibrous layer.

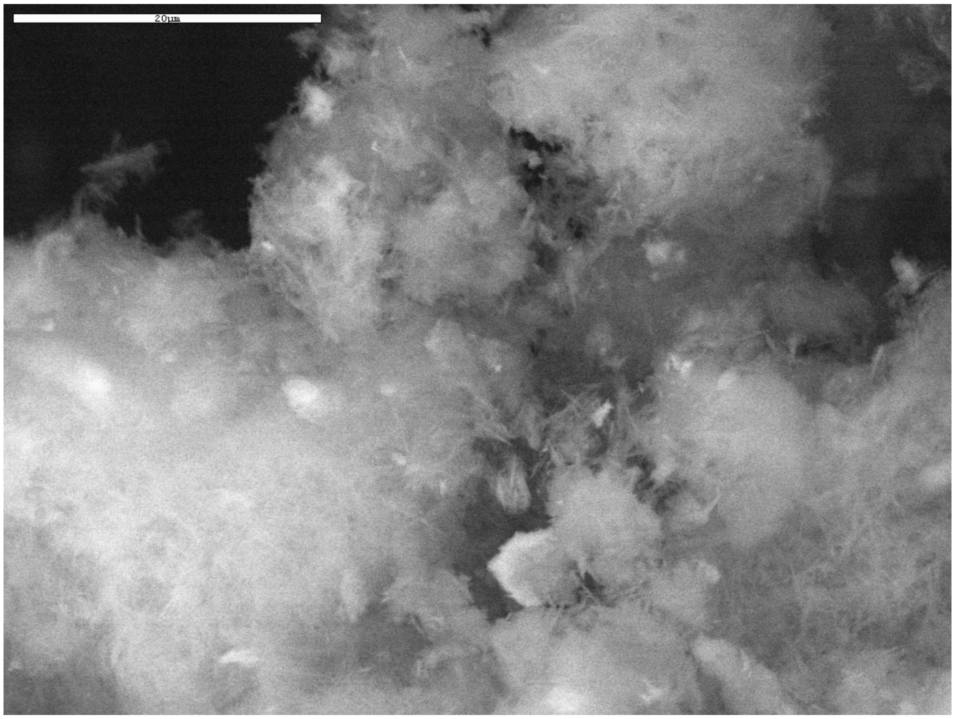

Figure VIII-2. Pretest SEM Photo of Calcium Silicate Particulate Debris

Because of the porous crystal lattice structure of the particulate, it is likely that these particles could deform under pressure. Figure VIII-3 shows a posttest photo that indicates that the calcium silicate particulate appears to have been pressed into a near continuous mat, which likely resulted in substantial reduction in porosity. If this particulate does deform under pressure, then the porosity through the continuous mat could decrease considerably. In addition, its specific surface area and density properties would not necessarily remain constant during this process. The debris bed in the test associated with Figure VIII-3 created a relatively high head loss across a thin layer of debris.

A calcium silicate debris bed can form in the same manner as a hardened particulate debris bed; however, calcium silicate is less dependent upon having a source of fibrous debris to filter it from the flow because calcium silicate has its own fibers (roughly 10 percent by mass). If the screen has a small enough mesh, it is likely that a bed of calcium silicate could form without any other fibers added to the bed. At first, the calcium silicate particulate might pass through the screen while the fibers from the calcium silicate accumulate. Then, if the fiber accumulation is sufficient, the fiber would filter the calcium silicate particulate. Existing test data are not sufficient to define the size of the screen mesh needed to form a debris bed with only calcium silicate. In addition, the screen would filter larger pieces of calcium silicate debris. To ensure conservative predictions, it is prudent to assume that debris beds with only calcium silicate will form unless adequate data are obtained to conservatively demonstrate otherwise.

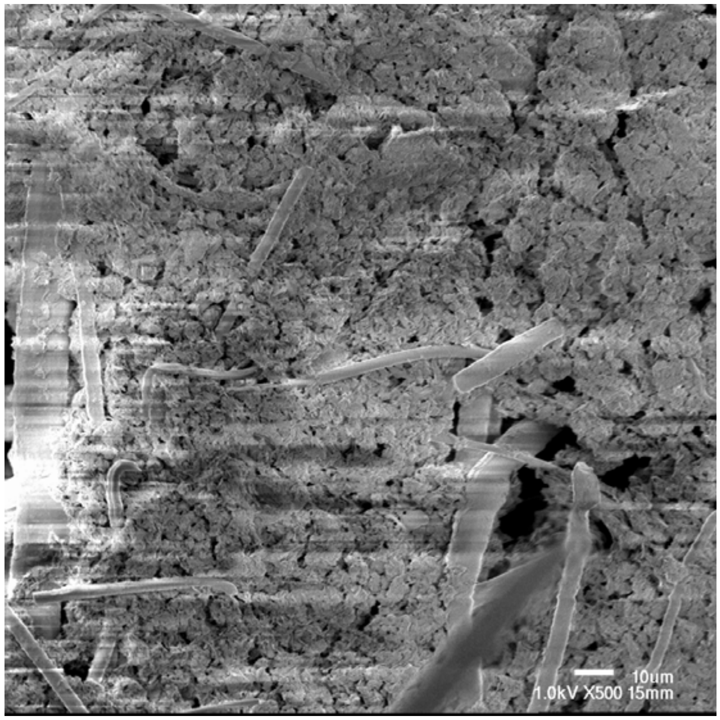

Figure VIII-3. Posttest SEM Photo of Calcium Silicate Debris from a Thin-Bed Test

Filtration efficiency is also an important aspect of head-loss behavior. As porosity decreases, finer particles may be filtered than before. When a thin bed exists, the filtration efficiency will increase so that the smaller particulate is filtered, which can further decrease porosity.

In summary, the parameters that affect the formation of a thin-bed debris bed and the resultant head loss include the following:

- existence of a sufficient quantity of fiber to filter the particulates
- porosity of the fibrous bed
- quantities of particulates
- size distribution and densities of the particulate that affect its porosity, specific surface area, and filtration efficiency
- whether the particulate is hardened or can deform under pressure
- sump screen mesh size
- flow approach velocity

VIII.4 <u>Thin-Bed Head-Loss Testing</u>

Various testing programs have demonstrated the thin-bed effect during head-loss testing. The following examples provide additional insights into thin-bed formations. The associated analyses were performed using the NUREG/CR-6224 head-loss correlation.

VIII.4.1 BWROG Test 7 (URG Technical Support Document, Vol. 1)

A truncated cone strainer with a screen area of 18 ft^2 was tested by first introducing 60 lbm of iron oxide corrosion products into the test tank, followed by 1 lbm of NUKON™ insulation debris about an hour later, at a pump flow of 5000 GPM and a water temperature of 63°F. The corresponding screen approach velocity was 0.62 ft/s. The particulate was allowed to circulate and become distributed before the fibers were added. Following the addition of the fibrous debris, the head loss increased rapidly to about 32 ft-water. The uncompressed thickness of the fibrous debris without the particulate would have been 0.28 in., but the debris bed formed with the particulate would have been about 0.63 in. thick if complete filtration were assumed. Based on the accepted sludge density of the corrosion products of 65 lbm/ft^3 and the material density of 324 lbm/ft^3, the porosity would have been about 80 percent. Analysis indicated the head loss should have been about 200 ft-water, which is much higher than the head loss actually measured. It is likely that holes developed in the debris because of the high pressure differentials that relieved the pressure across the bed. NUREG/CR-6224 notes that damage occurs to the fibrous bed whenever pressure drops exceed approximately 50 ft-water/in. (Note that 32-ft-water/0.63-in = 50.8 ft-water/in.) A layer of corrosion products held in place by the NUKON™ fibers formed the debris bed in this test. This debris bed consists primarily of a layer of particulate, its porosity would essentially be that of the sludge, and the resultant head loss is high; therefore, this bed is a thin-bed debris bed. The results of the test demonstrate the higher head losses that can be created by a thin bed even with the bed penetrations.

VIII.4.2 BWROG Test 8 (URG Technical Support Document, Vol. 1)

A truncated cone strainer with a screen area of 18 ft^2 was tested by first introducing 3 lbm of NUKON™ insulation debris, followed approximately an hour later by 16 lbm of iron oxide corrosion products, into the test tank at a pump flow of 5000 GPM and a water temperature of 61°F. The corresponding screen approach velocity was 0.62 ft/s. The particulate-to-fiber mass ratio was 5.3. The uncompressed thickness of the fibrous debris without the particulate would have been 0.83 in., and the debris bed formed with the particulate alone would have been about 0.16 in. thick if complete filtration were assumed. Based on the accepted sludge density of the corrosion products of 65 lbm/ft^3 and the material density of 324 lbm/ft^3, the porosity would have been about 80 percent. The measured head loss at 5000 GPM was quoted greater than 41.7 ft-water. It is likely that the debris bed lost integrity at these high head losses, which is indicated by the reported test measurement. In this test, the fibrous debris bed was formed at relatively high flow velocities before introducing the particulate; therefore, it is apparent that the fiber was well compacted before the arrival of the particulate and that the bed likely remained substantially stratified.

VIII.4.3 Latent Particulate (Surrogate) Test 17 (LA-UR-04-3970)

In this test, 15 gm of NUKON™ and 200 gm of particulate (less than 75 µm) were introduced into the test apparatus (fiber was introduced first, then the particulate). The particulate used included a clay component that appeared to break up in water into very fine particles. Posttest analyses of water clarity data indicated that approximately half of the particulate was not filtered from the flow, primarily because of the extreme fineness of the particulate; therefore, the subsequent analyses assumed that approximately 58 gm of particulate was in the debris bed, which resulted in a particulate to fiber mass ratio of 3.8 in the debris bed. A substantial uncertainty exists regarding the accuracy of the determination of the percentage of particulate not filtered from the flow. The 15-gm of NUKON™ formed a thin layer of fibrous debris 0.23 in. thick (at the as-manufactured density) but only about 0.07 in. thick at full test compression (analytical estimate). The particulate in the bed by itself would have formed a layer about 0.055 in. thick. At a flow approach velocity of 0.25 ft/s and a temperature of 94 °F, the measured head loss was 15.8 ft-water. Under these conditions, the analytically determined porosity was 77 percent, which is only slightly higher than the porosity of the particulate by itself (i.e., one minus the sludge density of 39-lbm/ft^3 divided by the particle material density of 166.6-lbm/ft^3 (1 – 39/166.6 = 0.766)). At faster approach velocities than the 0.25 ft/s that produced 15.9 ft-water head loss, the debris bed deteriorated, which was most likely because of the high pressure differential across the bed. Although substantial uncertainty is associated with the determination that approximately half of the particulate did not filter from the flow, a relatively thin layer of fibrous/particulate debris with bed porosity near that of the particulate alone caused a relatively high head loss.

VIII.4.4 Latent Particulate (Surrogate) Test 16 (LA-UR-04-3970)

In this test, 15 gm of NUKON™ bed and 600 gm of sand particulate ranging from 75 to 500 µm were introduced into the test apparatus (fiber was introduced first, then the particulate). Filtration of this relatively coarse sand was essentially complete. The particulate to fiber mass ratio for this test was 40. Figure VIII-4 shows the resultant bed of debris, approximately 0.23 in. thick, consisting mostly of the coarse sand with the fibers compressed underneath the sand (stratified). At a flow approach velocity of 0.46 ft/s and a temperature of 96.5°F, the measured head loss was 9.9 ft-water. Under these conditions, the analytically determined porosity was 41 percent, which is only slightly higher than the porosity of the particulate by itself (i.e., one minus the sludge density of 99-lbm/ft^3 divided by the particle material density of 166.6-lbm/ft^3 (1 – 99/166.6 = 0.406)). At a velocity of 0.25 ft/s, the head loss was 4.4 ft-water compared to 15.9 ft-water for latent particulate Test 17, even though the porosity of the coarse sand was much less than that of the fine particulate, because of the much smaller specific surface area of the coarse sand compared to the fine particulate. Although the porosity of the bed in Test 16 was much lower than the porosity in Test 17 (41 percent compared to 77 percent), the head loss for Test 16 was much lower than the head loss for Test 17. This outcome resulted from the much lower specific surface area of the coarse sand in Test 16 compared to the very fine particulate in Test 17.

VIII.4.5 Calcium Silicate Test 6H (LA-UR-04-1227)

In this test, 15 gm of NUKON™ debris and 7.5 gm of calcium silicate insulation particulate was introduced into the test apparatus (fiber was introduced first, then the particulate). The particulate to fiber mass ratio was 0.5. Posttest analyses of water clarity data indicate that all but the very finest particulate had filtered from the flow. The 15-gm of NUKON™ formed a thin layer of fibrous debris 0.23 in. thick (at the as-manufactured density), but the test bed under full compression was substantially thinner. Figure VIII-5 shows a photo of this debris bed. At a flow approach velocity of 0.4 ft/s and a temperature of 110°F, the measured head loss was 12.7 ft-water. An analysis deduced both the specific surface area and the sludge density for the calcium silicate. In the analysis, the sludge density was adjusted in the simulation until the particulate packing limit coincided with the rapid rise in head loss observed in the test data, which occurred when the approach velocity was increased beyond 0.35 ft/s. The working theory for the analysis of the calcium silicate thin-bed tests was that the formation of a relatively continuous layer of matted calcium silicate caused the rapid increases in the head losses as velocities increased. Figure VIII-3 shows the posttest SEM photo, which illustrates an apparent matted layer of calcium silicate. Under these conditions, the bed porosity apparently rapidly decreased with a corresponding increase in the bed's ability to filter finer particulate, which was demonstrated by the water clarity data. Under these conditions, the analytically determined porosity was 88 percent, which is significantly higher than the porosity of the particulate by itself (i.e., one minus the sludge density of 22-lbm/ft^3 divided by the particle material density of 115-lbm/ft^3 (1 – 22/115 = 0.808)). The most astounding feature of this thin-bed test was that such high head losses were achieved with a particulate to fiber mass ratio of only 0.5, even though the porosity apparently did not drop below approximately 0.8. To achieve such high head losses, the specific surface area had to be much higher than those determined for the hardened particulate. The analytically deduced specific surface area was 800,000-ft^2/ft^3. The higher specific surface areas were attributed to both the relative fineness of the particulate and internal voiding of the particles, whereby some flow potentially moved through these voids at higher pressure differentials.

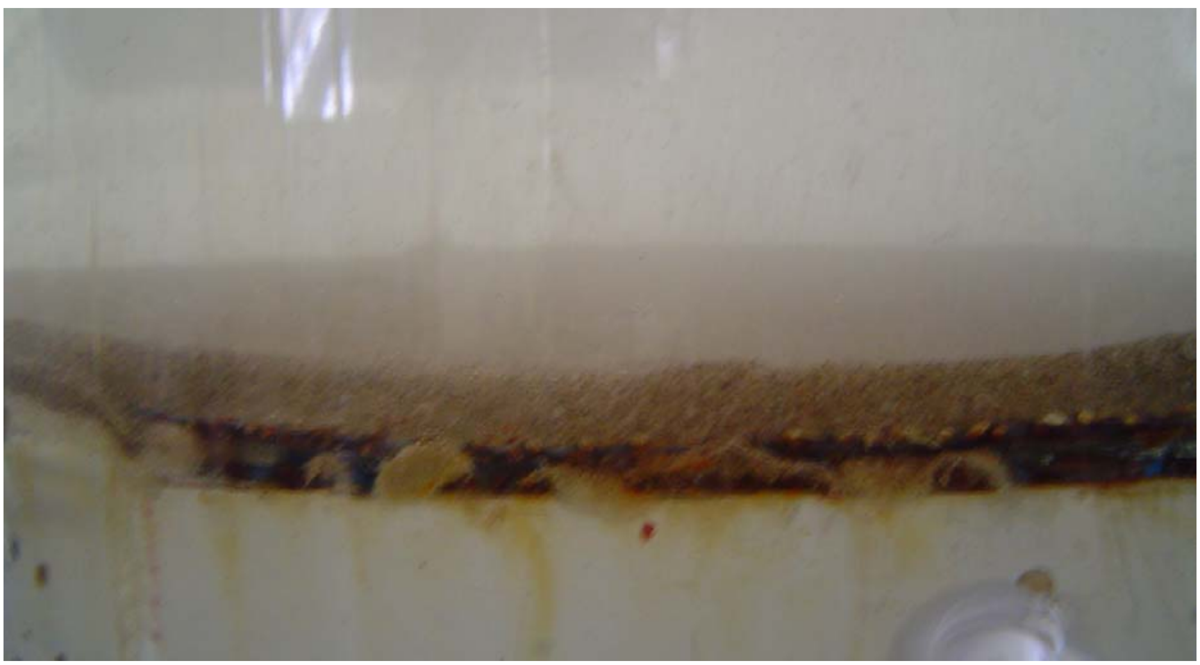

Figure VIII-4. Debris Bed for the Surrogate Latent Particulate Head-Loss Test 16

This set of relatively thin and relatively high head-loss tests illustrate the formation of debris beds whereby primarily the porosity of the particulate compacted into a sludge drives the head loss for four distinctly different particulate materials and a variety of particulate-to-fiber mass ratios. The two corrosion product tests involved head losses that became so high the debris bed probably developed penetrations that relieved the head loss; however, these thin-bed tests serve to illustrate how easily extreme head loss can occur. The latent thin-bed tests illustrate the differences between two distinctly different particulate size distributions. The calcium silicate test illustrated the potential effect of particulate deformation. Tests of this nature have been used to achieve an understanding of the thin-bed effect.

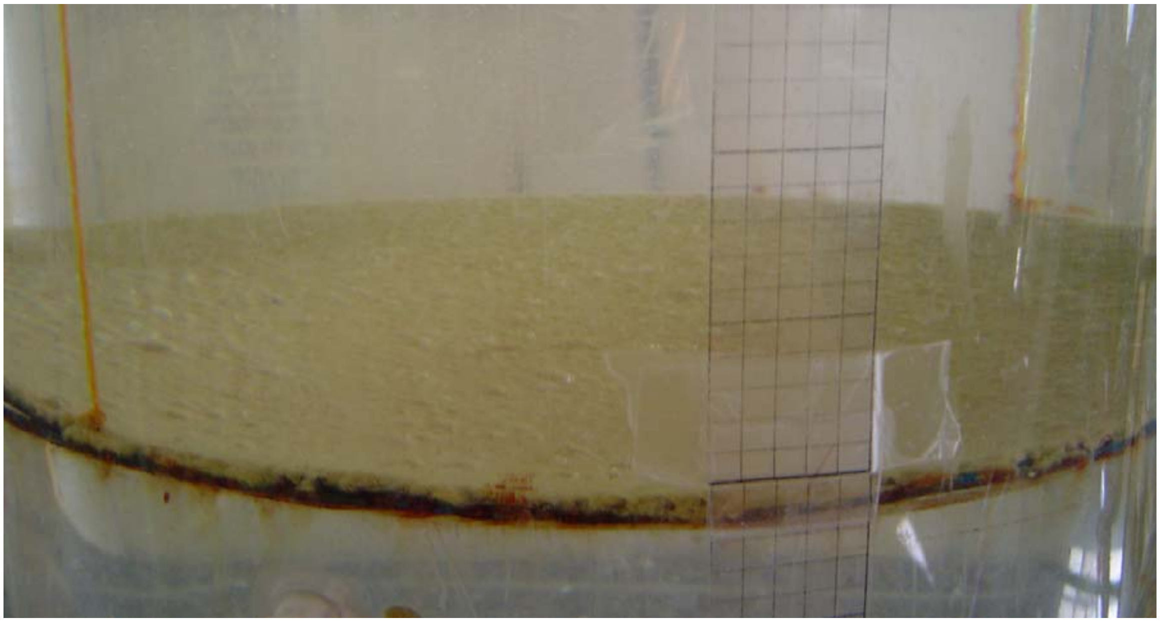

Figure VIII-5. Debris Bed for the Calcium Silicate Head-Loss Test 6H

VIII.5 Analytical Approach to Predicting Thin Beds

For a head-loss correlation to successfully predict the thin-bed behavior, as well as the porosity of a mixed debris bed, the correlation must have a debris bed porosity model that simulates not only mixed debris beds but also the porosity of the particulate by itself when enough of the particulate is in the debris bed to form a particulate layer. The NUREG/CR-6224 head-loss correlation porosity model contains a debris-packing limiting equation to limit bed compaction whenever the head loss and/or high quantities of particulate cause the bed compaction to reach the limit. The correlation porosity model includes a bed compaction term. When the particulate-to-fiber mass ratios become significantly large, the bed porosity from the porosity model approaches the porosity of the respective sludge.

The NUREG/CR-6224 correlation and its associated constitutive equations (porosity, compression function, and compression limiting) were developed assuming a uniform and a homogenous debris bed. Under thin-bed conditions, the fibrous debris could well be nonuniform because fiber would accumulate first before the particulate would filter from the flow; therefore, a layer of fiber next to the screen is likely. However, in a thin bed, the bed generally contains so much particulate that the fiber contribution to the head loss is small, thereby making the nonuniformity of the fibrous debris far less important.

Table VIII-1 (last page of this Appendix) compares head-loss prediction using the NUREG/CR-6224 correlation with the thin-bed tests presented herein. For the two corrosion products thin-bed tests, the tests were apparently conducted with so much particulate that penetrations developed in the beds such that head loss was substantially less than if a uniform debris bed had been maintained. As such, the NUREG/CR-6224 correlation overpredicted the head-loss results by a substantial margin. For the two latent (surrogate) particulate debris tests (i.e., less than 75 µm and 75 to 500 µm particulate), the NUREG/CR-6224 correlation was used to estimate specific surface area that agreed well with other tests, including mixed bed tests, in that test series. The latent sludge density and porosities determined experimentally agreed well with the correlation predictions. For the calcium silicate head-loss tests, input parameters were recommended for the NUREG/CR-6224 correlation that would cause the correlation to bound the head losses, even though the packing processes whereby the calcium silicate comes together to form a sort of matting layer are not well enough understood to formulate a model for those processes.

The NUREG/CR-6224 correlation was developed assuming the particulate properties would not be altered under head-loss pressures (i.e., constant densities and specific surface areas). With a particulate capable of deforming under pressure, the densities and surface areas are not necessarily constant. The correlation should not necessarily be expected to predict accurately the behavior of calcium silicate when compacted together in a thin-bed configuration. Therefore, the analytical approach is to estimate a bounding head loss. The bounding recommendation for calcium silicate was primarily based on the results of Test 6H, which produced the most severe head-loss conditions (i.e., the bounding specific surface area). Although a limited number of valid calcium silicate head-loss tests were conducted to determine the most severe head-loss conditions, the set of applicable tests supports the use of Test 6H in making bounding head-loss recommendations. Supporting tests accomplished the following:

- One test essentially reproduced the results with Test 6H.
- Two tests bracketed the thickness of the Test 6H fibrous debris bed (i.e., one test was slightly thinner and another slightly thicker). The associated head-loss parameters were more severe for Test 6H. In the thinner bed test, the filtration efficiency dropped off substantially relative to the efficiency of Test 6H. In the thicker bed test, the fibrous debris bed was thick enough that the amount of compaction needed to form a thin-bed matting of calcium silicate apparently did not occur within the flow capacity of the test apparatus.
- One test used the same quantity of fibrous debris as Test 6H but significantly more calcium silicate. In this test, the data indicate that a lower specific surface area than the 800,000/ft deduced from Test 6H is needed to simulate the test results even though the head losses were higher for this test.

Based on these results, it was judged that the 800,000/ft specific surface area bounded the test results and that Test 6H represents the more limited debris bed configuration. The recommended 880,000/ft specific surface area (in conjunction with a sludge density of 22 lbm/ft^3) included a 10-percent enhancement as a safety factor because of experimental uncertainties and variances in calcium silicate manufacturing.
In summary, the thin-bed effect, originally recognized with respect to the response of ECCS long-term cooling systems at nuclear power plants after three BWR operational events where strainer clogging occurred, has been experimentally reproduced for a variety of particulate debris. The experimental data were subsequently used to study the

physical processes whereby recommendations can be made for the application of the NUREG/CR-6224 correlation to this type of debris bed accumulation.

VIII.6 Addressing the Potential of Forming Stratified Debris Beds in Plant-Specific Evaluations

Plant accident scenarios do not anticipate the establishment of highly stratified debris beds because the debris is expected to arrive at the screens as a mixture of varied concentrations. However, it is possible for the debris bed makeup to have concentrations of particulate debris (i.e., the concentration of the particulate with respect to the fiber varies with the depth in the bed). Concentrations of the finer particles, which have a greater impact on head loss, would be more difficult to form than coarser particles because the finer particles have a greater potential to pass among the fibers.

The head loss across the concentrated layer would be higher than that predicted for the homogeneous debris bed, but then the lower head loss associated with the remaining correspondingly reduced concentration layer would compensate in part. The impact of these concentrations has not been thoroughly studied because of the large number of possible variations. In plant analyses, the conservatism associated with the estimates for the quantities of debris postulated to accumulate on the sump screen also compensates for the uncertainty associated with potential concentrations.

However, if a plant-specific analysis identifies conditions where the potential is indicated for a stratified debris bed to have a substantial impact on head-loss analyses, then that plant should assess the impact of that stratified bed. The determination of whether a stratified bed should be considered would involve the evaluation of the types of debris accumulation on the screens and the likelihood of one type of debris arriving in a preferential timeframe, such as the BWR example discussed below. The evaluation approach of a stratified debris bed would likely be specific to a particular bed structure. In a uniformly stratified debris bed, the head total head loss across the bed is the sum of the head losses across each of the stratified layers, but one of those layers could dominate the total head loss, especially if that layer was a layer of particulate. As an example, consider a debris bed consisting of an inner layer of fibrous debris, then a layer of particulate, followed by a layer of mixed debris. The head loss across the innermost layer of fibrous debris would assume a thickness of highly compressed fibrous debris because this layer would support the forces associated with the outer layers (a bounding compression can be estimated). The head loss across the particulate layer would adapt the porosity of the particulate sludge and the particulate layer thickness determined using the particulate mass and sludge density (assuming a layer of the particulate without fibers). For the head loss across the outer layer, the evaluation would use an approach applicable to that debris accumulation, which might be able to treat this layer as a normal fiber/particulate head-loss calculation. Then the three head losses would be summed, but the particulate layer would likely dominate the total head loss. This example illustrates how a plant-specific stratified head-loss analysis could adapt an approach that makes sense to the plant-specific postulated debris bed. Because head losses associated with stratified debris beds have not been thoroughly examined and procedures have not been developed for predicting head losses across these beds, plant specific head loss evaluations involving stratified debris beds must be conservatively validated based on experimental data.

For perspective, during the BWR strainer resolution, it was recognized that the particulate-to-fiber mass ratio would likely decrease as debris accumulation progressed because of the preferential settling of the particulate in the suppression pool relative to the settling of fibers (caused by the heavier densities of the corrosion products). However, most plant analyses generally assumed that debris would not settle in the suppression pool, thereby overpredicting debris accumulation and subsequently the head-loss calculations. Similar arguments could potentially apply to a PWR sump pool on a plant- and scenario-specific basis. For example, quantities of higher density failed coatings particulate washed into a relatively slow-moving sump pool could potentially settle and then remain in place such that the concentration of particulate arriving at the screen early in the scenario is higher than later in the scenario. However, these kinds of arguments are plant and scenario specific.

VIII.7 <u>Estimating Conservative Thin-Bed Head Losses</u>

VIII.7.1 Parametric Examples of Thin-Bed Head Loss Estimates

Plant-specific analyses are required to consider the potential for a thin-bed formation unless (1) that plant can substantiate the presence of insufficient fiber to form the initial bed of fibrous debris required to filter the particulate or (2) that plant implements a sump screen design that has experimentally demonstrated that a thin-bed debris bed is very unlikely to form because of its special geometry. The determination of the potential to form a thin bed must first assess the quantities of fibrous debris that could potentially accumulate on the screens from all sources, including insulation and fire barrier debris and latent fibers. If enough fibrous debris can accumulate to form a 1/8-in.-thick layer across the screen, then the potential to form a thin bed subsequently depends upon the availability of particulate debris from all sources, including latent particulate, particulate insulation debris, and failed coatings. If a plant determines that there is not sufficient fibrous debris to form a 1/8-in. layer across the screen, then that evaluation should have sufficient conservatism to compensate for uncertainties associated with the 1/8-in. specification. When integrated particulate/fiber insulation (e.g. calcium-silicate) debris can accumulate on the sump screen, it is conservatively assumed that this can form a debris bed without any supporting fiber beyond that fiber that is inherent in the manufacture of the integrated particulate/fiber insulation. The determination of sufficient particulate typically involves a parametric evaluation of the head loss versus mass and type of particulate in the bed to ascertain the conservatively minimum quantity of particulate needed to overcome the available net positive suction head. If the available quantities of particulate exceed the minimum quantity, then the potential for a thin-bed debris bed compromising the ECCS pumps exists.

The NUREG/CR-6224 head loss correlation has the capability of predicting the thin-bed head loss phenomena as illustrated in the following parametric examples. First, Figure VIII-6 and Figure VIII-1 show the head loss and corresponding bed porosity, respectively, predicted by the correlation for the input parameters of (1) a minimal thickness of LDFG (1/8-in.), and (2) particulate to fiber mass ratio of 5 and 130°F water. As the approach velocity was increased in the parametric, the debris bed was increasingly compressed until the particulate limited further compression. At this point, at velocity of about 0.16 ft/s, the debris bed became a thin-bed where the bed porosity approached that of the particulate without fiber (approximately 59%), as indicated by the rapid rise in head loss and corresponding drop in porosity. Note that head loss tests are typically conducted by forming the debris bed at a low velocity then incrementally increasing the velocity and measuring the corresponding head loss.

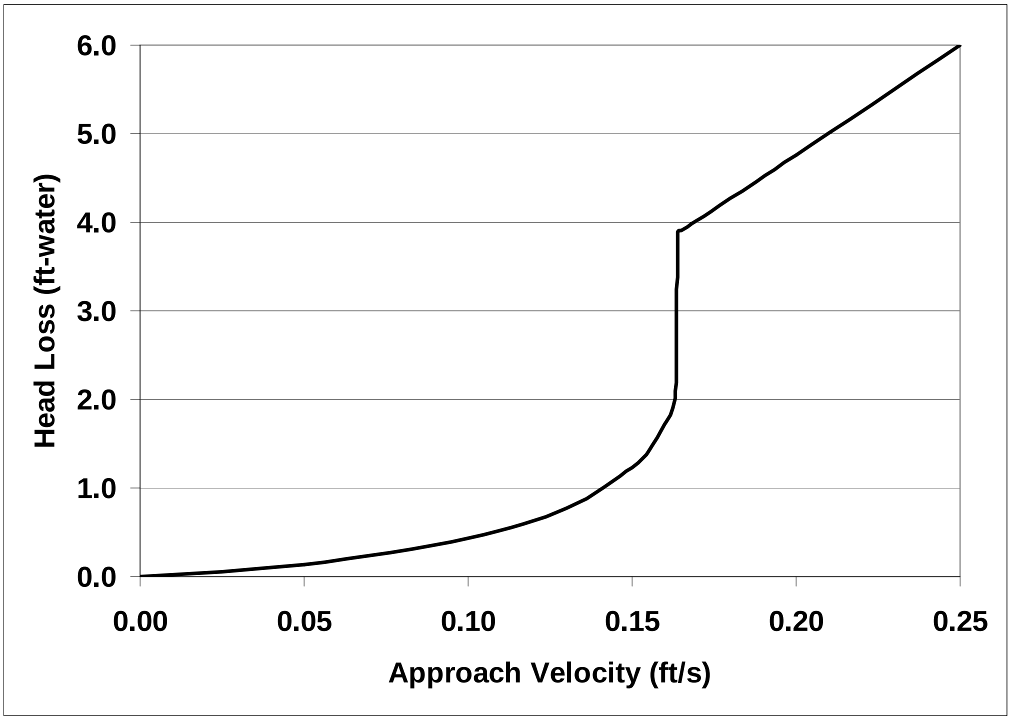

Figure VIII-6 Head Loss Example of Thin-Bed Formation Due to Bed Compression

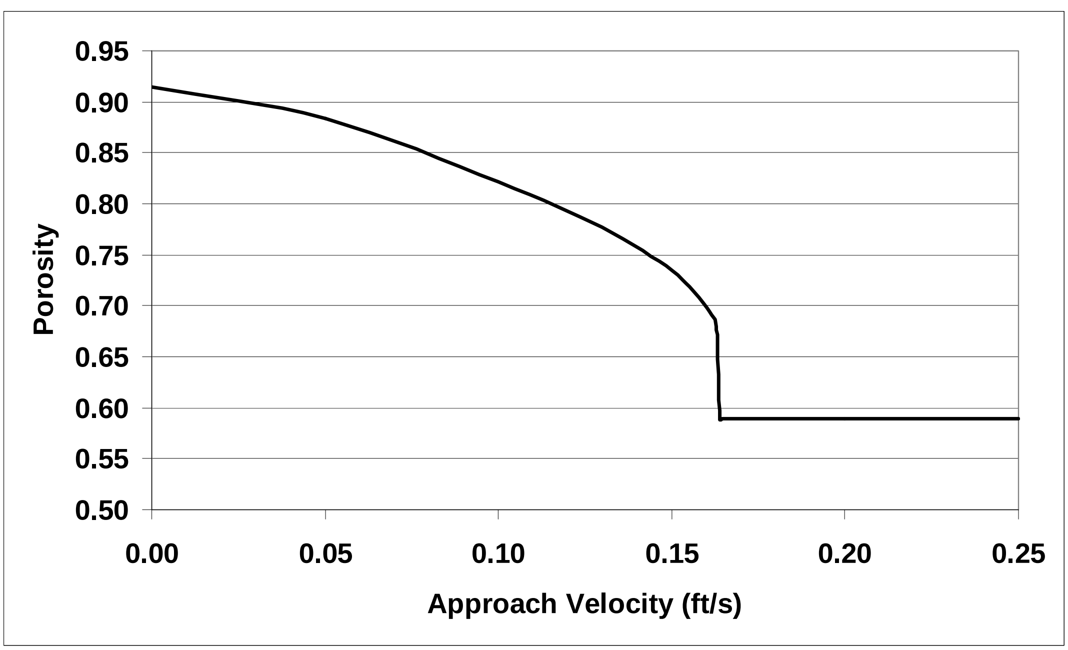

Figure VIII-7 Porosity Example of Thin Bed Formation Due to Bed Compression

In a second example, Figure VIII-8 shows a parametric example of the quantities of debris required in a thin-bed formation and the associated head losses (calculated using the NUREG/CR-6224 head-loss correlation). This example assumed the formation of a minimal thickness initial layer of fibrous debris (1/8 in. of NUKON™) and a variable quantity of latent particulate, as indicated by the particulate/fiber mass ratio. The figure shows the results for three approach velocities (i.e., 0.1, 0.3, and 1.5 ft/s). The debris bed was initially a mixed bed with relatively low head losses because the bed was primarily fibrous debris. As the particulate mass increased, the debris bed transitioned into a thin bed where the particulate dominated the porosity. This occurred at particulate-to-fiber mass ratios of 5.9, 4.0, and 2.0 for velocities of 0.1, 0.3, and 1.5 ft/s, respectively. If the screen area was 100 ft^2, the quantity of fibrous debris required to form a 1/8-in. bed would be 1.04 ft^3 (2.5 lb) and the mass of particulate needed to form a thin-bed debris bed would be 14.8, 10.0, and 5.0 lb, for velocities of 0.1, 0.3, and 1.5, respectively.

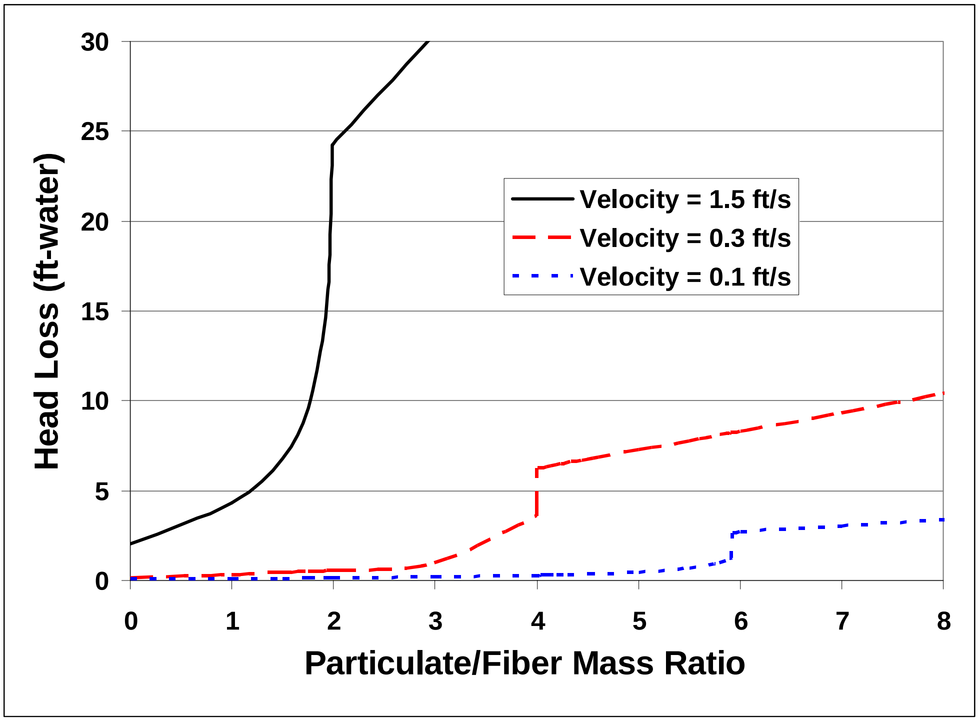

Figure VIII-8. Parametric Example of Thin-Bed Formation

Once it is determined that a thin-bed fiber/particulate debris bed can form, the maximum head loss based on the available particulate mass is determined by performing a parametric evaluation as demonstrated in Figure VIII-9. For an example approach velocity of 0.3 ft/s and three masses of available particulate, the figure shows the head loss as a function of the fiber bed thickness. If the postulated debris bed is less than 1/8 in., it was assumed that the fiber debris bed was too thin to filter the particulate from the flow. The head losses are shown to increase as additional fiber is added to the debris bed until enough fiber is in the bed to prevent the thin-bed effect from establishing. Figure VIII-9 illustrates the peak head loss for 10 and 20 lbs of latent particulate, which is the maximum head loss unless the volume of fibrous debris becomes so large that the fiber volumes dominate the head loss (Figure 7-2 of NUREG/CR-6808 provides an example). The peak head depends on the specific surface areas as well on the quantities. In this example, the specific surface area of the latent particulate is 106,000 ft^2/ft^3 compared to the NUKON™ specific surface area of 171,000 ft^2/ft^3. Therefore, increasing the quantity of fibrous debris increased the effective mixture specific area as well as the debris bed thickness. When the particulate surface area is greater than the fiber surface area, the maximum head loss would be closer to the head loss calculated for a 1/8-in.-thick bed than occurred in this example.

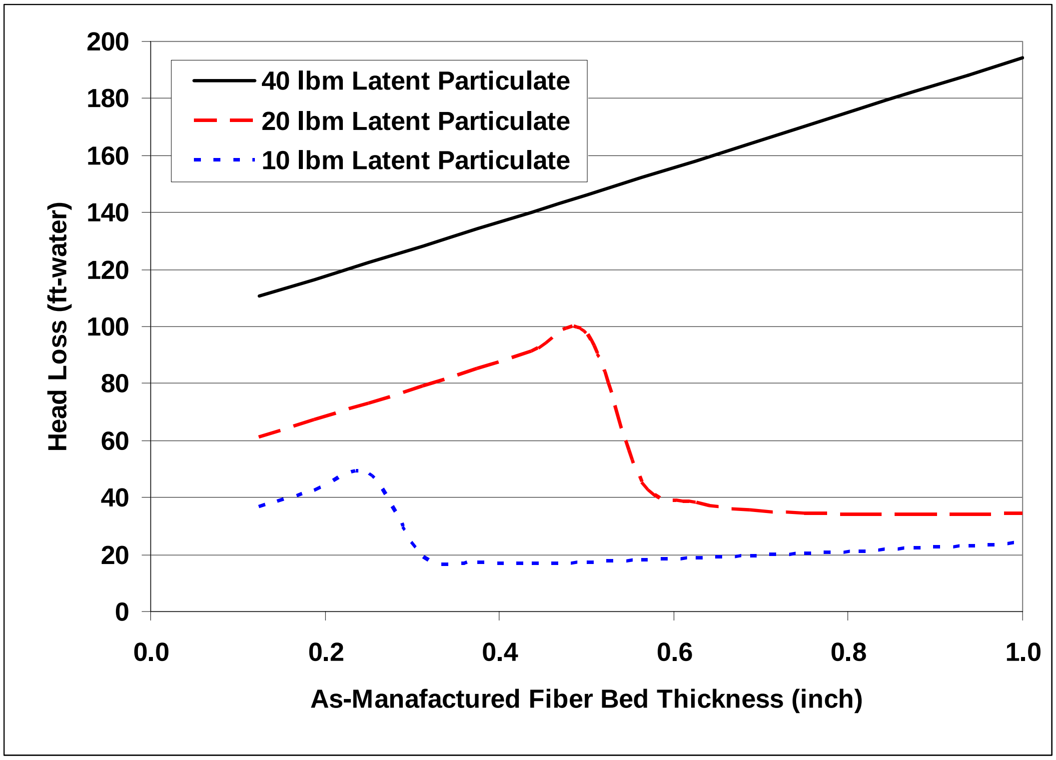

Figure VIII-9. Parametric Example of Peak Head-Loss for Given Mass of Particulate

The estimation of the peak thin-bed head loss is further demonstrated in a more specific example shown in Figure VIII-10. In this example, a maximum of 1000 ft^3 of LDFG and 300 lbs of latent particulate could accumulate in a 500 ft^2 sump screen. The approach velocity to the screen is 0.1 ft/s, the water temperature is 150 ^oF, and the containment does not contain any calcium silicate or other type of particulate insulation. If all the LDFG did accumulate on the screen, the resultant bed thickness would be 2-ft thick (uncompressed) resulting in a predicted head loss of 6.3 ft-water. In the figure, the debris bed thickness was varied, starting with a 1/8-in thickness, until a peak head loss of 8.8 ft-water was predicted at a thickness of approximately a 1/2-inch. This peak head loss is a thin-bed head loss with a porosity of approximately 59% (particulate sludge porosity). It would take a bed thickness nearly 3-ft thick to cause the same head loss as the peak thin-bed head loss.

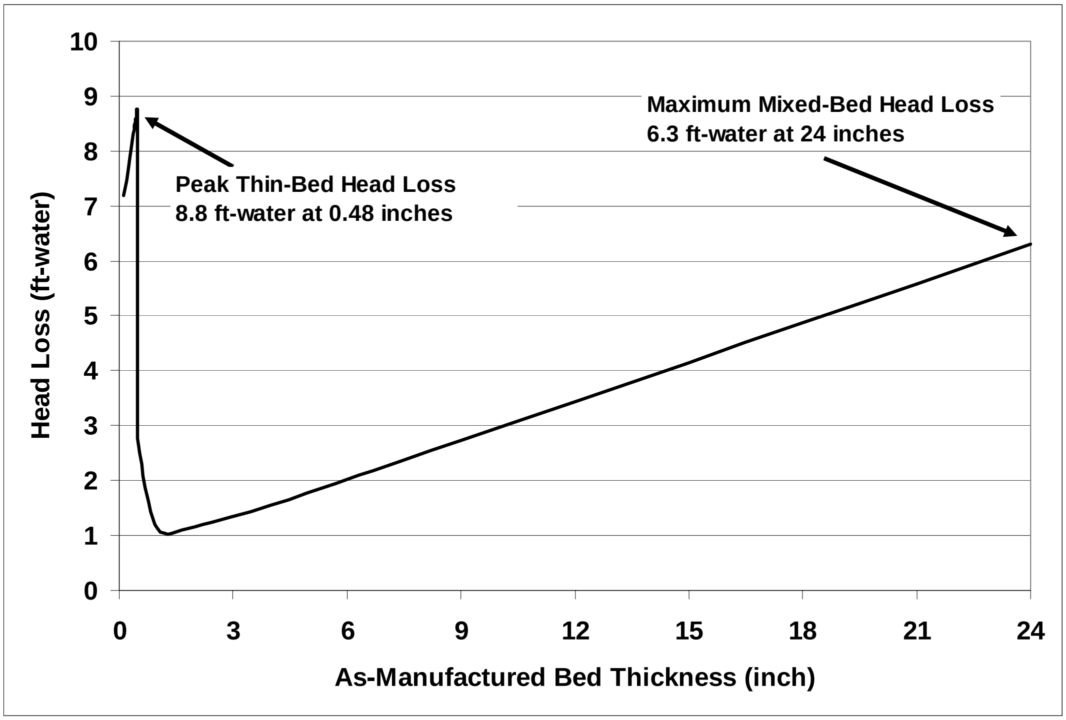

Figure VIII-10 Specific Example of Estimating Conservative Thin-Bed Head Losses

If a thin-bed debris bed cannot effectively form, then a continuous stratified bed should not be able to form. If the evaluation determines that there is not sufficient fiber to form a 1/8-in. layer of fibrous debris (without integrated particulate/fiber insulation debris present in the bed) required to establish a thin bed, then there is not sufficient fiber to establish a particulate layer in a stratified bed. If a thin bed cannot be established in a special geometry strainer because of nonuniform debris accumulation, then it is reasonable to assume that the same nonuniform accumulation in bed stratification would not lead to the continuous layer of stratification required to achieve the high head losses. If the plant sump screens have sufficient capability that a thin bed once formed does not compromise ECCS, then those screens should have enough capacity for a stratified particulate layer (same particulate mass) within a thicker debris bed. The establishment of a thin bed on a minimal fiber layer containing all available particulate should bound the head losses associated with a stratified layer of particulate within a mixed bed. The highest head loss is associated with the most concentrated and thickest layer of particulate, which corresponds to the establishment of the thin bed containing all available particulate. For all of these debris beds, the effects of other types of debris must be factored into a total head loss (e.g., reflective metallic installation and miscellaneous debris).

The term realistic in the above argument is used to acknowledge that total stratification is not realistic because fiber and particulate would arrive at the screen concurrently and the fine (most influential) particles have some ability to migrate within the fiber bed. However, one mechanism that could lead to stratification of some degree is late term erosion of larger debris in the sump pool (discussed in Appendix III.3.3.3). In such a scenario, the LOCA generated fiber and particulate would accumulate relatively early, then fibers from the erosion process could accumulate without significant embedded particulate. To demonstrate using the example above (Figure VIII-10): if after the peak thin-bed head loss was created, 1000 ft^2 of fiber were added to the top of the thin-bed (increasing the bed thickness to approximately 21 inches), an additional 5.6 ft-water head loss would be added to the peak thin bed head loss of 8.8 ft-water for a total head loss of about 14 ft-water. This shows that the head loss for worst-case bed stratifications can be estimated, however unlikely those debris beds are to form.

VIII.7.2 Procedure for Estimating Conservative Thin-Bed Head Losses

A procedure for estimating a conservative thin-bed head loss is illustrated in Figure VIII-11 and discussed in the following steps.

1. An assessment of the debris that could potentially transport and accumulate on the sump screen involves the generation of debris, an assessment of latent debris, and subsequent transport of that debris, as outlined in the appropriate sections of the GR and SER. This assessment would provide quantities for each type of debris and the appropriate characteristics of that debris.

2. The design of certain alternate geometry sump screens could preclude the formation of the thin-bed debris bed.   If sufficient data exists to determining that the particular screen design undergoing evaluation cannot form a thin-bed, then there is no need to proceed with this thin-bed evaluation. If this data does not exist, then proceed to the next step.

3. The minimum thickness of fiber needed to filter particulate from the flow stream and then support the formation of the debris bed must be specified.
    a. For debris types other than integrated particulate/fiber insulation debris, a thickness of 1/8-in (based on the as-manufactured density) has been specified as the minimum thickness required to form a uniform layer across the screen and effectively filter the particulate from the flow.
    b. For integrated particulate/fiber insulation debris (e.g., calcium silicate), the minimum thickness for supporting fibers (other than the fiber inherent to the manufacture of the integrated particulate/fiber insulation) has not been sufficiently determined to specify a minimum thickness because the fiber inherent to the integrated particulate/fiber insulation may be sufficient to form the bed. Therefore, the minimum thickness of fiber to form a debris layer when significant integrated particulate/fiber insulation debris is present is conservatively zero unless adequate data becomes available to specify otherwise.

4. Combining the fibrous debris available per the assessment with the minimum thickness required to form the debris bed, determine whether or not there would be sufficient fibrous debris to form a debris bed. If sufficient fibrous debris is available to form a debris bed then proceed to the next step.

5. The peak head loss associated with a debris bed is determined using a parametric evaluation where the fibrous debris is varied from the minimum from Step 3 to a value large enough that the bed transitions from a thin-bed into a mixed debris as illustrated in Figure VIII-10. All of the particulate is assumed to be in the debris bed. To ensure that the peak head loss is captured in the

parametric evaluation, the increments in fibrous debris must be small around the peak head loss. In a scenario involving calcium silicate or other integrated particulate/fiber insulation debris, all of the calcium silicate including its inherent fibers should be considered to be particulate because the recommended parameters for the NUREG/CR-6224 head loss correlation were based on this assumption. If fibrous debris, other than the fibers inherent in the calcium silicate, is present then the thickness of the bed formed is varied from zero to the maximum thickness possible using all the available fibers. In the unlikely case that there are no other fibers available, the debris bed would be formed as a layer of calcium silicate and any other particulate, which would automatically be a thin-bed. Therefore, the maximum bed thickness will be used to calculate the peak head loss assuming that the bed has been compressed to the particulate sludge limit. In this case, the NUREG/CR-6224 correlation compression equation would not apply.

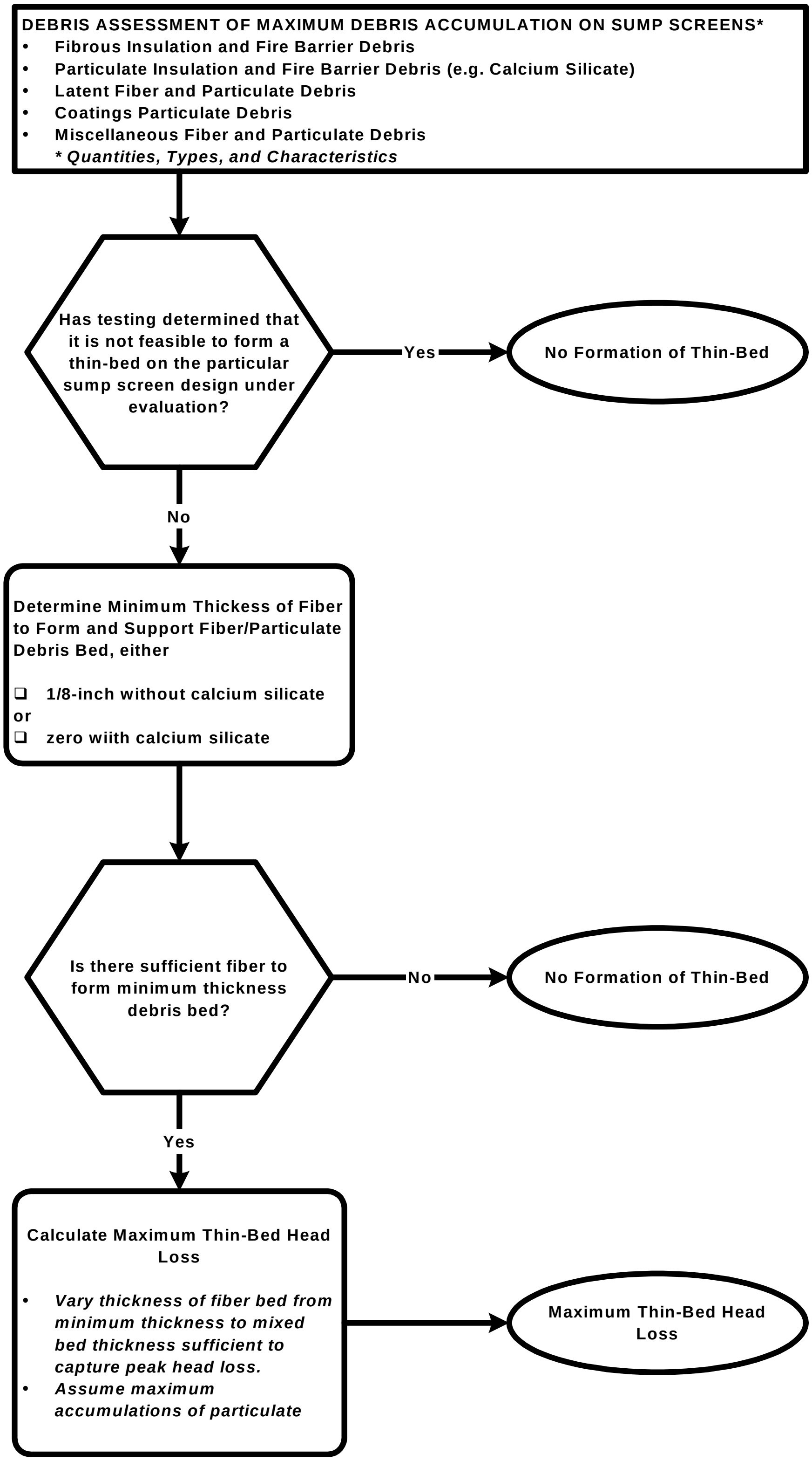

Figure VIII-11 Procedure for Estimating Conservative Thin-Bed Head Losses

VIII.8 References

Brinkman, K. W., and P. W. Brady, “Results of Hydraulic Tests on ECCS Strainer Blockage and Material Transport in a BWR Suppression Pool,” Pennsylvania Power and Light Company, EC-059-1006, Rev. 0, May 1994.

NRC Information Notice 93-34, “Potential for Loss of Emergency Cooling Function Due to a Combination of Operational and Post-LOCA Debris in Containment,” April 26, 1993.

NRC Information Notice 93-34, Supplement 1, “Potential for Loss of Emergency Cooling Function Due to a Combination of Operational and Post-LOCA Debris in Containment,” May 6, 1993.

NRC Information Notice 95-47, Revision 1, “Unexpected Opening of a Safety/Relief Valve and Complications Involving Suppression Pool Cooling Strainer Blockage,” November 30, 1995.

Table VIII-1. Comparison of Thin-Bed Test Data with NUREG/CR-6224 Simulations

Test No. and Particulate	Experimental Parameters					NUREG/CR-6224 Head-Loss Simulation Results				Comments
	Fiber[3] & Particulate[4] Bed Thicknesses (in.)	P/F Mass Ratio	Approach Velocity (ft/s)	Sludge Porosity and Density (lbm/ft_3)	Experimental Head Loss (ft-water)	NUREG/CR-6224 Head-Loss Prediction (ft-water)	Compacted Fiber/Part. Bed Thickness (in.)	Bed Porosity	Particulate Specific Surface Area (ft^2/ft^3)	
BWROG Test 7 Corrosion Products	0.28 (Fiber) 0.62 (Part.)	60	0.62	0.8 65	32	203	0.63	0.8	183,000	Debris Bed Damage Probable
BWROG Test 8 Corrosion Products	0.83 (Fiber) 0.16 (Part.)	5.3	0.62	0.8 65	> 41.7	83.3	0.19	0.8	183,000	Debris Bed Damage Probable
Latent Particulate Test 17 (< 75 µm)	0.23 (Fiber) 0.06 (Part.)	3.8	0.25	0.77 39	15.8	15.9	0.07	0.77	277,000	Uncertain in Debris Filtration Fraction
Latent Particulate Test 16 (75-500 µm)	0.23 (Fiber) 0.23 (Part.)	40	0.46	0.41 99	9.9	10.9	0.23	0.41	10,800	Stratified Debris Bed
Calcium Silicate Test 6H	0.23 (Fiber) 0.01 (Part.)	0.5	0.40	0.81 22	12.7	12.7	0.04	0.86	800,000	Bound Upper Head

[3] Experimental fiber beds thickness are based on the as-manufactured density without any bed compression.
[4] Experimental particulate bed thickness estimate assumed an equivalent thickness of particulate without the fiber present.

										Losses